Durham E-Theses

Antimicrobial Peptoids: Design, Synthesis and Biological Applications

BOLT, HANNAH,LOUISE

Antimicrobial Peptoids: Design, Synthesis and Biological Applications

A Thesis presented for the degree of Doctor of Philosophy

Hannah Louise Bolt

2016

Department of Chemistry, Durham University

Supervised by Dr Steven L. Cobb

Dr Steven Cobb

Department of Chemistry, University Science Laboratories, South Road, Durham, DH1 3LE, United Kingdom, +44 (0) 191 33 42086

s.l.cobb@durham.ac.uk

Abstract

The emergence of antimicrobial resistance is a severe threat to global health and new classes of antibiotics are desperately needed. Peptoids, or oligo-*N*-substituted glycines, are a group of peptidomimetics with increased structural stability and resistance to protease degradation compared to peptide analogues. In Chapter 1, peptoids are introduced and their antimicrobial properties reported to date are summarised. The synthesis and characterisation of one of the largest library of antimicrobial peptoids in existence is outlined in Chapter 2, comprising linear sequences and cyclic compounds. The development of synthetic methodology that allows the on-resin synthesis of novel peptoids containing both lysine- and arginine-type monomers is also described. In Chapter 3, the antiparasitic activity of the peptoid library is assessed against a variety of clinically relevant protozoan targets; including *Leishmania mexicana*, the causative agent of the neglected tropical disease cutaneous leishmaniasis. Active peptoids were identified against the insect and mammalian life stages of this parasite, including several with low micromolar potency against *L. mexicana* infected macrophages, an *in vivo* model of the disease. Additionally, peptoids that have selective activity at sub-micromolar concentrations against *Plasmodium falciparum* have been identified. Chapter 4 discusses the potent antibacterial and antifungal properties of the peptoid library against planktonic bacteria and also against mixed species, cross kingdom biofilms using a new quantitative polymerase chain reaction approach. Evaluation of peptoid toxicity to mammalian cells is also considered and conjugation of active sequences to the lantibiotic nisin is evaluated as a method to increase peptoid selectivity. To rationalise the activity of the peptoid library, Chapter 5 investigates the relationship between peptoid hydrophobicity, secondary structure and biological activity using circular dichroism spectroscopy and partitioning experiments. Finally, the antimicrobial mode of action is also examined using confocal fluorescence microscopy.

Acknowledgments

Memorandum

Work within this thesis has been presented by the author at the following meetings:

Poster presentation at the RSC Protein and Peptide Science Group, Early Stage Researcher Meeting, 11th November 2013, Durham University

Poster presentation at the RSC Bioorganic Group Postgraduate Symposium, 2nd April 2014, University of Warwick

Oral presentation at the Molecular Foundry Seminar Series (NanoBio Faculty), Molecular Foundry, 24th November 2014, Molecular Foundry, LBNL, Berkeley, CA, USA

Oral presentation at Van Mildert College, Destination 2015: Personal Research Journeys, 21st February 2015, Van Mildert College, Durham University

Oral presentation at RSC Chemical Biology and Bioorganic Postgraduate Symposium, 19th May 2015, Bristol University - *awarded a prize for the best overall student talk*

Lightning oral presentation and poster presentation at the Peptoid Summit, 7th and 8th August 2015, Molecular Foundry, LBNL, Berkeley, CA, USA

Poster presentation at the RSC Peptide and Protein Science Early Researcher Meeting, 13th November 2015, Durham University - *awarded a prize for the best poster*

Poster presentation at Science Engineering and Technology Award (SET Award), 7th March 2016, Westminster London

Poster presentation at the Durham University Early Researcher Poster Competition, 28th April 2016, Clayport Library, Durham City - *awarded the prize for best overall poster and the public's choice award*

Poster presentation at the British Society for Parasitology Autumn Symposium, 14-16th September 2016, Durham University

Poster presentation at the Chemistry and Biology of Peptides Symposium, 9th November 2016, University of Oxford - *awarded first prize for the poster presentations*

Publications resulting from work carried out as part of this thesis to date are listed below:

G.A. Eggimann, H.L. Bolt, P.W. Denny, S.L. Cobb*, Investigating the Anti-leishmanial Effects of Linear Peptoids, *ChemMedChem*, **2015,** *10* (2), 233-237.

G.A. Eggimann, K. Sweeney, H.L. Bolt, N. Rozatian, S.L. Cobb, P.W. Denny*, The Role of Phosphoglycans in the Susceptibility of *Leishmania mexicana* to the Temporin Family of Anti-Microbial Peptides, *Molecules*, **2015,** *20* (2), 2775-85.

H.L. Bolt, S.L. Cobb*, A practical method for the synthesis of peptoids containing both lysine-type and arginine-type monomers, *Org. Biomol. Chem.*, **2016,** *14* (4), 1211-1215.

H.L. Bolt, G.A. Eggimann, P.W. Denny, S.L. Cobb*, Enlarging the Chemical Space of Anti-leishmanials: a Structure-Activity Relationship Study of Peptoids against *Leishmania mexicana*, a Causative Agent of Cutaneous Leishmaniasis, *Med. Chem. Commun.,* **2016**, 7, 799 - 805.

H.L. Bolt*, P.W. Denny, S.L. Cobb, An efficient method for the synthesis of peptoids with mixed lysine-type/arginine-type monomers and evaluation of their anti-leishmanial activity, *J. Vis. Exp.*, **2016**, 117, e54750.

Y. Luo and H.L. Bolt, G.A. Eggimann, D.F. McAuley, R. McMullan, T. Curran, M. Zhou, C.A.B Jahoda, S.L. Cobb*, F.T. Lundy*, Peptoid efficacy against polymicrobial biofilms determined using propidium monoazide – modified quantitative PCR, *ChemBioChem*, accepted September **2016**, in press.

H.L. Bolt, C.E.J Williams, R.V. Brooks, R.N. Zuckermann, S. L. Cobb*, E.H.C Bromley*, Log *D* versus HPLC derived hydrophobicity: the development of predictive tools to aid in the rational design of bioactive peptoids, *Biopolymers* (*Peptide Science)*, accepted October **2016**, in press.

GB patent, GB1513444.8, H.L. Bolt and S.L. Cobb, Modified Peptoids, **2015**.

Abbreviations

AFM	Atomic force microscopy
Ahx	Aminohexanoic acid
AMP	Antimicrobial peptide
ANOVA	Analysis of variants
Ar	Aryl
BHI	Brain heart infusion broth
Boc	*tert*-Butyloxycarbonyl
BrAA	Bromoacetic acid
BSA	Bovine serum albumin
Bu	Butyl
CD	Circular dichroism
ClAA	Chloroacetic acid
CL	Cutaneous leishmaniasis
DAD	Diode array detector
DCM	Dichloromethane
Dde	*N*-(1-(4,4 Dimethyl-2,6-dioxocyclohexylidene)ethyl)
DIC	*N,N'*-diisopropylcarbodiimide
DIPEA	*N,N'*-diisopropylethylamine
DMAP	4-dimethylaminopyridine
DMF	*N,N'*-Dimethylformamide
DMSO	Dimethyl sulphoxide
DNA	Deoxyribonucleic acid
ED$_{50}$	Median effective dose

EPS	Extracellular polymeric substance
ERTG	Endo-Tracker™ Green
ESI-MS	Electrospray ionisation mass spectrometry
FBS	Foetal bovine serum
FDA	Food and Drug Administration
Fmoc	9-Fluorenylmethyl carbamate
FRET	Fluorescence resonance energy transfer
GPI	Glycosylphosphatidylinositol
h	Hour
HD$_{10}$	Hemolytic dose that lyses 10 % of erythrocytes
HEPES	4-(2-hydroxyethyl)-1-piperazineethanesulfonic acid
HFIP	Hexafluoroisopropanol
HIV	Human immunodeficiency virus
HPLC	High pressure liquid chromatography
HOMO	Highest occupied molecular orbital
HRMS	High resolution mass spectrometry
HSQC	Heteronuclear single quantum coherence spectroscopy
IC$_{50}$	Half maximal inhibitory concentration
LB	Lysogeny broth
LC-MS	Liquid chromatography mass spectrometry
LPG	Lipophosphoglycan
LRMS	Low resolution mass spectrometry
LTR	LysoTracker® Red
LUMO	Lowest unoccupied molecular orbital
MALDI	Matrix assisted laser desorption ionisiation mass spectrometry
MCL	Mucocutaneous leishmaniasis
MeCN	Acetonitrile

MeOH	Methanol
MEM	Minimim essential medium
MHB	Muller Hinton Broth
MHC	Minimum hemolytic concentration
MHz	Megahertz
MIC	Minimum inhibitory concentration
min	Minutes
MRE	Mean residue elipticity
mRNA	Messenger ribonucleic acid
MRSA	Methicillin-resistant *Staphylococcus aureus*
MS	Mass spectrometry
MTR	MitoTracker® Red
MW	Molecular weight
m/z	Mass to charge ratio
nd/nt	Not determined/not yet tested
NMP	*N*-methyl-2-pyrolidone
NMR	Nuclear magnetic resonance
NTD	Neglected tropical disease
Pbf	2,2,4,6,7-Pentamethyldihydrobenzofuran-5-sulfonyl
PBS	Phosphate buffered saline
PEG	Poly(ethylene glycol)
PCR	Polymerase chain reaction
PI	Propidium iodide
PMA	Propidium monoazide
PMC	2,2,5,7,8-pentamethylchroman-6-sulphonyl
PPG	Proteophosphoglycan
PPI/PPII	Polyproline type I/type II

PyBOP®	Benzotriazol-1-yl-oxytripyrrolidinophosphonium hexafluorophosphate
qPCR	Quantitative polymerase chain reaction
QSAR	Quantative structure activity relationship
QToF	Quadrupole time of flight
RCM	Ring closing metathesis
RNA	Ribonucleic acid
RP-HPLC	Reverse-phase high performance liquid chromatography
rpm	Revolutions per minute
RPMI	Roswell Park Memorial Institute medium
RT	Room temperature
SAR	Structure activity relationship
SI	Selectivity index
SEM	Scanning electron microscopy
SPPS	Solid phase peptide/peptoid synthesis
TBTA	Tris[(1-benzyl-1*H*-1,2,3-triazol-4-yl)methyl]amine
TFA	Trifluoroacetic acid
TIPS	Triisopropylsilane
tRNA	Transfer ribonucleic acid
TQD	Triple quadrupole
TOF	Time of flight
UPLC	Ultra-high performance liquid chromatography
UV-Vis	Ultraviolet-Visible
v/v	Volume concentration
VBNC	Viable but non-culturable
VL	Visceral leishmaniasis
WHO	World Health Organisation
XTT	2,3-bis-(2-methoxy-4-nitro-5-sulfophenyl)-2*H*-tetrazolium-5-carboxanilide

Contents

Chapter 1

An Introduction to Peptoids

1.1 Antimicrobial peptides

The discovery and deployment of antibiotics has had a dramatic positive impact on human and animal health since the introduction of penicillin in the 1940s. However, our ability to effectively treat bacterial diseases has gradually been eroded by the emergence of 'superbugs' that display resistance to multiple first line antibiotics. Increasing resistance, coupled with a dearth of new therapeutic molecules means the development of alternative antibacterial agents is imperative to prevent the onset of a post-antibiotic era where infection is rampant.[1]

Over the last few decades, an emerging class of molecules called antimicrobial peptides (AMPs) have been studied as potential antibiotic compounds. AMPs, also known as host-defense peptides, are found in nature and are part of the innate immune response of many organisms, as summarised by **Table 1.1**. They have been found to kill a large range of pathogens; including bacterial, fungal and parasitic species. In mammals, AMPs like the defensins and cathelicidin are found in leukocytes and are secreted by epithelia in skin and mucosal surfaces as part of the body's innate immune response. AMPs are also involved in other roles, such as wound repair, angiogenesis, inflammation responses and in the adaptive immune system. The potential applications of AMPs are already well reviewed, and these peptides have been recognised as highly selective and efficacious compounds.[2-4]

	Peptide	Origin	Structure	Number of amino acids
1	Magainin 2	Frog	α-helical	23
2	Cecropin A	Insect	α-helical	37
3	Cathelicidin	Mammal (human)	α-helical	37
4	α-defensins	Mammal (human)	β-sheet	29-35
5	β-defensin	Mammal (human)	β-sheet	36-47
6	Protegrin 1	Mammal (pig)	β-sheet	18
7	Indolicin	Mammal (bovine)	Extended structure	13
8	Lactoferricin	Mammal (bovine)	Loop (one disulphide)	25
9	Nisin	Bacteria	Polycyclic	34

Table 1.1. Examples of naturally occurring AMPs isolated from different sources with varying secondary structures.[5]

AMPs are short peptides (typically between ten and fifty amino acids) often with an amphipathic structure that allows permeabilisation of bacterial cytoplasmic membranes, leading to apoptosis. Many AMPs have α-helical domains and most are cationic with a high content of the amino acids lysine and/or arginine. Structure activity relationship studies have shown that factors such as sequence, size, helical content, charge and overall hydrophobicity can all affect the potency of AMPs. Understanding these related factors is key to designing new AMPs with increased potency and selectivity.[6,7]

AMPs often display greater selectivity towards bacterial membranes than eukaryotic membranes as their cationic character selectively targets prokaryotic membranes, which have a high proportion of negatively charged phospholipids. Perhaps the greatest advantage of AMPs over traditional small molecule drugs is that they are much less likely to be affected by bacterial resistance as they have been in use by nature for thousands of years without resistance emerging. Conventional antibiotics usually target specific bacterial processes, like cell wall synthesis, protein synthesis or replication. Bacteria undergo mutations rapidly and so can render entire classes of antibiotics ineffective in a short time period.[8,9]

Although the exact mechanisms are still debated within the field, antimicrobial peptides are thought to disrupt the cytoplasmic membrane, either causing the formation of aggregates, 'barrel-stave', 'carpet' or 'toroidal' pores that lead to cell lysis and apoptosis (see **Figure 1.1**). Alternatively, AMPs may permeate the membrane and target anionic intracellular substances like DNA, mRNA or specific proteins and interrupt cellular processes. Although bacteria have evolved certain strategies such as increased protease production, active efflux or modification of groups on the surface of bacterial membrane[*], many AMPs are able to evade these resistance mechanisms. As specific

---

[*] For example, surface polysaccharides may capture cationic AMPs before they reach the cell membrane.

receptors are not necessarily involved and an adaptation to alter the bacterial membrane composition is a substantial evolutionary change, AMPs are thought to be less susceptible to the development of bacterial resistance than typical small molecule antibiotics.[2,3,10-16]
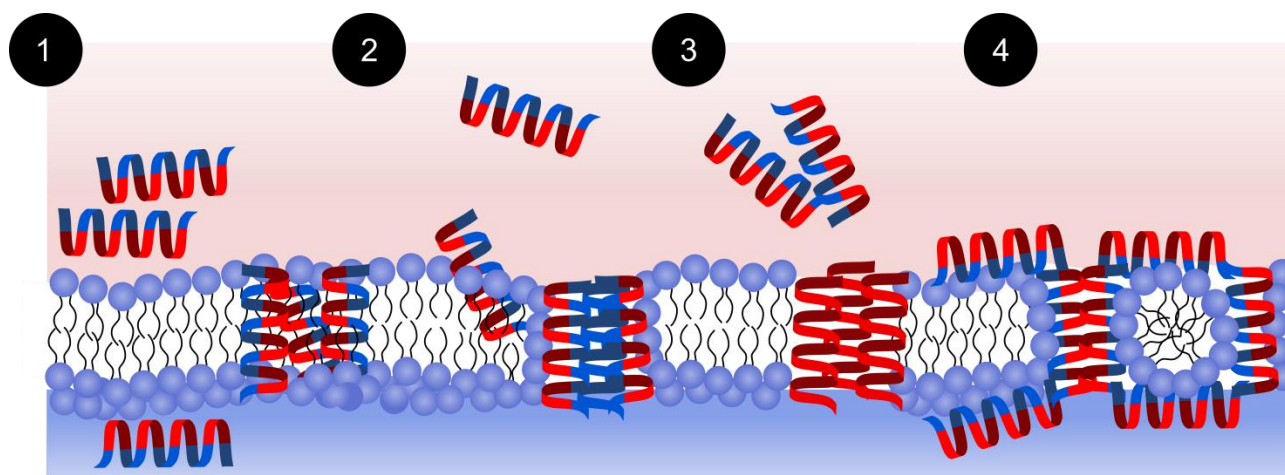
Figure 1.1. Proposed mechanism of action of AMP against a bacterial cell membrane, represented by the lipid bilayer. Peptides are represented by the blue and red helicies (although it should be noted that not all AMPs are helical, and not all are amphipathic) which suggest hydrophobic and hydrophilic regions of the peptide. **1**: aggregate model; **2**: toroidal pore model; **3**: barrel-stave model; **4**: carpet model.

More than 1,000 natural cationic peptides that display broad-spectrum activity have been identified to date.[†] Approved peptide therapeutics include antibiotics such as cyclic daptomycin[17], gramicidin[18] or the food preservative nisin (**9**).[19] Although about 140 peptides are being evaluated in the clinical trial process for various applications, few of these are antimicrobial peptides.[20] AMPs often show potent antimicrobial activity *in vitro* in controlled experiments, but there are many challenges in the clinical application of candidate peptides. For example, AMPs generally have poor oral bioavailability, a short half-life *in vivo* due to protease action and are rapidly excreted through the liver and kidneys so AMP drugs are usually unsuitable for systemic administration and tend to be proposed in topical applications only. Additionally, the synthesis of peptide based therapeutics can be costly which reduces their feasibility.[2,3,6,21-23]

Of the AMPs that pharmaceutical companies are developing, most are relatively small and the most cost-effective molecules which contain only the biologically active fragment of a larger parent peptide. AMPs have reached various stages of drug development, from preclinical studies to phase III trials (see **Table 1.2** for compounds **10–15** that are currently in clinical trials, **16** and **17** are in preclinical trials). However, despite encouraging results, as of 2015, no AMPs have been granted Food and Drug Administration (FDA) approval for clinical use.[5,20,24-26]

[†] The majority of these are documented in a variety of online databases, for example the Antimicrobial Peptide Database (URL: http://aps.unmc.edu/AP/main.php).

	Peptide	Clinical Trial Phase	Number of amino acids	Description and proposed use
10	Pexiganan acetate	III	22	Synthetic analogue of magainin 2; topical antibiotic for diabetic ulcers
11	Iseganan	III	17	Protegrin 1 analogue; prevention of oral mucositis
12	Omiganan	II/III	12	Synthetic cationic derivative of indolicidin; topical antiseptic for prevention of catheter infection
13	OP-145	II	24	LL-37 derivative for binding to lipopolysaccharides or lipoteichoic acid for the treatment of middle ear infection
14	LTX-109	I/II	3	Peptidiomimetic compound as a topical antibiotic for nasally colonised MRSA
15	hLF1-11	I/II	11	Lactoferrin analogue for the prevention of bacteria in the blood and fungal infections
16	Arenicin	preclinical	21	Rich in arginine and hydrophobic residues for use against multidrug resistant Gram positive bacteria
17	IMX924	preclinical	5	Synthetic peptide for use against both Gram positive and Gram negative bacteria

Table 1.2. Promising AMP candidates in clinical trials, as of 2015.[5,25]

Many groups have sought to optimise AMPs and their analogues in the pursuit of novel antimicrobial drugs, aiming to achieve improved metabolic stability and bioavailability, whilst retaining the activity and selectivity of the original peptide. For example, AMPs have been formulated as prodrugs or compounds have been developed that are structurally similar but distinct to peptides - these are collectively known as peptidomimetics.[27] Peptidomimetics can have additional advantageous properties, such as reduced rates of enzymatic degradation, the possibility to conformationally restrict the structure and enhance binding at desired receptors or provide the opportunity to add hydrophobic residues that can increase transport through cellular membranes.

Common strategies to improve peptide stability are summarised in **Figure 1.2**. These include cyclisation; the use of unnatural amino acids, for example, D- or β-amino acids; peptide stapling[28]; the addition of extra moieties to the peptide sequence, i.e. lipidation[29], methylation of sidechains[30,31] or PEGylation[32]; and modification of the peptide backbone such as use of *N*-acylated-*N*-aminoethyl amino acids[‡,33] or peptoids.[34] Additionally, many varied hybrid peptide-peptidomimetics have been synthesised to date. In particular the use of peptoids, oligomers of *N*-substituted glycine units, is becoming increasingly popular and the focus of this work.

[‡] α-AA peptides are based on the chiral peptide nucleic acid backbone.

Peptidomimetics
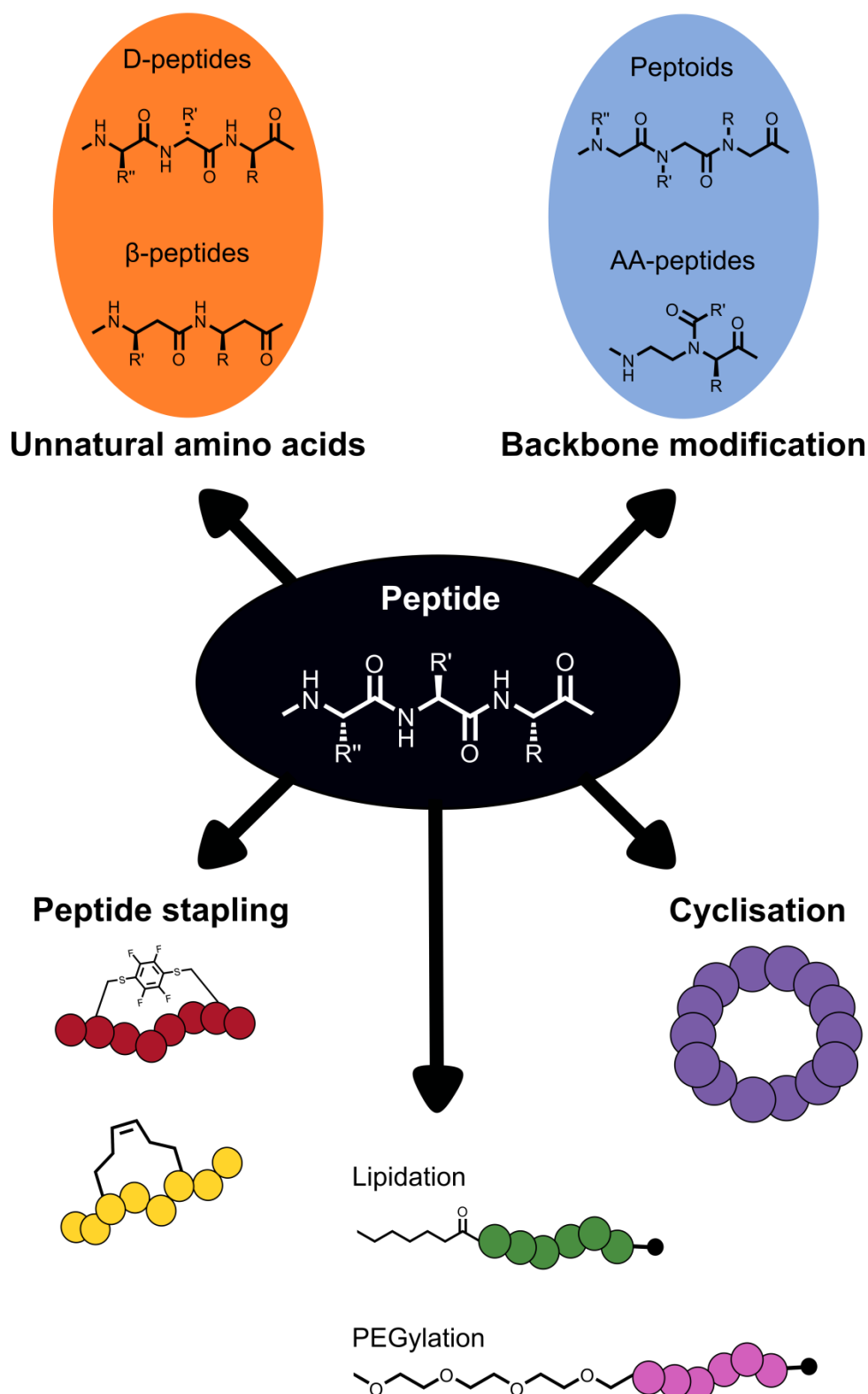
Figure 1.2. Common strategies to stabilise linear peptoids and examples of peptidomimetics that improve the *in vivo* stability of the compound compared to the parent peptide.

1.2 Peptoid structure

Peptoids are a class of peptidomimetics and as such share certain structural similarities with peptides, as illustrated in **Figure 1.3**. However, some aspects of peptoid structure are considerably different to that of peptides. In a peptoid, the polymer backbone consists of amide bonds where the side chain functionality is bonded to the nitrogen, rather than the α-carbon, so the repeating monomer of a peptoid is an *N*-substituted glycine. This means there are no stereogenic centres on the backbone of peptoids, compared to peptides that have a chiral backbone.[10,35]
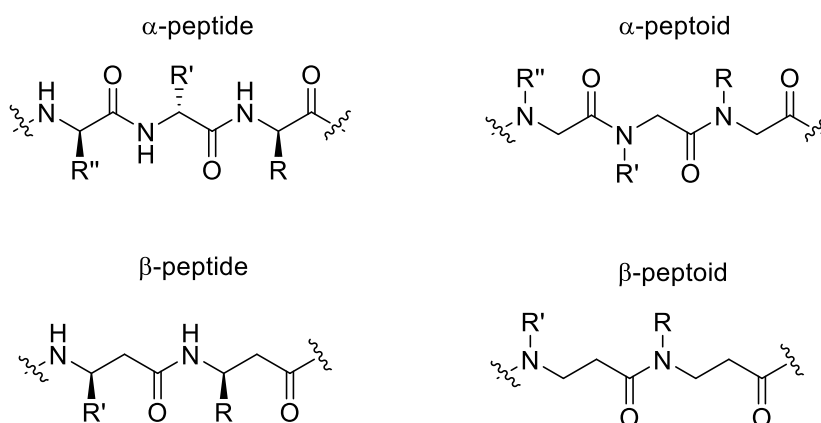
Figure 1.3. A comparison of the structures of generic α-peptoid and peptide oligomers. β-peptoids and β-peptides with the extra methylene unit in the backbone are also shown.

The lack of an amide hydrogen (due to the *N*-substitution) has several important effects on the structure of peptoids. In peptides and proteins, amide protons can undergo intra-chain hydrogen bonding which is key for the formation of the secondary structural motifs, such as α-helices and β-sheets. In peptoids, the absence of this amide proton leads to greater chain flexibility compared to peptides and prevents intra- and inter-chain hydrogen bonding. In addition, the lack of a hydrogen bonding donor on the backbone prevents backbone driven aggregation which can help to increase bioavailability. Therefore peptoid secondary structures are formed almost exclusively through electrostatic and steric interactions. As such peptoids are protease resistant and are not denatured by solvent changes or increased temperatures that usually disrupt hydrogen bonding patterns in peptides. Further discussion about peptoid secondary structure and strategies to stabilise such structures can be found in Chapter 2.[36]

The structures of generic alpha-peptoids and peptides are shown in **Figure 1.3**. Several research groups have also documented the synthesis and study of beta-peptoids, with an extra methylene group in the peptoid backbone.[37-39] The structure of β-peptoids is also shown above. Although they appear less frequently in the literature than the α-peptoids, β-peptoids will be considered briefly.

Due to their improved stability to proteases, peptoids have been used in a wide variety of biomedical applications, ranging from inhibitors of protein-protein interactions[40,41], molecular scaffolds[42,43], nucleic acid binders[44,45], lung surfactant protein mimics[46], biomimetic materials[43,47-50] or molecular transporters for drug delivery.[51-53] Example peptoids **18–21** for these applications are shown in **Figure 1.4**.

In particular, there is a wealth of literature detailing the antimicrobial activities of peptoids, with certain sequences displaying potent anti-infective properties against a wide variety of clinically relevant pathogens. This review seeks to summarise the field and will evaluate the antibacterial and antifungal properties of this exciting class of peptidomimetic molecules. The focus will be upon linear sequences but cyclic, lipidated peptoids, β-peptoids and hybrid peptoid-peptides will also be considered briefly.[10,54,55]

Inhibition of protein-protein interactions

18

rApaf protein K_d = 57 nM
Pérez-Payá, 2006

Cellular delivery agents

19

Cell penetrating peptoid sequence
with mitochondrial localisation
Bräse and Schepers, 2012

Molecular scaffolds

20

Anti-fouling peptoid and anchoring peptide
Messersmith, 2005

Biomimetic materials

21

Collagen triple helix mimetic
Boc(Gly-*N*Leu-Pro)$_7$-NH$_2$
Cai, 2007

Figure 1.4. Selected examples of peptoid structures and their varied applications.

1.3 Antibacterial peptoids

1.3.1 Linear sequences

The Barron group have conducted several structure-activity studies of peptoids against a wide variety of bacterial targets to probe the effect of characteristics such as chirality, chain length, overall sequence charge and hydrophobicity on the potency of peptoids as anti-infective compounds. In one study, peptoids were designed to mimic helical AMPs based broadly around a (*N*Lys*N*spe*N*spe)-motif (see **Figure 1.5**) and these peptoids were shown to have broad-spectrum activity with the best MICs of 1.6 µM for *E. coli* and 0.78 µM for *B. subtilis*.
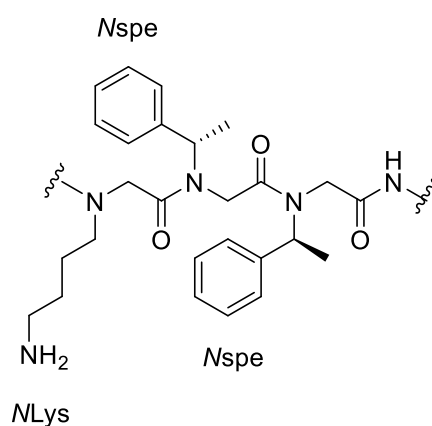
Figure 1.5. (*N*Lys*N*spe*N*spe)-motif within the antimicrobial peptoids synthesised by the Barron group.[56]

The hydrophobicity of the peptoids was altered by incorporation of different monomers; for example, *N*ssb monomers in peptoid **23** were replaced by the more hydrophobic monomers *N*smb and *N*sna in peptoids **28** and **29** respectively in **Table 1.3**. The increased hydrophobicity of the side chains in peptoids **28** and **29** led to greater antibacterial activity (MIC against *E. coli* decreases from 31 µM to 7 µM in peptoids **28** and **29**). However, incorporation of these more hydrophobic monomers also increased the hemolytic activity of the peptoids and the group also found that longer peptoid sequences are more cytotoxic against lung epithelial cells. The inclusion of the *N*His chain[§] in compound **31**, gave a peptoid with substantially decreased cytotoxicity *in vitro* and only a small reduction in antibacterial activity. To investigate the effect of charge, *N*Lys and *N*Glu monomers were used.

The lytic activity of peptoids against human erythrocytes was determined as a crude measure of selectivity. The most active peptoids showed good antibacterial activity against *B. subtillis* and *E. coli* and were also not significantly hemolytic, so the library was

---

[§] The imidazole group of the *N*His monomer is polar, but mostly uncharged at physiological pH with an isoelectric point of approximately pH 7.59.

extended in the group's later work (see **Table 1.3**). Successful compounds were then screened against six further clinically relevant bacterial pathogens and gave similar activities to pexiganan, **35**, a peptide optimised for biomedical applications.

It was demonstrated that the antimicrobial activity of these compounds was improved by moderate hydrophobicity, but high hydrophobicity and amphipathicity (i.e. peptoids **27**, **31** or **32**) led to poorly selective, hemolytic compounds. In addition, it was shown that that not only the hydrophobic, but also the positively charged side chains, have a great influence on the antibacterial potency; replacement of the positively charged side chain amines by carboxylic acids resulted in almost inactive compounds (see *N*Glu containing peptoid **33**). 12 residue sequences were identified as the optimal length for antibacterial activity – shorter peptoids were less potent and longer ones showed only an increase in hemolysis; for example, compare 9 reside peptoid **26** to 12 residue peptoid **22** with MIC values against *E. coli* of 9.1 µM to 3.5 µM respectively.

The overall peptoid helix stability was only slightly important for antimicrobial activity; the handedness of a helix does not alter its activity or selectivity as peptoids with the α-chiral monomer *N*spe and *N*rpe have the same activity (i.e. compound **22** and **24** both have equal MIC values against both *E. coli* and *B. subtilis*). Peptoids with strong and weak helical CD spectra all showed potent activity. Given that the peptoids which were strongly helical and amphipathic also had greater hemolytic activity, the overall sequence helicity should be considered when designing selective, antimicrobial peptoids in the future.[56]

Further sequences were made to mimic magainin-2 amide (**1**) and hits within this library gave MICs between 5.4–49 µM for *E. coli* and 0.82–7.8 for *B. subtilis*.[57]
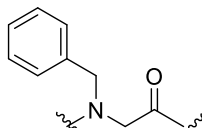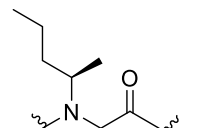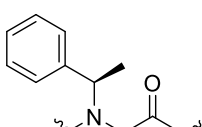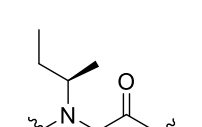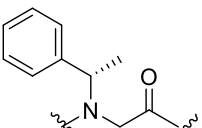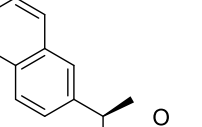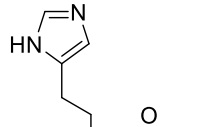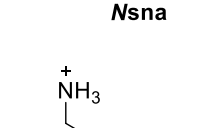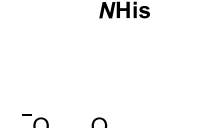
	Linear Sequence	Net Charge	MIC (µM)		Selectivity Ratio
			E. coli	*B. subtilis*	
22	(NLysNspeNspe)₄	+ 4	3.5	0.88	6.0
23	(NLysNssbNspe)₄	+ 4	31	3.9	> 3.9
24	(NLysNrpeNrpe)₄	+ 4	3.5	0.88	4.6
25	(NLysNspeNspe)₂	+ 2	27	27	> 8.1
26	(NLysNspeNspe)₃	+ 3	9.1	1.2	> 16
27	(NLysNspeNspe)₅	+ 5	5.5	1.4	0.55
28	(NLysNsmbNspe)₄	+ 4	7.4	0.95	> 16
29	(NLysNssbNspeNLysNssbNsna)₂	+ 4	7.2	0.93	7.6
30	(NLysNspeNspeNLysNspeNsna)₂	+ 4	3.3	1.6	1.2
31	(NLysNspeNspeNLysNspeNHis)₂	+ 4	3.5	6.9	> 31
32	(NLysNspeNspeNGluNspeNsna)₂	0	> 110	6.9	< 0.17
33	(NGluNspeNspe)₄	- 4	> 219	> 219	n/a
34	(NLysNpheNphe)₄	+ 4	12.5	1.6	14
35	*Pexiganan* (GIGKFLKKAKKFGKAVKILKK-NH₂)	+ 9	*3.1*	*1.6*	*24*

Table 1.3. A summary of selected peptoids and their associated antibacterial data from the Barron group. The selectivity ratio = 10 % hemolytic dose/MIC *E. coli*. The MIC values are obtained in assays with serum. The peptoid monomers used are also shown. All peptoids had C terminal amide groups.[56]

In other studies, peptoids related to the Barron group's initial study into helical AMP mimics were shown to be active against clinically relevant targets, *Pseudomonas aeruginosa* biofilms and *Mycobacterium tuberculosis* which are causes of pulmonary infection (see **Table 1.4**).[58,59]

These peptoids were shown to reduce the viability of established *P. aeruginosa* biofilms at their MICs, whereas antibiotics commonly used to treat this infection only showed comparable results at concentrations 8 to 30 times greater than their MIC. The most active peptoid tested, **22**, (*N*Lys*N*spe*N*spe)$_4$ had an MIC value of 12.5 µM, compared to 12.5–25 µM for pexiganan (**35**) which was used as a control. It was shown that the peptoids prevent biofilm formation by killing planktonic cells and the hydrophobic tail on the most active sequence, peptoid **38,** was proposed to act like a surfactant and interact strongly with the hydrophobic polysaccharide matrix on the cell surface, allowing the peptoid to penetrate deeper into the cell.[59]

The peptoids in **Table 1.4** showed appreciable activity against both *M. tuberculosis* and *M. tuberculosis* bacille Calmette-Guérin and displayed moderate toxicity against mammalian cells at their MIC. Similarly to the *P. aeruginosa* study, the cationic surfactant-like peptoid containing the C$_{13}$ chain, **38**, was the least cytotoxic and most active peptoid.[58]

	Linear Sequence	MIC (µM)		LD$_{50}$ (µM)
		P. aeruginosa	*M. tuberculosis*	
22	(*N*Lys*N*spe*N*spe)$_4$	12.5	14.1	20
36	(*N*Lys*N*spe*N*spe)$_3$*N*Lys*N*spe	12.5–25	14.46	40
37	(*N*Lys*N*spe*N*spe)$_2$*N*Lys*N*spe-LPro-*N*Lys*N*spe*N*spe	25–50	14.5	40
38	*N*tridec-*N*Lys*N*spe*N*spe*N*Lys	12.5–25	6.6	n/a

Table 1.4. Activities of selected peptoids against *P. aeruginosa* and *M. tuberculosis* and comparisons with their LD$_{50}$ against murine macrophages.[58,59]

Peptoids have also been proven to interact synergistically with antimicrobial peptides, suggesting a similar mechanism of action.[60]

A SAR study from the Shin group synthesised a peptoid analogue of a known tryptophan-rich antimicrobial peptide (see **39** in **Figure 1.6**). The cell selectivity of the peptide and peptoid were investigated against Gram positive and Gram negative bacteria, as well as their hemolytic activity against human red blood cells. Leakage of dye from liposomes designed to mimic the plasma membrane of bacteria was also measured to compare the mode of action between the peptide and peptoids. The peptoid and peptide tested showed very similar antimicrobial activities, with MIC ranging between 2

μM to 8 μM against a broad range of bacteria and neither showed significant hemolytic activity, even at 800 μM. Overall, the peptoid caused less dye leakage than the peptide and it was suggested that the target of both peptide and peptoid was intracellular rather than the cell membrane.[61]

Ac(*N*Lys*N*Leu*N*hTrp*N*Lys*N*hTrp*N*Lys*N*Lys*N*hTrp*N*Leu*N*Lys)

(*N*Lys*N*hTrp*N*Lys*N*Lys*N*hTrp*N*hTrp*N*Lys*N*hTrp*N*lLeu)
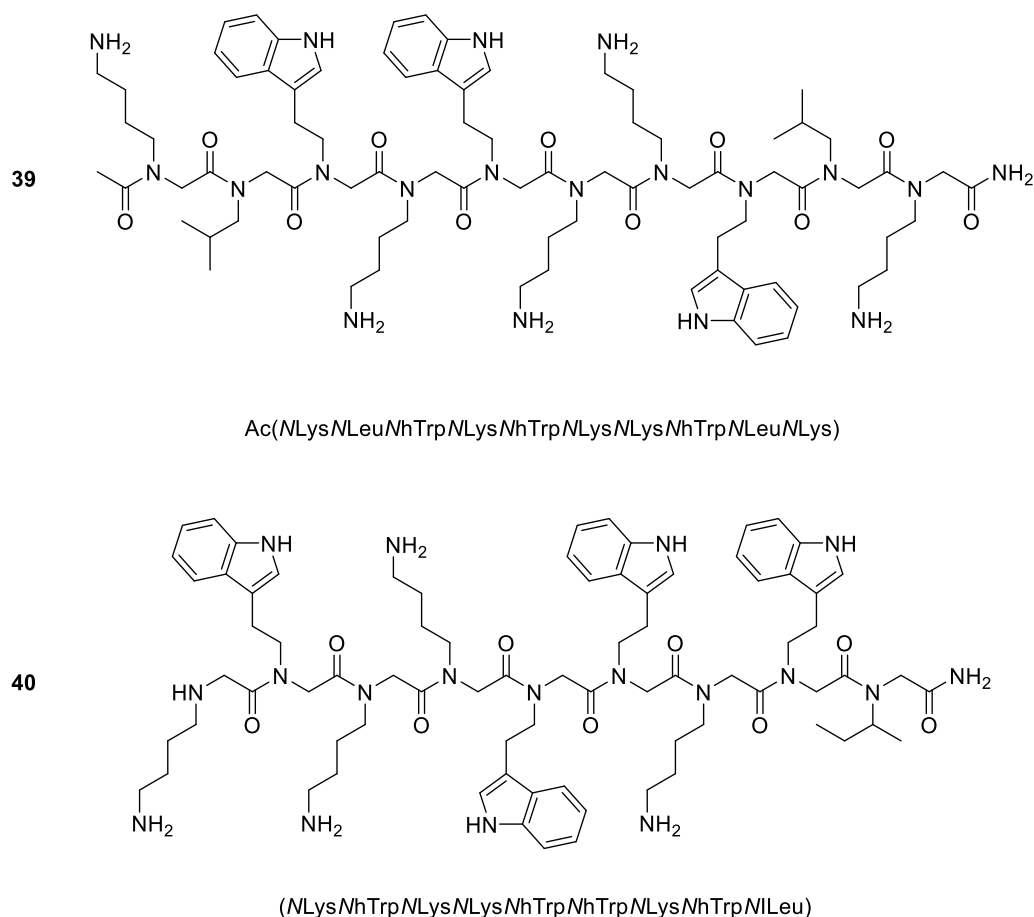
Figure 1.6. The tryptophan rich peptoid, **39**, synthesised by Shin *et al*. **40** is also shown, the GN2 peptoid made by Jenssen *et al*., of which derivatives were used in an SAR study on antimicrobial peptoids.[61,62]

The Jenssen group built upon the Shin study of the tryptophan rich peptoid by synthesising 22 cationic, amphipathic peptoids. These sequences were direct transformations of known typtophan rich antimicrobial peptides (see **Figure 1.6** for peptoid **40**, GN2) and the relationship between charge and hydrophobicity upon activity and cytotoxicity was examined. Screening against *E. coli*, *P. aeruginosa* and *S. aureus* showed MICs within the range of 2–64 μg mL^{-1} with moderate or improved activity in comparison to related antimicrobial peptides. It was shown that peptoids with high hydrophobicity (measured via HPLC retention time) are not always the most potent compounds against the Gram negative bacteria screened, but a linear relationship is seen for *S. aureus*. Furthermore, an increase in hydrophobicity (typically introduced by the

inclusion of highly aromatic residues like *N*-(2,2-diphenylethyl)glycine residues) reduces selectivity and increases toxicity against mammalian cells.[62]

The synthesis and characterisation of antibacterial tripeptoids found by screening of combinatorial chemistry libraries has identified peptoids with moderate activities against different bacteria strains.[63,64] The antimicrobial properties of peptoids have also been studied computationally, providing consistent results with biological testing[65] or via a mixture of modelling and NMR structural characterisation.[66] Another study compared the activity of a peptoid library using *in silico, in vitro* and *in vivo* techniques. In this study a QSAR model was able to correlate the antimicrobial activity (via MIC) of a peptoid from its structure.[67]

Finally, antimicrobial peptoids have also been immobilized onto titanium dioxide surfaces and shown to damage the cell membrane of adherent *E. coli* within 2 hours. In these systems both active antimicrobial peptoid and a passive antifouling peptoid coating was added with the view to use in implantable medical devices.[43]

1.3.2 Cyclic antimicrobial peptoids

Macrocyclisation enforces conformational ordering so reduces entropy losses upon binding to a biological target compared to a linear analogue and this is often linked to increased antimicrobial activity; for example, cyclic peptides like gramicidin are potent AMPs. An increased hydrophobic surface area in cyclic compounds compared to linear analogues and loss of charged termini is often attributed to an improvement in antimicrobial activity, via increased membrane permeability. In addition, the challenge of creating stable and defined secondary structures in linear peptoids due to their *cis-trans* isomerism means macrocyclisation is an attractive route. Therefore, there has been significant interest in the synthesis of cyclic peptoids as anti-infective agents, particularly because peptoids have been shown to cyclise more efficiently than peptides.[68-70]

The first cyclic peptoids with documented antimicrobial properties were synthesised by the De Riccardis lab. A small library of linear peptoids and their cyclised analogues was made to investigate activity against clinically relevant bacterial and fungal targets (*E. coli, S. aureus, Candida albicans* and *Cryptococcus neoformans*). Both protected and deprotected compounds were included in the study. Enhanced antimicrobial potency was seen following macrocyclisation and the moderate activity of cyclic molecules **41–46** are summarised in **Table 1.5**. Overall, their library showed better activity against the fungal targets compared to the bacteria and the antifungal potency increased with a greater number of charged amino groups, but this increased charge inhibited antimicrobial activity against both bacterial strains. It was also demonstrated that the amphiphilicity of the peptoids impacts significantly on the antimicrobial activity. The cyclic peptoids also show a selectivity against fungal strains and negligible toxicity to human red blood cells at the concentrations tested.[71]
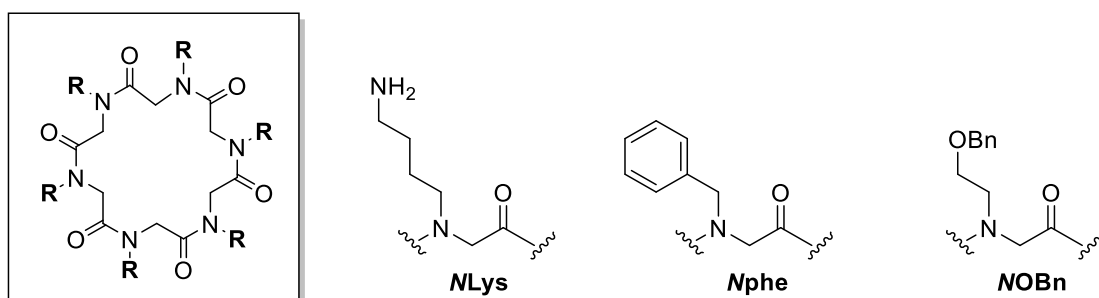
	Cyclic Peptoid	MIC (μM)		
		E. coli	*S. aureus*	*C. albicans*
41	cyclo (*N*Lys*N*OBn*N*OBn)$_2$	392	392	196
42	cyclo (*N*Lys*N*Lys*N*OBn)$_2$	383	383	184
43	cyclo (*N*phe*N*phe*N*phe)$_2$	> 1000	> 1000	> 1000
44	cyclo (*N*Lys*N*phe*N*phe)$_2$	465	465	232
45	cyclo (*N*Lys*N*Lys*N*phe)$_2$	786	> 1000	12
46	cyclo (*N*Lys*N*Lys*N*Lys)$_2$	> 1000	> 1000	5

Table 1.5. The antibacterial and antifungal properties of selected cyclic peptoids. The structure and side chains of the peptoids are also shown.[71]

The Kirschenbaum group have synthesised a large number of potent antimicrobial peptoids. The library was informed by X-ray crystal structures and designed with alternating cationic and hydrophobic monomers to lead to an amphiphillic structure with defined cationic/hydrophobic faces on opposing faces of the planar macrocycle. This was suggested to improve biological activity and may help cyclic peptoids to target cell membranes.[69,72]

Some peptoids screened were found to be inactive, but others showed potent antimicrobial properties; in particular peptoid **57** in **Table 1.6** with alternating phenyl and aminopropyl residues (*N*ap*N*phe)$_5$ had MIC values of 0.5 μg mL^{-1} and 7.8 μg mL^{-1} for *B. subtilis* and *E. coli*/*S. aureus* respectively. The potency of cyclic peptoids was compared to the activity of their linear precursors and as before, it was shown that cyclisation improves antibacterial properties. This is shown in **Table 1.6** and illustrated by **Figure 1.7** where it can be seen that the MIC values are lower for cyclic peptoids relative to their linear analogues.[72]
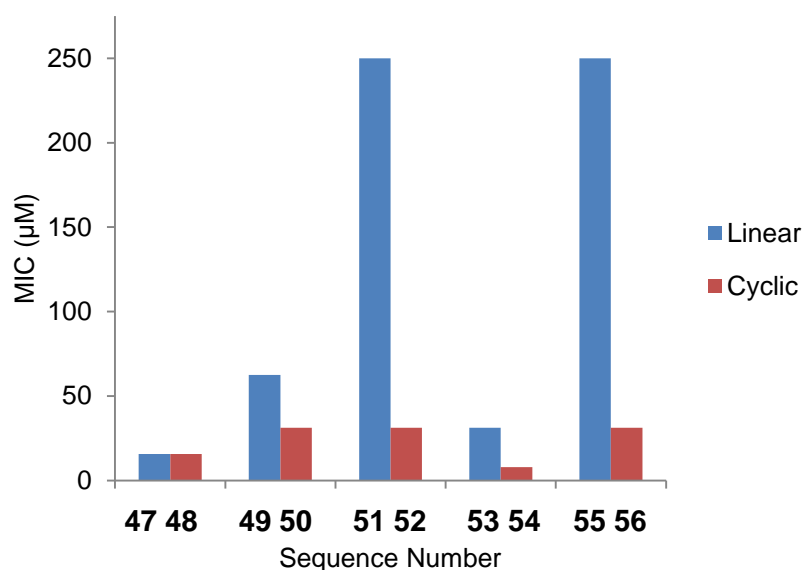
Figure 1.7. The MIC values for selected peptoids against *E. coli* (sequences shown in **Table 1.6**) and the increase in activity against shown by lower MIC values upon cyclisation.[72]

Longer peptoid sequences had increased activity in both cyclic and linear cases and the Kirshenbaum group concluded that there is a strong correlation between the hydrophobic surface area of a peptoid and activity by comparing sequences with side chains of varying hydrophobic surface area. For example, when comparing the napthyl, phenyl and diphenyl substituted peptoids (compounds **50**, **48** and **52** respectively) the napthyl peptoids have the greatest activity. However, increasing the hydrophobic area often also increases the hemolytic activity, so there should always be a balance between activity and selectivity. Finally in a resistance study using a potent cyclic peptoid, *S. aureus* was not able to develop resistance over a 21 day period, indicating the potential that peptoids provide as novel antimicrobials.[72]

The cyclic peptoids summarised in **Table 1.6** did not readily induce hemolysis of human erythrocytes ($HC_{50} > 250$ mg mL^{-1} for all compounds[**]) so were a promising starting point in the production of antibacterial peptoids.

[**] Where HC_{50} is the hemolytic concentration at which 50 % of the erythrocytes in solution are lysed.
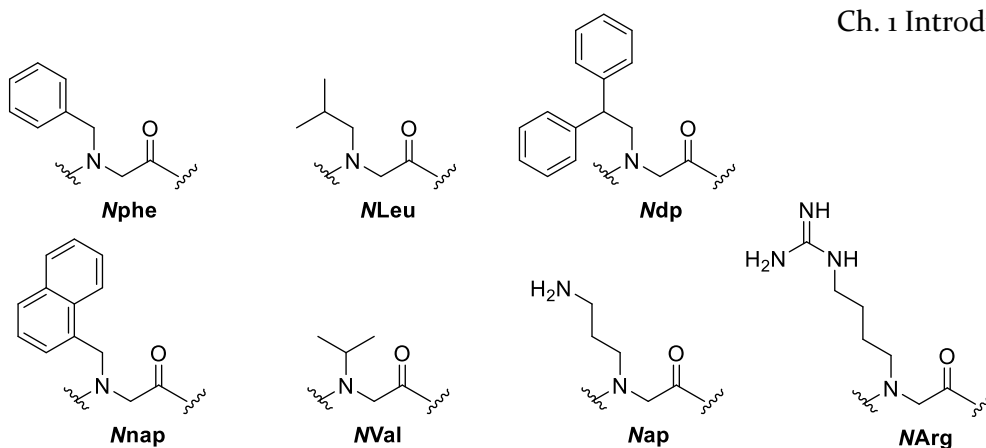
Peptoid Sequence	MIC (μM)	
	S. aureus	*E. coli*
47 linear Ac(Nap*N*dp)$_3$	15.6	15.6
48 cyclo (Nap*N*dp)$_3$	7.8	15.6
49 linear Ac(Nap*N*nap)$_3$	125	62.5
50 cyclo (Nap*N*nap)$_3$	31.3	31.3
51 linear Ac(Nap*N*phe)$_4$	250	250
52 cyclo (Nap*N*phe)$_4$	31.3	31.3
53 linear Ac(Nap*N*phe)$_3$	62.5	31.3
54 cyclo (Nap*N*phe)$_3$	7.8	7.8
55 linear Ac(Ndp*N*Leu*N*Arg*N*Val-Pro)$_2$	500	250
56 cyclo (Ndp*N*Leu*N*Arg*N*Val-Pro)$_2$	62.5	31.3
57 linear Ac(Nap*N*phe)$_5$	62.5	31.3
58 cyclo (Nap*N*phe)$_5$	7.8	7.8

Table 1.6. Selected peptoids from the Kirschenbaum study are tabulated to compare the effect of macrocyclisation. Peptoid monomers used are also illustrated.[72]

Further work from the Kirshenbaum group looked at the mode of action of cyclic antimicrobial peptoids against *S. aureus*. A new library of 5 and 6 residue cyclic peptoids was designed (see **Table 1.7**) to extend the previous library and these compounds included a greater variety of aromatic side chains for a more detailed SAR study.[73]

9 out of the 25 peptoids showed moderate or good antimicrobial activities and the relationship between hydrophobic surface area and activity was reinforced; i.e. for example, napthyl-based residues give higher potency than the phenyl-type monomers.

When comparing peptoids with diphenyl groups (i.e *N*dp monomer), sequences with three *N*dp residues show much better activity than those containing only two *N*dp monomers (i.e. scaffolds A/C **59** and **61** versus scaffold B **60**). Often compounds with increased hydrophobicity show increased toxicity towards host cells through non-specific interactions with mammalian membranes. However, most peptoids in this study had a good selectivity and moderate to low hemolysis (HD_{10} values in the range of 30–100 µM and selectivity ratios between 8 and 30).[73]
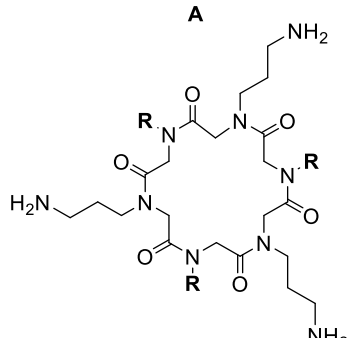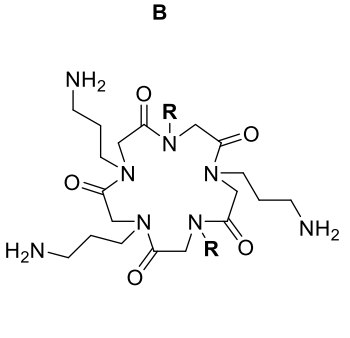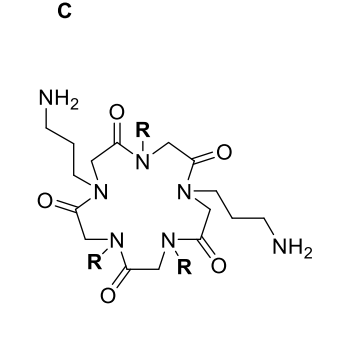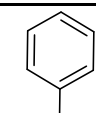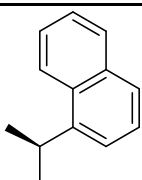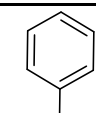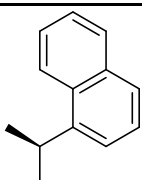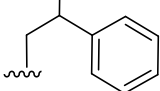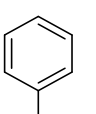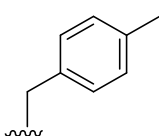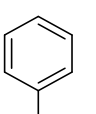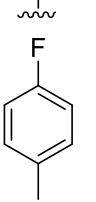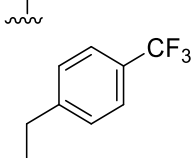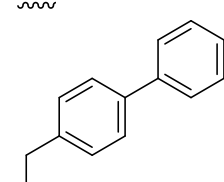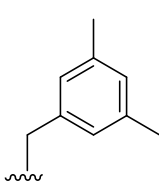
	R Group	Scaffold	MIC (µM)		R Group	Scaffold	MIC (µM)
59		A	3.9	**66**		A	3.9
60		B	250	**67**		B	> 500
61		C	3.9				
62		A	> 500	**68**		A	15.6
63		B	> 500				
64		A	31.3	**69**		A	3.9
65		A	3.9	**70**		A	3.9

Table 1.7. Peptoids from the Kirschenbaum study are tabulated with their MIC values against *S. aureus*. The cyclic scaffolds are shown above, with the 'R' groups shown in the table entries.[73]

Scanning electron microscopy (SEM) was used to confirm that the membrane of the bacteria, in this case *S. aureus*, was damaged upon treatment with cyclic peptoid. In **Figure 1.8**, it can be seen that pores and craters have been created in the bacterial cell walls in the cells treated with peptoid **59** at its MIC concentration.[73]
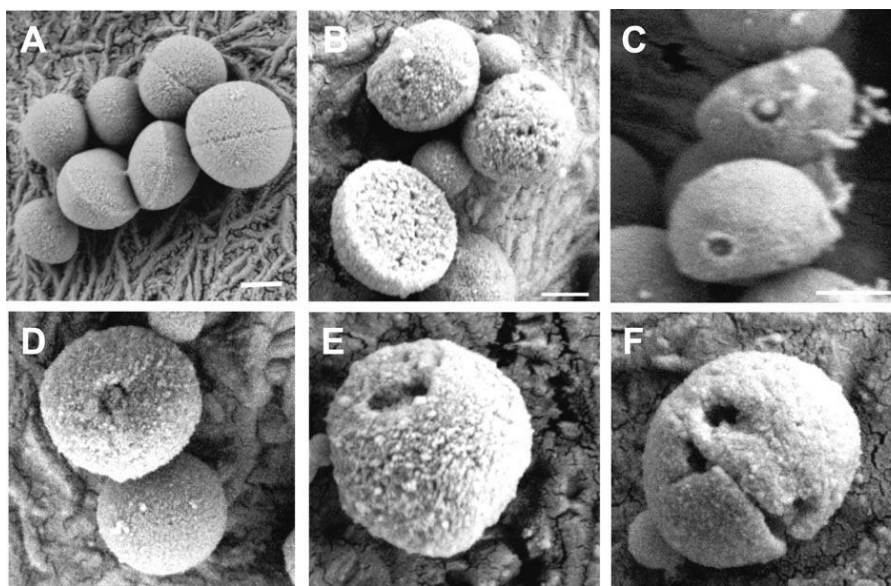
Figure 1.8. Scanning electron microscopy images to show the action of cyclic peptoids on bacterial cell membranes. **A** untreated cells; **B–F** cells incubated with peptoid **59** at the MIC value of 3.9 µM for 18 hours. Reprinted with permission, copyright 2013 John Wiley and Sons.[††,73]

The Kirschenbaum group have also used osmoprotective polymer additives to investigate the mechanism of action at the cell surface in more detail. It has been suggested that the creation of pores in a cell membrane leads to osmotic shock and the subsequent cell lysis and death. Adding osmoprotective layers to cells (in this case, polyethylene glycol) can prevent the influx of water that occurs after pore formation and therefore can protect against this process.

Both moderately active and potent cyclic peptoids were added to polymer protected methicillin-resistant *S. aureus* and SEM used to study morphological changes. Initial pores formed by the cyclic peptoids in the absence of osmoprotectant were between 2.0–3.8 nm in diameter but expanded to > 200 nm over 24 hours. After adding the osmoprotectant, the antimicrobial potency of the peptoids was diminished but pores were still seen via SEM. It is suggested by the authors that the polymer is able to protect the cells from the expansion of lethal pores attenuating the MIC and that the cell membrane of the MRSA is a primary target of their antimicrobial peptoids.[74]

[††] Image adapted from Huang *et al*, *Eur. J. Org. Chem.*, **2013**, *17*, 3560.

1.3.3 Lipopeptoids

Lipopeptides, such as daptomycin, or the polymyxin and echinocandin related antibiotics are becoming increasingly important antimicrobial peptides. These molecules all possess fatty acid chains that have been shown to be vital for their activities.[75] Lipopeptoids with different sequences and lipid tails have been synthesised to mimic these successful antimicrobial peptides and their toxicity and activity against both Gram positive and Gram negative bacteria strains studied by several groups.

The Barron group has taken linear peptoid sequences, previously used in their antibacterial studies, and added lipid-type chains to the N termini of the sequence with alkyl tails either 5, 10 or 13 carbons in length. A selection of these lipopeptoids and their activities against bacterial and fungal species have been summarised in **Table 1.8**. It was found that the 12 residue peptoid **22** (NLys$N$spe$N$spe)$_4$ with known antibacterial activity loses its activity against bacteria as the chain length of the lipid tail increases, i.e. C_5 chain on peptoid **70** yields an MIC of 15.5 μM against *E. coli* whereas with the C_{10} chain of compound **73** has an MIC value of 31.6 μM. However, the longer alkyl chains do shows display increased antifungal properties, with lower MIC values against *C. albicans*. It is suggested that the higher hydrophobicity needed for activity against fungal species stems from differences between zwitterionic eukaryotic membranes and the more anionic bacterial cell membranes.[76]

For the shorter peptoid sequences that were lipidated, an increased antimicrobial potency is seen against both bacteria and fungi compared to the analogous unalkylated peptoid **22** (i.e. peptoid **74** has lower MIC values of 8.8 μM against *E. coli* and *C. albicans* and MIC value of 2.2 μM against *B. subtilis*). Significantly, lipopeptoids as short as five residues showed good antimicrobial activity with promising selectivity ratios against human erythrocytes, with peptoid **74** having a selectivity ratio of 17.[76]

As expected, the longer lipid tails lead to more hydrophobic molecules with a higher toxicity towards eukaryotic cells. However, alkylation does not always cause detrimental hemolytic activity as the 5 residue Ndec peptoid **75** showed potent activity against Gram positive bacteria but negligible lysis of red blood cells at concentrations as high as 200 μg mL^{-1}. To extend the study, **38**, Ntridec-NLys$N$spe$N$spe$N$Lys was tested against a wide variety of clinically relevant pathogens including multi-drug resistant strains and showed broad spectrum activity.[76]

	Peptoid Sequence	MIC (μM)			HD$_{10}$ (μM)	Selectivity Ratio
		E. coli	*B. subtilis*	*C. albicans*		
22	(*N*Lys*N*spe*N*spe)$_4$	14.7	3.7	14.7	33	8.9
70	*N*pent(*N*Lys*N*spe*N*spe)$_4$	15.5	3.9	15.5	37	9.5
71	*N*pent(*N*Lys*N*spe*N*spe)$_3$	30.8	1.8	23.7	100	56
72	*N*pent(*N*Lys*N*spe*N*spe)$_2$	> 266	4.1	133	> 266	> 65
73	*N*dec(*N*Lys*N*spe*N*spe)$_4$	31.6	4.0	4.0	13	3.3
74	*N*dec(*N*Lys*N*spe*N*spe)$_2$	8.8	2.2	8.8	37.8	17
75	*N*dec-*N*Lys*N*spe*N*spe*N*Lys	> 108	6.8	108	> 215	> 32
38	*N*tridec-*N*Lys*N*spe*N*spe*N*Lys	14.0	1.8	14.0	73	41
35	Pexiganan (GIGKFLKKAKKFGKAVKILKK-NH$_2$)	7.8	3.9	124	181	46

Table 1.8. A summary of selected lipopeptoids and their associated antibacterial and antifungal properties. The selectivity ratio = 10 % hemolytic dose/*B. subtilis* MIC. The peptoid monomers are also summarised, where *N*dec = 10 carbon decane alkyl chain, *N*tridec = 13 carbon tridecyl chain and *N*pent = 5 carbon pentane chain. All peptoids had C terminal amide groups.[76]

A separate study looked into the effect of lipidation on a library of 19 very short antimicrobial peptoids. The sequences chosen were all based upon KKK, RRR, KGK or RGR tripeptides[‡‡] and therefore were cationic, made of *NLys* or *NhArg* residues. Sequences made exclusively of the cationic monomers had an overall charge of +3 and the sequences with a glycine between the two cationic residues had a net charge of +2. The lipid tails chosen are summarised in **Figure 1.9**; C_{11}, C_{14}, C_{16}, C_{20} or F_{11} chains (where the F_{11} backbone is comprised of CF_2 groups rather than CH_2).[77]
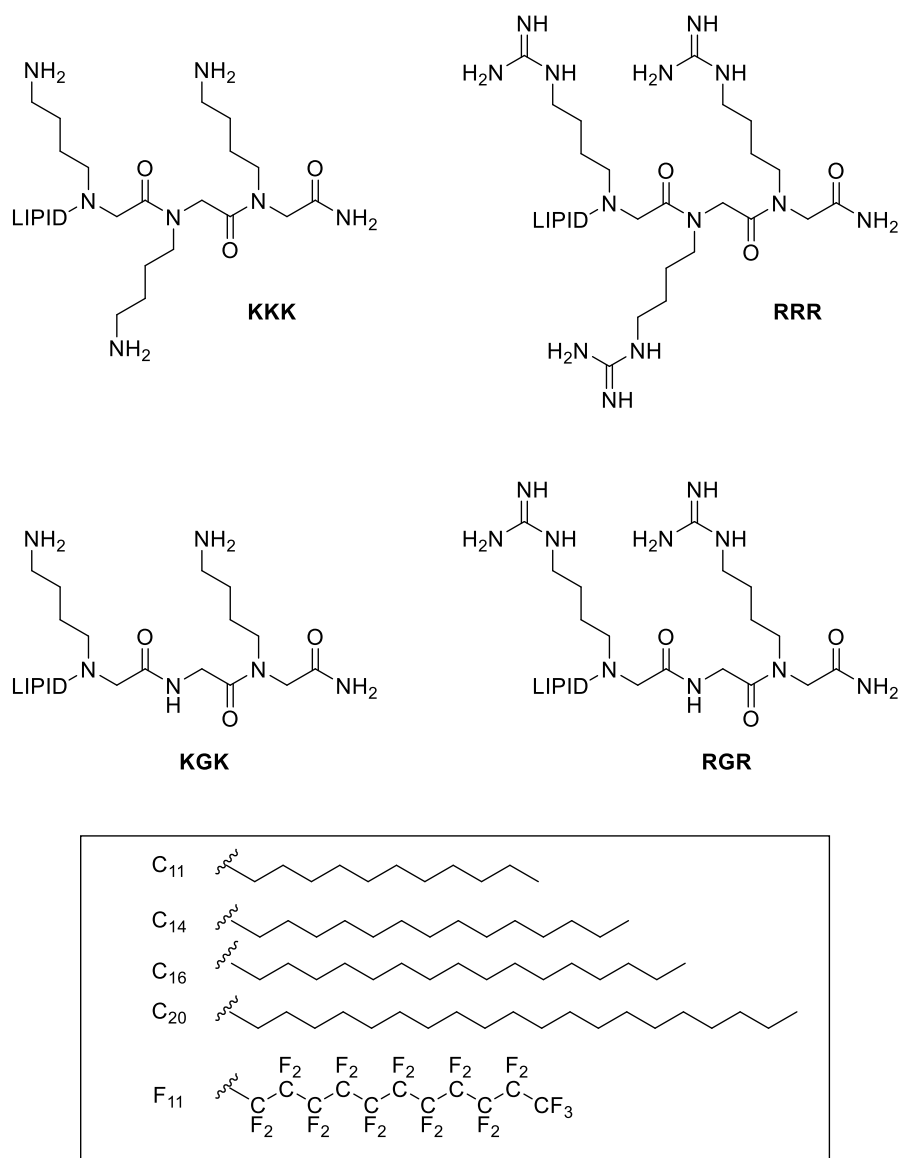
Figure 1.9. The short, three reside peptoids prepared by the Schweizer group with lipid tail groups.[77]

[‡‡] Where K is the amino acid lysine, R is arginine and G is glycine.

The compounds were tested against a variety of reference and clinical bacterial strains[§§] and were found to be moderately active against both Gram positive bacteria (MICs from 8 μg mL^{-1} for *S. aureus* and MRSA) and Gram negative species (for example, MICs from 16 μg mL^{-1} for *E. coli*, 64 μg mL^{-1} for *P. aeruginosa* and 16 μg mL^{-1} for *K. pneumoniae*). In comparison to the positive control (cetrimide, a cationic disinfectant), their most active peptoids were less able to inhibit Gram positive bacteria, but had a greater potency against the Gram negative bacteria.[77]

It was found that *E. coli* species were particularly susceptible to peptoids with the C_{16} chain. Overall, the fluorinated F_{11} chain was less effective than the C_{14} analogue on a mass basis and the homoarginine peptoids were more active but also more toxic than their analogous lysine peptoids. The hemolytic activity of compounds within the peptoid library was proportional to their antimicrobial activity, but the most hemolytic peptoids were still slightly less toxic than the cetrimide control. The antimicrobial assays were also repeated in the presence of bovine serum albumin (BSA) since hydrophobic proteins such as BSA are known to cause a reduction in antimicrobial activity through binding interactions. Both the control compound and the lipopeptoids were similarly inhibited with a reduction in antimicrobial potency.[77]

Other peptidomimetic structures based upon peptoids have also been lipidated to increase their antimicrobial activity, such as the α-AApeptides synthesised and tested by the Cai group.[78,79]

1.3.4 Peptide-peptoid hybrids

Several groups have tried to overcome the poor stability of peptides *in vivo* by synthesising peptoid-peptide hybrids. In one study using apidaecin Ib, **76**, an AMP with three arginine residues which are important for its antibacterial activity, single arginine or leucine residues were replaced with the equivalent peptoid residues. Basic residues often represent the attack site for trypsin-like enzymes so the mutation to a peptoid monomer had the potential to increase the half-life *in vivo*.[80]

The hybrids synthesised had arginine residues in one or more positions of the sequence replaced by *N*Arg *N*-(3-guanidinopropyl) glycine[***] or *N*nArg *N*-(2-guanidinoethyl) glycine[†††] at residue 17, 12 or 4, as shown in **Table 1.9**. These compounds were more resistant to proteolysis than unmodified apidacecin, which has a half-life of less than 60 minutes in a trypsin digest. No significant degradation of the peptide-peptoid hybrids **76–81** was detected after a 24 hour incubation with trypsin. Additionally, the hemolytic activity of the hybrids was shown to be less than 2 % at 300 μM for all compounds and as long as the C terminal residues were not altered, MIC values between 16–32 μM were achievable against *E. coli*.[80]

[§§] Data not shown
[***] i.e. compounds **77**, **78** and **79** in **Table 1.9**.
[†††] i.e. compound **81** in **Table 1.9**.

	Sequence	MIC (µM) *E. coli*	Hemolytic activity (%)
76	*Apidaecin Ib* GNNRPVYIPQPRPPHPRL	8	1.2
77	GNNRPVYIPQPRPPHP**NArg**L	> 128	0.44
78	GNNRPVYIPQP**NArg**PPHPRL	16	2
79	GNN**NArg**PVYIPQPRPPHPRL	16	0.06
80	GNNRPVYIPQPRPPHPR**NLeu**	> 128	nd
81	GNNRPVYIPQP**NnArg**PPHPRL	16–32	1.31

Table 1.9. Apidaecin analogues substituted with peptoid residues and their associated antibacterial activity against *E. coli* and the hemolytic activity against human erythrocytes at 300 µM. Peptoid residues are highlighted in bold.[80]

Some groups have incorporated a small number of peptoid resides into a peptide sequence for a specific purpose. For example, a synthetic mimic of naturally occurring AMPs papiliocin and magainin 2, **82**, was designed to have high antimicrobial activity. This peptide contained the N terminal residues of both peptides joined by a proline hinge, however caused significant lysis of human erythrocytes at 100 µM due to the rigid structure. By substituting this proline residue with the more conformationally flexible lysine peptoid residue in compound **83** the hemolytic activity was reduced so selectivity was increased two-fold; from 19 for the parent peptide **82** to 35 for **83**, as seen in **Table 1.10**.[81]

Proline residues play a critical role in determining peptide secondary structure and in other peptide-peptoid hybrids, proline residues have also been substituted by a peptoid monomer to reduce cytotoxicity (see **Table 1.10**). For example piscidin 1, **84**, is a cationic and cytotoxic peptide with α-helical secondary structure. Replacing the proline at position 8 with a peptoid lysine residue (**85**) reduces the rigidity of the sequence and leads to a hybrid compound with similar antibacterial activity but much increased selectivity compared to the parent peptide (selectivity ratio 1.6 for **84** compared to 140 for **85**).[82]

Additionally, proline residues in the tryptophan/proline-rich AMPs cathelicidin **86** and indolicidin **87** were substituted with the peptoid residue *N*Lys to increase the therapeutic index of the parent peptides. The minimal hemolytic concentrations (MHCs) of the *N*Lys peptide-peptoid hybrids, **88** and **89**, were drastically increased to > 200 µM, leading to improved selectivity indices in excess of 150 (**86** and **87** have selectivity factors of 59 and 7 respectively). It was proposed that these compounds have an intracellular target mechanism as no visible membrane depolarisation was seen when cells were treated at the MIC level.[83]

	Sequence	MIC (μM)		Minimal hemolytic concentration (μM)	Selectivity
		E. coli	*S. aureus*		
82	*Synthetic papiliocin/magainin 2 mimic* RWKIFKKIPKFLHSAKKF	2	4	100	19
83	RWKIFKKI***NLys***KFLHSAKKF	2	4	200	35
84	*Piscidin 1* FFHHIFRGIVHVGKTIHRLVTG	2	1	3.1	1.6
85	FFHHIFR***NLys***IVHVGKTIHRLVT	2	4	> 200	140
86	*Cathelicidin* KKFPWWWPFKK	4	1	100	59
87	*Indolicidin* ILPWLWPWWPWRR	8	1	25	7
88	KKF***NLys***WWW***NLys***FKK	1	1	> 200	235
89	IL***NLys***WLW***NLys***WW***NLys***WRR	4	1	>200	182
90	*Melittin* GIGAVLKVLTTGLPALISWIKRKRQQ	2	0.5	0.78	0.6
91	GIGAV***NAla***KVLTTG***NAla***PALISW***NAla***KRKRQQ	16	16	> 100	14
92	GIGAV***NLeu***KVLTTG***NLeu***PALISW***NLeu***KRKRQQ	4	4	> 100	50
93	GIGAV***Nphe***KVLTTG***Nphe***PALISW***Nphe***KRKRQQ	4	2	> 100	71
94	GIGAV***NLys***KVLTTG***NLys***PALISW***NLys***KRKRQQ	4	2	> 100	71

Table 1.10. Other peptide-peptoid hybrids and their associated biological activity against bacteria. The concentration at which minimal hemolytic activity is seen is also shown with a selectivity factor. Peptoid residues are highlighted in bold.[81,82,84,85]

Single peptoid residues were also introduced into the AMP melittin (**90**) to form other peptoid-peptide hybrids (compounds **91–94** in **Table 1.10**). Melittin, **90**, found in bee venom, is known to form an amphipathic structure with a leucine zipper motif that is thought to promote self-association and facilitate the formation of a transmembrane pore in cell membranes. Peptoid residues were substituted into key positions of the leucine zipper and showed strong antimicrobial activity against bacteria, even though CD studies showed that the helical structure was distorted by inclusion of these peptoid residues. Although the MIC values of the hybrid compounds against clinical isolates of MRSA[‡‡‡] were greater than the MIC of wild-type melittin (MIC = 2–8 μM and 2 μM respectively), the peptoid analogues **91–94** were far less hemolytic than melittin, with MHC values of > 100 μM compared to melittin itself that has an MHC of 0.78 μM. In particular substitution of leucine, phenylalanine or lysine for their peptoid counterparts in the leucine zipper were suggested as strategies to improve the antimicrobial action of peptides (i.e. *N*Leu in **92**, *N*phe in **93** or *N*Lys in **94**).[84]

In another study, a library of lysine-peptoid hybrids was synthesised as short analogues of cationic AMPs. All compounds incorporated the peptoid fragment **95** in **Figure 1.10** and multiple lysine residues were added at the C or N terminus and a selection of these sequences are shown in **Table 1.11**. The peptide-peptoid hybrids **96–100** exhibited broad-spectrum antimicrobial activity against clinically relevant bacteria. MIC values for the most active compounds in the library ranged between 2–8 μM and 4–20 μM for *S. aureus* and *E. coli* respectively. The hemolytic activity of these compounds at 50 μM was low in compounds with three or more lysine residues, for example **98–100**. In extension to the original study, more antibacterial lysine-peptoid hybrids based upon this structure were identified from a positional scanning combinatorial library.[86-88]
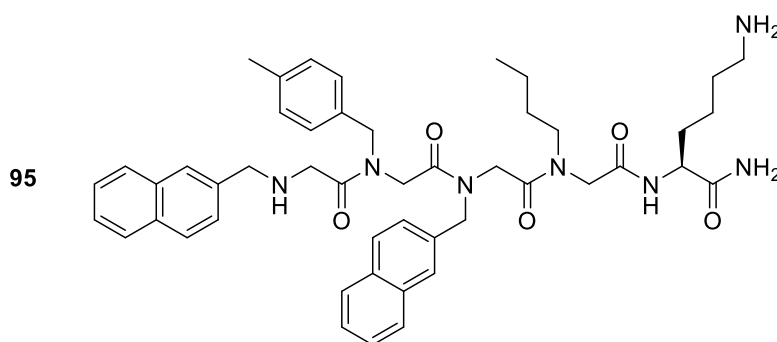
Figure 1.10. The peptoid fragment **95**, used in the Hansen study. Lysine residues were added either at the C or N terminus to form the peptide-peptoid hybrids.[86-88]

[‡‡‡] MIC values of compounds **91–94** against clinical isolates of MRSA are not shown in **Table 1.10**.

	Peptoid Sequence	MIC (µM)		Hemolysis (%)
		S. aureus	*E. coli*	
96	Fragment **95**-K	6.25	23	100
97	Fragment **95**-KK	6.25	21	51
98	Fragment **95**-KKK	3.12	17	5
99	Fragment **95**-KKKK	< 1.6	15	2
100	Fragment **95**-KKKKK	< 1.6	15	3
101	*Ampicillin*	1.25	62.5	nd

Table 1.11. Selected antimicrobial activities of some lysine-peptoid hybrids and hemolytic activity at 50 µM. All sequences were amidated at the C terminus.[86-88]

The peptide-peptoid hybrid **100** with five C terminal lysine peptide residues was used to investigate the mode of action against *S. aureus*. At concentrations much greater than the MIC, the compound disrupts the cell membrane and causes ATP leakage from the cells. At concentrations nearer the MIC the *S. aureus* growth is inhibited without ATP leakage. The hybrid can also bind to DNA, inhibiting DNA gyrase and topoisomerase IV causing the SOS response in *S. aureus* which indicates that this peptide-peptoid hybrid may have a dual mode of action.[89]

The Robinson group have reported the synthesis of macrocyclic peptide-peptoid compounds that have a β-hairpin backbone conformation. These antibiotics display antimicrobial activities against both Gram positive and Gram negative bacteria and have low hemolytic activity against human erythrocytes. The exchange of peptoid residues for peptide residues is shown to have no detrimental effect on biological activity or to the secondary structure.[90,91]

In another study, the cytotoxicity of peptide-peptoid hybrids was investigated. The library was comprised of sequences with alternating cationic amino acids and hydrophobic peptoid residues of varying lengths. Moderate activity against Gram positive strains was seen for those compounds with chiral peptoid residues, however, the presence of α-chiral side chains in the peptoid monomers was found to increase cytotoxicity. Both chiral and achiral peptoid monomers gave moderate activity against Gram negative *E. coli* with one compound having an MIC of 1 µM.[92]

1.3.5 β-peptoids

Several groups have also incorporated beta-peptoid residues into antimicrobial peptoids (i.e. poly-*N*-substituted β-alanine). These structures are isosteres of β-peptides and are similarly stable to proteases as the α-peptoids discussed above. β-peptoids have very different secondary structures to the linear α-peptoids described above and although many natural AMPs are helical, it has been shown that compounds without an amphiphillic, helical structure can also function as potent antimicrobials

Work by Du Pont in 2006 documented the synthesis of antimicrobial β-peptoids. In this study, 21 compounds between 9 and 18 residues in length were synthesised and tested against *E. coli.* In the library, functionalities included hydrophobic groups such as benzyl or isobutyl and cationic chains, such as aminoethyl, aminobutyl and 4-dimethylaminopyridine to probe effects like charge, the importance of overall side-chain composition and positioning of cationic and hydrophobic residues on their biological activity. A selection of these peptoids were shown to have moderate activity against *E. coli*, with the best sequence having an MIC of 128 μg mL^{-1}.[37]

A large number of antimicrobial β-peptoids have since been made by the Olsen group. In an early study, a library of β-peptoid α-peptide oligomers were made with α-chiral phenethyl side chains (β-*N*spe) and either the cationic amino acids lysine or arginine. A variety of both chiral and achiral containing β-peptoid residues were included in the sequence and the length of the chimeras varied between 10 and 16 residues (see **Figure 1.11**, peptoids **102–110**). For preliminary screening these compounds were tested against a range of Gram positive and negative bacteria[93] and also against the causative agent of malaria, *Plasmodium falciparum*.[94]

Later, an extended library was synthesised to test against a wider variety of pathogens, including drug resistant bacteria and the fungal species *C. albicans*.[95] This larger library included similar α-peptide β-peptoid motifs with the addition of the aliphatic monomer *N*-(*S*)-1-cyclohexylethyl-β-alanine (see **Figure 1.11**, peptoids **111** and **112**) to probe the effects of lipophilicity on activity.[95]
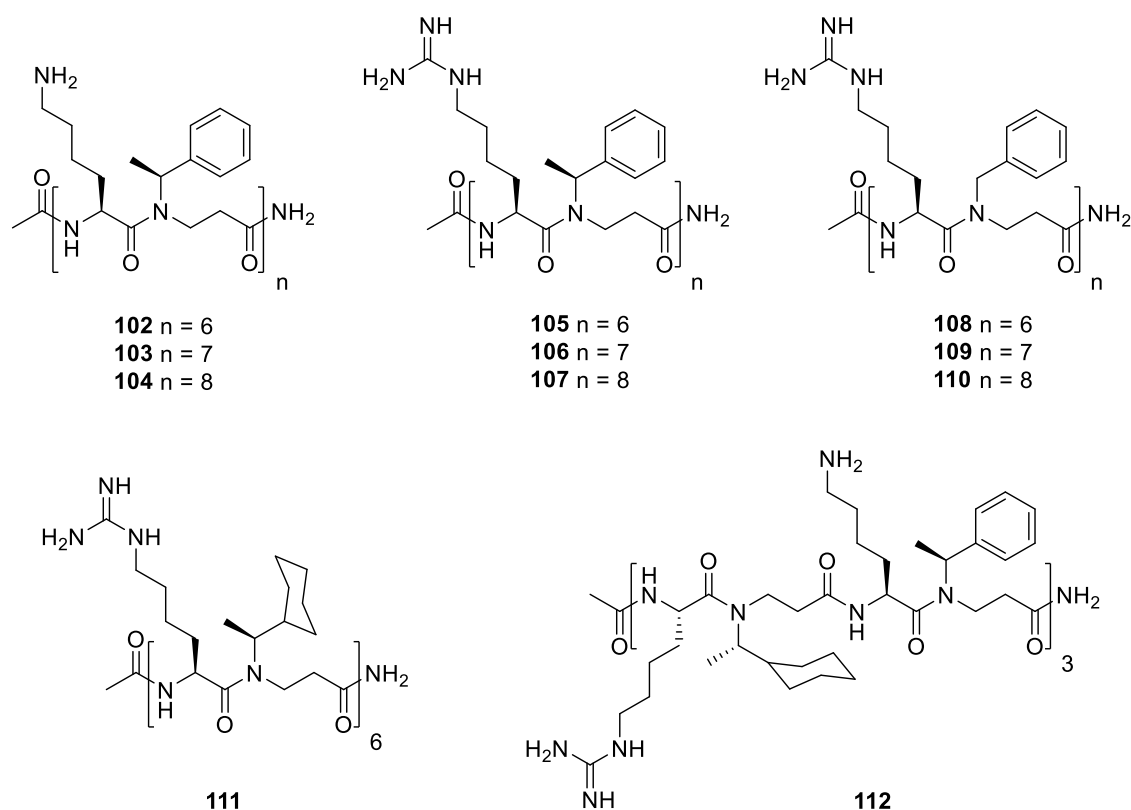
Figure 1.11. Example antimicrobial α-peptide β-peptoid hybrids synthesised by the Olsen group.[93-95]

Peptoid	MIC (µg/mL)						
	E. coli	*B. subtilis*	*S. aureus*	MRSA	VRE	*P. aeruginosa.*	*C. albicans*
102	63	63	> 200	500	250	63	125
103	63			250	125	31	63
104	31			125	63	16	63
105	16	16	125	16	16	63	125
106	16			9	9	37	148
107	16			16	8	31	31
108	4	8	32	67	17	67	33
109	16			64	16	64	32
110	34			64	9	34	34
111	8			8	4	64	16
112	32			16	8	128	32

Table 1.12. The biological activity for selected α-peptide β-peptoid dodecamers against a variety of resistant Gram positive and negative bacteria.[93-95]

Peptoids **102–110** were screened against *P. falciparum* and low IC$_{50}$ values were recorded for selected guanidinylated peptoids (IC$_{50}$ 4–6 µM for compounds **103** and **104**). Although the compounds showed considerably lower activity than the chloroquinine control, these peptoids were able to inhibit parasite growth at concentrations that AMPs magainin 1 and 2 could not. Most peptoids showed low hemolytic activity, but some erythrocyte

alterations could be seen at the IC_{50} value using microscopy. Additionally, the most active peptoids **103** and **104** showed hemolytic activity at concentrations near their IC_{50} values.[94]

Peptoids **102**, **105** and **108** were also moderately active against *E. coli*, *B. subtilis* and *S. aureus* (see **Table 1.12**). Sequences with arginine exhibited improved potencies to the lysine chimeras and the achiral β-*N*phe containing peptoid **108** is more potent to all bacteria tested than the chiral β-*N*spe variant **105**, suggesting that chirality is not necessarily required for antimicrobial action in these hybrid compounds. The chimeras were highly stable towards proteolysis and also showed no significant hemolysis of human red blood cells at concentrations up to 500 µg mL^{-1}.[93]

The results shown in **Table 1.12** demonstrate that longer oligomers generally resulted in improved biological activities towards most of the species tested (i.e. compare 12 residue **102** to 16 residue **104**). However, in the case of *E. coli* this trend was either diminished or reversed and some of the shorter compounds showed the most promising activities, for example peptoid **108** has more potent activity than the longer analogues **109** or **110**. Guanidino-functionalised sequences (**105/108**) showed a similarly better potency than the amino compounds (**102**) for all pathogens except *P. aeruginosa*. The link between secondary structure and biological activity was investigated using circular dichroism spectroscopy. Compounds with α-chiral β-peptoid residues show a greater degree of order than the achiral variants, so it was suggested that these compounds interact with cell membranes via an unstructured conformation. Peptoid **111** with higher lipophilic character showed at least a two fold increase in activity compared to the aromatic analogue **105** against all species tested. However, this was accompanied by an increase in hemolytic activity.[95]

Interestingly, *C. albicans* was significantly more susceptible to peptoids without α-chiral peptoid monomers (i.e. **108**) whereas methicillin-resistant *S. aureus* was more sensitive to those peptoids with more order, i.e. sequences containing α-chiral residues (i.e. **102** or **105**). All other pathogens showed no significant difference in activity between compounds with a higher or lower degree of order via CD. Toxicity against HeLa cells was also studied and all compounds were less hemolytic than pexiganan (**35**) which was used as a clinical comparison.[95]

Peptoids **102**–**110** in **Table 1.12** were also studied in more detail against both planktonic and biofilm cultures of *S. epidermis* using susceptibility and time-kill assays and confocal laser scanning microscopy respectively. At their minimum inhibitory concentration, all the α-peptide β-peptoids tested inhibited biofilm formation and at greater concentrations between 80–160 µg mL^{-1}, 6 hour old biofilms could be eradicated. As before, peptidomimetics containing guanidio functionalities and chiral β-peptoid residues (i.e. compound **105**) showed the best and fastest antimicrobial potencies and antibiofilm behaviour compared to those that with lysine and achiral peptoid residues. There was a clear relationship between increased sequence length and an increased antimicrobial activity and increased cytotoxicity, a trend that was more evident in amino-functionalised compounds than the guanidio-rich peptoids.[96]

Insertion assay experiments were performed using peptoids **102** and **105** and Langmuir monolayers to show that guanidino-containing peptide-peptoid hybrids are more readily able to compromise membrane integrity of monolayers that mimic Gram positive bacteria than amino-functionalised analogues. However, for the lipopolysaccharide monolayers that were used to represent a Gram negative system, the same trend was not observed.[97] Additionally, fluorescently labelled α-peptide β-peptoid chimeras related to **102**, **105** and **108** have been studied in cellular uptake studies and it was shown that these compounds were taken up more efficiently than the arginine rich peptide Tat_{47-57}[§§§] and subsequently localised in vesicular compartments.[98]

Finally, two of these α-peptide β-peptoid chimeras (compounds **102** and **105** in **Table 1.12**) were used to determine the potentiation of their antibacterial activity by human blood plasma. The activity of AMPs can be considered to be negatively impacted by the high salt content of blood plasma. However, in this study it was found that the antimicrobial activity of these peptidomimetics in 50 % blood plasma was increased (MIC improved by up to one order of magnitude) with respect to Gram negative *E. coli*; no effect was seen with Gram positive *S. aureus*. This enhancement of antibacterial activity is a promising characteristic of these peptidomimetics for therapeutic applications.[99]

1.4 Antifungal peptoids

Fungal infections are often more difficult to treat than infections caused by bacteria due to the limited number and greater toxicity of antifungal drugs. Additionally, infections caused by the fungal species *C. albicans* or *C. neoformans* are particularly common in at risk patient groups, such as the elderly or those with immunodeficiency. As with antibacterial drugs, resistance is developing against many of the currently available antifungal treatments.[100,101]

In combination with the Barron group, the Larabell research group have used soft X-ray tomography to study the cellular response of *C. albicans* to peptoids.[102] This technique allows imaging of the subcellular changes that occur due to phenotypic switching[****] and also to monitor changes resultant from antimicrobial treatment. In this study two peptoids **22** and **38** were used that had been previously used in antibacterial studies. The structures of these molecules are shown in **Figure 1.12**.

[§§§] Tat is HIV-1 transactivating protein; Tat_{47-57} sequence: YGRKKRRQRRR.
[****] In phenotypic switching the cellular type changes from a benign to an invasive, multi-cellular phenotype.

MIC *C. albicans* 3.0 μM

MIC *C. albicans* 13.0 μM
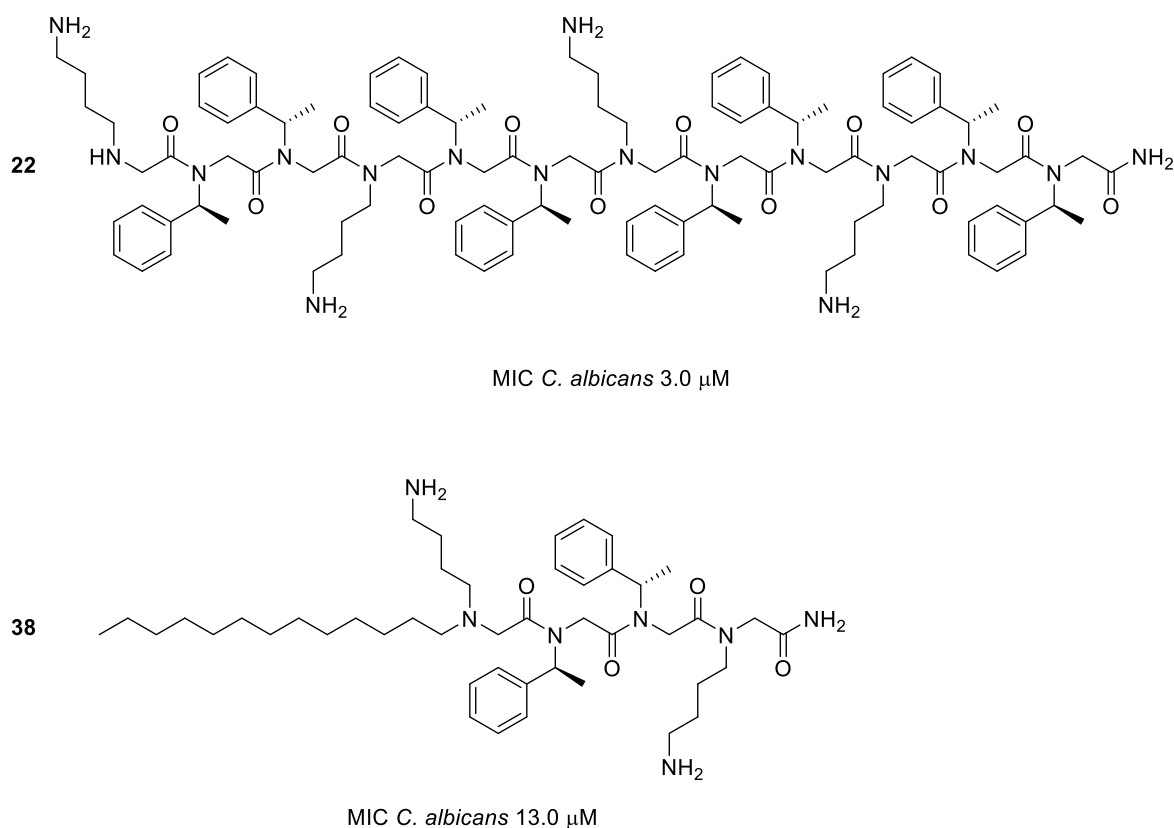
Figure 1.12. Peptoids used in the soft X-ray tomography study. Peptoid **22** and peptoid **38** have structural similarities to AMPs and were previously shown to have potent antifungal activities.[56,57]

Treatment with peptoids inhibited the formation of the pathogenic hyphal phenotype of *C. albicans* and led to significant changes in the cell and organelle morphology, particularly in the nucleus where lipidic bodies were seen to be embedded in the nucleus. Nucleoli in cells treated with peptoid also appeared to contain at least one hole that passed directly through the organelle in all cells imaged. The authors do not suggest a function or the consequences of this, but is a noteworthy addition to peptidomimetic research.[102]

Peptoids have also been shown to be promising antifungal candidates against plant pathogens, *Fusarium virguliforme* and *Fusarium lateritium* which both cause sudden death syndrome in soybean and are a threat to global food security. A library of 36 peptoids was designed to mimic ultrashort lipopeptides and synthesised using an Ugi four-component reaction. The peptoids have a tetrapeptoid backbones and an N-terminal palmitoyl residue, as shown by fragment **113** in **Figure 1.13**. In general *F. virguliforme* was more susceptible to the lipopeptoids and most compounds showed measurable antifungal activities against either or both *F. virguliforme* and *F. solani,* with MIC values ranging from 7–38 μM via a broth microdilution method (compared to a control commercial antifungal Benomyl that has an MIC of 2 μM).[103]
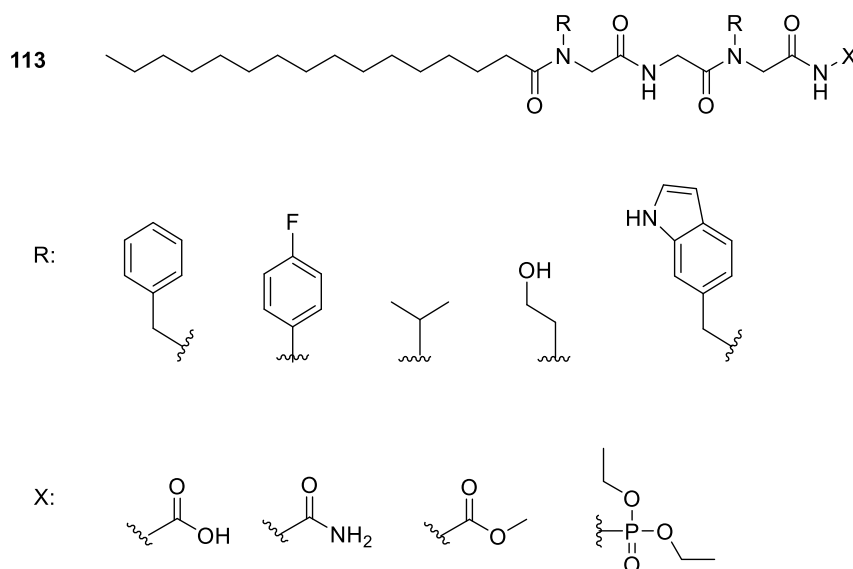
Figure 1.13. **113**, the general structure for the antifungal peptoids, with a selection of possible side chains which were employed in varying combinations. The C terminus of the peptoids was varied from acid, amide, ester to phosphoester.[103]

The group of Hansen have also studied antifungal properties of peptoids and developed their initial antibacterial studies previously described in section 1.3.1. Their lysine containing peptide-peptoid hybrids were tested against two common fungal species in immunocompromised patients; *C. albicans* and *C. neoformans*.

The potent antibacterial activity of this library has already been described above and these compounds were also active against the fungal targets. Most peptoids contained the central motif shown in **Figure 1.10**, with differing numbers of lysine residues at N- and C-termini or within the motif in varying combintions. In general, *C. neoformans* was more susceptible to the peptoids than amphotericin resistant *C. albicans* with MICs for active compounds in the range 1.6–6.25 µM and 3.1–12.5 µM respectively. The trends between active and less active compounds followed the trends described for the Gram positive bacteria and in most cases, an increased activity was seen with an increase in charge (i.e. for compounds with a greater number of lysine residues included in the sequence).[88]

More recently, another potent antifungal peptoid has been identified against *C. neoformans*, with a similar potency to antifungal agents in current clinical use. The structure of this tripeptoid **114** is shown in **Figure 1.14**. The peptoid identified was shown to have excellent stability, moderate cytotoxicity in mammalian cells (toxicity NIH-3T3 murine fibroblasts IC_{50} 48.6 μg/mL; toxicity HPLIA human peripheral lung epithelial cells IC_{50} 36.3 μg/mL) and a low hemolytic activity to human erythrocytes (HC_{10} 68.7 μg mL^{-1}). Against the *C. neoformans* lab strains, **114** had MIC values of 6.3 μg mL^{-1} and the compound was also evaluated against several clinical isolates and favourable MIC values between 12.5–65 μg mL^{-1} were recorded.[104]
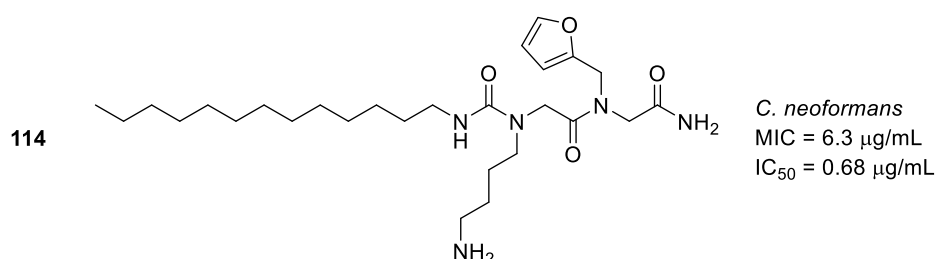
Figure 1.14. Structure of the antifungal peptoid **114**. MIC and IC_{50} values against *C. neoformans* H99S are shown.[104]

1.5 Conclusions and Project Aims

It has been shown that peptoids show significant promise in biomedical applications that is not just limited to their antimicrobial activity. Such applications are wide ranging from inhibitors for protein-protein interactions[40,41], lung surfactants[46], molecular scaffolds[42,43], biomimetic materials like collagen for biomedical devices and tissue engineering [43,47-50] or as molecular transporters for drug delivery.[51-53] Although a comprehensive review of such medicinal uses is not possible here, the area has been reviewed extensively by others.[10,105] Peptoids have also been proven as a novel class of anti-infective agents, displaying potent antibiotic, antifungal properties with advantageous properties such as their stability *in vivo*.

Some peptoids act via an amphiphilic arrangement of side chains in the folded state, others can mimic the side chains in natural protein surfaces. Structure-based design, combinatorial libraries with high throughput screening and sequence-based design have all been used to discover peptoids with useful biological activities. In some cases, a defined secondary structure was necessary to elicit a potent biological response but in other cases, potent compounds had no defined solution state secondary structure in the absence of cell membranes.

However, there are many challenges that must be addressed before biomedically useful peptoids can become a reality. Problems with selectivity or other side effects, such as immunogenicity, have not been fully evaluated and manufacture on a large scale may prove to be challenging or costly.

Whilst the secondary structure prediction of peptoids has advanced dramatically over the last few decades, our understanding of peptoid sequence-structure relationships are still not good enough to predict the secondary structure of complicated peptoids from scratch. Computational methods that can accurately predict peptoid conformations are in their infancy and improvements are needed urgently. Additionally, there is a lack of data concerning peptoid conformation in the literature; certain CD spectra published by other groups suggest that related peptoid sequences can form a range of stable helical conformations (the literature is examined in more detail in Chapter 2), however these have yet to be elucidated and characterised in detail. More information regarding peptoid secondary structure would allow the diversity of peptoid libraries to be improved. It is known that α-chiral substituents can induce helicity, but the requirement for approximately half of side chains to be bulky α-chiral monomers[106-108] places certain restrictions on the synthesis of diverse peptoid libraries. Future studies should look for novel side chain types that can stabilise peptoid folding to allow a more through exploration of chemical space.

The optimisation of the pharmacological properties of peptoids will be important in the future. Although peptoids have better stability than peptides *in vivo*, their oral availability will need to be improved for enteral administration and the fast excretion rates currently recorded[109] would have to be reduced for peptoids to be considered as pharmaceuticals. The ease of peptoid synthesis, the high cell permeability, *in vivo* stability among other pharmacokinetic properties are significant advantages in the search for peptoid pharmaceuticals. However, the issues outlined above need to be addressed before peptoids can be considered as viable drug candidates. A balance between activity and selectivity must also be achieved to avoid unwanted toxicity of any potentially useful pharmaceutical peptoids. As our understanding of the conformational control of peptoids increases, it is expected that many more promising pharmaceutical candidates will emerge which can be taken forward into clinical studies.[10,34,55,105]

Given the aforementioned points, the main aim of this research project was to build upon the work already undertaken into the antibiotic and antifungal properties of peptoids and to explore peptoids in more detail as a new class of anti-infective compounds.

In particular, a focus was placed upon developing peptoids as antiparasitic agents since no comprehensive investigation had yet been undertaken into the action of peptoids against protozoa. Our aim was to synthesise a large peptoid library, with increased chemical and biological stability compared to peptides. Following biological evaluation of this library, it was intended that active compounds against parasite targets would be identified and the structure activity relationships analysed to determine the most important features of antiparasitic peptoids.

Since peptoids are proposed to act against cell membranes, it was anticipated that peptoids that displayed potent antiparasitic activity would also be potential antibiotic compounds. Therefore, we planned to test the peptoid library against a variety of bacteria and fungi, particularly in their biofilm form due to limited studies into the fungicidal and bactericidal activity of peptoids against biofilms. This data would further help to elucidate the factors that contribute towards good antimicrobial activity in peptoid sequences.

Additionally, it has been highlighted that the mode of action of peptoids has not yet been conclusively determined and that the selectivity of many peptoids in the literature has either not been stated or has proven problematic. Therefore, a final objective was to examine the mode of action of peptoids in further detail using biophysical characterisation techniques and fluorescent microscopy experiments. In particular, the secondary structure of a wide variety of peptoids would be studied via circular dichroism spectroscopy to fill some of the aforementioned gaps in the literature and help to rationalise the biological activity of the library. It was hoped that these investigations would assist in the design of selective and potent antimicrobial peptoids, help to elucidate their mode of action and would strengthen the position of peptoids as a novel and promising class of compound, with potential antimicrobial applications within the pharmaceutical industry.

1.6 References

1. The World Health Organisation, *Antimicrobial Resistance* **2014**.
2. Y.J. Gordon, E.G. Romanowski, A.M. McDermott, *Curr. Eye Res.,* **2005**, *30*, 505.
3. L.O. Brandenburg, J. Merres, L.J. Albrecht, D. Varoga, T. Pufe, *Polymers,* **2012**, *4*, 539.
4. B. Mojsoska, H. Jenssen, *Pharmaceuticals,* **2015**, *8*, 366.
5. K. Midura-Nowaczek, A. Markowska, *Perspect. Med. Chem.,* **2014**, *6*, 73.
6. Y. Li, Q. Xiang, Q. Zhang, Y. Huang, Z. Su, *Peptides,* **2012**, *37*, 207.
7. K. Matsuzaki, *Biochim. Biophys. Acta,* **2009**, *1788*, 1687.
8. F. Guilhelmelli, N. Vilela, P. Albuquerque, L.d.S. Derengowski, I. Silva-Pereira, C.M. Kyaw, *Front. Microbiol.,* **2013**, *4*, 353.
9. M.R. Yeaman, N.Y. Yount, *Pharmacol. Rev.,* **2003**, *55*, 27.
10. J. Seo, B.C. Lee, R.N. Zuckermann In *Comprehensive Biomaterials*; P. Ducheyne, K.E. Healy, D.W. Hutmacher, D.W. Grainger, Kirkpatrick, C. J., Eds.; Elsevier: 2011; Vol. 2, p 53.
11. R.E.W. Hancock, D.S. Chapple, *Antimicrob. Agents Chemother.,* **1999**, *43*, 1317.
12. M. Zasloff, *Nature,* **2002**, *415*, 389.
13. D. Andreu, L. Rivas, *Biopolymers,* **1998**, *47*, 415.
14. M.J. Dawson, R.W. Scott, *Curr. Opin. Pharmacol.,* **2012**, *12*, 545.
15. A. Tossi, L. Sandri, A. Giangaspero, *Biopolymers,* **2000**, *55*, 4.
16. S. Gruenheid, H. Le Moual, *FEMS Microbiol. Lett.,* **2012**, *330*, 81.
17. C. Vilhena, A. Bettencourt, *Rev. Med. Chem.,* **2012**, *12*, 202.
18. D.A. Kelkar, A. Chattopadhyay, *Biochim. Biophys. Acta,* **2007**, *1768*, 2011.

19.   J.N. Hansen, *Crit. Rev. Food Sci. Nutrition,* **1994**, *34*, 69.
20.   P. Kosikowska, A. Lesner, *Expert Opin. Ther. Pat.,* **2016**, *26*, 689.
21.   A.T.Y. Yeung, S.L. Gellatly, R.E.W. Hancock, *Cell. Mol. Life Sci.,* **2011**, *68*, 2161.
22.   N.Y. Yount, M.R. Yeaman, *Annu. Rev. Pharma. Toxicol.,* **2012**, *52*, 505.
23.   K. Fosgerau, T. Hoffmann, *Drug Disc. Today,* **2015**, *20*, 122.
24.   H. Jenssen, P. Hamill, R.E. Hancock, *Clin. Microbiol. Rev.,* **2006**, *19*, 491.
25.   J.L. Fox, *Nat. Biotech.,* **2013**, *31*, 379.
26.   M.-D. Seo, H.-S. Won, J.-H. Kim, T. Mishig-Ochir, B.-J. Lee, *Molecules,* **2012**, *17*, 12276.
27.   J. Vagner, H. Qu, V.J. Hruby, *Curr. Opin. Chem. Biol.,* **2008**, *12*, 292.
28.   Y.H. Lau, P. de Andrade, Y. Wu, D.R. Spring, *Chem. Soc. Rev.,* **2015**, *44*, 91.
29.   B.P. Ward, N.L. Ottaway, D. Perez-Tilve, D. Ma, V.M. Gelfanov, M.H. Tschöp, R.D. DiMarchi, *Mol. Metab.,* **2013**, *2*, 468.
30.   Y. Linde, O. Ovadia, E. Safrai, Z. Xiang, F.P. Portillo, D.E. Shalev, C. Haskell-Luevano, A. Hoffman, C. Gilon, *Biopolymers,* **2008**, *90*, 671.
31.   J. Chatterjee, C. Gilon, A. Hoffman, H. Kessler, *Acc. Chem. Res.,* **2008**, *41*, 1331.
32.   I.W. Hamley, *Biomacromolecules,* **2014**, *15*, 1543.
33.   Y. Niu, H. Wu, Y. Li, Y. Hu, S. Padhee, Q. Li, C. Cao, J. Cai, *Org. Biomol. Chem.,* **2013**, *11*, 4283.
34.   J.A. Patch, K. Kirshenbaum, S.L. Seurynck, R.N. Zuckermann, A.E. Barron In *Pseudopeptides in Drug Development*; Nielsen, P. E., Ed.; Wiley-VCH: Germany, 2004, p 1
35.   R.N. Zuckermann, *Biopolymers,* **2011**, *96*, 545.
36.   D. Zhang, S.H. Lahasky, L. Guo, C.-U. Lee, M. Lavan, *Macromolecules,* **2012**, *45*, 5833.
37.   S.W. Shuey, W.J. Delaney, M.C. Shah, M.A. Scialdone, *Bioorg. Med. Chem. Lett.,* **2006**, *16*, 1245.
38.   O. Roy, S. Faure, V. Thery, C. Didierjean, C. Taillefumier, *Org. Lett.,* **2008**, *10*, 921.
39.   C.A. Olsen, *Biopolymers,* **2011**, *96*, 561.
40.   G. Malet, A.G. Martin, M. Orzaez, M.J. Vicent, I. Masip, G. Sanclimens, A. Ferrer-Montiel, I. Mingarro, A. Messeguer, H. O Fearnhead, E. Perez-Paya, *Cell Death Differ.,* **2006**, *13*, 1523.
41.   T. Hara, S.R. Durell, M.C. Myers, D.H. Appella, *J. Am. Chem. Soc.,* **2006**, *128*, 1995.
42.   W. Cai, J.P. Taulane, N.A. Sorto, A. Oganesyan, C.G. Gutierrez, M. Goodman, *Lett. Org. Chem.,* **2007**, *4*, 96.
43.   A.R. Statz, R.J. Meagher, A.E. Barron, P.B. Messersmith, *J. Am. Chem. Soc.,* **2005**, *127*, 7972.
44.   L.P. Labuda, A. Pushechnikov, M.D. Disney, *ASC Chem. Biol.,* **2009**, *4*, 299.
45.   M.M. Lee, A. Pushechnikov, M.D. Disney, *ASC Chem. Biol.,* **2009**, *4*, 345.
46.   S.L. Seurynck-Servoss, M.T. Dohm, A.E. Barron, *Biochem.,* **2006**, *45*, 11809.
47.   H. Tran, S.L. Gael, M.D. Connolly, R.N. Zuckermann, *J. Vis. Exp.,* **2011**, e3373.
48.   A.S. Knight, E.Y. Zhou, M.B. Francis, R.N. Zuckermann, *Adv. Mat.,* **2015**, *38*, 5665.
49.   X. Chen, K. Ding, N. Ayres, *Polym. Chem.,* **2011**, *2*, 2635.
50.   B.C. Lee, T.K. Chu, K.A. Dill, R.N. Zuckermann, *J. Am. Chem. Soc.,* **2008**, *130*, 8847.
51.   P.A. Wender, D.J. Mitchell, K. Pattabiraman, E.T. Pelkey, L. Steinman, J.B. Rothbard, *Proc. Natl. Acad. Sci. USA,* **2000**, *97*, 13003.
52.   Dominik K. Kölmel, Daniel Fürniss, Steven Susanto, Andrea Lauer, Clemens Grabher, Stefan Bräse, U. Schepers, *Pharmaceuticals,* **2012**, *5*, 1265.
53.   W. Huang, J. Seo, J.S. Lin, A.E. Barron, *Mol. Biosyst.,* **2012**, *8*, 2626.
54.   R.N. Zuckermann, T. Kodadek, *Curr. Opin. Mol. Ther.,* **2009**, *11*, 299.
55.   W.S. Horne, *Expert Opin. Drug Discov.,* **2011**, *6*, 1247.

56. N.P. Chongsiriwatana, J.A. Patch, A.M. Czyzewski, M.T. Dohm, A. Ivankin, D. Gidalevitz, R.N. Zuckermann, A.E. Barron, *Proc. Natl. Acad. Sci. USA,* **2008**, *105*, 2794.

57. J.A. Patch, A.E. Barron, *J. Am. Chem. Soc.,* **2003**, *125*, 12092.

58. R. Kapoor, P.R. Eimerman, J.W. Hardy, J.D. Cirillo, C.H. Contag, A.E. Barron, *Antimicrob. Agents Chemother.,* **2011**, 55, 3058.

59. R. Kapoor, M.W. Wadman, M.T. Dohm, A.M. Czyzewski, A.M. Spormann, A.E. Barron, *Antimicrob. Agents Chemother.,* **2011**, 55, 3054.

60. N.P. Chongsiriwatana, M. Wetzler, A.E. Barron, *Antimicrob. Agents Chemother.,* **2011**, 55, 5399.

61. J.-K. Bang, Y.H. Nan, E.K. Lee, S.Y. Shin, *Bull. Korean Chem. Soc,* **2010**, *31*, 2509.

62. B. Mojsoska, R.N. Zuckermann, H. Jenssen, *Antimicrob. Agents Chemother.,* **2015**.

63. S. Ng, B. Goodson, A. Ehrhardt, W.H. Moos, M. Siani, J. Winter, *Bioorg. Med. Chem.,* **1999**, 7, 1781.

64. B. Goodson, A. Ehrhardt, S. Ng, J. Nuss, K. Johnson, M. Giedlin, R. Yamamoto, W.H. Moos, A. Krebber, M. Ladner, M.B. Giacona, C. Vitt, J. Winter, *Antimicrob. Agents Chemother.,* **1999**, *43*, 1429.

65. F.S. Nandel, A. Saini, *Macromol. Theory Simul.,* **2007**, *16*, 295.

66. U. Sternberg, E. Birtalan, I. Jakovkin, B. Luy, U. Schepers, S. Brase, C. Muhle-Goll, *Org. Biomol. Chem.,* **2013**, *11*, 640.

67. A.M. Czyzewski, H. Jenssen, C.D. Fjell, M. Waldbrook, N.P. Chongsiriwatana, E. Yuen, R.E.W. Hancock, A.E. Barron, *PLOS ONE,* **2016**, *11*, e0135961.

68. K. Andreev, M. Lingaraju, A. Ivankin, M. Huang, K. Kirshenbaum, D. Gidalevitz, *Biophysical J.,* **2013**, *104*, 598A.

69. S.B.Y. Shin, B. Yoo, L.J. Todaro, K. Kirshenbaum, *J. Am. Chem. Soc.,* **2007**, *129*, 3218.

70. A.T. Bockus, C.M. McEwen, R.S. Lokey, *Curr. Top. Med. Chem.,* **2013**, *13*, 821.

71. D. Comegna, M. Benincasa, R. Gennaro, I. Izzo, F. De Riccardis, *Bioorg. Med. Chem.,* **2010**, *18*, 2010.

72. M.L. Huang, S.B.Y. Shin, M.A. Benson, V.J. Torres, K. Kirshenbaum, *ChemMedChem,* **2012**, 7, 114.

73. M.L. Huang, M.A. Benson, S.B.Y. Shin, V.J. Torres, K. Kirshenbaum, *Eur. J. Org. Chem.,* **2013**, 3560.

74. P.T. Smith, M.L. Huang, K. Kirshenbaum, *Biopolymers,* **2015**, *103*, 227.

75. G. Pirri, A. Giuliani, S.F. Nicoletto, L. Pizzuto, A.C. Rinaldi, *Eur. J. Biol.,* **2009**, *4*, 258.

76. N.P. Chongsiriwatana, T.M. Miller, M. Wetzler, S. Vakulenko, A.J. Karlsson, S.P. Palecek, S. Mobashery, A.E. Barron, *Antimicrob. Agents Chemother.,* **2011**, 55, 417.

77. B. Findlay, P. Szelemej, G.G. Zhanel, F. Schweizer, *PLOS ONE,* **2012**, 7, e41141.

78. Y. Niu, S. Padhee, H. Wu, G. Bai, Q. Qiao, Y. Hu, L. Harrington, W.N. Burda, L.N. Shaw, C. Cao, J. Cai, *J. Med. Chem.,* **2012**, 55, 4003.

79. Y. Hu, M.N. Amin, S. Padhee, R.E. Wang, Q. Qiao, G. Bai, Y. Li, A. Mathew, C. Cao, J. Cai, *ACS Med. Chem. Lett.,* **2012**, *3*, 683.

80. M. Gobbo, M. Benincasa, G. Bertoloni, B. Biondi, R. Dosselli, E. Papini, E. Reddi, R. Rocchi, R. Tavano, R. Gennaro, *J. Med. Chem.,* **2009**, *52*, 5197.

81. A. Shin, E. Lee, D. Jeon, Y.G. Park, J.K. Bang, Y.S. Park, S.Y. Shin, Y. Kim, *Biochem.,* **2015**, *54*, 3921.

82. J.-K. Kim, S.-A. Lee, S. Shin, J.-Y. Lee, K.-W. Jeong, Y.H. Nan, Y.S. Park, S.Y. Shin, Y. Kim, *Biochimica Et Biophysica Acta-Biomembranes,* **2010**, *1798*, 1913.

83. W.L. Zhu, K.S. Hahm, S.Y. Shin, *Journal of peptide science : an official publication of the European Peptide Society,* **2007**, *13*, 529.

84. W.L. Zhu, Y.M. Song, Y. Park, K.H. Park, S.-T. Yang, J.I. Kim, I.-S. Park, K.-S. Hahm, S.Y. Shin, *Biochim. Biophys. Acta,* **2007**, *1768*, 1506.
85. W.L. Zhu, K.-S. Hahm, S.Y. Shin, *J. Pept. Sci.,* **2007**, *13*, 529.
86. T.S. Ryge, P.R. Hansen, *Bioorg. Med. Chem.,* **2006**, *14*, 4444.
87. T.S. Ryge, P.R. Hansen, *J. Pept. Sci.,* **2005**, *11*, 727.
88. T.S. Ryge, N. Frimodt-Moller, P.R. Hansen, *Chemotherapy,* **2008**, *54*, 152.
89. S. Gottschalk, D. Ifrah, S. Lerche, C.T. Gottlieb, M.T. Cohn, H. Hiasa, P.R. Hansen, L. Gram, H. Ingmer, L.E. Thomsen, *BMC Microbiol.,* **2013**, *13*, 1.
90. S.C. Shankaramma, K. Moehle, S. James, J.W. Vrijbloed, D. Obrecht, J.A. Robinson, *Chem. Comm.,* **2003**, 1842.
91. S.C. Shankaramma, Z. Athanassiou, O. Zerbe, K. Moehle, C. Mouton, F. Bernardini, J.W. Vrijbloed, D. Obrecht, J.A. Robinson, *ChemBioChem,* **2002**, *3*, 1126.
92. R.D. Jahnsen, A. Sandberg-Schaal, K.J. Vissing, H.M. Nielsen, N. Frimodt-Møller, H. Franzyk, *J. Med. Chem.,* **2014**, *57*, 2864.
93. C.A. Olsen, G. Bonke, L. Vedel, A. Adsersen, M. Witt, H. Franzyk, J.W. Jaroszewski, *Org Lett,* **2007**, *9*, 1549.
94. L. Vedel, G. Bonke, C. Foged, H. Ziegler, H. Franzyk, J.W. Jaroszewski, C.A. Olsen, *ChemBioChem,* **2007**, *8*, 1781.
95. C.A. Olsen, H.L. Ziegler, H.M. Nielsen, N. Frimodt-Moller, J.W. Jaroszewski, H. Franzyk, *ChemBioChem,* **2010**, *11*, 1356.
96. Y. Liu, K.M. Knapp, L. Yang, S. Molin, H. Franzyk, A. Folkesson, *Int. J. Antimicrob. Agents,* **2013**, *41*, 20.
97. K. Andreev, C. Bianchi, J.S. Laursen, L. Citterio, L. Hein-Kristensen, L. Gram, I. Kuzmenko, C.A. Olsen, D. Gidalevitz, *Biochim. Biophys. Acta,* **2014**, *1838*, 2492.
98. C. Foged, H. Franzyk, S. Bahrami, S. Frokjaer, J.W. Jaroszewski, H.M. Nielsen, C.A. Olsen, *Biochimica Et Biophysica Acta-Biomembranes,* **2008**, *1778*, 2487.
99. L. Hein-Kristensen, K.M. Knapp, H. Franzyk, L. Gram, *BMC Microbiol.,* **2011**, *11*, 1.
100. K. Chiba, K. Kawakami, K. Tohyama, *Toxicol. in vitro,* **1998**, *12*, 251.
101. M.M. Harriott, M.C. Noverr, *Antimicrob. Agents Chemother.,* **2010**, *54*, 3746.
102. M. Uchida, G. McDermott, M. Wetzler, M.A. Le Gros, M. Myllys, C. Knoechel, A.E. Barron, C.A. Larabell, *Proc. Natl. Acad. Sci. USA,* **2009**, *106*, 19375.
103. M.D. Galetti, A.M. Cirigliano, G.M. Cabrera, J.A. Ramirez, *Mol Divers,* **2012**, *16*, 113.
104. A.E. Corson, S.A. Armstrong, M.E. Wright, E.E. McClelland, K.L. Bicker, *ACS Med. Chem. Lett.,* **2016**.
105. S.A. Fowler, H.E. Blackwell, *Org. Biomol. Chem.,* **2009**, *7*, 1508.
106. C.W. Wu, T.J. Sanborn, R.N. Zuckermann, A.E. Barron, *J. Am. Chem. Soc.,* **2001**, *123*, 2958.
107. C.W. Wu, T.J. Sanborn, K. Huang, R.N. Zuckermann, A.E. Barron, *J. Am. Chem. Soc.,* **2001**, *123*, 6778.
108. C.W. Wu, K. Kirshenbaum, T.J. Sanborn, J.A. Patch, K. Huang, K.A. Dill, R.N. Zuckermann, A.E. Barron, *J. Am. Chem. Soc.,* **2003**, *125*, 13525.
109. J. Seo, G. Ren, H. Liu, Z. Miao, M. Park, Y. Wang, T.M. Miller, A.E. Barron, Z. Cheng, *Bioconjugate Chem.,* **2012**, *23*, 1069.

Chapter 2

Peptoid Synthesis and Characterisation

2.1 The synthesis of α-peptoids

Peptoids were first made in the late 1980s as novel candidates for the drug discovery process by Protos Corporation. Ever since, there has been increasing interest and numerous developments in the field of peptoid synthesis.[1] In many respects, the synthesis of peptoids is very similar to that of peptides. Most often, the peptoid is built on resin using solid phase synthesis. This has the obvious advantage that using an excess of reagents can help to drive the reaction and that unused reagents and by-products are easily washed out after the reaction. Following synthesis of the whole sequence, acidic cleavage conditions remove the peptoid from the solid support to allow purification.

Due to their repetitive structure and high stability, the synthesis of many peptoids is fairly simple and can be automated. In early attempts at peptoid synthesis, a solid-phase monomer approach was taken. Later, an improved sub-monomer method was developed. Solution syntheses have also been attempted but will not be reviewed here.

2.1.1 Monomer approach

The synthesis of peptoid oligomers was first attempted using the monomer approach, where Fmoc protected monomers are incorporated into the growing peptoid chain on an insoluble, solid support using conventional coupling activators. The Fmoc group is then removed, analogous to peptide synthesis, and the next monomer added. The chain is built from the carboxy (C) to amino terminus (N), as illustrated by **Scheme 2.1**.[2]

These syntheses were successful on a wide variety of monomers. However, the Fmoc protected *N*-substituted glycine monomers are often very arduous and time consuming to make and the time needed to produce Fmoc-protected monomers often greatly exceeded the time taken to synthesise an entire library of peptoids on solid support.[1]
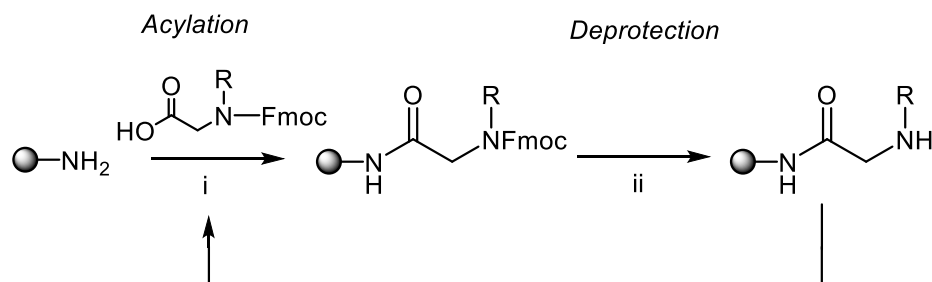
Scheme 2.1. The synthesis of a peptoid via the monomer approach, using Fmoc protected *N*-substituted glycine monomers; i. coupling using activating agent; ii. deprotection with 20 % piperidine in DMF.[1]

2.1.2 Submonomer approach

Due to the restrictions of the monomer approach, a sub-monomer method was developed in 1992 by Zuckermann *et al.*, and was a major breakthrough in peptoid synthesis. This approach involves acylation by a haloacetic acid (for example, bromo or chloroacetic acid) followed by a displacement step using a primary amine to introduce the side chain, as summarised in **Scheme 2.2**.[3]
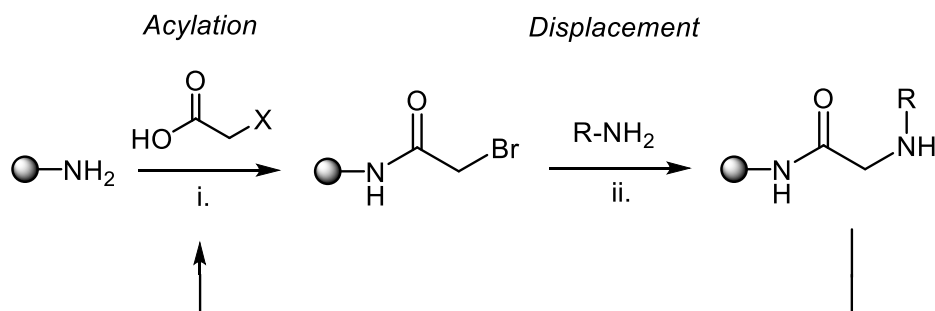
Scheme 2.2. The submonomer approach to peptoid synthesis; i. acylation with appropriate coupling agent and haloacetic acid (where X = Br or Cl); ii. S_N2 displacement with a primary amine.[3]

Generally, bromoacetic acid is used in the acylation step with an activating agent like *N,N'*-diisopropylcarbodiimide (DIC). However, for amines where there are unprotected heteroatoms on the side chain (for example, imidazoles or pyridines) chloroacetic acid is preferred because it is a poorer alkylating agent and prevents unwanted alkylation at side chain heteroatoms. The use of chloroacetic acid slows down the subsequent displacement step with the amine, but can be countered by addition of iodide, which forms a reactive iodoacetamide by Finklestein halide exchange *in situ*.[1,4-6] Importantly, protecting groups are generally not required[*] (except for certain amine side chain functionalities) and there are a large variety of inexpensive amines commercially available. Many new submonomers have been made for incorporation into peptoids. For example, chemical functionalities have been introduced that allow chemoselective

---

[*] i.e. compared to the Fmoc-protected amino acids used in standard solid-phase peptide synthesis.

conjugation and efficient ligations between peptoids.[7,8] Therefore, there are significant advantages to using this method as a vast range of chemical moieties can easily be introduced into peptoid libraries; potentially a much greater variety of side chains can be added than in traditional peptide chemistry. However, protecting group methodologies for peptoid side chains are not as advanced in peptoid studies, which can cause problems for many functionalities.

Today, the submonomer method is the most commonly used method for peptoid synthesis by the scientific community. The submonomer approach significantly increased the diversity of side chains available, increased efficiency in the reactions and improved synthetic yields. It has been shown that peptoids about 50 monomers long can be made, with yields for each coupling cycle in excess of 99 %.[1]

2.2 Synthesis of β-peptoids

Poly-*N*-alkylated β-alanines (or β-peptoids) have an extra methylene unit in the amide backbone compared to α-peptoids and this presents several challenges in the synthesis of these compounds. For an α-peptoid, the submonomer method of peptoid synthesis is very efficient. However, efficiency in the synthesis of β-peptoids is not as well established and may explain why β-peptoids appear less frequently in the literature than their α-peptoid equivalents

To date, two main synthetic routes to linear β-peptoids have been developed. The first utilises an aza-Michael reaction between a resin-bound acryloyl group and the required amine submonomer. For longer compounds, coupling protected building blocks on solid phase is often more sucessful.[9,10]

The aza-Michael addition (**Scheme 2.3**) first described by Hamper *et al.*[11], is a two-step submonomer approach. First, acryloyl chloride is used to acylate the resin. A subsequent conjugate aza-Michael reaction with a primary amine installs the required amine submonomer. However, this strategy is less efficient for the synthesis of β-peptoids greater than four monomers in length or that contain α-chiral amines, as poor yields are often achieved even with optimised reaction conditions.[9-12]
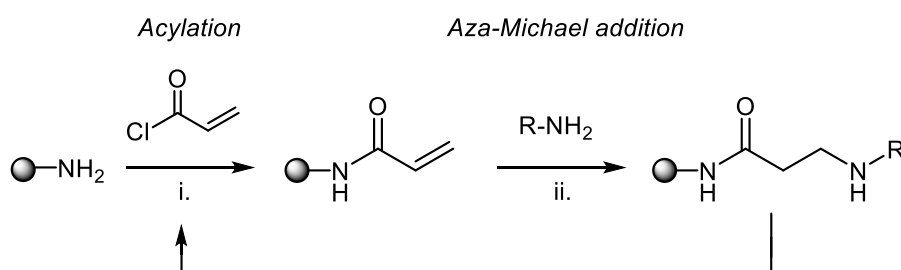
Scheme 2.3. A submonomer approach for the synthesis of β-peptoids using aza-Michael addition; i. acryloyl chloride with pyridine in DCM; ii. primary amine in THF/H$_2$O, 60 ˚C.[11]

Similar to the monomer approach of synthesis for α-peptoids, coupling protected β-peptoid building blocks on solid phase has been used by several groups to synthesise longer β-peptoid oligomers.[12-15] Typically Fmoc protected di- or tripeptoids are prepared, as Fmoc protection is a well-developed strategy in peptide synthesis. These can be prepared either via the solid-phase aza-Michael addition described above, or in solution via a cycle of aza-Michael reactions. In the latter approach, *t*-butyl acrylate is used as the starting material and intermediates are purified at each stage by flash chromatography (see **Scheme 2.4**). The final di/tripeptoids are then Fmoc-protected and the *t*-butyl protection removed to yield components for use in the synthesis of longer β-peptoid oligomers.[9,10,13,14]
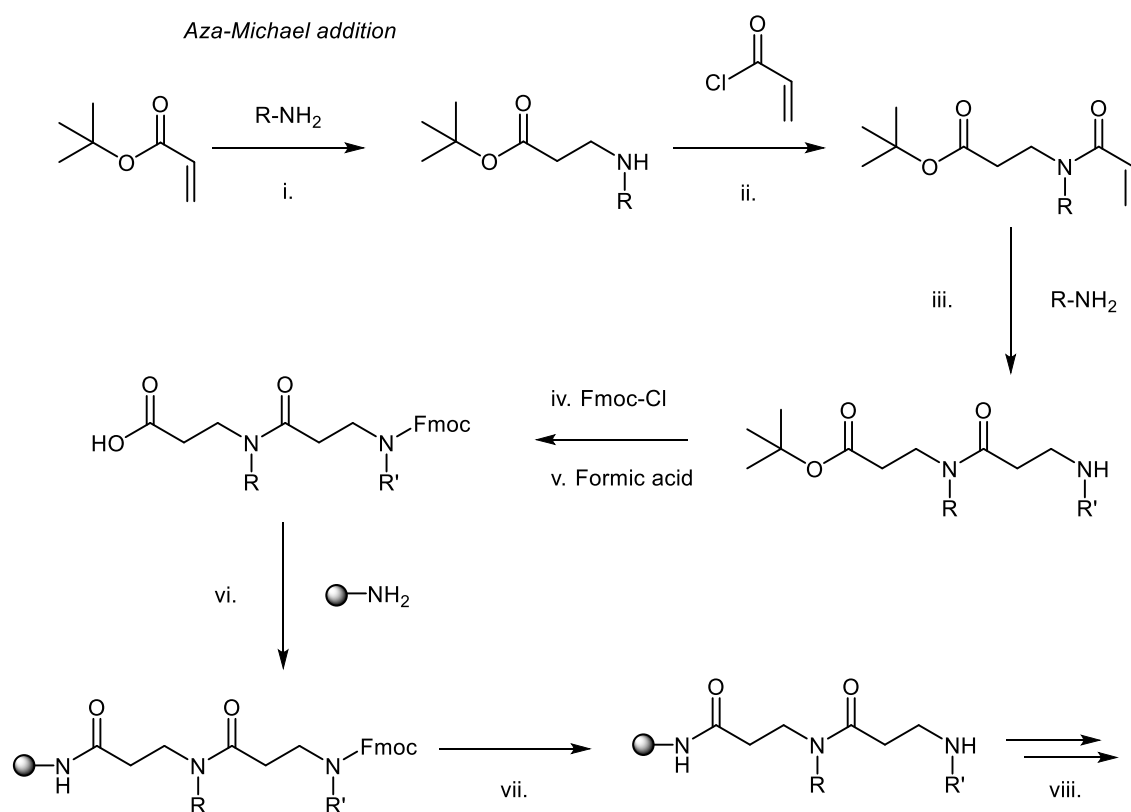
Scheme 2.4. Synthesis of an Fmoc-protected β-peptoid and its use in the solid phase synthesis of longer β-peptoid oligomers; i. aza-Michael addition with primary amine in THF/H$_2$O; ii. acryloyl chloride with pyridine in DCM; iii. aza-Michael addition with primary amine in THF/H$_2$O; iv. Fmoc protection using Fmoc-Cl; v. *t*-butyl deprotection using formic acid; vi. activating agent (i.e. HATU) with DIPEA in DMF at RT; vii. Fmoc deprotection using piperidine in DMF; viii. second coupling of Fmoc-protected monomer to extend sequence.[9,10,13,14]

Finally, efficient co-polymerisation of β-peptoids has also been reported, however the nature of this polymerisation means sequence specific compounds cannot be prepared.[16,17]

2.3 Cyclisation of linear peptoids

The syntheses discussed so far have all concerned the synthesis of linear peptoid structures. Whilst the first examples of cyclic peptoids only emerged in 2007, there has been significant interest within the scientific community to produce cyclic peptoids, and a wide variety of α-peptoid[18-22] and β-peptoid[23] macrocycles have been reported. Many cyclic peptoids are synthesised for their antibacterial properties because restricting the conformational flexibility of the peptoids often enhances biological activity and stability. A number of peptide macrocycles show potent antimicrobial activities and research groups are looking to mimic these with peptoid residues.[5,21,23-27]

It has been demonstrated that cyclisation can organise the peptoid side chains onto the opposite sides of a planar macrocycle, leading to an amphiphilic structure with well-defined lipophilic and cationic surfaces. This mimics natural antimicrobial peptides and therefore cyclic peptoids have the ability to be potent antimicrobials. Possibly because of this amphiphilic structure, cyclic peptoids may penetrate further into the lipid hydrophobic core of bacterial membranes than their linear equivalents and so show promise for use in drug discovery. [28]

Many examples of cyclic α- or β-peptoids have been documented and several methods to cyclise linear peptoids have been demonstrated, including head to tail cyclisation of the linear precursors in solution or side chain reactions on-resin. These are summarised in **Scheme 2.5**.

Head to tail cyclisation is currently the most common method used to synthesise these molecules, partly because mild conditions can be used in efficient reactions and give high yields. Typically in head to tail cyclisation, the linear precursors are synthesised on resin via the sub-monomer procedure, the peptoids cleaved from the resin and then cyclised in solution with a traditional coupling agent (see **Scheme 2.5**). In most cases, the terminal secondary amine of the peptoid chain is cyclised with a carboxylic acid formed following cleavage from the resin. Care needs to be taken to ensure that any reactive amine side chains are masked with appropriate protecting groups. Cyclisation of oligiomers from pentamer to 20mer lengths occurs very efficiently, with typical yields in excess of 90 %, due to the facile *cis-trans* isomerisation of the *N*-substituted amides. Interestingly, there is no requirement for high dilution, as the cyclisation reactions have been shown to proceed within 5 minutes at a 70 mM concentration. However, ring closures of tetramers have yet to be optimised and often leads to low yields (< 12 %).[27-29]

Similar to peptide chemistry, cyclisation of peptoids can also be achieved through chemoselective ligation of the side chains. Depending on where the reacting side chains are located in the sequence, truly cyclic peptoids or bridged compounds can be made.
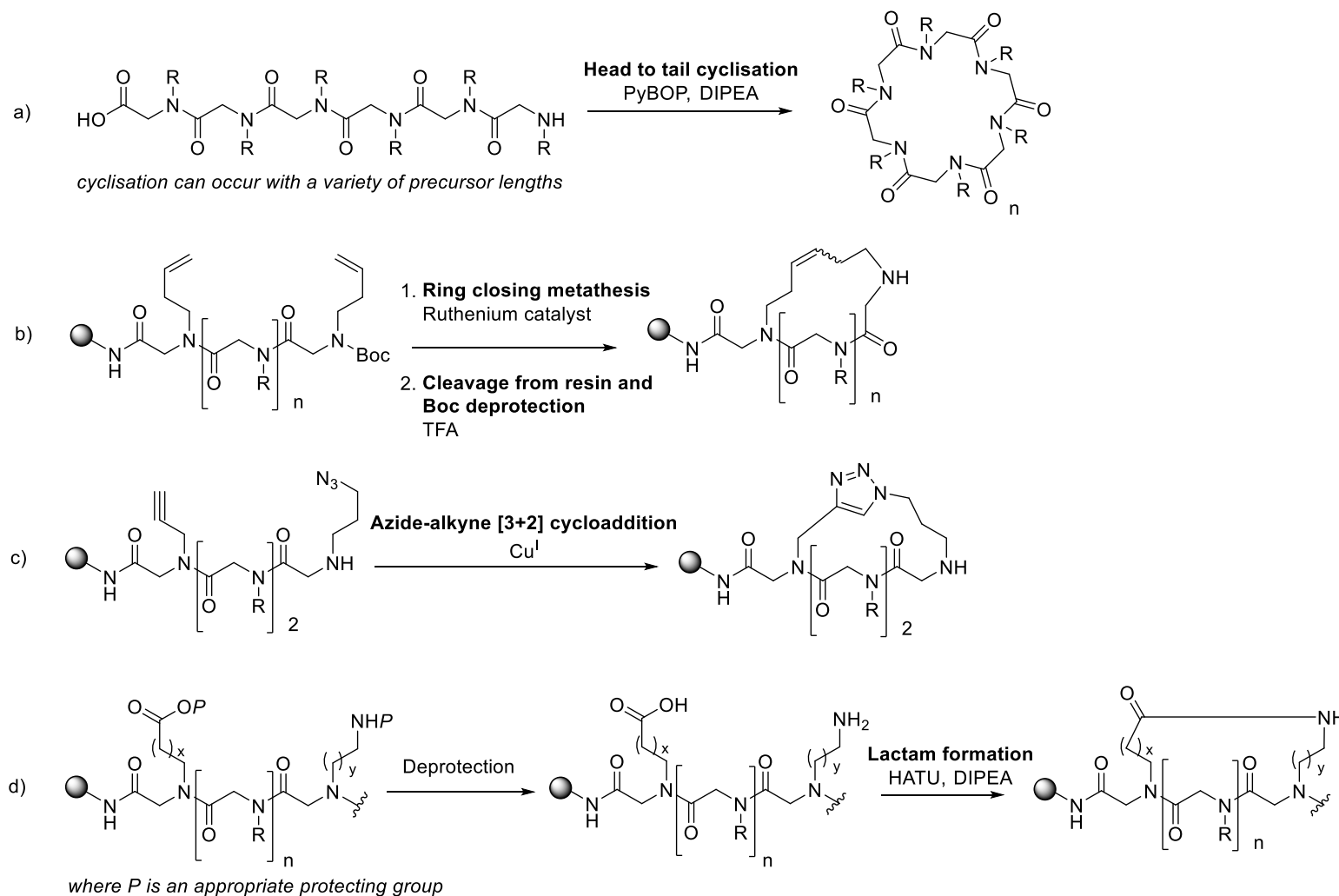
Scheme 2.5. A summary of the common methods of peptoid cyclisation and stapling. a) via head to tail cyclisation in solution; b) ring closing metathesis; c) azide-alkyne cycloaddition; d) amide bond formation.

One example of this is the formation of an amide bond, summarised in **Scheme 2.5d**. The formation of covalent bonds, for example, amides, disulphides or the use of sulphur as a nucleophile in S_N2 ring closing reactions are all well established. In one recent study, linear peptoids were synthesised and a covalent lactam bridge introduced by the formation of an amide bond, with the aim of stabilising the folding of helical peptoids in aqueous and organic solvents. When the reacting side chains were placed at positions *i* and *i* + 3, stabilisation of a helical secondary structure could be achieved.[30,31] Normally, helical secondary structures are formed by the inclusion of many aromatic α-chiral substituents in the peptoid sequence. However, this can restrict the diversity of a peptoid. The amide bond cyclisation strategy avoids the use of a high number these α-chiral substituents, allowing the peptoids to have a greater structural diversity. This has been particularly useful for the synthesis of helical peptoids with a large range of side chains for biological study.[30,32,33]

Another approach to cyclise peptoids via the covalent reaction of side chains is ring closing metathesis (RCM). In olefin metathesis a carbon-carbon bond is formed, usually using alkene groups on the substrate in combination with a ruthenium catalyst and has been used in many chemical reactions and in industry for many years. Although RCM is still challenging in solid-phase reactions, the cyclisation of peptoids (as in **Scheme 2.5b**) has been optimised through choice of the resin, solvent and catalyst. It was shown that ring sizes of 16–25 could be successfully made via this approach. [20]

Finally, click chemistry has also been used to ligate peptoid side chains and to form cyclic structures. This copper (I) catalysed [3+2] cycloaddition is shown in **Scheme 2.5c** and is regiospecific and high yielding under mild conditions. The formation of the triazole linkages and the macrocycle is assisted if the structure is preorganised so that the reactive groups are across one face of the helical secondary structure, i.e. at positions *i* and *i* +3.[34-38]

Due to the increased conformational ordering, many of these cyclised products have been crystallised[†], allowing X-ray diffraction structures of the cyclic peptoids to be obtained.[21,23,27-29,39]

[†] A comprehensive collection of all peptoid crystal structures can be found on the Peptoid Databank (maintained by the Kirshenbaum group at New York University) URL: https://wp.nyu.edu/kirshenbaumlab/peptoid-data-bank/

2.4 Common peptoid secondary structures

As seen in nature, a large variety of well-defined and ordered structures can be formed by peptides and proteins. For peptoids, there is a great deal of conformational diversity in their secondary structures due to the flexibility of their backbones and lack of hydrogen bonding capacity. Currently, the folding of peptoids into global hierarchical structures is not completely understood. However, if the secondary structure of a particular peptoid can be predicted or controlled, the biological function and properties of these molecules can be exploited and enhanced.

Many of the mechanisms that allow the folding of normal peptides are absent in peptoids. Peptoids cannot undergo extensive hydrogen bonding which stabilises the secondary structures of peptides. As the peptoid backbone has no chiral centres, peptoids have no inherent handedness and their secondary structures are usually controlled by non-covalent local interactions, such as steric and electronic effects. Despite the lack of hydrogen bond donors and the achirality of the peptoid backbone, stable secondary structures in solution have been achieved. Within the area of peptoid chemistry, common structural motifs in peptide chemistry have been seen like helices or turns for α-peptoids. Defined structures have also been designed for β-peptoids but will not be discussed for brevity.[40-42]

2.4.1 Stable peptoid helices

By far the most studied peptoid secondary structure is the peptoid helix. The chemistry of such structures is well established and these helices show excellent chemical and thermal stability.[43] Chemists can now design helical peptoids as AMP mimics with specific functions, as it is possible to predict which sequences will form stable helices in solution.

It has been shown that bulky, chiral side chain groups adjacent to the nitrogen on the main chain can induce a helical structure in peptoids as short as 5 residues long in solution.[44] Several common monomers used for this purpose are shown in **Figure 2.1**. Helices can also be stabilised by side chain reactions that effectively staple peptoid chains to enforce a helical structure

Nspe   **Nssb**   **Nsch**
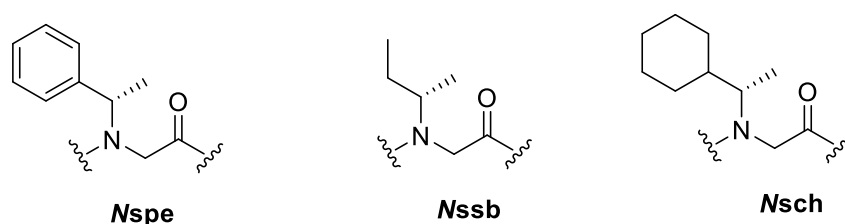
Figure 2.1. Common α-chiral sub-monomers used to induce a helical secondary structure in peptoid oligomers.

Peptoid helices have been shown to contain 3 residues per turn and have a pitch of about 6 Å (however, the pitch can vary by as much as 10 % depending on the specific side chains used). A model structure for a peptoid helix of compound **115** is shown in **Figure 2.2**. These helices have similar structures to the type-I polyproline (PPI) peptide helices that are commonly seen in proteins and contain all *cis*-amide bonds. The direction of this helix in peptoids is usually controlled by the handedness of the chiral building blocks used.[44-46]

Helical peptoids are regularly studied using circular dichroism (CD) spectroscopy (see section 2.5). Normally, greater helical characteristics are observed if the bulky side chain contains an aromatic group at the *i* and *i* + 3 positions, but heterooligomeric peptoids can fold into stable helices if at least 50 % of the monomers contain a chiral centre.[33] Furthermore, the helices are stabilised if the C-terminal residue is α-chiral and also as the peptoid chain increases in length, i.e. decamers and longer.[32,33,44,45,47]
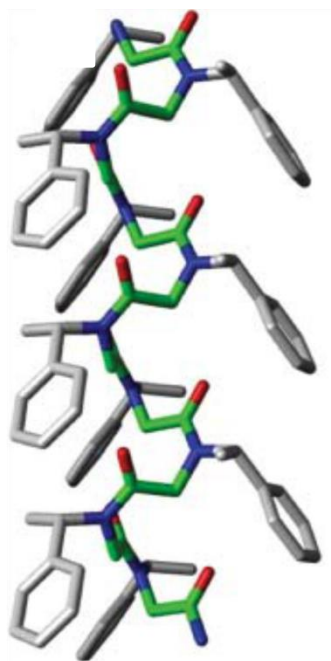
Figure 2.2. A representative model of the peptoid helix for peptoid **115**, Nspe$_{10}$. The structure has been generated using molecular mechanics. The backbone is highlighted in green. Image adapted and reprinted with permission from The Royal Society of Chemistry.[‡,47]

Where sequences contain aromatic, α-chiral monomers, the peptoid helix is induced as the large groups significantly reduce the conformational freedom of the peptoid backbone. The backbone is limited to a certain range of angles to prevent electronic repulsions with the aromatic rings of the side chain and neighbouring carbonyl groups of the peptoid backbone. Therefore, the helix formation is largely controlled by the steric and electronic properties of the submonomers used.[32,33,44,45,48-50]

---

‡ Image reproduced from Fowler and Blackwell, *Org. Biomol. Chem.*, **2009**, 7, 1508.

More recently, it was shown that the peptoid helix could also be controlled using the electronic properties of the side chains, which can affect an electronic n → π* interaction and alter the cis/trans ratio of the backbone amide bonds.[49,51-53] In the PPI-type helix, all the amide bonds should be present as the *cis* isomer in order to achieve a homogeneous helix. The less common type II polyproline helix has also been synthesised, which contains all *trans* amide bonds from repeated *N*-aryl glycine residues (see **Figure 2.3**) that cause a greater steric clash with the corresponding backbone carbonyls.[.51]
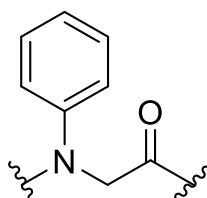
Figure 2.3. *N*-aryl glycine peptoid monomer, shown to induce a PPI-II helix with *trans* amide bonds.[51]

This *cis/trans* amide bond ratio is attributed to a balance between n → π* interactions between the backbone carbonyl and aromatic side chain or the carbonyl to carbonyl n → π* interaction of the amide bond, favouring the cis amide and *trans* amide isomers respectively. Therefore, including an electron deficient substituent submonomer can enhance the proportion of *cis* conformations in a peptoid by lowering the HOMO (n) – LUMO (π*) gap. Whereas an electron rich substituent will favour the *trans* conformation as the n → π*$_{Ar}$ interactions become less favourable. These interactions are shown in **Figure 2.4** and could be exploited in the design of new peptoid structures.[49,52,54]

trans-amide
n → π* amide
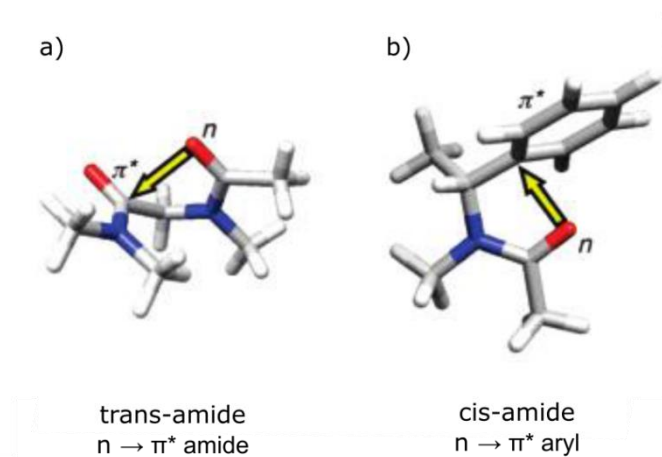
cis-amide
n → π* aryl

Figure 2.4. The n → π* interactions are shown between a) the carbonyls of the backbone stabilising the *trans* amide conformation; b) the backbone carbonyl and the aromatic residue stabilising the cis conformation. The nitrogen of the amide is shown in blue and oxygen in red. Adapted with permission, copyright 2007 American Chemical Society[§,52]

[§] Image reproduced from Gorske *et al.*, *J. Am. Chem. Soc.*, **2007**, *129*, 8928.

For example, in model peptoids the $K_{cis/trans}$ ratio was examined by Blackwell *et al*. Values for selected dipeptoids (in this case capped with piperidine or a methyl group) are shown in **Table 2.1**. The model peptoid structures and monomers utilised are shown in **Figure 2.5**.[52] Relative to the *N*spe dipeptoid (**116**), electron withdrawing groups on the aromatic ring (i.e. pentafluoro-functionalised *N*pfe in compound **117** or nitro-functionalised *N*snp residue in **118**) stabilise the *cis* amide, suggesting the influence of n → π*$_{Ar}$ interactions. In comparison, inclusion of the sterically bulkier cyclohexyl peptoid (**120**) or more electron-rich phenolate monomer (*N*mph in **121**) cause a decrease in the *cis* amide rotamer population compared to the analogous *N*spe dipeptoid, **119**.[52]
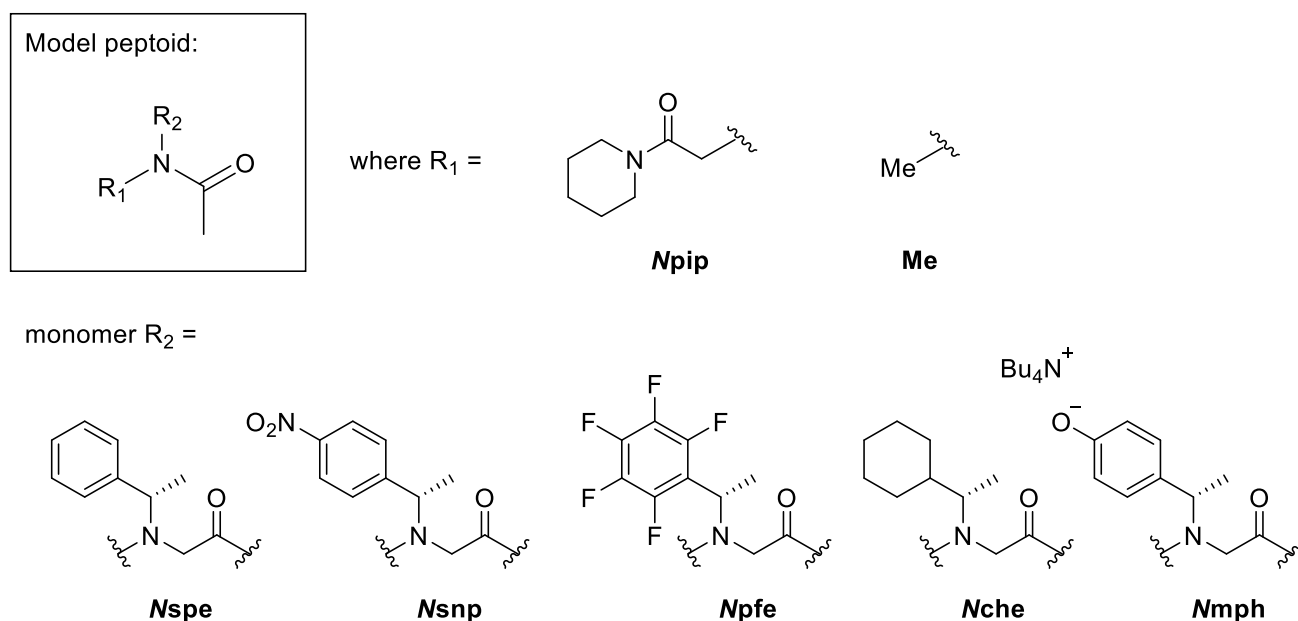
Figure 2.5. The structure of the model dipeptoids synthesised to study the effect of monomer functionalisation on the *cis/trans* amide ratio. The different resides utilised in the R* position are also shown.

	R_1	R_2	$K_{cis/trans}$	$\Delta G_{cis/trans}$ (kcal mol^{-1})
116	*N*pip	*N*spe	2.04	- 0.42
117	*N*pip	*N*snp	3.43	- 0.73
118	*N*pip	*N*pfe	3.84	- 0.79
119	Me	*N*spe	2.12	- 0.44
120	Me	*N*che	1.30	- 0.15
121	Me	*N*mph	1.25	- 0.13

Table 2.1. Model dipeptoids containing monomers with different steric and electronic characters and the associated *cis/trans* ratio and free energy.

2.4.2 The 'threaded loop' conformation

In previous studies of peptoid helices, an anomalous result had been seen in the CD spectra of a group of peptoid nonamers. The CD spectra were distinct from the peptoid helices with a single broad peak at 203 nm, suggesting a novel structure type. NMR spectroscopy studies in d³-acetonitrile revealed a new structure with well-defined local interactions, known as the 'threaded loop' conformation, where the C- and N-termini of the peptoid are held in close proximity by hydrogen bonds.[47,55]
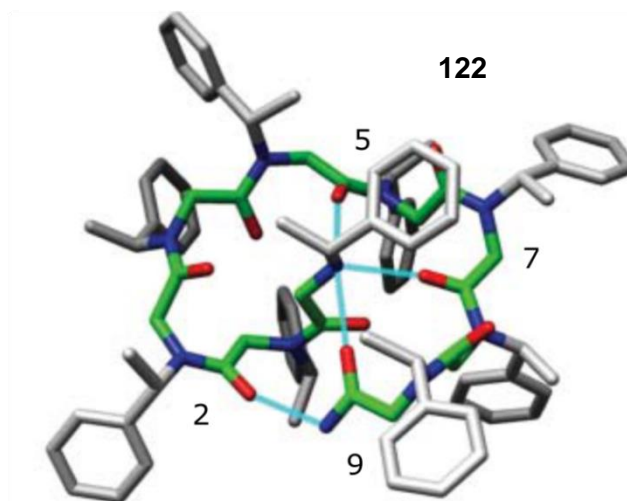
Figure 2.6. The NMR structure of the threaded loop conformation of peptoid **122**, Nspe$_9$, structure obtained in d³-acetonitrile. Hydrogen bonds shown in blue. Image adapted and reprinted with permission from The Royal Society of Chemistry.[**,47]

So far, the threaded loop conformation has been found to be unique for peptoid nonamers with α-chiral side chains, such as **122**, and it is stabilised by four intramolecular hydrogen bonds, as shown in **Figure 2.6**. Three of these hydrogen bonds are between the backbone carbonyl groups of residue 5, 7 and 9 to the N-terminal secondary amine and the fourth is from the carbonyl of residue 2 to the C-terminal primary amide. The threaded loop contains four *cis* and four *trans* amide bonds.[55] In the threaded loop conformation, solvophobic interactions direct the polar amide bonds to the interior of the loop. This secondary structure can be easily converted into a helix by the addition of a polar solvent that can disrupt the hydrogen bonding patterns (e.g. methanol) showing that the strength of hydrogen bonding is very important in stabilising the threaded loop conformation.

The Blackwell group has also manipulated the secondary structure of this peptoid 'threaded loop' using electronic effects, for example with the nitro-aromatic residues Nsnp and Ns2ne (**Figure 2.7**). By placing these monomers at strategic points in the peptoid nonamer, the hydrogen bonding at key positions in the structure can be modulated and the loop structure stabilised or disassembled.[54,56-58]
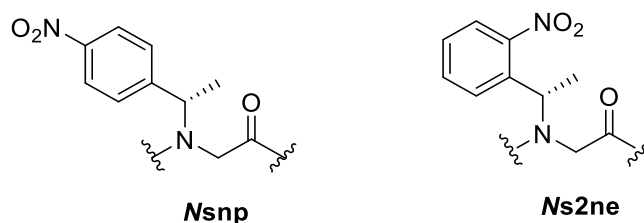
Figure 2.7. Nitro-aromatic residues used in the Nspe$_9$ threaded loop by Blackwell *et al.* Placement of the Nsnp in an N-terminal position stabilises the threaded loop, whereas inclusion of Ns2ne destabilises the structure.

2.4.3 Turn structures

Peptoid turn structures are not as well studied as the two motifs already discussed, however progress has been made to manipulate peptoid structures in this way. In the literature, turns have been achieved either by macrocyclisation (techniques for cyclisation are discussed in detail in section 2.3) or by the introduction of a heterocyclic turn-inducing monomer.[21,47,59-61]

Firstly, the head-to-tail macrocyclisation of achiral peptoids can form units which resemble native peptide β-turns. For hexamer and octamer peptoids with alternating aromatic and alkyl sub-monomers, the two types of side chain are segregated to opposite faces of the macrocycle, as illustrated in **Figure 2.8A**. The enforced cyclic structure closely resembles both type I and type III β-turns. The two amide bonds in the turn region are both *cis*, and *trans* in the rest of the structure.[21,47,58]

An alternative way to induce a peptoid turn in a linear oligomer is through the use of specific monomer units that mimic turn structures. Triazole monomers have been used for this purpose, as shown by compound **124** in **Figure 2.9**. The triazole is geometrically constrained and introduces a tight turn in peptoid structures. If bulky α-chiral groups neighbour the triazole ring, the structural stability can be further increased by rigidifying the turn. Other monomers have also been used to create the same effect. For example, N-aryl side chains with hydrogen bond donors in the ortho position can form hydrogen bonds to the peptoid backbone and enable an acyclic peptoid reverse-turn structure.[47,59-61]

a)

b)

c)

123
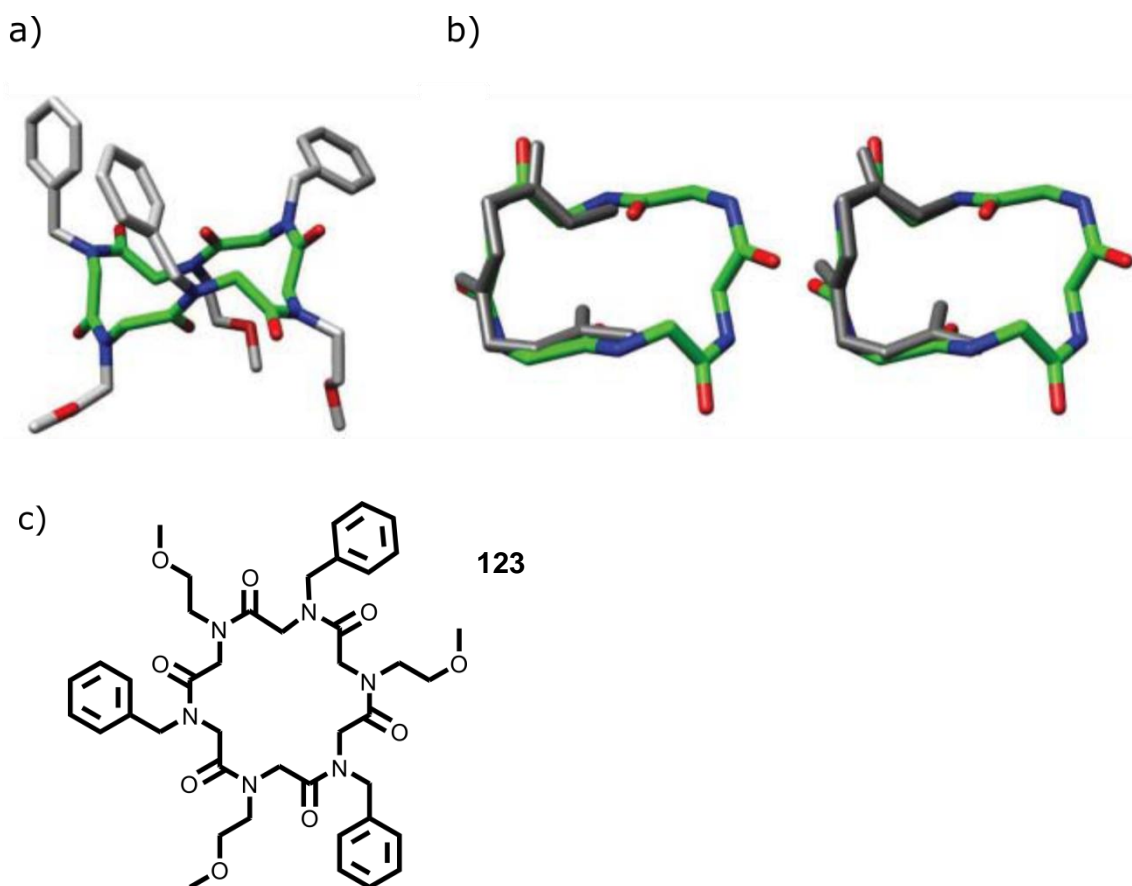
Figure 2.8. a) The X-ray crystal structure of an example cyclic hexamer **123**; b) the backbone of the cyclic peptoid, shown in green, is overlaid with a peptide type I (left) and type III β-turn (right), both shown in grey; c) chemical structure of the peptoid macrocycle **123**. Image adapted and reprinted with permission from The Royal Society of Chemistry. [††,47]

a)

b)

124
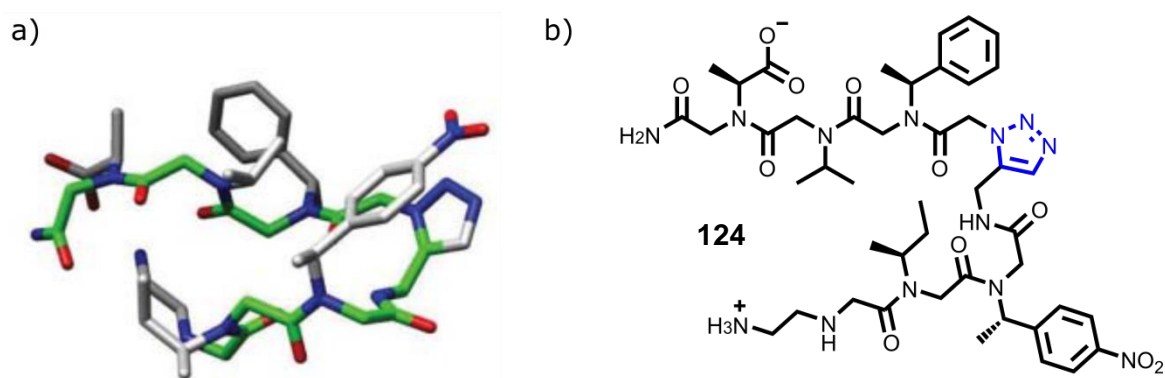
Figure 2.9. The NMR structure of the highly ordered turn induced by the triazole unit in compound **124**, where the peptoid backbone is highlighted in green. The structure of peptoid **124** is also shown, with the triazole moiety highlighted in blue. Image adapted and reprinted with permission from The Royal Society of Chemistry. [‡‡,47]

[††] Image reproduced from Fowler and Blackwell, *Org. Biomol. Chem.*, **2009**, 7, 1508.
[‡‡] Image reproduced from Fowler and Blackwell, *Org. Biomol. Chem.*, **2009**, 7, 1508.

2.4.4 Self-assembly of peptoid nanostructures

Another peptoid structural motif that has been well documented by the Zuckermann group is peptoid nanosheets and related nanotubes, which were discovered well over a decade later than peptoid helices. Nanosheets have been suggested as β-sheet mimetics and are typically comprised of amphiphillic diblock copolymers.[62-64] To form these nanosheets, chain-chain interactions are necessary and this introduces a greater level of complexity into the design of peptoid nanosheets as peptoid backbones cannot undergo intramolecular hydrogen bonds like peptides.

The Zuckermann group synthesised the first peptoid nanosheet which was formed of two separate, oppositely charged 36 residue peptoids that self-assemble into a bilayer in high yield under aqueous conditions. The two amphiphilic 36mers alternated a polar ionic sub-monomer and nonpolar aromatic monomer and this regular sequence was repeated. These nanosheets were characterised by atomic force microscopy, X-ray diffraction and transmission electron microscopy to show that the layers were 3 nm thick and consistent with a bilayer model, where hydrophobic groups are buried in the interior of the sheet and ionic groups exposed to the surface. This two dimensional structure is shown in **Figure 2.10**. The bilayers were stable over a broad pH range and various temperatures, but dissolve in the presence of greater than 50 % acetonitrile.[8,62,65-68]

The sheet formation was found to be highly dependent on the two-fold periodicity (i.e. three and four-fold repeating units didn't lead to self-assembling polymers) and also on peptoid chain lengths; in general, the longer the chain the more stable the nanosheets formed.

a)

b)
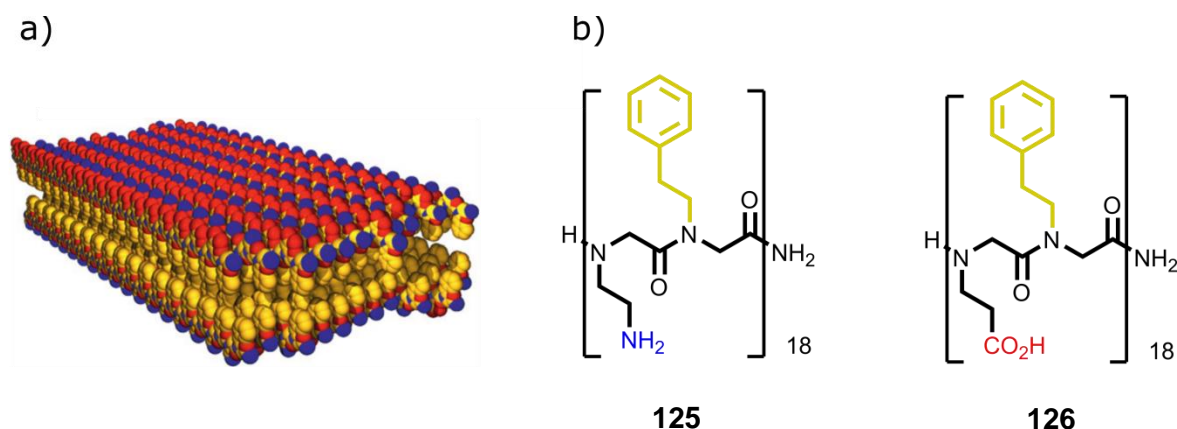
Figure 2.10. a) The structure of the two dimensional nanosheet described, as taken from molecular modelling. Oxygen is shown in red, nitrogen in blue and carbon in yellow. b) The chemical structure of the two, oppositely charged amphiphilic peptoids **125** and **126**, i.e. the positively charged peptoid **125** (*NaeN*phe)$_{18}$ and the negatively charged peptoid **126** (*NceN*phe)$_{18}$.[65,67] Image adapted and reprinted with permission, copyright 2010 Nature Publishing Group. [§§]

[§§] Image of nanosheet reproduced from Nam *et al.*, *Nat. Mater.*, **2010**, *9*, 454.

More sophisticated nanosheets have also been made by the Zuckermann group, who sought to form a nanosheet from a single peptoid chain. They combined the critical design elements from the first nanosheets to successfully form a block charge structure (Nae$N$phe)$_9$(Nce$N$phe)$_9$ and also a peptoid with alternating charge (Nae$N$pheNce$N$phe)$_9$. Both designs formed nanosheets and as expected the block charge motif had the best stability against pH change and chemical denaturation.[65,67]

Additionally, monodisperse amphiphillic diblock polypeptoids have also recently been shown to spontaneously assemble into hollow, crystalline nanotubes.[69] Such structures have no central hydrophobic core, which is dissimilar to the nanosheets described above and van der Waals interactions provide the dominant interaction. The motif used in these nanosheets contains a hydrophobic block of poly-N-decylglycines and a hydrophilic domain made of 2-(2o(2-methoxyethoxy)ethoxy)ethylglycine monomers. The ethyleneoxy and aliphatic packing interactions are strong enough to crystallise the thin nanotube domains, with significant curvature and provide materials that can be adapted for many potential applications in the nanotechnology or pharmaceutical fields.[69]

2.5 Characterisation of peptoid secondary structure

Mass spectrometry is usually used to confirm the sequence of peptoids but characterising the secondary structure of peptoids needs further analytical techniques which are briefly explained below. In particular, circular dichroism spectroscopy (CD), X-ray crystallography and nuclear magnetic resonance (NMR) spectroscopy have been regularly used and other techniques such as fluorescence resonance energy transfer (FRET) or computational methods have also been used.

CD spectroscopy is probably the most commonly used procedure to study the secondary structures of peptoids as measurements are quick to obtain and only require low sample concentrations (typically 1–10 mg mL^{-1}). CD spectroscopy can be used to evaluate the stability as well as conformation of the peptoids under many conditions such as temperature, solvents or the effect of denaturants. A source of circularly polarised light is used and for optically active samples the left and right components of circularly polarised light are absorbed to different extents leading to characteristic absorption bands.[70]

CD spectroscopy is used extensively to study helical peptoids, as intense and characteristic absorption signals due to low energy electronic transitions within the N-substituted amide backbone can be seen (corresponding to n $\rightarrow$ π* and π$_o$ $\rightarrow$ π* transitions). Peptoids as short as five residues long can exhibit helical CD spectra, although the signals intensify as chain length increases. In helical peptoids with α-chiral aromatic side chains, well-defined double minima are seen around 202 and 218 nm, similar to peptide helices and it is suggested that these helicies are structurally similar to a type-I polyproline helix.[32,33,50,71]

The handedness of helices is controlled by the chirality of the monomers chosen, so peptoids with side-chains of opposing handedness exhibit mirror-image CD spectra. Only molecules without a plane of symmetry show the characteristic absorptions, therefore in peptides the chirality in the backbone allows measurements to be taken regardless of the sequence. However, with peptoids, if no α-chiral sub-monomers are present, CD measurements cannot be obtained.[32,33,50,71]

Where it has been possible to crystallise peptoids, single crystal X-ray diffraction techniques have been used to study their conformation. The first crystal structure of a peptoid (an *N*-(1-cyclohexylethyl)glycine pentamer) was reported in 2003.[50] Linear peptoids tend to be difficult to crystallise due to their flexibility, therefore far more X-ray structures have been solved for conformationally restrained cyclic peptoids than linear ones.[21,32,33,50]

Finally, NMR spectroscopy has also been used to characterise peptoid secondary structures, often in combination with CD spectroscopy or X-ray structures. Often 2D-NMR is used to gain a better understanding of the solution state conformations of peptoids; NOESY was used to confirm the n → π^*_{Ar} interactions discussed earlier. ^{1}H–^{13}C HSQC spectra have also been used to show that there is more than one helical conformation in solution, as far more peaks are seen on the proton-carbon correlation than expected. This arises due to the lack of backbone hydrogen bonding in peptoids, which means that the amide bonds can readily populate *cis* and *trans* forms. In general, in longer peptoids, the *cis* form is favoured. The ratio between *cis* and *trans* states can be altered by inclusion of monomers with different steric or electronic character (as discussed in section 2.4.1) and the ratio $K_{cis/trans}$ can be determined via integration of the NMR spectra.[32,33,50,52,72,73]

Overall, great progress has been made in understanding and synthesising new peptoid structures over the last decade. Common motifs from peptide chemistry have been copied and successfully transferred into peptoids, such as the helix and more complicated structures such as self-assembling microspheres and nanosheets. It has been shown that subtle sequence variations can influence long-range structural interactions, giving chemists a handle to help design peptoids for specific applications.[66,74]

Several groups have accurately predicted the structure of peptoids from their sequence, but there is still much work to be completed in this area. In the future, the *de novo* design of functional peptoids, for example for biological applications, will depend upon the ability to predict the structure of peptoids from their sequence. As peptoids lack regular hydrogen bonding patterns, this is very challenging. To date, steric, hydrophobic, electrostatic and stereoelectronic effects have all been implicated in the folding of peptoids and these additional forces all vary greatly for the hundreds of potential peptoid side chains. Further research is needed to thoroughly understand the complicated molecular interactions that are necessary to fold peptoids into helices, turns and larger global structures that would resemble peptoid protein mimics.[46,72]

2.6 Peptoid library synthesis

Over 200 peptoids have been synthesised as part of this project, this includes simple linear peptoids including those that have been lipidated or PEG-ylated, sequences with novel chemical functionalities and cyclic compounds. The synthesis of these compounds will be discussed, including the development of novel methodology for the synthesis of sequences containing both lysine- and arginine-type monomers, a new class of peptoid. The synthesis of fluorescently tagged peptoids will be discussed in Chapter 5, where they are used to facilitate investigations into peptoid mode of action.

2.6.1 Library design

Our initial peptoid library was designed to incorporate three key properties known to lead to biological activity in antimicrobial peptides (AMPs); positive charge, amphipathicity and a defined secondary structure. By mimicking these key attributes of AMPs, it was hoped that potent anti-infective behaviours could also be replicated in the peptoid sequences.

Firstly, most sequences included residues that could provide an overall cationic charge to the sequence. In naturally occurring AMPs, inclusion of lysine and arginine is highly conserved as they facilitate interaction with bacterial cell membranes. Both bacterial and parasitic cell membranes tend to be more negatively charged than mammalian cells as they have a greater proportion of phospholipids on their surface. It was hoped that cationic peptoids may have a greater selectivity to pathogenic cells over mammalian cells.

A large proportion of potent AMPs are helical, so sequences within this library were designed to encourage the formation of peptoid helicies. Given the lack of backbone chirality and the amide bound proton that can undergo hydrogen bonding to stabilise peptide secondary structure, bulky, aromatic residues were included in the peptoid sequences in order to induce a helical secondary structure, as described in section 2.4.1 Many of our peptoids include the N-(S-phenylethyl)glycine residue (Nspe) as this has been shown to induce a helical peptoid conformation. CD studies on our library[***] confirm that most sequences display at least some helical character.[75-77]

Typically sequences used a repeat motif of three residues, i.e. (NxNyNz)$_n$ where Nx is typically a charged or hydrophilic monomer. Ny/z is usually a hydrophobic monomer such as the Nspe monomer so the motif often was similar to that shown in **Figure 2.11**. Peptoid helices are reported to be wound slightly tighter than the typical peptide α-helix, with 3.0 residues per turn. Use of the three monomer motif in **Figure 2.11** should encourage the formation of an amphiphilic structure where all the hydrophilic groups

---

[***] Data in section 2.10

are positioned on the same side of the helix. This has often been shown to aid antimicrobial action in AMPs.[47,77]
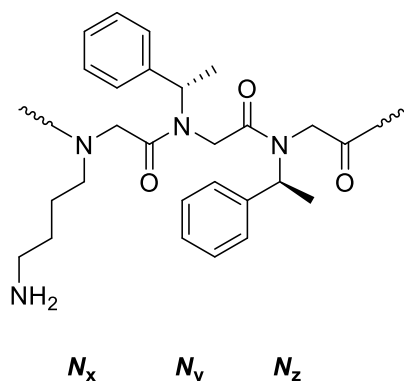
Figure 2.11. Typical repeating peptoid motif of hydrophilic monomer, *N*x, followed by two hydrophobic monomers, *N*y and *N*z (that don't necessarily have to be the same).

In initial peptoid syntheses, a limited variety of monomers were incorporated into the library using cheap and commercially available amines, including aromatics like substituted-benzylamines and simple alkyl amines. Successive generation libraries were designed to add differing functionalities and to expand the chemical space achieved by the peptoid sequences. For example, residues containing heteroatoms reminiscent of natural amino acids were included (i.e. histidine, tryptophan or cysteine-type monomers) or those with suspected beneficial pharmacokinetic properties (i.e. fluorine containing monomers). **Figure 2.12** shows a representative selection of the wide variety of peptoid residues included in our library.

By including a wide variety of side chain functionalities in the peptoid library, structure-activity relationship investigations have been investigated against a variety of biological targets.

As well as examining the effect of different monomer functionalisation, other features were designed into the sequences to investigate other attributes that are necessary for potent, anti-infective peptoids. These alterations will be discussed as specific compounds are introduced, but include changes such as:

- Peptoid sequence length

- Overall peptoid charge

- Placement of charge in the peptoid sequence

- Length and nature of hydrophilic side chains

- The effect of α-chiral monomers

- Differing motifs (i.e. pattern of hydrophilic and hydrophobic residues)

'hydrophillic' residues   aromatic residues   alkyl residues   heteroatom containing residues
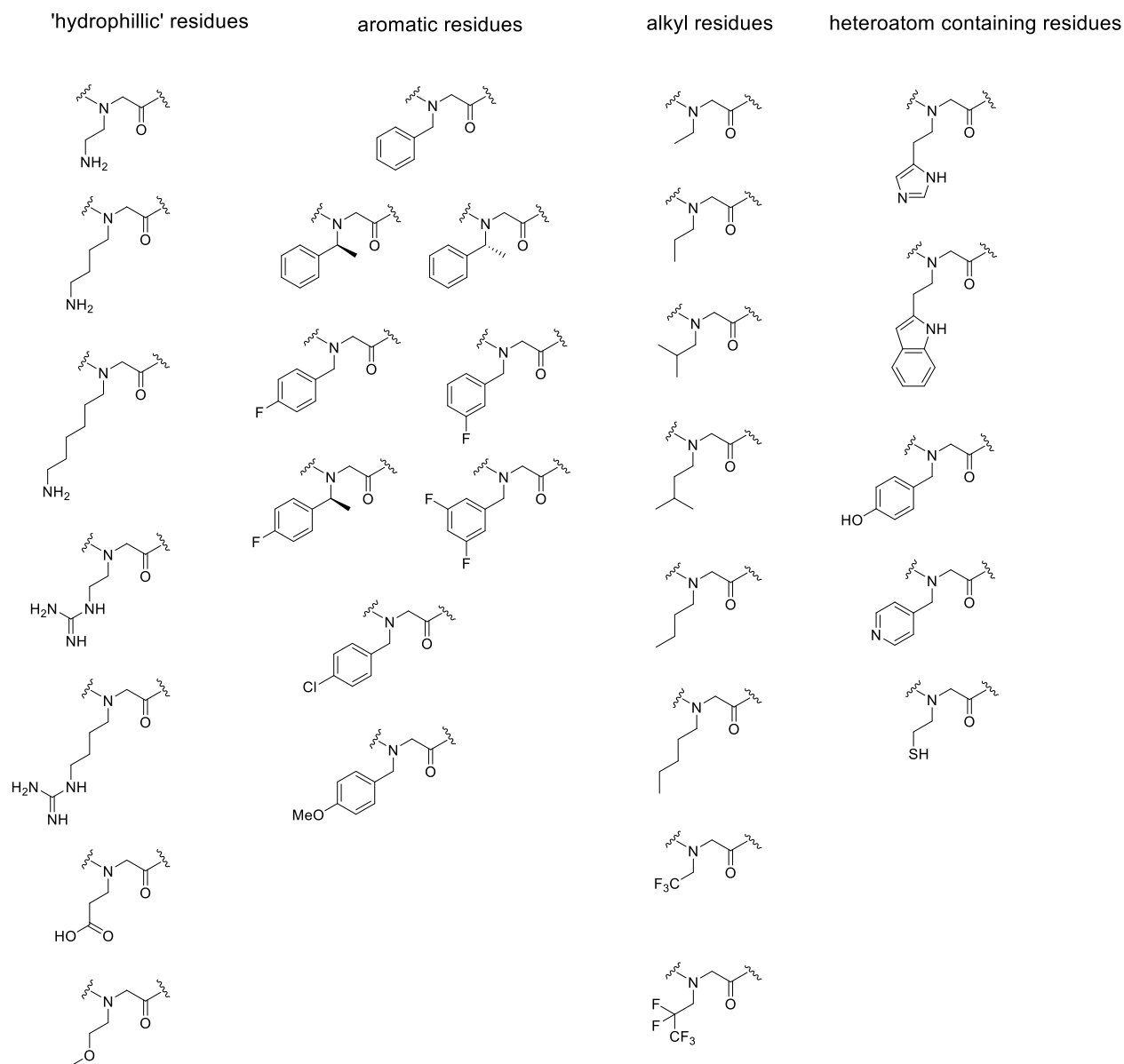
Figure 2.12. Representative selection of the most common monomers used as an example of the chemical diversity within the library.

2.6.2 Peptoid nomenclature

Within the scientific literature, there exists many different ways to name a single peptoid sequence. Unlike peptides, where each amino acid in the sequence has a distinctive name and one letter amino acid code, the naming of peptoid monomers is far more ambiguous. In part, this is due to the great diversity within peptoid sequences and also because no group has yet published guidelines for the naming of peptoids. As such, different research groups use different terminology for the same peptoid monomer.

In an effort to implement a consistent nomenclature across peptoid building blocks within this project, the following conventions have been adopted. Peptoid monomers are typically named after the amine that they are derived from (unless the side chains are reminiscent of a natural amino acid). Building blocks with side chains analogous to those of amino acids are named after the corresponding amino acid if the N-terminal nitrogen of the building block bears those atoms attached to the alpha carbon of the corresponding amino acid (not including the alpha carbon), e.g. *N*Arg. Building blocks with side chains analogous to those of amino acids but differing by one carbon are named after the corresponding amino acid with 'h' (homo) preceding the amino acid code if the building block contains one carbon extra, e.g. *N*hArg, or 'n' (nor) preceding the amino acid code if the building block contains one carbon less, e.g. *N*nArg (see **Figure 2.13**). Capitalization within building blocks is in line with the literature where possible and amino acid components of peptoid building block names are capitalized.
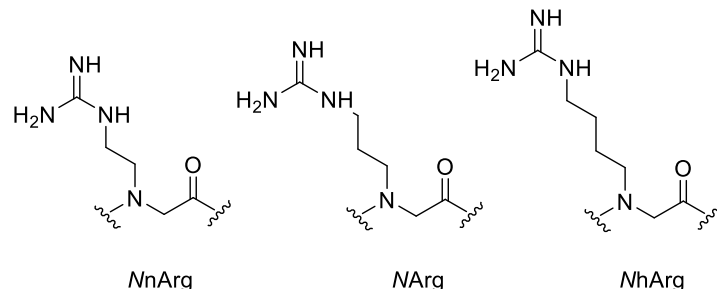
Figure 2.13. Nomenclature for peptoid monomers similar to the peptide amino acid arginine.

Where possible, this building block nomenclature has been chosen to be as similar as possible to that found in the literature. While some building block names may differ from those found in the literature in some cases, it is envisaged that the naming scheme chosen will result in more consistent and understandable naming. In collaboration with Sam Lear (Cobb group, Durham University), this nomenclature has been used in an online web utility for the calculation of peptoid molecular weights and assignment of mass spectrometry data. This site can be found at www.pep-calc.com/peptoid and also includes residues not used in this project, but commonly found in the literature.[78] Additionally, a table to show peptoid monomers and the primary amine they are derived from can be found in the Appendix.

2.6.3 Synthesis of linear peptoids

All peptoids were made using solid-phase synthesis and the submonomer procedure pioneered by Zuckermann *et al* introduced in section 2.1.2.[3] A schematic for the synthesis and cleavage from the resin is shown in **Scheme 2.6**. In the submonomer method, the peptoid is built up sequentially to form a monodisperse sequence by acylation of the resin using a haloacetic acid and subsequent displacement by a primary amine. The submonomer procedure is then repeated until a peptoid of the required sequence and length has been achieved.
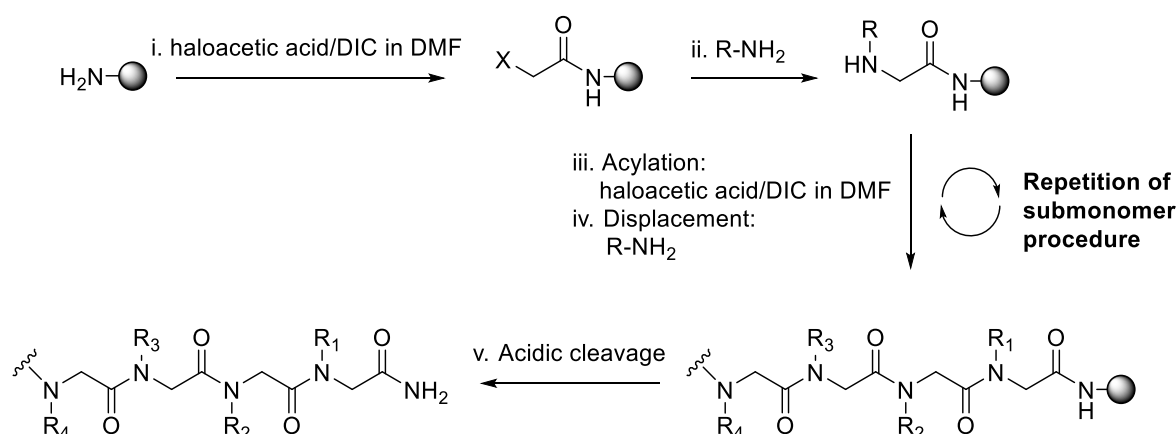
Scheme 2.6. The sub-monomer synthesis of a peptoid on solid phase; i. acylation step; ii. displacement using a primary amine; iii/iv. repetition of submonomer method; iv. acidic cleavage from the resin using TFA. 'R' represents the side-chains and where necessary, monomers are protected by a suitable protecting group.

Typically, bromoacetic acid was chosen as the acetylating agent and *N,N'*-diisopropylcarbodiimide (DIC) as the activator in the first coupling. For certain sequences where side chain functionality included unprotected heteroatoms, chloroacetic acid was used instead. The chloroacetic acid was used to synthesise the peptoids using amines with unprotected side-chains such as imidazole, indole or pyridyl groups.

Due to the unprotected heteroatoms, there is the potential for sequence propagation on the side chain heterocycles as shown in **Scheme 2.7**. It is expected that activated bromoacetic acid will temporarily acylate most side chain aromatic nitrogens. However, this reaction is readily reversed in the presence of base and because the second step of the submonomer procedure involves a high concentration of amine, unwanted side products from acylation are removed. Bromoacetic acid can also alkylate the unprotected heteroatoms. Normally, this side reaction is not observed on the propagating chain because acylation of an N-terminal secondary amine is not reversible and is approximately 1,000 times faster than alkylation. However, the reversibility of side-chain

heterocycle acylation allows accumulation of the irreversible alkylation byproduct. To avoid this, chloroacetic acid was used in the acylation step when monomers were used that had unprotected heteroatoms.[4]
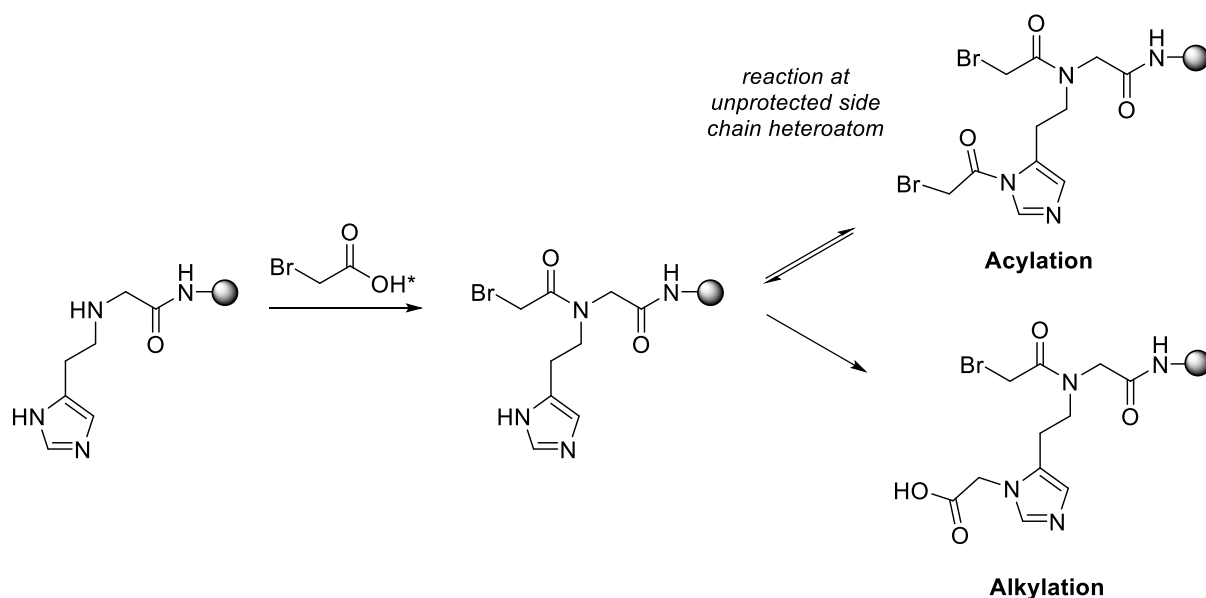
Scheme 2.7. The two potential side reactions that can occur at unprotected, side chain heteroatoms when treated with an activated haloacetic acid; acylation (transient) and alkylation (irreversible).

Chloroacetic acid is a poorer alkylating agent than bromoacetic acid so reduces the unwanted alkylation reaction, but it also slows down the following displacement reactions. Therefore, in syntheses using chloroacetic acid, the displacement steps were extended to 90 minutes. After the synthesis, a final piperidine deprotection ensured that any side-products from acylation were removed.

Following successful acylation, in the second step of the submonomer method, a variety of primary amines were used to undertake the S_N2 displacement of the halide atom to form the peptoid monomer. All coupling steps were undertaken in DMF as both haloacetic acids, DIC and most amines have good solubility in DMF, although NMP was used to solubilise certain amines that had poor solubility in DMF.

Most amines were commercially available, either as protected amines (i.e. *N*ae from *N*-Boc-1,2-diaminoethane) or could be used without protection. Several monomers needed treatment before use in peptoid synthesis and are shown in **Figure 2.14**. The glutamic acid peptoid residue *N*Glu was derived from ^{t}Bu-protected β-alanine which is purchased as a hydrochloride salt and must be free-based prior to synthesis to give **127**. In order to add a cysteine monomer, commercially available thioethylamine was trityl protected to yield **128**. The *N*Lys monomer was derived from *N*-Boc-1,4-diaminobutane, compound **129**, which was either synthesised from the unprotected diamine (as described in section 2.6.4), or purchased from commercial sources. Protocols for monomer preparation can be found in the Experimental chapter.
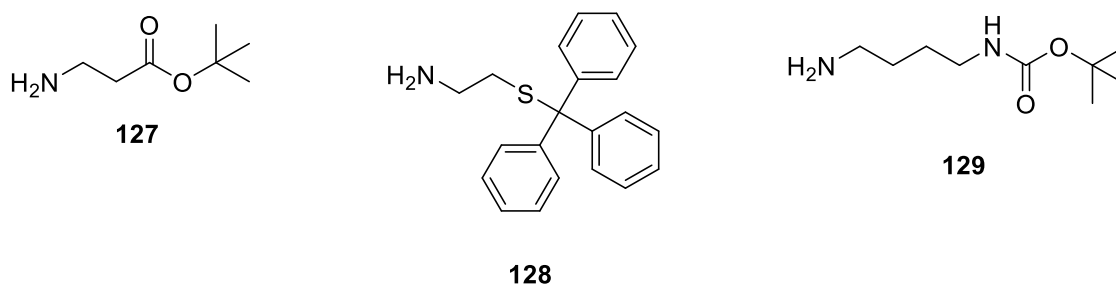
Figure 2.14. Protected monomers synthesised for use in the submonomer method of peptoid synthesis.

Typically, Rink Amide resin was used to build the peptoids from the C terminus, as it is a versatile resin and following cleavage from the resin results in a C terminal carboxamidine. However, in the synthesis of cyclic precursors or specialised sequences (discussed in section 2.6.5) other resins were chosen. Removal of the final compound from the resin is undertaken using acidic cleavage conditions that depend on the particular resin chosen (see Chapter 7).

In general, the peptoids in this library were cleaved for no longer than 90 minutes (most commonly 45–60 minutes) due to the potential for acid induced degradation of the *N*-(*S*/*R*-phenylethyl)glycine residue monomer. In comparison to peptide synthesis where cleavages of 6 hours are routine, this is a much shorter time period but provided peptoids in the greatest purity with adequate overall yield.

Peptoids were synthesised both manually in the Cobb Group[†††] and using a customised, automated parallel synthesiser in the Zuckermann lab[‡‡‡] using different conditions (see **Table 2.2**). A list of peptoids synthesised in this peptoid library and detailed experimental procedures for these syntheses can be found in the Experimental chapter. All peptoids were purified to > 95 %, as characterised by analytical RP-HPLC.

At the outset of this project, most synthetic peptoid papers referenced the original 1992 submonomer paper from the Zuckermann group[2] and a statement was made that adapted conditions were used but these were rarely stated. Therefore, there was no overall consensus within the literature on the exact method that should be used for the synthesis of generic peptoids. The literature suggested that the time taken for the addition of each submonomer (both acylation and displacement) can vary between several minutes and several hours, dependent on the amines used, which becomes problematic in the synthesis of longer peptoids. It had been shown that couplings occurred faster when the reactions were heated; either manually or using microwave irradiation. In particular, microwave heating is reported to be useful for α-branched primary amines and where electronically deactivated amines are used. In these cases, gentle microwave heating was

[†††] At Durham University
[‡‡‡] At the Molecular Foundry, Lawrence Berkeley National Laboratory, USA

reported to give a modest increase in purity relative to control experiments carried out at room temperature.[79,80]

Table 2.2 summarises the three reactions conditions used for the synthesis of linear peptoids. Due to the suggestion that conventional or microwave heating could aid the submonomer synthesis of peptoids; early syntheses in this project used a heated shaker platform or microwave to accelerate reactions. In heated reactions, 15 minute couplings at 50 °C (condition 1) were chosen to balance the time of reaction and product purity (crude product purity between 40 and 70% by RP-analytical HPLC). Pure samples were obtained following HPLC using these conditions, however additions and deletions were seen in the crude products and it was anticipated that the yields could be improved with optimisation.

At this point, the synthesis of peptoids was undertaken using an automated peptoid synthesiser that had no heating element, so other conditions were necessary. In automated syntheses the acylation and displacement steps were carried out at room temperature for 20 minutes and 60 minutes respectively (condition 2), following advice from the Zuckermann group. The longer coupling times and lower concentration of bromoacetic acid led to high yielding, clean syntheses with crude purities approximated between 75–95 % by RP-analytical HPLC. Final purification was substantially easier using condition 2a so subsequent manual syntheses also followed the optimised conditions used in the automated syntheses.

In syntheses using chloroacetic acid (condition 3), the crude products were not as clean and had crude purities between 50–75 % by RP-analytical HPLC. However, enough material was obtained following preparative HPLC at > 95 % purity for biological testing so the reactions were not optimised further.

	Condition 1		Condition 2	Condition 3

Manual Synthesis	Heated shaker
	50 ˚C
	
	Acylation 15 min
	   8 eq. 2 M BrAA in DMF
	   8 eq. 2 M DIC in DMF
	
	Displacement 15 min
	   4 eq. 1 M amine in DMF
		Microwave (power 20W)
		50 ˚C
		
		Acylation 15 min
		   8 eq. 2 M BrAA in DMF
		   8 eq. 2 M DIC in DMF
		
		Displacement 15 min
		   4 eq. 1 M amine in DMF
			Shaker platform
			Room temperature
			
			Acylation 20 min
			   1 mL 0.6 M BrAA in DMF
			   0.20 mL 50 % DIC in DMF *v/v*
			
			Displacement 60 min
			   1 mL 0.8–2.0 M amine in DMF
				Shaker platform
				Room temperature
				
				Acylation 20 min
				   1 mL 0.6 M ClAA in DMF
				   0.20 mL 50 % DIC in DMF *v/v*
				
				Displacement 90 min
				   1 mL 0.8–2.0 M amine in DMF

Automated Synthesis			Robot
			Room temperature
			
			Acylation 20 min
			   1 mL 0.6 M BrAA (or ClAA) in DMF
			   0.18 mL 50 % DIC in DMF *v/v*
			
			Displacement 60 min
			   1 mL 0.8 – 2.0M amine in DMF
				Robot
				Room temperature
				
				Acylation 20 min
				   1 mL 0.6 M ClAA in DMF
				   0.18 mL 50 % DIC in DMF *v/v*
				
				Displacement 90 min
				   1 mL 0.8–2.0 M amine in DMF

Table 2.2. A comparison of manual and automated synthesis procedures. NMP is used as a solvent for poorly soluble amines, BrAA is bromoacetic acid and ClAA is chloroacetic acid. Condition 2 is recommended for all syntheses (or condition 3 where residues containing unprotected heteroatoms are introduced).

2.6.4 Boc protection of 1,4-diaminobutane

The lysine-mimetic *N*Lys submonomer is derived from 1,4-diaminobutane, which must be mono-protected to prevent unwanted reactions and chain propagation along the side chain groups.

Boc (*tert*-butyloxycarbonyl) protection was chosen, similar to the Boc protection of Fmoc-Lys(Boc)-OH used in peptide synthesis, as the Boc group can be removed under the same acidic conditions used to cleave products from the resin. A literature procedure was followed to achieve the synthesis of mono-*N*-Boc-1,4-diaminobutane, **129**.[81]

The reaction shown in **Scheme 2.8** uses high-dilution synthesis; large volumes of solvent, low temperatures and slow addition of Boc anhydride to the 10-fold excess of 1,4-diaminobutane to encourage formation of the mono-protected product over the di-substituted amine. Unreacted 1,4-diaminobutane is readily removed from the product by washing with water. Following extraction and solvent removal, **129** is found as a colourless oil and ready for use in solid phase synthesis, without further purification.
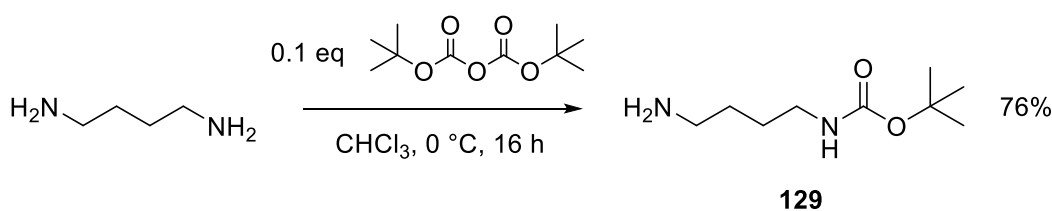
Scheme 2.8. Mono-Boc protection of 1,4-diaminobutane using high dilution synthesis.

Later in the project, it was decided to purchase *N*-Boc-1,4-diaminobutane (**129**) from commercial sources to save time and reduce reagent costs. Although **129** synthesised in house looked identical to the commercially bought compound via ^{1}H and ^{13}C NMR spectroscopy, the purchased amine was less viscous, therefore easier to handle and more soluble in DMF (the solvent used in the sub-monomer synthesis of peptoids) which was advantageous.

2.6.5 Cyclic peptoids

As previously explained in Chapter 1, cyclisation often increases the biological activity of molecules. This is attributed in part to a more rigid structure, therefore conformational entropy losses are minimised upon target binding. When considering peptides and peptoids, cyclisation also removes charged termini which can increase membrane permeability.[82]

A small library of cyclic peptoids was synthesised in this project to investigate if these compounds would have an improved biological activity compared to their linear analogues. The five cyclic peptoids synthesised as part of this project are summarised in **Figure 2.15**. Since the cyclisation itself enforces a defined secondary structure inclusion of the α-chiral *N*-(*S*-phenylethyl)glycine residue monomer, which was used frequently in the linear sequences to achieve a stable secondary structure, was unnecessary.

130
cyclo (*N*Lys*N*phe*N*phe)$_2$

131
cyclo (*N*Lys*N*pfb*N*pfb)$_2$

132
cyclo (*N*Lys*N*phe)$_3$

133
cyclo (*N*hArg*N*phe)$_3$

134
cyclo (*N*Lys*N*phe*N*hArg*N*phe*N*Lys*N*phe)
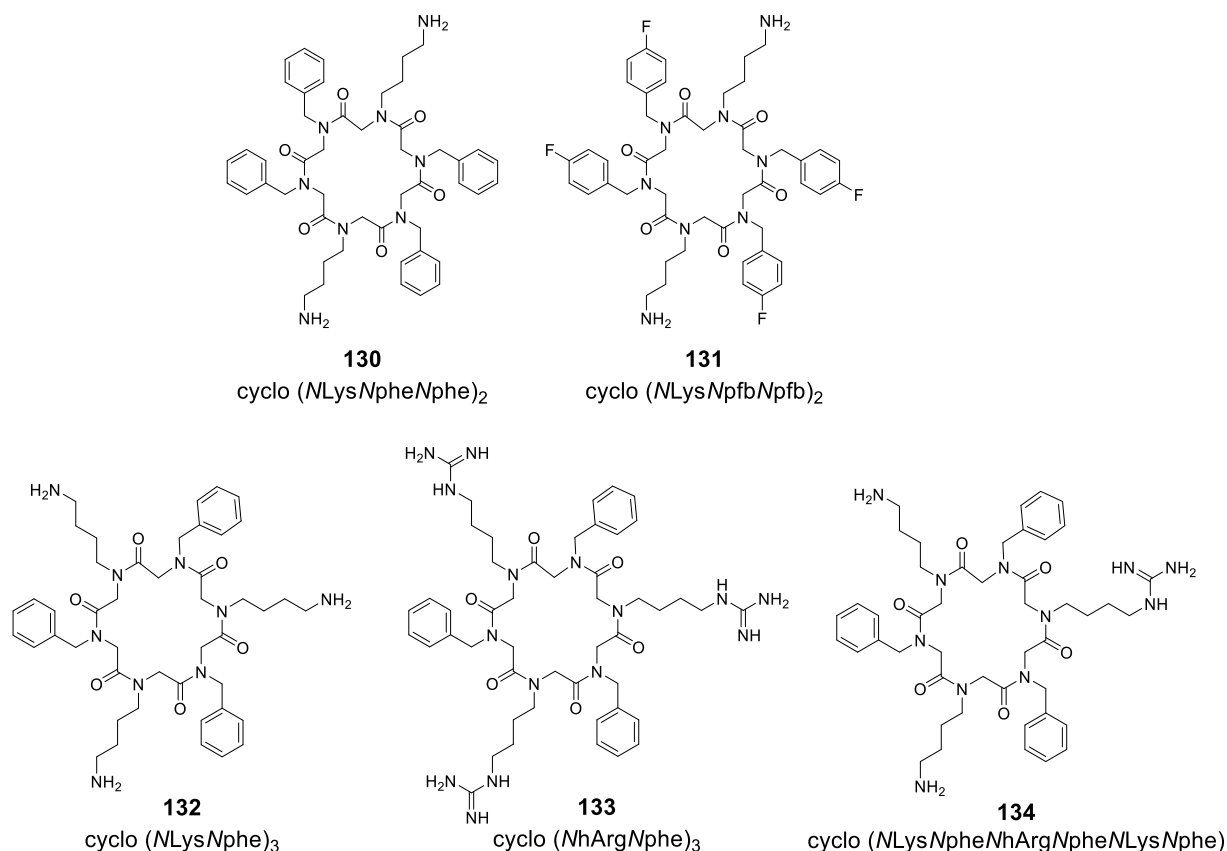
Figure 2.15. The cyclic peptoids synthesised with a range of cationic functionalities represented.

Peptoids **130** and **131** with the $N_x N_y N_y$ motif were synthesised as direct comparisons to 6 residue peptoids from the linear library, (*N*Lys*N*phe*N*phe)$_2$ and (*N*Lys*N*pfb*N*pfb)$_2$. However, X-ray diffraction data collected from various cyclic peptoids in the literature show that if the linear sequence has alternating hydrophobic/phillic residues, the

hydrophobic chains are organised onto one face of the macrocycle and the hydrophilic chains will be directed towards the opposite face. This should form an amphiphilic structure with well-defined lipophilic and cationic surfaces.[28,29] Therefore, three peptoids based upon an alternating N_xN_y motif, **132**, **133** and **135** were also synthesised. As well as being more highly charged, it was anticipated that these peptoids may have more distinct hydrophobic and hydrophilic faces compared to **130** and **131**, which may increase biological activity.

A wide variety of techniques have been developed for the cyclisation of peptoids (summarised in 2.3). In this project, a head-to-tail cyclisation strategy was employed. As shown in **Scheme 2.9**, the linear precursor peptoid is made using the submonomer procedure on solid phase, cleaved from the resin and then cyclised in solution.[28,39]

Protected linear peptoid on resin

Protected peptoid off resin

Deprotected cyclic peptoid

Protected cyclic peptoid
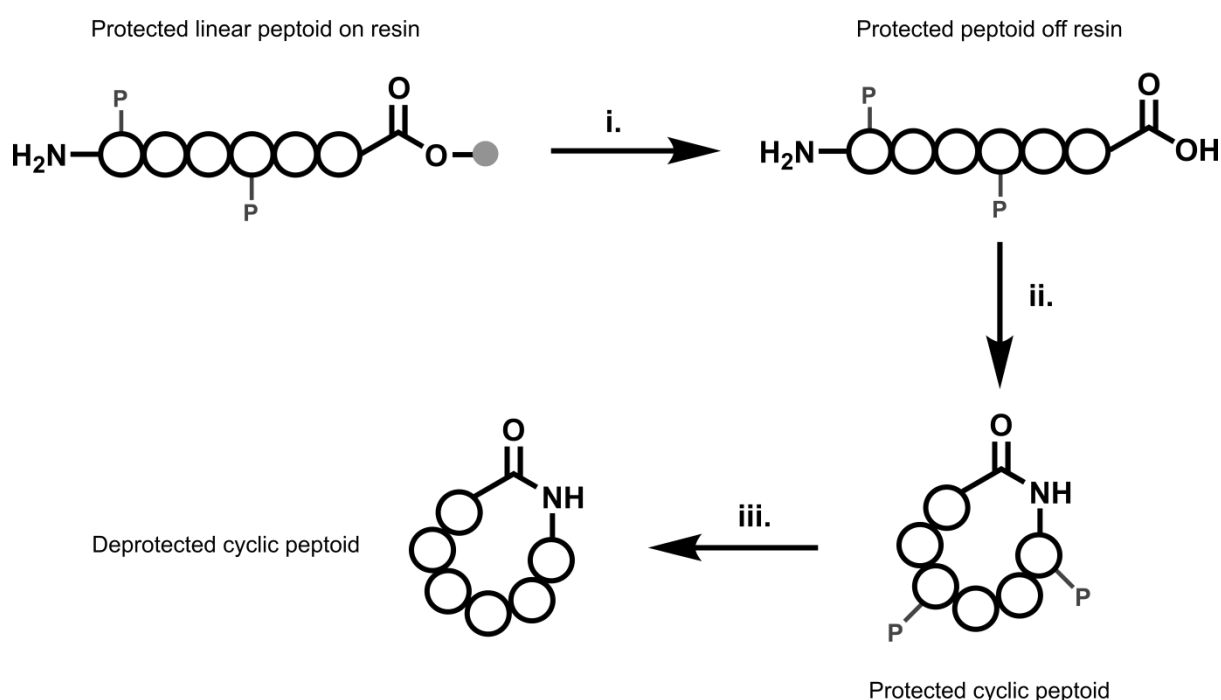
Scheme 2.9. A schematic to represent the stages involved in the cyclisation of linear peptoids, where 'P' represents protected side-chains. i. cleavage from resin under mildly acidic conditions; ii. cyclisation using an activating agent; iii. removal of side-chain protecting groups.

In order to facilitate a head-to-tail cyclisation, 2-chlorotrityl chloride resin was used for the synthesis of linear precursors. This resin produces a C-terminal carboxylic acid group upon cleavage from the solid-support, which can be easily activated to facilitate cyclisation. To load the resin, bromoacetic acid and DIPEA are used and all subsequent couplings follow as for Rink Amide resin. As this resin contains a fairly acid and moisture sensitive linker and because a concentrated bromoacetic acid solution is used in the acylation step, couplings were undertaken at room temperature. These conditions were adequate to produce a crude peptoid that didn't need purification before cyclisation.

To cleave the peptoid from the resin, hexafluoroisopropanol, HFIP (20 % *v/v* in DCM) was used. This cocktail causes cleavage under mild conditions that does not remove protecting groups on the side-chain amino groups (i.e. Boc protection remains intact). This is necessary to prevent unwanted side-reactions upon cyclisation.

Cyclisation was carried out on the crude, protected peptoids using PyBOP and DIPEA in DMF, which form an activated ester to assist the head-to-tail attack of the terminal amine. Finally, the Boc groups are removed from the *N*Lys residues using a TFA cocktail. Full conditions for the cleavage, cyclisation and deprotection of **130** are shown in **Scheme 2.10**.
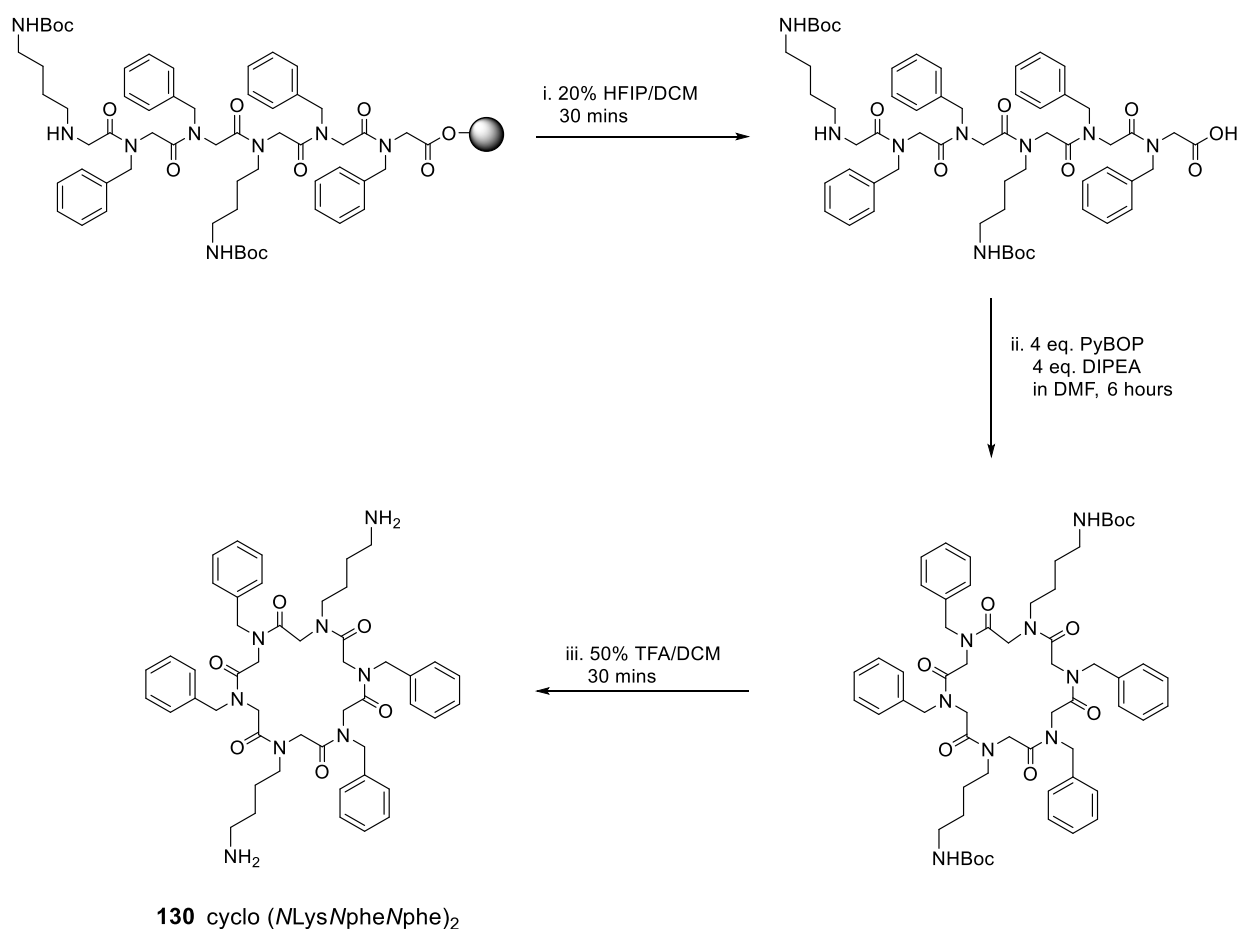
Scheme 2.10. The synthesis of the cyclic peptoid **130**. The linear precursor is made on 2-chlorotrityl chloride resin as previously described; i. cleavage from the resin; ii. cyclisation under high-dilution synthesis conditions; iii. deprotection of Boc groups.

For small molecules, intramolecular reactions should be much faster than intermolecular processes. Although literature precedents[28,39] suggested that there was no need for high-dilution conditions to encourage cyclisation over the formation of oligomers, reactions were carried out in a larger volume of solvent than necessary (typically 10 mL for 100 μmol peptoid) and the peptoid solution was added dropwise over several hours.

DMF was used in initial cyclisations, but as it has a boiling point of 153 °C it is difficult to remove at the end of the reaction *in vacuo*, so a trial cyclisation was carried out in DCM. However, no appreciable cyclic product was seen on the crude reaction mixture via LC-MS or recovered following work up so further reactions continued using DMF.

Purification was necessary following the cyclisation and also a final purification was undertaken after Boc deprotection to yield the peptoids in > 95 % purity (see **Figure 2.16**). See Experimental chapter for further detail regarding the cyclisation.
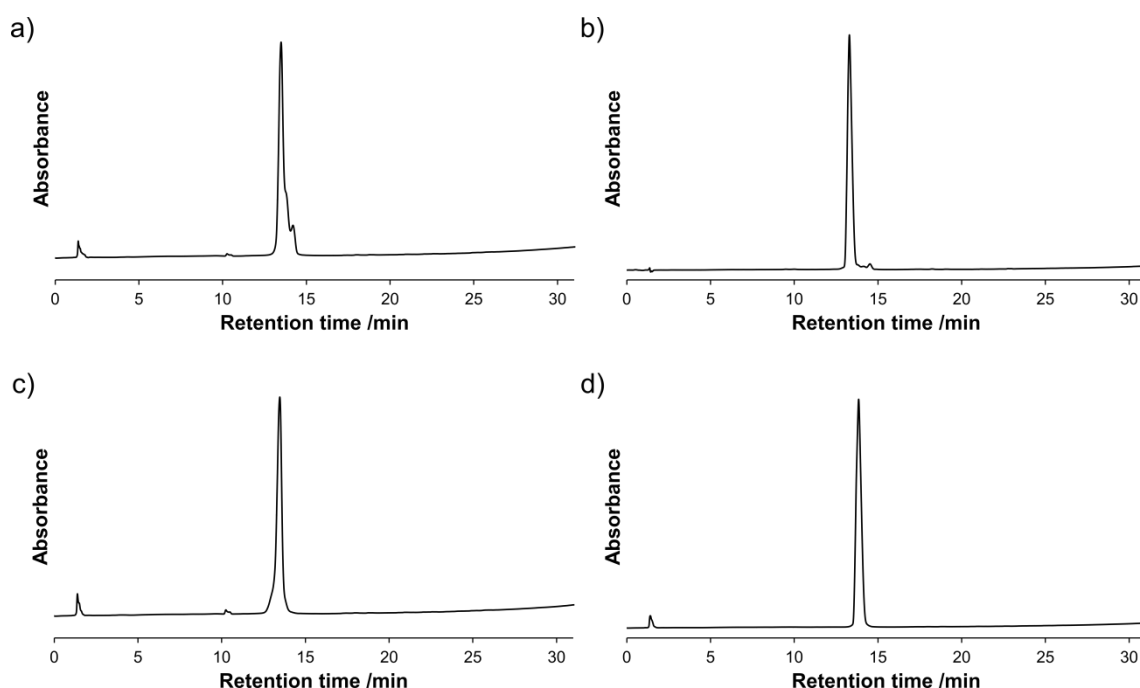
Figure 2.16. Analytical RP-HPLC traces for a) **130** cyclo (*N*Lys*N*phe*N*phe)$_2$; b) **132** cyclo (*N*Lys*N*phe)$_3$; c) **133** cyclo (*N*hArg*N*phe)$_3$; d) **134** cyclo (*N*Lys*N*phe*N*hArg*N*phe *N*Lys*N*phe). See Experimental chapter for gradient and solvent conditions.

Crystallisation of the peptoids **130–134** was attempted to investigate their structural conformation further. This was carried out using a sitting drop method in a sparse matrix crystallisation screen with 24 different buffers, pH conditions and salts or additives conditions[§§§]. The crystallisation was attempted with several peptoid concentrations and with plates stored at room temperature and in various temperature fridges. However, to date, no suitable crystals have been produced.

[§§§] Using a crystallisation screen developed for peptides by Dr Ehmke Pohl, Durham University.

A collaboration with the laboratory of Professor Kent Kirshenbaum (New York State University, USA) provided an additional library of ten cyclic peptoids synthesised by Alan-Yao Liu to compliment those synthesised in Durham. Compounds **135-144** expand the library of cyclic peptoids and include larger ring sizes (6, 8 and 10 residue peptoids) and differently functionalised monomers to form very different scaffolds to those made as part of this project. These cyclic products are shown in **Figure 2.17** and were also synthesised by the head-to-tail cyclisation of linear precursor peptoids.[28]
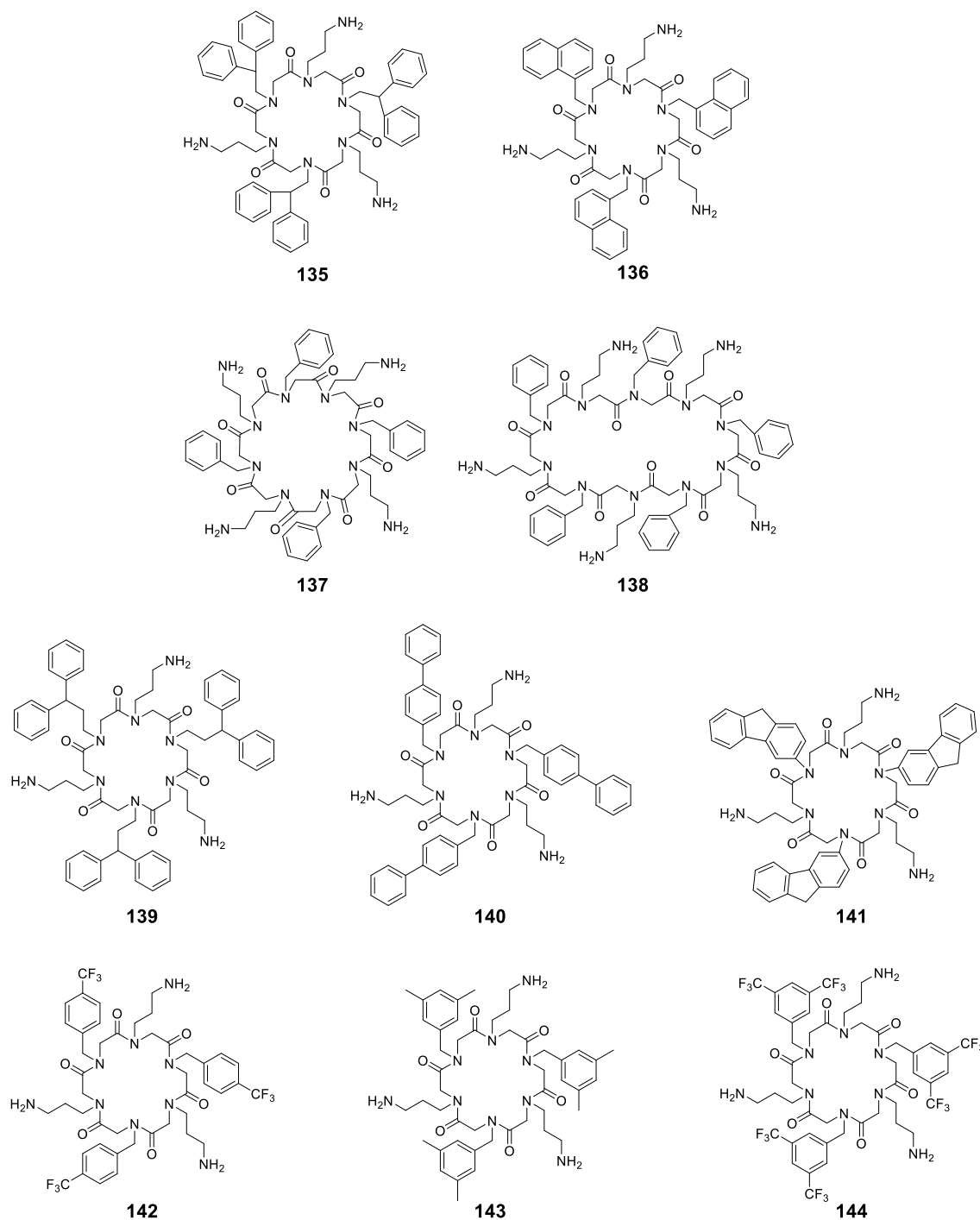
Figure 2.17. The structure of the ten cyclic peptoids provided by the Kirshenbaum Group and synthesised by Alan-Yao Liu.

2.7 Novel chemical methodology for the introduction of arginine-type monomers

As seen in Chapter 1, antimicrobial peptoids are often designed to mimic naturally occurring AMPs and contain a mixture of hydrophobic and cationic monomers to mimic the amphipathic structures of many AMPs. The presence of cationic side chains within the peptoid sequence can provide a degree of selectivity between zwitterionic mammalian cell membranes and the more negatively charged prokaryotic cell membranes. In biologically active peptoids, either lysine- or arginine-type monomers provide this net positive charge and there are many examples within the literature of cationic anti-infective peptoids that contain either lysine-type or arginine-type monomers (see **Figure 2.18**).[28,77,83-86]

Lysine-type monomer   Arginine-type monomer
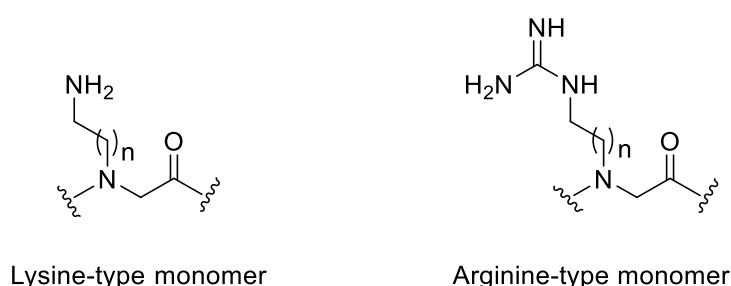
Figure 2.18. A representation of the amino functionalised lysine-type monomers and guanido functionalised arginine-type monomers, where different length side chains are possible and n = 1-6.

Beyond their anti-infective applications, cationic peptoids have been applied in other areas of medicinal chemistry. For example, peptoids rich in guanidine functionalised arginine monomers have been used as molecular transporters,[87-89] cell-penetrating vehicles,[29,89-91] heparin binding agents,[92] and as analogues of Lung Surfactant Protein B.[93] It has been shown that cellular uptake can be affected by the use of either lysine or arginine type monomers; in general guanidine containing peptoids can translocate into the cell more quickly than their amino analogues. Additionally, it has been suggested that sequences including arginine-type monomers may have an increased biological activity, however this is typically accompanied by an increased toxicity towards mammalian cells.[94]

Therefore, it would be advantageous to investigate the biological activities of peptoids that contain mixtures of lysine- or arginine-type monomers in order to fine tune the balance between toxicity and activity. However, with the exception of one example,[95] all of the peptoids investigated to date have sequences consisting exclusively of either the amino functionalised lysine monomer or the guanido functionalised arginine residues exclusively.**** The lack of a suitable synthetic route to prepare such mixed cationic

---

**** Although peptoid-peptide hybrids have been made with mixed cationic functionality introduced using the amino acids lysine and arginine.

peptoids has meant that their biological potential has remained almost largely unexplored.[96,97]

Polyarginine-type peptoids reported in the literature have mostly been synthesised using the method developed by Rothbard and co-workers.[98] This approach uses pyrazole-1-carboxamidine to transform lysine-type monomers into their arginine-type analogues (i.e. an amino to guanido transformation) in a post-synthetic modification of unprotected amino moieties. This reaction can only be carried out after the peptoid has been cleaved from the resin and Boc protecting groups removed. Therefore, it is not possible to use this approach to synthesise sequences containing both amino (i.e. *N*Lys) and guanido (i.e. *N*Arg*)* functionalities as every lysine-type residue with the peptoid chain is transformed into an arginine-type residue.

The Zuckermann group has previously synthesised a PMC (2,2,5,7,8-pentamethylchroman-6-sulphonyl) protected guanidinopropyl amine monomer.[17] Barron *et al.*, attempted to use this PMC protected monomer in the on-resin synthesis of a linear peptoid functionalised with both amino and guanidine cationic groups.[95] However, poor solubility of the PMC protected monomer in solvents commonly used for on-resin reactions led to a low coupling efficiency in the submonomer method. The extended cleavage times necessary for this protecting group also proved problematic, causing acid-induced degradation of the mixed peptoid (in particular, deterioration of the commonly used *N*spe monomer) preventing the full isolation and purification of the target peptoid sequences with both arginine/lysine-type residues.

Therefore to the best of our knowledge an efficient generally applicable method for the synthesis of mixed arginine/lysine-type peptoids was yet to be reported. In this work, an effective synthetic route was developed that allowed novel linear and cyclic cationic peptoids to be synthesised that contained both lysine-type and arginine-type monomers within the same sequence.[99] This has allowed the biological activity of this novel class of peptoids to be investigated; in particular, the relationship between antimicrobial properties and cytotoxicity probed in more detail (discussion in Chapters 3 and 4).

2.7.1 Synthesis of Dde-protected amine submonomers

In order to incorporate both amino and guanido functionalised side chains (lysine-type and arginine-type monomer residues respectively) within the same sequence using solid phase synthesis, it was planned to utilise orthogonal protection of monomers. Commonly, *N*-Boc protected amines are used in peptoid synthesis for the protection of amino groups; for example *N*-Boc-1,4-diaminobutane. For the other protecting group, Dde (*N*-(1-(4,4-dimethyl-2,6-dioxocyclohexylidene)ethyl) was chosen.

Dde is commonly used to protect free primary amines in peptide synthesis and provides orthogonal protection to the acid cleavable Boc group.[100,101] The Dde group is removed using 2 % hydrazine in DMF which allows these residues to be selectively deprotected (leaving the Boc protection on the other lysine-type monomers intact). Following complete synthesis of the peptoid using the submonomer method, selective deprotection of the Dde amine on-resin enables the guanidinylation reaction at specific positions using pyrazole-1-carboxamidine. Finally, cleavage from the resin under acidic conditions simultaneously deprotects the remaining Boc protected amino chains to yield a mixed peptoid, containing both lysine-type and arginine-type peptoid residues (See **Scheme 2.12**, steps iv. to vi.).

A variety of mono-*N*-Boc protected amines are available to purchase from commercial sources, or can be made in high dilution syntheses using Boc anhydride and the required diamine, as for **129**.[23] Initially, it was planned to synthesise a mono Dde-protected amine in a similar manner so it could be synthesised in bulk and used directly in the submonomer procedure.

In the first attempt to synthesise *N*-Dde-1,4-diaminobutane, the literature procedure[81] previously used to synthesise mono-Boc protected diamines in this project (section 2.6.4) was followed under similar high-dilution conditions with 1,4 diaminobutane and 2-acetyldimedone (Dde-OH). Several conditions, as summarised by **Table 2.3**, were used to attempt the synthesis of mono *N*-Dde-1,4-diaminobutane (**145**). However, in all cases the major product of the reaction and the only compound isolated was the doubly protected amine (**146**), shown in **Scheme 2.11**. Therefore, this procedure was deemed to be ineffective as the protection of the amines with Dde-OH was so efficient and an alternative route to mixed arginine/lysine peptoids using on-resin protection of the amine was developed.
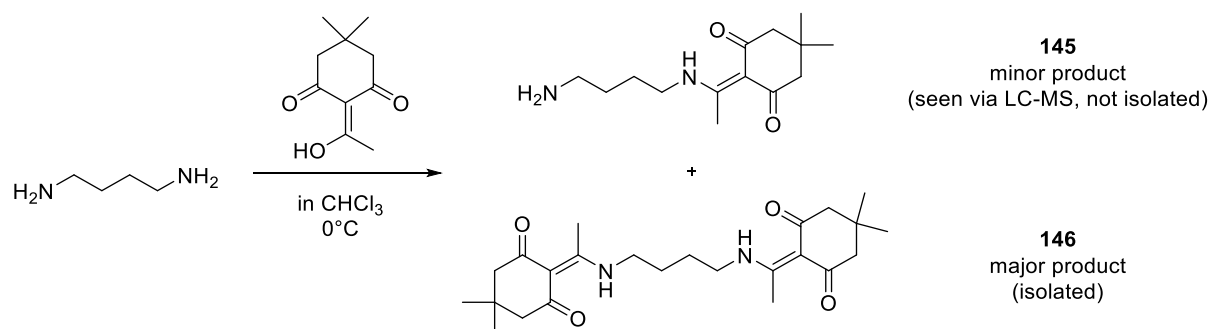
Scheme 2.11. The attempted synthesis of *N*-Dde-1,4-diaminobutane using high dilution synthesis.

Reaction	Equivalents diaminobutane	Equivalents Dde-OH	Solvent	Addition Time (hours)	Reaction Time (hours)
1				1	18
2			CHCl₃	6	18
3	10	1		10	18
4			CH₂Cl₂	6	18
5				10	18

Table 2.3. Conditions used in the attempted solution synthesis of *N*-Dde-1,4-butanediamine.

Coupling conditions were developed that permitted an unprotected diamine to be added to the peptoid sequence during the displacement stage of the sub-monomer method. One extra step was then introduced to protect this free amine on resin using Dde-OH (2-acetyldimedone). This is shown in **Scheme 2.12**, steps i. to iii.

Adding the Dde group on resin has been used in peptide synthesis, but has never been used to make mixed arginine- and lysine-type peptoid residues as far as we are aware.[100,101] Addition of Dde-OH to the free amine on resin was complete by LC-MS after 60 minutes at room temperature (10 eq. Dde-OH with respect to the resin, in the minimum volume of DMF necessary to dissolve the reagent fully). The submonomer procedure could then be resumed to lengthen the peptoid chain successfully as the Dde-protected sidechains are stable to the conditions used in the submonomer method. Following completion of the sequence, selective deprotection of the Dde enables the on-resin guanidinylation reaction to take place at specific positions in the sequence.
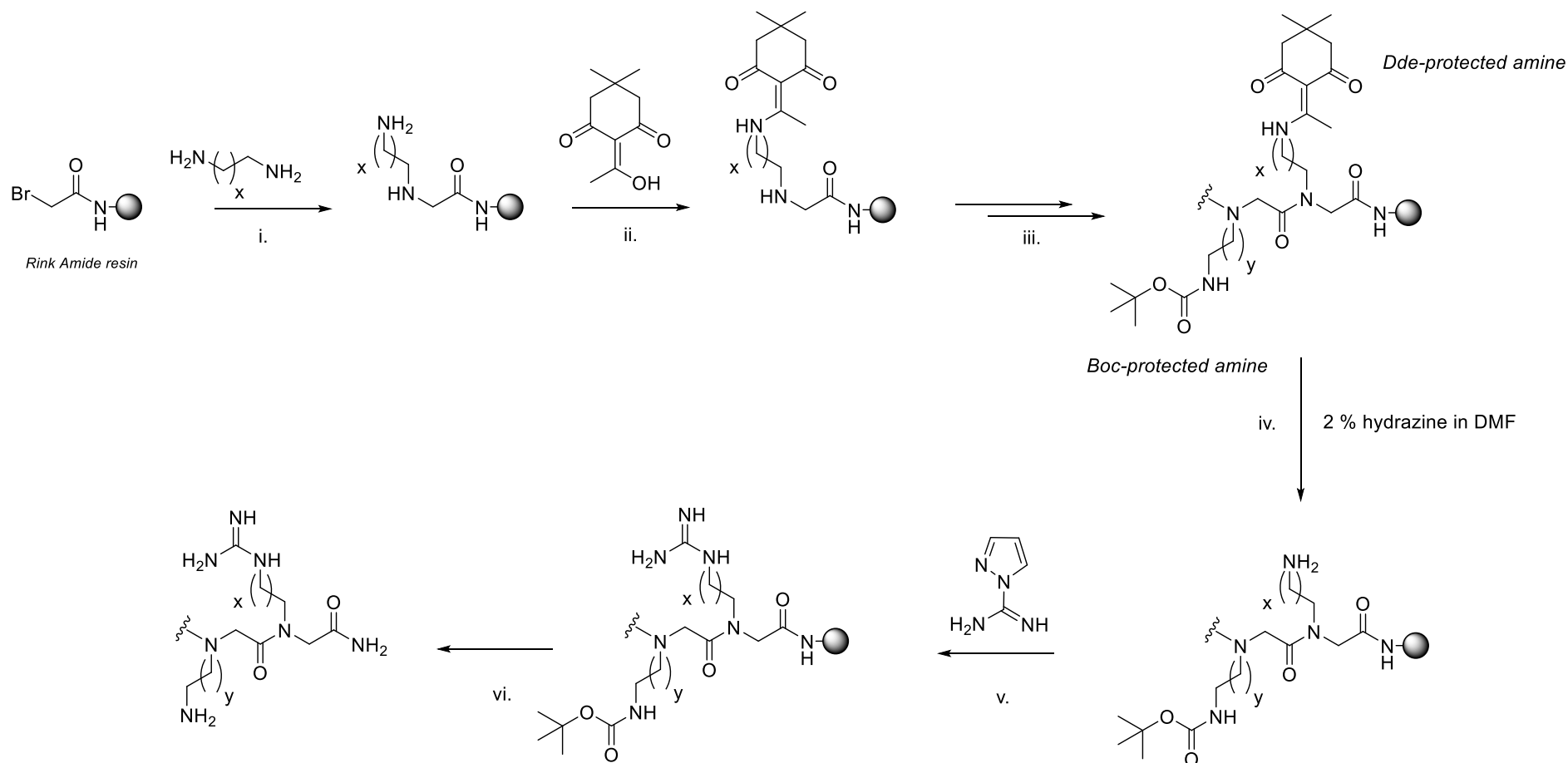
Scheme 2.12. The method used to synthesise mixed arginine/lysine peptoids, where x and y = 1-5; i. standard displacement step in the submonomer method with diamine, 1.5 M in DMF, 60 min, RT; ii. addition of Dde-OH, 10 eq. wrt resin in minimum volume DMF, 60 min at RT to protect free amine; iii. further additions to extend the peptoid chain, using the normal sub-monomer procedure; iv. deprotection of Dde using 2 % hydrazine in DMF 4 x 3 min; v. guanidinylation of free amine, on resin, using 6 eq. pyrazole-1-carboxamidine per free amine and 6 eq. DIPEA per free amine in the minimum volume DMF, 60 min, RT; vi. acidic cleavage from the resin and deprotection of Boc groups.

2.7.2 On resin guanidinylation

Following the on-resin protection of specific amine submonomers with Dde and completion of the peptoid sequence on resin, the Dde group was deprotected using a 2 % hydrazine solution in DMF. This yields free amino groups that can be selectively transformed into guanido groups, or arginine-type monomers.

Pyrazole-1-carboxamidine is a convenient reagent for the guanidinylation of simple primary amines that leaves secondary amines unaffected, even when used in large excess and is therefore suitable for use with peptoid side chains.[102] The guanidinylation reaction with pyrazole-1-carboxamidine previously reported by Rothbard *et al.* must be carried out on fully deprotected peptoids in solution and additionally, water was used as a solvent with sodium bicarbonate as a base. The procedure developed as part of this project uses reaction conditions which are more compatible with solid-phase synthesis (e.g. DMF with DIPEA). Carrying out the guanidinylation reaction on resin is preferable as the excess reagents used can be washed away at the end of the synthesis making the final purification easier. Finally, cleavage from the resin simultaneously deprotects lysine chains and yields the mixed peptoid, containing both lysine and arginine peptoid residues.

Additionally, this approach benefits from being compatible with the submonomer solid-phase synthesis of peptoids, which is utilised by the majority of the scientific community. Although not reported here, the methodology developed should be well-suited for use with automated peptoid synthesisers as it adds only one step to the commonly used sub monomer method and the Dde group is easily introduced under room temperature conditions.

To demonstrate the versatility and synthetic utility of the methodology, a library of linear peptoids containing both amino and guanido moieties within the same sequence were synthesised (see **Table 2.4** and **Figure 2.19** for monomer abbreviations). To illustrate Dde addition, deprotection and guanidinylation steps this process, mass spectra taken from each stage of the synthesis of two peptoids can be found in the Appendix.

	Peptoid	Sequence
Mixed Lysine/Arginine	**147**	(*N*Lys*N*spe*N*spe)₂(*N*hArg*N*spe*N*spe)₂
	148	(*N*hArg*N*spe*N*spe)₂(*N*Lys*N*spe*N*spe)₂
	149	(*N*Lys*N*spe*N*spe)(*N*hArg*N*spe*N*spe)(*N*Lys*N*spe*N*spe)₂
	150	[(*N*hArg*N*spe*N*spe)(*N*Lys*N*spe*N*spe)]₂
	151	[(*N*nArg*N*spe*N*spe)(*N*Lys*N*spe*N*spe)]₂
	134	cyclo (*N*Lys*N*phe*N*hArg*N*phe*N*Lys*N*phe)
All Arginine	**152**	(*N*hArg*N*spe*N*spe)₄
	153	(*N*hArg*N*mfb*N*mfb)₄
	154	[(*N*amy*N*spe*N*spe)(*N*hArg*N*spe*N*spe)]₂
	155	(*N*nArg*N*spe*N*spe)₄

Table 2.4. Sequences of the all arginine-type and the mixed lysine- /arginine-type peptoids prepared in this study.
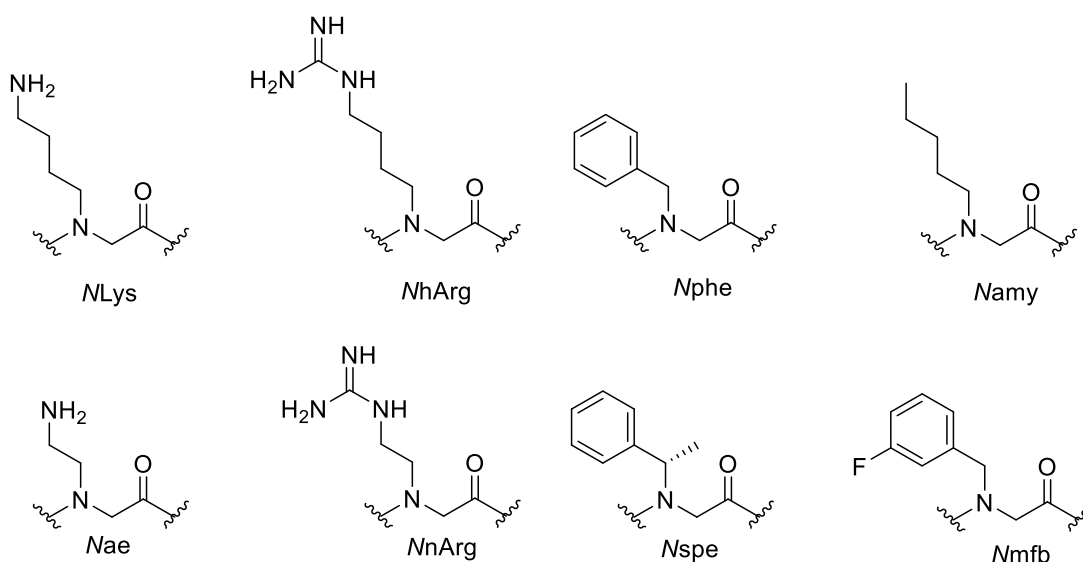
Figure 2.19. Monomers used in the synthesis of the arginine-containing peptoids **147–155**. The *N*hArg and *N*nArg monomers were formed from a post-synthetic transformation, all other monomers were introduced from standard displacement step in the submonomer method of peptoid synthesis.

Initially, 'mixed' lysine/arginine-type peptoids (Table 2.4, **147–150**) were prepared with monomers containing 4 carbons in the side chain (i.e. *N*Lys and *N*hArg monomers derived from 1,4-diaminobutane). The Dde group was introduced at a variety of positions within the sequence. It was found that the Dde protection reaction on resin was efficient, it could be carried out near the resin linker at the C terminus and other Dde-protected residues in the same sequence were tolerated. The synthesis was also carried out using the shorter, 2 carbon amine monomer (*N*ae, **Table 2.4, 151**) to highlight that the methodology works with side chains of varying lengths (i.e. *N*ae and *N*nArg, derived from 1,2-diaminoethane).

Four all arginine-type peptoids were also synthesised on resin using the Dde protection strategy developed (**Table 2.4, 152–155**). Carrying out the guanidinylation reaction on resin significantly simplified the final purification of these peptoids compared to those made using the Rothbard method. The preparation of these mixed peptoids illustrates that the Dde methodology is compatible not just with *N*phe and *N*spe but also with other commonly used amine monomers (i.e. *N*mfb and *N*amy).

A cyclic peptoid (**134**) with both lysine- and arginine-type residues was also synthesised via a Dde-protected linear precursor (**Scheme 2.13**). The linear peptoid protected by the Dde-group was successfully cleaved from 2-chlorotrityl chloride resin and cyclised in a solution phase head-to-tail cyclisation, as in section 2.6.5. Subsequent Dde-deprotection of the cyclic peptoid allowed guanidinylation in solution, prior to a final acidic TFA deprotection of remaining Boc-protected amines. Despite the bulky nature of the Dde group, the cyclisation still occurred efficiently at room temperature.

134 cyclo (*N*Lys*N*phe*N*Lys*N*phe*N*hArg*N*phe)
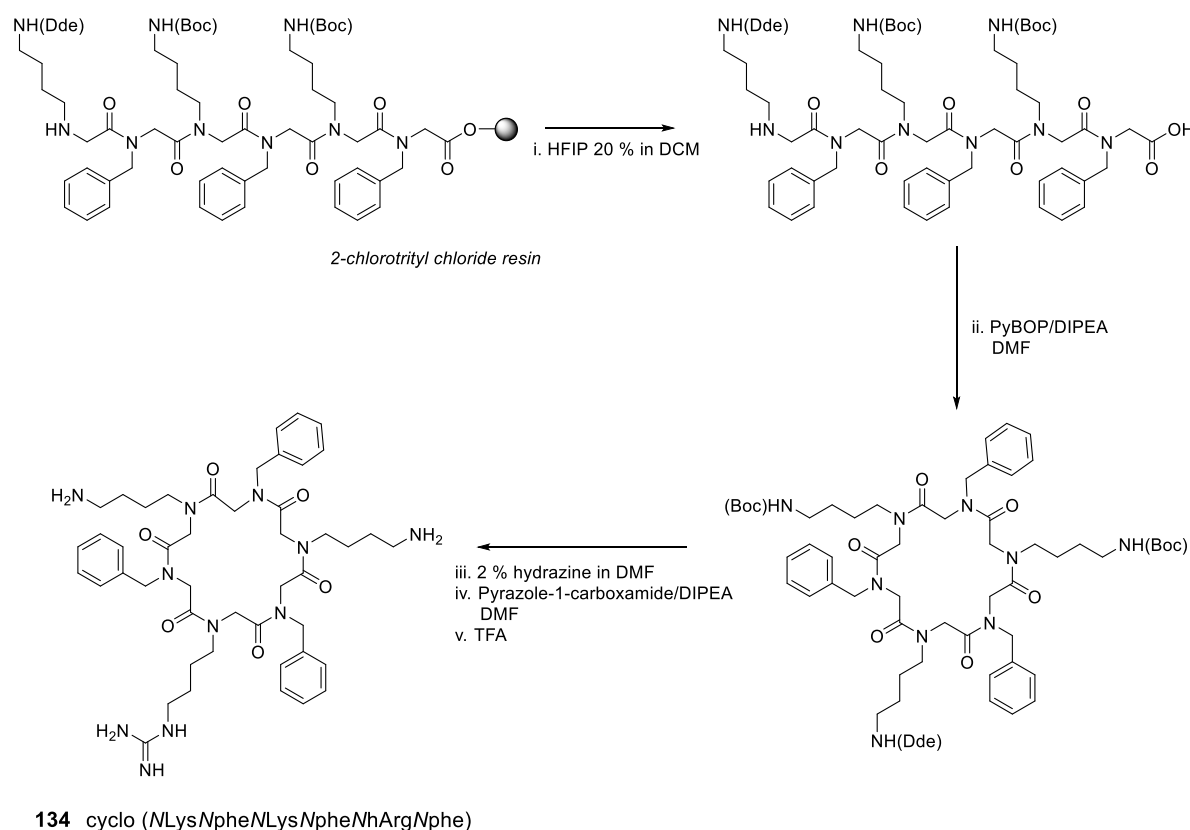
Scheme 2.13. The synthesis of a cyclic peptoid **134**, containing both arginine/lysine-type residues; i. linear precursor made on 2-chlorotrityl chloride resin using sub-monomer method and cleaved under mildly acidic conditions (20 % HFIP in DCM, 20 min); ii. head-to-tail cyclisation of peptoid in solution (6 eq. PyBOP, 6 eq. DIPEA in DMF), 6 hours; iii. deprotection of Dde (2 % hydrazine in DMF, 4 x 3 mins); iv. guanidinylation in solution (6 eq. pyrazole carboxamidine per free amine in the minimum volume of DMF, 6 eq. DIPEA, RT, 60 min); v. deprotection of N-Boc groups (TFA, 60 min).

Analytical RP-HPLC purification of all final compounds was undertaken, to yield the peptoids in > 95 % purity, as shown by **Figure 2.20** where chromatograms for representative compounds from the library are shown (the chromatogram for the mixed cyclic compound **134** is shown in **Figure 2.16d**).
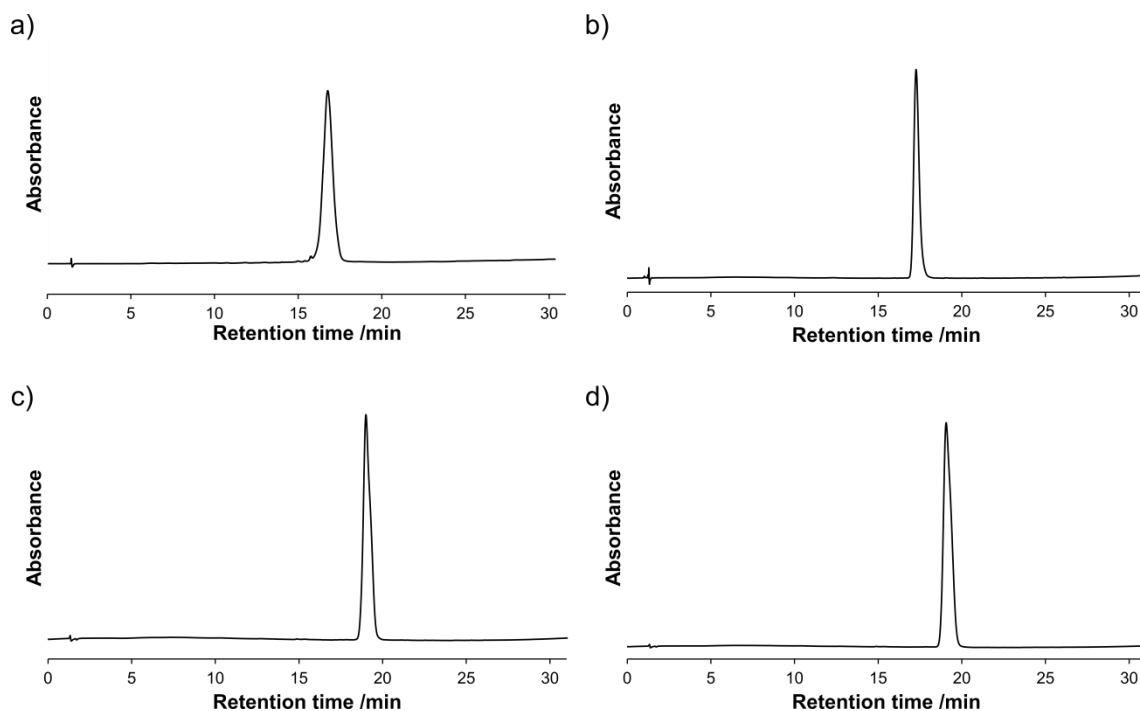
Figure 2.20. Analytical RP-HPLC chromatograms for selected peptoids; a) **148** (*N*hArg*N*spe*N*spe)$_2$(*N*Lys*N*spe*N*spe)$_2$; b) **153** (*N*hArg*N*mfb*N*mfb)$_4$; c) **151** [(*N*nArg*N*spe*N*spe)(*N*Lys*N*spe*N*spe)]$_2$; d) **155** (*N*nArg*N*spe*N*spe)$_4$. Gradient 0–100 % solvent B (solvent A = 95 % H$_2$O, 5 % MeCN, 0.1 % TFA; solvent B = 95 % MeCN, 5 % H$_2$O, 0.1 % TFA); column oven at 40 °C; λ = 220 nm.

In conclusion, a practical synthetic procedure has been developed that can synthesise linear and cyclic peptoids that contain both arginine- and lysine-type residues within the same sequence. This has enabled the preparation of a small library of peptoids that contain combinations of peptoid monomers not previously reported in the literature. The methodology developed uses orthogonal *N*-Boc and *N*-Dde protection and pyrazole-1-carboxamidine as a guanidinylation reagent. The final identities of all peptoids was confirmed using accurate QToF mass spectrometry and the peptoids were all estimated to be > 95 % pure by RP-analytical HPLC. Significantly, this process is amenable for use with acid sensitive monomers (i.e. *N*spe) and it is compatible with the commonly used submonomer method of peptoid synthesis.

2.8 Expanding peptoid chemical space: end group modification

In an attempt to enhance the efficacy of the peptoid sequences synthesised, modifications were made to the termini. In particular, moieties similar to simple lipid chains were added to either the C or N terminus of a peptoid to mimic lipopeptides, biologically active peptide derivatives often found in nature.

Lipopeptides are typically comprised of an aliphatic, fatty acid-derived chain, covalently linked to a the N terminus of a short linear or cyclic oligopeptide. A large structural diversity of lipid chains can be found in nature, with chains between 6 and 18 carbon units in length, including branched and non-branched, saturated and unsaturated chains. In nature, these lipopeptides are synthesised nonribosomally in bacteria and fungi and can be highly active against multidrug resistant species of bacteria and fungi.[103]

Compounds like daptomycin, micafungin or colistin are all approved lipopeptide antibiotics. A range of isolated lipopeptides are now being used in research into novel antimicrobials; particularly relevant to this project are several families of lipopeptides, such as the ciliatamides or dragonamides, that have been shown to display potent anti-leishmanial activities less than 10 μM.[104,105]

In addition to use as commercial antibiotics, certain lipopeptides are now being increasingly used in areas such as the cosmetics industry for their surfactant properties or as emulsifiers in certain food technology applications. The mode of action of lipopeptides on microorganisms has been suggested to include disruption of the plasma cell membrane as well as targeting specific processes, like inhibition of ATPases or D-glucan synthase used in fungal cell wall synthesis. This dual mode of action may help to explain the low number of reported cases of bacterial resistance in lipopeptide antibiotics compared to traditional small molecule drugs.[103,106,107]

Despite the attractive characteristics of the lipopeptides, they are still limited by the *in vivo* stability of their peptide components. Although certain cyclic lipopeptides are proteolytically stable, the majority of linear sequences are not, therefore the development of novel, lipopeptide analogues that are resistant to proteolysis is a rapidly increasing area of research. As with peptides, one potential strategy for stabilisation is the introduction of *N*-substituted glycine monomers. Indeed, to date a few peptoids with lipid tails have also been made to mimic these successful antimicrobial lipopeptides.

As described in Chapter 1 (Lipopeptoids), the Barron group has added lipid-type chains of either 5, 10 or 13 carbons in length to the N-terminus of linear peptoid sequences and found sequences with potent antimicrobial activities.[108] A separate study looked into the effect of lipidation on a library of 19 very short antimicrobial peptoids based upon KKK, RRR, KGK or RGR tripeptides and therefore were cationic with *N*Lys or *N*hArg (homoarginine) residues. The compounds were tested against a variety of reference and clinical bacterial strains and were found to be moderately active against both Gram positive bacteria and Gram negative species.[94]

Another common strategy used to enhance the antimicrobial action of therapeutics is the addition of polyethylene glycol (PEG) polymer chains, known as PEGylation. Many PEGylated pharmaceuticals now exist on the market since the covalent addition of PEG to a compound, has multiple advantageous effects and typically improves the pharmacokinetic profile of a drug. PEG is FDA approved, non-toxic and non-immunogenic, PEGylation can mask a pharmaceutical from the host immune system, can increase the circulatory time of a drug by increasing retention time in the blood and minimising renal excretion and the addition of the PEG chains imparts water solubility to hydrophobic sequences.[109-111]

Although peptoids are not susceptible to proteolysis like peptides, reduction of immunogenicity, reduced renal excretion or increased solubility may be advantageous for any future medicinal applications. A handful of PEGylated peptoids have been previously reported in materials applications.[112,113] Additionally, it has been reported that the addition of a short PEG chain to a peptide-peptoid hybrid had no detrimental effect on the antibacterial profile of a peptoid.[114]

2.8.1 Synthesis of lipopeptoids and PEG-ylation of sequences

To enhance the chemical space of our peptoids and in an attempt to modulate their biological activity and toxicity, a suite of lipopeptoids were synthesised. The two peptoid sequences chosen were identified as having good antibacterial and antiparasitic activity, which is discussed in more detail in Chapters 3 and 4. Peptoid **156** (*N*ae*N*spe*N*spe)$_4$ and peptoid **157** [(*N*Lys*N*pfb*N*pfb)(*N*Lys*N*spe*N*spe)]$_2$ were both lipidated and PEGylated to give the compounds listed in **Table 2.5.** Example structures are provided in **Figure 2.21**.

The lipid-like amines added to the peptoid sequences were heptylamine (**158**, **163**, **168**, **173**), dodecylamine (**160**, **165**, **170**, **175**), hexadecylamine (**161**, **166**, **171**, **176**) and cycloheptylamine (**159**, **164**, **169**, **174**). As no specific target was specified, this variety of amines introduced a range of saturated, unbranched lipid chain lengths (C$_7$ to C$_{16}$), as well as a cyclic moiety to examine the SAR. The C$_{16}$ chains were chosen because of their previously proven activity[94] against *E. coli* and the shorter chains for their potential to give good selectivity ratios.[108] 2-2(2-methoxyethoxy)ethoxy ethylamine was also chosen to represent a short chain PEG-mimic to determine the effect of PEGylation on peptoid antimicrobials (peptoids **162**, **167**, **172**, **177**).

Adding these five amines to both the C and N terminus of the two peptoid sequences afforded 20 novel lipopeptoids. The synthesis of sequences with a lipid head or tail group is shown by **Scheme 2.14**. Whilst the addition of lipid tail groups is standard practice, as far as we are aware, this is the first time that lipid groups have been added to the C terminus of a peptoid sequence.

Compound number	Sequence
158	$NC_7(NaeNspeNspe)_4$
159	$NcycloC_7(NaeNspeNspe)_4$
160	$NC_{12}(NaeNspeNspe)_4$
161	$NC_{16}(NaeNspeNspe)_4$
162	$Nte(NaeNspeNspe)_4$
163	$NC_7[(NLysNpfbNpfb)(NLysNspeNspe)]_2$
164	$NcycloC_7[(NLysNpfbNpfb)(NLysNspeNspe)]_2$
165	$NC_{12}[(NLysNpfbNpfb)(NLysNspeNspe)]_2$
166	$NC_{16}[(NLysNpfbNpfb)(NLysNspeNspe)]_2$
167	$Nte[(NLysNpfbNpfb)(NLysNspeNspe)]_2$
168	$(NaeNspeNspe)_4\text{-}C_7H_{15}$
169	$(NaeNspeNspe)_4\text{-}C_7H_{13}$
170	$(NaeNspeNspe)_4\text{-}C_{12}H_{25}$
171	$(NaeNspeNspe)_4\text{-}C_{16}H_{33}$
172	$(NaeNspeNspe)_4\text{-}C_9H_{21}O_3$
173	$[(NLysNpfbNpfb)(NLysNspeNspe)]_2\text{-}C_7H_{15}$
174	$[(NLysNpfbNpfb)(NLysNspeNspe)]_2\text{-}C_7H_{13}$
175	$[(NLysNpfbNpfb)(NLysNspeNspe)]_2\text{-}C_{12}H_{25}$
176	$[(NLysNpfbNpfb)(NLysNspeNspe)]_2\text{-}C_{16}H_{33}$
177	$[(NLysNpfbNpfb)(NLysNspeNspe)]_2\text{-}C_9H_{21}O_3$

On the left side the rows are grouped: rows 158–167 are labelled **Tail group — Modification at N terminus**, and rows 168–177 are labelled **Head group — Modification at C terminus**.

Table 2.5. Peptoid sequences modified with C and N terminal lipid or PEG chains.

163 $NC_7[(NLysNpfbNpfb)(NLysNspeNspe)]_2$
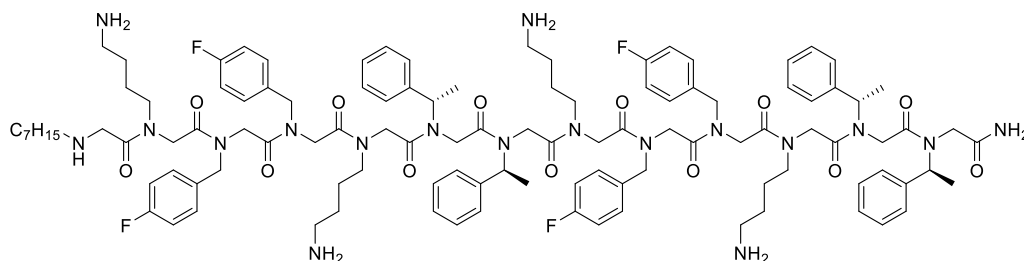
169 $(NaeNspeNspe)_4\text{-}C_7H_{13}$
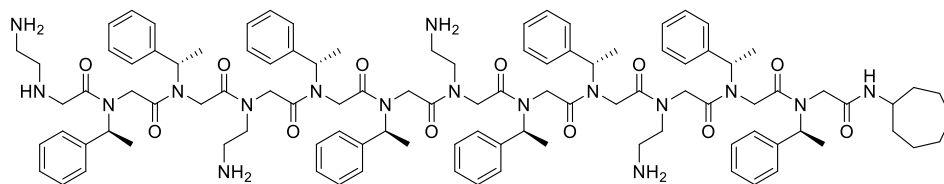
Figure 2.21. Example structures of the lipopeptoids synthesised. **163** shows the heptyl amine tagged to the N terminus and **169** is an example of peptoid with cycloheptane lipid head group.
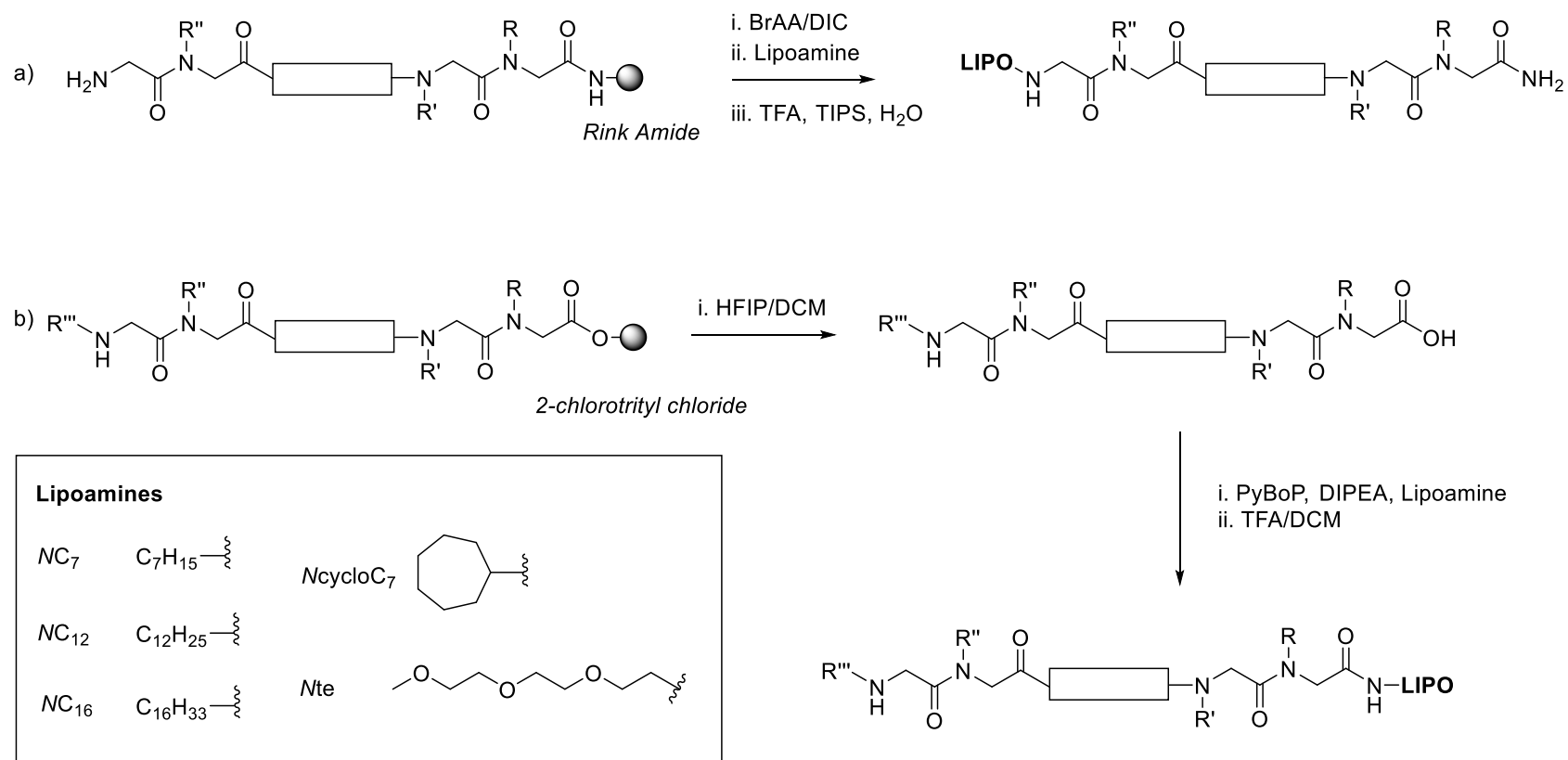
Scheme 2.14. The synthesis of lipidated peptoids **158–177** with a) peptoid tail groups; b) lipid head groups. The four lipoamines and the short PEG-type amine introduced are shown in the box.

For the N terminal tagged sequences **158–167**, the lipoamines were added to the sequence using an on resin coupling using Rink Amide resin. Following acylation with bromoacetic acid, the lipoamine was introduced in the displacement step of the submonomer method. All couplings were undertaken under standard conditions; 60 minute displacement, 1–2 M amine concentration at RT. However, the hexadecylamine was added at 0.5 M in 50 % DCM in DMF *v/v* due to a decreased solubility compared to the other amines. Following acidic resin cleavage, the lipopeptoids were obtained as a crude powder.

To add a lipid head group to a peptoid C terminus (peptoids **168-177**) the sequence was synthesised on 2-chlorotrityl chloride resin and cleaved from the support using 50 % HFIP in DCM, to afford a C-terminal carboxy-functionalised peptoid sequence. Using these cleavage conditions, the Boc protection of lysine monomers remains intact. Subsequently, the crude material was used in a solution phase coupling between the peptoid and the lipoamine in DMF, with PyBOP as an activator. 4 equivalents of PyBOP with respect to the crude peptoid were used with DIPEA (4 equivalents) and the amine (4 equivalents), as in **Scheme 2.14b**.

Using these conditions, all coupling reactions had reached completion after 90 minutes by LC-MS, without further optimisation. A subsequent organic/aqueous extraction removed excess primary amine from the mixture and the Boc protection of the peptoid side chains was removed using TFA.

The compounds shown in **Table 2.5** were purified by RP-HPLC to afford the material in > 95 % purity for biological evaluation. **Figure 2.22** shows a representative selection of analytical HPLC traces for the lipopeptoids.

As explained in more detail in Chapter 7, the purification used a linear gradient from 0–100 % solvent B (where solvent A = 95 % water, 5 % acetonitrile, 0.1 % TFA; solvent B = 95 % acetonitrile, 5 % water, 0.1 % TFA). Typically, in the purification of linear peptides a gradient is set up from 0–100 % solvent B over 60 minutes, dependent on the exact sequence and purity of the crude sequence. However, due to the hydrophobic nature and reduced solubility of peptoids with lipid chains of 12 or 16 carbons in length (peptoids **160/161**, **165/166**, **170/171**, **175/176**), injections were made to the column during an isocratic step at 40 % solvent B and the following gradient to 100 % B was undertaken over 60 minutes.

a)

b)

c)

d)

e)

f)
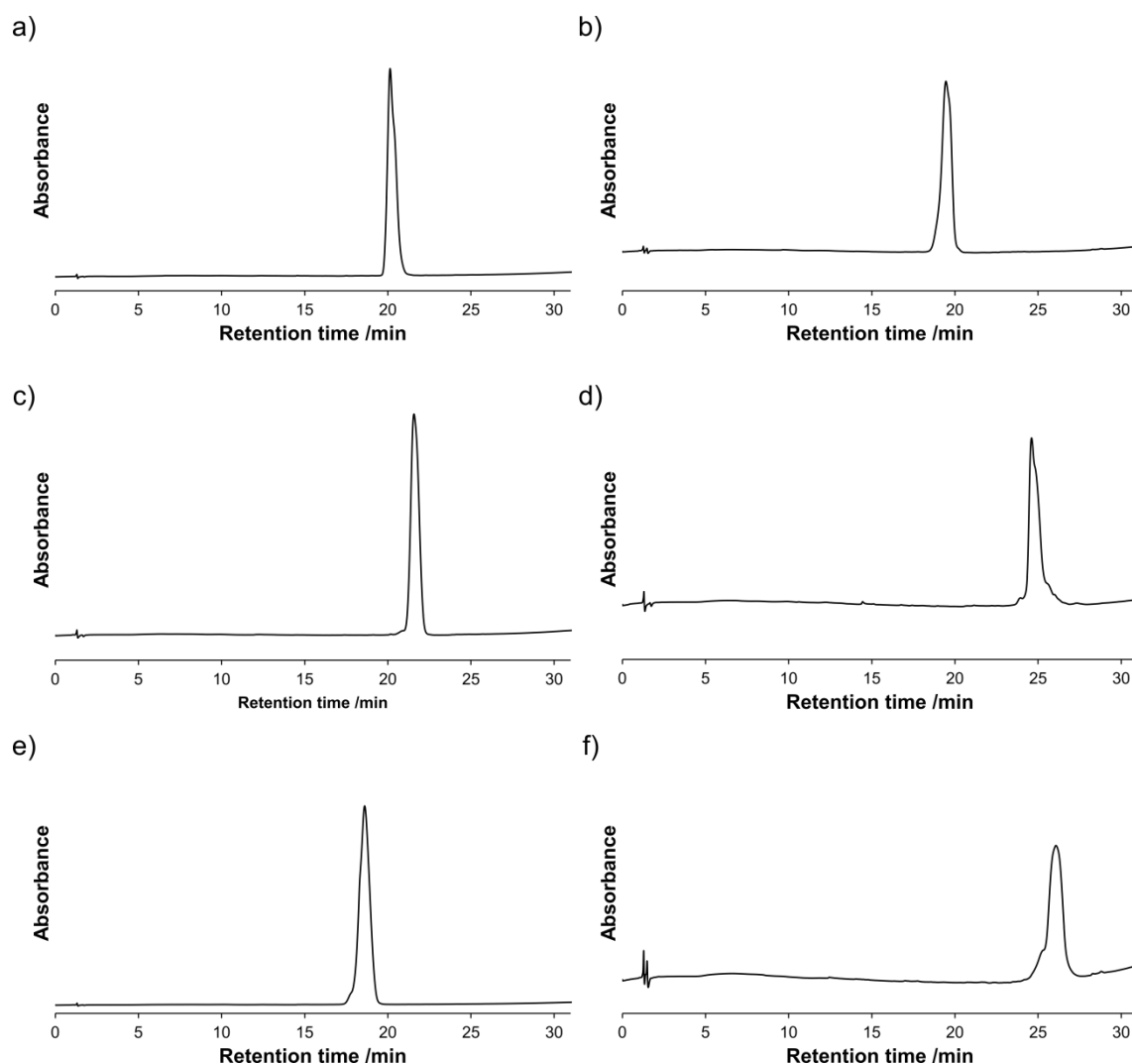
Figure 2.22. Analytical RP-HPLC chromatograms for selected compounds from the lipopeptoid library so show peptoids with lipid head and tail groups. One of example of a peptoid with each lipid chain is shown; a) **158** $NC_7(NaeNspeNspe)_4$; b) **169** $(NaeNspeNspe)_4$-C_7H_{13}; c) **165** $NC_{12}[(NLysNpfbNpfb)(NLysNspeNspe)]_2$; d) **170** $(NaeNspeNspe)_4$-$C_{12}H_{25}$; e) **162** $Nte(NaeNspeNspe)_4$; f) **176** $[(NLysNpfbNpfb)(NLysNspeNspe)]_2$-$C_{16}H_{33}$. Gradient 0–100 % solvent B (solvent A = 95 % H_2O, 5 % MeCN, 0.1 % TFA; solvent B = 95 % MeCN, 5 % H_2O, 0.1 % TFA); column oven at 40 °C; λ = 220 nm.

2.9 Peptoid proteolytic stability

Stability testing using MALDI described in this section was undertaken by Dr Yu Luo and Dr Fionnuala Lundy (Queen's University, Belfast). The stability investigation using HPLC was assisted by Emily Corlett (undergraduate project student at Durham University).

Many groups are investigating peptoids for biomedical or materials applications due to their reported stability against proteolysis. This gives peptoids longer half-lives *in vivo* when compared to a given peptide sequence. However, very few studies within the literature have data to support the increased enzymatic stability and pharmacokinetic properties of peptoids.[43,115]

In pharmacokinetic studies of labelled peptoids, it was shown that peptoids are largely absorbed in the liver, similar to other high molecular weight drugs. If the peptoids were made less hydrophobic, increased kidney uptake could be achieved. Although peptoids show similarly poor bioavailability to peptides when administered orally, their passage through the gastrointestinal tract is slower and peptoids are generally excreted whole in urine rather than being broken down by proteases.[116,117]

The main paper published to date investigating the superior stability of peptoids tested L-peptides, D-peptides and peptoids against a range of enzymes from the four major classes of proteases; metallo, cysteine, aspartyl and serine proteases. Hexa- or tetrapeptide and peptoid sequences were prepared for each enzyme, including retro sequences to cover both possible reading frames, and were incubated with the enzymes under approximate physiological conditions. All L-peptides designed were indeed substrates for their respective enzymes, whereas the D-peptides displayed only minimal degradation to 3 of the 6 enzymes tested. The peptoids were unaffected by all enzymes tested and this data has formed the evidence for increased peptoid stability to proteolysis.[43]

Due to the lack of data available in the literature, as a proof of concept stability assays were undertaken to check that the specific sequences synthesised in this peptoid library were also stable to degradation. A small selection of representative peptoids were tested in a quantitative enzymatic HPLC assay and the digestion profile of a peptoid was examined via mass spectrometry.

The stability of peptoids and peptides were first compared by a chymotrypsin digestion assay using RP-HPLC. Chymotrypsin, a digestive enzyme which is found in the pancreatic juice to perform proteolysis, is known to preferentially cleave peptide amide bonds at aromatic residues like tyrosine, tryptophan or phenylalanine which fit into a hydrophobic pocket in the enzyme. All peptoid sequences tested contained peptoid monomers equivalent to phenylalanine *N*-(*S*-phenylethyl)glycine residue or *N*-benzyl glycine (*N*spe or *N*phe) and a variety of sequences and building blocks were analysed in this study. In this assay, a solution of chymotrypsin was added to the peptoid samples and time-points taken approximately every 2 hours over a 24 hour period. Experiments

were performed in triplicate to ensure that a robust data set was taken. The absorbance of the peptoid or peptide was quantitatively monitored by RP-HPLC at 215 nm (corresponding to absorbance of the amide backbone).

As seen in **Figure 2.23**, within the bounds of error (not shown), the peptoids are stable to chymotrypsin as the overall amount of peptoid does not change over time. Half-lives could not be calculated as no decay, exponential or otherwise, was seen during the experiment. In comparison, a native p53 peptide[††††] (**178**) was degraded rapidly, so time points could only be collected for approximately 4 hours. The resultant half-life of the native p53 peptide was calculated to be 58 minutes ± 6 minutes.

Additionally, collaborators at Queens University Belfast have compared the digestion profile of peptoid **180** (*Nae*N*phe*N*phe*)$_4$ by trypsin against a naturally occurring α-helical antimicrobial peptide, LL-37 compound (**179**), derived from human cathelicidin.[‡‡‡‡] Trypsin is another enzyme typically found in the mammalian digestive system and belongs to the family of serine proteases. In contrast to chymotrypsin, trypsin cleaves peptides primarily at the C terminal side of lysine or arginine residues – peptoid **180** tested has four *N*ae lysine-mimetic residues within the sequence.

The samples were treated with trypsin for 24 hours and their MALDI spectra compared to the untreated sample. As seen in **Figure 2.24** peptoid **180** at *m/z* = 1596 showed no appreciable degradation, whereas the peptide **179** showed complete loss of the parent ion at *m/z* = 4492 and was degraded into many smaller molecular weight peptide fragments.
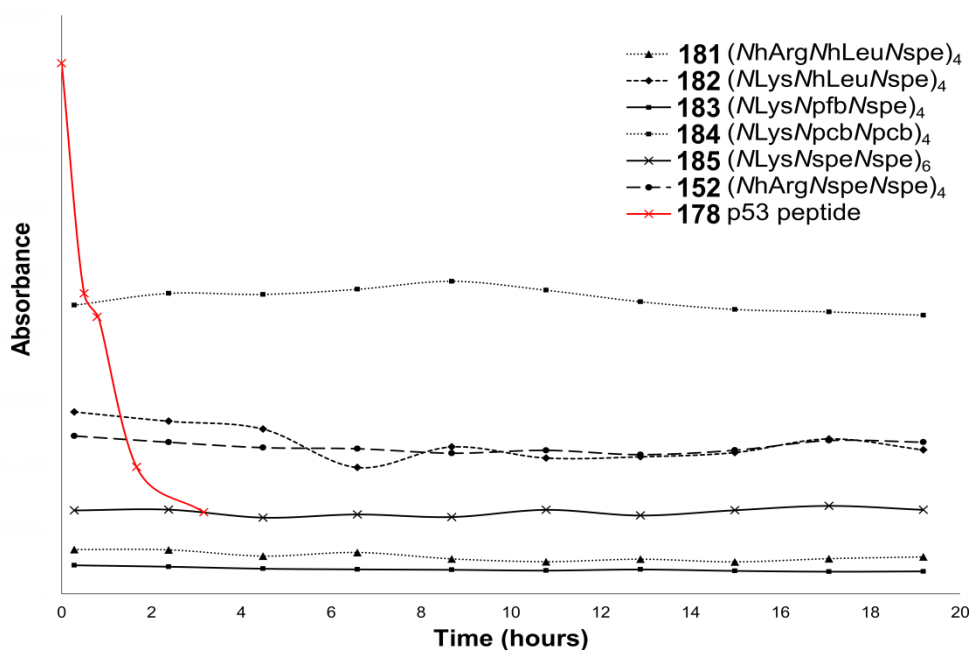
Figure 2.23. The results of the stability assay (absorbance monitored via RP-HPLC at 215 nm) show that all six peptoids tested are stable to chymotrypsin as no degradation is seen over time. In comparison, p53 peptide **178** has a half-life of approximately 1 hour.

[††††] **178** native p53 peptide sequence: LTFCHYWCQLTS-NH$_2$
[‡‡‡‡] **179** LL-37 peptide sequence: LLGDFFRKSKEKIGKEFKRIVQRIKDFLRNLVPRTES-NH$_2$

a) Peptoid (*NaeNpheNphe*)4 (180)
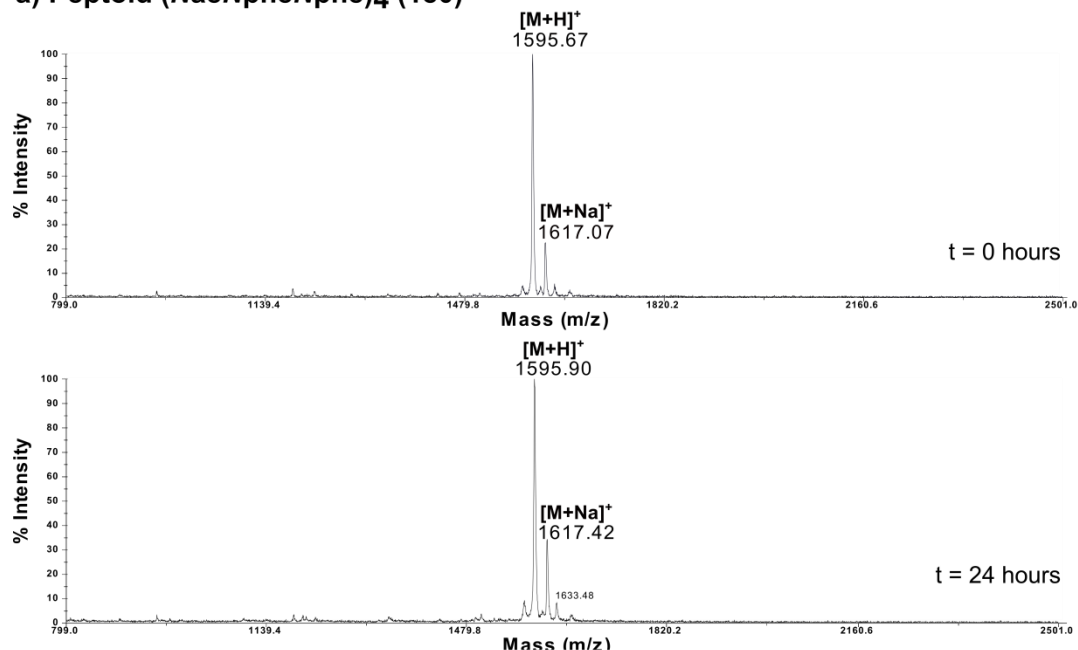
b) Peptide LL-37 (179)
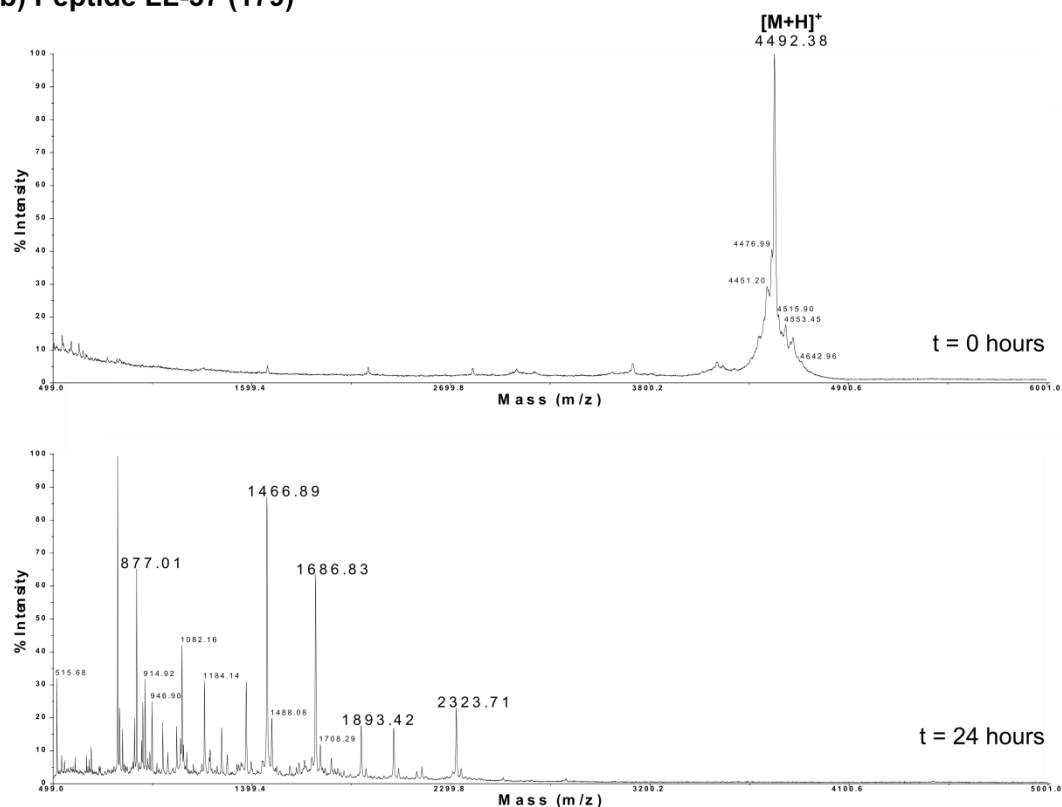
Figure 2.24. Tryptic degradation profile of a) peptoid (*NaeNpheNphe*)4 **180** and b) peptide LL-37, compound **179**. **180** shows no degradation after 24 hours in trypsin, whereas peptide **179** shows complete loss of parent ion and degradation into many smaller molecular weight peptide fragments.

2.10 Analysis of peptoid library secondary structure

Circular dichroism (CD) spectroscopy was introduced in section 2.4 and this technique has previously been used by the Barron group, among others, to identify helical peptoids. The secondary structures of a number of peptoids synthesised within this library were characterised in order to help rationalise the biological activity of the sequences, as it is known that helical peptoids may have increased biological activities.[50,77]

For simple first round analysis, all spectra were collected at 50 µM concentration in 1 mol dm^{-3} phosphate buffered saline solution[§§§§] (PBS). This low concentration was chosen to prevent intermolecular interactions which may affect the CD values obtained. CD data for a small selection of peptoids are shown in **Figure 2.25** and **Figure 2.26** as an example of the characteristic CD spectra for helical peptoids. Data is presented in mean residue ellipticity units which take into account the chain length and concentration of samples.

The CD spectra of peptoids **186–188** without a chiral reporter do not show any discernible secondary structure as shown in **Figure 2.25**, where the ellipticity values are all around zero across the wavelength range studied. The lack of secondary structure seen could arise due to the samples forming random conformations in solution or because any helices formed are racemic and therefore signals for left-handed and right-handed helices cancel each other out. However, it should be noted that even if a compound doesn't show helicity in solution, it may spontaneously self-assemble into a helix when in contact with a cell membrane.

At 50 µM, the CD spectra of compounds in **Figure 2.26** show two minima at approximately 202 nm and 218 nm, which indicate that these peptoids are forming PPI-type helices in solution. This data matches results reported by the Barron group.[32,33] For the 6 residue peptoid, there are small minima at 202 nm and 218 nm, suggesting **25** (*N*Lys*N*spe*N*spe)$_2$ is weakly helical. As peptoid helices have 3.0 residues per turn, it is unsurprising that a 6 residue peptoid only shows weak helicity as it is too short to form a fully stabilised helix. The ellipticity values are more negative for the longer peptoids (**26/22**), suggesting that longer chains stabilise the helices formed.

CD data has been collected for other selected sequences (data in the electronic supplementary information). Most sequences containing α-chiral monomers show a defined folded structure, suggestive of a peptoid helix. This will be discussed in more detail in Chapter 5 where a greater investigation of peptoid secondary structure is undertaken.

[§§§§] pH 7.4

186 (*N*Lys*N*phe*N*phe)$_4$
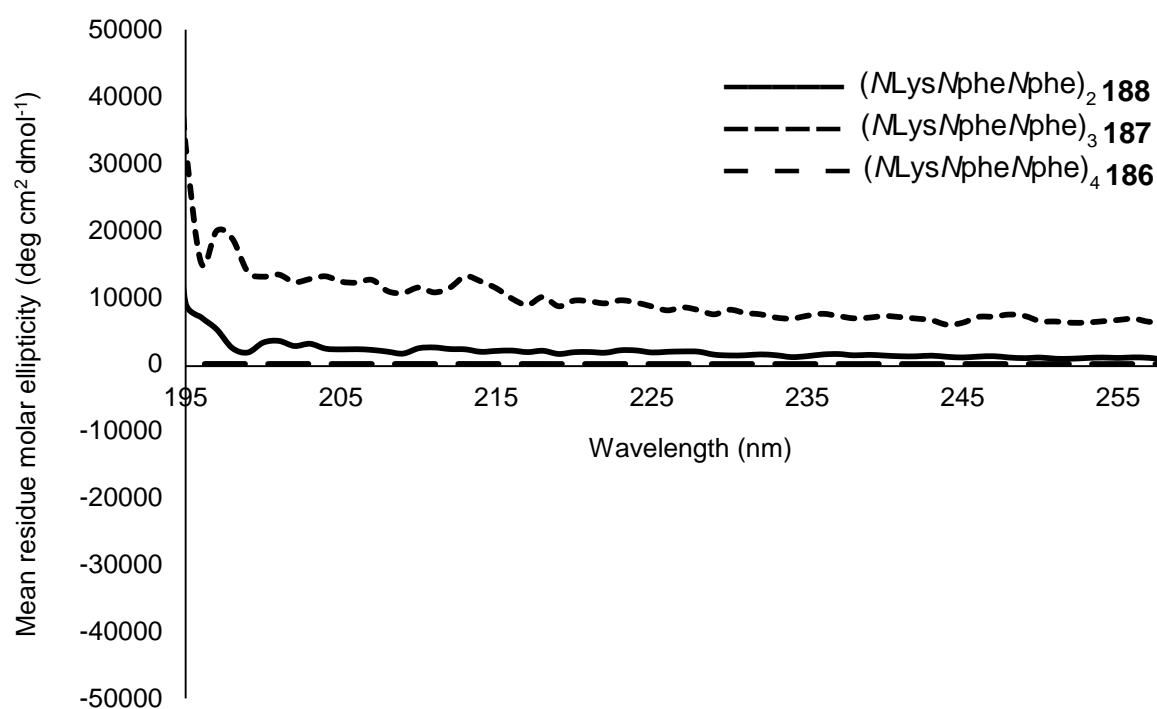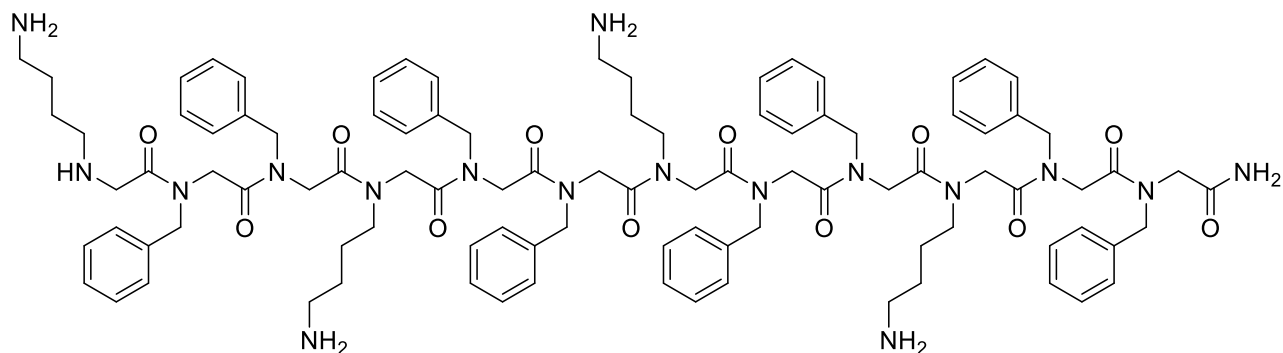
Figure 2.25. CD spectra for peptoid sequences of different lengths containing the achiral *N*phe monomer, peptoids **186–188**. Data collected at 50 µM in PBS (pH 7.4) at 22 °C. The structure of the 12 residue sequence **186** is shown. The secondary structure of these samples in solution cannot be determined – described in text.

22   (*N*Lys*N*spe*N*spe)$_4$
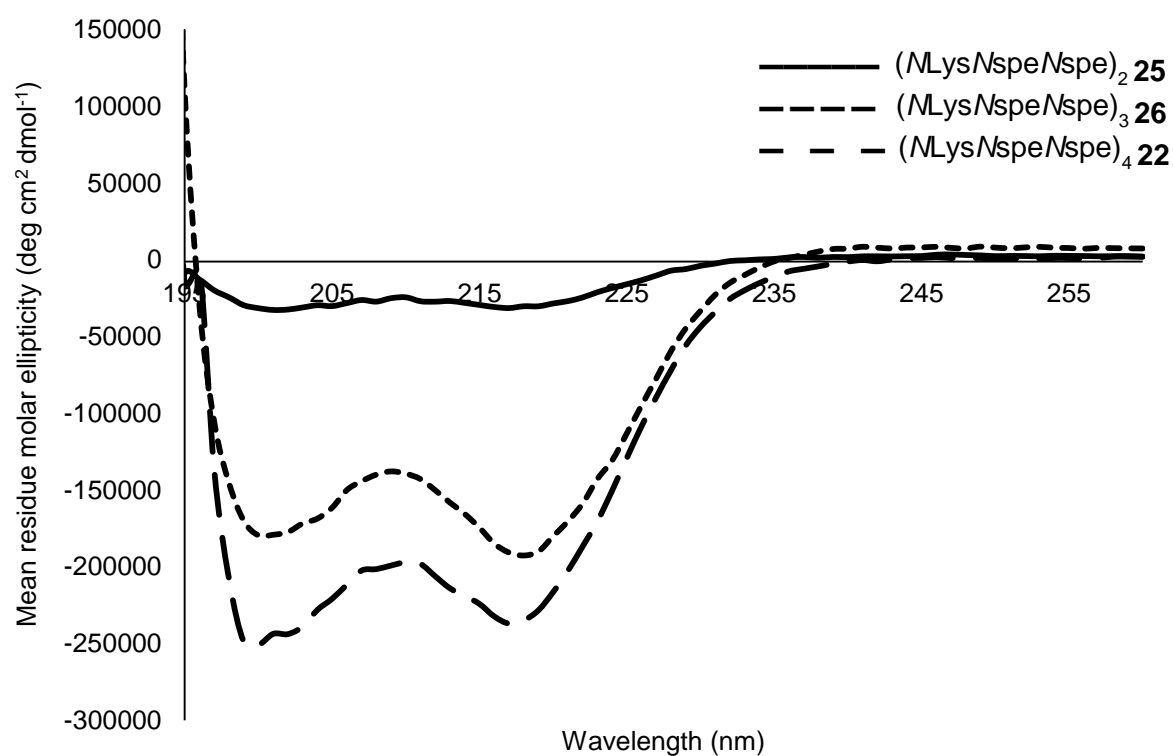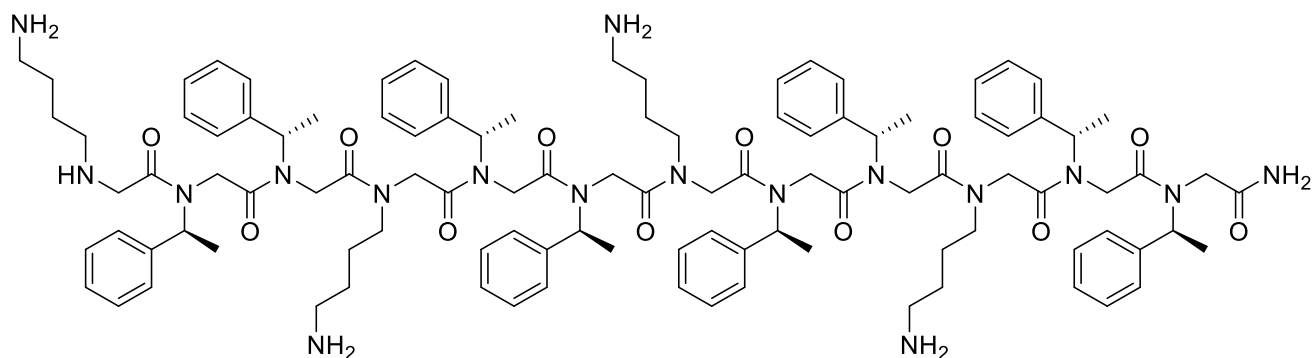
Figure 2.26. CD spectra for peptoid sequences of different lengths containing the α-chiral *N*spe monomer, peptoids **22**, **25**, **26**. Data collected at 50 μM in PBS (pH 7.4) at 22 °C. The structure of the 12 residue sequence **22** is shown. The samples show characteristic signals of peptoid helicies.

2.11 References

1.   R.N. Zuckermann, *Biopolymers,* **2011**, *96*, 545.
2.   R.J. Simon, R.S. Kania, R.N. Zuckermann, V.D. Huebner, D.A. Jewell, S. Banville, S. Ng, L. Wang, S. Rosenberg, C.K. Marlowe, D.C. Spellmeyer, R.Y. Tan, A.D. Frankel, D.V. Santi, F.E. Cohen, P.A. Bartlett, *Proc. Natl. Acad. Sci. USA,* **1992**, *89*, 9367.
3.   R.N. Zuckermann, J.M. Kerr, S.B.H. Kent, W.H. Moos, *J. Am. Chem. Soc.,* **1992**, *114*, 10646.
4.   T.S. Burkoth, A.T. Fafarman, D.H. Charych, M.D. Connolly, R.N. Zuckermann, *J. Am. Chem. Soc.,* **2003**, *125*, 8841.
5.   J. Seo, B.C. Lee, R.N. Zuckermann In *Comprehensive Biomaterials*; P. Ducheyne, K.E. Healy, D.W. Hutmacher, D.W. Grainger, Kirkpatrick, C. J., Eds.; Elsevier: 2011; Vol. 2, p 53.
6.   J.A.W. Kruijtzer, R.M.J. Liskamp, *Tetrahedron Lett.,* **1995**, *36*, 6969.
7.   T. Uno, E. Beausoleil, R.A. Goldsmith, B.H. Levine, R.N. Zuckermann, *Tetrahedron Lett.,* **1999**, *40*, 1475.
8.   R.N. Zuckermann, M. Lebl In *Proceedings of the 22nd American Peptide Symposium* 2011.
9.   C.A. Olsen, *Biopolymers,* **2011**, *96*, 561.
10.   C.A. Olsen, *ChemBioChem,* **2010**, *11*, 152.
11.   B.C. Hamper, S.A. Kolodziej, A.M. Scates, R.G. Smith, E. Cortez, *J. Org. Chem.,* **1998**, *63*, 708.
12.   A.C. Olsen, M. Lambert, M. Witt, H. Franzyk, W.J. Jaroszewski, *Amino Acids,* **2008**, *34*, 465.
13.   S.W. Shuey, W.J. Delaney, M.C. Shah, M.A. Scialdone, *Bioorg. Med. Chem. Lett.,* **2006**, *16*, 1245.
14.   C.A. Olsen, G. Bonke, L. Vedel, A. Adsersen, M. Witt, H. Franzyk, J.W. Jaroszewski, *Org Lett,* **2007**, *9*, 1549.
15.   L. Vedel, G. Bonke, C. Foged, H. Ziegler, H. Franzyk, J.W. Jaroszewski, C.A. Olsen, *ChemBioChem,* **2007**, *8*, 1781.
16.   S. Lin, X. Yu, Y. Tu, H. Xu, S.Z.D. Cheng, L. Jia, *Chem. Comm.,* **2010**, *46*, 4273.
17.   L. Jia, H. Sun, J.T. Shay, A.M. Allgeier, S.D. Hanton, *J. Am. Chem. Soc.,* **2002**, *124*, 7282.
18.   J.H. Lee, A.M. Meyer, H.-S. Lim, *Chem. Comm.,* **2010**, *46*, 8615.
19.   Y.-U. Kwon, T. Kodadek, *Chem. Comm.,* **2008**, 5704.
20.   S.N. Khan, A. Kim, R.H. Grubbs, Y.-U. Kwon, *Org. Lett.,* **2011**, *13*, 1582.
21.   S.B.Y. Shin, B. Yoo, L.J. Todaro, K. Kirshenbaum, *J. Am. Chem. Soc.,* **2007**, *129*, 3218.
22.   J.H. Lee, H.-S. Kim, H.-S. Lim, *Org. Lett.,* **2011**, *13*, 5012.
23.   O. Roy, S. Faure, V. Thery, C. Didierjean, C. Taillefumier, *Org. Lett.,* **2008**, *10*, 921.
24.   K. Andreev, M. Lingaraju, A. Ivankin, M. Huang, K. Kirshenbaum, D. Gidalevitz, *Biophysical J.,* **2013**, *104*, 598A.
25.   C. Caumes, C. Fernandes, O. Roy, T. Hjelmgaard, E. Wenger, C. Didierjean, C. Taillefumier, S. Faure, *Org. Lett.,* **2013**, *15*, 3626.
26.   E. De Santis, T. Hjelmgaard, S. Faure, O. Roy, C. Didierjean, B.D. Alexander, G. Siligardi, R. Hussain, T. Javorfi, A.A. Edwards, C. Taillefumier, *Amino Acids,* **2011**, *41*, 663.
27.   B. Yoo, S.B.Y. Shin, M.L. Huang, K. Kirshenbaum, *Chem. Eur. J.,* **2010**, *16*, 5528.
28.   M.L. Huang, S.B.Y. Shin, M.A. Benson, V.J. Torres, K. Kirshenbaum, *ChemMedChem,* **2012**, *7*, 114.

29. M.L. Huang, M.A. Benson, S.B.Y. Shin, V.J. Torres, K. Kirshenbaum, *Eur. J. Org. Chem.,* **2013**, 3560.

30. B. Vaz, L. Brunsveld, *Org. Biomol. Chem.,* **2008**, *6*, 2988.

31. E. Nnanabu, K. Burgess, *Org. Lett.,* **2006**, *8*, 1259.

32. C.W. Wu, T.J. Sanborn, R.N. Zuckermann, A.E. Barron, *J. Am. Chem. Soc.,* **2001**, *123*, 2958.

33. C.W. Wu, T.J. Sanborn, K. Huang, R.N. Zuckermann, A.E. Barron, *J. Am. Chem. Soc.,* **2001**, *123*, 6778.

34. J.M. Holub, M.J. Garabedian, K. Kirshenbaum, *QSAR Comb. Sci.,* **2007**, *26*, 1175.

35. J.M. Holub, H.J. Jang, K. Kirshenbaum, *Org. Biomol. Chem.,* **2006**, *4*, 1497.

36. R. Jagasia, J.M. Holub, M. Bollinger, K. Kirshenbaum, M.G. Finn, *J. Org. Chem.,* **2009**, *74*, 2964.

37. J.M. Holub, H. Jang, K. Kirshenbaum, *Org. Lett.,* **2007**, *9*, 3275.

38. S.B.L. Vollrath, S. Braese, K. Kirshenbaum, *Chem. Sci.,* **2012**, *3*, 2726.

39. D. Comegna, M. Benincasa, R. Gennaro, I. Izzo, F. De Riccardis, *Bioorg. Med. Chem.,* **2010**, *18*, 2010.

40. J.S. Laursen, J. Engel-Andreasen, P. Fristrup, P. Harris, C.A. Olsen, *J. Am. Chem. Soc.,* **2013**, *135*, 2835.

41. J.S. Laursen, P. Harris, P. Fristrup, C.A. Olsen, *Nature Communications,* **2015**, *6*, 7013.

42. J.S. Laursen, J. Engel-Andreasen, C.A. Olsen, *Accounts Chem. Res.,* **2015**, *48*, 2696.

43. S.M. Miller, R.J. Simon, S. Ng, R.N. Zuckermann, J.M. Kerr, W.H. Moos, *Drug Dev. Res.,* **1995**, *35*, 20.

44. P. Armand, K. Kirshenbaum, R.A. Goldsmith, S. Farr-Jones, A.E. Barron, K.T.V. Truong, K.A. Dill, D.F. Mierke, F.E. Cohen, R.N. Zuckermann, E.K. Bradley, *Proc. Natl. Acad. Sci. USA,* **1998**, *95*, 4309.

45. K. Kirshenbaum, A.E. Barron, R.A. Goldsmith, P. Armand, E.K. Bradley, K.T.V. Truong, K.A. Dill, F.E. Cohen, R.N. Zuckermann, *Proc. Natl. Acad. Sci. USA,* **1998**, *95*, 4303.

46. M. Wetzler, A.E. Barron, *Biopolymers,* **2011**, *96*, 556.

47. S.A. Fowler, H.E. Blackwell, *Org. Biomol. Chem.,* **2009**, *7*, 1508.

48. J. Seo, A.E. Barron, R.N. Zuckermann, *Org. Lett.,* **2010**, *12*, 492.

49. C.B. Gorske, R.C. Nelson, Z.S. Bowden, T.A. Kufe, A.M. Childs, *J. Org. Chem.,* **2013**, *78*, 11172.

50. C.W. Wu, K. Kirshenbaum, T.J. Sanborn, J.A. Patch, K. Huang, K.A. Dill, R.N. Zuckermann, A.E. Barron, *J. Am. Chem. Soc.,* **2003**, *125*, 13525.

51. N.H. Shah, G.L. Butterfoss, K. Nguyen, B. Yoo, R. Bonneau, D.L. Rabenstein, K. Kirshenbaum, *J. Am. Chem. Soc.,* **2008**, *130*, 16622.

52. B.C. Gorske, B.L. Bastian, G.D. Geske, H.E. Blackwell, *J. Am. Chem. Soc.,* **2007**, *129*, 8928.

53. G.L. Butterfoss, P.D. Renfrew, B. Kuhlman, K. Kirshenbaum, R. Bonneau, *J. Am. Chem. Soc.,* **2009**, *131*, 16798.

54. B.C. Gorske, J.R. Stringer, B.L. Bastian, S.A. Fowler, H.E. Blackwell, *J. Am. Chem. Soc.,* **2009**, *131*, 16555.

55. K. Huang, C.W. Wu, T.J. Sanborn, J.A. Patch, K. Kirshenbaum, R.N. Zuckermann, A.E. Barron, I. Radhakrishnan, *J. Am. Chem. Soc.,* **2006**, *128*, 1733.

56. S.A. Fowler, R. Luechapanichkul, H.E. Blackwell, *J. Org. Chem.,* **2009**, *74*, 1440.

57. B.C. Gorske, H.E. Blackwell, *J. Am. Chem. Soc.,* **2006**, *128*, 14378.

58. B. Yoo, K. Kirshenbaum, *Curr. Opin. Chem. Biol.,* **2008**, *12*, 714.

59. J.R. Stringer, J.A. Crapster, I.A. Guzei, H.E. Blackwell, *J. Org. Chem.,* **2010**, *75*, 6068.

60. J.K. Pokorski, L.M.M. Jenkins, H. Feng, S.R. Durell, Y. Bai, D.H. Appella, *Org. Lett.,* **2007**, *9*, 2381.

61. M. Rainaldi, V. Moretto, M. Crisma, E. Peggion, S. Mammi, C. Toniolo, G. Cavicchioni, *J. Pept. Sci.,* **2002**, *8*, 241.

62. B. Sanii, R. Kudirka, A. Cho, N. Venkateswaran, G.K. Olivier, A.M. Olson, H. Tran, R.M. Harada, L. Tan, R.N. Zuckermann, *J. Am. Chem. Soc.,* **2011**, *133*, 20808.

63. H. Tran, S.L. Gael, M.D. Connolly, R.N. Zuckermann, *J. Vis. Exp.,* **2011**, e3373.

64. R.V. Mannige, T.K. Haxton, C. Proulx, E.J. Robertson, A. Battigelli, G.L. Butterfoss, R.N. Zuckermann, S. Whitelam, *Nature,* **2015**, *526*, 415.

65. K.T. Nam, S.A. Shelby, P.H. Choi, A.B. Marciel, R. Chen, L. Tan, T.K. Chu, R.A. Mesch, B.-C. Lee, M.D. Connolly, C. Kisielowski, R.N. Zuckermann, *Nature Materials,* **2010**, *9*, 454.

66. A.A. Fuller, B.A. Yurash, E.N. Schaumann, F.J. Seidl, *Org. Lett.,* **2013**, *15*, 5118.

67. R. Kudirka, H. Tran, B. Sanii, N. Ki Tae, P.H. Choi, N. Venkateswaran, R. Chen, S. Whitelam, R.N. Zuckermann, *Biopolymers,* **2011**, *96*, 586.

68. B. Sanii, R. Kudirka, A. Cho, N. Venkateswaran, G.K. Olivier, A.M. Olson, H. Tran, R.M. Harada, L. Tan, R.N. Zuckermann, *Biophysical Journal,* **2012**, *102*, 269A.

69. J. Sun, X. Jiang, R. Lund, K.H. Downing, N.P. Balsara, R.N. Zuckermann, *Proc. Natl. Acad. Sci. USA,* **2016**, *113*, 3954.

70. D.H.A. Correa, C.H. I. Ramos, *Afr. J. Biochem. Res.,* **2009**, *3*, 164.

71. J.A. Patch, K. Kirshenbaum, S.L. Seurynck, R.N. Zuckermann, A.E. Barron In *Pseudopeptides in Drug Development*; Nielsen, P. E., Ed.; Wiley-VCH: Germany, 2004, p 1

72. G.L. Butterfoss, B. Yoo, J.N. Jaworski, I. Chorny, K.A. Dill, R.N. Zuckermann, R. Bonneau, K. Kirshenbaum, V.A. Voelz, *Proc. Natl. Acad. Sci. USA,* **2012**, *109*, 14320.

73. U. Sternberg, E. Birtalan, I. Jakovkin, B. Luy, U. Schepers, S. Brase, C. Muhle-Goll, *Org. Biomol. Chem.,* **2013**, *11*, 640.

74. M.L. Hebert, D.S. Shah, P. Blake, J.P. Turner, S.L. Servoss, *Org. Biomol. Chem.,* **2013**, *11*, 4459.

75. H.-M. Shin, C.-M. Kang, M.-H. Yoon, J. Seo, *Chem. Comm.,* **2014**, *50*, 4465.

76. J.A. Patch, A.E. Barron, *J. Am. Chem. Soc.,* **2003**, *125*, 12092.

77. N.P. Chongsiriwatana, J.A. Patch, A.M. Czyzewski, M.T. Dohm, A. Ivankin, D. Gidalevitz, R.N. Zuckermann, A.E. Barron, *Proc. Natl. Acad. Sci. USA,* **2008**, *105*, 2794.

78. S. Lear, S.L. Cobb, *Journal of Computer-Aided Molecular Design,* **2016**, 1.

79. M.A. Fara, J.J. Díaz-Mochón, M. Bradley, *Tetrahedron Lett.,* **2006**, *47*, 1011.

80. H.J. Olivos, P.G. Alluri, M.M. Reddy, D. Salony, T. Kodadek, *Org. Lett.,* **2002**, *4*, 4057.

81. D. Muller, I. Zeltser, G. Bitan, C. Gilon, *J. Org. Chem.,* **1997**, *62*, 411.

82. A.T. Bockus, C.M. McEwen, R.S. Lokey, *Curr. Top. Med. Chem.,* **2013**, *13*, 821.

83. B. Mojsoska, R.N. Zuckermann, H. Jenssen, *Antimicrob. Agents Chemother.,* **2015**.

84. H.L. Bolt, G.A. Eggimann, P.W. Denny, S.L. Cobb, *MedChemComm,* **2016**, *7*, 799.

85. G.A. Eggimann, H.L. Bolt, P.W. Denny, S.L. Cobb, *ChemMedChem,* **2015**, *10*, 233.

86. T.S. Ryge, N. Frimodt-Moller, P.R. Hansen, *Chemotherapy,* **2008**, *54*, 152.

87. T. Jong, A.M. Pérez-López, E.M.V. Johansson, A. Lilienkampf, M. Bradley, *Bioconjugate Chem.,* **2015**, *26*, 1759.

88. S.B.L. Vollrath, D. Fuerniss, U. Schepers, S. Braese, *Org. Biomol. Chem.,* **2013**, *11*, 8197.

89. W. Huang, J. Seo, J.S. Lin, A.E. Barron, *Mol. Biosyst.,* **2012**, *8*, 2626.

90.	C.Y. Huang, T. Uno, J.E. Murphy, S. Lee, J.D. Hamer, J.A. Escobedo, F.E. Cohen, R. Radhakrishnan, V. Dwarki, R.N. Zuckermann, *Chem. Biol.,* **1998**, *5*, 345.

91.	Dominik K. Kölmel, Daniel Fürniss, Steven Susanto, Andrea Lauer, Clemens Grabher, Stefan Bräse, U. Schepers, *Pharmaceuticals,* **2012**, *5*, 1265.

92.	B.K. Ford, M. Hamza, D.L. Rabenstein, *Biochem.,* **2013**, *52*, 3773.

93.	S.L. Seurynck-Servoss, M.T. Dohm, A.E. Barron, *Biochem.,* **2006**, *45*, 11809.

94.	B. Findlay, P. Szelemej, G.G. Zhanel, F. Schweizer, *PLOS ONE,* **2012**, *7*, e41141.

95.	M.T. Dohm, R. Kapoor, A.E. Barron, *Curr. Pharm. Des.,* **2011**, *17*, 2732.

96.	M. Gobbo, M. Benincasa, G. Bertoloni, B. Biondi, R. Dosselli, E. Papini, E. Reddi, R. Rocchi, R. Tavano, R. Gennaro, *J. Med. Chem.,* **2009**, *52*, 5197.

97.	C.A. Olsen, H.L. Ziegler, H.M. Nielsen, N. Frimodt-Moller, J.W. Jaroszewski, H. Franzyk, *ChemBioChem,* **2010**, *11*, 1356.

98.	P.A. Wender, D.J. Mitchell, K. Pattabiraman, E.T. Pelkey, L. Steinman, J.B. Rothbard, *Proc. Natl. Acad. Sci. USA,* **2000**, *97*, 13003.

99.	H.L. Bolt, S.L. Cobb, *Org. Biomol. Chem.,* **2016**, *14*, 1211.

100.	I.A. Nash, B.W. Bycroft, W.C. Chan, *Tetrahedron Lett.,* **1996**, *37*, 2625.

101.	B. Rohwedder, Y. Mutti, P. Dumy, M. Mutter, *Tetrahedron Lett.,* **1998**, *39*, 1175.

102.	M.S. Bernatowicz, Y.L. Wu, G.R. Matsueda, *J. Org. Chem.,* **1992**, *57*, 2497.

103.	S.M. Mandal, A.E. Barbosa, O.L. Franco, *Biotechnol. Adv.,* **2013**, *31*, 338.

104.	Y. Nakao, S. Kawatsu, C. Okamoto, M. Okamoto, Y. Matsumoto, S. Matsunaga, R.W.M. van Soest, N. Fusetani, *J. Nat. Prod.,* **2008**, *71*, 469.

105.	M.J. Balunas, R.G. Linington, K. Tidgewell, A.M. Fenner, L.D. Urena, G.D. Togna, D.E. Kyle, W.H. Gerwick, *J. Nat. Prod.,* **2010**, *73*, 60.

106.	S.K. Straus, R.E.W. Hancock, *Biochim. Biophys. Acta,* **2006**, *1758*, 1215.

107.	T. Schneider, A. Müller, H. Miess, H. Gross, *Int. J. Med. Microbiol.,* **2014**, *304*, 37.

108.	N.P. Chongsiriwatana, T.M. Miller, M. Wetzler, S. Vakulenko, A.J. Karlsson, S.P. Palecek, S. Mobashery, A.E. Barron, *Antimicrob. Agents Chemother.,* **2011**, *55*, 417.

109.	F.M. Veronese, G. Pasut, *Drug Discov Today,* **2005**, *10*, 1451.

110.	S. Jevsevar, M. Kunstelj, V.G. Porekar, *Biotechnol. J.,* **2010**, *5*, 113.

111.	F.M. Veronese, A. Mero, *BioDrugs,* **2008**, *22*, 315.

112.	X. Chen, K. Ding, N. Ayres, *Polym. Chem.,* **2011**, *2*, 2635.

113.	S.H. Lahasky, X. Hu, D. Zhang, *ACS Macro. Lett.,* **2012**, *1*, 580.

114.	R.O. Jahnsen, A. Sandberg-Schaal, N. Frimodt-Møller, H.M. Nielsen, H. Franzyk, *Eur. J. Pharmaceut. Biopharmaceut.,* **2015**, *95, Part A*, 40.

115.	R.N. Zuckermann, T. Kodadek, *Curr. Opin. Mol. Ther.,* **2009**, *11*, 299.

116.	Y.F. Wang, H. Lin, R. Tullman, C.F. Jewell, M.L. Weetall, F.L.S. Tse, *Biopharm. Drug Dispos.,* **1999**, *20*, 69.

117.	J. Seo, G. Ren, H. Liu, Z. Miao, M. Park, Y. Wang, T.M. Miller, A.E. Barron, Z. Cheng, *Bioconjugate Chem.,* **2012**, *23*, 1069.

Chapter 3

Antiparasitic Peptoids

Neglected tropical diseases (NTDs) represent a significant global health burden, affecting approximately one-sixth of the world's population.[1] The illnesses classified as NTDs by the World Health Organisation (WHO) include diverse conditions that have historically been overlooked by international public health efforts, leading to insufficient prevention and treatment options. Currently, seventeen NTDs have been prioritised by the WHO and are caused by a variety of pathogens, including protozoa, bacteria, viruses or helminths, as summarised in **Table 3.1**.[1]

Prokaryotic	Eukaryotic		Viral
	Protozoa	*Helminth*	
Treponematoses (yaws)	Human African Trypanosomiasis	Dracunculiasis (guinea-worm disease)	Dengue
Leprosy	Chagas	Lymphatic Filariasis	Rabies
Trachoma	Leishmaniases	Onchocerciasis (river blindness)	
Buruli ulcer		Echinococcosis	
		Foodbourne trematodiases	
		Schistosomiasis	
		Soil-transmitted helminthiases	
		Taeniasis/cysticercosis	

Table 3.1. The seventeen neglected tropical diseases prioritised by the WHO. The conditions are split to illustrate the causative pathogen, where the protozoa are unicellular eukaryotes and the helminth are multicellular eukaryotes.[1]

These conditions present a severe threat to global health and they affect the world's poorest populations, particularly in tropical and sub-tropical regions, as illustrated by **Figure 3.1**. NTDs are typically endemic in resource-poor, developing countries where populations have limited access to healthcare, deprived living conditions and a lack of resources to tackle the disease. In addition to the mortality of these diseases, they can cause long-term disability and have significant social and economic consequences.

Often treatments for these NTDs are limited in their efficacy, cause severe side effects that can be detrimental to patient compliance and increasingly face problems such as drug resistance, so many NTDs may become untreatable in the future.[1,2] Given the lack of licensed vaccines and the disadvantages associated with many of the current drugs on the market, there is a clear need for the development of new therapies for NTDs. This urgency is highlighted by recent initiatives such as the 2012 London Declaration on Neglected Tropical Diseases that encourages partnerships between public and private institutions, with the aim of eradicating and controlling neglected diseases. In 2015, the Ross Fund was announced by the UK government, providing over £1 billion to combat serious disease, including NTDs, and antimicrobial resistance in developing counties.[3,4]
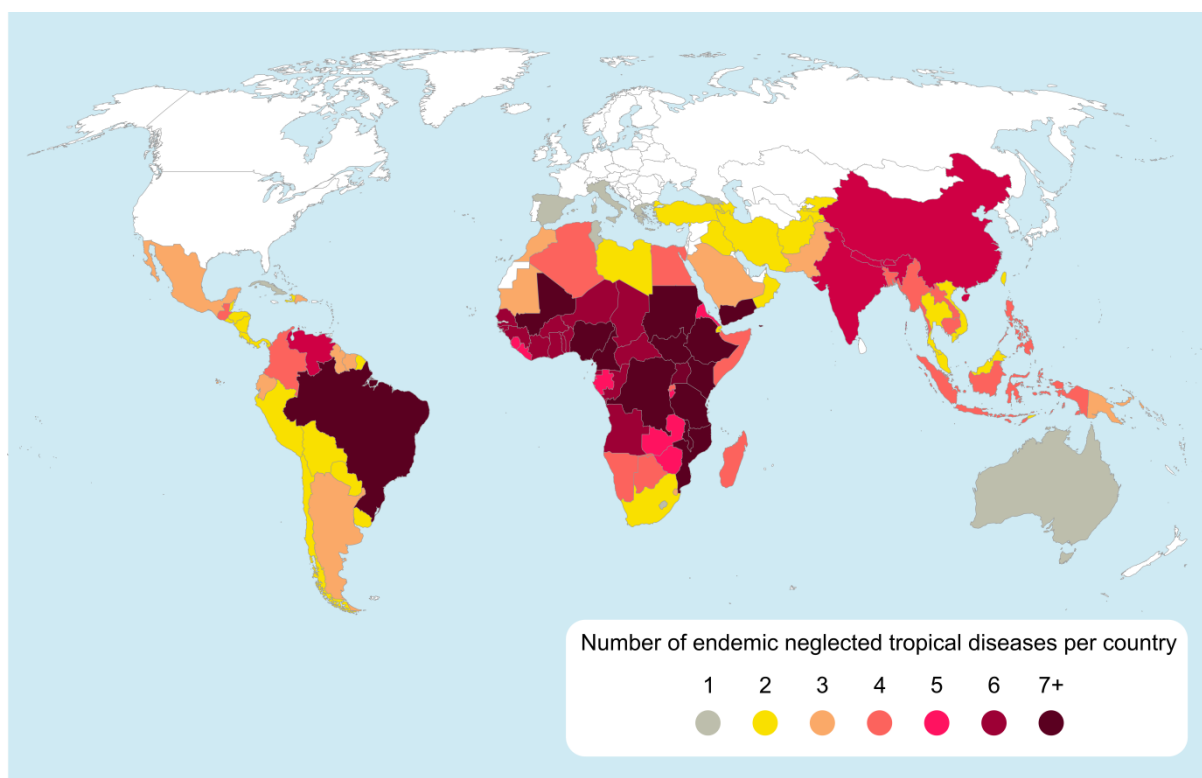
Figure 3.1. A map to illustrate the global burden of neglected tropical diseases. Data is taken from 2010 estimates of global endemicity of the 17 WHO classified NTDs.

Research into the development of vaccines against parasitic tropical diseases has mainly been focused on malaria but despite this, only one vaccine has been licensed for malaria to date.[5-7] With no vaccines approved for clinical use against parasitic NTDs, eradication of their transmission vector is the main preventative strategy. If infection does occur, the frontline treatments in current use often have significant limitations and severe side effects. In addition, increasing drug resistance to many of the available treatments means that these diseases may become untreatable in the near future.[8-12]

Access to the genome sequences of many clinically relevant parasites opens the possibility for drug discovery based upon the identification of novel molecular drug targets. For example, trypanothione reductase has been identified as a potential target for the kinetoplastids[13], a selection of kinases for *Plasmodium falciparum*[9] and very recently the inhibition of the kineoplastid proteasome has been muted as a potential conserved target across *Leishmania*, and *Trypanosoma* species.[14] Despite the fact that many potential, parasite specific biochemical targets and pathways have now been identified for the treatment of infections caused by protozoa, adequate treatments for many of these NTDs are still elusive. Bringing new treatments to market for diseases caused by protozoa is challenging because of the complicated lifecycle of these parasites, with multiple stages that have drastic differences in their membrane composition and that exhibit distinct metabolic processes or protein expression.[9,15]

This project focussed on the development of peptoids as novel antiparasitic agents against *Leishmania* species, the causative agents of the NTD leishmaniasis. Other vector-borne protozoa were also considered, such as those that cause malaria or the NTDs Chagas disease and African sleeping sickness and these will also be discussed in the following chapter.

3.1   Leishmanaisis

Leishmaniasis is one of the WHO's classified neglected tropical diseases and is caused by insect vector-borne protozoan parasites of the genus *Leishmania.* Endemic in over 80 countries worldwide, it is estimated that there are 1.3 million new cases each year, causing 20,000 to 30,000 deaths annually. In 2010, it was approximated that 12 million people were infected and a further 350 million at risk of disease across five continents.[16,17]

Leishmaniasis has three main clinical forms; visceral leishmaniasis (VL) which causes life threatening organ damage and is typically accompanied by fever; cutaneous leishmaniasis (CL) which leads to significant scarring and mucosal damage and mucocutaneous leishmaniasis (MCL) which causes the partial or total destruction of mucous membranes (see **Figure 3.2**).

VL is typically fatal in approximately 95 % of untreated cases and is characterised by irregular bouts of fever, enlargement of the liver and spleen, dramatic weight loss and anaemia. The visceral form is highly endemic in the Indian subcontinent and East Africa, with over 90 % of cases occurring in Bangladesh, Brazil, India, Ethiopia, South Sudan and Sudan. CL is the most common form of the disease, causing mild to severe skin infections that can cause disfigurement and life-long disability. 95 % of CL infections are found in America, the Middle East, Central Asia and more recently southern Europe. Although CL is not fatal itself, it can lead to complications from secondary infections. Most cases of MCL occur in Bolivia, Brazil and Peru and if untreated can progress to the ulcerative destruction of the nose and mouth area.[17,18]

Figure 3.2. a) and b) skin ulcers caused by cutaneous leishmaniasis; c) destruction of the mouth and nose area by mucocutaneous leishmaniasis.[*]

---

[*]   Images reproduced from a) https://www.emaze.com/@AIIWFRCF/Leishmaniasis; b) https://en.wikipedia.org/wiki/Leishmaniasis   c)   http://www.medicalrealm.net/what-is-microbiology---leishmaniasis.html

Leishmaniasis typically affects the poorest people around the globe and is often associated with malnutrition, poor access to housing and healthcare and population mobility, as illustrated by the recent explosion of CL cases in the Middle East due to the refugee crisis.[19] As well as the physical symptoms of the disease, patients often suffer from long-term disability and social exclusion. Leishmaniasis is particularly problematic where patients have *Leishmania*-HIV coinfection since patients are more likely to develop a serious disease and display high relapse and fatality rates.[18,20]

3.1.1   Life cycle

As a vector-borne disease, leishmaniasis is transmitted by the bite of a female phlebotomine sandfly. *Leishmania* are digenetic parasites with distinct life stages involving two hosts, both insect and vertebrate, as shown in **Figure 3.3**.

In a mammalian host, *Leishmania* are present as intracellular amastigotes, and multiply within various tissue cells or macrophages and the presence of these amastigotes causes the clinical symptoms of leishmaniasis. Host cells with a large parasite burden are often prone to lysis which release the amastigotes and can lead to the infection of further macrophages. Upon taking a blood meal from an infected mammalian host, a sandfly may ingest infected macrophages. As these are digested in the gut of the insect vector, the *Leishmania* parasites undergo a transformation into the promastigote stage. In this phenotype, the parasite survives as a motile extracellular parasite with a single flagellum. Promastigotes divide in the insect midgut and migrate to the proboscis, where the metacyclic promastigotes can be transferred back to a mammalian host during feeding and cause further infection in the new host.[21,22]

There are substantial differences between the promastigote and pathogenic amastigote forms of the parasite, including significant modifications to the cell surface which are suspected to cause different susceptibilities when treated with drugs and AMPs. The insect stage promastigotes are surrounded by a thick glycocalyx layer composed of macromolecules; mainly lipophosphoglycan (LPG) and also cell surface proteophosphoglycan (PPG). The LPG layer is made of anionic phosphorylated disaccharides and bound to the cell membrane via a glycosylphosphoinositol (GPI) anchor. In contrast, in the mammalian form of the parasite expression of both LPG and PPG is down-regulated so amastigotes display very low or negligible cell surface quantities of LPG and PPG.[23-25]

Recent work by our group with mutant *Leishmania mexicana* has shown that the presence of PPG is a major factor that contributes to promastigote sensitivity to a family of AMPs, whereas the presence of LPG has little effect on the sensitivity of the protozoa to treatment. It is suggested that the anionic charge of the PPG helps to attract the cationic AMPs and may help to explain why the pathogenic amastigotes (that have a lack of PPG on their cell surface) often display greater resistance to treatment than the insect stage promastigotes. Although this work is not discussed in detail here, a publication resulting from this work can be found in the Appendicies.[26]
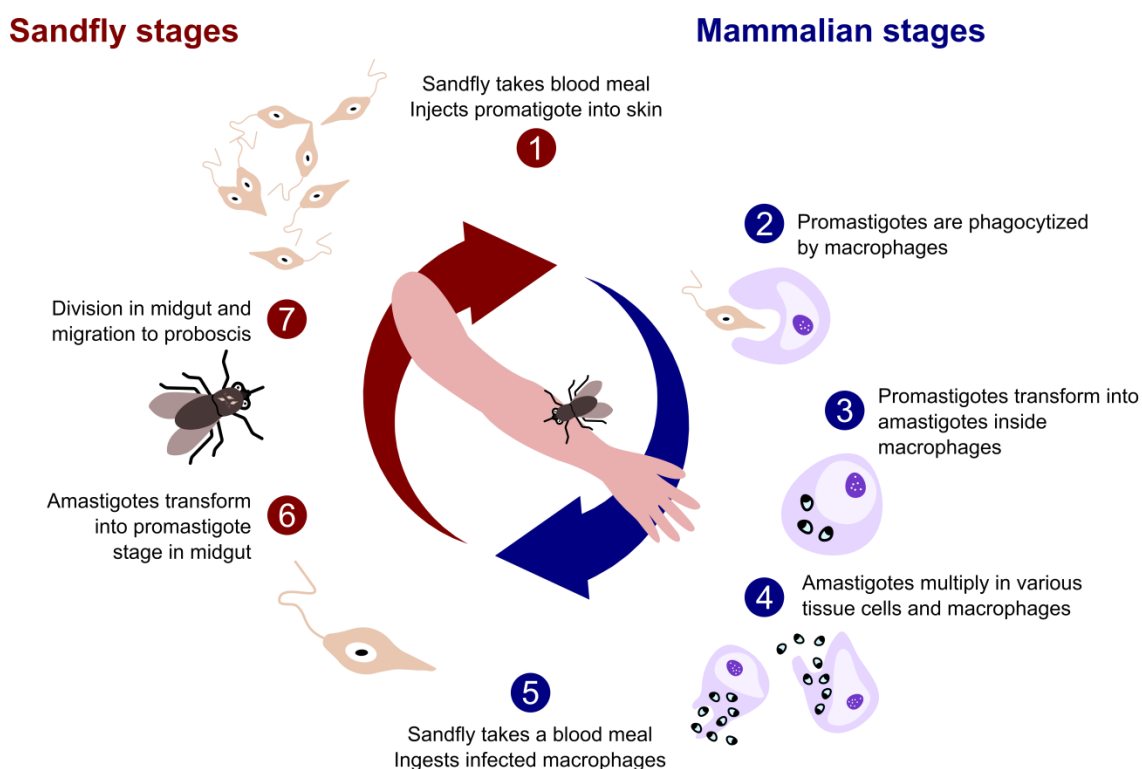
Figure 3.3. Lifecycle of *Leishmania spp.* including promastigote stage inside the insect vector and transformation to the mammalian amastigote form inside mammalian macrophages.

3.1.2 Current treatments for leishmaniasis

Preventative measures deployed against leishmaniasis commonly use vector control, such as the use of insecticides, the culling of animal reservoir populations or the use of insecticide-treated nets. However, these tactics are commonly ineffective since control of the disease involves a complex biological system, involving human host, multiple parasite life stages, a sandfly vector and various animal reservoir hosts.

Currently, there is no approved vaccine for the prevention of either CL or VL in humans, although several promising candidates are in development.[12,27] There has been extensive investigation into vaccines using killed or attenuated parasites, second generation vaccines based upon recombinant or antigenic proteins and a third generation of

immunisations derived from antigen-encoding DNA plasmids. Those based upon recombinant protein or antigen-encoding plasmids have given very promising results and a few vaccines have now been licensed for use against visceral leishmaniasis in canines. Several candidate vaccines have made phase I and II clinical trials, and others are currently ongoing.[12,27-30] It seems very likely that a vaccine for leishmaniasis in humans will be developed in the near future. However, even with a successful vaccine in hand, deployment to affected populations will take time and considerable expense.

Chemotherapy is the basis for current treatment in all three major forms of leishmaniasis; VL, CL and MCL. The main treatments in clinical use are shown in **Figure 3.4** and have already been well reviewed.[31,32] These treatments are often unsatisfactory with high toxicity, long durations of treatment and severe side effects that lead to poor patient compliance, as summarised in **Table 3.2**. Additionally, the distinct species of *Leishmania* have very different susceptibilities to the drugs in current use; for example, paramomycin (**193**), a drug effective against VL in India shows poor efficacy against VL in East Africa.[33]

Options include the use of the pentavalent antimonials like sodium stibogluconate (**189**) or meglumine antimoniate (**190**), which have been in clinical use since the 1940s. This class of drugs contains antimony and have very severe side effects, including cardiotoxicity. Pentavalent antimonials must also be administered intravenously, which is a disadvantage in areas where Leishmaniasis is prevalent because patients often have poor access to healthcare.[11,20,31,32,34,35]

Amphotericin B (**191**) is a widely used antifungal polyene that is also commonly used drug in the fight against leishmanaisis and binds to the parasite specific sterol, ergosterol. However, the drug also has toxic side effects and must be administered parenterally. Amphotericin B formulations (in particular the liposomal form) were developed to reduce these adverse effects and lead to improvements in pharmacokinetic properties. However these have limitations for use in developing countries since they are costly and unstable at higher temperatures.[11,20,31,32,34,35]

Miltefosine (**192**) is another front-line treatment for Leishmaniasis. Although this drug can be administered orally, it must be refrigerated and is also a teratogen so cannot be prescribed to pregnant women. With resistance to this drug developing in the Indian sub-continent and high levels of treatment failure, this drug also has severe disadvantages.[11,20,31,32,34,35]

Paromomycin (**193**) is an alternative drug but is also associated with severe toxicity. Pentamidine (**194**) has an unknown mechanism of action and is only used infrequently due to the appearance of resistant cases of leishmaniasis. It is highly toxic and can trigger severe side effects, such as diabetes mellitus or severe hypoglycaemia. Typically it is only recommended when used in combination therapy.[11,20,31,32,34,35]

Pentavalent antimonials

189 Sodium stibogluconate

190 Meglumine antimoniate

191
Amphotericin B

192
Miltefosine

193
Paromomycin

194
Pentamidine
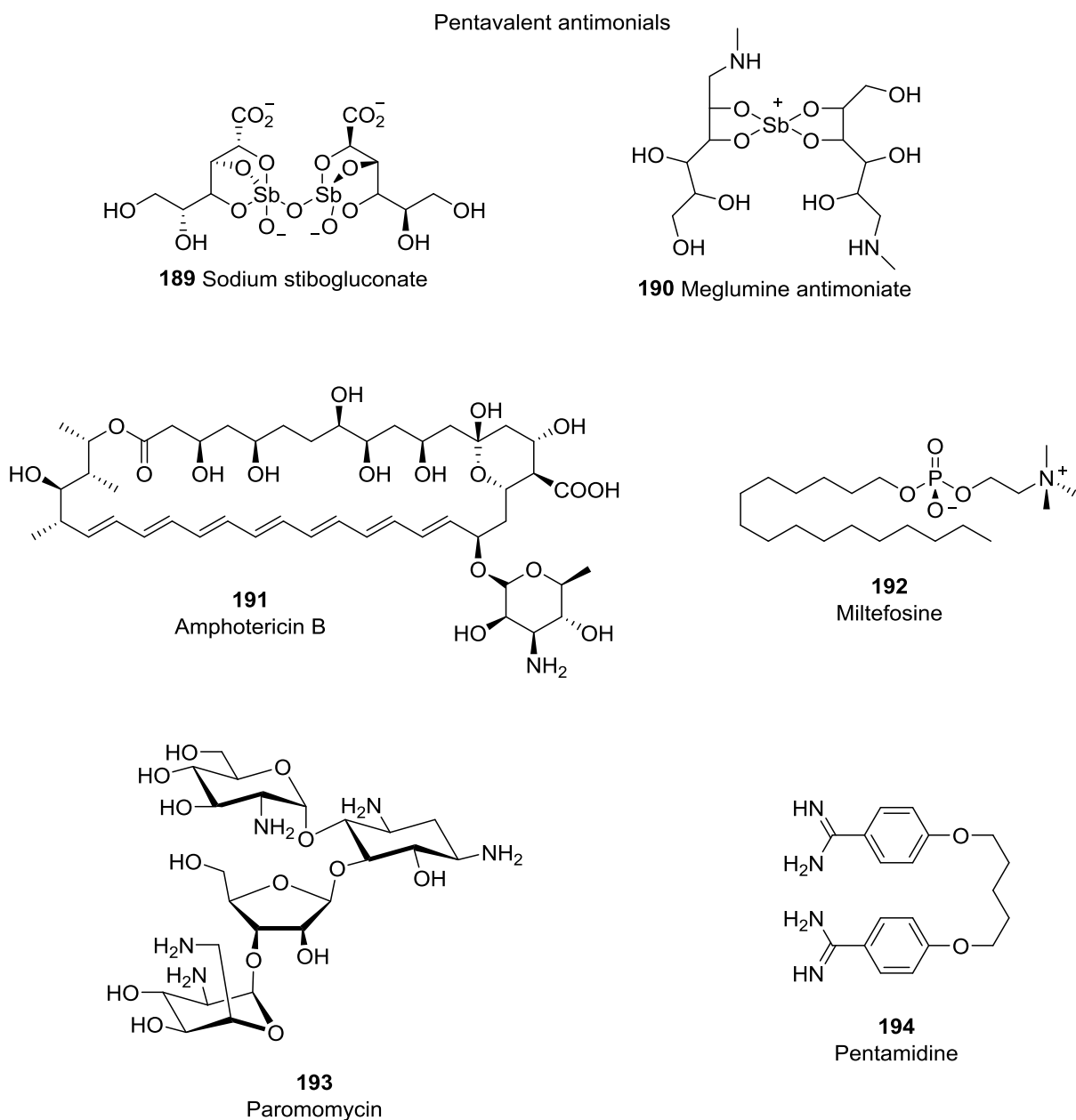
Figure 3.4. Chemical structures of the frontline treatments in clinical use for leishmaniasis.

Structure(s)	Drug	Administration	Side effects	Resistance
189 **190**	Pentavalent antimonials	Intramuscular or Intravenous	Severe cardiotoxicity, pancreatitis, toxic to liver and kidney, painful injection and stiff joints, gastrointestinal problems	Common (> 65 % in India) Efficacy 35–95 % depending on area
191	Amphotericin B	Intravenous	Severe toxicity to kidney, high fever, potassium deficiency, bone pain, cardiac arrest (rare)	Seen in laboratory strains Efficacy > 90 %
	Liposomal amphotericin B	Intravenous Must be stored below 25 ˚C	Mild toxicity to kidney	Not documented Efficacy > 97 %
192	Miltefosine	Oral Must be refrigerated	Vomiting and diarrhoea, toxicity to liver and kidney, teratogenic	Seen in laboratory strains *L. braziliensis, L. guyanensis* and *L. mexicana* are insensitive to miltefosine Efficacy 60–93 % in Africa; 94 % in India
193	Paromomycin	Intramuscular for VL Topical for CL	Severe toxicity to ear, liver and kidney, pain at injection site, abdominal cramp and diarrhoea	Seen in laboratory strains against *L. donovani* Efficacy 46–85 % in Africa; 94 % in India
194	Pentamidine	Intramuscular	Hyperglycemia via pancreatic damage, hypotension, pain at injection site, death	Resistance emerging, particularly with HIV-coinfection Efficacy 35–96 % dependent on species

Table 3.2. A summary of the current anti-leishmanial drugs in clinical use, administration routes, evidence of drug resistance and their associated toxicity.[31,32]

With developing drug resistance, toxicity issues and the requirement to treat diverse patient populations, there is a real need to develop new, improved therapeutics for leishmaniasis. However, bringing novel treatments to market for diseases caused by protozoa is challenging because of the complicated lifecycle of these parasites, with multiple stages that have drastic differences in their membrane composition and that exhibit distinct metabolic processes or protein expression. In particular, for leishmaniasis, the disease has several manifestations so is a complex disease, particularly in patients with co-infections. Additionally, the fact that *Leishmania* parasites residue inside a compartment within an intracellular target means there are many membranes that a potential drug must pass. Even for CL pharmacokinetics are complex since drugs must pass into the dermal layer, compared to bacterial of fungal infections that are present in the upper and more easily reachable epidermal skin layers.[9,36]

In recent years, the development of safer, more effective treatments for VL has become a priority following the London Declaration in 2012. In contrast, CL remains relatively overlooked and new treatments are desperately needed. One rich source of potential drug scaffolds and pharmacophores are natural products. A wide variety of these have been shown to have mild anti-leishmanial activities, including plant-derived compounds such as alkaloids[37], flavonoids[32] or terpenes[38,39] and products isolated from marine sponges.[40,41] In particular, antimicrobial peptides (AMPs) have been proposed as targets for the development of new treatments for leishmaniasis due to their broad spectrum antimicrobial activities and as yet resistance has not emerged to these compounds.[42,43] A wide variety of AMPs derived from mammalian sources,[44-50] invertebrates,[51-66] amphibians[26,43,67] or synthetic AMPs[68,69] have been shown to have activity against protozoan species. These antiparasitic peptides include promising activity against *Leishmania spp.*, from AMPs such as the cathelicidins, indolicidins, histatins and bombinins (see **Table 3.3**).[42,43,70]

It is suspected that most cationic AMPs target the protozoan plasma membrane by association with the acidic phospholipids on the outer membrane of the protozoa, but other modes of action have been demonstrated such as interaction with intracellular targets, immunomodulatory effects or the induction of biochemical changes that lead to apoptosis. The relative specificity of the AMPs towards the parasite over host cells is accounted for by the more anionic cell membrane structure compared to mammalian cells.[42,43,70]

Previous work in the Cobb group has shown that the temporins, a versatile group of AMPs, are effective against *Leishmania mexicana,* the causative agent of cutaneous leishmaniasis. The temporins are short AMPs isolated from frog skin secretions and they have an exceptionally low number of positively charged amino acids (net charges between neutral and +3). Temporin A, B and 1Sa were shown to have activity against *L. mexicana* in the low micromolar range for promastigotes, but poor activity against the clinically relevant amastigote form.[67]

However, the biological and chemical stability of short, linear peptides is often problematic for their application as pharmaceuticals. Peptides are rapidly degraded *in vivo* by the wide variety of proteases and peptidases in the body, leading to short biological half-lives and a low bioavailability.[67] Therefore, this project aimed to investigate peptoids as potential improved antiparasitic agents against *L. mexicana* and cutaneous leishmaniasis.

		AMP	*Leishmania* spp.	IC_{50} (μM)
Invertebrate	195	CA(1-8)M(1-18) *KWKLFKKIGIGAVLKVLTTGLPALIS*	*L. donovani* promastigotes	1–5
	196	CA(1-7)M(2-9) *KWKLFKKIGAVLKVL*	*L. donovani* and *L. pifanoi* axenic amastigotes	< 1
	197	Oct-CA(1-7)M(2-9) *Oct-KWKLFKKIGAVLKVL*	*L. infantum* blood circulating amastigotes	< 1
	198	Gomesin *pECRRLCYKQRCVTYCRGR_{NH2}*	*L. amazonensis* promastigotes	2.5
	199	Sandfly defensin-1 *ATCDLLSAFGVGHAACAAHCIGHGYRGG YCNSKAVCTCRR*	*L. amazonensis* and *L. major* promastigotes	> 50
Amphibian	200	Bombinin H2 and H4 *IIGPVLGLVGSALGGLLKKI*	*L. donovani* and *L. pifanoi* promastigotes/axenic amastigotes	7/11
	201	Dermaseptin-S1 *ALWKTMLKKLGTMALHAGKAALGAAAD TISQGTQ*	*L. amazonensis* and *L. major* promastigotes/amastigotes	4.5/13.5
	202	Skin peptide-TyrTyr *YPPKPESPGEDASPEEMNKYLTALRHYINL VTRERY*	*L. major* promastigotes/amastigotes	5.9/6.2
	203	Phylloseptin-1 *FLSLIPHAINAVSAIAKHN*	*L. amazonensis* promastigotes	0.5
	204	Temporin A *FLPLIGRVLSGIL*	*L. infantum* and *L. mexicana* promastigotes/ amastigotes	12/50
Mammalian	6	β-defensin-1 *DHYNCACMGG*	*L. amazonensis* and *L. major* promastigotes/amastigotes	20/50
	205	Histatin 5 *DSHAKRHHGYKRKFHEKHHSHRGY*	*L. donovani* promastigotes/amastigotes	7.3/14.2

Table 3.3. A selection of anti-leishmanial AMPs, their peptide sequence in grey and their recorded antiparasitic activity. All peptides are amidated at the C terminus. *pE* represents pyroglutamic acid and R_{NH2} post-translational amidation of arginine.[70]

3.2   Antiparasitic peptoids in the literature

As discussed in Chapter 1, in recent years, a number of peptoids have been shown to be potent and promising antimicrobials against a wide variety of clinically relevant fungi, Gram negative and Gram positive bacteria with activities similar to leading AMPs.[71-80] However as yet, very few groups have investigated the effect of peptoids against parasites therefore there is little information available to aid the rational design of antiparasitic peptoids.

A study from the Olsen group tested α-peptide β-peptoid chimeras against *Plasmodium falciparum*, one of the causative agents of malaria. The compounds were designed with alternating β-peptoids and α-amino acids to give lipophilicity and side-chain functionality respectively. For certain sequences, sub-hemolytic doses showed anti-plasmodial activities, with the best IC_{50} of 3.6 µM for **206** shown in **Figure 3.5**, however it was noted that although these chimeras had low hemolytic activity, they caused severe membrane alterations in human red bloods cells observed via phase-contrast light microscopy.[81]

Peptoids have also been investigated as inhibitors of trypanothione reductase, vital for *Trypanosoma* and *Leishmania* species. These parasites use trypanothione instead of the glutathione redox based defence system in mammalian organisms and as this enzyme is not present in mammals, selective inhibition of trypanothione reductase has been proposed as a drug target. The Douglas and Fairlamb groups had previously shown that peptides could act as strong inhibitors of trypanothione reductase and modelled peptoids on these leads. Successful inhibition was seen with several peptoids in kinetic enzymatic assays and the most successful peptoid (see **207** in **Figure 3.5**) only weakly inhibited glutathione reductase in human erythrocytes giving a promising selectivity ratio.[82]

206
IC_{50} = 3.6 µM

207
K_i = 179 µM
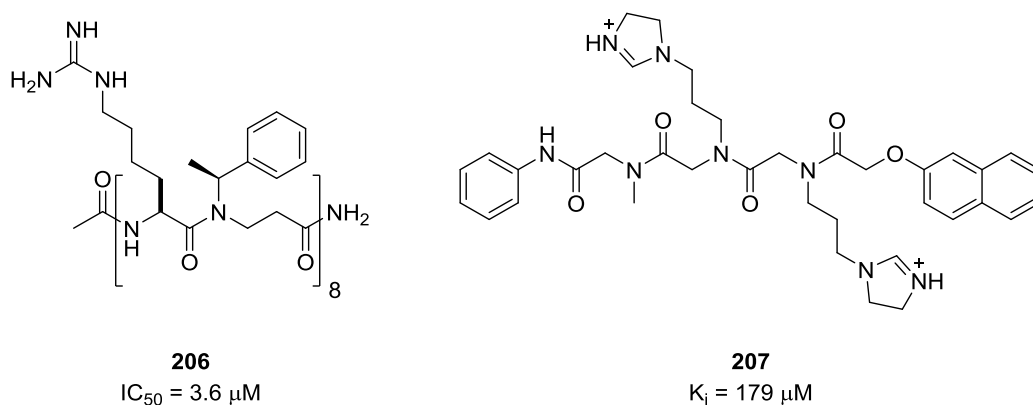
Figure 3.5. Structures of **206** the peptide-peptoid chimera with activity against *P. falciparum* and **207** the trypanothione reductase inhibitor.[81,82]

3.3 Determination of peptoid activity against *Leishmania mexicana*

In order to assess the potential leishmanicidal activity of peptoids, the library synthesised in chapter 2 was screened against insect and mammalian stage parasites of *Leishmania mexicana*, the causative agent of CL.

3.3.1 Leishmania testing

The peptoids were screened against MYNC/BZ/62/M379 *L. mexicana* in a high throughput alamarBlue® assay with results described in sections 3.3.4, 3.3.5 and 3.3.6. This is the first time that peptoids have been tested in whole cell, phenotypic parasite cytotoxicity assays. Due to the vast differences between *Leishmania* lifestages, compounds were screened against both the procyclic promastigote and the axenic amastigotes. Promising compounds were also tested against mammalian macrophages infected with *L. mexicana* amastigotes in section 3.3.8 as a more realistic model of the disease *in vivo*.

The detailed and optimised experimental protocol for these assays can be found in Chapter 7. However, in brief, compounds to be tested were added to 96 well plates in triplicate and serial dilutions carried out from 100 µM to 3 µM. Appropriate controls were also added to the plate; amphotericin B (**191**) as positive control, DMSO vector only negative controls and wells containing medium only to allow correction for background fluorescence. Parasites were subcultured, added to the plates in appropriate media and incubated with the peptoids for 60 minutes. After the incubation time, the wells were diluted ten-fold, followed by a further incubation of 24 hours. In order for quantitative results to be obtained at the end of the assay, the cell viability reagent alamarBlue® was added to each well[†] and incubated for 4 hours at the appropriate temperature for the parasite culture; 26 °C for promastigotes and 32 °C for amastigotes.
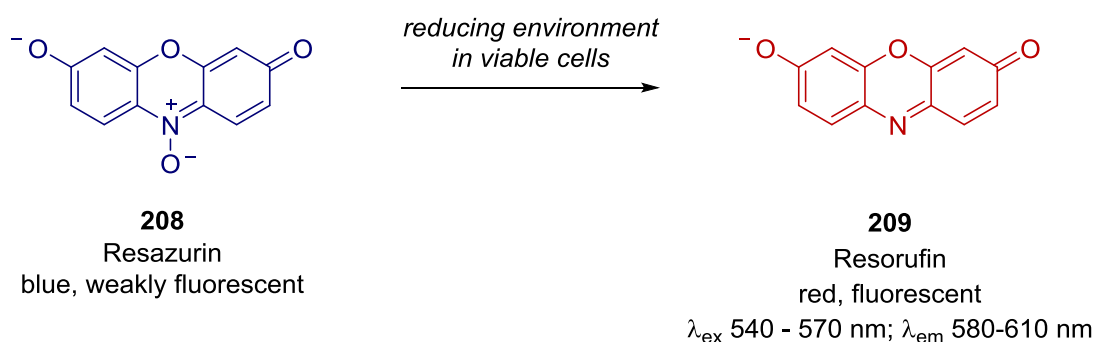
Scheme 3.1. The reduction of resazurin to the fluorescent resorufin, used as the active ingredient in alamarBlue® cell viability reagent.

[†] 10 % of well volume, following the recommended protocol from the manufacturer.

AlamarBlue® quantitatively assesses cell viability using the reducing activity of living cells via a fluorescent or colorimetric detection technique. The active ingredient of alamarBlue® is resazurin, a non-toxic and cell permeable compound that is blue and non-fluorescent. When the dye enters living cells, the resazurin (**208**) is reduced to a red and highly fluorescent compound, resorufin (**209**) as shown by **Scheme 3.1**. The cell viability can then be calculated from the fluorescence emission intensity, larger values correlate to increased total metabolic activity from the cells.[83]

Although the *in vitro* alamarBlue® assay has limitations (i.e. exposure times will be very different *in vivo*, pharmacokinetic factors such as excretion and tissue penetration are not considered and suppressed cell proliferation cannot be quantified) the assay was used for first round toxicity evaluation.

Seeding tests and growth curves were also carried out to ensure that the seeding density and conditions were appropriate for the cell line. Since different amounts of foetal bovine serum (FBS) are required for the culture of promastigote and amastigotes[‡], several peptoids were also tested in serum-free conditions in the first 60 minute incubation to determine the effect, if any, of FBS on antiparasitic activity. Results showed that the serum had little effect on the anti-leishmanial effect of the peptoids (see data in the Appendices) so future assays were all undertaken with serum as these conditions are more representative of biological conditions. This is in contrast to many previous studies with AMPs, where clear and measurable differences are seen between serum and serum-free assays due to the higher susceptibility of AMPs to proteases.[67,84,85]

3.3.2   Cytotoxicity assays against mammalian cell lines

Alongside the parasite assays, the same high throughput alamarBlue® screening was adapted for two mammalian cell lines[§] to determine the cytotoxicity of the peptoid library. The ultimate aim of this project is to develop compounds that could be used as new therapeutics, in the case of cutaneous leishmaniasis (CL) this would be as a topical application. Ideally, any drug should be selective to the target and balance desired activity with toxicity to human cells.

Compounds in the peptoid library were tested against human epithelial cell lines, HaCaT and HepG2, to model toxicity against skin cells and liver cells respectively. The HaCaT line consists of spontaneously transformed aneuploid keratinocytes and the HepG2 are human liver carcinoma cells. Cultures of both cell lines are frequently used in *in vitro* studies of cytotoxicity or cell function as they are both immortal cell lines and because cells have high and reproducible proliferation and differentiation rates *in vitro*.[86-89]

HaCaT or HepG2 cells were subcultured and prepared in 96 well plates prior to the assay then incubated in the presence of peptoid solutions in DMSO for 1 hour (concentrations

---

[‡] 15 % FBS in pH 7.0 promastigote culture and 20 % FBS in pH 5.5 amastigote culture.
[§] Specific adaptations used in mammalian cytotoxicity assay are summarised in the Experimental Chapter 7.

between 3 and 100 μM). Solutions were then removed from the plates, the cells washed with PBS and new medium added. Cells were incubated for a further 24 hours and the viability of cells measured by addition of alamarBlue®. DMSO vector controls were used and as with the results from the *L. mexicana* assays, all compounds were screened in triplicate on a minimum of two occasions to ensure that a robust data set was collected.

3.3.3 Library design

For initial screening purposes, the peptoid sequences were designed around a linear *N*x*N*y*N*y motif, which was repeated to give 6, 9 or 12 residue peptoids. This repeating motif was used as peptoid helices are reported to have 3.0 residues per turn. By placing a hydrophilic residue in the *N*x position and hydrophobic monomers for *N*y, the formation of an amphiphillic structure may be encouraged where all the hydrophilic groups are positioned on the same side of the helix. This has often been shown to aid antimicrobial action in AMPs.[76,90]

Due to the lack of information available to aid in the design of antiparasitic peptoids, the initial peptoid library synthesised included only five monomers combined in the *N*x*N*y*N*y motif. In these sequences, the *N*y monomer was either the chiral aromatic *N*-(*S*)-(1-phenylethyl) glycine residue (*N*spe) or the achiral *N*-(benzyl) glycine (*N*phe). As discussed in Chapter 2, inclusion of sterically bulky and aromatic monomers in close proximity can favour the formation of a helical structure, another factor known to enhance activity in antimicrobial peptides.[91,92] For the hydrophilic *N*x, cationic lysine-type monomers were chosen with varying length of side chain; *N*-(2-aminoethyl) glycine, *N*-(4-aminobutyl) glycine or *N*-(6-aminohexyl) glycine (*N*ae, *N*Lys and *N*ah with 2, 4 and 6 carbons respectively as shown in **Figure 3.6A**). This first generation library[93] allows the effect of overall sequence length, sequence chirality and the nature of the cationic *N*x monomer on the anti-leishmanial activity to be determined.

In a second generation library,[94] a further 30 novel linear peptiods were synthesised to include a range of substituted aromatic and aliphatic monomers (monomer structures shown in **Figure 3.6A**). This library contains more varied side chain substituents to provide a more in depth investigation of structure activity relationships. To add extra diversity to these peptoids, sequences were also designed around four motifs (**Figure 3.6B**). The first was the *N*x*N*y*N*y motif used in the first generation library, again repeated two, three or four times to give 6, 9 or 12 residue peptoids respectively. In a further iteration, a second hydrophobic building block was introduced into each sequence (motif 2), i.e. *N*x*N*y*N*z where *N*y and *N*z were either an aromatic or alkyl residue. To investigate if the sequence specific position if *N*y or *N*z influenced the activity, they were also placed in a co-block manner (motif 3). In the final motif 4, the overall charge of a 12 residue peptoid was reduced by replacing one or two of the charged *N*Lys residues with the uncharged *N*amy monomer. The five carbon *N*amy monomer has the same molecular weight and has a side chain five carbons in length, so differs only in the chemical functionality.

A

'Charged' residues

Nae

NLys

Nah

Aromatic residues

Nspe

Nphe

Npfb

Nmfb

Npcb

Npmb

Alkyl residues

NnVal

NLeu

NhLeu

Namy

B

Motif 1 — 12mer, 9mer, 6mer

Motif 2 — 12mer, 9mer, 6mer

Motif 3 — 12mer, 9mer, 6mer

Motif 4 — 12mer, 12mer, 12mer, 12mer
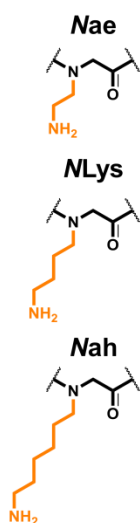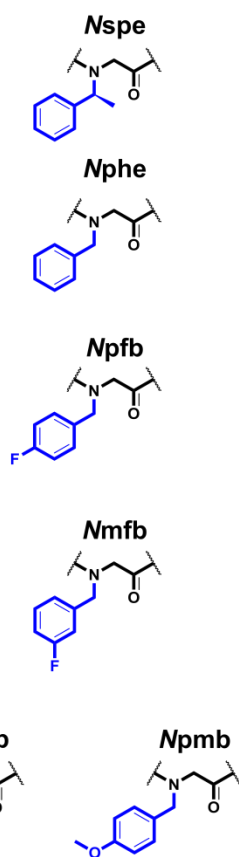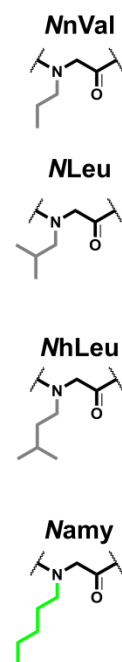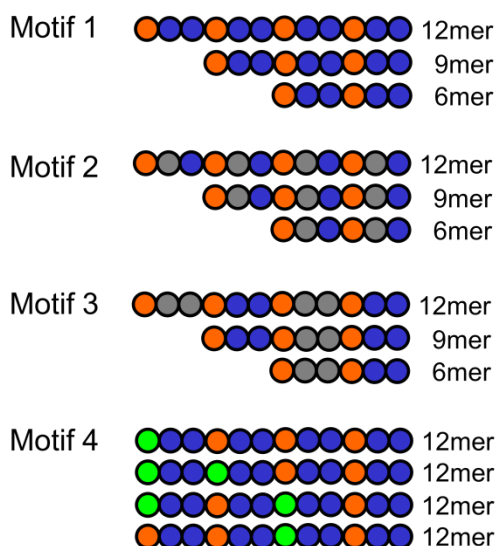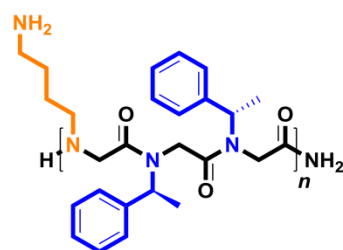
Example structure:

where n = 2, 3 or 4

Figure 3.6. **A** The chemical structures of the monomers used in this peptoid library with their abbreviations; **B** Different structural motifs used in the SAR study are also shown with an example of the repeating trimer repeat.

3.3.4 First generation library screening: the effect of sequence length, chirality and cationic monomer on anti-leishmanial activity

From the anti-leishmanial assay described in section 3.3.1, the parasite viabilities can be determined following treatment with peptoids of different concentrations. From this data, the effective median dose (ED_{50}) for each compound can be calculated and this data is tabulated in **Table 3.4** for the first generation peptoid library. The amphotericin B control used in the assay behaved as expected, with a reduction in nearly 100% of parasites at the lowest concentration tested to give an ED_{50} less than 2 μM.

	Compound	ED_{50} *L. mexicana* (μM)		ED_{50} mammalian cells (μM)	
		Promastigotes	Amastigotes	HaCaT	HepG2
191	*Amphotericin B*	*< 2*	*< 2*	*> 100*	*> 100*
210	(Nah*N*phe*N*phe)$_4$	21	> 100	> 100	> 100
211	(Nah*N*phe*N*phe)$_3$	> 100	> 100	> 100	> 100
212	(Nah*N*phe*N*phe)$_2$	> 100	> 100	> 100	> 100
186	(*N*Lys*N*phe*N*phe)$_4$	15	> 100	36	> 100
187	(*N*Lys*N*phe*N*phe)$_3$	> 100	> 100	> 100	> 100
188	(*N*Lys*N*phe*N*phe)$_2$	> 100	> 100	> 100	> 100
180	(Nae*N*phe*N*phe)$_4$	21	> 100	> 100	> 100
213	(Nae*N*phe*N*phe)$_3$	> 100	> 100	> 100	> 100
214	(Nae*N*phe*N*phe)$_2$	> 100	> 100	> 100	> 100
215	(Nah*N*spe*N*spe)$_4$	11	> 100	23	41
216	(Nah*N*spe*N*spe)$_3$	25	> 100	> 100	> 100
217	(Nah*N*spe*N*spe)$_2$	> 100	> 100	> 100	> 100
185	(*N*Lys*N*spe*N*spe)$_4$	8	> 100	20	29
22	(*N*Lys*N*spe*N*spe)$_3$	15	> 100	> 100	> 100
26	(*N*Lys*N*spe*N*spe)$_2$	> 100	> 100	> 100	> 100
25	(Nae*N*spe*N*spe)$_4$	7	17	26	41
156	(Nae*N*spe*N*spe)$_3$	10	> 100	> 100	> 100
218	(Nae*N*spe*N*spe)$_2$	> 100	> 100	> 100	> 100

Table 3.4. Activity of the first generation peptoid library against *L. mexicana* pro and amastigotes, including their toxicity to mammalian cell lines. Please see the Appendices for side chain abbreviations.

Effect of sequence length

The results show that the longest peptoid sequences show the lowest ED_{50} values against *L. mexicana* and therefore the most potent activity with the activity increasing as the sequence is lengthened. For example, all of the shortest 6 residue peptoids (**212**, **188**, **214**, **217**, **25** and **219**) were completely inactive against both promastigotes and amastigotes, even at the highest 100 μM concentration tested. The 9 residue peptoids show intermediate activity to the promastigotes, with some sequences with the chiral *N*spe monomer showing good activity against the insect stage promastigotes (ED_{50} 25 μM,

15 µM and 10 µM for **216**, **26** and **218**). Following this pattern, the 12 residue peptoids displayed the best leishmanicidal activities against the promastigotes, with peptoid **156** being the only compound in this library to show any activity against the amastigotes (ED_{50} 17 µM, structure as in **Figure 3.7**).
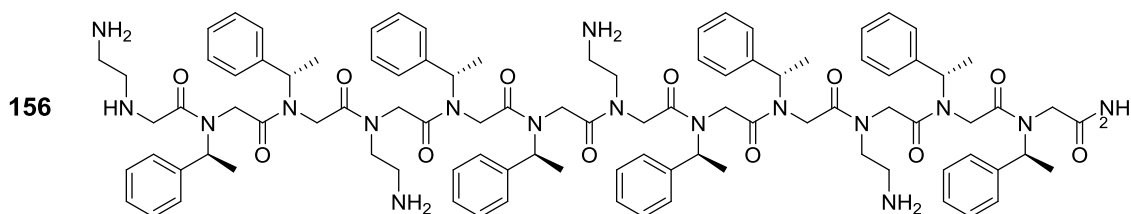
Figure 3.7. Structure of peptoid **156** that shows activity against *L. mexicana* promastigotes ED_{50} 7 µM and amastigotes ED_{50} 17 µM.

Effect of sequence chirality

To examine the effect of chirality peptoids with the *N*spe and the achiral *N*phe monomers were compared and it can be concluded that those peptoid with the chiral monomer display better activity (data in **Table 3.4**). Amongst the 12 residue peptoids the *N*spe analogues show significantly lower ED_{50} values than those containing *N*phe; for example compare peptoids **22** and **186** (*N*spe and *N*phe respectively) with activity of 8 µM and 15 µM or **156** and **180** with ED_{50} 7 µM and 21 µM. However, the extra contribution to hydrophobicity from the additional methyl group of *N*spe could also provide an explanation for this trend. Therefore, further investigations into the hydrophobicity of chiral and achiral peptoids was therefore undertaken to aid the rationalisation of the biological activity of our libraries and this is discussed in Chapter 5.

Effect of cationic monomer choice

The anti-leishmanial activity of the peptoids was also increased as the chain length of the cationic monomer in the *N*x position is decreased. Therefore the *N*ae monomer has better activity against the *L. mexicana* than the *N*Lys monomer, which itself has better activity than *N*ah. I.e. activity *N*ae > *N*Lys > *N*ah, as evidenced by comparing **156**, **22** and **215** (**Table 3.4**). These differences in activity could stem from the greater flexibility of the longer side chains

The *N*ae peptoid **218** is the most potent 9 residue peptoid in the library (ED_{50} 10 µM), followed by the *N*Lys analogue then the *N*ah sequence (ED_{50} of 15 µM for **26** and 25 µM for **216**). Peptoid **156** (*N*ae*N*spe*N*spe)$_4$ is the only member of the library to show activity against the axenic amastigotes with an ED_{50} of 17 µM. Analogous peptoids **22** (*N*Lys) and **215** (*N*ah) decrease parasite viability by 70 % and 80 % respectively at 100 µM but at

lower concentrations activity was negligible. Notably, the ED_{50} for **218** is similar to the activity recorded for AMPs against various amastigote-stage *Leishmania* spp.[70]

All the peptoids are more potent against promastigotes (insect stage) than amastigotes (mammalian stage parasites) of *L. mexicana*. This trend was also seen in previous work from our group with the temporin family of antimicrobial peptides.[67] Differences in the membrane structure of the two life stages could explain this behaviour since amastigotes have a minimalist surface glycocalyx and the LPG and PPG layer, found on promastigotes, is down-regulated. It is thought that the PPG layer may help to target cationic compounds to the cell membrane. Due to the significantly different behaviour of the compounds against the two parasitic life stages, mechanistically it is proposed that the peptoids act on the cell membranes, although further work is needed to confirm this.[21]

Toxicity to mammalian cells

Only the longest 12 residue sequences (**186**, **215**, **22**, **156**) displayed a level of toxicity to either of the mammalian cell lines tested (**Table 3.4**). Most sequences showed no toxicity, even at the highest concentration tested (100 µM). Logically, the most active compounds in this library were those that were mildly cytotoxic. However in all cases, the peptoids showed a greater potency against *L. mexicana* than the mammalian cells. For example, the most active peptoid **156** (ED_{50} 7 µM and 17 µM against promastigote and amastigote respectively) shows toxicity of 26 µM and 41 µM against HaCaT and HepG2 so some selectivity is seen in the peptoids.

Photographs of the wells were taken before and after compound treatment to check whether cell growth was inhibited by compounds that were not toxic to the cells, as this is not always reflected in the results of the alamarBlue® assay. **Figure 3.8** compares untreated cells before and after the assay when peptoid **156** is added at different concentrations.
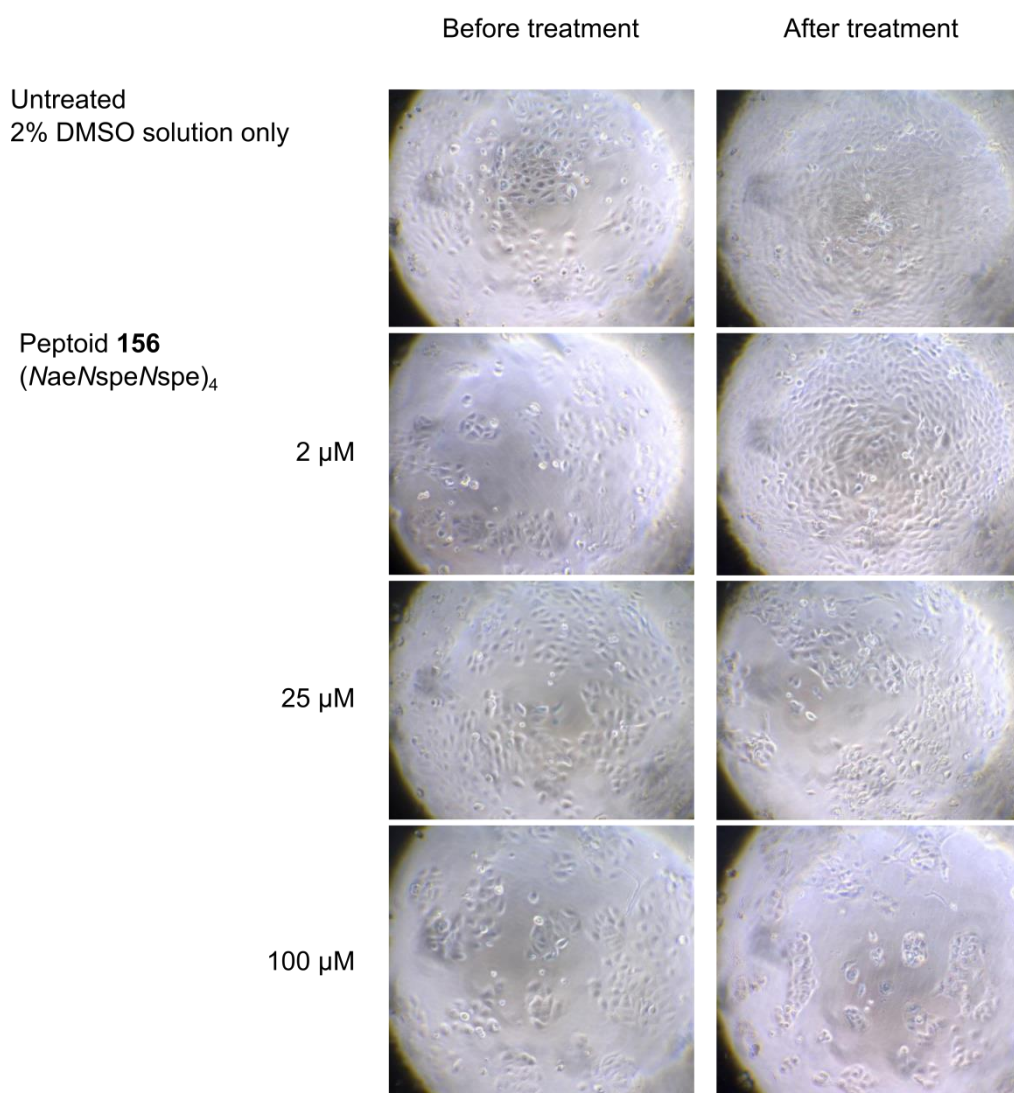
Figure 3.8. Photographs taken of HaCaT in 96 well plates treated by DMSO (control) and peptoid **156**; a) before treatment following a 24 hour subculture and b) after 1 hour incubation with compound, a PBS wash then further 24 hour incubation/recovery time.

As shown by the photos taken of cells incubated with DMSO only, plates were seeded at a density that allowed cell growth over the course of the assay. Peptoid **156,** shown to be cytotoxic (ED$_{50}$ 26 μM) allows the HaCaT to proliferate at 2 μM, similar to the growth seen in the control wells. At the ED$_{50}$, it is noticeable that cell growth is reduced or stalled. Following peptoid treatment at 100 μM, far fewer cells are present in the well and although some cells are still alive[**] they look very different to the healthy HaCaT; cells have a different morphology and granularities around the cell nuclei.

[**] As the cells are still adhered to the plate.

3.3.5 Second generation library screening: the effect of monomer substitutions to anti-leishmanial activity

Peptoids synthesised as part of the extended, second generation library are shown in **Table 3.5**. In these compounds, the cationic monomer was *N*Lys exclusively to allow comparison between the whole library and a variety of commercially available amines were incorporated into the sequences to provide sequence diversity. The peptoids prepared were also tested against both *L. mexicana* promastigotes and amastigotes, with many showing improved activity compared to the first generation library.

Substitution of aromatic residues in the peptoid sequence

The effect of substitution on the aromatic residues was investigated through the inclusion of *N*pmb, *N*pcb, *N*pfb and *N*mfb monomers. Peptoids with the achiral *N*pmb (methoxy substitution in the para position) residue showed significantly reduced potency against the *L. mexicana* promastigotes (see **Table 3.5**). For the 12 residue sequence **220** the ED_{50} was 42 µM, which is a three-fold reduction in activity compared to the *N*phe analogue (**186** ED_{50} 15 µM). The shorter 6 and 9 residue *N*pmb peptoids, **221** and **222**, did not show any activity to the promastigotes and no activity was found against the amastigotes for any sequence length of the *N*pmb peptoids.

In contrast, the peptoids substituted with halogens on the aromatic monomers showed enhanced activity against the axenic amastigotes and maintained activity against the insect stage promastigotes (peptoids **184** and **223–230**) *cf* the unsubstituted analogues (**186–188** in **Table 3.5**). Peptoids with a chloro substitutent in the para position of the phenyl ring (*N*pcb) were all active against the promastigotes, but only the longer 9 and 12 residue sequences, **223** and **184**, showed any activity against the axenic amastigotes, with ED_{50} values of 85 and 44 µM respectively.

For peptoids substituted with fluorine there is little overall effect on activity whether the fluorine atom is in the para or meta position (*N*pfb or *N*mfb) and only the longest 12 residue sequences showed any activity against the amastigotes (ED_{50} **225** 75 µM and **228** 69 µM in **Table 3.5**). However, these achiral fluorinated peptoids were efficacious against the promastigotes with similar potency to the chiral, non-halogenated sequences **186–188**. The 9 residue sequences **226** and **229** showed antiparasitic activity in the low micromolar range (19 µM and 17 µM), although the shortest 6 residue peptoids didn't show any activity to either stage of the parasite. This provided compelling evidence that fluorination of peptoids may be a good strategy to increase the biological activity of sequences.

Compound		ED$_{50}$ *L. mexicana* (μM)		ED$_{50}$ mammalian cells (μM)	
		Pro	Ama	HaCaT	HepG2
191	*Amphotericin B*	< 2	< 2	> 100	> 100
220	(*N*Lys*N*pmb*N*pmb)$_4$	42	> 100	41	>100
221	(*N*Lys*N*pmb*N*pmb)$_3$	> 100	> 100		
222	(*N*Lys*N*pmb*N*pmb)$_2$	> 100	> 100		
184	(*N*Lys*N*pcb*N*pcb)$_4$	28	44	18	22
223	(*N*Lys*N*pcb*N*pcb)$_3$	22	85	22	23
224	(*N*Lys*N*pcb*N*pcb)$_2$	29	> 100		
225	(*N*Lys*N*pfb*N*pfb)$_4$	15	75	46	30
226	(*N*Lys*N*pfb*N*pfb)$_3$	19	> 100	> 100	45
227	(*N*Lys*N*pfb*N*pfb)$_2$	> 100	> 100		
228	(*N*Lys*N*mfb*N*mfb)$_4$	14	69	25	17
229	(*N*Lys*N*mfb*N*mfb)$_3$	17	> 100	64	43
230	(*N*Lys*N*mfb*N*mfb)$_2$	> 100	> 100		
183	(*N*Lys*N*pfb*N*spe)$_4$	8	27	20	26
231	(*N*Lys*N*pfb*N*spe)$_3$	13	> 100	52	36
232	(*N*Lys*N*pfb*N*spe)$_2$	> 100	> 100		
157	[(*N*Lys*N*pfb*N*pfb)(*N*Lys*N*spe*N*spe)]$_2$	6	21	78	55
233	(*N*Lys*N*spe*N*spe)(*N*Lys*N*pfb*N*pfb)(*N*Lys*N*spe*N*spe)	13	> 100	65	43
234	(*N*Lys*N*pfb*N*pfb)(*N*Lys*N*spe*N*spe)	> 100	> 100		
235	(*N*Lys*N*nVal*N*spe)$_4$	> 100	> 100	> 100	
236	(*N*Lys*N*nVal*N*spe)$_3$	> 100	> 100		
237	(*N*Lys*N*nVal*N*spe)$_2$	> 100	> 100		
238	(*N*Lys*N*Leu*N*spe)$_4$	> 100	> 100	> 100	
239	(*N*Lys*N*Leu*N*spe)$_3$	> 100	> 100		
240	(*N*Lys*N*Leu*N*spe)$_2$	> 100	> 100		
182	(*N*Lys*N*hLeu*N*spe)$_4$	12	> 100	> 100	
241	(*N*Lys*N*hLeu*N*spe)$_3$	52	> 100		
242	(*N*Lys*N*hLeu*N*spe)$_2$	> 100	> 100		
243	(*N*amy*N*spe*N*spe)[(*N*Lys*N*spe*N*spe)]$_3$	8	21	12	15
244	(*N*amy*N*spe*N*spe)$_2$(*N*Lys*N*spe*N*spe)$_2$	11	16	20	18
245	[(*N*amy*N*spe*N*spe)(*N*Lys*N*spe*N*spe)]$_2$	10	17		
246	(*N*Lys*N*spe*N*spe)$_2$(*N*amy*N*spe*N*spe)(*N*Lys*N*spe*N*spe)	10	15	20	22

Table 3.5. Activity of the second generation peptoid library against *L. mexicana* pro and amastigotes, including their toxicity to mammalian cell lines.

From the data collected in the first screening, it was determined that peptoids with the chiral and aromatic *N*spe monomer show better activity than those containing the achiral *N*phe. Therefore, a further set of fluorinated peptoids were synthesised where *N*spe was combined with the *N*pfb building block in two motifs (peptoids **183**, **157 231–234**; motifs 2 and 3 in **Figure 3.6**). When comparing peptoids of the same length in these motifs, both versions had similar activity against both lifestages of *L. mexicana*. For example, **183** (*N*Lys*N*pfb*N*spe)$_4$ had an ED$_{50}$ value of 8 μM against the promastigotes and the co-block peptoid **157** [(*N*Lys*N*pfb*N*pfb)(*N*Lys*N*spe*N*spe)]$_2$ displayed an activity of

6 µM. This level of activity against the promastigotes is comparable to the unsubstituted, chiral peptoid **22** (NLysNspeNspe)$_4$ that has an ED$_{50}$ of 8 µM and is two-fold better than the sequence containing Npfb exclusively, peptoid **225**, which had an ED$_{50}$ of 15 µM. However, the activity between **183/157** and **22** against the axenic amastigotes was improved. The NspeNpfb peptoids showed good activities (ED$_{50}$ 27 µM and 21 µM respectively) but the Nspe-only peptoid was inactive and peptoid **225** showed only moderate activity of 75 µM.

The toxicity data collected for these compounds is also shown in **Table 3.5**. From this data, it appears that sequences containing the Npcb residue are more toxic to mammalian cells than either Npfb or Nmfb. For example, when comparing the 12 residue peptoids **184** (NLysNpcbNpcb)$_4$ and **225** (NLysNpfbNpfb)$_4$, lower ED$_{50}$ values are recorded for **225** against L. mexicana (28 µM cf 15 µM), yet the less active **184** has greater toxicity to both HaCaT and HepG2 than **225** (ED$_{50}$ HaCaT 18 µM cf 46 µM; ED$_{50}$ HepG2 22 µM cf 30 µM). This trend also holds for the shorter sequences in the library and when comparing Npcb to Nmfb.

In sequences where Nspe is used in combination with Npfb in motif 2, in general lower ED$_{50}$ values are seen against the mammalian cell lines so these compounds are more cytotoxic (i.e. compare the 12 residue peptoids **225** with **183**, ED$_{50}$ against HaCaT 46 µM and 20 µM respectively). However, less toxicity is seen when these residues are combined in a coblock manner, as in motif 3. In this case, peptoid **157** is illustrative (see **Figure 3.9**), with ED$_{50}$ values of 76 µM for HaCaT and 55 µM against HepG2.
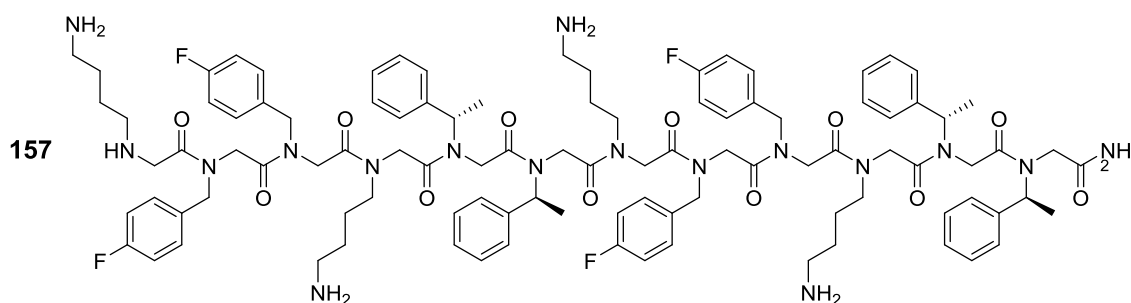
Figure 3.9. Structure of peptoid **157** [(NLysNpfbNpfb)(NLysNspeNspe)]$_2$, the most active compound screened from peptoids with substituted aromatic groups.

Therefore, the combination of the chiral Nspe monomer with the fluorinated Npfb residue helps to improve the overall activity of the sequence against L. mexicana. In particular, combining these two monomers in a coblock manner (motif 3) can help to reduce toxicity to mammalian cells, whilst maintaining potent antiparasitic behaviour. Peptoid **157** was the most active compound from this part of the SAR study with an ED$_{50}$ of 6 µM (promastigotes) and 21 µM (axenic amastigotes).

The effect of alkyl peptoid monomers

The second generation library also included sequences that combine one aromatic residue with one alkyl monomer; either a propyl, isobutyl or isopentyl pentyl side chain (*N*nVal, *N*Leu and *N*hLeu correspondingly). These peptoids were based upon motif 2, compounds **235–242**.

As shown by **Table 3.5**, none of these peptoids showed much activity against either life stage of *L. mexicana.* Only the 12 and 9 residue peptoids containing the *N*hLeu building block showed any activity (ED$_{50}$ promastigotes: **182** 12 µM and **241** 52 µM). The toxicity of the longest 12 residue peptoids containing these alkyl monomer were also assessed against the HaCaT keratinocytes and none showed any effect at the highest concentration tested.

The reduced activity of peptoids **235–242** to both *L. mexicana* and the mammalian cells could be due to a lack of stable helical structure. Only a third of residues in each sequence are aromatic and previous work has shown that sequences should have at least half aromatic residues, preferably α-chiral, to induce a helix.[95] Alternatively, the poor biological activity may be explained by the reduced overall hydrophobicity of the compounds. This result highlights that as expected, the size and chemical functionality of peptoid monomers is highly important for anti-leishmanial efficacy.

Reduction of overall sequence charge

In the further design iteration of motif 4, *N*Lys residues in the *N*x position were replaced by the alkyl building block *N*amy. In peptoids **243–246**, the terminal amino group of either one or two *N*Lys monomers was replaced by a methyl group. Thus, the net positive charge of the peptoid is reduced but the overall molecular weight remains unchanged. Despite the poor activity seen when alkyl chains replaced an aromatic residue in motif 2, peptoids **243–246** following motif 4 were the most potent in the library. An example structure for these peptoids is shown in **Figure 3.10**.
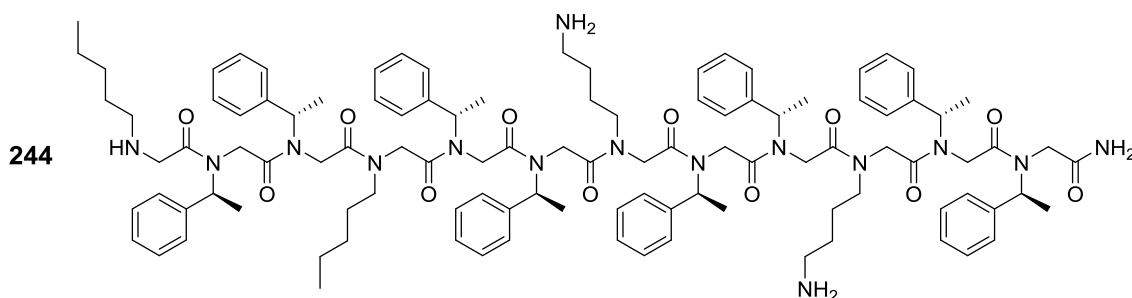
Figure 3.10. Structure of peptoid **244** (*N*amy*N*spe*N*spe)$_2$(*N*Lys*N*spe*N*spe)$_2$ where several cationic monomers are replaced by the uncharged *N*amy residue.

For all compounds in the first and second generation library discussed so far, the promastigotes are more susceptible to peptoid treatment than the axenic amastigotes. As already mentioned, this is probably due to the large differences in the cell surface coat of each parasite. However, for all four peptoids with a reduced net charge (**243–246**) there is a smaller difference between potencies against promastigotes and amastigotes, as seen by ED_{50} values in **Table 3.5**. For example, against the promastigotes ED_{50} values were between 8 μM and 10 μM for peptoids **243–246**. The activity against the amastigotes for these peptoids was also in the low micromolar range (ED_{50} 15–21 μM). These results suggest that the increased hydrophobicity and reduced charge of the *N*amy residue can increase the biological activity when compared to the amino groups found on *N*Lys. No significant difference was seen if the overall positive charge was reduced by 1 or 2, or in which position the residue(s) were replaced.

Unfortunately the four peptoids **243–246** also show elevated cytotoxicity against the mammalian cells ($ED_{50} < 20$ μM for all compounds against both HaCaT and HepG2). This indicates that the increase in efficacy is a generic effect. However, the sequences were still slightly more potent against *L. mexicana* than the mammalian cells.

Initial summary

In conclusion, following analysis of the first and second generation linear peptoid libraries active peptoids were identified against *L. mexicana* for the first time (**Table 3.4** and **Table 3.5** respectively).[93,94] Efficacious compounds were found against both promastigotes (insect-stage parasites) and against the axenic amastigotes (mammalian-stage parasites). In this group of 50 peptoids, over 20 were identified with ED_{50} values in the low micromolar range against the promastigote stage of the parasite. Seven compounds also showed low micromolar potencies against the clinically relevant amastigotes, including peptoid **246**, (*N*Lys*N*spe*N*spe)$_2$(*N*amy*N*spe*N*spe)(*N*Lys*N*spe*N*spe), with the best ED_{50} of 15 μM (**Table 3.5**).

A comparison of the active and inactive sequences shows that the overall length of a peptoid and the nature of the individual monomers have a large influence on biological activity. As the peptoid sequence length is increased more potent activity was observed against both lifestages of *L. mexicana*. The chiral aromatic monomer *N*spe, known to stabilise the formation of a helical secondary structure in peptoids, was found to increase the antiparasitic effect compared to the achiral *N*phe analogues. It is also clear that the more hydrophobic a compound is, the more potent it becomes, presumably due to greater membrane permeability. When examining the effect of different amino-functionalised side chains, it was found that the shorter chain lengths (*N*ae) gave rise to the most active peptoids and the longest (*N*ah) had the least potent activity.

The investigation also demonstrated a clear difference in the sensitivity of the two life stages of *L. mexicana* to treatment by peptoids, with amastigotes being significantly more resistant. This is also observed with AMPs and is highly likely caused by the different molecules displayed on each of the parasite membranes and how these

influence sensitivity to both peptoids and peptides.[26,51,67] Due to this, it is probable that the active peptoids screened in this study target the cellular membrane of the parasites.

Many sequences in the library display only mild or negligible toxicity to the mammalian cell lines tested. However, the most active peptoids also display the greatest toxicities, with **246** having an ED_{50} of 20 µM and 22 µM against HaCaT and HepG2 respectively. This is a point for improvement, however, in applications against *L. mexicana*, some level of toxicity in a topical treatment may be acceptable. These results provide a basis to begin further SAR studies to explore the activity, mode of action and toxicity of this new class of potential anti-leishmanial compounds. Conclusions drawn from the SAR data were used in the design of a third generation linear peptoid library, which provided an opportunity to further probe the therapeutic window of bioactive peptoids.

3.3.6 Enlarging the chemical space of linear anti-leishmanial peptoids

In a third generation library, most peptoids were prepared using automated synthesisers in collaboration with Professor Ron Zuckermann at the Lawrence Berkeley National Laboratory. This allowed a greater number of compounds to be synthesised with a much larger subset of peptoid monomers included in the sequences.

In the third generation library, a focus was placed on 12 residue peptoids as this length of sequence was shown to have the best activity in the first and second generation libraries. Monomer abbreviations and chemical structures for the sequences outlined in **Table 3.6** are shown in **Figure 3.11**. Firstly, this library contained peptoids with arginine only or the peptoids synthesised by the methodology developed in Chapter 2 to synthesise mixed lysine- and arginine-type monomers within the same sequence.[96] This allowed comparison of the biological activity of these sequences to the amino-only functionalised peptoids of the previous libraries (i.e *N*ae/*N*Lys and *N*nArg/*N*hArg, peptoids **147–155**).

As fluorinated monomers showed increased efficacy, a variety of peptoids were synthesised containing fluorinated building blocks. For example, a variety of aliphatic fluorine monomers were introduced into achiral peptoids (peptoids **247–251**) and chiral analogues of the previous *N*pfb library with the cationic *N*ae residue instead of *N*Lys to further investigate the effect of the length of the cationic sidechain (**252–258**). Other fluorine containing monomers in peptoids **261–267** included the α-chiral fluorinated residue *N*sfb, or achiral monomers such as *N*dfb, *N*tfe or *N*pfp that were used in combination with *N*spe to induce an overall helical peptoid.

As many of the monomers included in the library so far are not representative of natural amino acids, a variety of residues were added to sequences that have moieties seen in amino acids. Peptoids **284–292** include groups such as the imidazole of histidine (*N*hHis), phenolic group from tyrosine (*N*hTyr), the indole of tryptophan-mimic *N*hTrp or thiol from the cysteine-type monomer, *N*hCys. However, it should be noted that these resides have an extra methylene group in the sidechain compared to their peptide equivalents, which may cause significant differences in activity.

	Sequence	Average viability *L. mexicana* (%)	ED$_{50}$ HaCaT (µM)
147	(*N*Lys*N*spe*N*spe)$_2$(*N*hArg*N*spe*N*spe)$_2$	84	> 100
148	(*N*hArg*N*spe*N*spe)$_2$(*N*Lys*N*spe*N*spe)$_2$	7	15
149	(*N*Lys*N*spe*N*spe)(*N*hArg*N*spe*N*spe) (*N*Lys*N*spe*N*spe)$_2$	61	33
150	[(*N*hArg*N*spe*N*spe)(*N*Lys*N*spe*N*spe)]$_2$	50	33
151	[(*N*nArg*N*spe*N*spe)(*N*ae*N*spe*N*spe)]$_2$	76	35
155	(*N*nArg*N*spe*N*spe)$_4$	23	18
247	(*N*ae*N*spe*N*dfea)(*N*ae*N*phe*N*dfea)$_3$	100	> 100
248	(*N*ae*N*spe*N*ea)(*N*ae*N*phe*N*ea)$_3$	100	> 100
249	(*N*ae*N*spe*N*ea)$_4$	100	> 100
250	(*N*ae*N*phe*N*ea)$_2$(*N*ae*N*spe*N*ea)(*N*ae*N*phe*N*ea)	90	> 100
251	(*N*ae*N*phe*N*dfea)$_2$(*N*ae*N*spe*N*dfea)(*N*ae*N*phe*N*dfea)	100	> 100
252	(*N*ae*N*pfb*N*spe)$_4$	7	32
253	[(*N*ae*N*pfb*N*pfb)(*N*ae*N*spe*N*spe)]$_2$	84	7
254	(*N*Lys*N*pfb*N*Lys*N*spe)$_3$	95	> 100
255	(*N*ae*N*pfb*N*ae*N*spe)$_3$	89	> 100
256	(*N*Lys*N*pfb*N*rpe)$_4$	55	11
257	(*N*ae*N*pfb*N*rpe)$_4$	16	34
258	[(*N*ae*N*pfb*N*spe)(*N*Lys*N*pfb*N*spe)]$_2$	71	25
259	(*N*Lys*N*spe)$_6$	100	> 100
260	(*N*ae*N*spe)$_6$	87	> 100
261	(*N*Lys*N*dfb*N*spe)$_4$	23	25
262	(*N*ae*N*dfb*N*spe)$_4$	2	28
263	(*N*Lys*N*sfb*N*sfb)$_4$	2	36
264	(*N*ae*N*sfb*N*sfb)$_4$	4	24
265	(*N*Lys*N*sfb*N*spe)$_4$	38	34
266	(*N*ae*N*tfe*N*spe)$_4$	98	> 100
267	(*N*ae*N*pfp*N*spe)$_4$	42	52
268	[(*N*Glu*N*pfb*N*spe)(*N*Lys*N*pfb*N*spe)]$_2$	22	73
269	(*N*Glu*N*pfb*N*spe)(*N*Lys*N*pfb*N*spe)$_3$	40	37
270	(*N*Glu*N*spe*N*spe)(*N*Lys*N*spe*N*spe)$_3$	52	28
271	(*N*Glu*N*spe*N*spe)(*N*Lys*N*spe*N*spe)$_2$(*N*Glu*N*spe*N*spe)	46	31
272	(*N*Lys*N*spe*N*spe)(*N*Glu*N*spe*N*spe)$_2$(*N*Lys*N*spe*N*spe)	89	27
273	(*N*Glu*N*spe*N*spe)$_2$(*N*Lys*N*spe*N*spe)$_2$	77	28
274	(*N*Glu*N*spe*N*spe)$_2$(*N*ae*N*spe*N*spe)$_2$	62	25
275	(*N*Glu*N*spe*N*spe)(*N*ae*N*spe*N*spe)$_2$(*N*Glu*N*spe*N*spe)	2	75
276	(*N*ae*N*spe*N*spe)(*N*Glu*N*spe*N*spe)$_2$(*N*ae*N*spe*N*spe)	44	> 100
277	(*N*Glu*N*spe*N*spe)(*N*ae*N*spe*N*spe)$_3$	0	8
278	[(*N*Glu*N*spe*N*spe)(*N*ae*N*spe*N*spe)]$_2$	6	49
279	[(*N*Glu*N*spe*N*spe)(*N*Lys*N*spe*N*spe)]$_2$	8	26
280	(*N*Lys*N*but*N*spe)$_4$	100	> 100
281	(*N*ae*N*but*N*spe)$_4$	100	> 100
282	(*N*but*N*spe*N*spe)$_2$(*N*Lys*N*spe*N*spe)$_2$	1	25
283	[(*N*but*N*spe*N*spe)(*N*Lys*N*spe*N*spe)]$_2$	0	19
284	(*N*Lys*N*hHis*N*spe)$_4$	100	> 100
285	(*N*ae*N*hHis*N*spe)$_4$	100	> 100
286	[(*N*ae*N*spe*N*spe)(*N*ae*N*hHis*N*spe)]$_2$	80	> 100
287	(*N*ae*N*hTyr*N*spe)$_4$	82	86
288	(*N*Lys*N*hTyr*N*spe)$_4$	89	> 100
289	[(*N*Lys*N*spe*N*spe)(*N*Lys*N*hTrp*N*spe)]$_2$	65	18
290	[(*N*ae*N*spe*N*spe)(*N*ae*N*hTrp*N*spe)]$_2$	66	10
291	[(*N*Lys*N*spe*N*spe)(*N*Lys*N*pyr*N*spe)]$_2$	93	> 100
292	(*N*Lys*N*hCys*N*spe)$_4$	100	> 100

Table 3.6. Percentage viability *L. mexicana* amastigotes when treated with 100 µM peptoid. ED$_{50}$ values against the mammalian HaCaT cell line also displayed.

It was previously recognised that a reduction in the charge of a peptoid may increase its antimicrobial properties against *L. mexicana* (i.e. the *N*amy peptoids **243–246**). Therefore, peptoids **280–283** were synthesised with the *N*but monomer either in position *N*y of motif 2, or replacing a cationic monomer in position *N*x, as in motif 4. This was to examine whether reducing the charge of peptoids with this alkyl chain could retain activity but decrease toxicity to mammalian cells. A series of peptoids were also synthesised with the glutamic acid analogue *N*Glu to investigate the effect of substitution by an anionic residue (peptoids **268–279**).

Finally, in several peptoids, the repeating three residue repeat unit was changed, either to an alternating *N*x*N*y motif (i.e. peptoids **254**, **255**, **259** and **260**) to examine the effect of this charge: hydrophobicity ratio on activity against *L. mexicana*.
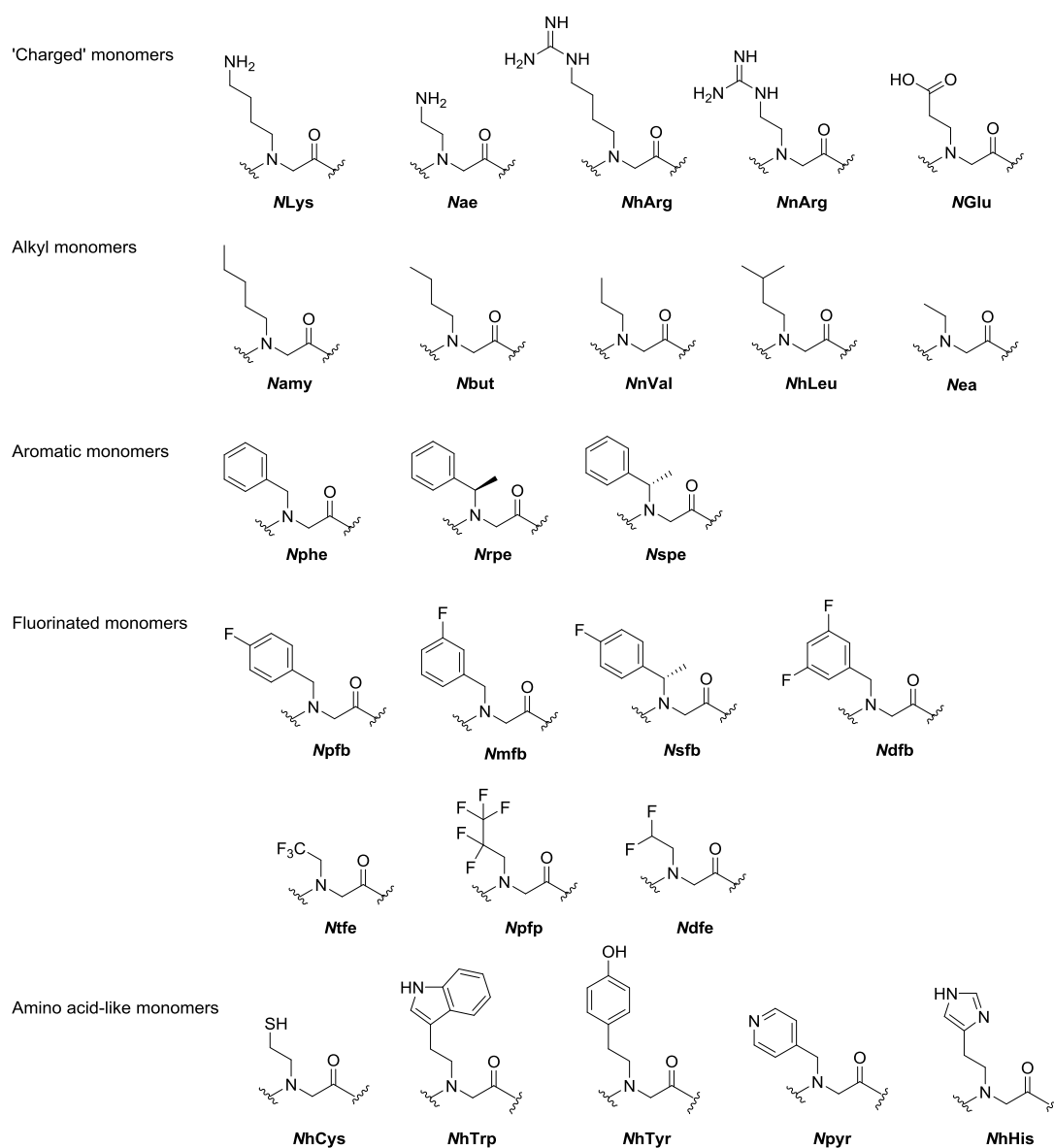
Figure 3.11. Monomers used in the third generation peptoid library and accompanying monomer abbreviations, as discussed in the text.

Following synthesis, cleavage and purification of the library as described in Chapter 2, the peptoids were initially tested in a screen against the *L. mexicana* amastigotes at 100 µM. Assays were only undertaken against amastigotes as it had already been determined that sequences that were active against amastigotes would also almost certainly have some level of activity against the promastigotes, as promastigotes were more susceptible to peptoid treatment in all prior screening.

Peptoids were tested as before in the alamarBlue® high-throughput assay at a concentration of 100 µM against the *L. mexicana* and the population viability reported following treatment compared to positive and negative controls. Additionally, cytotoxicity screening against the HaCaT keratinocytes was undertaken to identify compounds that merited further investigation. The results are shown in **Table 3.6** as a percentage viability of *L mexicana* amastigotes following treatment.

As seen from the data in **Table 3.6**, varying activities are seen for the peptoid library against *L. mexicana* amastigotes and in general, the compounds that showed the greatest percentage reduction in parasite viability also tended to have lower ED_{50} values against HaCaT. Some of the SAR drawn from this testing agrees with the conclusions made previously. For example, as seen in the second generation library, (section 3.3.5) peptoids containing alkyl chains in motif 2 showed little activity (i.e. peptoids **247–251** and **280–281**).

The fluorinated peptoids showed enhanced activities; in particular the inclusion of the α-chiral *N*sfb monomer seemed to increase activity. In peptoids **263** and **264** (in motif 1) the activity was significantly enhanced, decreasing parasite viability to 2 % and 4 %. In motif 2 i.e. compound **265**, the *N*sfb activity was not so strong but still reduced parasite viability to 38 % after 100 µM treatment. However, significant toxicity to the HaCaT was also recorded (ED_{50} of 36 µM, 24 µM and 34 µM respectively for **263**, **264** and **265** respectively).

Similar to the peptoids with a reduced net charge, replacing cationic *N*Lys or *N*ae monomers with either *N*but or *N*Glu residues yields peptoid sequences that can considerably reduce the viability of *L. mexicana*. In the peptoids with the *N*Glu monomers, the net charge is reduced due to the anionic charge of the carboxylic acid side chain and a range of activities were seen depending on the specific positioning of the *N*Glu residues. The most active peptoids reduced parasite viability by nearly 100 % when added at 100 µM (i.e. peptoids **277**, **275**, **278** and **279**). Similar reductions in parasite viability were also seen for the *N*but peptoids **280** and **281**.

When considering the effect of monomers that mimic amino acids upon antiparasitic activity it can be seen that some of these peptoids display negligible toxicity to HaCaT but the parasite population is not greatly affected by treatment of 100 µM. The only significant reduction in viability is seen for the *N*hTrp peptoids (peptoids **289** and **290**, reducing viability to approximately 65 %) but these also are cytotoxic to HaCaT with ED_{50} values of 18 µM and 10 µM respectively.

To help identify peptoids for further investigation, the viability data obtained for each compound was plotted against the ED_{50} value against HaCaT, as shown by **Figure 3.12**. Ideally, any potential future antiparasitic treatment would significantly reduce cell viability of *L. mexicana* but have low toxicity to mammalian cells.

Many peptoids display no activity against either the parasites or the mammalian cells (in the top right corner) and others show toxicity but little activity against *L. mexicana*. The area highlighted on the graph shows a handful of peptoids that show lower toxicity to mammalian cells but have potent activity against the parasites.[††]
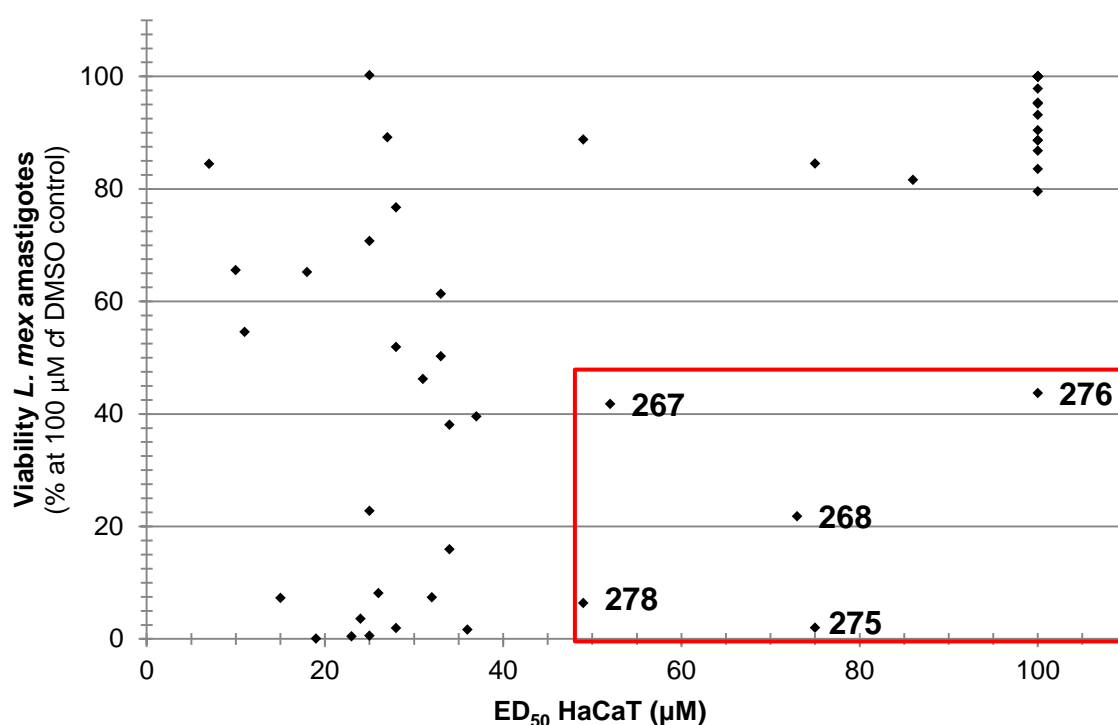
Figure 3.12. Correlation of *L. mexicana* amastigote viability when treated with 100 µM peptoid (sequences as shown in **Table 3.6**) against the median effective dose against HaCaT. Compounds which reduce parasite viability by at least 50 % with an ED_{50} > 40 µM against HaCaT are labelled. **267** (Nae*N*pfp*N*spe)$_4$, **268** [(*N*Glu*N*pfb*N*spe)(*N*Lys*N*pfb*N*spe)]$_2$, **275** (*N*Glu*N*spe*N*spe)(Nae*N*spe*N*spe)$_2$ (*N*Glu*N*spe*N*spe), **276** (Nae*N*spe*N*spe)(*N*Glu*N*spe*N*spe)$_2$(Nae*N*spe*N*spe) and **278** [(*N*Glu*N*spe*N*spe)(Nae*N*spe*N*spe)]$_2$.

Following the identification of peptoids **267**, **276**, **278**, **268** and **275**, ED_{50} determination was undertaken. Other peptoids, such as the arginine-only and mixed lysine- and arginine-type peptoids **293–155** and a few extra sequences **298–303** were also tested to allow a more rigorous SAR discussion.

[††] ED_{50} HaCaT > 50 µM; ED_{50} *L. mexicana* < 50 µM.

Some compounds that had been identified as promising in the viability assay, were subsequently shown to have ED_{50} in excess of 100 μM as no activity was seen at concentrations less than 100 μM. Therefore an ED_{50} value could not be calculated; for example **267** reduces parasite viability to 42 % at 100 μM, but has an ED_{50} > 100 μM.

	Sequence	ED_{50} (μM)	
		L. mexicana amastigotes	HaCaT
293	(*N*hArg*N*phe*N*phe)$_4$	> 100	> 100
294	(*N*hArg*N*phe*N*phe)$_2$	> 100	> 100
152	(*N*hArg*N*spe*N*spe)$_4$	51	20
295	(*N*hArg*N*spe*N*spe)$_3$	> 100	> 100
153	(*N*hArg*N*mfb*N*mfb)$_4$	42	28
296	(*N*hArg*N*mfb*N*mfb)$_3$	> 100	> 100
181	(*N*hArg*N*hLeu*N*spe)$_4$	> 100	> 100
297	(*N*hArg*N*hLeu*N*spe)$_3$	> 100	> 100
154	[(*N*amy*N*spe*N*spe)(*N*hArg*N*spe*N*spe)]$_2$	30	36
147	(*N*Lys*N*spe*N*spe)$_2$(*N*hArg*N*spe*N*spe)$_2$	37	> 100
148	(*N*hArg*N*spe*N*spe)$_2$(*N*Lys*N*spe*N*spe)$_2$	34	15
149	(*N*Lys*N*spe*N*spe)(*N*hArg*N*spe*N*spe)(*N*Lys*N*spe*N*spe)$_2$	> 100	33
150	[(*N*hArg*N*spe*N*spe)(*N*Lys*N*spe*N*spe)]$_2$	37	33
151	[(*N*nArg*N*spe*N*spe)(*N*ae*N*spe*N*spe)]$_2$	> 100	35
155	(*N*nArg*N*spe*N*spe)$_4$	74	18
267	(*N*ae*N*pfp*N*spe)$_4$	> 100	52
268	[(*N*Glu*N*pfb*N*spe)(*N*Lys*N*pfb*N*spe)]$_2$	62	73
275	(*N*Glu*N*spe*N*spe)(*N*ae*N*spe*N*spe)$_2$(*N*Glu*N*spe*N*spe)	33	75
276	(*N*ae*N*spe*N*spe)(*N*Glu*N*spe*N*spe)$_2$(*N*ae*N*spe*N*spe)	41	> 100
278	[(*N*Glu*N*spe*N*spe)(*N*ae*N*spe*N*spe)]$_2$	20	49
298	(*N*Lys*N*spe*N*spe*N*spe)$_3$	33	44
299	(*N*Lys*N*phe*N*spe)$_4$	> 100	> 100
300	(*N*ae*N*phe*N*spe)$_4$	> 100	> 100
301	(*N*Lys*N*rpe*N*rpe)$_4$	> 100	75
302	(*N*ae*N*rpe*N*rpe)$_4$	36	87
303	(*N*ae*N*rpe*N*rpe)$_3$	> 100	> 100

Table 3.7. Median effective dose against *L. mexicana* amastigotes and cytotoxicity data against HaCaT for selected peptoids within the third generation library.

To study the effect of the cationic monomer (i.e. arginine- or lysine-type residues), peptoids **293–154** (arginine-only) can be compared to the mixed functionality sequences **147–155** and the lysine-only analogues from sections 3.3.4 and 3.3.5. Overall, sequences with the arginine-type residues show more potent activity against *L. mexicana* amastigotes, although there are several exceptions, so this effect is sequence dependent. For example, for peptoids with the (*N*x*N*spe*N*spe)$_4$ motif, sequences **152** (*N*hArg) and **22** (*N*Lys) have ED_{50} values of 51 μM and > 100 μM respectively so the arginine-type peptoid

has a greater activity. For sequences with *N*mfb monomers **153** and **228**, again the *N*hArg peptoids show a greater activity than their *N*Lys equivalents (ED$_{50}$ against amastigotes 42 μM compared to 69 μM), although neither of the 9 residue peptoids following this design (**296** and **229**) show any activity with either cationic residue. Equally, the introduction of the arginine-type monomers doesn't make inactive sequences active, i.e. compare the (*N*x*N*phe*N*phe)$_4$ or (*N*x*N*hLeu*N*spe)$_4$ motifs – peptoids **186/293** or **182/181** where neither the *N*Lys or *N*hArg analogues show any activity at 100 μM.

However, when looking at the shorter lysine- or arginine-type monomers, *N*ae and *N*nArg, peptoid **156** has an ED$_{50}$ of 17 μM against *L. mexicana* amastigotes whereas the guanido-functionalised **155** has less potent activity of 74 μM. Therefore, it appears that amino lysine-type residues are more potent at the shorter 2-carbon side chain length than the arginine-type monomers, however this trend is reversed for the longer *N*Lys or *N*hArg building blocks (4 carbons in length). Other exceptions are also seen (for example, peptoids **243** and **154** where the *N*Lys analogue shows the most potent activity) so whether the lysine- or arginine-type monomers induce the greatest activity against the parasites is a sequence-dependent effect.

The peptoids containing the *N*Glu monomers (**268–278**) show intermediate activity against *L. mexicana* axenic amastigotes, but lower toxicity to HaCaT compared to the parent (*N*ae*N*spe*N*spe)$_4$ sequence, peptoid **156** which has ED$_{50}$ values of 17 μM against *L. mexicana* and 26 μM against HaCaT. In the case of peptoid **278**, activity against the amastigotes is at 20 μM, similar to peptoid **156** but the toxicity is reduced two-fold to 49 μM. Therefore, reducing the charge of a sequence with an *N*Glu monomer may retain biological activity but reduce toxicity to mammalian cells, especially when compared to reducing the sequence charge by substitution alkyl monomers like *N*amy.
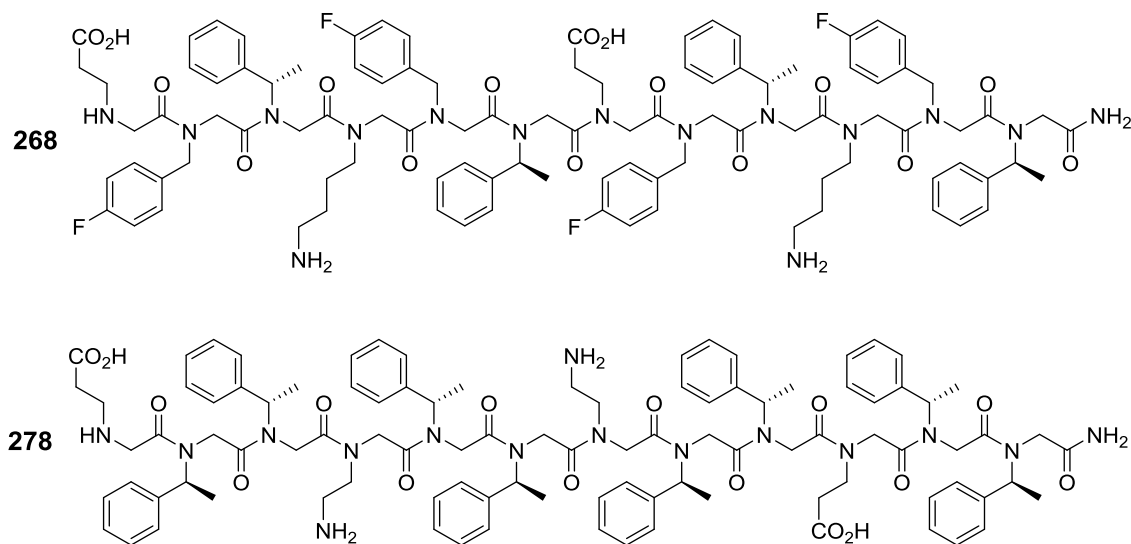
Figure 3.13. Structures of the *N*Glu peptoids **268** and **278**.

Although AMPs are typically cationic to target cell membranes, it is suggested that these *N*Glu peptoids in particular may be interesting candidates for leishmanicidal activity due

to the unique environment in which *Leishmania* parasites reside. The parasites are typically found in acidic parasitophorous vacuoles which are produced by the parasites when inside their host cells, to allow growth whilst protected from host cell defence mechanisms. It has previously been shown that basic drugs can accumulate in these low pH vacuoles and shift the pH higher, which increases the efficacy of the drug against *Leishmania*.[97] Since these peptoids are the sequences with the least positive net charge in the library and *N*Glu residues have basic character, they may also be able to act in a similar manner. Therefore, in section 3.3.8 these sequences were tested in a study of *Leishmania* infected macrophages.

Finally, peptoids **298–303** were synthesised to compare to the simple library in **Table 3.4**. Peptoid **298** (*N*Lys*N*spe*N*spe*N*spe)$_3$ deviates from the typical three monomer repeat unit seen in **22** (*N*Lys*N*spe*N*spe)$_4$ but is still 12 residues in length overall. By changing the periodicity of the sequence, peptoid **298** it is significantly more hydrophobic[‡‡] and shows improved activity against the parasites but less toxicity; ED$_{50}$ *L. mexicana* 33 μM and > 100 μM, ED$_{50}$ HaCaT 44 μM and 20 μM for **298** and **22** respectively.

Peptoids **299** and **300** were synthesised with both *N*spe and *N*phe monomers in an attempt to reduce the toxicity, however neither sequence showed any activity against the parasites. The *N*rpe peptoids **301–303** are enantiomers of the *N*spe peptoids and as expected, show a very similar pattern in activity, although are slightly less potent than the *N*spe sequences **22**, **156** and **218**.

In conclusion, further factors that are necessary for leishmanicidal activity have been elucidated. It has been confirmed that the reduction of net charge from the typical + 4 in the peptoid **22** (*N*Lys*N*spe*N*spe)$_4$ and its analogues can increase the antimicrobial action of peptoids; either by replacement of cationic monomers with alkyl residues such as *N*amy or *N*but or the anionic carboxyl moiety *N*Glu. In the case of replacement by alkyl chains, this is often associated by increased toxicity to mammalian cells. However, in certain sequences where the compound charge is reduced by the inclusion of *N*Glu monomers, the peptoids show negligible toxicity to HaCaT.

The introduction of fluorine is often highly advantageous in pharmaceutical compounds. As a small atom, substitution of hydrogen atoms with a fluorine only causes a small steric change but can modulate lipophilicity, basicity and bioavailability of compounds.[98] Peptoid sequences in this library with fluorinated monomers also display good antiparasitic activities. Since our assay is a simple cell based *in vitro* assay, presumably the increased activity of the fluorine-containing monomers is due to the altered lipophilicity of these sequences.

Finally, it was shown that most active compounds had a significant proportion of α-chiral residues (such as *N*spe, *N*rpe or *N*sfb). As previously reported, the inclusion of such residues can help to induce a helical secondary structure and increase antimicrobial effect.[76,95,99-101]

[‡‡] RP-HPLC retention time 20.0 min for peptoid **298** *cf* 17.6 min for peptoid **22** over a 30 minute gradient.

3.3.7 Cyclic peptoids

Cyclic peptoids **135–144** *were synthesised by Alan-Yao Liu in the laboratory of Professor Kent Kirshenbaum, New York University, USA.*

Cyclisation has been shown to increase the biological activity of peptoids against various bacteria and fungi which is attributed to restricted structures and the removal of charged termini which can increase membrane permeability.[102] Since the smallest, 6 residue peptoids in the first and second generation libraries displayed no activity against *L. mexicana* (see section 3.3.4 and 3.3.5), a few cyclic peptoids were synthesised to investigate if cyclisation could affect an improved biological activity.

The synthesis and design of this library has already been discussed in Chapter 2 and the structures of all cyclic compounds are shown in **Figure 3.14**. Peptoids **130** and **131** were analogues of linear 6 residue peptoids already tested and peptoids **132–134** contain similar monomers but have two-fold periodicity. Compounds **132–134** have a greater net charge and literature studies suggest these compounds will organise with all hydrophobic and hydrophilic residues on opposing faces of the macrocycle, which may increase biological activity.[72,73] The laboratory of Professor Kent Kirshenbaum from New York State University, USA also provided ten cyclic peptoids (compounds **135–144**) to expand the study into the anti-leishmanial properties of cyclic peptoids. In these compounds larger ring sizes and utilisation of different monomers created different scaffolds to peptoids **130–134**.

The results from the biological evaluation of all cyclic peptoids against *L. mexicana* promastigotes and amastigotes can be found in **Table 3.8**. Peptoids **130–134** unfortunately showed no activity at the highest 100 µM concentration tested to either life stage of the parasite. Peptoids **130** and **131** are cyclic versions of peptoids **188** (*N*Lys*N*phe*N*phe)$_2$ and **227** (*N*Lys*N*pfb*N*pfb)$_2$. The linear analogues also show no activity against *L. mexicana* so in this case the cyclisation does not improve biological activity.

Peptoids **132–134** also showed no activity against *L. mexicana* despite the increased compound charge and potentially more amphipathic structure. All of these cyclic compounds also showed no toxicity to the mammalian keratinocytes HaCaT at 100 µM, so these compounds are probably not suited to cause parasitic membrane disruption.
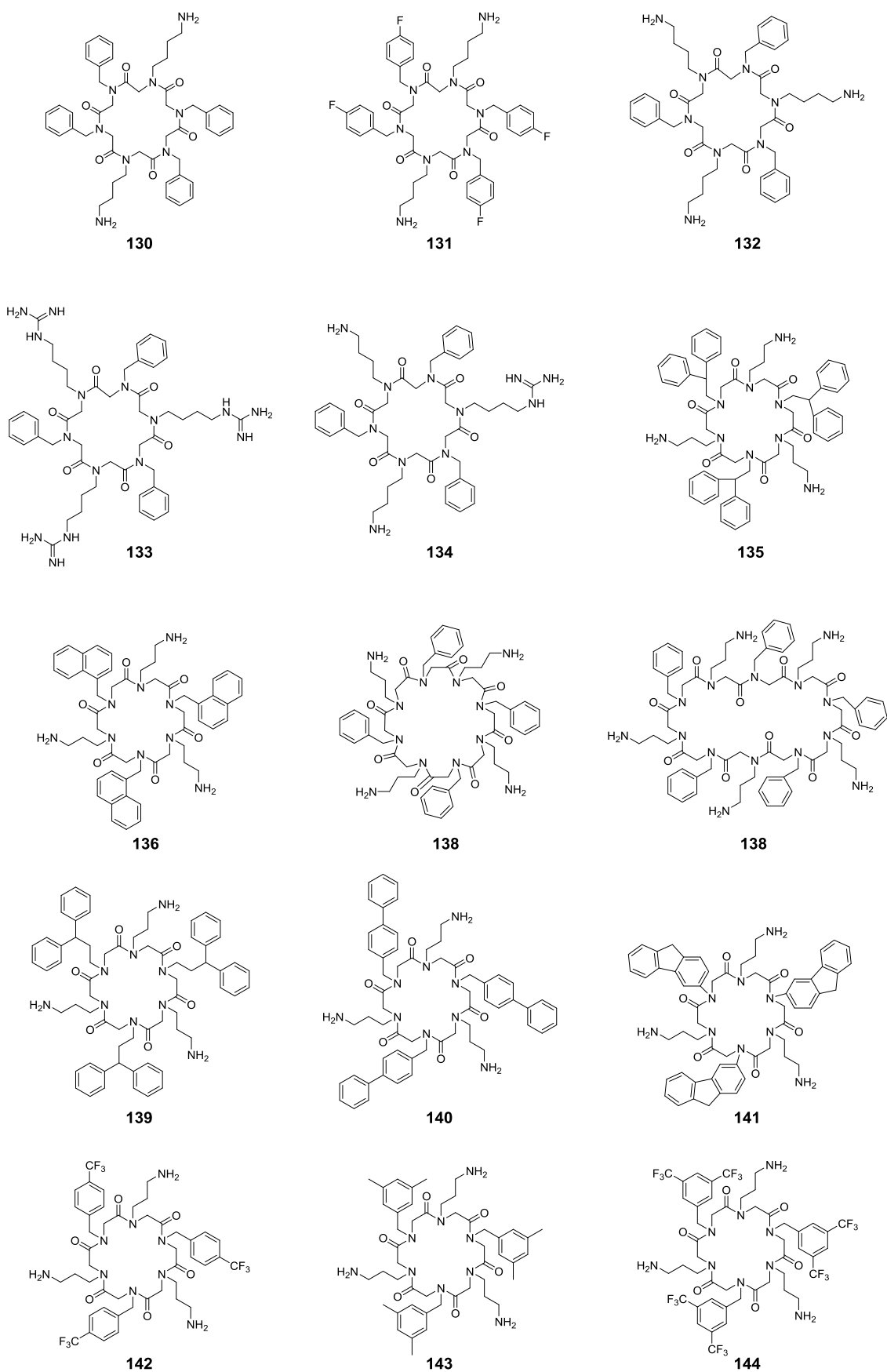
Figure 3.14. Structures of cyclic compounds synthesised (**130–134**) and compounds synthesised by Alan-Yao Liu in the Kirshenbaum lab (**135–144**).

Compound	ED$_{50}$ (μM)	
	Promastigotes	Amastigotes
191 *Amphotericin B*	< 2	< 2
130	> 100	> 100
131	> 100	> 100
132	> 100	> 100
133	> 100	> 100
134	> 100	> 100
135	> 100	43
136	40	> 100
137	> 100	> 100
138	46	> 100
139	17	63
140	19	> 100
141	> 100	> 100
142	> 100	> 100
143	46	> 100
144	38	> 100

Table 3.8. Median effective dose of cyclic peptoid library against *L. mexicana* promastigotes and amastigotes tested in a 1 hour cytotoxicity assay.

For peptoids **135–144**, some display good activity against the promastigote stage of the parasites. In particular, **139** and **140** show potent activity with ED$_{50}$ values 17 μM and 19 μM respectively. These peptoids are both 6 monomers in size, with an alternating pattern of hydrophilic (*N*-(4-aminopropyl) glycine monomers (*N*ap) and hydrophobic residues that have either a biphenyl or diphenyl sidechain (*N*bpe or *N*dpe). Other 6 residue cyclic compounds with substituted phenyl groups (**136**, **143** and **144**) and the 10 monomer peptoid **138** also showed moderate activity against the promastigotes.

However, activity against the axenic amastigotes is marginal for these compounds, which was consistent with results seen for linear peptoids within this molecular weight range. Although several sequences show a reduction in parasite viability at concentrations of 100 μM and 50 μM, only peptoids **135** and **139** have measurable ED$_{50}$ values and these are only moderately active at 43 μM and 63 μM respectively.

Due to the lack of activity against *L. mexicana*, the toxicity of these compounds to mammalian cells was not assessed. Overall, there is no evidence that cyclic peptoids display good antiparasitic activity against *L. mexicana*. Peptoids **135–144** have been previously proven to have potent antibacterial activities, i.e. peptoids **139** and **140** each have an MIC of 3.9 μg mL^{-1} against *S. aureus*. It is possible that all cyclic peptoids have a mechanism of action that is ineffective against protozoa.[72,73]

3.3.8 Validation of peptoids against intracellular *L. mexicana*

Screening undertaken in sections 3.3.4 to 3.3.7 all collected data against axenic *Leishmania mexicana*, i.e. extracellular, cultured amastigotes. These *in vitro* promastigote and axenic amastigote assays are often used in anti-leishmanial drug screening. However, due to the significant cellular, biochemical and physiological differences between these parasites and intracellular amastigotes, more representative assays can be useful. In the clinical stage of leishmaniasis, amastigotes reside within macrophages and therefore macrophage-amastigote models are considered to be more representative.[103,104] This section describes an assay developed to test peptoids against *L. mexicana* infected macrophages.

A parasite-rescue and transformation assay system was recently described by Jain *et al.*[105] for screening compounds against *L. donovani* infected differentiated THP1 cells (visceral leishmaniasis) and was modified to suit *L. mexicana*.[103,105,106]

Briefly, RAW 264.7 murine macrophages were subcultured in 96-well plates and incubated with *L. mexicana* amastigotes for 24 hours. The macrophages were then washed to removed non-viable cells that had not adhered to the plates and the macrophages are treated with peptoid solutions at varying concentrations for 24 hours, before being lysed by SDS solution to release the parasites. Following a further 48 hour incubation, the parasite viability was assessed using the alamarBlue® reagent. To assess the cytotoxicity of the peptoid sequences against RAW 264.7 only, in addition to the assay against *L. mexicana* infected macrophages, the protocol was carried out simultaneously in the absence of parasites.

Sufficient controls were added to each plate to ensure results were significant; for example, RAW 264.7 only, *L. mexicana* only, medium only and a *L. mexicana*/RAW positive control. At the end point of the assay viable parasites can be seen in wells which were treated with non-active compounds. These parasites resemble the infective, metacyclic promastigotes and were rescued from the lysed RAW macrophages.[§§] In these wells, the parasite population appears healthy, with plenty of cell division occurring. In wells treated by intermediately active compounds, some viable parasites are seen, but at a reduced cell density. In wells treated by amphotericin B or active peptoids, few or no parasites are rescued from the assay.

Triage from the axenic screening of the first and second generation libraries against *L. mexicana* highlighted promising sequences to take forwards into the infected assay. Peptoids **180** (Nae*N*phe*N*phe)$_4$ and **156** (Nae*N*phe*N*phe)$_4$ are from the first generation library, with **156** showing low micromolar activity against both the promastigotes and axenic amastigotes. **180** is the achiral analogue and shows only mild activity against the insect stage of the parasite so was used as a negative control. Peptoids **157** and **244** were also chosen to investigate the effect of using the *N*pfb and *N*amy building blocks, which as discussed in section 3.3.5 were shown to increase efficacy of sequences against both

---

§§ The appendix contains a photograph to illustrate the appearance of rescued parasites.

life stages of the parasite, where peptoid **157** is [(*N*Lys*N*pfb*N*pfb)(*N*Lys*N*spe*N*spe)]$_2$ and peptoid **244** (*N*amy*N*spe*N*spe)$_2$(*N*Lys*N*spe*N*spe)$_2$ with a reduced net charge and greater hydrophobicity.

In a second round of screening, compounds were identified from the third generation library that were able to significantly reduce the viability of *L. mexicana* amastigotes at 100 µM but had reduced toxicity to the mammalian cell line HaCaT, as highlighted in **Figure 3.12**. These peptoids, **268**, **275**, **276** and **278** all include the glutamic acid peptoid mimic, *N*Glu, and so have a reduced net charge due to the anionic character of this residue. The identification of these sequences was particularly surprising, because the action of AMPs is often attributed to their net positive charge. However, given previous studies that showed accumulation of Tamoxifen, a basic drug, in parasitophorous vacuoles and its ability to raise the pH of the compartment to induce leishmanicidal activity[97], these compounds were also used in the infected assay to examine the effect of pH on the compounds. Peptoid **268** has *N*pfb residues in combination with *N*spe/*N*Lys. Peptoids **275**, **276** and **278** are based around an *N*ae*N*spe*N*spe motif with certain *N*ae residues replaced with *N*Glu.

The results discussed below were obtained in triplicate from at least two independent assays to ensure a robust data set was obtained. The reduction in cell populations of *L. mexicana* and the macrophages when treated by the peptoid sequences can be found in the Appendix A4. The ED$_{50}$ values obtained from peptoid action against intracellular *L. mexicana* and RAW 264.7 are shown in **Table 3.9**.

From this data, it can be seen that peptoids with activity against axenic amastigotes tend to retain activity against the intracellular amastigotes, i.e. peptoid **278** has an ED$_{50}$ of 20 µM against axenic amastigotes and ED$_{50}$ of 12 µM against intracellular amastigotes. Overall, the effect of peptoid treatment on the intracellular amastigotes tends to be larger than the axenic amastigotes (as demonstrated by lower ED$_{50}$ values). As expected, peptoid **180** shows no activity under all concentrations tested, showing that peptoids with little activity against the axenic amastigotes are also likely to show no activity to intra-macrophage amastigotes. Peptoids **156** and **157** show some activity against the intracellular parasites at 5 µM, the highest concentration measured, reducing viability to 50 % and 70 % respectively. However, at lower concentrations activity was negligible. Peptoid **244** has the lowest ED$_{50}$ value against the axenic amastigotes (16 µM) and is also the most active against the intracellular amastigotes with an ED$_{50}$ of 1.6 µM.

A similar story was seen for peptoids **268**, **275**, **276** and **278**. For these compounds, screening was undertaken from 0.2 µM to 50 µM and ED$_{50}$ values were obtained that were in all cases lower than the values against axenic amastigotes. For these compounds, the best activity was seen in sequence **268** containing the fluorinated *N*pfb monomer.

	Sequence	ED$_{50}$ (µM)			
		Promastigotes	Axenic amastigotes	Intracelluar amastigotes	RAW
Amphotericin B		< 2	< 2	0.195	> 100
DMSO		>100	> 100	>100	> 100
180	(*Nae*N*phe*N*phe*)$_4$	21	> 100	> 5	> 5
156	(*Nae*N*spe*N*spe*)$_4$	7	17	> 5	3
157	[(*N*Lys*N*pfb*N*pfb)$_2$(*N*Lys*N*spe*N*spe)]$_2$	6	21	> 5	5
244	(*N*amy*N*spe*N*spe)$_2$(*N*Lys*N*spe*N*spe)$_2$	11	16	1.6	1.7
268	[(*N*Glu*N*pfb*N*spe)(*N*Lys*N*pfb*N*spe)]$_2$		62	10	14
275	(*N*Glu*N*spe*N*spe)(*Nae*N*spe*N*spe)$_2$(*N*Glu*N*spe*N*spe)		33	14	13
276	(*Nae*N*spe*N*spe)(*N*Glu*N*spe*N*spe)$_2$(*Nae*N*spe*N*spe)		41	>25	>25
278	[(*N*Glu*N*spe*N*spe)(*Nae*N*spe*N*spe)]$_2$		20	12	8

Table 3.9. Biological data for the intracellular *L. mexicana* amastigote assay. ED$_{50}$ values against the intracellular amastigotes (*L. mexicana* M379) and against the murine macrophages (RAW 264.7) are tabulated. Values are also shown for the *in vitro* assays against promastigotes and axenic amastigotes for comparison.

However, although potent activities were recorded against the intracellular *L. mexicana*, there was also significant toxicity against RAW 264.7. For example, peptoids **156** and **157** demonstrated greater toxicity against the macrophages than the intracellular, and axenic, amastigotes ($ED_{50} > 5$ μM for the intracellular parasite compared to ED_{50} of 3 μM and 5 μM against the macrophages respectively). Peptoid **244** is equivalently cytotoxic to both host and parasite (ED_{50} of 1.7 μM and 1.6 μM respectively). For peptoids **268–278**, little difference was seen in the activity of the peptoids against both the *L. mexicana* and RAW macrophages.

This toxicity is consistent with studies from other groups, where peptoids with increased antimicrobial activity also demonstrate increased host cell cytotoxicity,[71,76,81,107] although these groups have not explicitly drawn attention to the hemolytic activity or toxicity to mammalian cell lines. It was also highlighted in section 3.3.5 that activity against the parasites was accompanied by a certain level of toxicity to the mammalian cell lines HaCaT and HepG2. Clearly, overcoming this selectivity issue is a general problem for peptoids therefore further investigations into the toxicity of peptoids is examined in Chapter 5.

However, the fact that several peptoids did display low micromolar activity against *L. mexicana* infected macrophages provides a starting point for future studies into the antimicrobial and cytotoxic effects of peptoids. Despite the host cell toxicity, this data has helped to elucidate the key characteristics required for anti-leishmanial peptoid development and are the first peptoids with potent activity against *L. mexicana* promastigotes and amastigotes that retain activity against the clinically significant infected macrophages.

3.4 Further investigations into peptoid action against trypanosomatids

Biological testing in this section was carried out by Dr Marcel Kaiser at the Swiss Tropical and Public Health Institute, Basel.

Other important neglected tropical diseases are also caused by protozoa and these comprise a significant percentage of the 1 billion people affected by NTD's worldwide. In particular, diseases caused by trypanosomatids, kinetoplastid protozoa with a characteristic single flagellum, are particularly significant. *Leishmania* spp. are counted within this class alongside *Trypanosoma brucei* spp. and *Trypanosoma cruzi,* the causative agents of African sleeping sickness and Chagas disease.

Peptoids are proposed to disrupt the cell membrane of mammalian, bacterial and parasitic species. The major surface molecules of the trypanosomatids are related displaying glycosylphosphatidylinositol (GPI)-anchored glycoproteins. However, the membranes are significantly different with predominant variant surface glycoproteins

seen on *T. brucei*, surface mucins on *T. cruzi* with more complex glycophospholipids such as the lipophosphoglycans and glycoinositolphospholipids seen in *Leishmania* spp.[108]

Given the similarity between the trypanosomatids, both in biology, cell surface molecules and genomic sequences, it has been suggested that Chagas disease, sleeping sickness and leishmaniasis could be targeted by a drug that can modulate a conserved target across all three species. Although a broad spectrum drug to treat infections across species has not yet been discovered to date, a promising and selective kinetoplastid proteasome inhibitor has recently been identified for all three diseases.[14] Due to the similarities between these parasite species a selection of our peptoid library were tested against other species by the Swiss Tropical and Public Health Institute in Basel.

Leishmaniasis has already been introduced in section 3.1; over 20 distinct *Leishmania* species can cause visceral, cutaneous or mucocutaneous Leishmaniasis. Of these, the visceral form is the most serious, causing fatalities in 95 % of untreated cases. In particular, *L. donovani* causes VL in East Africa and the Indian subcontinent and *L. infantum* is the species responsible for the disease in Europe, North Africa and Latin America. AMPs that are active against one species of *Leishmania* are not always active against other species. Therefore, the work into CL was extended and peptoid compounds were tested against *L. donovani* as a representative species for VL.[10,16,94]

Human African trypanosomiasis (or sleeping sickness) is transmitted by tsetse flies in rural sub-Saharan Africa and is caused by *T. brucei* species. Fewer than 4,000 cases were reported in 2014, but the disease is usually fatal if left untreated. African sleeping sickness causes acute and intermittent fever that develops into a second meningo-encephalitic stage with symptoms including sleep disturbance and the onset of psychiatric disorders. Diagnosis relies on laboratory examination of samples; treatment requires parenteral administration and can cause serious adverse side-effects.[109]

Chagas disease (or American trypanosomiasis) is another life-threatening disease caused by *T. cruzi*. Occurring in Latin America, the disease affects an estimated 7 million people and is becoming an emerging problem in previously unaffected areas due to increased population mobility. The insect vector is a triatomine bug that spreads disease by faecal contamination of the eyes, mouth or open skin, which includes blood meal sites. The initial acute phase is often asymptomatic but can cause fever and abdominal and chest pain. During the chronic phase, complications of the digestive system or destruction of the cardiac and nervous systems can lead to sudden death. Although current treatments are reasonably effective, alternative drugs are needed as severe adverse reactions can develop in up to 40 % of cases and these drugs are not suitable for pregnant women.[110]

Due to the limited number of studies where peptoids are tested against protozoa and the promising results from our investigations with *L. mexicana*, a diverse library of peptoids was chosen to screen against *T. b. rhodesiense*, *T. cruzi* and *L. donovani*, the trypanosomatids that cause some of the world's most prevalent and significant parasitic NTDs.

3.4.1 Biological evaluation of peptoid library

The 54 sequences tested in this study were selected from peptoids that had already been evaluated for their leishmanicidal properties against *L. mexicana*. As so little information is available concerning the antiparasitic properties of peptoids, a diverse library of compounds were screened which included a large number of monomers to represent as many chemical functionalities as possible.

Due to the similarity of the trypanosomatid species, the sequences chosen included peptoids that had been identified with good activity against *L. mexicana*, in particular with α-chiral monomers, like *N*-(*S/R*-phenylethyl) glycine which induce stable peptoid helicies[76,95,100] and were previously shown to increase antimicrobial activity in section 3.3. The previous investigations against *L. mexicana* also showed that 12 residue peptoids were the most efficacious, so mainly peptoids of 12 residues in length were chosen, with some shorter sequences included for comparison. Other factors that contribute towards promising biological activity were also identified, such as the inclusion of fluorinated monomers so a variety of sequences containing fluorine-containing residues were also tested as well as those that are similar to amino acids to further expand our understanding of biologically active peptoid monomers.

To further enhance the chemical space accessed by the library, several design motifs were included to investigate the effect of sequence periodicity further (i.e. sequences with two, three and four monomer repeat units). As before, the cationic monomers utilized were also varied; lysine-type (*N*Lys, *N*ae), arginine-type (*N*hArg, *N*nArg) or peptoids containing both functionalities in the same sequence and in some sequences the overall charge was reduced by placing an alkyl chain in the third position of the motif (i.e. *N*amy or *N*but).

Peptoid sequences tested and the IC$_{50}$ values obtained from biological testing against *L. donovani*, *T. b. rhodesiense* and *T. cruzi* are shown in **Table 3.10**. In all assays, an appropriate reference drug (**304–307**) was used as a positive control and the relevant infective life stage was tested; i.e. for the *Trypanosoma* species trypomastigotes and for *L. donovani* axenic amastigotes were used. The detailed procedures for these assays can be found in the Experimental Chapter 7.

		Peptoid Sequence	IC$_{50}$ (μM)			
			T. b. rhodesiense	*T. cruzi*	*L. donovani*	L-6
Reference Drug	304 *Melarsoprol*		0.01			
	305 *Benznidazole*			1.99		
	192 *Miltefosine*				0.27	
	306 *Podophyllotoxin*					0.01
Peptoid	186	(*N*Lys*N*phe*N*phe)$_4$	10.1	10.5	nd	9.8
	180	(*N*ae*N*phe*N*phe)$_4$	10.6	10.3	15.0	10.8
	299	(*N*Lys*N*phe*N*spe)$_4$	3.0	4.1	10.8	3.7
	300	(*N*ae*N*phe*N*spe)$_4$	10.2	8.1	15.7	7.5
	25	(*N*Lys*N*spe*N*spe)$_2$	32.3	59.3	nd	76.4
	22	(*N*Lys*N*spe*N*spe)$_4$	3.3	5.0	6.8	3.6
	301	(*N*Lys*N*rpe*N*rpe)$_4$	3.2	3.8	12.5	3.5
	219	(*N*ae*N*spe*N*spe)$_2$	60.8	60.2	nd	60.9
	156	(*N*ae*N*spe*N*spe)$_4$	8.6	5.4	6.1	4.3
	302	(*N*ae*N*rpe*N*rpe)$_4$	12.1	9.7	10.9	8.6
	235	(*N*Lys*N*nVal*N*spe)$_4$	23.2	34.8	nd	30.4
	182	(*N*Lys*N*hLeu*N*spe)$_4$	2.8	4.0	14.2	3.6
	259	(*N*Lys*N*spe)$_6$	29.9	26.9	nd	26.6
	260	(*N*ae*N*spe)$_6$	31.7	30.3	nd	33.3
	183	(*N*Lys*N*pfb*N*spe)$_4$	3.5	3.5	5.8	2.7
	157	[(*N*Lys*N*pfb*N*pfb)(*N*Lys*N*spe*N*spe)]$_2$	8.4	5.3	5.0	4.0
	256	(*N*Lys*N*pfb*N*rpe)$_4$	9.9	5.2	15.7	5.4
	257	(*N*ae*N*pfb*N*rpe)$_4$	11.6	7.5	8.0	7.6
	252	(*N*ae*N*pfb*N*spe)$_4$	11.0	7.7	8.3	5.8
	254	(*N*Lys*N*pfb*N*Lys*N*spe)$_3$	28.6	24.4	nd	29.0
	255	(*N*ae*N*pfb*N*ae*N*spe)$_3$	31.7	29.8	nd	30.9
	261	(*N*Lys*N*dfb*N*spe)$_4$	9.0	5.2	11.9	5.7
	262	(*N*ae*N*dfb*N*spe)$_4$	21.7	7.6	8.2	8.1
	263	(*N*Lys*N*sfb*N*sfb)$_4$	8.4	6.0	6.9	3.8
	264	(*N*ae*N*sfb*N*sfb)$_4$	19.8	6.2	6.7	5.8
	265	(*N*Lys*N*sfb*N*spe)$_4$	8.5	6.6	9.8	7.2
	266	(*N*ae*N*tfe*N*spe)$_4$	26.2	29.4	nd	37.3
	152	(*N*hArg*N*spe*N*spe)$_4$	2.2	4.8	4.0	3.2
	154	[(*N*amy*N*spe*N*spe)(*N*hArg*N*spe*N*spe)]$_2$	2.4	6.7	5.1	5.8
	147	(*N*Lys*N*spe*N*spe)$_2$(*N*hArg*N*spe*N*spe)$_2$	3.5	6.5	5.9	7.2
	150	[(*N*hArg*N*spe*N*spe)(*N*Lys*N*spe*N*spe)]$_2$	8.8	11.3	10.5	11.0
	151	[(*N*nArg*N*spe*N*spe)(*N*ae*N*spe*N*spe)]$_2$	3.6	3.7	5.3	3.9
	155	(*N*nArg*N*spe*N*spe)$_4$	3.4	6.2	6.2	6.5
	271	(*N*Glu*N*spe*N*spe)(*N*Lys*N*spe*N*spe)$_2$(*N*Glu*N*spe*N*spe)	9.9	13.4	22.2	17.2
	275	(*N*Glu*N*spe*N*spe)(*N*ae*N*spe*N*spe)$_2$(*N*Glu*N*spe*N*spe)	10.0	10.4	17.4	10.5
	276	(*N*ae*N*spe*N*spe)(*N*Glu*N*spe*N*spe)$_2$(*N*ae*N*spe*N*spe)	24.6	15.4	27.9	25.4
	268	[(*N*Glu*N*pfb*N*spe)(*N*Lys*N*pfb*N*spe)]$_2$	28.0	10.8	22.0	15.8
	243	(*N*amy*N*spe*N*spe)[(*N*Lys*N*spe*N*spe)]$_3$	7.4	7.0	5.7	4.4
	244	(*N*amy*N*spe*N*spe)$_2$(*N*Lys*N*spe*N*spe)$_2$	6.0	8.5	6.9	9.4
	280	(*N*Lys*N*but*N*spe)$_4$	7.0	14.9	nd	19.4
	281	(*N*ae*N*but*N*spe)$_4$	9.2	17.7	nd	28.8
	308	(*N*but*N*spe*N*spe)$_2$(*N*ae*N*spe*N*spe)$_2$	8.8	6.9	7.8	9.0
	284	(*N*Lys*N*hHis*N*spe)$_4$	nd	41.7	nd	nd
	285	(*N*ae*N*hHis*N*spe)$_4$	nd	43.7	nd	nd
	286	[(*N*Lys*N*spe*N*spe)(*N*Lys*N*hHis*N*spe)]$_2$	31.8	25.0	nd	32.9
	287	[(*N*ae*N*spe*N*spe)(*N*ae*N*hHis*N*spe)]$_2$	30.4	24.8	nd	34.5
	288	(*N*Lys*N*hTyr*N*spe)$_4$	10.3	25.0	nd	16.9
	309	(*N*ae*N*hTyr*N*spe)$_4$	10.6	19.4	nd	27.9
	291	[(*N*Lys*N*spe*N*spe)(*N*Lys*N*pyr*N*spe)]$_2$	10.4	25.4	nd	29.3
	310	[(*N*ae*N*spe*N*spe)(*N*ae*N*pyr*N*spe)]$_2$	10.6	23.0	nd	36.0
	292	(*N*Lys*N*hCys*N*spe)$_4$	30.7	30.6	nd	32.4
	311	(*N*ae*N*spe*N*moe*N*spe)$_3$	11.8	20.9	nd	31.4
	290	[(*N*ae*N*spe*N*spe)(*N*ae*N*hTrp*N*spe)]$_2$	11.3	7.5	8.4	7.6
	289	[(*N*Lys*N*spe*N*spe)(*N*Lys*N*hTrp*N*spe)]$_2$	9.9	7.5	12.8	6.9

Table 3.10. Biological activity of the peptoid library against the causative parasites of the following diseases; *T. b. rhodesiense* STIB 900 trypomastigotes for African sleeping sickness; *T. cruzi* Tulahuen C4 strain amastigotes for Chagas disease; *L. donovani* MHOM-ET-67/L82 amastigotes for visceral leishmaniasis. Cytotoxicity was carried out against L6 rat myoblasts (skeletal tissue) and all tests were also carried out on multiple occasions using relevant reference drugs for controls. *nd* indicates that no IC$_{50}$ value could be calculated due to negligible activity at the highest concentrations tested.

In general, across the trypanosomatids tested, some potent sequences were found against each species. For example, against *T. b. rhodesiense* and *T. cruzi* a few IC_{50} values of less than 10 μM were recorded; for each parasite the best peptoid was **152** with activity at 2.2 μM and **151** at 3.7 μM respectively. For *L. donovani* several compounds had IC_{50} values less than 10 μM (for example, peptoids **22**, **156**, **183**, **157**, **264** and peptoid **152** with the lowest IC_{50} against *L. donovani* of 4.0 μM).

The peptoids were also tested against L-6 myoblasts (rat skeletal tissue) as a representative mammalian cell line in order for a selectivity index (SI) to be calculated for each sequence.[***] The SI provides a measure to ascertain which sequences are the most selective peptoids and several promising sequences for each species of parasite tested are highlighted in **Table 3.11**.

	Peptoid Sequence	IC_{50} (μM)	Selectivity Index	HPLC RT (min)
African sleeping sickness (*T. b. rhodesiense*)				
304 *Melarsoprol*		0.01	2260	
25	(*N*Lys*N*spe*N*spe)$_2$	32.3	2.4	14.4
154	[(*N*amy*N*spe*N*spe)(*N*hArg*N*spe*N*spe)]$_2$	2.4	2.4	22.4
280	(*N*Lys*N*but*N*spe)$_4$	7.1	2.7	16.5
281	(*N*ae*N*but*N*spe)$_4$	9.2	3.1	16.9
309	(*N*ae*N*hTyr*N*spe)$_4$	10.6	2.6	14.8
291	[(*N*Lys*N*spe*N*spe)(*N*Lys*N*pyr*N*spe)]$_2$	10.4	2.8	13.4
310	[(*N*ae*N*spe*N*spe)(*N*ae*N*pyr*N*spe)]$_2$	10.6	3.4	14.1
311	(*N*ae*N*spe*N*moe*N*spe)$_3$	11.8	2.7	16.8
Chagas disease (*T. cruzi*)				
305 *Benznidazole*		1.99	193	
261	(*N*Lys*N*dfb*N*spe)$_4$	5.2	1.1	17.9
151	[(*N*nArg*N*spe*N*spe)(*N*ae*N*spe*N*spe)]$_2$	3.7	1.1	19
276	(*N*ae*N*spe*N*spe)(*N*Glu*N*spe*N*spe)$_2$(*N*ae*N*spe*N*spe)	15.4	1.7	20.5
281	(*N*ae*N*but*N*spe)$_4$	17.7	1.6	16.9
308	(*N*but*N*spe*N*spe)$_2$(*N*ae*N*spe*N*spe)$_2$	6.9	1.3	21.9
290	[(*N*ae*N*spe*N*spe)(*N*ae*N*hTrp*N*spe)]$_2$	7.5	1.0	17.8
Visceral Leishmaniasis (*L. donovani*)				
192 *Miltefosine*		0.27	499	
157	[(*N*Lys*N*pfb*N*pfb)(*N*Lys*N*spe*N*spe)]$_2$	5.0	0.8	17.6
154	[(*N*amy*N*spe*N*spe)(*N*hArg*N*spe*N*spe)]$_2$	5.1	1.1	22.4
244	(*N*amy*N*spe*N*spe)$_2$(*N*Lys*N*spe*N*spe)$_2$	6.9	1.4	22.8
308	(*N*but*N*spe*N*spe)$_2$(*N*ae*N*spe*N*spe)$_2$	7.8	1.2	21.9

Table 3.11. Summary of selected peptoids and their biological activities against trypanosomatid parasites and SI, which can be compared to reference drugs. Analytical HPLC retention times from compounds > 95 % pure and are recorded from the centre of the peak; gradient = 0–100% solvent B over 30 minutes, column oven set to 40 °C, where A = 95 % H_2O, 5 % acetonitrile, 0.1 % TFA, B = 95 % acetonitrile, 5 % H_2O, 0.1 % TFA.

[***] Selectivity index is defined as the toxicity to L6 rat myoblast cells divided by the IC_{50} against the parasite concerned.

Although none of the peptoids had better activity than the reference drugs, many of the peptoids tested were found to have comparable or improved antiparasitic activity to AMPs reported in the literature. For example, the leishmanicidal CA(1-8)M(1-18)[62] peptide (compound **195**) has IC_{50} values between 1 - 5 μM against *L. donovani* promastigotes (our assay tests against the less vulnerable amastigote life stage) and histatin 5[111] (compound **205**) is reported to have an IC_{50} of 14.2 μM against *L. donovani* amastigotes. The most active peptoids highlighted in **Table 3.11** against *L. donovani* amastigotes have IC_{50} values from 5.0–7.8 μM. However, it should be noted that the SI for these compounds is not ideal as they are all around 1, showing that the peptoids that have shown good activity against *L. donovani* are not very selective and display equal toxicity to the L-6 cells. For *T. cruzi*, the AMPs cecropin[60] (compound **2**) and meucine-24[61] have IC_{50} values of 0.2 μM and 10–20 μM respectively. Although our peptoids cannot match the activity of cecropin, most of the peptoids with the highest SIs around 2 have low micromolar activity below 10 μM.

Against *T. b. rhodesiense*, the SIs were slightly higher, between 2–3, with peptoid **154** showing the best activity of 2.4 μM. In two of the most efficacious compounds selected for this parasite, peptoids have the *N*but alkyl monomer in the second position of the trimer repeat, so these compounds have less aromatic character than other members of the library. These peptoids (**280** and **281**) have IC_{50} values of 7.0 μM and 9.2 μM. They also display activity against *T. cruzi* (14.9 μM and 17.7 μM) but no activity against *L. donovani*.

Most of the compounds selected with the best SIs for *L. donovani* have alkyl residues in the third position of the trimer motif. In these compounds (**154, 244, 308**), the hydrophobicity of the compound is increased, as evidenced by the increased RP-HPLC retention times, and are also less charged than other members of the library. Encouragingly, peptoid **244** identified in the infected macrophage study (section 3.3.8) has also been highlighted here as a promising lead against *L. donovani*, although the SI is a point for improvement.

It is not possible to directly compare the ED_{50} values obtained against *L. mexicana* in section 3.3 with the IC_{50} values against *L. donovani*, due to drastically different assay procedures; against *L. donovani* peptoids are incubated with amastigotes for 70 hours, however, against *L. mexicana* a quick-kill assay is used with the amastigotes incubated with compound for 1 hour, then at ten-fold reduced concentration for 24 hours. However, trends in activity can still be compared and it can be concluded that the factors identified for activity against *L. mexicana* are also applicable to *L. donovani*. For example, inclusion of α-chiral monomers or those containing fluorine and peptoids designed around the threefold repeating motif tend to be the most effective against *L. mexicana* (CL) and also *L. donovani* (VL). Reduction in overall sequence charge by replacing a cationic moiety with an alkyl group also remains a good strategy to increase antiparasitic activity.

These generalised trends are also applicable to *T. cruzi* and *T. b. rhodesiense*. Overall, for the best peptoids identified in **Table 3.11**, *Trypanosoma* species have slightly lower IC_{50} values, and better SIs compared to *L. donovani*. Although the selectivity of these sequences is a point for future improvement, these peptoids provide a starting point for further enhancements and also demonstrate that the peptoids have trypanocidal activity against more than one parasitic species.

3.5   Targeting malaria: peptoids against *Plasmodium falciparum*

Biological testing in this section was carried out by Dr Marcel Kaiser at the Swiss Tropical and Public Health Institute, Basel. Hemolysis data was collected by Dr Russel Luo and Dr Fionnuala Lundy (Queen's University, Belfast).

Although malaria is not classified as a NTD by the World Health Organisation and the rates of incidence have decreased substantially in recent years, malaria remains the most prevalent and debilitating protozoan infection in the world, affecting populations in South and Central America, Africa and Asia. Malaria is an infection of red blood cells caused by various *Plasmodium* spp. that are transmitted by the bite of an infected *Anopheles* mosquito. Malaria can cause severe fever, nausea or seizures but when treated promptly, uncomplicated infections have a low mortality rate of ~0.1 %. Despite the favourable prospects for treatment and deployment of insecticide-treated mosquito nets, in 2015, there were 214 million new cases of the disease and it caused an estimated 438,000 fatalities.[6,70,112]

Most cases of malaria are caused by *Plasmodium vivax* or *Plasmodium falciparum*, which is responsible for approximately 90% of malaria deaths. The *Plasmodium* spp. are quite different to the trypanosomatids discussed above, with a more complex infectious cycle and very different cell surface coats.[6,70]

The same peptoid library discussed in section 3.4 tested against the causative parasites of Chagas disease, leishmaniasis and African sleeping sickness was also evaluated against *P. falciparum* to see if any sequences have the potential to be developed as selective antimalarial compounds and to draw comparisons between the activity of peptoids against the *Trypanosoma* and *Leishmania* parasites.

3.5.1   Results from biological screening

In the assays against *P. falciparum*, chloroquinine was used as a positive control in the antimalarial assays as it is one of the drugs prescribed for malaria prevention and treatment, although widespread resistance of *P. falciparum* to the drug is now seen in endemic areas.[113] The IC_{50} values following screening of the peptoid library against *P. falciparum* are tabulated in **Table 3.12**.

		Peptoid Sequence	IC$_{50}$ (µM)		Selectivity Index
			P. falciparum	L-6	
Drug	307 *Chloroquine*		0.0047		41500
	306 *Podophyllotoxin*			0.01	-
Peptoid	186	(NLysNpheNphe)$_4$	4.05	9.8	2.4
	180	(NaeNpheNphe)$_4$	2.85	10.8	3.8
	299	(NLysNpheNspe)$_4$	1.48	3.7	2.5
	300	(NaeNpheNspe)$_4$	1.51	7.5	5.0
	25	(NLysNspeNspe)$_2$	34.20	76.4	2.2
	22	(NLysNspeNspe)$_4$	0.56	3.6	6.5
	301	(NLysNrpeNrpe)$_4$	0.41	3.5	8.6
	219	(NaeNspeNspe)$_2$	27.55	60.9	2.2
	156	(NaeNspeNspe)$_4$	0.68	4.3	6.3
	302	(NaeNrpeNrpe)$_4$	0.79	8.6	10.9
	235	(NLysNnValNspe)$_4$	nd	30.4	nd
	182	(NLysNhLeuNspe)$_4$	0.85	3.6	4.3
	259	(NLysNspe)$_6$	2.60	26.6	10.2
	260	(NaeNspe)$_6$	0.68	33.3	49.2
	183	(NLysNpfbNspe)$_4$	0.73	2.7	3.6
	157	[(NLysNpfbNpfb)(NLysNspeNspe)]$_2$	1.53	4.0	2.6
	256	(NLysNpfbNrpe)$_4$	1.05	5.4	5.1
	257	(NaeNpfbNrpe)$_4$	1.49	7.6	5.1
	252	(NaeNpfbNspe)$_4$	1.51	5.8	3.8
	254	(NLysNpfbNLysNspe)$_3$	8.50	29.0	3.4
	255	(NaeNpfbNaeNspe)$_3$	2.40	30.9	12.9
	261	(NLysNdfbNspe)$_4$	1.34	5.7	4.3
	262	(NaeNdfbNspe)$_4$	0.99	8.1	8.1
	263	(NLysNsfbNsfb)$_4$	0.69	3.8	5.5
	264	(NaeNsfbNsfb)$_4$	0.72	5.8	8.0
	265	(NLysNsfbNspe)$_4$	1.21	7.2	6.0
	266	(NaeNtfeNspe)$_4$	8.06	37.3	4.6
	152	(NhArgNspeNspe)$_4$	0.22	3.2	14.6
	154	[(NamyNspeNspe)(NhArgNspeNspe)]$_2$	0.05	5.8	124.8
	147	(NLysNspeNspe)$_2$(NhArgNspeNspe)$_2$	0.79	7.2	9.2
	150	[(NhArgNspeNspe)(NLysNspeNspe)]$_2$	1.43	11.0	7.7
	151	[(NnArgNspeNspe)(NaeNspeNspe)]$_2$	0.55	3.9	7.0
	155	(NnArgNspeNspe)$_4$	0.59	6.5	11.1
	271	(NGluNspeNspe)(NLysNspeNspe)$_2$(NGluNspeNspe)	4.83	17.2	3.6
	275	(NGluNspeNspe)(NaeNspeNspe)$_2$(NGluNspeNspe)	3.06	10.5	3.4
	276	(NaeNspeNspe)(NGluNspeNspe)$_2$(NaeNspeNspe)	6.88	25.4	3.7
	268	[(NGluNpfbNspe)(NLysNpfbNspe)]$_2$	4.78	15.8	3.3
	243	(NamyNspeNspe)[(NLysNspeNspe)]$_3$	0.19	4.4	22.4
	244	(NamyNspeNspe)$_2$(NLysNspeNspe)$_2$	0.19	9.4	49.0
	280	(NLysNbutNspe)$_4$	5.66	19.4	3.4
	281	(NaeNbutNspe)$_4$	2.74	28.8	10.5
	308	(NbutNspeNspe)$_2$(NaeNspeNspe)$_2$	0.23	9.0	39.1
	284	(NLysNhHisNspe)$_4$	nd	> 50	nd
	285	(NaeNhHisNspe)$_4$	nd	> 50	nd
	286	[(NLysNspeNspe)(NLysNhHisNspe)]$_2$	nd	32.9	nd
	287	[(NaeNspeNspe)(NaeNhHisNspe)]$_2$	22.35	34.5	1.5
	288	(NLysNhTyrNspe)$_4$	14.44	16.9	1.2
	309	(NaeNhTyrNspe)$_4$	9.74	27.9	2.9
	291	[(NLysNspeNspe)(NLysNpyrNspe)]$_2$	23.23	29.3	1.3
	310	[(NaeNspeNspe)(NaeNpyrNspe)]$_2$	12.76	36.0	2.8
	292	(NLysNhCysNspe)$_4$	nd	32.4	> 50
	311	(NaeNspeNmoeNspe)$_3$	8.53	31.4	3.7
	290	[(NaeNspeNspe)(NaeNhTrpNspe)]$_2$	1.56	7.6	4.8
	289	[(NLysNspeNspe)(NLysNhTrpNspe)]$_2$	1.63	6.9	4.2

Table 3.12. Biological activity of the peptoid library against *P. falciparum* NF54 IEF stage. Cytotoxicity was carried out against L-6 rat myoblasts (skeletal tissue) and all tests were also carried out on multiple occasions using relevant reference drugs for controls. *nd* indicates that no IC$_{50}$ value could be calculated due to negligible activity at the highest concentrations tested.

Overall, the peptoids tested show greater activity against *P. falciparum* compared to the trypanosomatids *T. cruzi*, *L. donovani* and *T. b. rhodesiense.* Many IC_{50} values were recorded against *P. falciparum* that were significantly lower than 1 μM, for example peptoid **154** at 0.05 μM. Although activity at this level is significantly less than chloroquine, when comparing the activity of peptoid sequences to natural AMPs, it can be seen that several of the peptoids in **Table 3.12** have improved activities. The AMPs cecropin[57,58] (compound **2**) and gomesin[64] are reported to have IC_{50} values of 1.5 μM and 50 μM respectively against *P. falciparum,* whereas selected peptoids from the library have sub-micromolar activities.

The selectivity of the library has been determined in a similar manner to section 3.4 by calculating a selectivity index[†††] and a selection of the most promising compounds has been highlighted in **Table 3.13**. From this data, it can be seen that the SIs against *P. falciparum* are much improved compared to those against the trypanosomatids and this stems from the more potent activity against *Plasmodium.*

	Peptoid Sequence	IC_{50} (μM)	Selectivity Index	HPLC RT (min)
Malaria (*P. falciparum*)				
307 *Chloroquine*		0.0047	41500	
259	(*N*Lys*N*spe)$_6$	2.60	10.2	13.7
260	(*N*ae*N*spe)$_6$	0.68	49.2	14.1
152	(*N*hArg*N*spe*N*spe)$_4$	0.22	14.6	17.8
154	[(*N*amy*N*spe*N*spe)(*N*hArg*N*spe*N*spe)]$_2$	0.05	124.8	22.4
147	(*N*Lys*N*spe*N*spe)$_2$(*N*hArg*N*spe*N*spe)$_2$	0.79	9.2	16.5
244	(*N*amy*N*spe*N*spe)$_2$(*N*Lys*N*spe*N*spe)$_2$	0.19	49.0	22.8
308	(*N*but*N*spe*N*spe)$_2$(*N*ae*N*spe*N*spe)$_2$	0.23	39.1	21.9

Table 3.13. Summary of selected peptoids and their biological activities against specific parasites. Selectivity index is defined as the toxicity to L6 rat myoblast cells divided by the IC_{50} against *P. falciparum* and can be compared to the selectivity index of the reference drugs. Analytical HPLC retention times from compounds > 95 % pure and are recorded from the centre of the peak; gradient = 0–100% solvent B over 30 minutes, column oven set to 40 °C, where A = 95 % H$_2$O, 5 % acetonitrile, 0.1 % TFA, B = 95 % acetonitrile, 5 % H$_2$O, 0.1 % TFA.

In particular, compound **154** [*N*amy*N*spe*N*spe)(*N*hArg*N*spe*N*spe)]$_2$ with the very potent 0.05 μM activity has a selectivity index in excess of 100. Since this sequence has toxicity to L-6 at 5.8 μM and similar activity against *T. b. rhodesiense, T. cruzi* and *L. donovani,* poor SIs were recorded for these species. However, due to the excellent anti-plasmodial activity of **154**, it has a large selectivity window against *P. falciparum.*

Peptoids **244** and **308** also have good SIs and sub-micromolar activity, although are not quite as potent as **154**. In these three sequences, cationic residues in the trimer repeat motif have been replaced by a monomer with alkyl functionality (for **154** and **244** *N*amy,

---

[†††] Selectivity index is defined as the toxicity to L6 rat myoblast cells divided by the IC_{50} against the parasite concerned.

for **308** *N*but). Therefore these sequences are more hydrophobic, as seen by the longer RP-HPLC retention times in **Table 3.13**, and are less highly charged than other members of the library (i.e. overall +2 charge instead of the standard +4 net charge).

It is worth noting that the most promising anti-malarial peptoids also mostly contain guanido-functionalised *N*hArg residues instead of the amino analogues (*N*Lys), i.e. compare the activity of **152** to peptoid **22**, (*N*Lys*N*spe*N*spe)$_4$. In this case, the inclusion of the arginine-type residues doesn't change the toxicity to the L-6 mammalian cells (both around 3 µM), but does significantly increase the activity against *P. falciparum*. This is in agreement with the only other study of anti-plasmodial peptoids, where peptide-β-peptoid hybrids[‡‡‡] with the amino acid arginine had more potent activity than lysine analogues.[81]

Interestingly, peptoids **259** and **260** shown in **Figure 3.15** were also highlighted amongst the peptoids with the best SI. Although the activity against *P. falciparum* is not as good as others in **Table 3.13**, these sequences display much reduced toxicity to the mammalian L-6 cells. The sequences of both peptoids are based upon an alternating pattern of cationic (*N*Lys or *N*ae) and hydrophobic aromatic residues (*N*spe), with the shorter *N*ae monomers in compound **260** being the most efficacious. It is interesting to note that both **259** and **260** do not have the common three-fold repeat motif, which has previously been suggested to impart an amphipathic, helical structure and thus lead to increased antimicrobial effects.[76,99]
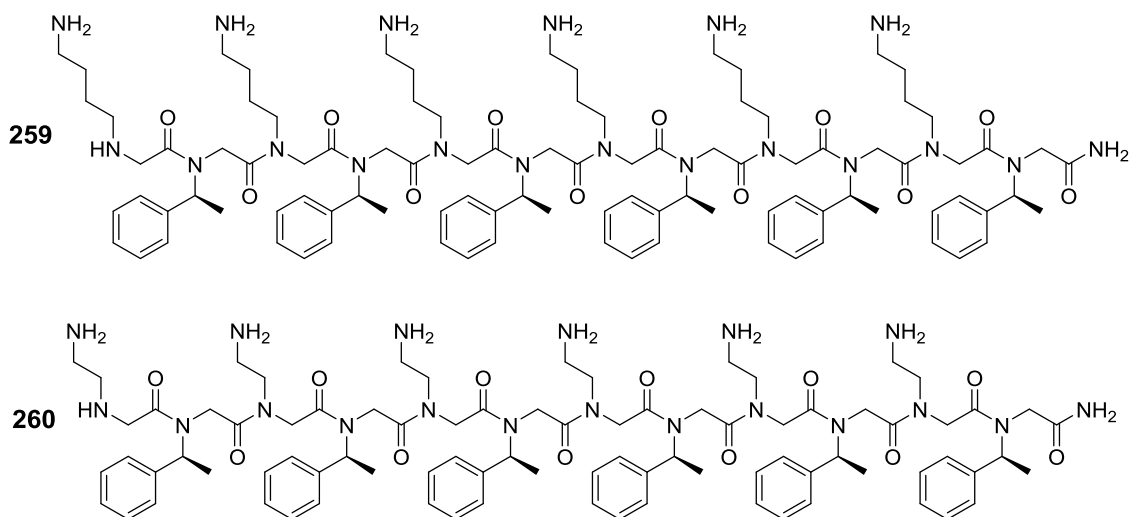
Figure 3.15. Chemical structures for peptoids **259** (*N*Lys*N*spe)$_6$ and **260** (*N*ae*N*spe)$_6$, that both show promising SI against *P. falciparum*.

[‡‡‡] In these peptide-peptoid hybrids, peptoid monomers were used for the hydrophobic monomers and peptide amino acids for the cationic residues of lysine or arginine.

3.5.2 Hemolytic activity of selected peptoids

The compounds identified as the most promising anti-plasmodial peptoids (in **Table 3.13**) were also tested for their hemolytic activity to investigate toxicity of peptoids to human erythrocytes, in addition to their selectivity index. Briefly human whole blood was diluted in PBS to form a clear 8 % erythrocyte suspension and peptoid solutions were added and incubated for 1 hour at 37 °C before analysis (detailed protocol for the standard hemolysis assay can be found in Chapter 7). The hemolytic activities of the 7 peptoid sequences and chloroquine diphosphate (as a reference drug) are shown in **Figure 3.16**.

As expected by the variety of residues present in this library, a variety of hemolytic activities were recorded. Some of the compounds screened showed significant hemolytic activity, such as peptoids **152**, **244** and **147** causing approximately 80 % hemolysis at 12.5 µM. Sequences **154** and **308** had even stronger detrimental activity to the human erythrocytes, even at the lowest concentration tested (6.25 µM). However, peptoids **259** and **260** show little hemolytic activity in the same range as the chloroquine control, even at 100 µM.
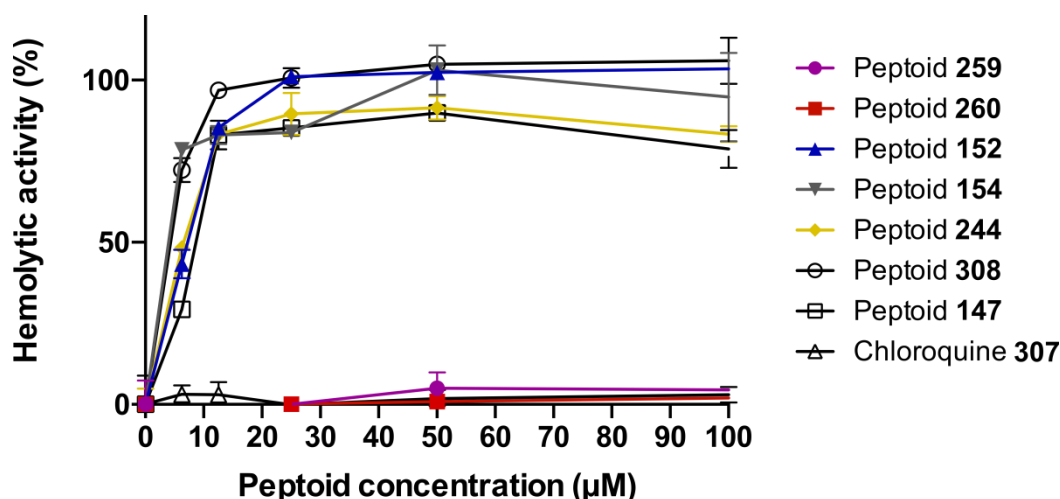
Figure 3.16. Hemolytic assay of peptoids selected in **Table 3.13**. Chloroquine diphosphate salt was tested as a control. Human erythrocytes treated with compounds from 6.25–100 µM. Data collected from three independent experiments, each undertaken in triplicate.

These findings highlight the need for multiple assessments of toxicity since peptoid **154** has a very high selectivity index using the *in vitro* testing against the mammalian cells, but shows over 50 % hemolytic activity even at the lowest concentration tested. As already eluded to in section 3.3.8, other groups have also identified peptoid toxicity as an issue but few people have attempted to overcome this challenge. In particular, for some of the most active peptide-β-peptoid hybrids tested by Olsen *et al.* against *P. falciparum*, their sequences also showed hemolytic activity at concentrations lower than 10 µM. Additionally, human red blood cells were also examined in this study using microscopy

and even peptoids that had low hemolytic activity caused severe membrane alterations at low concentrations. Therefore, in the future the appearance of the erythrocytes should be studied following treatment by peptoids **259** and **260**.[81]

Peptoids **259** and **260** have only mild toxicity to mammalian cells (around 30 μM against L-6), and show low hemolytic activity but potent activity against *P. falciparum*. Therefore sequences **259** (IC_{50} 2.60 μM and SI of 10.2) and **260** (IC_{50} 0.68 μM and SI of 49.2) may be interesting candidates for further development. These sequences both follow an alternating design of hydrophobic and charged monomers which is different to the typical three residue repeat often seen in antimicrobial peptoids. Therefore in the future, it would be useful to evaluate the toxicity, hemolytic activity and antiparasitic activity of a variety of peptoids with different charge : hydrophobicity ratios and to change the hydrophobic monomer (for both **259** and **260**, α-chiral *N*spe is used). This would allow further investigation into whether it is the increased net cationic charge, or the increased number of hydrophobic residues that causes the improved antimicrobial effect and lower toxicity/hemolytic activities.

3.6 Conclusions

In conclusion, the work presented in this chapter represents the first comprehensive investigation into the use of peptoids as a novel class of antiparasitic agents. Initial work focussed on the effect of peptoids against the causative agent of cutaneous leishmaniasis, *Leishmania mexicana*. In this work, the first examples of peptoids were found that were active against both insect stage promastigotes and mammalian axenic amastigotes. Additionally, this work identified the first peptoids that were active against intracellular parasites (in this case inside infected macrophages), with peptoid **244** (*N*amy*N*spe*N*spe)$_2$(*N*Lys*N*spe*N*spe)$_2$ having an ED_{50} of 1.6 μM.

A variety of other protozoa responsible for disease were also studied and active sequences were identified against *Trypanosoma brucei rhodesiense*, *Trypanosoma cruzi*, *L. donovani* and *P. falciparum*. In particular, peptoids **259** (*N*Lys*N*spe)$_6$ and **260** (*N*ae*N*spe)$_6$ have been identified that display significant anti-plasmodial activity (IC_{50} of 2.68 μM and 0.68 μM respectively), low toxicity to L-6 mammalian cells and negligible hemolytic activity. Despite the similarity of the surface GPI-anchored glycoproteins and GPI-related complex glycophospholipids of the trypanosomatids, each species does have different cell surface molecules, which is the most likely cause of the different susceptibility of each species to specific peptoid sequences.

The peptoids have an increased resistance to proteolysis than peptide-based therapeutics and show comparable or improved antimicrobial activity to many common AMPs in the literature. Therefore, the increased stability of the peptoids makes them promising candidates for further investigation as they overcome the problematic *in vivo* biostability typically displayed by AMPs. Additionally, since the predicted mode of action of peptoids is plasma membrane disruption or pore formation, the risk of parasite resistance

development is low. This is advantageous compared to the small molecule drugs currently in clinical use, to which drug resistance is developing.

Hydrophobicity has been identified as a very important property that can contribute towards antimicrobial activity. Many potent sequences had a large proportion of hydrophobic residues, fluorine substitution or a reduced net charge compared to inactive compounds. To help rationalise biological activity and correlate this to hydrophobicity of sequences, a detailed study of peptoid hydrophobicity was undertaken in Chapter 5.

The selectivity of peptoids can be problematic as many active sequences presented here in Chapter 3 have been shown to be toxic to mammalian cells or to have significant hemolytic activity. This is a point for improvement in the future and is discussed further in Chapter 5, where the mode of action of antimicrobial peptoids is investigated in more detail. However, in applications against cutaneous leishmaniasis, potential treatments can be formulated for a topical application, where a certain level of toxicity to host cells may be acceptable. Many of the treatments in current clinical use against NTDs also show some level of toxicity or severe side effects and this point emphasises the drastic need for new therapeutics to be developed against these diseases.

Finally, this library represents the largest, and most functionally varied, library of antiparasitic peptoids reported to date and thus it should help inform and direct future research into biologically active peptoids. Given that many studies in the literature have found a low hit rate in whole cell parasite screens against the trypanosomatids, peptoids are presented as very promising drug candidates. For example, in the GlaxoSmithKline Tres Cantos facility, over 1.8 million small molecule compounds were screened to find around 200 potent hits against each of *L. donovani, T. cruzi* or *T. brucei.*[114] In the case of the peptoid library presented as part of this project, around 200 compounds were screened to find many sequences with potent activity, particularly against *P. falciparum*. The study should also benefit the scientific field as it provides the largest toxicity screening of peptoids to date and it is anticipated that the data may aid the design of bioactive peptoids in the future.

3.7   References

1.   The World Health Organisation, **2016**.
2.   T.K. Mackey, B.A. Liang, R. Cuomo, R. Hafen, K.C. Brouwer, D.E. Lee, *Clin. Microbiol. Rev.,* **2014**, *27*, 949.
3.   The World Health Organisation, *London Declaration on Neglected Tropical Diseases,* **2012**.
4.   Department for International Development and Department of Health, *The Ross Fund,* **2015**.
5.   J.M. Bethony, R.N. Cole, X. Guo, S. Kamhawi, M.W. Lightowlers, A. Loukas, W. Petri, S. Reed, J.G. Valenzuela, P.J. Hotez, *Immunol. Rev.,* **2011**, *239*, 237.
6.   N.J. White, S. Pukrittayakamee, T.T. Hien, M.A. Faiz, O.A. Mokuolu, A.M. Dondorp, *Lancet,* **2014**, *383*, 723.
7.   V.S. Moorthy, J.-M. Okwo-Bele, *Lancet,* **2015**, *386*, 5.

8. A.R. Renslo, J.H. McKerrow, *Nat. Chem. Biol.,* **2006**, *2,* 701.
9. R. Pink, A. Hudson, M.-A. Mouries, M. Bendig, *Nat. Rev. Drug Discov.,* **2005**, *4,* 727.
10. S.L. Croft, S. Sundar, A.H. Fairlamb, *Clin. Microbiol. Rev.,* **2006**, *19,* 111.
11. S.L. Croft, M.P. Barrett, J.A. Urbina, *Trends Parasitol,* **2005**, *21,* 508.
12. L. Kedzierski, *J. Glob. Infect. Dis.,* **2010**, *2,* 177.
13. A.H. Fairlamb, A. Cerami, *Annu. Rev. Microbiol.,* **1992**, *46,* 695.
14. S. Khare, A.S. Nagle, A. Biggart, Y.H. Lai, F. Liang, L.C. Davis, S.W. Barnes, C.J.N. Mathison, E. Myburgh, M.-Y. Gao, J.R. Gillespie, X. Liu, J.L. Tan, M. Stinson, I.C. Rivera, J. Ballard, V. Yeh, T. Groessl, G. Federe, H.X.Y. Koh, J.D. Venable, B. Bursulaya, M. Shapiro, P.K. Mishra, G. Spraggon, A. Brock, J.C. Mottram, F.S. Buckner, S.P.S. Rao, B.G. Wen, J.R. Walker, T. Tuntland, V. Molteni, R.J. Glynne, F. Supek, *Nature,* **2016**, *advance online publication*.
15. A.R. Renslo, J.H. McKerrow, *Nat. Chem. Biol.,* **2006**, *2,* 701.
16. J. Alvar, I.D. Vélez, C. Bern, M. Herrero, P. Desjeux, J. Cano, J. Jannin, M.d. Boer, The World Health Organisation Leishmaniasis Control Team, *PLOS ONE,* **2012**, *7,* e35671.
17. The World Health Organisation, *Leishmaniasis* **2014**.
18. B.L. Herwaldt, *Lancet,* **1999**, *354,* 1191.
19. R. Du, P.J. Hotez, W.S. Al-Salem, A. Acosta-Serrano, *PLOS Negl. Trop. Dis.,* **2016**, *10,* e0004545.
20. P. Desjeux, *Comp. Immunol. Microb.,* **2004**, *27,* 305.
21. T. Naderer, M.J. McConville, *Cell. Microbiol.,* **2008**, *10,* 301.
22. S.M. Gossage, M.E. Rogers, P.A. Bates, *Int. J. Parasitol.,* **2003**, *33,* 1027.
23. T. Naderer, J.E. Vince, M.J. McConville, *Curr. Mol. Med.,* **2004**, *4,* 649.
24. V. Bahr, Y.D. Stierhof, T. Ilg, M. Demar, M. Quinten, P. Overath, *Mol. Biochem. Parasitol.,* **1993**, *58,* 107.
25. D.L. Sacks, G. Modi, E. Rowton, G. Spath, L. Epstein, S.J. Turco, S.M. Beverley, *Proc. Natl. Acad. Sci. USA,* **2000**, *97,* 406.
26. G.A. Eggimann, K. Sweeney, H.L. Bolt, N. Rozatian, S.L. Cobb, P.W. Denny, *Molecules,* **2015**, *20,* 2775.
27. R.N. Coler, M.S. Duthie, K.A. Hofmeyer, J. Guderian, L. Jayashankar, J. Vergara, T. Rolf, A. Misquith, J.D. Laurance, V.S. Raman, H.R. Bailor, N.D. Cauwelaert, S.J. Reed, A. Vallur, M. Favila, M.T. Orr, J. Ashman, P. Ghosh, D. Mondal, S.G. Reed, *Clin. Trans. Immunol.,* **2015**, *4,* e35.
28. H. Rezvan, M. Moafi, *Vet. Res. Forum,* **2015**, *6,* 1.
29. K. Jain, N.K. Jain, *J. Immunol. Methods,* **2015**, *422,* 1.
30. R. Kumar, C. Engwerda, *Clin. Trans. Immunol.,* **2014**, *3,* e13.
31. J.P.B. de Menezes, C.E.S. Guedes, A.L. Petersen, A.F. de Oliveira, V. Deborah Bittencourt, T. Patrcia Sampaio, *BioMed. Res. Int.,* **2015**, *2015,* 11.
32. J.N. Sangshetti, F.A. Kalam Khan, A.A. Kulkarni, R. Arote, R.H. Patil, *RSC Adv.,* **2015**, *5,* 32376.
33. A. Hailu, A. Musa, M. Wasunna, M. Balasegaram, S. Yifru, G. Mengistu, Z. Hurissa, W. Hailu, T. Weldegebreal, S. Tesfaye, E. Makonnen, E. Khalil, O. Ahmed, A. Fadlalla, A. El-Hassan, M. Raheem, M. Mueller, Y. Koummuki, J. Rashid, J. Mbui, G. Mucee, S. Njoroge, V. Manduku, A. Musibi, G. Mutuma, F. Kirui, H. Lodenyo, D. Mutea, G. Kirigi, T. Edwards, P. Smith, L. Muthami, C. Royce, S. Ellis, M. Alobo, R. Omollo, J. Kesusu, R. Owiti, J. Kinuthia, *PLOS Negl. Trop. Dis.,* **2010**, *4,* e709.
34. S.L. Croft, V. Yardley, *Curr. Pharm. Des.,* **2002**, *8,* 319.

35. Centres for Disease Control and Prevention; Centres for Disease Control and Prevention; Vol. 2014.

36. M.N. Martinez, G.L. Amidon, *J. Clin. Pharmacol.,* **2002**, *42*, 620.

37. I. Muhammad, D.C. Dunbar, S.I. Khan, B.L. Tekwani, E. Bedir, S. Takamatsu, D. Ferreira, L.A. Walker, *J. Nat. Prod.,* **2003**, *66*, 962.

38. H. Fuchino, T. Koide, M. Takahashi, S. Sekita, M. Satake, *Planta Medica,* **2001**, *67*, 647.

39. M. Sairafianpour, J. Christensen, D. Staerk, B.A. Budnik, A. Kharazmi, K. Bagherzadeh, J.W. Jaroszewski, *J. Nat. Prod.,* **2001**, *64*, 1398.

40. Y. Nakao, S. Kawatsu, C. Okamoto, M. Okamoto, Y. Matsumoto, S. Matsunaga, R.W.M. van Soest, N. Fusetani, *J. Nat. Prod.,* **2008**, *71*, 469.

41. M.J. Balunas, R.G. Linington, K. Tidgewell, A.M. Fenner, L.D. Urena, G.D. Togna, D.E. Kyle, W.H. Gerwick, *J. Nat. Prod.,* **2010**, *73*, 60.

42. A.K. Marr, B.S. McGwire, W.R. McMaster, *Future Microbiol.,* **2012**, 7, 1047.

43. S.L. Cobb, P.W. Denny, *Curr. Opin. Investig. Drugs,* **2010**, *11*, 868.

44. B.S. McGwire, C.L. Olson, B.F. Tack, D.M. Engman, *J. Infect. Dis.,* **2003**, *188*, 146.

45. B.S. McGwire, M.M. Kulkarni, *Exp. Parasitol.,* **2010**, *126*, 397.

46. M.M. Kulkarni, W.R. McMaster, E. Kamysz, W. Kamysz, D.M. Engman, B.S. McGwire, *Mol. Microbiol.,* **2006**, *62*, 1484.

47. C. Maciel, V.X. de Oliveira Junior, M.A. Fázio, R. Nacif-Pimenta, A. Miranda, P.F.P. Pimenta, M.L. Capurro, *PLOS ONE,* **2008**, *3*, e3296.

48. A. Bera, S. Singh, R. Nagaraj, T. Vaidya, *Mol. Biochem. Parasitol.,* **2003**, *127*, 23.

49. L.R. Haines, J.M. Thomas, A.M. Jackson, B.A. Eyford, M. Razavi, C.N. Watson, B. Gowen, R.E. Hancock, T.W. Pearson, *PLOS Negl. Trop. Dis.,* **2009**, *3*, e373.

50. M.A. Lynn, J. Kindrachuk, A.K. Marr, H. Jenssen, N. Panté, M.R. Elliott, S. Napper, R.E. Hancock, W.R. McMaster, *PLOS Negl. Trop. Dis.,* **2011**, 5, e1141.

51. A.F. Lacerda, P.B. Pelegrini, D.M. de Oliveira, E.A. Vasconcelos, M.F. Grossi-de-Sa, *Front. Microbiol.,* **2016**, 7, 91.

52. P. Diaz-Achirica, J. Ubach, A. Guinea, D. Andreu, L. Rivas, *J. Biochem.,* **1998**, *330*, 453.

53. C. Chicharro, C. Granata, R. Lozano, D. Andreu, L. Rivas, *Antimicrob. Agents Chemother.,* **2001**, 45, 2441.

54. J. Alberola, A. Rodriguez, O. Francino, X. Roura, L. Rivas, D. Andreu, *Antimicrob. Agents Chemother.,* **2004**, *48*, 641.

55. C. Tian, B. Gao, C. Rodriguez Mdel, H. Lanz-Mendoza, B. Ma, S. Zhu, *Mol. Immunol.,* **2008**, *45*, 3909.

56. M. Shahabuddin, I. Fields, P. Bulet, J.A. Hoffmann, L.H. Miller, *Exp. Parasitol.,* **1998**, *89*, 103.

57. R.W. Gwadz, D. Kaslow, J.Y. Lee, W.L. Maloy, M. Zasloff, L.H. Miller, *Infect. Immun.,* **1989**, 57, 2628.

58. H.G. Boman, D. Wade, I.A. Boman, B. Wahlin, R.B. Merrifield, *FEBS Lett.,* **1989**, *259*, 103.

59. R. Carballar-Lejarazu, M.H. Rodriguez, F. de la Cruz Hernandez-Hernandez, J. Ramos-Castaneda, L.D. Possani, M. Zurita-Ortega, E. Reynaud-Garza, R. Hernandez-Rivas, T. Loukeris, G. Lycett, H. Lanz-Mendoza, *Cell. Mol. Life Sci.,* **2008**, *65*, 3081.

60. A. Fieck, I. Hurwitz, A.S. Kang, R. Durvasula, *Exp. Parasitol.,* **2010**, *125*, 342.

61. B. Gao, J. Xu, C. Rodriguez Mdel, H. Lanz-Mendoza, R. Hernandez-Rivas, W. Du, S. Zhu, *Biochimie,* **2010**, *92*, 350.

62. K. Konno, M. Hisada, H. Naoki, Y. Itagaki, R. Fontana, M. Rangel, J.S. Oliveira, M.P. Cabrera, J.R. Neto, I. Hide, Y. Nakata, T. Yasuhara, T. Nakajima, *Peptides,* **2006**, *27,* 2624.

63. S.E. Lofgren, L.C. Miletti, M. Steindel, E. Bachere, M.A. Barracco, *Exp. Parasitol.,* **2008**, *118,* 197.

64. C.K. Moreira, F.G. Rodrigues, A. Ghosh, P. Varotti Fde, A. Miranda, S. Daffre, M. Jacobs-Lorena, L.A. Moreira, *Exp. Parasitol.,* **2007**, *116,* 346.

65. M. Rangel, M.P. Cabrera, K. Kazuma, K. Ando, X. Wang, M. Kato, K. Nihei, I.Y. Hirata, T.J. Cross, A.N. Garcia, E.L. Faquim-Mauro, M.R. Franzolin, H. Fuchino, K. Mori-Yasumoto, S. Sekita, M. Kadowaki, M. Satake, K. Konno, *Toxicon,* **2011**, *57,* 1081.

66. J. Vizioli, P. Bulet, J.A. Hoffmann, F.C. Kafatos, H.M. Muller, G. Dimopoulos, *Proc. Natl. Acad. Sci. USA,* **2001**, *98,* 12630.

67. F.L. Chadbourne, C. Raleigh, H.Z. Ali, P.W. Denny, S.L. Cobb, *J. Pept. Sci.,* **2011**, *17,* 751.

68. A.L. Souza, R.X. Faria, K.S. Calabrese, D.J. Hardoim, N. Taniwaki, L.A. Alves, S.G. De Simone, *PLOS ONE,* **2016**, *11,* e0157673.

69. T. Jacobs, H. Bruhn, I. Gaworski, B. Fleischer, M. Leippe, *Antimicrob. Agents Chemother.,* **2003**, *47,* 607.

70. M. Torrent, D. Pulido, L. Rivas, D. Andreu, *Curr. Drug Targets,* **2012**, *13,* 1138.

71. B. Mojsoska, R.N. Zuckermann, H. Jenssen, *Antimicrob. Agents Chemother.,* **2015**.

72. M.L. Huang, S.B.Y. Shin, M.A. Benson, V.J. Torres, K. Kirshenbaum, *ChemMedChem,* **2012**, *7,* 114.

73. M.L. Huang, M.A. Benson, S.B.Y. Shin, V.J. Torres, K. Kirshenbaum, *Eur. J. Org. Chem.,* **2013**, 3560.

74. T.S. Ryge, P.R. Hansen, *J. Pept. Sci.,* **2005**, *11,* 727.

75. T.S. Ryge, N. Frimodt-Moller, P.R. Hansen, *Chemotherapy,* **2008**, *54,* 152.

76. N.P. Chongsiriwatana, J.A. Patch, A.M. Czyzewski, M.T. Dohm, A. Ivankin, D. Gidalevitz, R.N. Zuckermann, A.E. Barron, *Proc. Natl. Acad. Sci. USA,* **2008**, *105,* 2794.

77. R. Kapoor, P.R. Eimerman, J.W. Hardy, J.D. Cirillo, C.H. Contag, A.E. Barron, *Antimicrob. Agents Chemother.,* **2011**, *55,* 3058.

78. R. Kapoor, M.W. Wadman, M.T. Dohm, A.M. Czyzewski, A.M. Spormann, A.E. Barron, *Antimicrob. Agents Chemother.,* **2011**, *55,* 3054.

79. C.A. Olsen, H.L. Ziegler, H.M. Nielsen, N. Frimodt-Moller, J.W. Jaroszewski, H. Franzyk, *ChemBioChem,* **2010**, *11,* 1356.

80. K. Andreev, C. Bianchi, J.S. Laursen, L. Citterio, L. Hein-Kristensen, L. Gram, I. Kuzmenko, C.A. Olsen, D. Gidalevitz, *Biochim. Biophys. Acta,* **2014**, *1838,* 2492.

81. L. Vedel, G. Bonke, C. Foged, H. Ziegler, H. Franzyk, J.W. Jaroszewski, C.A. Olsen, *ChemBioChem,* **2007**, *8,* 1781.

82. C. Chan, H. Yin, J.H. McKie, A.H. Fairlamb, K.T. Douglas, *Amino Acids,* **2002**, *22,* 297.

83. J. Mikus, D. Steverding, *Parasitol. Int.,* **2000**, *48,* 265.

84. M.T. McCrudden, D.F. Orr, Y. Yu, W.A. Coulter, G. Manning, C.R. Irwin, F.T. Lundy, *J. Clin. Periodontol.,* **2013**, *40,* 933.

85. D.T. McLean, M.T. McCrudden, G.J. Linden, C.R. Irwin, J.M. Conlon, F.T. Lundy, *Regul. Pept.,* **2014**, *194-195,* 63.

86. V.M. Schoop, N. Mirancea, N.E. Fusenig, *J. Invest. Dermatol.,* **1999**, *112,* 343.

87. P. Boukamp, R.T. Petrussevska, D. Breitkreutz, J. Hornung, A. Markham, N.E. Fusenig, *The Journal of Cell Biology,* **1988**, *106,* 761.

88. S. Wilkening, F. Stahl, A. Bader, *Drug Metab. Dispos.,* **2003**, *31,* 1035.

89. S. Costantini, G. Di Bernardo, M. Cammarota, G. Castello, G. Colonna, *Gene,* **2013**, *518*, 335.
90. S.A. Fowler, H.E. Blackwell, *Org. Biomol. Chem.,* **2009**, 7, 1508.
91. C.W. Wu, K. Kirshenbaum, T.J. Sanborn, J.A. Patch, K. Huang, K.A. Dill, R.N. Zuckermann, A.E. Barron, *J. Am. Chem. Soc.,* **2003**, *125*, 13525.
92. R. Kapoor, *Biophysical J.,* **2010**, *98*, 277A.
93. G.A. Eggimann, H.L. Bolt, P.W. Denny, S.L. Cobb, *ChemMedChem,* **2015**, *10*, 233.
94. H.L. Bolt, G.A. Eggimann, P.W. Denny, S.L. Cobb, *MedChemComm,* **2016**, *7*, 799.
95. C.W. Wu, T.J. Sanborn, K. Huang, R.N. Zuckermann, A.E. Barron, *J. Am. Chem. Soc.,* **2001**, *123*, 6778.
96. H.L. Bolt, S.L. Cobb, *Org. Biomol. Chem.,* **2016**, *14*, 1211.
97. D.C. Miguel, J.K.U. Yokoyama-Yasunaka, S.R.B. Uliana, *PLoS Neglected Tropical Diseases,* **2008**, *2*, e249.
98. D.E. Yerien, S. Bonesi, A. Postigo, *Org. Biomol. Chem.,* **2016**.
99. J.A. Patch, A.E. Barron, *J. Am. Chem. Soc.,* **2003**, *125*, 12092.
100. K. Kirshenbaum, A.E. Barron, R.A. Goldsmith, P. Armand, E.K. Bradley, K.T.V. Truong, K.A. Dill, F.E. Cohen, R.N. Zuckermann, *Proc. Natl. Acad. Sci. USA,* **1998**, *95*, 4303.
101. C.W. Wu, T.J. Sanborn, R.N. Zuckermann, A.E. Barron, *J. Am. Chem. Soc.,* **2001**, *123*, 2958.
102. A.T. Bockus, C.M. McEwen, R.S. Lokey, *Curr. Top. Med. Chem.,* **2013**, *13*, 821.
103. P.A. Bates, *Parasitol.,* **1994**, *108*, 1.
104. C. Peters, T. Aebischer, Y.D. Stierhof, M. Fuchs, P. Overath, *J. Cell. Sci.,* **1995**, *108*, 3715.
105. S.K. Jain, R. Sahu, L.A. Walker, B.L. Tekwani, *J. Vis. Exp.,* **2012**, e4054.
106. D. Paape, A.S. Bell, W.P. Heal, J.A. Hutton, R.J. Leatherbarrow, E.W. Tate, D.F. Smith, *PLOS Negl. Trop. Dis.,* **2014**, *8*, e3363.
107. A.M. Czyzewski, H. Jenssen, C.D. Fjell, M. Waldbrook, N.P. Chongsiriwatana, E. Yuen, R.E.W. Hancock, A.E. Barron, *PLOS ONE,* **2016**, *11*, e0135961.
108. M.A. Ferguson, *Phil. Trans. Royal Soc. Biol. Sci.,* **1997**, *352*, 1295.
109. R. Brun, J. Blum, F. Chappuis, C. Burri, *Lancet,* **2009**, *375*, 148.
110. A. Rassi Jr, A. Rassi, J.A. Marin-Neto, *Lancet,* **2010**, *375*, 1388.
111. J.R. Luque-Ortega, W. van't Hof, E.C. Veerman, J.M. Saugar, L. Rivas, *FASEB J.,* **2008**, *22*, 1817.
112. R.W. Snow, C.A. Guerra, A.M. Noor, H.Y. Myint, S.I. Hay, *Nature,* **2005**, *434*, 214.
113. A.-C. Uhlemann, S. Krishna In *Malaria: Drugs, Disease and Post-genomic Biology*; Compans, R. W., Cooper, M. D., Honjo, T., Koprowski, H., Melchers, F., Oldstone, M. B. A., Olsnes, S., Potter, M., Vogt, P. K., Wagner, H., Sullivan, D. J., Krishna, S., Eds.; Springer Berlin Heidelberg: Berlin, Heidelberg, 2005, p 39.
114. I. Pena, M. Pilar Manzano, J. Cantizani, A. Kessler, J. Alonso-Padilla, A.I. Bardera, E. Alvarez, G. Colmenarejo, I. Cotillo, I. Roquero, F. de Dios-Anton, V. Barroso, A. Rodriguez, D.W. Gray, M. Navarro, V. Kumar, A. Sherstnev, D.H. Drewry, J.R. Brown, J.M. Fiandor, J. Julio Martin, *Sci. Rep.,* **2015**, *5*, 8771.

Chapter 4

Antibacterial and Antifungal Peptoids

Since the discovery of penicillin in 1928, a large range of antibiotics have been successfully developed to combat a wide variety of infections. However, as discussed earlier for the neglected tropical diseases, antimicrobial resistance is an extreme threat to global public health. Statements from organisations like the World Health Organisation highlight the real possibility of entering a new era with a lack of suitable antibiotics. Recent initiatives such as the 10 x 20 Initiative in 2010 and the 2015 Global Antimicrobial Resistance Research Innovation Fund encourage investment and a commitment to the development of new antibacterial drugs.[1]

Antibiotic resistance is reported frequently in the media, with a high proportion of hospital acquired infections caused by multi-drug resistant bacteria. Resistance to these antibiotics is increasing at a remarkable rate and is a significant problem. Clinically noteworthy antibiotic resistance has developed against every single antibiotic in use and as illustrated by **Figure 4.1**, the first observations of drug resistant bacteria often occurs very soon after the first clinical use of the drugs. For example, in the case of daptomycin (discovered in 2004), resistance was seen only one year later in 2005. Despite this, the development of new classes of antibiotics has stalled even though the need for such drugs has increased dramatically.[2-9]
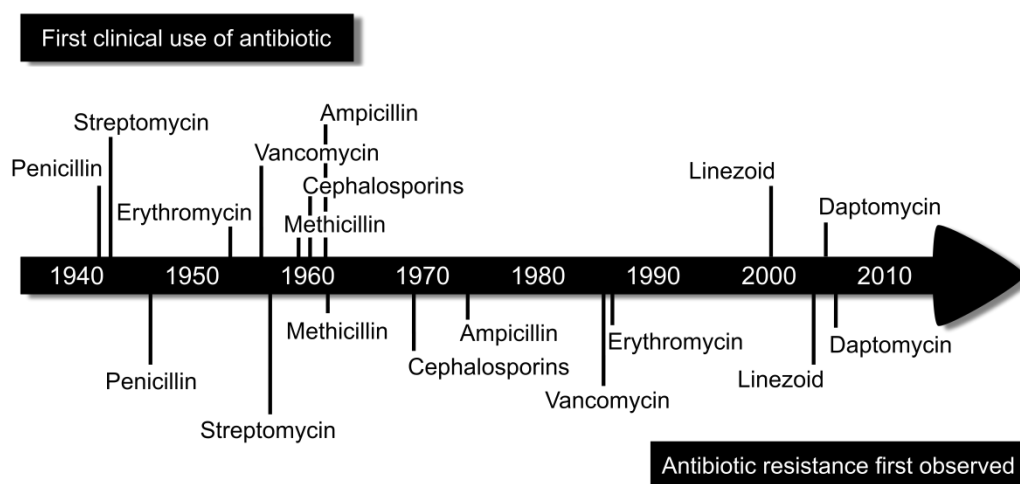
Figure 4.1. Timeline to show the deployment of key antibiotics in the clinic and the first reported occurrence of antibiotic resistance to these drugs.

The problem of antibiotic resistance will only escalate in the future, therefore there is a desperate need to design, make and test new antibiotic compounds. AMPs have been extensively studied as new antibiotic compounds with different modes of action to traditional small molecule drugs that may decrease the chance of resistance developing. As discussed in Chapter 1, peptoids have also been shown as very promising new antibiotic compounds with a greater resistance to proteolysis than peptide counterparts. Therefore, the peptoid sequences designed for antiparasitic activity were also tested as novel antibiotics in this project.

Bacteria can be classified as either Gram positive or Gram negative, dependent on their membrane structure. Gram positive bacteria have a thick, multi-layered peptidoglycan membrane that protects a single cytoplasmic membrane. The Gram negative bacteria have a single peptidoglycan layer but an extra outer membrane made of glycolipids (especially lipopolysaccharides), which can provide protection against toxins and makes the Gram negative bacteria less susceptible to antibiotics. In addition to these layers, bacterial cell membranes are decorated with other molecules and proteins, as shown in **Figure 4.2**.[6,10]
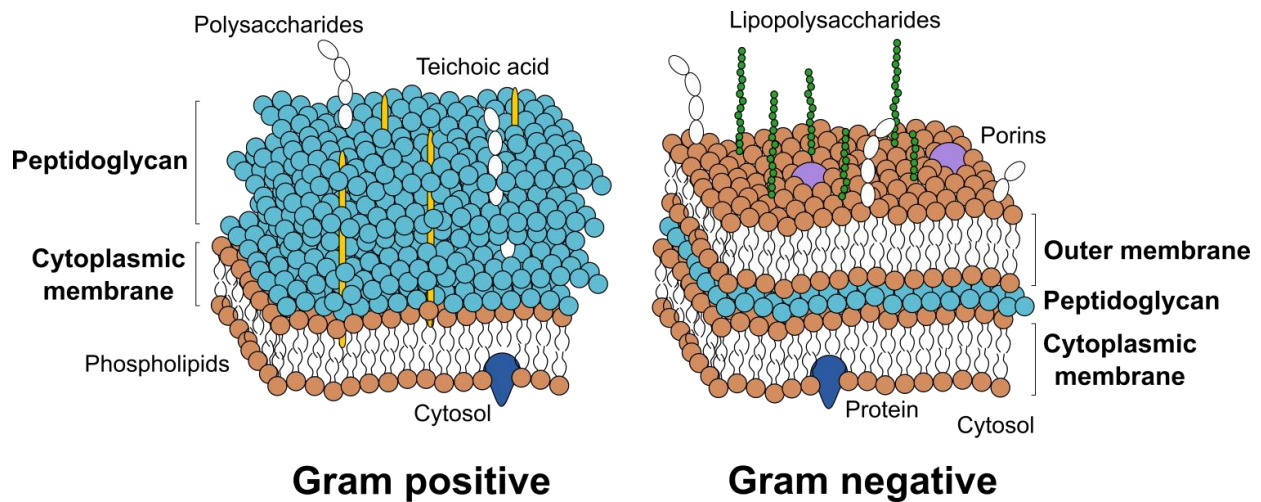
Figure 4.2. A comparison of the membrane structures of Gram positive and Gram negative bacteria.

Clinically relevant microorganisms often exist naturally in complex biofilms that are substantially different in phenotype to planktonic bacteria. A biofilm is an aggregate of microorganisms that can comprise a mixture of bacterial or fungal species. In the biofilm, cells typically adhere to each other, or to a surface, and are frequently embedded in a self-produced matrix of extracellular polymeric substances (EPS) (see **Figure 4.3**). Biofilms are not easily washed from any surfaces they adhere to as the EPS matrix, typically made of polysaccharides, protects the biofilm.[11-13]
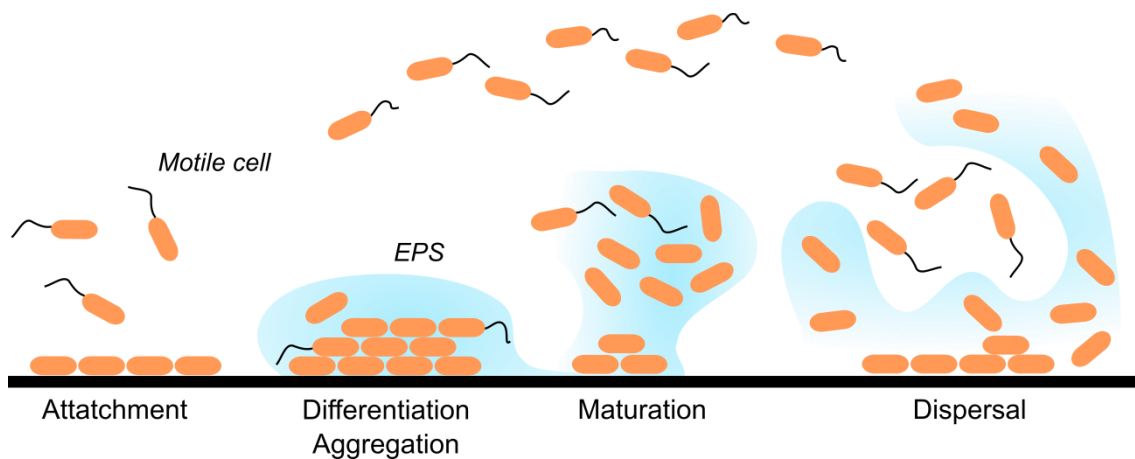
Figure 4.3. The lifecycle of a biofilm; bacteria populate and attach to a surface, bacteria produce EPS, aggregate and grow in the biofilm community then after maturation, single cells are released to start new colonies.

Biofilms are responsible for many device related infections in a hospital setting, i.e. on catheters or surgical implants, and also cause tissue infections including dental plaques or chronic wound infections. Conventional antibiotics that work well against planktonic bacteria are often inadequate for the treatment of biofilms. The extracellular matrix provides some protection for the biofilm as any drug may fail to penetrate beyond the surface layer of the biofilm. Additionally, biofilms are often not as metabolically active as planktonic species so therefore might not respond so well to antibiotics that target metabolic processes. Multiple species can exist within a biofilm, so any antibiotic would have to target multiple bacterial or fungal strains and certain genes may be up- or down-regulated in the biofilms.[14]

Consequently any investigation into new antibiotics should ideally target both planktonic and biofilm bacterial phenotypes, and across both Gram negative and Gram positive strains. Therefore, peptoids were evaluated as novel antibiotic compounds in tests against bacteria in both their planktonic (section 4.1) and biofilm form (section 4.2). It is suspected that peptoids disrupt the cell membrane and since Gram negative and Gram positive bacteria have significantly different membrane structures, a selection of bacterial strains were tested that represented both classes of bacterial cell envelope. The action of peptoids against biofilms was then investigated in both single and multispecies biofilms. Following these investigations into the antibacterial and fungicidal properties of the peptoid library, a method to potentially improve the selectivity index of peptoids was explored in section 4.3, via conjugation of peptoid sequences to the lantibiotic nisin.

4.1   Bacterial minimum inhibitory concentration determination

Antibacterial screening was undertaken in collaboration with Dr Gary Sharples in the Biosciences Department at Durham University, and contributions to the collection of bacterial MIC data were made by Dr Gabriela Eggimann (postdoctoral research assistant, Cobb group), Mark Laws (undergraduate project student, Cobb group) and Sophia Schwartz (Erasmus student, Cobb group).

To assess the antibacterial properties of a selection of peptoids, minimum inhibitory concentrations (MICs) were determined for the peptoids against *Staphylococcus aureus* and *Staphylococcus epidermidis* (Gram positive), *Escherichia coli* and *Pseudomonas aeruginosa* (Gram negative). Certain strains of *E. coli* and *S. aureus* are responsible for food poisoning and *S. aureus* can also cause respiratory disease or skin infections. *S. epidermis* is part of the normal skin flora, however in patients with compromised immune systems, infections can develop especially within biofilms on surgical implants or catheters. *P. aeruginosa* is another opportunistic pathogen that can colonise medical devices and is also associated with serious illnesses. It typically infects the respiratory tract, urinary tract or open wounds, particularly in patients with a weakened immune system, and can lead to sepsis.[15]

The MIC is defined as the lowest concentration of peptoid that completely inhibits bacterial growth after incubation at 38 °C for 16 hours, using the procedure by Andrews *et al.*[16] Ampicillin (**101**) was used as a comparative as it is a commonly used antibiotic and results were quantified via absorbance values.

Peptoids assessed in this study were chosen from the library already tested against *L. mexicana* to gain a broader understanding of the factors that lead to effective and selective antimicrobial peptoids. Since the mode of action of peptoids against bacteria is assumed to be membrane disruption, the sequences selected contained a wide variety of side chain functionalisation to help elucidate the factors necessary for activity. As before, sequences 6, 9 and 12 residues in length were included and the library included residues with alkyl character, substituted aromatic monomers and different cationic functionality; such as the mixed lysine- and arginine- type peptoids. All sequences were designed around the trimer motif previously described and reported to promote amphipathic structures, where the third monomer was typically a cationic monomer (since the peptoid helix turn is reported to be every three residues in a polyproline type I helix).[17-19]

In addition to the MIC data, as a measure of toxicity against mammalian cells the peptoid library was also tested against the epithelial HaCaT and HepG2 cell lines introduced in Chapter 3. From these ED_{50} values obtained a selectivity index[*] was calculated for the action of the peptoids against each pathogen. The results from the biological evaluation of the peptoid library are shown in **Table 4.1**. To the best of our knowledge this library is the single largest library of linear antibacterial peptoids to date and many of the sequence motifs and monomers included have not yet been reported in antibacterial peptoids.

---

[*] Selectivity index is defined as toxicity/activity and represented as an average of the selectivity to HaCaT and HepG2.

Peptoid Sequence	ED₅₀ (µM)		MIC (µM)				Average Selectivity Index			
	HaCaT	HepG2	E.coli	P.aeruginosa	S.aureus	S.epidermidis	E.coli	P.aeruginosa	S.aureus	S.epidermidis
210 (NahNpheNphe)₄	100	100	13	100	2	6	8	1	50	17
211 (NahNpheNphe)₃	100	100	50	100	6	3	2	1	17	33
212 (NahNpheNphe)₂	100	100	100	100	100	100	1	1	1	1
186 (NLysNpheNphe)₄	36	100	13	50	3	2	6	2	23	34
187 (NLysNpheNphe)₃	100	100	50	100	25	6	2	1	4	17
188 (NLysNpheNphe)₂	100	100	100	100	100	100	1	1	1	1
180 (NaeNpheNphe)₄	100	100	13	50	2	6	8	2	50	17
213 (NaeNpheNphe)₃	100	100	100	100	13	100	1	1	8	1
214 (NaeNpheNphe)₂	100	100	100	100	100	100	1	1	1	1
215 (NahNspeNspe)₄	23	41	25	50	2	2	2	1	16	17
216 (NahNspeNspe)₃	100	100	25	100	3	2	4	1	33	50
217 (NahNspeNspe)₂	100	100	100	100	100	25	1	1	1	4
22 (NLysNspeNspe)₄	20	29	25	50	2	1	1	1	13	25
26 (NLysNspeNspe)₃	100	100	13	100	2	2	8	1	50	50
25 (NLysNspeNspe)₂	100	100	100	100	100	25	1	1	1	4
156 (NaeNspeNspe)₄	26	41	100	50	2	2	0	1	17	17
218 (NaeNspeNspe)₃	100	100	25	100	2	13	4	1	50	8
219 (NaeNspeNspe)₂	100	100	100	100	100	100	1	1	1	1
220 (NLysNpmbNpmb)₄	41	100	100	100	3	2	1	1	24	36
184 (NLysNpcbNpcb)₄	18	22	100	100	25	6	0	0	1	4
223 (NLysNpcbNpcb)₃	22	23	50	25	3	2	0	1	8	12
225 (NLysNpfbNpfb)₄	46	30	13	25	2	1	3	2	19	38
226 (NLysNpfbNpfb)₃	100	45	13	25	3	3	6	3	24	24
228 (NLysNmfbNmfb)₄	25	17	25	25	6	3	1	1	4	7
229 (NLysNmfbNmfb)₃	64	43	13	25	6	2	4	3	9	27
183 (NLysNpfbNspe)₄	20	26	13	13	2	2	2	2	12	12
231 (NLysNpfbNspe)₃	52	36	25	25	3	2	2	2	15	22
157 [(NLysNpfbNpfb)(NLysNspeNspe)]₂	100	55	6	50	2	1	13	2	39	78
233 (NLysNspeNspe)(NLysNpfbNpfb)(NLysNspeNspe)	65	43	13	25	3	2	4	3	21	28
243 (NamyNspeNspe)[(NLysNspeNspe)]₃	12	15	50	50	2	2	0	0	7	7
244 (NamyNspeNspe)₂(NLysNspeNspe)₂	20	18	100	100	2	1	0	0	10	19
245 (NLysNspeNspe)₂(NamyNspeNspe)(NLysNspeNspe)	20	22	100	100	6	2	0	0	4	11
293 (NhArgNpheNphe)₄	100		6	25		2	17	4		50
152 (NhArgNspeNspe)₄	20	12	6	13	1	1	3	2	16	16
295 (NhArgNspeNspe)₃			6	50	2	2				
153 (NhArgNmfbNmfb)₄	28	21	13	13	2	2	2	2	12	12
296 (NhArgNmfbNmfb)₃			6	25	2	1				
181 (NhArgNhLeuNspe)₄			13	25	1	2				
297 (NhArgNhLeuNspe)₃				100	3	2				
154 [(NamyNspeNspe)(NhArgNspeNspe)]₂	31	24	100	100	3	6	0	0	9	5
147 (NLysNspeNspe)₂(NhArgNspeNspe)₂	100		17	34	17		6	3	6	
148 (NhArgNspeNspe)₂(NLysNspeNspe)₂	15		17	17	17		1	1	1	
149 (NLysNspeNspe)(NhArgNspeNspe)(NLysNspeNspe)₂	33		17	17	17		2	2	2	
150 [(NhArgNspeNspe)(NLysNspeNspe)]₂	33		17	67	17		2	0	2	

Table 4.1. The minimum inhibitory concentrations for the peptoid library against *S. aureus* and *S. epidermidis* (Gram positive), *E. coli* and *P. aeruginosa* (Gram negative). Toxicity against two mammalian cell lines (HaCaT and HepG2) is also shown to calculate selectivity values. The selectivity index is represented as an average of the selectivity to HaCaT and HepG2. MIC values recorded at 100 µM have true MIC values > 100 µM.

As seen from the data summarised in **Table 4.1**, many peptoids within the library have low MIC values against both Gram negative and Gram positive bacteria, ranging from the most active at less than 1 μM to inactive peptoids with no activity even at 100 μM. Some of the MIC values obtained are within the same range of selected natural antimicrobial peptides described in the literature. For example, the AMP cecropin A[†] (compound **2**) was shown to kill 90 % of *E. coli* at 2 μM and peptoids **293**, **152**, **295** and **296** all have an MIC against *E. coli* of 6 μM.[20] Magainin 2[‡] (compound **1**), an amphibian derived AMP, was reported to have MIC values against *E. coli*, *S. epidermidis* and *S. aureus* of 5 μg mL⁻¹ (20 μM), 10 μg mL⁻¹ (4 μM) and 50 μg mL⁻¹ (2 μM) respectively and many of the peptoids in **Table 4.1** exhibit even better antibacterial activities than this (see **Figure 4.4**).[21,22]
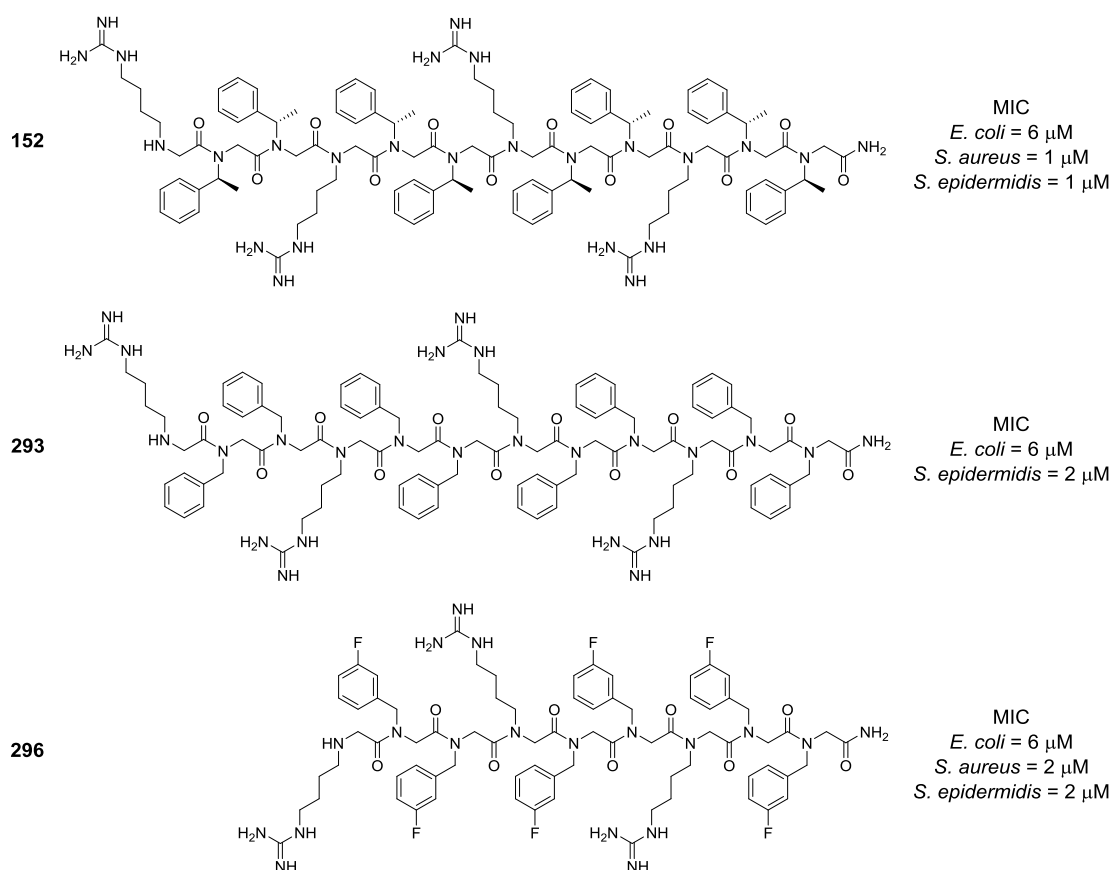
Figure 4.4. Structures of peptoids **152**, **293**, **296** with *N*hArg functionalisation.

Unsurprisingly, the activity of most peptoids is significantly greater against the Gram positive species (*S. aureus* and *S. epidermidis*) than Gram negative species (*E. coli* or *P. aeruginosa*). This differential activity is most probably due to the presence of the lipopolysaccharide-rich outer membrane of Gram negative bacteria, which presents a significant permeability barrier to many hydrophobic molecules. Certain compounds within the library displayed selectivity for certain bacterial species, however no Gram negative specific peptoids were identified. Any sequences that can selectively target Gram negative bacteria are highly sought after due to rising concerns about antibiotic resistance.[2,9,23-26]

[†] **2** cecropin A sequence: KWKLFKKIEKVGQNIRDGIIKAGPAVAVVGQATQIAK-NH₂
[‡] **1** magainin 2 sequence: GIGKFLHSAKKFGKAFVGEIMNS-NH₂

4.1.1 Structure activity relationships in antibacterial peptoids

First generation peptoid library – effect of sequence length and chirality

As a starting point, the first generation peptoid library (compounds **210–219**), previously tested for activity against *L. mexicana*[27] was also examined. In the work against the parasites, it was determined that factors such as overall sequence length and inclusion of chiral monomers could enhance the antimicrobial effect of the peptoid. It was also shown that the length of cationic side chain was important, with the shortest *N*ae monomer imparting better activity than *N*Lys and the longest *N*ah residue having the least potent antiparasitic activity.

These trends are also replicated in the activity of the peptoid library against the bacteria in **Table 4.1**. The longest 12 residue peptoids (**210**, **186**, **180**, **215**, **22** and **156**) were always more active than their 9 residue analogues, which were themselves more active than the 6 residue peptoid sequences. Hexapeptoids **212**, **188**, **214**, **217**, **25** and **219** showed generally limited antibacterial activity against the bacteria tested with MICs of 100 μM, although it is interesting to note that *S. epidermidis* did show some sensitivity to peptoids **25** and **219.**

Interestingly, the effect of monomer chirality was less important to achieve antibacterial activity than with *L. mexicana*; in many cases, sequences comprised exclusively from achiral monomers had comparable or better activity than analogues containing the chiral *N*spe building block (see **Table 4.1**). For example, comparing peptoid **186** to **22** (structures in **Figure 4.5**) which are achiral and chiral analogues of the same sequence, similar MIC values are observed against *P. aeruginosa* (50 μM for both) and *S. aureus* (MIC 3 μM and 2 μM). However, against *E. coli*, the achiral peptoid **186** has an MIC of 12 μM compared to 25 μM for the chiral equivalent **22**. A similar pattern is apparent with peptoids **180** and **156** (sequences with the shorter *N*ae monomer and either *N*phe or *N*spe respectively), with the peptoids having similar activity against both *P. aeruginosa* and *S. aureus* but the achiral sequence **180** shows better activity against *E. coli* (MIC 13 μM and > 100 μM respectively).

186 where R = H
22 where R = CH₃
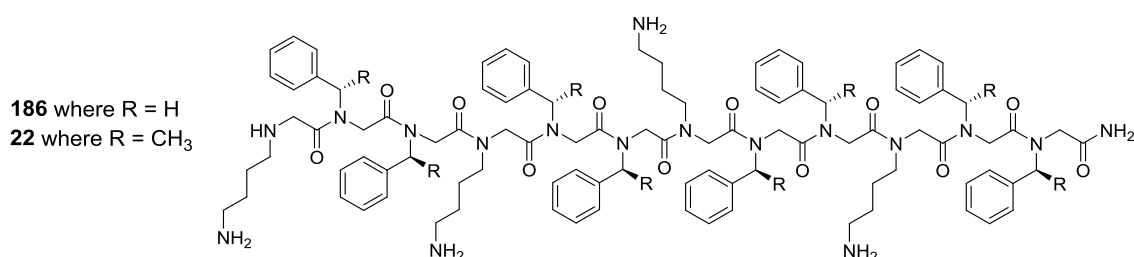
Figure 4.5. Structures of the achiral peptoid **186** (where R = H) and chiral peptoid **22** (where R = CH$_3$).

When comparing sequences containing the different amino-functionalised cationic monomers, *N*ae, *N*Lys and *N*ah, it is not possible to draw a simple conclusion about the optimum length of side chain for the best antibacterial activity as promising activity is seen for all three cationic residues (monomer structures given in **Figure 4.6**). Peptoids based upon the (*NxN*phe*N*phe)$_4$ motif **210** (*N*x = *N*ah), **186** (*N*x = *N*Lys) and **180** (*N*x = *N*ae) all have an MIC of 13 μM against *E. coli* and good activity against both *Staphylococcus* species. However, when comparing the chiral analogues of the same motif (*NxN*spe*N*spe)$_4$, the sequences with *N*ah and *N*Lys (**215** and **22**) have an MIC of 25 μM against *E. coli* but peptoid **156** with the shortest *N*ae residue has negligible activity. For these peptoids **215**, **22** and **156**, the activity against *P. aeruginosa*, *S. aureus* and *S. epidermidis* is similar regardless of the choice of cationic monomer (see **Table 4.1**).
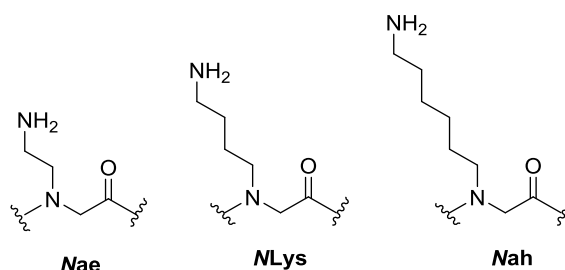
Figure 4.6. Cationic monomers used in sequences **210–219** with 2, 4 and 6 carbons in the side chain.

Effects of substitution to aromatic monomers

The effect of additional substituents to the aromatic groups on peptoid sequences within the library was examined in a similar way to those described in Chapter 3.[28] Monomer substitutions included a methoxy group in the para position of the benzyl group (*N*pmb), chlorine in the para position (*N*pcb) or fluorine in either the para or meta position (*N*pfb or *N*mfb). Against *L. mexicana*, it was shown that halogenated monomers (in particular fluorinated ones) improve the efficacy of the sequence against amastigotes.

Based upon these observations, the screening of peptoids against bacteria focused on the halogenated sequences so only the longest 12 residue methoxy substituted peptoid was tested, compound **220** in **Table 4.1**. Addition of the –OMe group to the ring had a negligible effect to the Gram negative bacteria and no improvement in action was seen against the Gram positive bacteria compared to the unsubstituted analogue, peptoid **186**.

Addition of chlorine in the para position of the benzyl ring was shown to increase toxicity to the mammalian cell lines but improved activity against axenic amastigotes. However, a similar increase in activity was not seen against the bacteria. For example, compound **184** has an MIC of > 100 μM against *E. coli*, whereas the unsubstituted analogue **186** shows potent activity at 13 μM (see **Table 4.1**).

The fluorinated peptoid sequences were more successful at targeting the various bacterial species. Peptoids containing the achiral *N*mfb or *N*pfb (**225–229**) show

marginally improved antibacterial activities compared to the unsubstituted peptoids (**186–188**). There is no significant difference on antibacterial activity for monomers substituted in the para or meta position and interestingly, the 9 residue peptoids **226** and **229** have a similar level of broad spectrum antibacterial activity as the longer 12 residue peptoids, **225** and **228**, but have a reduced toxicity to the mammalian cells. In this case, it appears that the shorter 9 residue sequences may be better antibacterial candidates with a larger therapeutic window.

The peptoids containing the chiral *N*spe monomer in combination with the fluorinated monomer *N*pfb (**183–233**, **Table 4.1**) show slightly more potent activity against the bacterial species than the achiral fluorinated peptoids **225–229**, however also tend to be more toxic to the mammalian cells. In particular the 12 residue peptoid **157** is promising, where the *N*spe and *N*pfb are designed in a coblock manner. [(*N*Lys*N*pfb*N*pfb)(*N*Lys*N*spe*N*spe)]$_2$ has good activity towards *E. coli* (MIC 6 μM), *S. aureus* and *S. epidermidis* (MIC 2 μM and < 1 μM) but shows a reduced toxicity towards HaCaT and HepG2 compared to the sequences made of *N*spe or *N*pfb exclusively.

Peptoids with alkyl substitution

To probe the relationship between net charge and hydrophobicity of a peptoid and its biological activity, analogues of peptoid **22** (*N*Lys*N*spe*N*spe)$_4$ were synthesised where the alkyl monomer *N*amy was substituted in the place of the cationic *N*Lys monomers. In these analogues (peptoids **243–245**, **Table 4.1**), the charge is replaced either at the *N* terminal end of the sequence or in two positions within the sequence (see **Figure 4.7** for an example structure).

The parent sequence **22** shows moderate activity against *E. coli* and *P. aeruginosa* (MIC 25 μM and 50 μM respectively) and potent micromolar activity against the Gram positive bacteria. Substitution of the cationic *N*Lys monomer with *N*amy retains activity against both Gram positive bacteria, but leads to a reduction of overall activity against Gram negative bacteria. To illustrate this, peptoids **243–245** have MIC values of 50 μM or > 100 μM against *E. coli* and similar reductions in activity are seen for *P. aeuriginosa*.
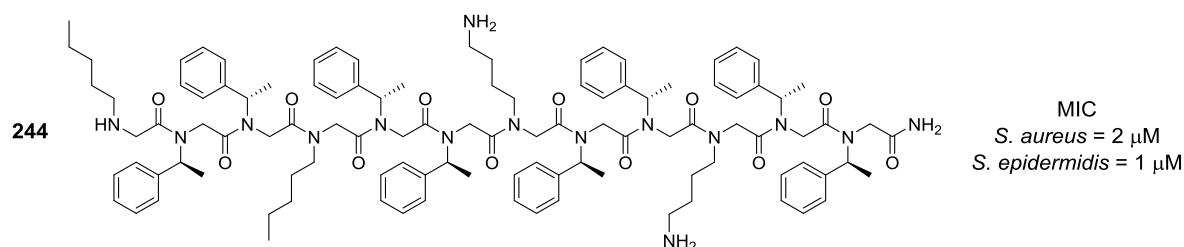
Figure 4.7. Example structure for peptoid **244** where charged *N*Lys residue is replaced by *N*amy.

The effect of lysine- or arginine-type monomers on antibacterial activity

Arginine containing peptoids have been shown to increase membrane permeability and antibacterial activity in the literature[29-31] so sequences containing arginine peptoid monomers were included in the library. This allowed the comparison of differently functionalised cationic residues on the peptoid sequences (i.e. the amino *N*Lys peptoids or the guanidine groups of *N*hArg). It has also been suggested that arginine in peptide sequences can increase antibacterial potency but also will have an associated rise in toxicity.[29,32] In an attempt to modulate the biological properties of the peptoid library, for the first time, peptoids with both lysine and arginine in the same sequence have been evaluated against bacterial targets using the new methodology developed in this project.[33]

This sub-library of peptoids can be split between sequences exclusively containing arginine residues (**Table 4.1**, peptoids **293–154**) and those that contain a mixture of both lysine and arginine-type side chains (**Table 4.1**, peptoids **147–150**). In these compounds *N*hArg has been introduced, which is the equivalent side chain to the *N*Lys residue, with 4 carbons in the backbone and the terminal guanidine moiety. An example structure for peptoid **150** is shown in **Figure 4.8**.
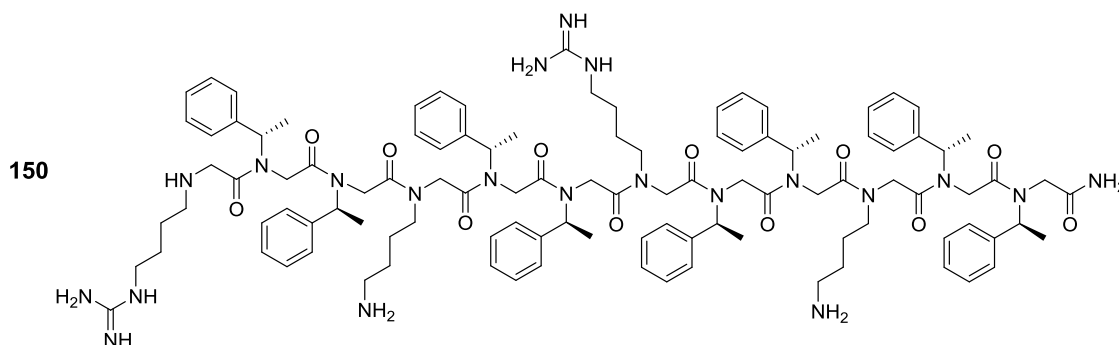
Figure 4.8. Structure of peptoid **150** [(*N*hArg*N*spe*N*spe)(*N*Lys*N*spe*N*spe)]$_2$, that contains both amino-functionalised lysine-type monomers and the arginine-mimetic residues.

In contrast to peptoids that contain amino-functionalised *N*Lys residues, the sequences with *N*hArg exclusively tend to have an increased toxicity to the mammalian cell lines tested but do display improved activity against the bacteria tested (see **Table 4.1**). For example, when comparing the fluorinated peptoids **153** and **296** to their lysine-equivalents (**228** and **229** respectively) we see an approximate 2-fold increase in antibacterial activity for all species tested; for the longest 12 residue sequence (*N*x*N*mfb*N*mfb)$_4$ activity against *E. coli* is 13 µM in **153** (where *N*x is *N*hArg) compared to 25 µM in **228** (where *N*x is *N*Lys). Against *S. aureus* the arginine-type peptoid has an MIC of 2 µM contrasting with 6 µM for the lysine equivalent. However, in sequences that were inactive with lysine residues, replacement by *N*hArg does not make the sequence active (see peptoid **154**, where the sequence is not active against Gram negative bacteria at any concentration), but in these cases the inclusion of the guanidine group does increase the toxicity.

As predicted, sequences with a combination of lysine and arginine-type residues show a balance between toxicity to mammalian cells and antibacterial activity compared to sequences with the *N*Lys or *N*hArg residues only. For example, in related peptoids containing all arginine residues (**152**), all lysine residues (**22**) and both lysine/arginine monomers within the same sequence (peptoids **148-150**), we see toxicity to the HaCaT keratinocytes at 11 µM, 20µM and 15–33 µM respectively. The general antibacterial activity follows a similar trend for example against *E. coli*, the lysine-only peptoid **22** has the lowest activity at 25 µM, the arginine-only peptoid **152** has the most potent activity with an MIC of 6 µM and the mixed sequences **148–150** have intermediate activity at 17 µM.

The observation that guanidine-only peptoids display the most potent biological activities is in agreement with previous studies into arginine-rich peptides, which are able to bind membrane-bound lipids more readily than their amino-functionalised lysine equivalents. In this case it was proposed that the arginine-type side chains can form bidentate hydrogen bonds with the phospholipid head groups. This has also been concluded in studies with antimicrobial peptide-peptoid hybrids containing both lysine and arginine.[29,34]

4.1.2 Conclusions from antibacterial MIC determination

In summary, the peptoids within this library that have antiparasitic activity are also successful antibacterial compounds. In general, all peptoids were far more active towards the Gram positive species tested than to the Gram negative bacteria, in keeping with their differing envelope structures. Hence the peptoid library has much better selectivity indices against *S. aureus* and *S. epidermidis*.

The best activity against *E. coli* reported was 6 µM for peptoids **293** (*N*hArg*N*phe*N*phe)$_4$, **152** (*N*hArg*N*spe*N*spe)$_4$ and **295** (*N*hArg*N*spe*N*spe)$_3$ and 17 µM against *P. aeruginosa* for peptoids **148** (*N*hArg*N*spe*N*spe)$_2$(*N*Lys*N*spe*N*spe)$_2$ and **149** (*N*Lys*N*spe*N*spe)-(*N*hArg*N*spe*N*spe)(*N*Lys*N*spe*N*spe)$_2$. Many peptoids also showed micromolar activities against *S. aureus* and *S. epidermidis* with both species showing a similar pattern of sensitivity; although *S. aureus* did show a tendency to be more resistant than *S. epidermidis* possibly due to minor differences in cell surface charge and hydrophobicity.[35,36] In many cases, *P. aeruginosa* also proved more peptoid-resistant than *E. coli*. This may reflect differences in the lipid composition of each species or the ability of *P. aeruginosa* to form biofilms, which has been observed previously with AMPs such as LL-37 (compound **179**).[37]

Factors contributing to enhanced antimicrobial activity include the overall length of sequence, with longer 12 residue peptoids typically displaying the best activity, although in many cases the 9 residue peptoids also display broad spectrum activity against bacteria. As seen in Chapter 3, substitution of fluorine in peptoid monomers also enhances activity.

In many cases, achiral sequences displayed potent activity, especially against the Gram positive bacteria. For example, peptoid **153** (*N*hArg*N*mfb*N*mfb)$_4$ contains achiral *N*-(3-fluorophenylmethyl) glycine residues and has MIC values of 13 µM against *E. coli* and 2 µM against *S. aureus*. Interestingly, from our library most compounds that are active against the bacteria but exhibit no/low toxicity to mammalian cells contain achiral monomers, or at least a reduced frequency of chiral monomers within the sequence compared to the standard *NxN*spe*N*spe motif. Whether through the presumed increase in hydrophobicity, or through other effects, the addition of chiral *N*spe residues in a sequence often has a detrimental effect on overall toxicity. Since many of the achiral sequences show potent antibacterial activity and these peptoids are not expected to form fully folded peptoid helicies, secondary structure is perhaps not as important as predicted. However, it should be noted that this is not replicated in activity against protozoa, where chirality has been shown to be far more important. Therefore, a larger potential therapeutic window may exist for antibacterial peptoids compared to antiparasitic peptoids.

Additionally, in Chapter 3, some of the best sequences were identified when a cationic monomer was replaced with an alkyl chain, resulting in a reduced net charge and increased overall hydrophobicity, as measured by RP-HPLC. No effect is seen for this substitution against Gram positive bacteria. However, such substitutions by the *N*amy residue are detrimental to the activity of the library against *E. coli* and *P. aeruginosa*. Peptoid **22** (*N*Lys*N*spe*N*spe)$_4$ has MIC values of 25 µM and 50 µM against *E. coli* and *P. aeruginosa* respectively, however peptoid **244** (*N*amy*N*spe*N*spe)$_2$(*N*Lys*N*spe*N*spe)$_2$.is inactive against both species at 100 µM.

This peptoid library was designed to mimic natural antimicrobial peptides, which are proposed to act on cell membranes, among other targets. For certain compounds, particularly the more hydrophobic sequences that are both active against bacteria but toxic to mammalian cells, this may be the case. However, other compounds exhibited negligible toxicity to mammalian cells but good activity against bacteria and this may indicate that cell membrane disruption is not the only mechanism at work. Selectivity of the peptoids has also proved slightly problematic, with some of the best antibacterial compounds also having equipotent toxicity to mammalian cells, resulting in poor selectivity indices. Overall, there is more work to be done to elucidate the mode of action of antimicrobial peptoids and this is explored in further detail in Chapter 5.

4.2   Peptoid activity against bacterial and fungal biofilms

Biofilm testing was carried out at Queens University, Belfast by Dr Yu Luo (postdoctoral research assistant), under the supervision of Dr Fionnuala Lundy.

The preliminary data presented in section 4.1 shows that many peptoid sequences have excellent MIC values against planktonic bacteria, as determined in broth culture. However as discussed in the introduction, the majority of infections *in vivo* involve biofilms which may be comprised of multiple bacterial and/or fungal species. Microbes growing in their biofilm form differ significantly from their planktonic equivalent; such as the production of EPS matrix that can protect the biofilm and often have slower growth rates. Biofilms also tend to display high mutation rates, so resistance to conventional antibiotics is a significant problem. Therefore, the MIC value may not always be an accurate predictor for activity against more complicated biofilms and it is important that anti-biofilm properties are also studied.[11,14,38]

Chapter 1 reviews the previous studies into the antibacterial and antifungal properties of peptoids and they have been shown to be efficacious against a range of planktonic micro-organisms[19,39,40] and bacterial biofilms.[41] However, to date, the activity of peptoids against fungal biofilms, and in particular, polymicrobial bacterial and bacterial-fungal biofilms has yet to be determined.

In addition to the bacteria studied in MIC determination (*S. aureus* and *E. coli*), the fungal species *Candida albicans* was incorporated into anti-biofilm activity assays to represent the natural complexity of a biofilm. Although *C. albicans* is common in the gastrointestinal and genitourinary flora of a large proportion of the human population, it is an opportunistic pathogen that can cause candidiasis ranging from superficial to life-threatening systemic infection, particularly in immunocompromised patients. Biofilms containing *C. albicans* are responsible for a large number of clinical infections on both biological and abiotic surfaces; for example the cornea or endotracheal tubes.[42-44]

In polymicrobial infections *in vivo*, species have been shown to influence each other, through sensing and signalling or the formation of the biofilm architecture.[45,46] *C. albicans* has been shown to dramatically affect the physical environment of any biofilm it is present in and can influence interspecies protein expression.[47,48] Additionally, as with most fungal pathogens, *C. albicans* is becoming increasingly resistant to antibiotics so new treatments for cross-kingdom biofilms are desperately needed.[49,50]

Traditionally, the efficacy of a compound against a biofilm can be determined using a crystal violet assay or based upon the metabolic activity of the biofilm. The crystal violet assay uses a triarylmethane dye (see compound **312**, **Figure 4.9**) that when solubilised adheres to proteins and DNA and can quantify the total biofilm mass present. The biomass counted typically includes the EPS matrix, extracellular or dead cells, as well as the live biofilm so can lead to an overestimation of the biomass present. The metabolic

assay is similar to the alamarBlue® assay described in Chapter 3. For biofilms, a tetrazolium-based dye is used (commonly XTT, **313**) which is reduced in the mitochondria to the formazan product and can reflect the number of viable cells present colourimetrically. This assay only measures living microorganisms, but different strains of the same pathogen may have very different metabolic activities which can make comparisons between discrete assays difficult.[51] In addition, neither of these assays are useful for application to mixed species biofilms as they cannot distinguish between species, for example, if the treatment has killed one species selectively.

312
Crystal violet

313
XTT

314
PMA
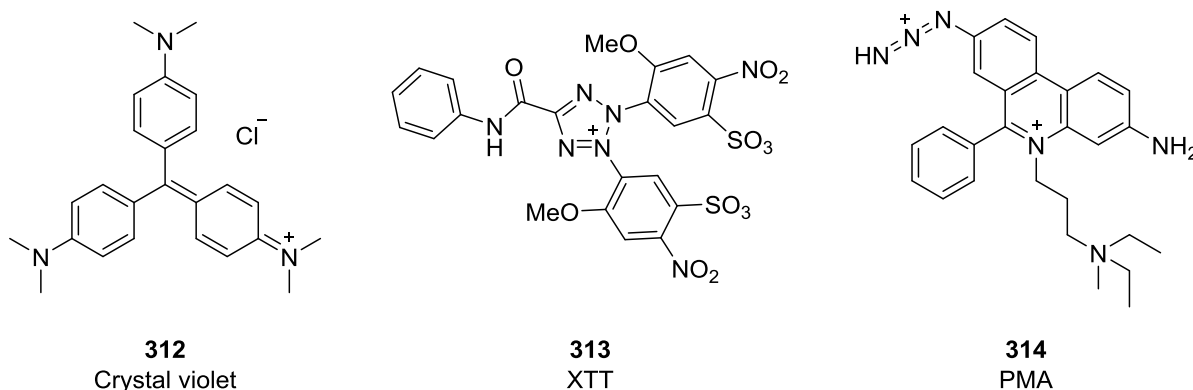
Figure 4.9. Dyes used in the crystal violet assay, metabolic assay and in PMA-qPCR (discussed below).

Recently, the Lundy group at Queen's University Belfast has adapted a quantitative polymerase chain reaction (qPCR) based assay to aid in the quantification of mixed species biofilms. Briefly, PCR is a technique used to amplify DNA. Through several steps DNA is denatured to a single stranded form that complementary primers can bind to. Following the primer annealing step, DNA polymerase is used to produce a complimentary copy of the target DNA strand. In qPCR, the reaction is followed using a fluorescent reporter to measure DNA generation in real-time.[52]

This qPCR approach used by the Lundy group is also modified by the use of propidium monoazide (**314**, PMA in **Figure 4.9**), a photoreactive dye that is able to intercalate DNA with high affinity upon exposure to intense visible light. PMA can only bind to extracellular DNA or in cells with compromised membranes and forms irreversible covalent linkages to the DNA. This means the PMA-qPCR only amplifies DNA from viable cells so results are potentially more accurate than those obtained from a crystal violet assay or metabolic assay.[51,53]

Additionally, since PCR uses primers specific to each bacteria or fungi, viable organism numbers for each species within the polymicrobial biofilm can be quantified. It also allows quantification of viable, but non-culturable microorganisms (VBNC), which biofilms are very likely to contain. Microorganisms have been reported to enter a VBNC

state when exposed to antibiotic treatment so the use of a non-cultivation based assay in this case is very appealing.[53,54]

Initially, the efficacy of the peptoid library was determined against monospecies biofilms containing *C. albicans*, *S. aureus* or *E. coli* using a crystal violet assay for preliminary screening purposes. The anti-biofilm properties of selected peptoids were then determined against polymicrobial bacterial-fungal biofilms using the PCR approach.Peptoid action against single species biofilms

For initial screening of the entire peptoid library, a crystal violet assay was used to quantify the change in biofilm mass following peptoid treatment. Peptoids were added at a concentration of 100 µM to established single species biofilms of *C. albicans*, *S. aureus* and *E. coli*. It was assumed that if a peptoid could reduce viable biofilm mass, it would also be useful to prevent biofilms.

The peptoids used in this study are shown in **Table 4.2** and are all sequences initially synthesised for testing against *Leishmania*. As before, the peptoids were typically designed with a repeat of three residues where the third residue has cationic functionality to induce an amphipathic structure with bulky *N*phe and *N*spe residues to encourage formation of a helical structure which may improve the antimicrobial effect.

	Sequence		Sequence
186	$(NLysNpheNphe)_4$	**228**	$(NLysNmfbNmfb)_4$
187	$(NLysNpheNphe)_3$	**182**	$(NLysNhLeuNspe)_4$
188	$(NLysNpheNphe)_2$	**245**	$[(NamyNspeNspe)(NLysNspeNspe)]_2$
22	$(NLysNspeNspe)_4$	**293**	$(NhArgNpheNphe)_4$
26	$(NLysNspeNspe)_3$	**152**	$(NhArgNspeNspe)_4$
25	$(NLysNspeNspe)_2$	**153**	$(NhArgNmfbNmfb)_4$
180	$(NaeNpheNphe)_4$	**181**	$(NhArgNhLeuNspe)_4$
213	$(NaeNpheNphe)_3$	**154**	$[(NamyNspeNspe)(NhArgNspeNspe)]_2$
214	$(NaeNpheNphe)_2$	**147**	$(NLysNspeNspe)_2(NhArgNspeNspe)_2$
156	$(NaeNspeNspe)_4$	**148**	$(NhArgNspeNspe)_2(NLysNspeNspe)_2$
218	$(NaeNspeNspe)_3$	**149**	$(NLysNspeNspe)(NhArgNspeNspe)(NLysNspeNspe)_2$
219	$(NaeNspeNspe)_2$	**150**	$[(NhArgNspeNspe)(NLysNspeNspe)]_2$
210	$(NahNpheNphe)_4$	**132**	Cyclo $(NLysNphe)_3$
211	$(NahNpheNphe)_3$	**133**	Cyclo $(NhArgNphe)_3$
212	$(NahNpheNphe)_2$	**134**	Cyclo $(NLysNpheNhArgNpheNLysNphe)$
215	$(NahNspeNspe)_4$		
216	$(NahNspeNspe)_3$		
217	$(NahNspeNspe)_2$		

Table 4.2. Peptoid library tested for efficacy against single species fungal and bacterial biofilms. Anti-biofilm activity of peptoids in the first column can be found in **Figure 4.11**; those in the second column are illustrated in **Figure 4.12**.

The library contains 18 peptoids (**186–217**) to examine the effect of overall sequence length, cationic monomer functionality and chirality on the biofilm growth to be investigated. Additionally, selected peptoids from the second generation library were tested using a crystal violet assay to compare the effect of lysine-type monomers with the arginine-type monomers (peptoids **228–150**). Three cyclic peptoids, **132–134** were also considered. A planktonic culture of microorganism was prepared in 96 well plates and incubated for 4 hours at 37 °C to allow initial biofilm formation. After washing to remove planktonic cells, 100 µM of compound were added to the plate wells and incubated for a further 24 hours to allow biofilm maturation. The peptoids show variable antifungal and antibacterial activities when screened for inhibitory activity against monospecies biofilms of *C. albicans*, *S. aureus* and *E. coli*.

Many sequences show good efficacy with a large percentage reduction in overall biofilm mass, as shown in **Figure 4.11** and **Figure 4.12**. In particular, peptoids **26**, **180**, **156**, **218**, **210** and **245** show over 75 % reductions in biofilm mass across the different species. **Figure 4.12** also shows a comparison to a synthetic peptide with repeating lysine-leucine-alanine residues (KLA peptide **315** in **Figure 4.10**) with potent anticancer properties.[55] **315** has only mild activity against the *E. coli* biofilm and no activity against *S. aureus* or *C. albicans*.

315
(KLAKLAKLA)$_2$-NH$_2$
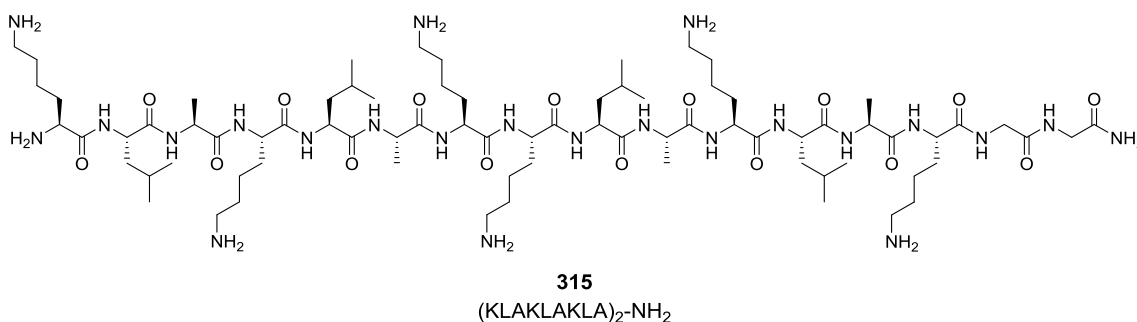
Figure 4.10. Structure of the KLA AMP, **315**.

Sequence length effects

To examine the effect of sequence length, the peptoids in **Figure 4.11** were compared. In agreement with the antiparasitic testing undertaken in Chapter 3, the longest peptoids tend to show the greatest activities; the longest 12 residue peptoids are more efficacious than the 9 residue peptoids that have an intermediate activity and the shortest 6 residue peptoids are mostly inactive. For example, against *C. albicans* peptoids based upon the *N*ae*N*phe*N*phe motif show the most activity for the longest sequence **180** and the least potent compound is the 6 reside peptoid **214**. Against *S. aureus*, the longer peptoids had good activity and no activity for the shortest peptoids, but interestingly it was the comparable shorter 9 residue analogues that caused the greatest reduction in biofilm mass (see peptoids **213** and **180** or **218** and **156**). For *E. coli*, the trends are split where the longest peptoids are the most active with *N*ae or *N*Lys residues, however with the *N*ah monomer the intermediate 9 residue peptoids are the most active (i.e. compare peptoids **210** and **216**).
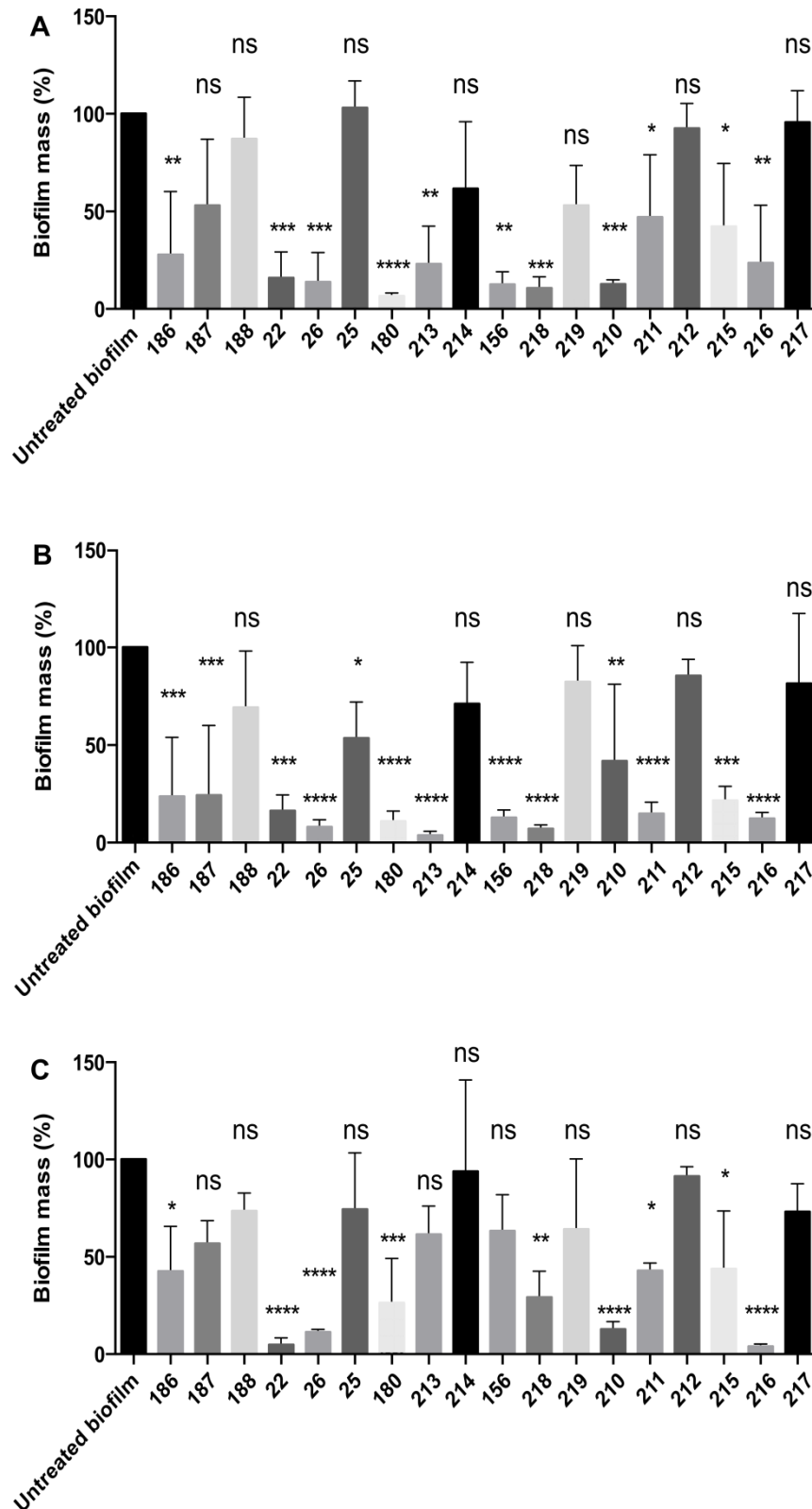
Figure 4.11. Efficacy of peptoids **186–217** against **A**; *C. albicans* **B**; *S. aureus* **C**; *E. coli* monospecies biofilms determined by crystal violet assay. Biofilms were treated with peptoids at 100 µM and compared with untreated, control biofilms. The results (average of 3 independent experiments) were plotted as percent biomass of controls. Statistical analysis was determined by one-way ANOVA followed by Tukey's post hoc correction for multiple comparisons (ns: p > 0.05; *: p < 0.05; **: p < 0.01; ***: p < 0.001; ****: p < 0.0001).
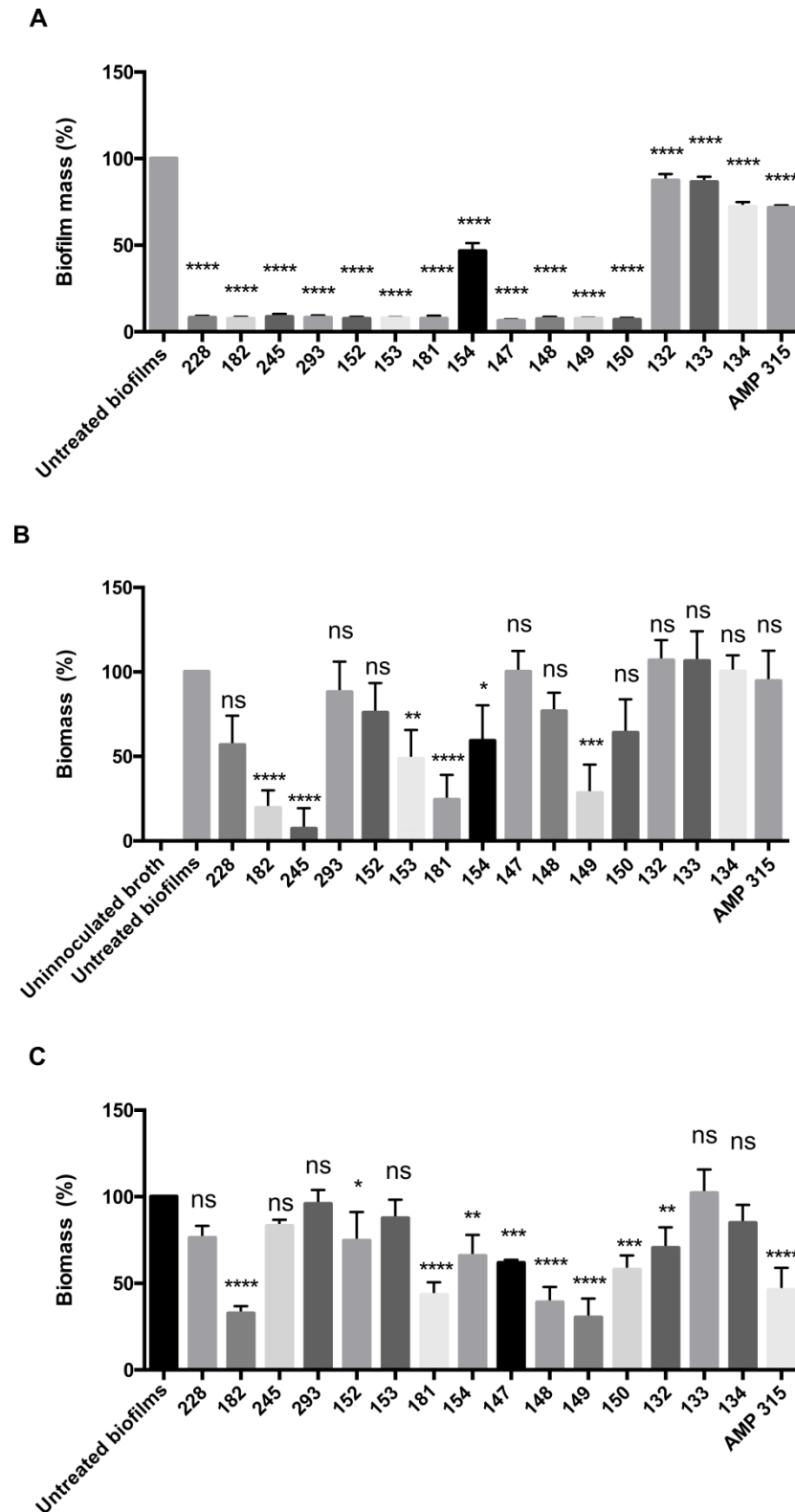
Figure 4.12. Efficacy of peptoids **228** to **134** and the AMP **315** against **A**; *C. albicans* **B**; *S. aureus* **C**; *E. coli* monospecies biofilms determined by crystal violet assay. The peptoid treated biofilms were compared with untreated, control biofilms, the AMP KLA and the results (average of 3 independent experiments) were plotted as percent biomass of controls. Statistical analysis was determined by one-way ANOVA followed by Tukey's post hoc correction for multiple comparisons (ns: $p > 0.05$; *: $p < 0.05$; **: $p < 0.01$; ***: $p < 0.001$; ****: $p < 0.0001$).

Chirality

The peptoid library in **Figure 4.11** was also designed to include sequences containing either the chiral *N*spe or the achiral *N*phe monomer to determine the effect of sequence chirality on the anti-biofilm activities of the compounds. Overall, sequences containing *N*spe were more efficacious than their achiral analogues across all three biofilm species tested (e.g. compare achiral peptoid **186** and chiral peptoid **22**). However, for peptoids containing the *N*ae monomer, there was little difference in activity between the chiral and achiral peptoids against *S. aureus* or *C. albicans* (i.e. compare peptoid families **156**–**219** and **180**–**214** respectively). The differences in activity for chiral and achiral members of the entire peptoid library were even less pronounced against *E. coli*.

Effect of cationic monomers

The success of many AMPs is attributed to their overall cationic charge that allows them to target the membranes of prokaryotes over mammalian cells.[48] Within the library, the effect of different cationic monomers was investigated when comparing the amino-functionalised *N*ae, *N*Lys and *N*ah residues (2, 4 and 6 carbons in length respectively) to the *N*hArg monomers with guanidine moieties – see **Figure 4.13**. Results for sequences decorated with these cationic monomers are shown in both **Figure 4.11** and **Figure 4.12**.
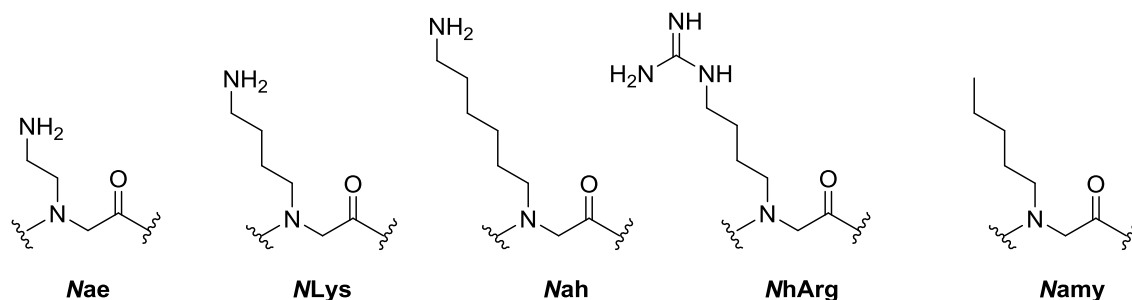
Figure 4.13. Monomers used to examine the effect of different cationic residues on the anti-biofilm activity of sequences.

When comparing peptoid sequences of the same overall length (i.e. 12 residues), peptoids containing the shortest *N*ae monomer tended to be more active than the longer *N*Lys monomer for all species (e.g. compare peptoid **186** and peptoid **180**). On the whole, peptoids containing the *N*ah monomer were less active than those containing either *N*ae or *N*Lys, as shown by the greater reduction in biofilm mass for *N*ae or *N*Lys sequences in **Figure 4.11**. However, peptoid **216** (*N*ah*N*spe*N*spe)$_3$ is an exception as it can be seen that **216** reduced *E. coli* biofilm by around 95 % or a *S. aureus* biofilm by approximately 75 %. The *N*ah peptoids are also less effective in our anti-leishmanial testing and potentially the reduced activity of the *N*ah*N*y*N*y motif could stem from the greater flexibility of the longer aminohexane chain.

To examine the effect of cationic functionalisation, peptoid sequences containing *N*Lys and *N*hArg can be compared. For example, peptoids containing the achiral *N*phe or *N*spe residues with either *N*Lys or *N*hArg cationic residues (**186/228** and **293/153** respectively) the lysine-type peptoids **186/293** show greater anti-biofilm activities compared to the arginine-type analogues across all species. This is an interesting conclusion, since against planktonic bacteria it was shown that the arginine peptoids often displayed the most potent activity. The achiral sequences containing the fluorinated monomer *N*mfb show little activity with either type of cationic residue. As can be seen from **Figure 4.12**, for sequences with both lysine- and arginine-type residues (i.e. **147**, **148**, **150**, **149**) intermediate activity is seen for both *S. aureus* and *E. coli*, greater than the guanido-only peptoids (**152**) but less than the amino-only peptoid (**22**).

Finally, the charge of certain sequences was reduced through substitution of the *N*amy monomer (i.e. **245** and **154**) as this had shown to be a useful strategy for developing anti-leishmanicidal peptoids. It can be seen from **Figure 4.12** that peptoid **245** has potent activity at 100 µM against *C. albicans* and *S. aureus*, reducing the biofilm mass more than **22** (the analogous sequence where *N*amy residues are substituted for *N*Lys). However **245** shows no activity against *E. coli* monospecies biofilms whereas peptoid **22** reduces biofilm mass by approximately 95% at the same concentraion. In sequence **154** containing *N*amy and *N*hArg residues, a similar trend is seen (no activity for *E. coli* but substantial activity against *C. albicans* and *S. aureus* compared to the all *N*hArg peptoid **152**). Overall, as seen with the other peptoids where lysine- and arginine-type residues are compared, the amino-functionalised **245** causes a greater reduction in biofilm mass than the *N*hArg peptoid.

Cyclisation

Cyclisation is often used as a strategy to increase antimicrobial activity, but as mirrored by the antibacterial MIC and antiparasitic ED_{50} values already determined in Chapters 3 and 4, cyclic peptoids were inactive even at the 100 µM concentrations in the biofilm activity assays. The cyclic peptoids **132–134** were all 6 residues in length, and similar to their linear analogues showed no significant activity against any of the monospecies biofilms, as shown by **Figure 4.12**.

4.2.1 Mixed species biofilm assay using PMA-modified qPCR

All results discussed above were obtained from the crystal violet assay described. Although routinely used by the scientific community for biofilm quantification, this approach detects both live and dead organisms alongside matrix components. Therefore, PMA modified qPCR was developed to selectively and quantitatively determine the antimicrobial activity of selected peptoids against single- and multi-species biofilms. The activity of the peptoids against polymicrobial biofilms is particularly interesting, as these systems are more representative of clinically relevant biofilms. First the PMA-qPCR was validated against monospecies biofilms and then used in the multi-species biofilm assays.

Three sequences were chosen for further study, which represented some of the most active peptoids in the single species crystal violet assays discussed in section 4.2; peptoids **26** (*N*Lys*N*spe*N*spe)$_3$, **180** (*Nae*N*phe*N*phe)$_4$, and **216** (*Nah*N*spe*N*spe)$_3$ (results as in **Figure 4.11** and **Figure 4.12**, structures in **Figure 4.14**). One peptoid was chosen from each class of cationic residue and two chiral and one achiral peptoids were used. These compounds also displayed negligible toxicity of > 100 μM to mammalian cell lines, HaCaT and HepG2.[§]
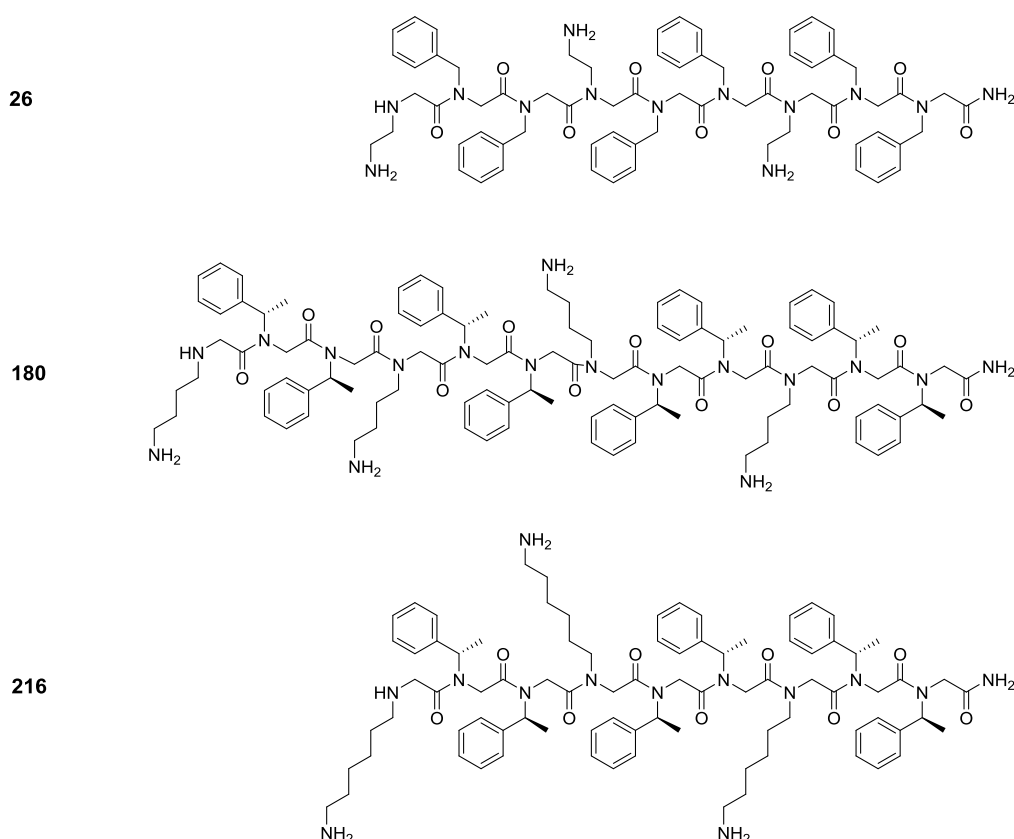
Figure 4.14. Structures of the peptoids **26**, **180**, **216** chosen for evaluation in mixed species biofilms.

[§] Description of the toxicity evaluation can be found in Chapter 3.

As predicted from the significant activity seen in the crystal violet assay, the monospecies biofilms treated with peptoid all showed significant reduction in cell numbers. This indicates strong antibacterial and fungicidal activity of peptoids **26**, **180** and **216** and the data is shown in **Figure 4.15**.

Treatment by peptoid had a potent effect against *C. albicans*, with peptoids **26** and **180** reducing the cell number by over 4 orders of magnitude. In agreement with the crystal violet assay results, the *N*ah containing peptoid **216** did not perform quite as well against *C. albicans*, although it still caused a significant reduction in the fungal biofilm. All three peptoids also considerably reduced the cell counts of the *S. aureus* and *E. coli* biofilms, but cell counts were reduced to a smaller extent than with the fungal biofilm. For *S. aureus*, all peptoids had a similar effect but in the *E. coli* monospecies biofilms, peptoid **216** was the most effective. This leads to the interesting conclusion that peptoid **216** may be more specific to the fungal biofilm over *E. coli* and *S. aureus* and would be very useful given increasing bacterial resistance.
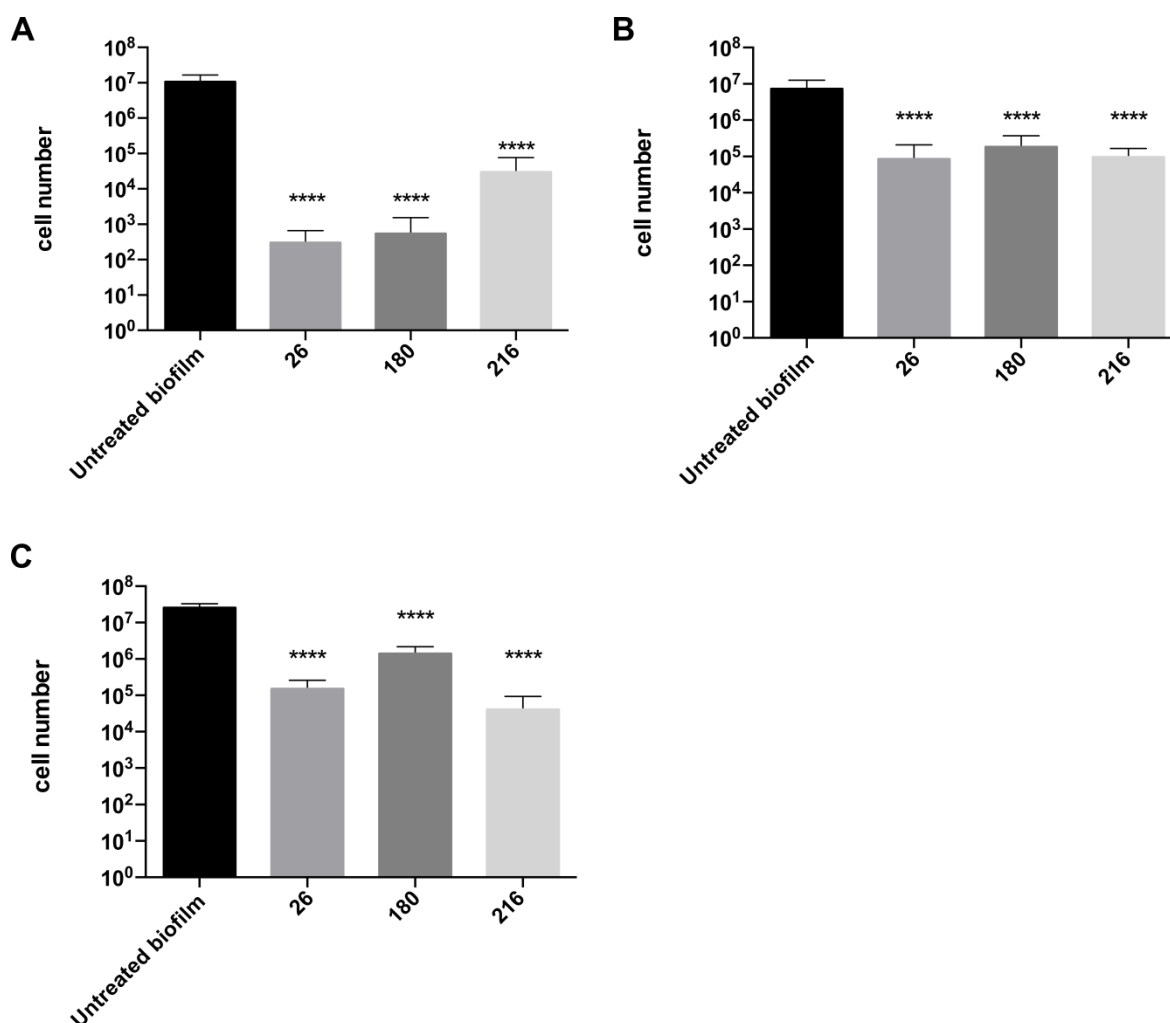
Figure 4.15. PMA-qPCR quantification of cell number following peptoid treatment of monospecies biofilms. Cell numbers of **A**; *C. albicans* **B**; *S. aureus* **C**; *E. coli* treated with 100 μM peptoid **26**, **180** and **216** (****: p < 0.0001.).

Peptoids **26**, **180** and **216** were also tested against mixed species biofilms containing *C. albicans* and either *S. aureus* or *E. coli*, with results from testing at 100 µM shown in **Figure 4.16**. In the mixed species biofilm containing *C. albicans* and *S. aureus* (**Figure 4.16A and B**), cell numbers were reduced more for the bacteria than fungi. Peptoid **26** was better able to reduce the cell count of *S. aureus* than the other peptoids and peptoid **180** showed the greatest reduction in *C. albicans* cell numbers. In the polymicrobial biofilm with *C. albicans* and *E. coli* (**Figure 4.16C and D**), the biofilm cell numbers were reduced more for *C. albicans* than *E. coli* with treatment by all three peptoids. In this polymicrobial biofilm, the *N*ah sequence **216** was the most active against both species, followed by peptoid **180** and then **26**.
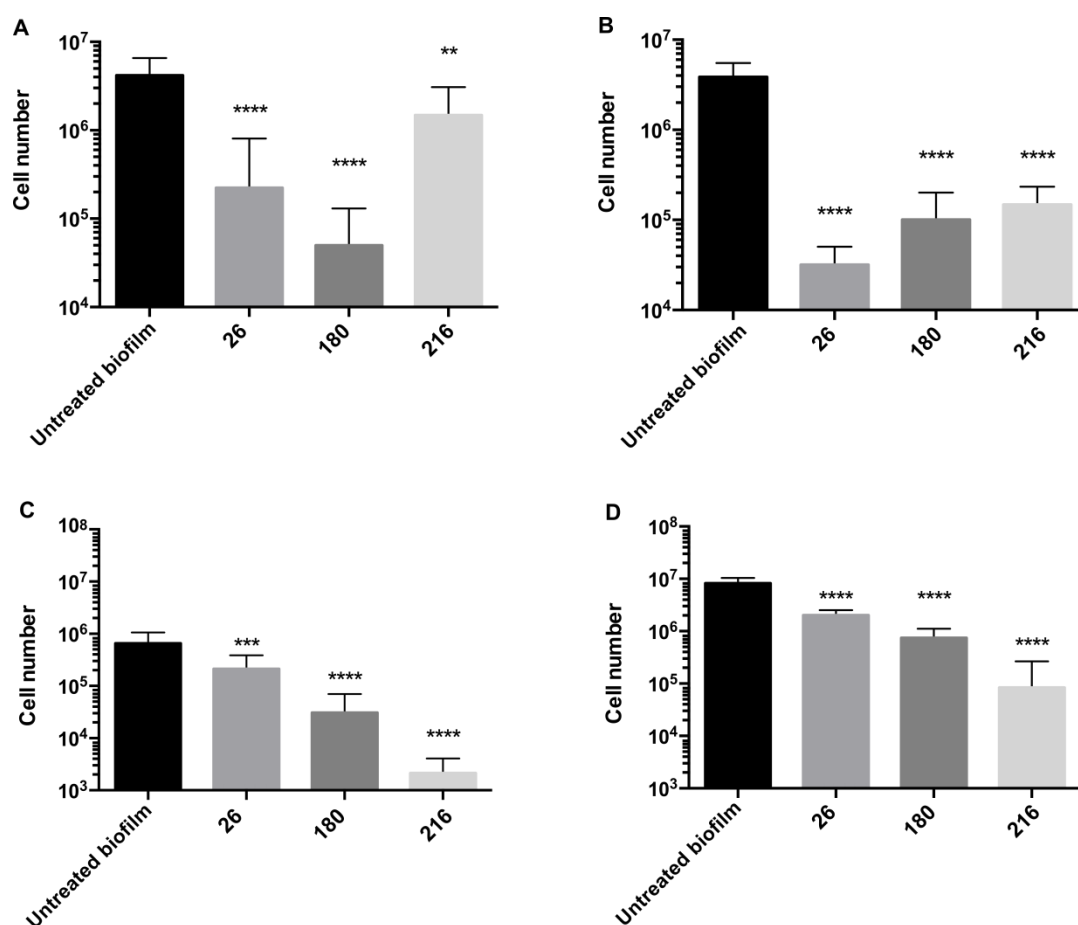
Figure 4.16. PMA-qPCR quantification of cell numbers following 100 µM peptoid treatment of polymicrobial biofilms made of *C. albicans* and either *S. aureus* or *E. coli*. Cell numbers of **A**; *C. albicans* and **B**; *S. aureus* within the same polymicrobial biofilm, following treatment with peptoids. Cell numbers of **C**; *C. albicans* and **D**; *E. coli* within the same polymicrobial biofilm, following treatment with peptoids (**: $p < 0.01$; ****: $p < 0.0001$.).

When present in a biofilm with *S. aureus, C. albicans* appeared to be less susceptible to treatment with 100 µM peptoid **216** than in a single species biofilm (section 4.2) or in a polymicrobial biofilm with *E. coli*. Since there has been very limited work on peptoid efficacy in polymicrobial biofilms it remains to be determined if this is a unique phenomenon.

Finally, when cross-kingdom biofilms were treated with peptoids **26**, **180** and **216** at concentrations lower than 100 µM a dose dependent effect was seen. In the mixed species biofilms, all three peptoids significantly reduced the cell numbers of *S. aureus* by approximately 100%, even when treated at 10 µM. Reduction in cell viability for *C. albicans* or *E. coli* were negligible at 10 µM, but considerable reduction in cell numbers were seen at 25 µM and 50 µM respectively. For all three species present in the cross-kingdom biofilms, achiral peptoid **216** showed the greatest reduction in cell number.
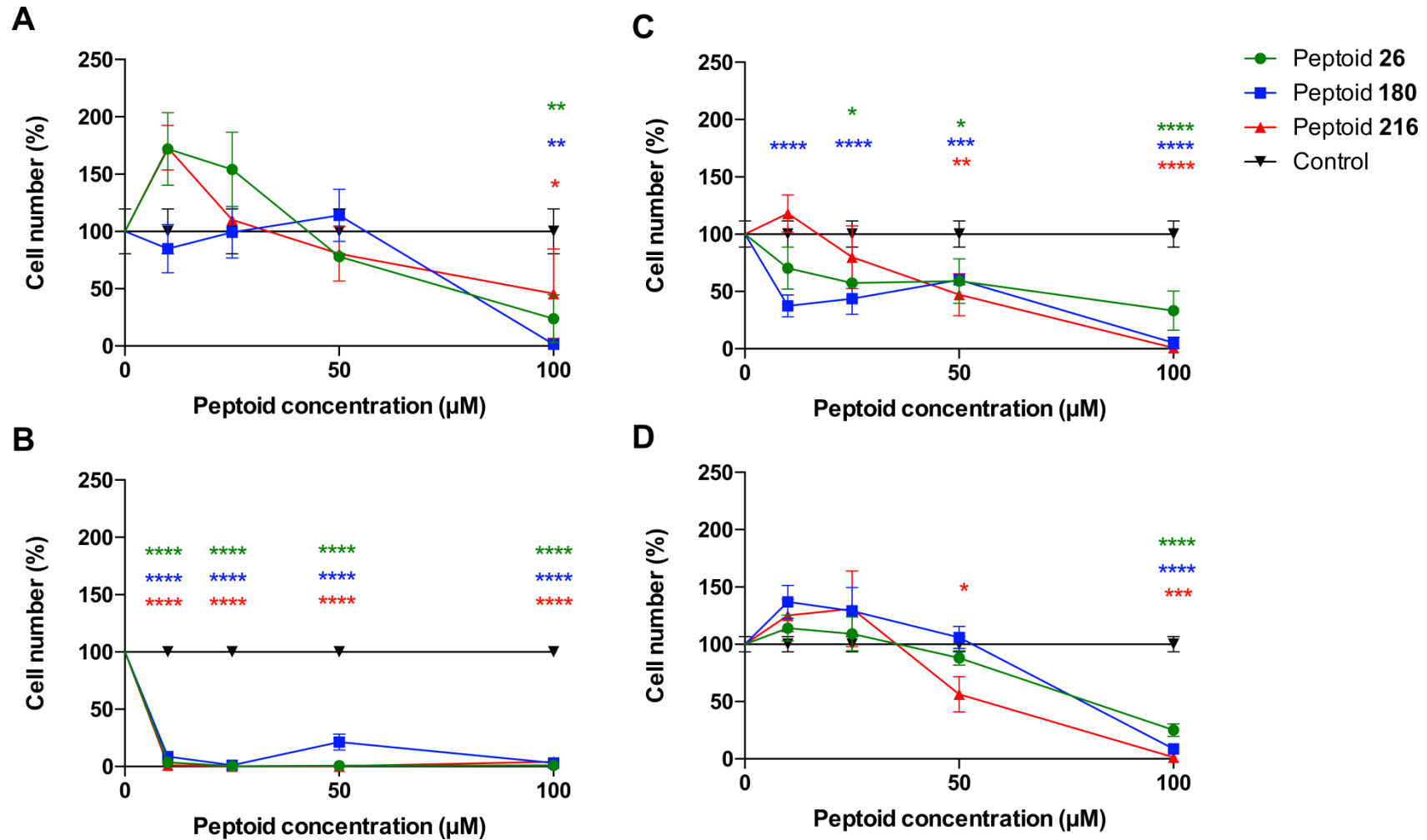
Figure 4.17. PMA-qPCR quantification of cell numbers following peptoid treatment of polymicrobial biofilms following treatment with peptoids **26**, **180** and **216** at concentrations of 10, 25, 50 and 100 μM. Within *C. albicans* and *S. aureus* biofilms; cell numbers (percentage of untreated control) for **A** *C. albicans* and **B** *S. aureus*. Within *C. albicans* and *E. coli* biofilms cell numbers (percentage of untreated control) for **C** *C. albicans* and **D** *E. coli* (*: $p < 0.05$; **: $p < 0.01$; ****: $p < 0.0001$. One-way ANOVA followed by Tukey's post hoc correction for multiple comparisons, N=3 independent experiments, 3 replicates in each. Statistical analysis was performed independently for each peptoid).

4.2.2 Permeablisation of cell membranes by peptoids

A large proportion of antimicrobial peptides have been shown to disrupt cell membranes which, at least in part, may cause their antimicrobial effects. Several proposed mechanisms of action for AMPs on cell membranes have already been described in Chapter 1. It is thought that the mode, or modes, of action of antimicrobial peptoids are mechanistically very similar to AMPs and therefore may also involve membrane disruption, although currently there are only a few studies to support this.[23,56-59]

To help elucidate the mode of action of peptoids, a membrane permeabilisation assay was performed with peptoids from the library against *C. albicans*, *S. aureus* and *E. coli*. The assay is designed to show whether the peptoids are capable of causing cell lysis and if the cell membranes of these pathogens are a target.
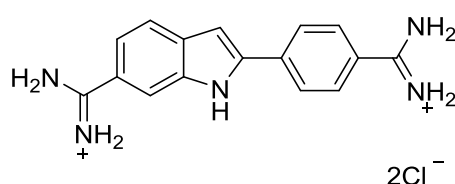
316
SYTOX Green
λ_{ex} = 504 nm; λ_{em} = 523 nm

Figure 4.18. SYTOX® Green, the nucleic acid stain and unsymmetrical cyanine dye used to assess the integrity of cell membranes.

The dye SYTOX® Green (**316**) is able to bind nucleic acids but is impermeable to living eukaryotic and prokaryotic cells. Therefore, this dye is routinely used to assess the integrity of plasma membranes and used as an indicator of dead cells. If a microbial cell membrane has been compromised, for example by treatment with a compound, SYTOX® Green can bind the cellular nucleic acids. This association event increases the fluorescence of the dye and renders cells with compromised membranes as brightly green fluorescent. After binding, the fluorescence emission of the dye can be enhanced by as much as one thousand fold and is proportional to the fraction of permeabilised cells in the population.[60,61]

For the three peptoids used in the qPCR study in section 4.2.1, the propensity to permeabilise the cell membranes was assessed using SYTOX® Green, as shown in **Figure 4.19** (peptoids **26**, **180** and **216**, with structures shown in **Figure 4.14**). Sufficient controls were undertaken and other measurements to determine the background levels of fluorescence, for example untreated cells permeabilised by heat treatment as a positive control, the Mueller Hinton Broth (MHB) growth medium alone and also each peptoid in the uninoculated broth. All peptoid treatments were at 100 μM, the screening concentration used in the anti-biofilm evaluations described in section 4.2
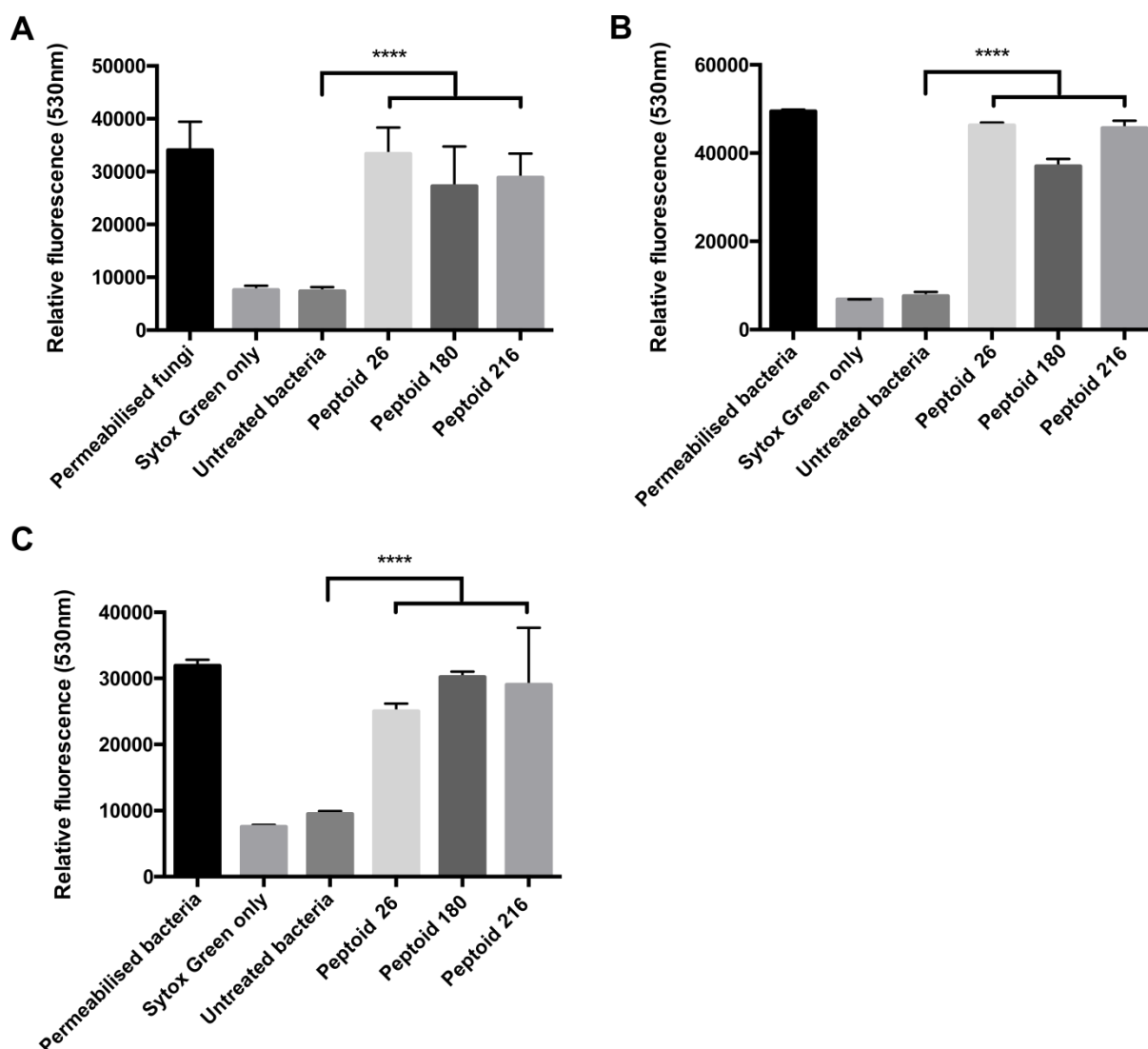
Figure 4.19. Propensity for peptoids **26**, **180** and **216** to permeabilise the microbial membranes of; **A** *C. albicans*; **B** *E. coli*; **C** *S. aureus,* as determine by the SYTOX® Green assay. The efficacy of membrane permeabilisation by peptoids was compared with untreated controls and the results (average of 3 independent experiments) were analysed by ANOVA followed by Tukey's post hoc correction for multiple comparisons (****: $p < 0.0001$). Cells permeabilised by heat treatment were used as positive controls.

In all cases, a significant increase in fluorescence was seen following treatment with 100 µM peptoid for the bacteria and fungi, suggesting that the peptoids cause significant membrane permeabilisation in *C. albicans*, *E. coli* and *S. aureus*. This test also validates use of the PMA-qPCR (since the PMA can only bind to DNA within cells that have compromised membranes). The results show that the peptoids that have the greatest antimicrobial effect against single species biofilms (**Figure 4.15**) also cause the greatest membrane permeabilisation via the SYTOX® Green assay (**Figure 4.19**). For example, against *C. albicans* peptoid **26** causes the greatest reduction in cell number and causes the greatest increase in fluorescence.

An additional five peptoids from **Table 4.2** (**186**, **182**, **293**, **181**, **149**) were also tested using the SYTOX® Green assay, with structures shown in **Figure 4.20**. Although in all cases, an enhancement of fluorescence was seen following peptoid treatment, the data show that there were some differences in the ability of specific peptoids to permeablise bacterial and fungal cell membranes. When *C. albicans* was incubated in the presence of SYTOX® Green and each of the five peptoids, a substantial enhancement of fluorescence was seen in all cases, demonstrating that the peptoids are all able to significantly permeablise the cell membrane of the fungal species (see **Figure 4.21A**).

Results for Gram positive *S. aureus* are shown in **Figure 4.18B** and Gram negative *E. coli* in **Figure 4.18C**. For both bacteria, the peptoids also caused considerable membrane disruption, but a smaller increase in fluorescence intensity was seen compared to *C. albicans*, suggesting a smaller extent of membrane permeabilisation. Although still statistically significant, peptoids **293**, **181**, **149** were less efficacious against *S. aureus* and *E. coli* than **186** and **182**.

186 where R = NH$_2$
293 where R = NHC(NH)NH$_2$
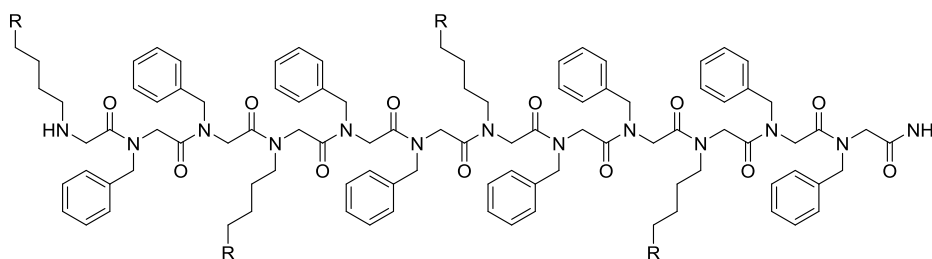
182 where R = NH$_2$
181 where R = NHC(NH)NH$_2$
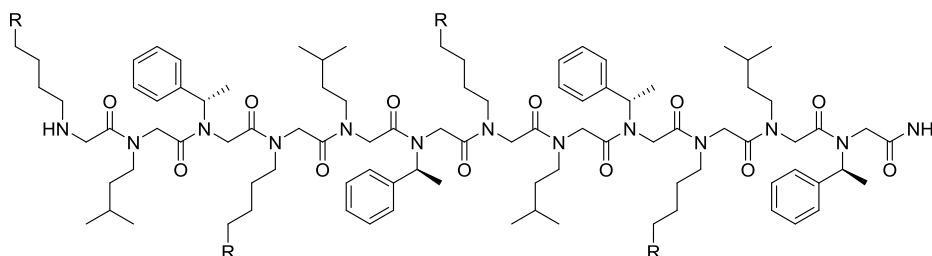
149
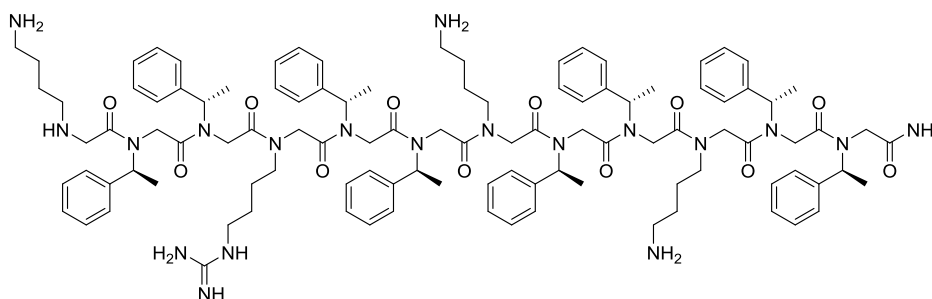
Figure 4.20. Structures of peptoids **186**, **182**, **293**, **181** and **149** studied in the SYTOX® Green assay.
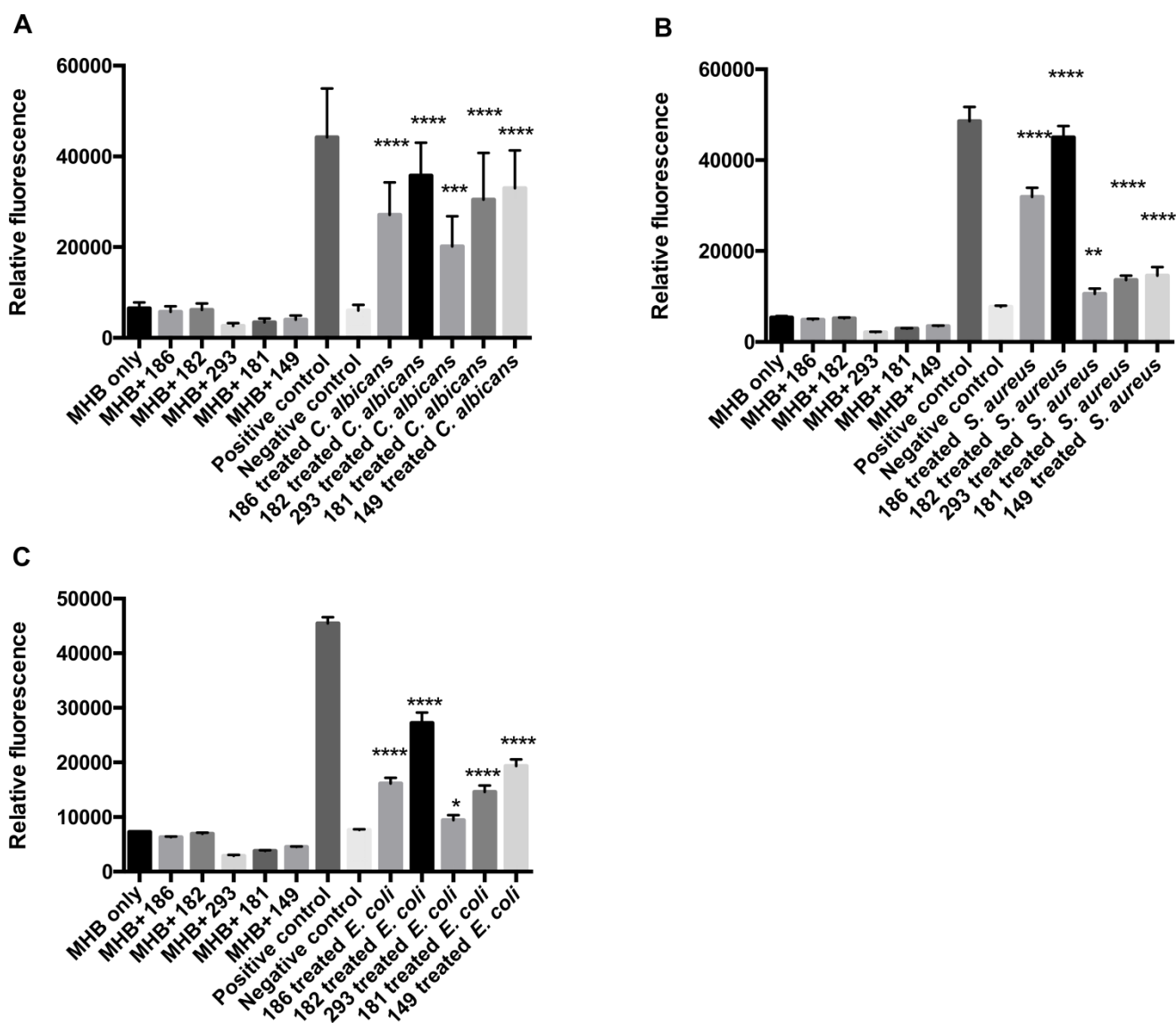
Figure 4.21. Membrane permeabilization activities of selected peptoids at 100 µM against planktonic cultures of **A**; *C. albicans* **B**; *S. aureus* **C**; *E. coli*. One-way ANOVA followed by Tukey's post hoc correction for multiple comparisons from three independent experiments, where: *p< 0.5; **p<0.05, ***p< 0.001; **** p< 0.0001.

A small number of peptoids were tested so detailed conclusions regarding SARs cannot be drawn, however peptoid **182** (*N*Lys*N*hLeu*N*spe)$_4$ appears to cause the largest increase in fluorescence across the second SYTOX® Green assay. For the analogous peptoid **181** with *N*hArg residue instead of *N*Lys, a similar increase in fluorescence is seen when *C. albicans* is treated with both peptoids. However, **181** is less able to disrupt the cell membranes of *S. aureus* and *E. coli* than **182**. Peptoids **186** and **293,** also differing only by the cationic monomers (*N*Lys and *N*hArg respectively) and show a similar pattern where the amino-functionalised sequence causes a greater increase in fluorescence than the guanido-functionalised sequence for both bacteria, but little difference against *C. albicans*.

From this data, it appears that sequences with lysine-type monomers may cause more disruption to the cell membranes of *S. aureus* and *E. coli* than those with arginine-type monomers. This is an interesting conclusion since several studies investigating the potential application of peptoids as molecular transporters have suggested that the guanidinium group of arginine can enhance cellular uptake.[31,62]

From the biofilm inhibition data obtained from Crystal Violet assays (section 4.2), it can be seen that all peptoids have a greater effect against *C. albicans* than the bacterial biofilms. This agrees with the SYTOX® Green assay, where the enhancement of fluorescence seen is much greater for the fungi than *S. aureus* or *E. coli*. The propensity of these peptoids to disrupt cell membranes via SYTOX® Green assay also correlates to their anti-biofilm activity. As shown in **Table 4.3** peptoid **182** causes the greatest membrane disruption and the best antibacterial and fungicidal activity of the five studied. Sequence **293**, shows the smallest increase in fluorescence and also the least significant reductions in biomass, with no effect seen against *S. aureus* and *E.coli*.

	Sequence	Approximate reduction in biomass (%)		
		C. albicans	*S. aureus*	*E. coli*
186	(*N*Lys*N*phe*N*phe)$_4$	25	20	45
182	(*N*Lys*N*hLeu*N*spe)$_4$	10	25	25
293	(*N*hArg*N*phe*N*phe)$_4$	10	*ns*	*ns*
181	(*N*hArg*N*hLeu*N*spe)$_4$	10	25	40
149	(*N*Lys*N*spe*N*spe)(*N*hArg*N*spe*N*spe)(*N*Lys*N*spe*N*spe)$_2$	10	40	40

Table 4.3. Peptoids studied in SYTOX® Green assay and their approximate anti-biofilm activity against fungal and bacterial biofilm, as determined by Crystal Violet assay.

In conclusion, the SYTOX® Green assay has identified that the plasma membranes of *C. albicans*, *S. aureus* and *E. coli* are a target for antimicrobial peptoids. The results strongly support that the microbial action of peptoids **5**, **7** and **17** is due to membrane disruption, but additional action via a secondary intracellular target cannot be completely ruled out. The data obtained helps to rationalise some of the anti-biofilm activities recorded, with the best antimicrobials showing the largest membrane disruption, as expected. Further work to elucidate the mechanism of action of these peptoids is described in Chapter 5, which extends this work using fluorescent microscopy experiments to further pinpoint cellular targets of peptoids.

4.2.3 Conclusions from biofilm activity screening

For the first time, peptoids have shown to be efficacious against fungal biofilms and also against polymicrobial biofilms. The peptoid library tested displays excellent bactericidal and fungicidal activities *in vitro* against *C. albicans, S. aureus* and *E. coli* biofilms using both a traditional crystal violet assay and novel PMA-modified qPCR. On the whole, the peptoid library showed similar activity patterns across the three species tested, i.e. peptoids that were active at some level against one species also tended to be active against the others. In general, the peptoids studied in multispecies assays cause the greatest reduction in biomass against *S. aureus*, followed by *C. albicans*, with *E. coli* showing the least effect following peptoid treatment. This trend is in agreement with other studies in the literature that conclude planktonic *E. coli* is more difficult to target with peptoids than Gram positive bacteria or fungi and is due to the extra outer membrane leaflet in Gram positive bacteria.[63,64] Peptoid **216** (Nah*N*spe*N*spe)$_3$ was identified with significant activity against *S. aureus* in a mixed biofilm with *C. albicans* at 10 µM and also shows good activity against both species within the *C. albicans* and *E. coli* cross-kingdom biofilm when treated at higher concentrations.

The sequences with arginine-type monomers are typically less efficacious against the biofilms than peptoids containing lysine-type monomers. This is supported by the SYTOX® Green assay, which shows that sequences with lysine-type monomers are able to cause a greater extent of membrane disruption. This is a potential point for further investigation, since against planktonic bacteria in section 4.1.1, this trend is reversed and peptoids containing arginine-type monomers have lower MIC values (therefore more potent activity).

Another important conclusion from this study is the identification of peptoids such as **216** (Nah*N*spe*N*spe)$_3$, **150** [(Nh*Arg*N*spe*N*spe)(*N*Lys*N*spe*N*spe)]$_2$ and **147** (*N*Lys*N*spe*N*spe)$_2$(Nh*Arg*N*spe*N*spe)$_2$ that are effective against *C. albicans* but have a less significant effect against either *S. aureus* or *E. coli*. These compounds could be useful as probes to determine if inhibition of *C. albicans* alone can perturb polymicrobial biofilm formation. Given the recent suggestions that *C. albicans* has a significant influence on local biofilm environment this may be a noteworthy direction of research.[47,48] More discussion about these compounds and potential future studies can be found in the Future Work section in Chapter 6.

Initially, this study aimed to determine whether MIC is predictive of anti-biofilm activity. From the data gathered, it has confirmed that MIC determination is unsuitable to predict which peptoids may display potent activity against biofilms. To choose one example, peptoids **215** (Nah*N*spe*N*spe)$_4$ and **216** (Nah*N*spe*N*spe)$_3$ both have an MIC of 25 µM against planktonic *E. coli* but very different activity against the *E. coli* biofilm, as determined from the crystal violet assay.

An improved knowledge of the treatment of clinically relevant polymicrobial biofilms *in vitro* should ultimately translate to better treatment of infections *in vivo* and provides further support for investigating peptoids as future antimicrobial agents.

4.3   Peptoids with a dual mode of action: nisin-peptoid conjugates

4.3.1   The lantibiotic nisin

Nisin is a polycyclic peptide produced by several strains of the Gram positive bacterium *Lactococcus lactis* and is an antimicrobial against other Gram positive bacteria with nanomolar potency. Nisin (compound **9**) is frequently used as a food preservative (E234) due to its high antibacterial activity and negligible toxicity to humans and provides a potential scaffold for the development of novel antibacterial agents. However, due to its susceptibility to proteolytic degradation use as a general antibiotic has been hindered.[65]
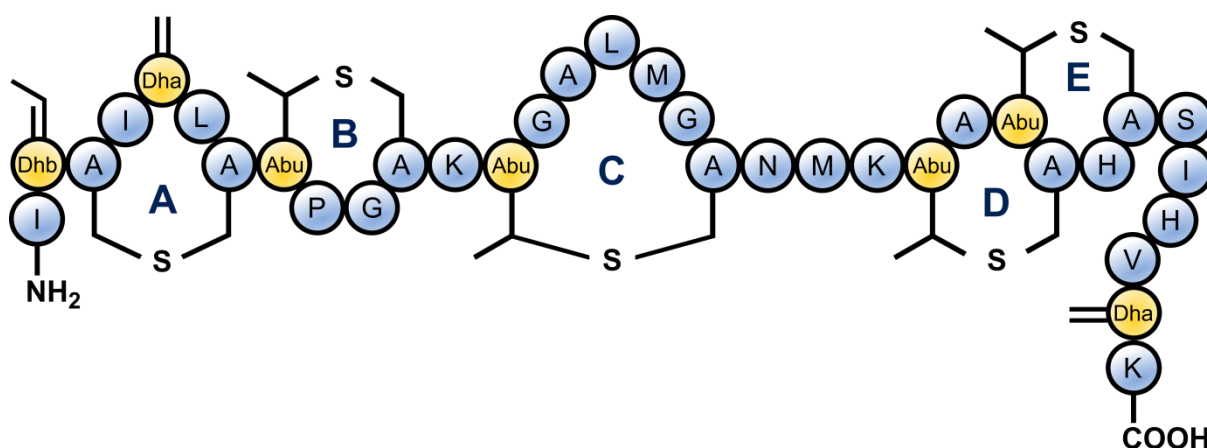
Figure 4.22. The lantibiotic nisin (**9**), where Dhb = dehydrobutyrine, Dha = dehydroalanine and Abu = aminobutyric acid.

Nisin (**9**) shares similar characteristics to typical antimicrobial peptides, such as overall positive charge and amphipathic structure. Classified as a lantibiotic due to the presence of unusual lanthionine rings in its structure, nisin also contains unsaturated amino acids introduced by posttranslational modifications, such as dehydroalanine and 2-aminobutyric acid. In total, nisin has five lanthione rings (labelled *A – E* in **Figure 4.22**) and these rings impart a conformation that is key to nisin's ability to act as a potent antimicrobial. The A/B ring system at the N terminus has been shown to bind to lipid II, which is a crucial membrane component used in bacterial cell wall synthesis. Following lipid II binding, the nisin can insert into the bacterial membrane and create pores that leads to cell death.[65-68]

Nisin provides an excellent starting point for the design new antibiotics, however, due to its peptide-based structure, several problems arise in the application of the full length sequence. These include immunogenicity issues, the susceptibility of nisin to proteolytic degradation *in vivo* and consequent poor pharmacokinetics. Some groups have sought to overcome these by the total chemical synthesis of nisin analogues with improved properties.[69,70]

It has been shown that C-terminally truncated peptides containing the A/B ring system can still display significant activity, as it is the A/B ring system that is essential for lipid II binding.[71] A vast library of truncated nisin peptides have now been biologically evaluated, including very promising semi-synthetic lipopeptides. These peptides contain the crucial N terminal nisin[A/B] fragment that is reported to be stable to further enzymatic degradation and have lipid-type groups coupled to the C terminus. Example structures are shown in **Figure 4.23** and these products show potent inhibition of bacterial growth, including against clinical isolates, comparable to nisin itself.[68]

317

MIC MRSA USA 300 = 64 µg/mL

318

MIC MRSA USA 300 = 8 µg/mL
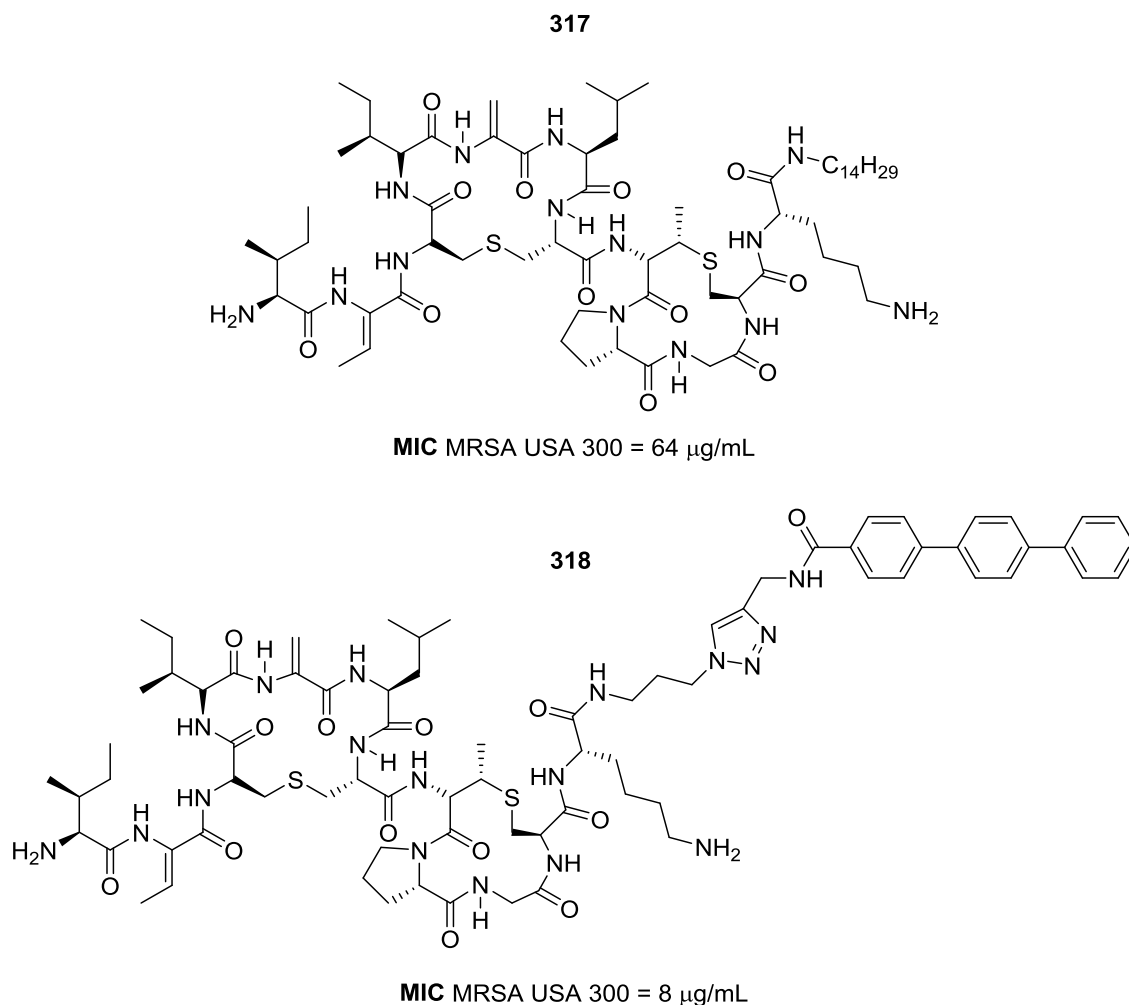
Figure 4.23. Structures of two example semi-synthetic lipopeptides, **317** and **318**, based upon the nisin[A/B] rings.[68]

In this project, we wished to exploit the antibacterial activity of nisin by the addition of peptoid sequences to the N terminal A/B ring (residues 1-12). By linking a peptoid with the truncated nisin ring fragment, it was hoped that the antibacterial action could be amplified. The combination of the lipid II targeting ring system of nisin[A/B] with peptoids, known to disrupt cell membranes non-specifically, may produce a potent antibiotic with a dual mode of action, similar to that seen in the full nisin sequence. As for peptoids in

general, these hybrids would have a different mode of action from current antibiotics and as they would target the bacterial cell envelope, the potential for drug resistance would be low.

The protocol for the synthesis of lipopeptides derived from nisin provides an efficient synthetic route to the nisin-peptoid conjugates. Nisin[A/B] is obtained from the chemoenzymatic degradation of the full length nisin and this fragment can then be modified at the C terminus.[68] In particular, an azide functionality can be installed that provides a convenient handle for ligation to alkynes via a copper catalysed click cycloaddition. The peptoid sequences are stable by their nature, since the nisin[A/B] ring is itself formed as a product of digestion and compounds like **317** and **318** have been shown to have improved stability in serum relative to nisin, the whole conjugate should be stable to proteolysis. These peptide-peptoid hybrids could therefore potentially form a new class of potent antibiotic compounds to help combat emerging antimicrobial resistance.

4.3.2   Azide-alkyne click-reactions

The azide-alkyne cycloaddition is an example of a simple 'click' reaction and is used to form 1,2,3 triazoles. A thermally activated Huisgen 1,3-dipolar cycloaddition between an azide and terminal alkyne (**Scheme 4.1a**) often forms a mixture of two regioisomers when using asymmetric alkynes. However, when the reaction is catalysed, either by copper(I) or ruthenium, the reaction follows a different mechanism and allows regioselective products to be obtained. As shown in **Scheme 4.1b** and **Scheme 4.1c**, the copper catalysed conditions form a 1,4-disubstituted triazole and the ruthenium catalysed reaction preferentially creates the 1,5- triazole.[72-74]
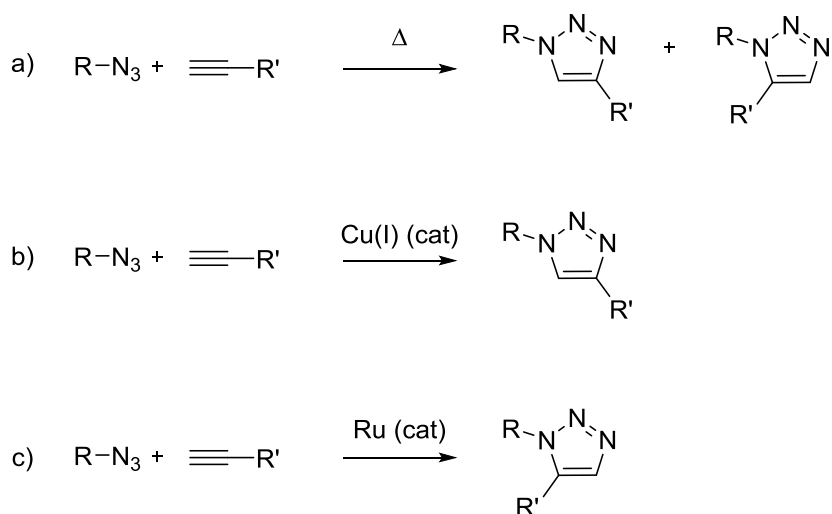
Scheme 4.1. Azide-alkyne cycloadditions a) thermal; b) copper(I) catalysed click reaction to form 1,4-triazole; c) ruthenium catalysed click reaction yielding 1,5-triazole.

This click reaction between an azide and a terminal alkyne is compatible with a range of conditions, tolerates a broad range of chemical functionalities and provides a robust strategy for chemical ligations. As an isostere of the amide bond (see **Figure 4.24**), the triazole formed by click reactions is not just a passive connector, but provides a biocompatible linker that readily associates with biological targets through hydrogen bonding and dipole interactions. Additionally, the copper(I) catalysed click reaction can be performed under aqueous conditions at room temperature, so is well suited for use with peptide-based reagents. For these reasons, the copper catalysed click reaction is ideal for the ligation of nisin with peptoid sequences.[75]

Hydrogen bond acceptors

Hydrogen bond donor
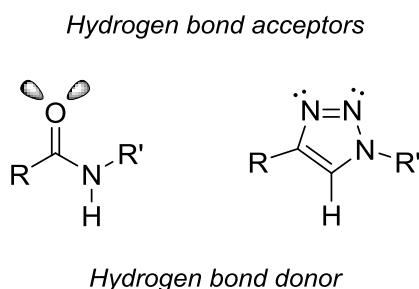
Figure 4.24. The similarity between an amide bond and the 1,2,4 triazole formed in a copper catalysed click reaction.

4.3.3 Synthesis of nisin-peptoid conjugates

This synthetic work was carried out by HLB in collaboration with the group of Dr Nathaniel Martin and assisted by Laurens Kleijn (Utrecht University).

Nisin was digested using a protocol developed in the Martin lab with trypsin and the fragment containing the A/B ring system isolated by preparative HPLC. The nisin[A/B] was then coupled to azidopropylamine and a second RP-HPLC purification undertaken to yield nisin with an azide linker (compound **321**, as in **Scheme 4.2**). This azide linker provides a handle to allow further functionalisation, in this case the addition of a peptoid sequence to nisin[A/B].[68]

Peptoid sequences were prepared using the submonomer procedure for the solid phase synthesis of peptoids and an alkyne tail added to the sequence using propargylamine under standard coupling conditions. Peptoids were then cleaved from the resin and purified by RP-HPLC prior to the click reaction. Ligation of nisin[A/B]-azide and the alkyne tagged peptoids were assisted by microwave irradiation using a copper(I) catalysed 'click' cycloaddition. The active Cu(I) catalyst is generated from the Cu(II) salt using sodium ascorbate as a reducing agent and with Tris[(1-benzyl-1*H*-1,2,3-triazol-4-yl)methyl]amine (TBTA) as a ligand to cleanly afford the expected product. The general reaction is shown in **Scheme 4.2** and forms a 1,2,3-triazole linker.
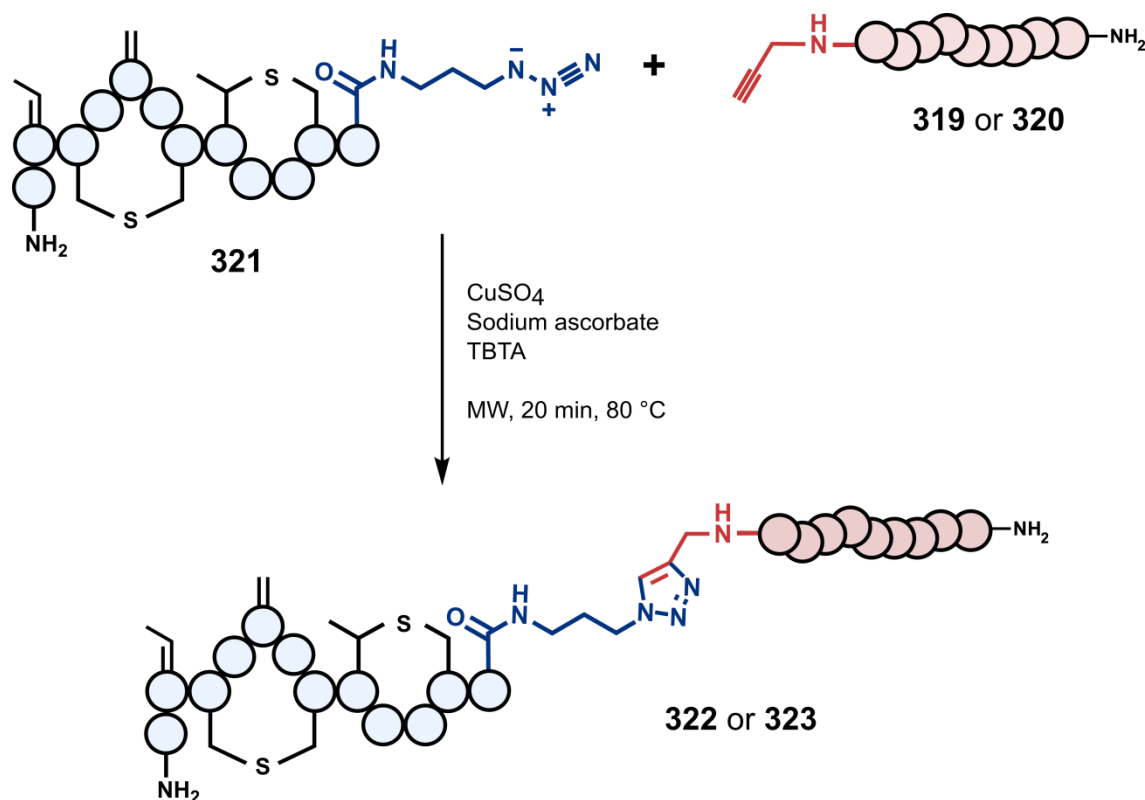
Scheme 4.2. Click reaction of nisin[A/B]-azide and an alkyne-tagged peptoid sequence.

Two peptoid sequences were chosen to click with nisin[A/B] which had previously shown promising antibacterial activities. The two peptoids used in the click reaction were compound **319** *N*prp*N*spe*N*spe(*N*ae*N*spe*N*spe)₄ derived from **156** (MIC 2 μM against *S. aureus*) and peptoid **320** *N*prp*N*spe*N*spe[(*N*Lys*N*pfb*N*pfb)(*N*Lys*N*spe*N*spe)]₂ from **157** (MIC 2 μM against *S. aureus* and 5 μM against *E. coli*). Both **319** and **320** were 15 monomers in length; the 12 residue parent sequence followed by an extra two *N*spe monomers to lengthen the chain between the last cationic residue and an N terminal *N*prp monomer with alkyne functionality.

The click reaction between the nisin[A/B]-azide (**321**) and either peptoid **319** or **320** was catalysed by Cu(I) and therefore the 1,4 regioisomer is the expected product of the reaction, with the two resulting peptide-peptoid conjugates, **322** and **323**. No optimisation of the reaction was needed, with completion seen via LC-MS after 20 minutes reaction at 80 °C. Following a final RP-HPLC purification, the expected conjugates were obtained in >99% purity for biological testing, as shown by **Figure 4.25**. Full experimental details can be found in Chapter 7.
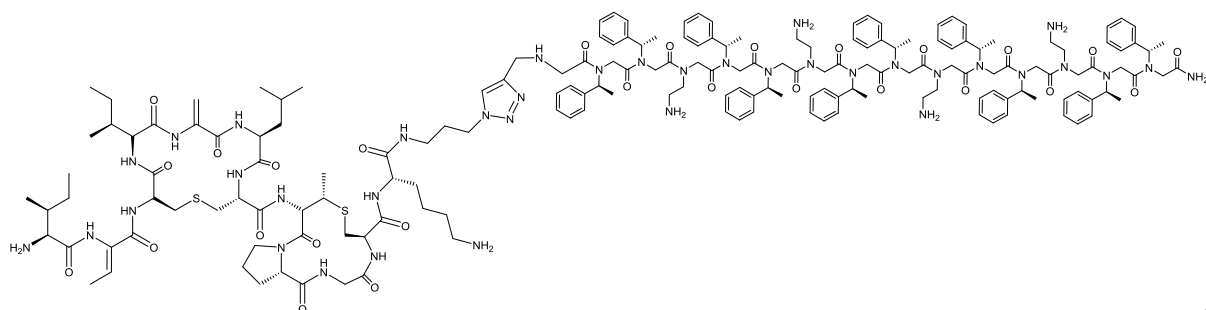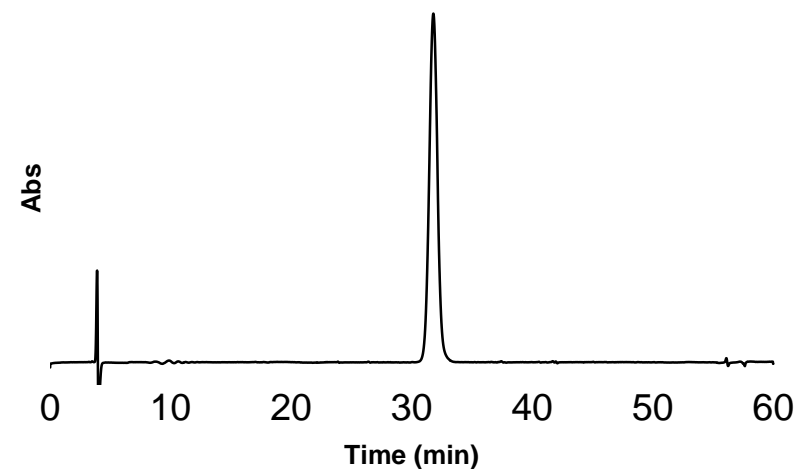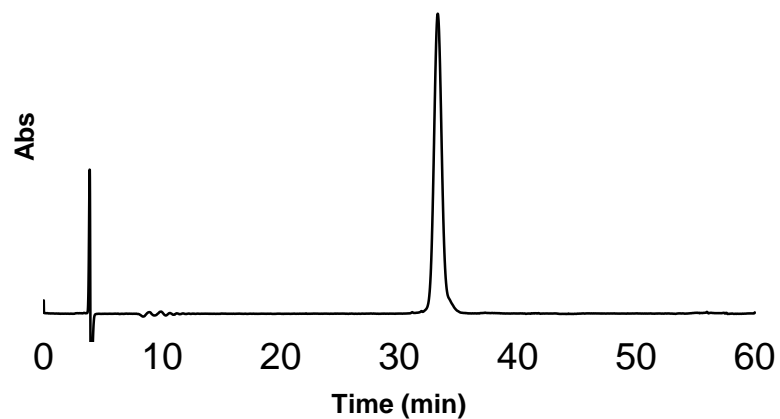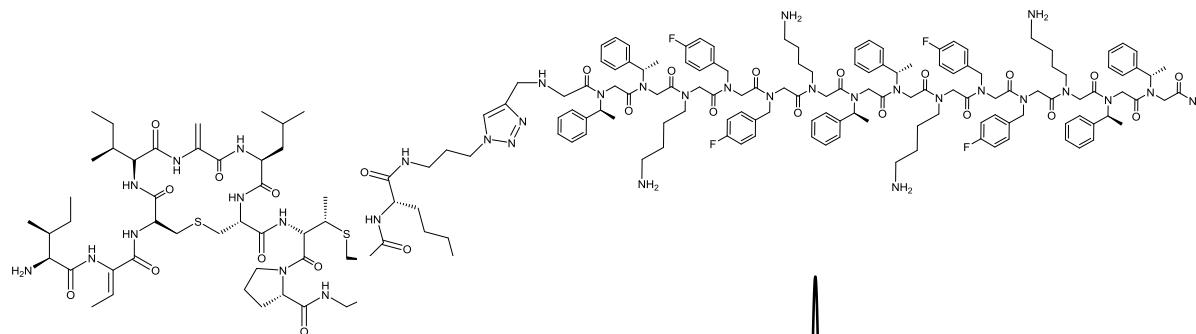
Figure 4.25. Analytical HPLC traces for the two click linked nisin[A/B]-peptoid conjugates, **322** and **323**. Products are expected to be the 1,4 regioisomer and were obtained as a homogeneous sample via RP-HPLC; 60 minute gradient; 0–100 % solvent B, where A = 100 % H₂0, 0.1 % TFA; B = 100 % acetonitrile, 0.1 % TFA.

4.3.4 Antibacterial and toxicity testing

Bacterial MIC determination was carried out by Laurens Kleijn (Utrecht University, Martin group) and cytotoxicity assays were carried out by HLB at Durham University.

The antibacterial activity of the nisin-peptoid conjugates was determined against methicillin-resistant *S. aureus* (USA 300); the predominant strain associated with community-acquired MRSA infection in the United States of America.[76] The minimum inhibitory concentrations were calculated and compared to the peptide antibiotic vancomycin (compound **324**) and nisin (compound **9**), as shown by **Table 4.4**.

	Sequence	MIC (μM)	ED_{50} (μM)	
		S. aureus (USA300)	HaCaT	HepG2
324	Vancomycin	1		
9	Nisin	5		
321	Nisin[1–12]-azide	26		
156	(Nae*N*spe*N*spe)$_4$	2	26	15
157	[(*N*Lys*N*pfb*N*pfb)(*N*Lys*N*spe*N*spe)]$_2$	2-4	53	18
319	*N*prp*N*spe*N*spe(Nae*N*spe*N*spe)$_4$	4	20	12
320	*N*prp*N*spe*N*spe[(*N*Lys*N*pfb*N*pfb)(*N*Lys*N*spe*N*spe)]$_2$	4–7	15	17
322	Nisin[1–12]-*N*spe*N*spe(Nae*N*spe*N*spe)$_4$	5–10	24	15
323	Nisin[1–12]-*N*spe*N*spe [(*N*Lys*N*pfb*N*pfb)(*N*Lys*N*spe*N*spe)]$_2$	9–18	22	23

Table 4.4. Biological evaluation of peptide-peptoid conjugates and other fragments for comparison. Antibacterial activity against methicillin-resistant *S. aureus* and toxicity against HaCaT and HepG2 cell lines are also recorded.

The parent peptoids without the alkyne linker show excellent activity against the methicillin resistant *S. aureus*, with **156** and **157** displaying MICs of 2 μM and 2–4 μM respectively, which are better than the 5 μM MIC of nisin itself. Functionalising these sequences with the alkyne linker reduces the activity by approximately half for both **319** (4 μM) and **320** (4–7 μM), although these compounds compare favourably to the nisin-azide **321** which has an MIC of 26 μM.

Unfortunately, the nisin-peptoid hybrids **322** and **323** show additional diminished activity and are overall less active than the unconjugated peptoids. When comparing **322** to **156**, the nisin-peptoid conjugate is approximately five-fold less active than the parent peptoid (i.e. MIC 5–10 μM compared to 2 μM) and this reduction in activity is similar for the second peptoid sequence with fluorinated monomers, **323** and **157** (MIC 9–18 μM vs 2–4 μM). Potentially, the peptoid tail may interfere with lipid II binding of the nisin[A/B] rings and could explain the reduced activity.

However, despite the reduction in activity compared to the peptoids alone, the MIC values are still in the low micromolar range and promising against a resistant bacterium. Interestingly **321**, the nisin[1-12]-azide, exhibits a reduced biological activity when

compared to nisin itself, potentially due to interference in the lipid II binding by the azide. For **322**, the MIC is similar to nisin (compound **9**) at approximately 5 μM. However, none of the compounds display as potent activity as vancomycin (compound **324**) with an MIC of < 1 μM.

The toxicity of the peptoid library has been discussed throughout Chapters 3 and 4, and as discussed is often overlooked in other literature regarding antimicrobial peptoids. From our initial investigations, it has become apparent that the toxicity of peptoids is something that needs to be carefully considered alongside their biological activity. Despite the somewhat disappointing antibacterial activity of nisin-peptoid hybrids, it was proposed that conjugation to nisin may be a potential strategy to manipulate the cytotoxicity of the peptoid sequences to mammalian cells and increase their selectivity.

In order to ascertain whether the decreased activity displayed by the nisin-peptoid conjugates (when compared to their parent peptoid sequences) was accompanied by a beneficial reduction in toxicity, cytotoxicity assays were performed against HaCaT keratinocytes and epithelial HepG2 cells. These assays were all undertaken in triplicate on a minimum of three occasions to ensure a robust data set was obtained and the ED_{50} values are presented as the average over the multiple assays in **Table 4.4**.

The peptoid sequences **319** and **320** with the N terminal alkyne were the most cytotoxic to both mammalian cell lines tested (ED_{50} values of < 20 μM). Regrettably, the nisin-conjugated peptoid sequences **322** and **323** were also moderately cytotoxic to both mammalian cell lines tested around 20 μM. The ED_{50} values obtained show that the nisin-peptoids have a similar level of toxicity to the peptoid sequences **156** and **157**. Given that nisin is known to show negligible toxicity and no observable adverse activity in *in vivo* studies, this was a disappointing result. In an attempt to rationalise the unexpected toxicity and the reduced antibacterial activity compared to the parent peptoids, enzymatic stability assays were undertaken.[77]

4.3.5 Stability of peptide-peptoid conjugates to enzymatic degradation

The stability of the nisin[A/B]-peptoid conjugates **322** and **323** was assessed using a trypsin degradation assay. This assay was based upon the same conditions used to obtain the nisin[A/B] ring from chemoenzymatic degradation of the full nisin sequence.[68] Compounds **322** and **323** were incubated with TPCK[**] trypsin for 24 hours at 37 °C in tris-HCl buffer (50 mM at pH 7.8, with 5 mmol CalCl$_2$[††]). The peptoid sequences **156** and **157** were also subjected to the same digestion procedure for comparison.

The digestion was monitored using a combination of analytical RP-HPLC and MALDI mass spectrometry. For analysis using mass spectrometry, a 10 μL aliquot was removed from incubation and analysed spotted to the MALDI target immediately (as a mixture with α-cyano-4-hydroxycinnamic acid matrix). After 24 hour incubation with the enzyme, no significant change is seen in the MALDI spectra of **156** or **157**.

However, for the nisin-peptoid conjugates **322** and **323**, ions are seen that were not present in initial MALDI spectra before digestion and these appear at lower *m/z* values than the molecular ion, suggesting that the initial conjugates are being digested into lower molecular weight fragments (see **Figure 4.26** and **Figure 4.27**).
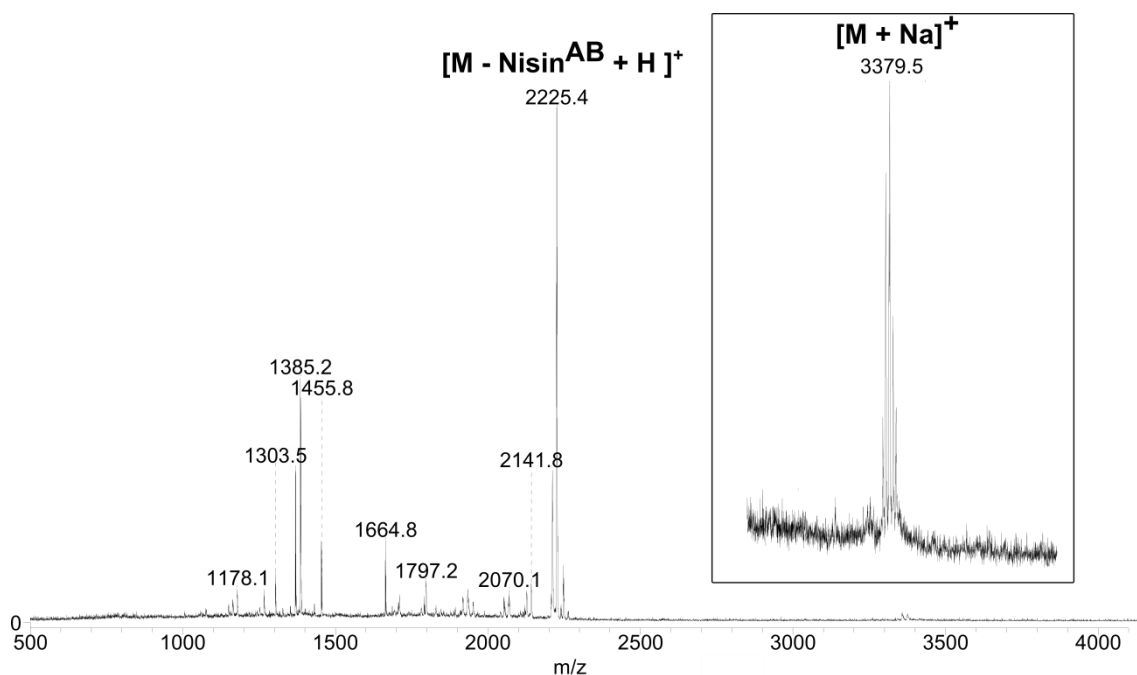
Figure 4.26. MALDI mass spectrum showing products following 24 hour trypsin degradation of peptoid **322** with ions labelled. The spectrum has been expanded to show the weak molecular ion peak at *m/z* 3379.5. Suppression of ions at *m/z* < 1000.

[**] TPCK trypsin: *N*-tosyl-L-phenylalanyl chloromethyl ketone treated to inhibit any chymotrypsin activity which may be present.

[††] CaCl$_2$ added to reduce trypsin autolysis.
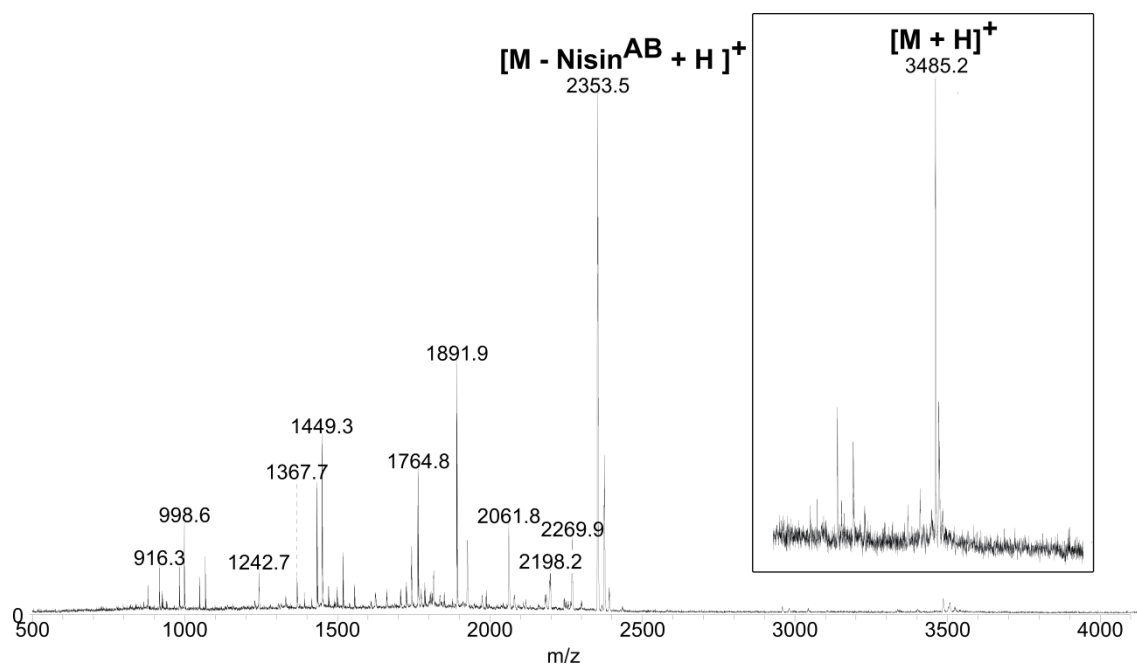
Figure 4.27. MALDI mass spectrum showing products following 24 hour trypsin degradation of peptoid **323** with ions labelled. The spectrum has been expanded to show the weak molecular ion peak at *m/z* 3379.5. Suppression of ions at *m/z* < 1000.

As shown by both MALDI spectra, the peaks corresponding to molecular ion after trypsin degradation are significantly decreased and can only be seen fully using an expanded view[‡‡]. In the spectra for **322** and **323**, peaks appear at *m/z* 2225.4 and 2353.5, which correspond to peptoid fragments produced by the cleavage of the Lys_{12} residue attached to the $nisin^{A/B}$ ring (**325** and **326** in **Scheme 4.3**). A peak at *m/z* 1150 corresponding to the $nisin^{A/B}$ fragment **327** can be seen in the MALDI spectrum following digestion of **322** in **Figure 4.26**.[§§]

[‡‡] Although the smaller peak intensity cannot be correlated to the amount of sample present.

[§§] The peak at *m/z* 1150 cannot be seen in the MALDI following digestion of **323,** possibly due to the suppression of low molecular weight ions.

R₁ = **322** *m/z* = 3356
R₂ = **323** *m/z* = 3485

R₁ = *Nspe**Nspe(**Nae**Nspe**Nspe)*₄
R₂ = *Nspe**Nspe**[(**NLys**Npfb**Npfb)(**NLys**Nspe**Nspe)]*₂

Trypsin, 37 °C
Cleavage at Lys₁₂

327 *m/z* = 1150

R₁ = **325** *m/z* = 2224
R₂ = **326** *m/z* = 2352
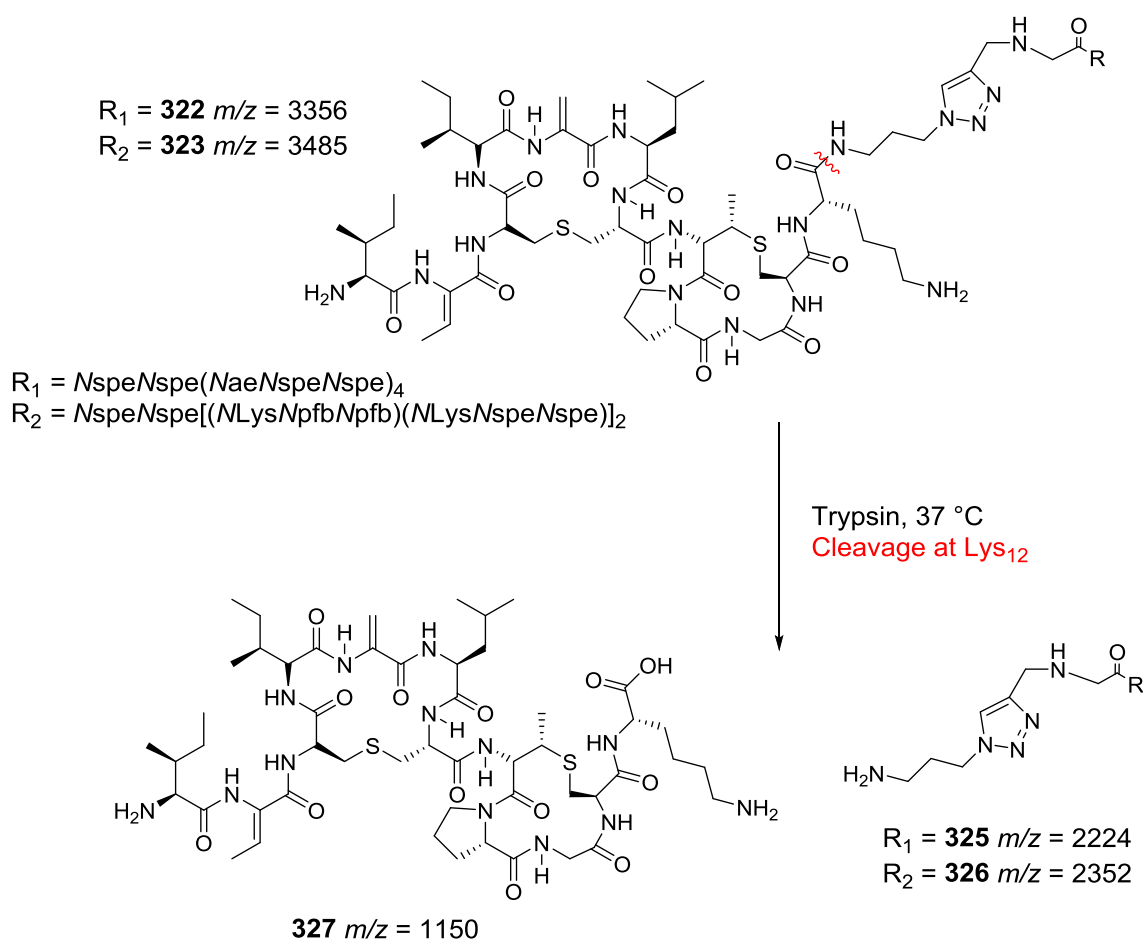
Scheme 4.3. Proposed cleavage of the Lys₁₂ residue on nisin[AB] ring into peptoid and peptide fragments (**325** and **326** are seen via MALDI).

MS/MS experiments are commonly used to aid in the sequencing of peptides or peptoids[78-80] and commonly lead to fragmentation at the amide bond of the backbone resulting in a series of product ions. These ions either appear to extend from the N-terminus (termed 'b ions', containing the carbonyl part of the CO-NH bond) or the C-terminus ('y ions', with the nitrogen atom of the amide bond). To confirm the identity of the peaks at *m/z* 2225.4 and 2353.5, MALDI LIFT-ToF/ToF MS/MS was used. This LIFT technique allows the detection of product ions resulting from fragmentation of a specified ion, as a result of elevated laser power.[81]

The product ions seen from fragmentation of *m/z* 2225.4 and 2353.5 are summarised in **Figure 4.28a** and **Figure 4.28b** respectively and the annotated MALDI LIFT spectra obtained for both can be found in the Appendix. Since some fragmentations are preferred over others, certain ions are absent and the abundance of observed peaks varies. Overall, the fragmentation observed in both cases is consistent with the proposed compounds **325** or **326** formed by cleavage at the Lys₁₂ residue, as shown in **Scheme 4.3**.

A $C_8H_{15}N_5O$ | *N*spe | *N*spe | *N*ae | *N*spe | *N*spe | *N*ae | *N*spe | *N*spe | *N*ae | *N*spe | *N*spe | *N*ae | *N*spe *N*spe

y ions (N-terminal to C): y_{14}, y_{13}, y_{12}, y_{11}, y_{10}, y_9, y_8, y_7, y_6, y_5, y_3, y_2

b ions: b_2, b_4, b_5, b_6, b_7, b_9, b_{10}, b_{11}, b_{12}, b_{13}

B $C_8H_{15}N_5O$ | *N*spe | *N*spe | *N*Lys | *N*pfb | *N*pfb | *N*Lys | *N*spe | *N*spe | *N*Lys | *N*pfb | *N*pfb | *N*Lys | *N*spe *N*spe

y ions: y_{14}, y_{13}, y_{12}, y_{11}, y_{10}, y_9, y_8, y_7, y_6, y_5, y_3

b ions: b_2, b_4, b_5, b_8, b_9, b_{11}, b_{12}, b_{13}
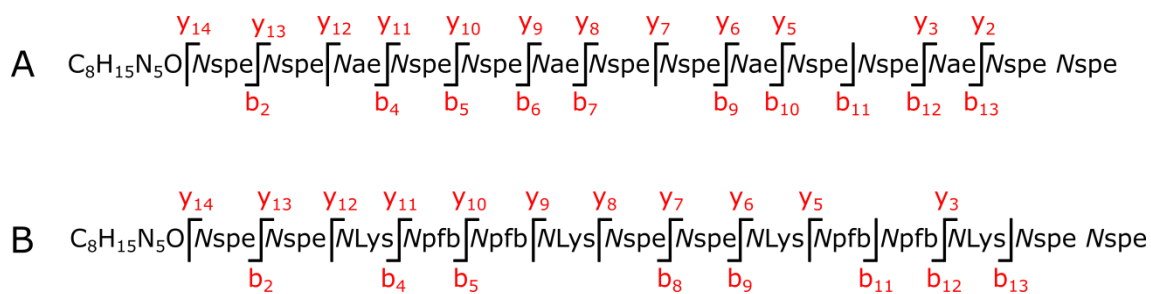
Figure 4.28. Summary of ions observed via MALDI LIFT-ToF/ToF, where ions resulting from amide cleavage are observed as b ions or y ions; A following fragmentation of ion at *m*/z 2225.4 in sample obtained following digestion of **322**; B following fragmentation of ion at *m*/z 2353.5 in sample obtained following digestion of **323**.

The digestion of **322** and **323** can also be monitored using analytical RP-HPLC to investigate the relative amounts of cleaved versus intact compound in greater detail. In control peptoids **156** and **157**, no significant change is seen in the RP-HPLC chromatogram after 24 hour incubation with the enzyme (see **Figure 4.29a** and **Figure 4.29c**).

However, for the nisin-peptoid conjugates **322** and **323**, significant differences are seen in the appearance of RP-HPLC chromatograms before degradation (t = 0 h) and afterwards (t = 24 h). As shown in **Figure 4.29b** and **Figure 4.29d,** the chromatograms for both nisin-peptoid conjugates show several peaks following incubation with trypsin which suggests that substantial digestion is occurring under these conditions. For example, for both conjugates (**322** and **323**) the single peak seen at t = 0 h (at retention time ~ 20 min) is significantly decreased at t = 24 h and extra peaks appear on the chromatogram at reduced retention times; ~ 15 min from the nisin$^{A/B}$ rings (compound **327**) and at ~ 18 min is also seen, which is attributed to the peptoid fragments **325** or **326**.

To study the rate of digestion, at several time points an aliquot was removed (100 µL), 10 µL TFA added to quench enzyme activity and a 10 µL injection made to the HPLC instrument. Further conditions are described in Chapter 7 and the chromatograms obtained for digestion of conjugate **322** are plotted in **Figure 4.30** (a similar time point plot for **323** can be found in the Appendix). The data obtained suggest that the half-life of the nisin-peptoid conjugates is between 2-3 hours, based upon integration of the RP-HPLC chromatograms, with the majority of the conjugate cleaved into peptide and peptoid fragments after 6 hours.
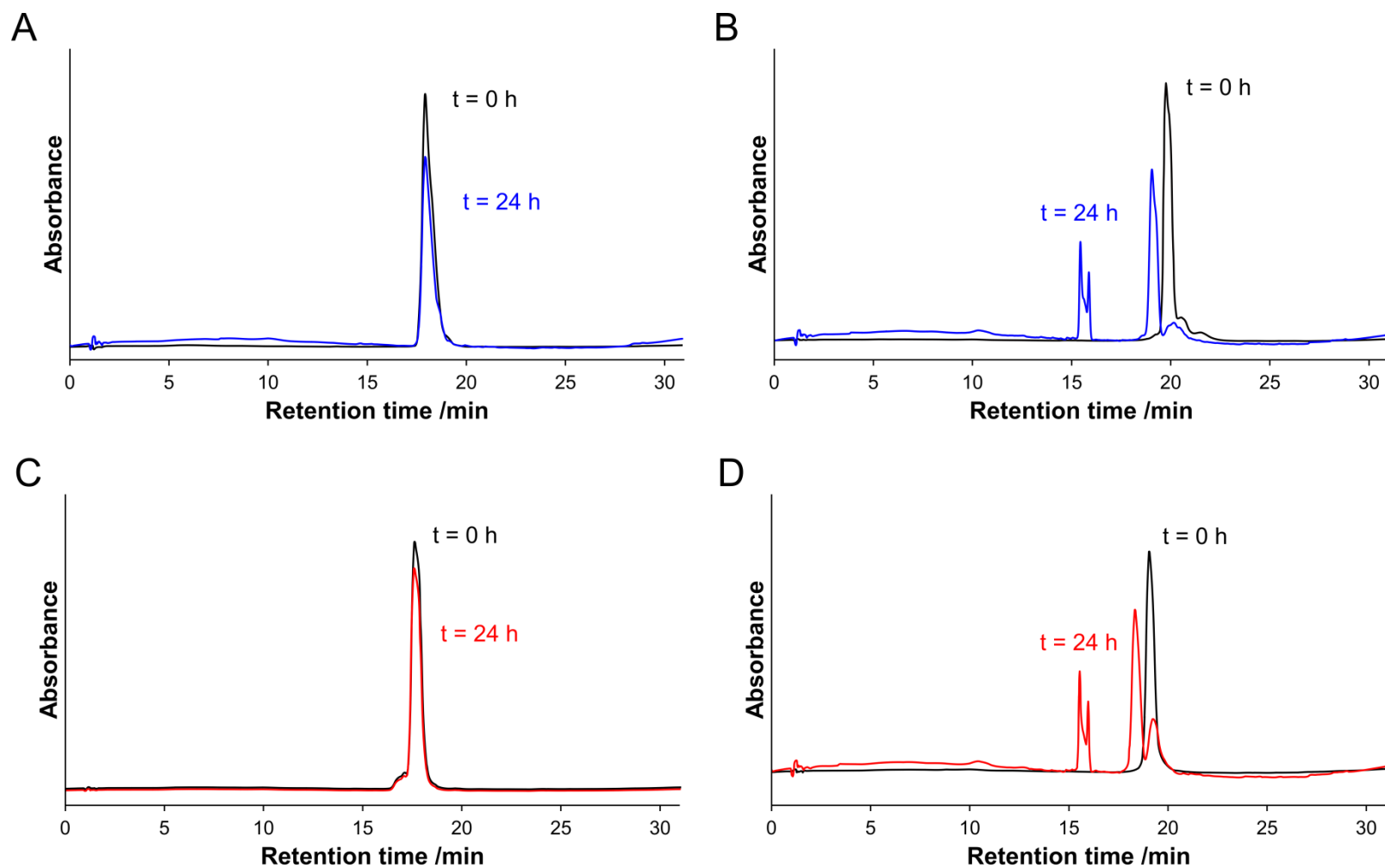
Figure 4.29. RP-HPLC chromatograms for the digestion of nisin-peptoid conjugates by trypsin over a 24 hour time period in tris-HCl buffer (50 mM at pH 7.8, with 5 mmol CalCl$_2$) A peptoid **156**; B peptoid **157**; C nisin-peptoid conjugate **322**; D nisin-peptoid conjugate **323** where black chromatogram shows the trace at t = 0 h (i.e. with no digestion) and coloured traces at t = 24 h.
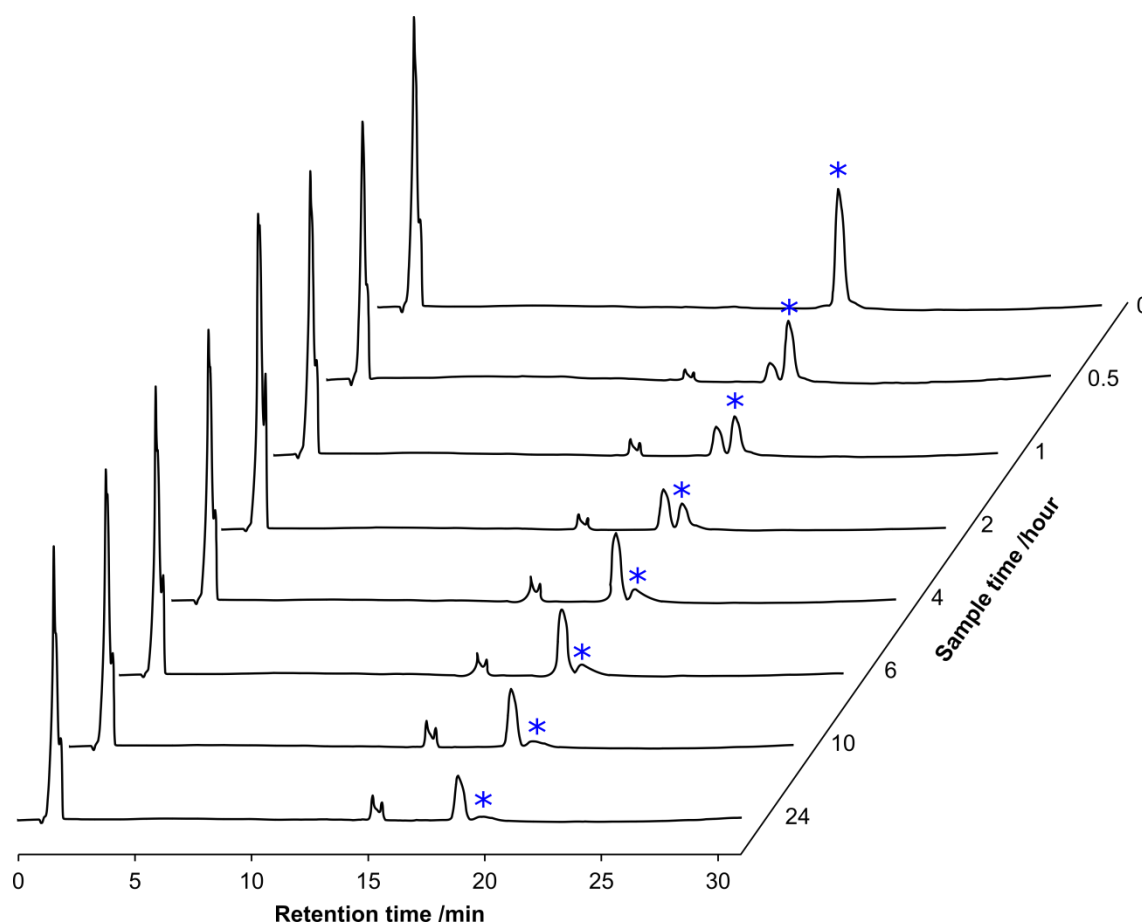
Figure 4.30. RP-HPLC chromatograms for the digestion of **322** by trypsin in tris-HCl buffer (50 mM at pH 7.8, with 5 mmol CalCl$_2$) over a 24 hour time period. Intense peak at retention time = 2 min corresponds to the TFA added to quench enzyme activity. The initial nisin-peptoid conjugate **322** is labelled with a star in each chromatogram to show its digestion to fragments **325** and **327** at reduced retention times.

Therefore, it is evident that under the conditions used, the nisin$^{A/B}$-peptoid conjugates are not stable to enzymatic degradation by trypsin. This is perhaps unsurprising due to the C-terminal lysine residues on the nisin$^{A/B}$ ring system, however previously biologically active semi-synthetic lipopeptides have been prepared using the same methodology and also contain the Lys$_{12}$ amide bond (see examples **317** and **318** in **Figure 4.23**).[68] Both **317** and **318** were tested for their stability and were shown to be stable for over 10 hours in serum and also showed potent antimicrobial activity. It would be interesting to perform the same trypsin degradation on these compounds to determine their enzymatic stability.

The poor stability seen for the nisin$^{A/B}$-peptoid conjugates **322** and **323** is a possible explanation for their unexpectedly high toxicity and poor antibacterial activity, since these compounds may also be unstable in the biological assays they were applied in or in serum (although this remains to be determined). If the Lys$_{12}$ residue is cleaved the peptide **327** and peptoid fragments **325** or **326** would be formed.

Cleavage into these fragments could explain why the antibacterial activity of both **322** and **323** is reduced compared to the peptoids **156** (Nae$N$spe$N$spe)$_4$ and **157** [(NLys$N$pfb$N$pfb)(NLys$N$spe$N$spe)]$_2$ alone, as the peptoid fragments **325** and **326** have an N-terminal triazole group. The activity of the Nprp compounds with N-terminal alkynes (**319** and **320** MIC 4 and 4–7 μM respectively) are two-fold less potent than **156** or **157** (MIC 2 and 2–4 μM) and this may also be the case for **325**/**326**. Cleavage into the peptoid fragments would also explain why the ED$_{50}$ values against HepG2 and HaCaT are similar for **156** and the conjugate **322** or **157** and the conjugate **323**, as the peptoid sequences are not conjugated to the nisin$^{A/B}$ rings in either case. Additionally, the peptoid chain may interfere with the ability of the A/B ring fragment of nisin to bind to lipid II, which could explain the reduced activity of the conjugates. Lipid II binding assays should be completed to test this hypothesis in the future.

In conclusion, conjugation of a peptoid sequence to a peptide (in this case, nisin[1-12]-azide) is simple using copper catalysed click methodology and the peptide-peptoid hybrids **322** and **323** were obtained in good yield and purity. However, for the sequences illustrated here, there is no advantage to conjugating the peptoids to nisin$^{A/B}$; the peptoid sequences themselves would be better antibacterial candidates and both the peptoid sequences and the peptide-peptoid hybrids display similar levels of toxicity to mammalian cells.

The nisin$^{A/B}$-peptoid hybrids are not stable to tryptic degradation and it has been shown that enzymatic cleavage occurs at the Lys$_{12}$ residue. The poor stability of the peptide-peptoid conjugates is the likely explanation for their poor antibacterial activity and the unexpected toxicity to mammalian cells. Cleavage at Lys$_{12}$ during the course of the assay forms the nisin$^{A/B}$ rings which are not themselves active and a peptoid fragment similar to **319** or **320** which have poorer activity than the parent peptoids **156** and **157**.

4.4   Conclusions

In conclusion, the peptoids presented in this chapter have been shown to display potent antibacterial activity against planktonic bacteria, and also against bacteria and fungi in their biofilm form. This is the first time that peptoids have been shown to be efficacious against fungal biofilms and also against cross-kingdom, polymicrobial biofilms.

Certain members of this library provide promising starting points for the development of lead compounds and confirm that peptoids may be a promising new class of antibiotics that could potentially help to combat the increasing problem of antibiotic resistance. For example, peptoid **153** (*N*hArg*N*mfb*N*mfb)$_4$ has MIC values against planktonic *E. coli* and *P. aeruginosa* of 13 μM; for both *S. aureus* and *S. epidermidis* the MIC is 2 μM. Against bacteria or fungi in their biofilm form, peptoid **216** (*N*ah*N*spe*N*spe)$_3$ was identified with significant activity against *S. aureus*, *E. coli* and *C. albicans* in mixed species biofilms. Factors that enhance antibacterial activity against Gram positive and Gram negative bacteria, and those within biofilms, have been highlighted in the appropriate sections. It has also been demonstrated that MIC determination is generally unsuitable to predict which sequences may display potent activity against biofilms.

The peptoid library tested was designed to mimic helical and cationic antimicrobial peptides, found in nature as part of the innate immune response of many organisms. Many of the AMPs are proposed to cause membrane disruption, among other possible mechanisms of action, and it is thought that peptoids also behave in a similar manner. It has been shown that the cell membranes of bacteria and fungi in biofilms are indeed disrupted following treatment by selected peptoids from the library, using the SYTOX® Green assay. The peptoids which cause the largest plasma membrane permeabilisation also tend to display the largest antimicrobial activities, such as peptoid **182** (*N*Lys*N*hLeu*N*spe)$_4$, which causes the greatest increase in fluorescence in the SYTOX® Green assay against *S. aureus*, *E. coli* and *C. albicans* (> 3,000 fold increase in fluorescence for all three species). Treatment by peptoid **182** also causes significant reductions in biomass within single species biofilms by 25 % for *S. aureus*, 25 % for *E. coli* and 10 % for *C. albicans*, as measured by the Crystal Violet assay. Further work to elucidate the mechanism of action of these peptoids is described in Chapter 5, and aims to further clarify the cellular targets of these antimicrobial peptoid sequences.

Finally, the peptoid community is clearly able to design and synthesise potent antimicrobial peptoids. Sequences designed as part of this project and those already in the literature display very good activities against a wide range of bacterial and fungal pathogens. However, many of these peptoids are also toxic towards host and mammalian cells. Chapter 5 examines the selectivity of antimicrobial peptoid sequences in more detail, in an attempt to overcome this challenge.

4.5   References

1.   The 10 x '20 Initiative: pursuing a global commitment to develop 10 new antibacterial drugs by 2020, *Clin. Infect. Dis.,* **2010**, *50*, 1081.

2.   H.C. Neu, *Science,* **1992**, *257*, 1064.

3.   A.E. Clatworthy, E. Pierson, D.T. Hung, *Nat. Chem. Biol.,* **2007**, *3*, 541.

4.   The World Health Organisation, *Antimicrobial Resistance* **2014**.

5.   D.J. Payne, M.N. Gwynn, D.J. Holmes, D.L. Pompliano, *Nat. Rev. Drug Discov.,* **2007**, *6*, 29.

6.   R. Tommasi, D.G. Brown, G.K. Walkup, J.I. Manchester, A.A. Miller, *Nat. Rev. Drug Discov.,* **2015**, *14*, 529.

7.   O. Cars, L.D. Hogberg, M. Murray, O. Nordberg, S. Sivaraman, C.S. Lundborg, A.D. So, G. Tomson, *BMJ,* **2008**, *337*, a1438.

8.   L. Czaplewski, R. Bax, M. Clokie, M. Dawson, H. Fairhead, V.A. Fischetti, S. Foster, B.F. Gilmore, R.E.W. Hancock, D. Harper, I.R. Henderson, K. Hilpert, B.V. Jones, A. Kadioglu, D. Knowles, S. Ólafsdóttir, D. Payne, S. Projan, S. Shaunak, J. Silverman, C.M. Thomas, T.J. Trust, P. Warn, J.H. Rex, *Lancet Infect. Dis.,* *16*, 239.

9.   C.T. Walsh, T.A. Wencewicz, *J. Antibiot.,* **2014**, *67*, 7.

10.   T.J. Silhavy, D. Kahne, S. Walker, *Cold Spring Harb. Perspect. Biol.,* **2010**, *2*, a000414.

11.   H.-C. Flemming, J. Wingender, *Nat. Rev. Microbiol.,* **2010**, *8*, 623.

12.   J.W. Costerton, P.S. Stewart, E.P. Greenberg, *Science,* **1999**, *284*, 1318.

13.   P. Stoodley, K. Sauer, D.G. Davies, J.W. Costerton, *Annu. Rev. Microbiol.,* **2002**, *56*, 187.

14.   P.S. Stewart, J.W. Costerton, *Lancet,* **2001**, *358*, 135.

15.   *Medical Microbiology*; 4th ed.; University of Texas Medical Branch: Galveston Texas, 1996.

16.   J.M. Andrews, *J. Antimicrob. Chemother.,* **2001**, *48*, 5.

17.   C.W. Wu, T.J. Sanborn, R.N. Zuckermann, A.E. Barron, *J. Am. Chem. Soc.,* **2001**, *123*, 2958.

18.   C.W. Wu, T.J. Sanborn, K. Huang, R.N. Zuckermann, A.E. Barron, *J. Am. Chem. Soc.,* **2001**, *123*, 6778.

19.   N.P. Chongsiriwatana, J.A. Patch, A.M. Czyzewski, M.T. Dohm, A. Ivankin, D. Gidalevitz, R.N. Zuckermann, A.E. Barron, *Proc. Natl. Acad. Sci. USA,* **2008**, *105*, 2794.

20.   R.W. Gwadz, D. Kaslow, J.Y. Lee, W.L. Maloy, M. Zasloff, L.H. Miller, *Infect. Immun.,* **1989**, *57*, 2628.

21.   M. Zasloff, *Proc. Natl. Acad. Sci. USA,* **1987**, *84*, 5449.

22.   L. Silvestro, J.N. Weiser, P.H. Axelsen, *Antimicrob. Agents Chemother.,* **2000**, *44*, 602.

23.   F. Guilhelmelli, N. Vilela, P. Albuquerque, L.d.S. Derengowski, I. Silva-Pereira, C.M. Kyaw, *Front. Microbiol.,* **2013**, *4*, 353.

24.   S. Gruenheid, H. Le Moual, *FEMS Microbiol. Lett.,* **2012**, *330*, 81.

25.   M. Vaara, M. Nurminen, *Antimicrob. Agents Chemother.,* **1999**, *43*, 1459.

26.   N. Ruiz, D. Kahne, T.J. Silhavy, *Nat. Rev. Microbiol.,* **2006**, *4*, 57.

27.   G.A. Eggimann, H.L. Bolt, P.W. Denny, S.L. Cobb, *ChemMedChem,* **2015**, *10*, 233.

28.   H.L. Bolt, G.A. Eggimann, P.W. Denny, S.L. Cobb, *MedChemComm,* **2016**, *7*, 799.

29.   L. Vedel, G. Bonke, C. Foged, H. Ziegler, H. Franzyk, J.W. Jaroszewski, C.A. Olsen, *ChemBioChem,* **2007**, *8*, 1781.

30.   K. Andreev, C. Bianchi, J.S. Laursen, L. Citterio, L. Hein-Kristensen, L. Gram, I. Kuzmenko, C.A. Olsen, D. Gidalevitz, *Biochim. Biophys. Acta,* **2014**, *1838*, 2492.

31. P.A. Wender, D.J. Mitchell, K. Pattabiraman, E.T. Pelkey, L. Steinman, J.B. Rothbard, *Proc. Natl. Acad. Sci. USA,* **2000**, *97*, 13003.

32. C.A. Olsen, H.L. Ziegler, H.M. Nielsen, N. Frimodt-Moller, J.W. Jaroszewski, H. Franzyk, *ChemBioChem,* **2010**, *11*, 1356.

33. H.L. Bolt, S.L. Cobb, *Org. Biomol. Chem.,* **2016**, *14*, 1211.

34. J.B. Rothbard, T.C. Jessop, P.A. Wender, *Adv. Drug. Deliv. Rev.,* **2005**, *57*, 495.

35. L.A. Rawlinson, J.P. O'Gara, D.S. Jones, D.J. Brayden, *J. Med. Microbiol.,* **2011**, *60*, 968.

36. N. Malanovic, K. Lohner, *Biochim. Biophys. Acta,* **2015**.

37. J. Turner, Y. Cho, N.N. Dinh, A.J. Waring, R.I. Lehrer, *Antimicrob. Agents Chemother.,* **1998**, *42*, 2206.

38. N. Hoiby, T. Bjarnsholt, M. Givskov, S. Molin, O. Ciofu, *Int. J. Antimicrob. Agents,* **2010**, *35*, 322.

39. J.A. Patch, K. Kirshenbaum, S.L. Seurynck, R.N. Zuckermann, A.E. Barron In *Pseudopeptides in Drug Development*; Nielsen, P. E., Ed.; Wiley-VCH: Germany, 2004, p 1

40. R. Kapoor, P.R. Eimerman, J.W. Hardy, J.D. Cirillo, C.H. Contag, A.E. Barron, *Antimicrob. Agents Chemother.,* **2011**, *55*, 3058.

41. R. Kapoor, M.W. Wadman, M.T. Dohm, A.M. Czyzewski, A.M. Spormann, A.E. Barron, *Antimicrob. Agents Chemother.,* **2011**, *55*, 3054.

42. F.L. Mayer, D. Wilson, B. Hube, *Virulence,* **2013**, *4*, 119.

43. N.C. Lim, D.K. Lim, M. Ray, *Eye Contact Lens,* **2013**, *39*, 348.

44. S. Cairns, J.G. Thomas, S.J. Hooper, M.P. Wise, P.J. Frost, M.J. Wilson, M.A. Lewis, D.W. Williams, *PLOS ONE,* **2011**, *6*, e14759.

45. K.A. Brogden, J.M. Guthmiller, C.E. Taylor, *Lancet,* **2005**, *365*, 253.

46. F.L. Short, S.L. Murdoch, R.P. Ryan, *Trends Microbiol.,* **2014**, *22*, 508.

47. M.L. Falsetta, M.I. Klein, P.M. Colonne, K. Scott-Anne, S. Gregoire, C.H. Pai, M. Gonzalez-Begne, G. Watson, D.J. Krysan, W.H. Bowen, H. Koo, *Infect. Immun.,* **2014**, *82*, 1968.

48. B.M. Peters, M.A. Jabra-Rizk, M.A. Scheper, J.G. Leid, J.W. Costerton, M.E. Shirtliff, *FEMS Immunol. Med. Microbiol.,* **2010**, *59*, 493.

49. B.C. Monk, A. Goffeau, *Science,* **2008**, *321*, 367.

50. M.M. Harriott, M.C. Noverr, *Antimicrob. Agents Chemother.,* **2010**, *54*, 3746.

51. K. Chiba, K. Kawakami, K. Tohyama, *Toxicol. in vitro,* **1998**, *12*, 251.

52. T.C. Lorenz, *J. Vis. Exp.,* **2012**, e3998.

53. S. Tavernier, T. Coenye, *PeerJ,* **2015**, *3*, e787.

54. S. Pasquaroli, G. Zandri, C. Vignaroli, C. Vuotto, G. Donelli, F. Biavasco, *J. Antimicrob. Chemother.,* **2013**, *68*, 1812.

55. R.J. Boohaker, M.W. Lee, P. Vishnubhotla, J.M. Perez, A.R. Khaled, *Curr. Med. Chem.,* **2012**, *19*, 3794.

56. H. Jenssen, P. Hamill, R.E. Hancock, *Clin. Microbiol. Rev.,* **2006**, *19*, 491.

57. S.K. Straus, R.E.W. Hancock, *Biochim. Biophys. Acta,* **2006**, *1758*, 1215.

58. M. Torrent, D. Pulido, L. Rivas, D. Andreu, *Curr. Drug Targets,* **2012**, *13*, 1138.

59. M.R. Yeaman, N.Y. Yount, *Pharmacol. Rev.,* **2003**, *55*, 27.

60. B.L. Roth, M. Poot, S.T. Yue, P.J. Millard, *Appl. Environ. Microbiol.,* **1997**, *63*, 2421.

61. D.T. McLean, F.T. Lundy, D.J. Timson, *Biochimie,* **2013**, *95*, 875.

62. W. Huang, J. Seo, J.S. Lin, A.E. Barron, *Mol. Biosyst.,* **2012**, *8*, 2626.

63. B. Mojsoska, R.N. Zuckermann, H. Jenssen, *Antimicrob. Agents Chemother.,* **2015**.

64. T.S. Ryge, N. Frimodt-Moller, P.R. Hansen, *Chemotherapy,* **2008**, *54*, 152.

65. E. Breukink, I. Wiedemann, C. van Kraaij, O.P. Kuipers, H.G. Sahl, B. de Kruijff, *Science,* **1999**, *286*, 2361.

66.   L. Zhou, A.J. van Heel, M. Montalban-Lopez, O.P. Kuipers, *Front. Cell Dev. Biol.,* **2016**, *4*, 7.
67.   C.J. Arnusch, A.M.J.J. Bonvin, A.M. Verel, W.T.M. Jansen, R.M.J. Liskamp, B. de Kruijff, R.J. Pieters, E. Breukink, *Biochem.,* **2008**, *47*, 12661.
68.   T. Koopmans, T.M. Wood, P. t Hart, L.H.J. Kleijn, A.P.A. Hendrickx, R.J.L. Willems, E. Breukink, N.I. Martin, *J. Am. Chem. Soc.,* **2015**, *29*, 9382.
69.   N. Ghalit, J.F. Reichwein, H.W. Hilbers, E. Breukink, D.T.S. Rijkers, R.M.J. Liskamp, *ChemBioChem,* **2007**, *8*, 1540.
70.   J.C. Slootweg, N. Peters, H.L. Quarles van Ufford, E. Breukink, R.M. Liskamp, D.T. Rijkers, *Bioorg. Med. Chem.,* **2014**, *22*, 5345.
71.   R. Rink, J. Wierenga, A. Kuipers, L.D. Kluskens, A.J. Driessen, O.P. Kuipers, G.N. Moll, *Appl. Environ. Microbiol.,* **2007**, *73*, 5809.
72.   F. Himo, T. Lovell, R. Hilgraf, V.V. Rostovtsev, L. Noodleman, K.B. Sharpless, V.V. Fokin, *J. Am. Chem. Soc.,* **2005**, *127*, 210.
73.   B.C. Boren, S. Narayan, L.K. Rasmussen, L. Zhang, H. Zhao, Z. Lin, G. Jia, V.V. Fokin, *J. Am. Chem. Soc.,* **2008**, *130*, 8923.
74.   C.W. Tornøe, C. Christensen, M. Meldal, *J. Org. Chem.,* **2002**, *67*, 3057.
75.   H.C. Kolb, K.B. Sharpless, *Drug Discov. Today,* **2003**, *8*, 1128.
76.   C. Margaret, N.P. Eli, Z.D. Michael, *Emerging Infect. Dis.,* **2015**, *21*, 1973.
77.   A. Hagiwara, N. Imai, H. Nakashima, Y. Toda, M. Kawabe, F. Furukawa, J. Delves-Broughton, K. Yasuhara, S.-m. Hayashi, *Food Chem. Toxicol.,* **2010**, *48*, 2421.
78.   R. Ruijtenbeek, C. Versluis, A.J.R. Heck, F.A.M. Redegeld, F.P. Nijkamp, R.M.J. Liskamp, *J. Mass Spectrom.,* **2002**, *37*, 47.
79.   B. Bogdanov, X.N. Zhao, D.B. Robinson, J.H. Ren, *J. Am. Soc. Mass Spectrom.,* **2014**, *25*, 1202.
80.   A. Thakkar, A.S. Cohen, M.D. Connolly, R.N. Zuckermann, D. Pei, *J. Comb. Chem.,* **2009**, *11*, 294.
81.   D. Suckau, A. Resemann, M. Schuerenberg, P. Hufnagel, J. Franzen, A. Holle, *Anal. Bioanal. Chem.,* **2003**, *376*, 952.

Chapter 5

Investigations into Peptoid Mode of Action

Within Chapters 3 and 4 a large number of peptoid sequences were evaluated as antimicrobial compounds and structure activity data was analysed. Particularly against parasitic targets, there was little data already available in the literature to aid in the design of antiparasitic peptoids. From the work carried out in Chapters 3 and 4, several factors important for activity were elucidated but it was also shown that biophysical characteristics of the peptoids, such as hydrophobicity, have a large impact upon their biological activity and little information is available to help rationalise this activity.

Peptoids are thought to cause membrane disruption as their primary mechanism of action, although this has not been conclusively determined or confirmed as the only mode of action. Previously, cyclic peptoids have been shown to disrupt *S. aureus* membranes using scanning electron microscopy. Cells treated with sub-MIC, MIC or supra-MIC concentrations of selected peptoids showing cell surface damage and/or pore formation, which is consistent with the proposed mode of action against the membrane.[1,2]

A lysine-peptoid hybrid, **328** shown in **Figure 5.1**, has been shown to inhibit DNA replication and induce the SOS response in *S. aureus*[*] leading to inhibition of cell growth.[3] In a separate study with *S. aureus*, peptides substituted with *N*Lys monomers have been shown to cause a much weaker membrane depolarisation compared to parent peptides that cause significant depolarisation of the cell membrane at their MIC. This suggests that the antibacterial action of these peptide-peptoid hybrids is probably not due to disruption of the bacterial cytoplasmic membrane, but perhaps inhibition of intracellular components.[4,5]

Short fluorescently-tagged cell penetrating peptoids (**329** and **330** in **Figure 5.1** are examples) have also been shown specifically target cellular organelles such as mitochondria, nuclei or endosomes.[6] Although the cell penetrating peptoids are much shorter than the typical antimicrobial sequences and the hybrid compounds have greater

---

[*] The SOS response is triggered following DNA damage to a cell. As part of the response the cell cycle is arrested and DNA repair and mutagenesis processes are activated.[3]

peptide character, it is therefore probable that peptoids could be directed towards an intracellular target, in addition to the cell membrane.
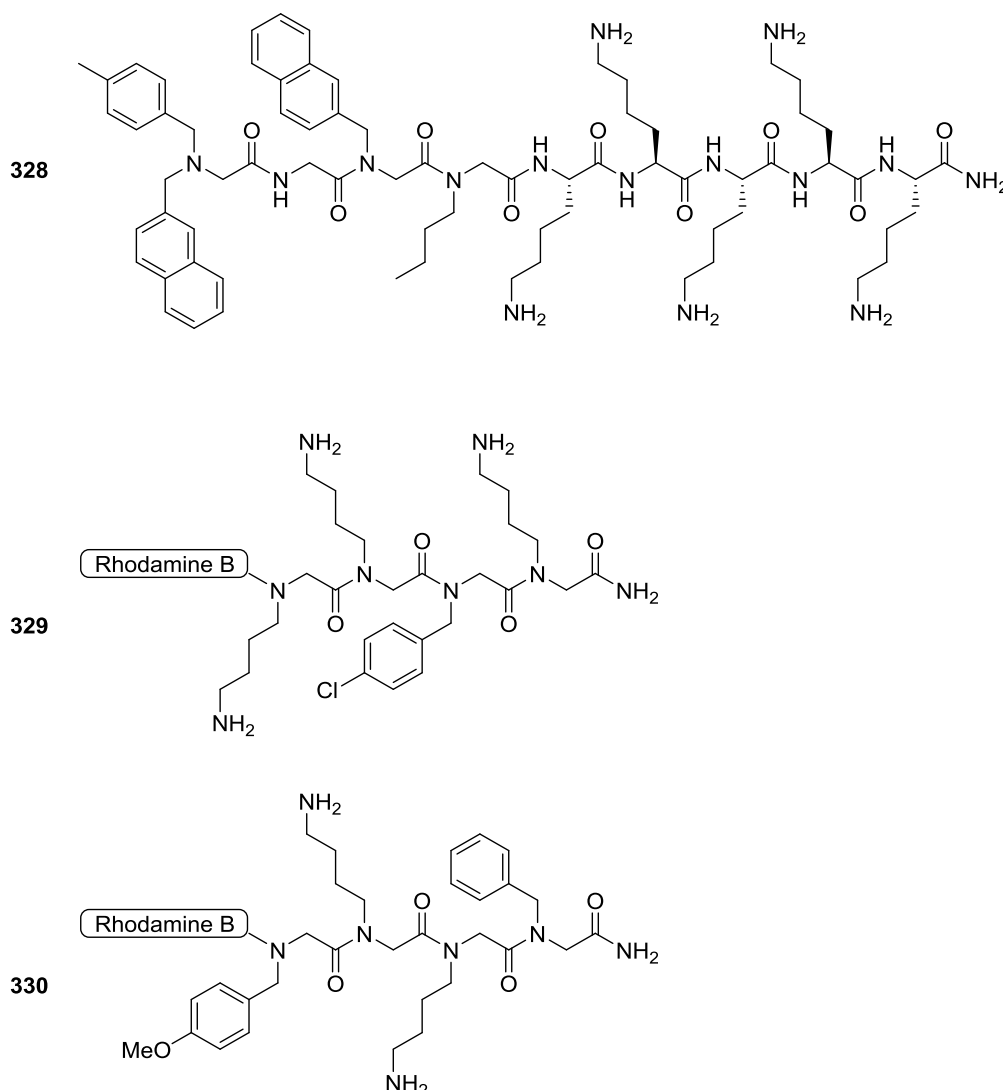
Figure 5.1. Chemical structure of the lysine-peptoid hybrid, **328** and two fluorescently-tagged cell-penetrating peptoids, **329** and **330**, that target mitochondria and endosomes respectively.[4-6]

This chapter describes several investigations into peptoid mode of action and an attempt to develop methods that may assist in the rational design of antimicrobial peptoids. With the data set obtained from the antibacterial MIC determination, a correlation between activity, toxicity and hydrophobicity was undertaken in section 5.1 to examine how these parameters affect the selectivity of peptoids and in an attempt to address the challenge of host-cell toxicity. Following on from issues highlighted, a detailed study into the hydrophobicity of peptoid sequences via partitioning experiments is described in section 5.2. Finally, given the inconclusive evidence in the literature, fluorescent microscopy is used in section 5.3 to probe the biological mode of action of the particular peptoid sequences synthesised as part of this project.

5.1 Further exploration of peptoid antimicrobial activity and toxicity

In Chapters 3 and 4, an antimicrobial peptoid library was screened to explore the structure-activity relationships against protozoa, bacteria and fungi. The selectivity indices of the peptoids were also determined to help to evaluate the true potential of peptoids as novel anti-infective compounds. However, it was shown that many potent sequences also displayed significant host-cell toxicity or hemolytic activity (Chapter 3). In order to progress the clinical development of peptoids, a more detailed understanding of their toxicity must be established.

From the data in section 4.1 (antibacterial MIC determination), many promising peptoids were identified that showed little or no toxicity to either of the mammalian cell lines tested. For example, compounds such as **180** (*NaeNpheNphe*)$_4$, **226** (*NLysNpfbNpfb*)$_3$ and **157** [(*NLysNpfbNpfb*)(*NLysNspeNspe*)]$_2$ display negligible toxicity to HaCaT or HepG2 at the highest concentrations tested and are also broad spectrum antibacterial agents. However, many sequences did display significant toxicity to mammalian cells, and in general these compounds were similarly toxic to both HaCaT and HepG2. On the whole, as the antimicrobial action of a compound increases, the associated toxicity is also increased. This is a problem found in other recent studies that focus on the biological applications of peptoids, however often attention is not directed towards the issue of toxicity.[7-9]

Many assessments of peptoid toxicity currently reported in the literature have been evaluated by hemolytic activity, however these assays cannot necessarily be accurately used to predict toxicity more generally against mammalian cells. For example, many peptoids in the literature are based upon peptoid **22** (*NLysNspeNspe*)$_4$ which exhibits excellent antimicrobial properties, with a reported selectivity ratio of > 6 and acceptable 50 % hemolytic dose (HD$_{50}$ of 100 µM).[10] However, in toxicity screening undertaken as part of this project, peptoid **22** was found to have ED$_{50}$ of 20 µM and 29 µM against HaCaT and HepG2 respectively.[11] More recently, other research groups have carried out *in vitro* mammalian assays and seen toxicity of peptoid **22** at 5.1 µM against NIH-3T3 murine fibroblast cells.[9] Therefore, there is a clear need to scrutinise the relationship between peptoid antimicrobial activity and toxicity towards mammalian cells in greater detail.

5.1.1 Correlations between antibacterial activity, toxicity and hydrophobicity

The selectivity of sequences was highlighted as a particular challenge for the design of antimicrobial peptoids in Chapters 3 and 4. To explore the relationship between activity, and toxicity a comparison was made between the MIC values gathered in Chapter 4.1 against each bacterial species against the average toxicity of each peptoid to HaCaT and HepG2 (shown in **Figure 5.2**).
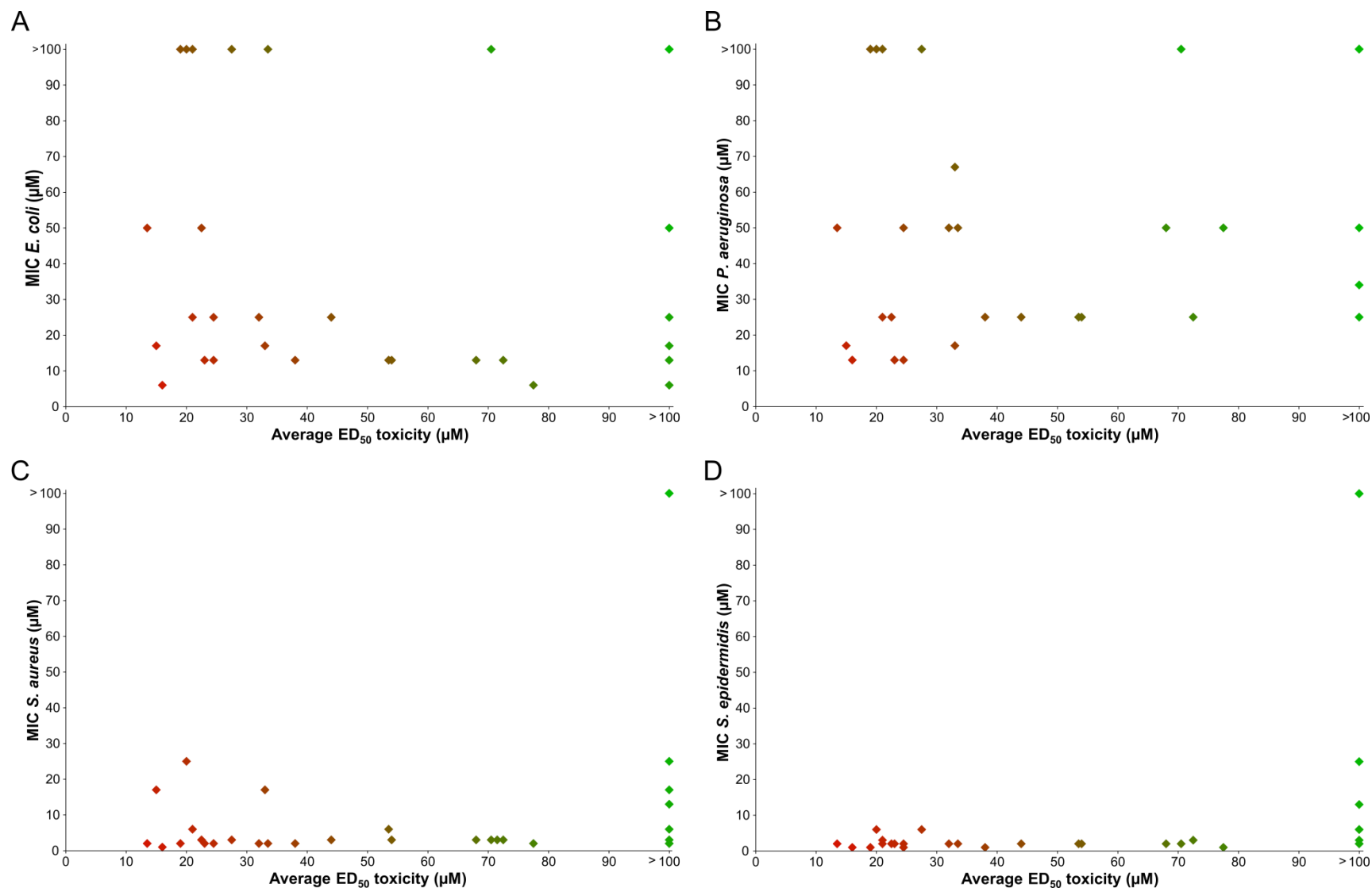
Figure 5.2. Correlations antibacterial activity of compounds with the average toxicity to mammalian cell lines (averaged for HaCaT and HepG2) where; **A** *E. coli*; **B** *P. aeruginosa*; **C** *S. aureus*; **D** *S. epidermidis*. Multiple compounds had MIC > 100 μM and ED_{50} > 100 μM. Compounds indicated in green show activity against prokaryotes or less toxicity to eukaryotes, those in red show increased toxicity to mammalian cells and/or weaker activity against the bacteria.

The data in **Figure 5.2** shows that a handful of peptoids have been identified that show respectable antibacterial activity and also display low toxicity to mammalian cells (i.e. compounds indicated in green on the bottom right hand quadrant of each graph in **Figure 5.2**). These compounds have the potential to be future selective antibiotic compounds. However, a large proportion of the peptoids within this library do display significant toxicity (those indicated in red to the left hand side of each graph). There are also many sequences that are toxic to the mammalian cells, but show little activity against Gram negative bacteria. It is likely that the external lipopolysaccharide layer on the outer cell membranes of *E. coli* and *P. aeruginosa* (absent in Gram positive bacteria) prevents these peptoids from reaching the cell membrane. To investigate a possible explanation for this observation, the hydrophobicity of the compounds was considered.

In Chapters 3 and 4, hydrophobicity was shown to be an important characteristic of peptoids, so to examine the relationship between hydrophobicity and the activity or toxicity of peptoids, retention times of the library were assessed using analytical reverse-phase HPLC. Although this approach can only provide a relatively crude measure of hydrophobicity and will not translate into predictions about how a compound will interact with the cell membranes of biological systems, certain interesting trends were evident.

The correlation of peptoid antibacterial activity against the HPLC retention times is shown in **Figure 5.3**. Since the activity of peptoids is much greater against Gram positive bacteria than Gram negative bacteria, the graphs are predominantly populated by peptoids for *E. coli* and *P. aeruginosa* due to their higher MIC values. There appears to be a linear relationship between activity and retention time for the Gram positive bacteria, where the peptoids at longer retention times (therefore more hydrophobic) have the lowest MIC values against *S. aureus* or *S. epidermidis*.

However, for the Gram negative bacteria, there is no clear correlation between hydrophobicity and activity of the peptoid library. Some compounds with the longest retention times (presumably the most hydrophobic) are inactive against these bacteria, whereas others with shorter retention times display good activity. It has previously been suggested that highly hydrophobic sequences may have lower activities due to self-association that prevents full contact with the cell membrane.[7] However, this may be an overly simplistic explanation as the same is not seen against Gram positive bacteria, where the same hydrophobic peptoid sequences result in low MIC values.

The conclusion that peptoids with high hydrophobicity do not always appear as the most potent hits against *E. coli* and *P. aeruginosa*, but against *S. aureus* a linear relationship is seen between hydrophobicity and activity, has been corroborated by one recent report in the literature.[7]
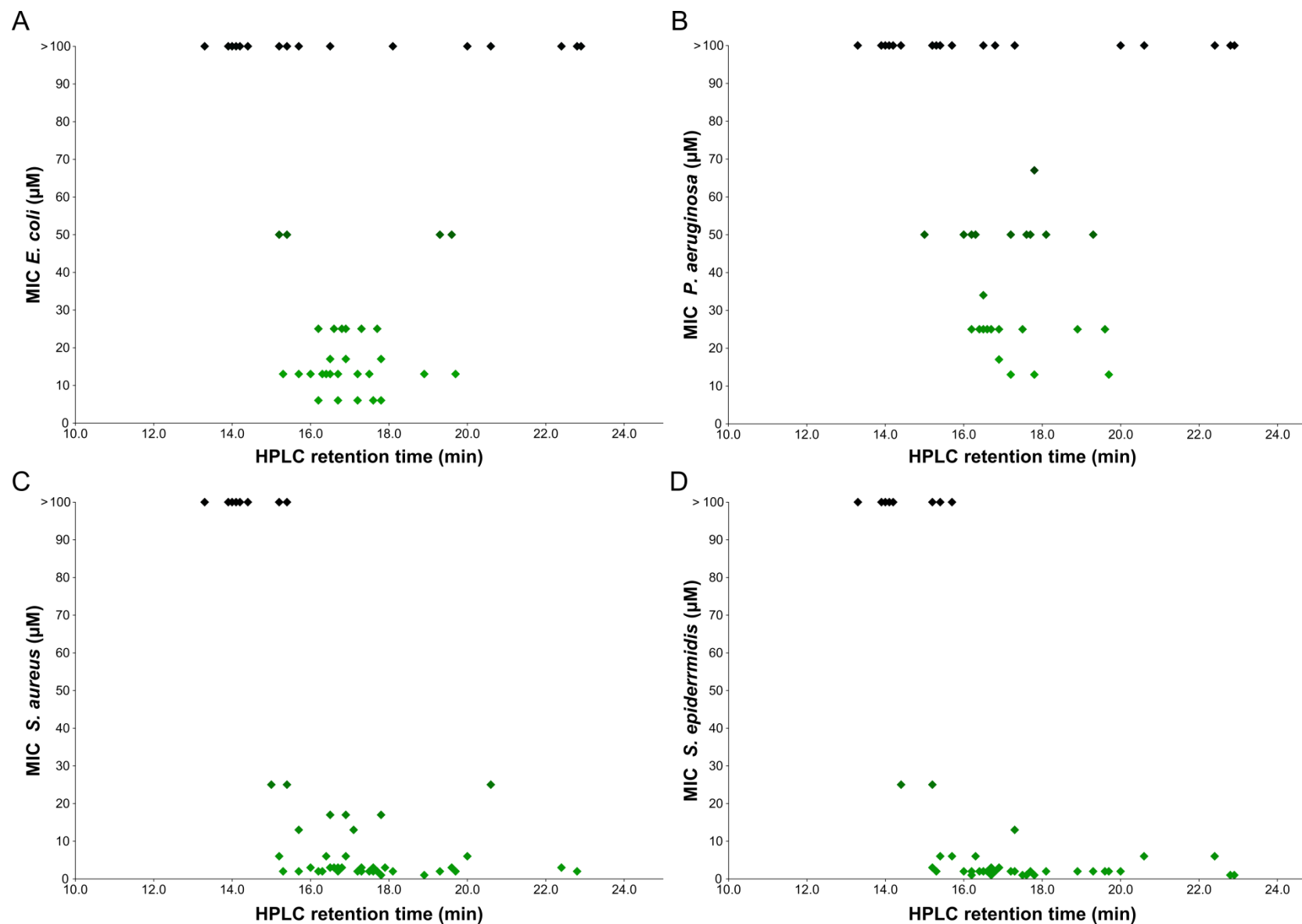
Figure 5.3. Antibacterial activity of compounds plotted against the HPLC retention times where; **A** *E. coli*; **B** *P. aeruginosa*; **C** *S. aureus*; **D** for *S. epidermidis*. HPLC gradient from 0–100 % B over 30 minutes, column oven at 40 ˚C, where solvent A = 95% H2O, 5% MeCN, 0.1% TFA; solvent B = 95% MeCN, 5% H2O, 0.1% TFA. Peptoids shown in green show antibacterial activity, those in black have negligible activity.

When comparing the toxicity of the peptoid library (via mammalian ED_{50} values) to the HPLC derived retention times, there is a linear relationship between toxicity and hydrophobicity (see **Figure 5.4**). A similar profile of toxicity is seen for both HaCaT and HepG2 cell lines and the least hydrophobic compounds tend to be the least toxic, with those at highest retention times showing the lowest ED_{50} values.

Figure 5.4. Average peptoid toxicity (values for HaCaT and HepG2 averaged) plotted against their retention time, obtained via analytical RP-HPLC; HPLC gradient from 0–100 % B over 30 minutes, column oven at 40 ˚C, where solvent A = 95 % H2O, 5 % MeCN, 0.1 % TFA; solvent B = 95 % MeCN, 5 % H2O, 0.1 % TFA. Compounds indicated by green show negligible toxicity, those in red show toxicity to the mammalian cells.

In the literature, HPLC retention times are used to rationalise antimicrobial activity[7,10,12] and also in *in silico* predictions of activity.[9] From the data presented, it is suggested that HPLC retention time alone cannot estimate or rationalise activity. For Gram negative bacteria, HPLC retention time is not predictive of activity and although peptoids with longer retention times may have an increased efficacy against Gram positive bacteria, these compounds may also have a concomitant and undesirable increased toxicity.

This emphasises the need for the community to develop extra tools to predict and understand peptoid activities. Other parameters to evaluate the activity of antimicrobial peptiods and guide the design of bioactive peptoids need to be considered. In an attempt to rationalise the activity of the library a detailed investigation into the hydrophobicity of the peptoids using partitioning experiments was undertaken and this is described in section 5.2.1.

5.1.2   *In vivo* peptoid toxicity using a *Galleria mellonella* model

Testing was carried out at Queens University, Belfast by Dr Yu Luo (postdoctoral research assistant), under the supervision of Dr Fionnuala Lundy.

Once a compound has shown to be effective in *in vitro* models, such as those described in Chapters 3 and 4, its efficacy is typically evaluated in an animal model. However, there are significant ethical considerations before mammalian models can be used and these are often expensive and time consuming. Therefore, ethically more acceptable invertebrate models are being used increasingly. Insects have a complex innate immune system similar to mammals, for example many species produce small antibacterial peptides and such insect models have provided useful tools for investigation into the pathogenesis of a wide range of microbial infections. One such model uses the larvae of the greater wax moth, *Galleria mellonella* which provides a reliable investigation into compound toxicity and efficacy *in vivo* and is an inexpensive and rapid alternative to the use of animal models.[13,14]

A small selection of peptoids were tested against *G. mellonella* via a direct injection of 100 μM peptoid solution through the cuticle and the number of larvae alive after 72 hours treatment time were counted to assess the toxicity of peptoids *in vivo*. Photographs showing larvae following treatment by peptoids and positive and negative controls are shown in **Figure 5.5**. The results obtained for other compounds are recorded in **Table 5.1** and show that none of the peptoid sequences were toxic in the *Galleria* model; all larvae treated are still alive after 72 hours treatment.
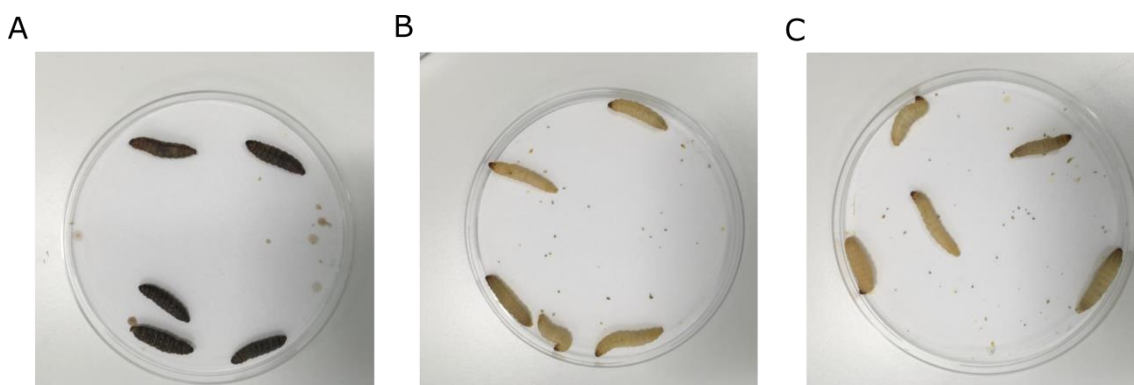
Figure 5.5. Investigation of *in vivo* peptoid toxicity using a *Galleria mellonella* model. **A** positive control, *G. mellonella* injected with 20 μL *E. coli* (10^8 colony forming units mL^{-1}) causing death of 5/5; **B** negative control, *G. mellonella* injected with 20 μL PBS, 5/5 alive; **C** *G. mellonella* treated with 20 μL of 100 μM peptoid **186**, 5/5 alive after 72 hours treatment.

Treatment	Toxicity to *G. mellonella* (no larvae alive/5)	ED$_{50}$ HaCaT (µM)
E. coli	0	*nd*
PBS	5	> 100
186 (*N*Lys*N*phe*N*phe)$_4$	5	36
182 (*N*Lys*N*hLeu*N*spe)$_4$	5	> 100
293 (*N*hArg*N*phe*N*phe)$_4$	5	> 100
181 (*N*hArg*N*hLeu*N*phe)$_4$	5	28
149 (*N*Lys*N*spe*N*spe)(*N*hArg*N*spe*N*spe)(*N*Lys*N*spe*N*spe)$_2$	5	33

Table 5.1. Effect of 72 h peptoid treatment (20 µL, 100 µM sample) on *G. mellonella*. 5 moth larvae were treated for each sample and for all peptoids 5/5 larvae were alive following 72 h treatment. The ED$_{50}$ against HaCaT is shown for comparison.

Through this simple *G. mellonella* model, it has been shown that peptoids have low *in vivo* toxicity to the larvae. Interestingly, although none of the peptoids caused death to the moth larvae, several of the peptoids showed moderate toxicity to HaCaT keratinocytes at concentrations much lower than the 100 µM treatment used in the *G. mellonella* assay (see **Table 5.1**). This work is, to the best knowledge, one of the first studies carried out to evaluate the *in vivo* toxicity of peptoids and shows that toxicity considerations are a complex issue and the need for system specific evaluation.

5.2   Investigation of peptoid secondary structure

This work was carried out in collaboration with Dr Beth Bromley and students (Durham University, Physics Department). All compounds were designed, synthesised, and purified by HLB and their biophysical properties investigated by Charlotte Williams (MPhys student) and Dr Lara Small (Postdoctoral Research Assistant).

5.2.1 Hydrophobicity as a predictive tool in the rational design of bioactive peptoids

In nature, systems that have efficient and specific functions are often accompanied by well-defined structures that support their applications. Within the field of biochemistry, proteins are a perfect example. The knowledge of how a sequence determines its fully folded structure is key to the *de novo* design of such molecules and the ability to synthesise stable folded compounds is key for a wide variety of applications from drug discovery to the development of new materials.

Natural proteins and peptides explore a variety of conformational states from fully stabilised to unfolded global structures; peptoids are no different. Peptoids have already been shown to adopt stable and well defined folds in solution, such as the peptoid helix[10,15-17] or peptoid nanosheets[18-20], as in Chapter 2. Unlike peptides where regular backbone hydrogen bonding helps to stabilise the secondary structures adopted, peptoids typically rely upon the local steric[17,21] or electronic effects[22-24] of side chains to help stabilise any secondary structures formed. The positioning of the side chains on the nitrogen of the amide (as opposed to the α-carbon) also renders the backbones of peptoid sequences achiral and the tertiary amides are more easily isomerised between *cis* and *trans* conformations than the secondary amides of a peptide. As discussed in Chapter 2, this means that the secondary structures adopted by peptoids are influenced heavily by the choice of side-chains. Peptoids that contain chiral monomers (e.g. *N*spe) often have helical structures, with a range of different circular dichroism (CD) spectra that are dependent on the side chains used. The chemistry of such structures is well established and these helical states show excellent stability to chemical and thermal denaturation. As shown in previous chapters, this has enabled chemists to design helical peptoids with specific functions as it is possible to predict which sequences will form stable helices in solution, for example the antimicrobial peptide mimics in the literature and Chapters 3 and 4.[7,10-12,25]

Additionally, classification of the hydrophobicity of a compound is often extremely useful in the prediction of drug efficacy in small molecule drug development. Knowledge of such physiochemical properties at an early stage of compound development can help in assessment of how well a potential drug can cross biological membranes to reach its target *in vivo*. Often values such as log *P* or log *D* values (the partition coefficient for the compound between octanol and water or buffer respectively) are determined for small

molecules, or predicted using a variety of software tools. However log P is not a simple additive property and these predictive programmes can be overly simplistic; other effects such as hydrogen bonding or specific electronic properties all play a part. For larger molecules, including peptoids, where folding is possible, the situation is far more complicated.[26,27]

To date, there have been few studies that link the secondary structure of peptoids with their biophysical properties such as intrinsic hydrophobicity.[28] Knowledge of such parameters would provide very useful tools to rationalise, and potentially predict, the behaviour and/or biological properties of peptoids. Typically, researchers have referred to the reverse-phase HPLC retention times of compounds as a crude measure of average hydrophobicity and it has been suggested that the hydrophobicity of a given peptoid sequence has a large effect on both toxicity and antimicrobial activity.[7,8,10]

However, in sequences where a peptoids global structure is dependent on environment, the hydrophobicity of the folded molecule, may be very different; analogous to the exposed hydrophobic area in a folded protein being very different to that seen in the unfolded state. With few exceptions, using HPLC to predict log P or log D is mostly unsuitable, since properties responsible for retention in chromatography are different to those responsible for partitioning – in particular the contribution from hydrogen bonding. Additionally, our HPLC system has 0.1 % added TFA so retention times are based at pH 2.2 (very different to typical biological systems), whereas the partitioning is carried out in PBS at approximately pH 7.4. Although these pH values are different, basic amino-functionalised side chains typically included in antimicrobial peptoids will be protonated in both cases. However, in other peptoids with acidic side chains or those with a lower pKa, the discrepancy between HPLC pH conditions and partitioning may become more important. We believe that the partitioning experiments will be very useful in these cases, as the hydrophobicity measured from log D values may be more representative of biological conditions.

Therefore, partitioning experiments were carried out on a small peptoid library to compare the hydrophobicity determined from partitioning to their HPLC-derived hydrophobicity and investigate peptoid conformation in solution by CD spectroscopy. The partitioning experiments were carried out to calculate log D values and to provide a measure of the 'folded hydrophobicity'.

The peptoids tested in this study were based upon the simple three-fold repeat motif NxNyNy, previously synthesised for biological testing (see **Table 5.2**); where Nx is a hydrophilic monomer with primary amine functionality, either NLys or Nae; Ny is a hydrophobic residue comprising either Nspe or Nphe. 6, 9 and 12 residue peptoids based on this motif were synthesised to examine the effects of sequence length, chirality and cationic side chain length.
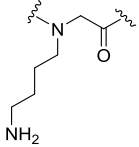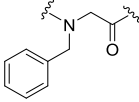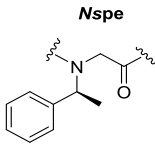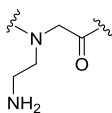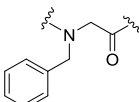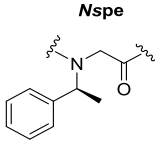
N$_x$	N$_y$	Peptoid	Sequence
*N*Lys	*N*phe	**186**	(*N*Lys*N*phe*N*phe)$_4$
		187	(*N*Lys*N*phe*N*phe)$_3$
		188	(*N*Lys*N*phe*N*phe)$_2$
	*N*spe	**22**	(*N*Lys*N*spe*N*spe)$_4$
		26	(*N*Lys*N*spe*N*spe)$_3$
		25	(*N*Lys*N*spe*N*spe)$_2$
*N*ae	*N*phe	**180**	(*N*ae*N*phe*N*phe)$_4$
		213	(*N*ae*N*phe*N*phe)$_3$
		214	(*N*ae*N*phe*N*phe)$_2$
	*N*spe	**156**	(*N*ae*N*spe*N*spe)$_4$
		218	(*N*ae*N*spe*N*spe)$_3$
		219	(*N*ae*N*spe*N*spe)$_2$

Table 5.2. The peptoids tested in partitioning experiments of differing lengths, containing either chiral (*N*spe) or achiral (*N*phe) residues and containing either shorter (*N*ae) or longer (*N*Lys) positive side chains. All sequences have a C-terminal amide group and N-terminal free amine.

A peptoid solution (between 10 and 100 μM) in PBS was added to octanol and the system allowed to equilibrate under gentle agitation for 150 hours. At this point it is assumed that the peptoid has partitioned between these two phases, such as to minimise its free energy. A combination of UV spectrometry and dynamic light scattering were used to determine that no aggregation was taking place in either phase (data shown in the Appendix). The peptoid concentrations of both phases were then determined using UV-Vis spectroscopy and the logarithm of the ratio of concentration in PBS over concentration in octanol (log *D*) was calculated.

Peptoids with higher hydrophobicity
More soluble in octanol

Peptoids with lower hydrophobicity
More soluble in PBS

octanol

PBS

octanol

PBS

ΔG° (PBS to octanol) < 0
spontaneous forward reaction
log D = negative

ΔG° (PBS to octanol) > 0
spontaneous reverse reaction
log D = positive
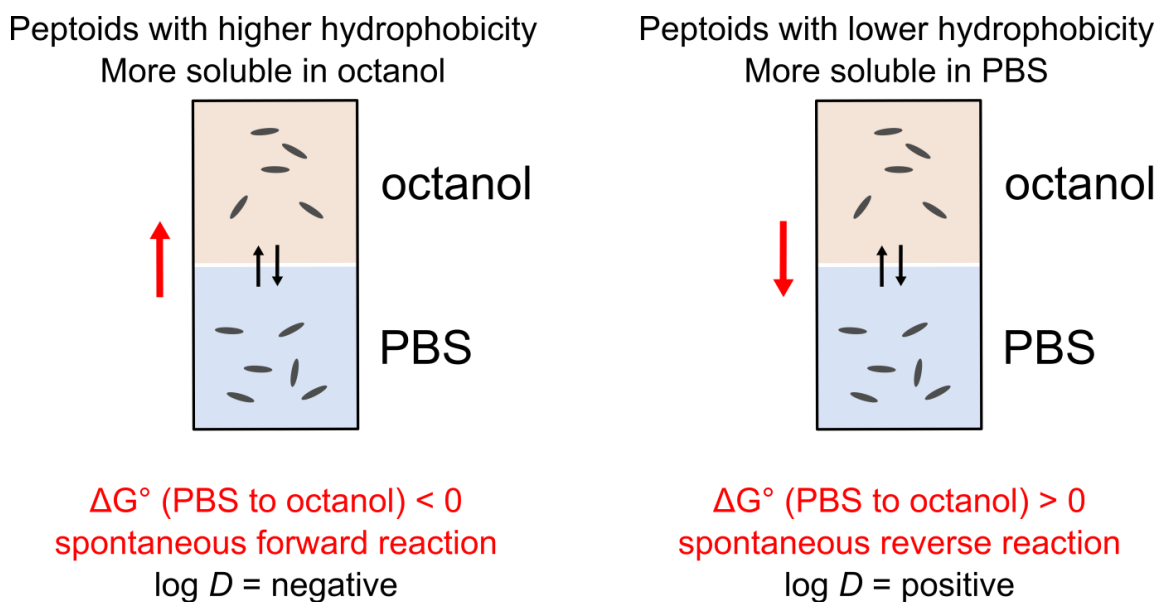
where log D = log ([PBS]/[octanol])

Figure 5.6. Illustration of peptoid partitioning between aqueous (PBS) and organic (octanol). When ΔG˚ < 0, the partitioning is spontaneous with a PBS to octanol transition being favoured. The more negative ΔG˚, the more hydrophobic peptoid; when ΔG˚ > 0, the reaction is not spontaneous and the reverse reaction (octanol to PBS) is favoured and peptoids largely remain in the PBS phase.

It has already been highlighted that reverse phase HPLC retention times of compounds are used as a crude measure of average hydrophobicity to rationalise behaviour (for example, antibacterial properties).[7,9,10] The HPLC retention times for the compounds tested in **Figure 5.7A** indicate that the peptoids become more hydrophobic as the chain is increased in length. There is also an increase in hydrophobicity caused by switching from the achiral *N*phe monomer to the chiral *N*spe monomer, e.g. compare **186** (*N*Lys*N*phe*N*phe)$_4$ and **22** (*N*Lys*N*spe*N*spe)$_4$. It has previously been suggested that this change may be due to the extra α-CH$_3$ group present in *N*spe monomer. However, it may be that this is a too simplistic an explanation given that there is a decrease in the hydrophobicity when the *N*ae monomer is replaced in a sequence by the longer *N*Lys, e.g. peptoids **186** (*N*Lys*N*phe*N*phe)$_4$ and **180** (*N*ae*N*phe*N*phe)$_4$ respectively.

The trends in hydrophobicity observed from analysis of the HPLC retention times are not reproduced in the folded hydrophobicity data collected from the partitioning data. In **Figure 5.7B** it can be seen that the partition coefficients are similar for all peptoids except for the 9 and 12 residue peptoids with the combination of both *N*ae and *N*spe (**156** and **218**). Peptoids **156** (*N*ae*N*spe*N*spe)$_4$ and **218** (*N*ae*N*spe*N*spe)$_3$ are the only peptoids in the library to show significant movement into the hydrophobic phase (e.g. they have negative log D values). It can also be seen from comparison of **156** and **218** that, increasing the sequence length gives rise to an increase in partitioning to the hydrophobic phase (i.e. **156** partitions into the octanol layer more than **218**).

The dramatic differences in the two descriptions of hydrophobicity suggest that the folding of peptoids in both the aqueous and hydrophobic phases is important to their biophysical properties. In particular it is clear that the difference in energy between the folded state adopted in PBS and the folded state adopted in octanol is greater when the peptoid is longer, there are chiral residues present, and the positive side chains are shorter (i.e. *N*ae perfered over *N*Lys).

The conformation of the chiral peptoids in both phases was investigated by circular dichroism (CD). All of the peptoids gave a significant CD signal and hence were found to be adopting helical folded conformations in both PBS and octanol (see **Figure 5.7 C/D**), however, the shapes of the curves suggest different solution conformations. The peptoids in PBS show a change in the shape of the CD spectra as the length increases, perhaps indicating that the lowest energy conformation changes as the peptoid becomes longer. The CD spectra of the peptoids in octanol show a different shape to those in PBS and again exhibits a variation with peptoid length. Again this indicates a difference in the details of the helical structure being adopted.

For the two longest chiral peptoids, **22** [(*N*Lys*N*spe*N*spe)$_4$] and **156** [(*N*ae*N*spe*N*spe)$_4$] there is no difference in the CD spectrum in either PBS or octanol as function of cationic side chain length. The large difference in folded hydrophobicity between these two peptoids must therefore stem from a difference in energy of the same folded state with short (*N*ae) or long (*N*Lys) cationic side chains. It cannot be determined from these data whether the long side chain stabilises the aqueous folded state or destabilised the hydrophobic folded state or if both are occurring. A likely reason for this difference is that the folded conformation may enable increased shielding of the positive charge from the solvent in the short chained case that would be energetically unfavourable in PBS and energetically favourable in octanol.

This difference in energy of the folded state is highly likely to be implicated in difference in the antimicrobial efficacy between these two peptoids. To consider how log D could be used to help rationalise and predict the antimicrobial properties of peptoids, **22** (*N*Lys*N*spe*N*spe)$_4$ and **156** (*N*ae*N*spe*N*spe)$_4$ were selected as they have the same overall net charge (+4) but very different log D values (+1.21 and -1.85). As shown in **Table 5.3**, the HPLC retention time can indeed be potentially predictive of biological activity, for example in the case of the *L. mexicana* amastigotes, where peptoid **156** has a longer HPLC retention time than **22** and greater biological activity (ED$_{50}$ 17 compared to >100 µM).

However, when screening against other microbes which have different membrane compositions, the hydrophobicity as predicted by log D may prove to be more significant in determining the activity. The activity of the peptoids against *E. coli* illustrates this, where Peptoid **156** with the longer retention time is inactive, but **22** has an MIC of 25 µM. These differences in activity cannot be rationalised in terms of HPLC retention time, but the clear difference in the log D values does offer a route by which to probe the link between physical properties and biological activity in more detail.
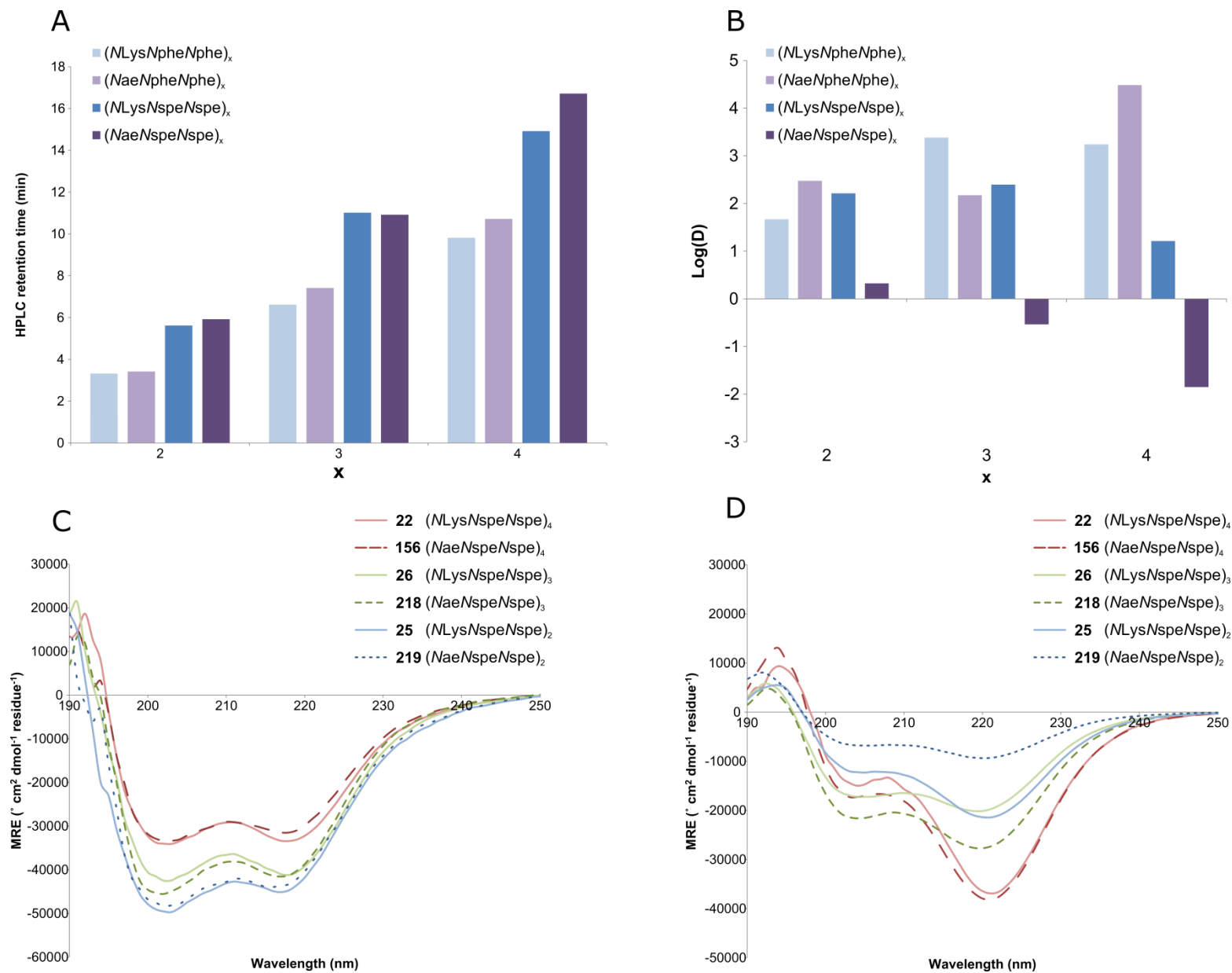
Figure 5.7. A comparison of HPLC and partitioning-derived hydrophobicity for peptoids **186–219**; **A** reverse phase HPLC retention times; **B** log *D* values as calculated from partition experiments. Also, a comparison of CD spectra for all of the chiral peptoids; **C** in PBS; **D** in octanol.

Peptoid	Sequence	ED$_{50}$ (µM)		MIC (µM)		HPLC RT (min)	log D (pH 7.4)
		L. mex promastigotes	*L. mex amastigotes*	*E.coli*	*S. aureus*		
22	(*N*Lys*N*spe*N*spe)$_4$	8	>100	25	2	14.9	1.21
156	(*N*ae*N*spe*N*spe)$_4$	7	17	>100	2	16.7	- 1.85

Table 5.3. A comparison of the biological activity of the peptoids **22** and **156** with the analytical HPLC retention times and log D values at pH 7.4. Gradient: 0–100 % solvent B over 30 min at 220 nm, column oven at 40 ˚C (where solvent A = 95 % H$_2$O, 5 % MeCN 0.1 % TFA; solvent B = 95 % MeCN, 5 % H$_2$O, 0.1 % TFA). All biological screening in triplicate on a minimum of two separate occasions to ensure a robust data set was collected

In conclusion, in this study the hydrophobicity of peptoids that mimic antimicrobial peptides have been measured via partition experiments for the first time. This method produces a measure of the hydrophobicity of the folded state of the peptoids via log D values. Analysis shows that the folding of peptoids can have a significant impact on their biophysical characteristics; in particular their folded hydrophobicity can be significantly different to that measured by HPLC retention time. The partitioning experiments are therefore an important addition to the toolbox for drug efficacy prediction alongside the measures normally used, including measures of average hydrophobicity such as HPLC retention time. The influence of folding on the efficacy of a peptoid as a drug could be profound and here it has been shown that the log D values could be an important additional predictor to use in the rational design of biologically active peptoid sequences in the future.

More work is now being carried out to optimise these partitioning experiments, through use of a NanoDrop spectrophotometer to reduce the volumes necessary and hence amount of peptoid sample needed. This will allow more repeats can be carried out, a reduced equilibration time and the possibility to examine a greater number of compounds in a high throughput process. Using this modified protocol, the Bromley group is now investigating a larger subset of the peptoid library to further probe the potential applications of log D values as a predictive tool to assist with rational design of biologically active peptoids in the future.

5.3 Mode of action studies using confocal fluorescence microscopy

Peptides 342 and 343 synthesised with assistance from Sophia Schwartz (Erasmus student) and microscopy experiments in collaboration with Dr Robek Pal (Durham University, Chemistry department).

Fluorescently labelled molecules are highly useful compounds and can be used, among many other applications, to help determine the mechanism of action of a compound. Using confocal fluorescence microscopy, these fluorescent compounds can be visualised in live cells and organelle specificity examined using one of many commercially available stains in co-localisation experiments.

A number of studies have already performed detailed spectroscopic characterisation of fluorescently labelled peptoids and studied these in cell based microscopy, such as peptoids **329** and **330** (see **Figure 5.1** for structures).[6,29-32] In particular, the Bräse and Schepers groups have used confocal microscopy to investigate the cell penetrating properties of peptoid sequences. In this work it was shown that highly charged peptoids enter the cells by endocytosis and are subsequently released back into the cytoplasm. For peptoids with a higher proportion of hydrophobic residues, localisation is seen in the mitochondria. Amino-functionalised peptoids tend to accumulate in the cytosol, whereas arginine-mimetic peptoids with guanidinium groups collect preferentially in the nucleus.[6,30]

However, the sequences studied in the literature to date tend to be shorter than the most active compounds in our library and our sequences display very different charge to hydrophilic ratio and patterns. As the typical sequences found in our library are both highly charged and have many lipophilic monomers, a series of fluorescence microscopy experiments were planned to determine if our compounds are also transported to specific organelles, which would be a very powerful tool for targeted drug delivery. Determination of where these peptoids localise, whether at the cell membrane or inside specific organelles within the cell, should also enable more detailed information to be gathered about their mechanism of action.

5.3.1 Synthesis of fluorescent compounds

There are thousands of commercially available dyes available to add to compounds. The existing library is vast, covering wide emission wavelengths with dyes of diverse structures, chemical functionality and provide a range of photophysical properties. Some of the most commonly used fluorophores are those structurally related to fluorescein, i.e. compounds **331–333 Figure 5.8.**

331
Fluorescein
λ_{ex} 490 nm, λ_{em} 514 nm

332
5(6) - carboxyfluorescein
λ_{ex} 492 nm, λ_{em} 517 nm

333
Rhodamine B
λ_{ex} 553 nm, λ_{em} 627 nm
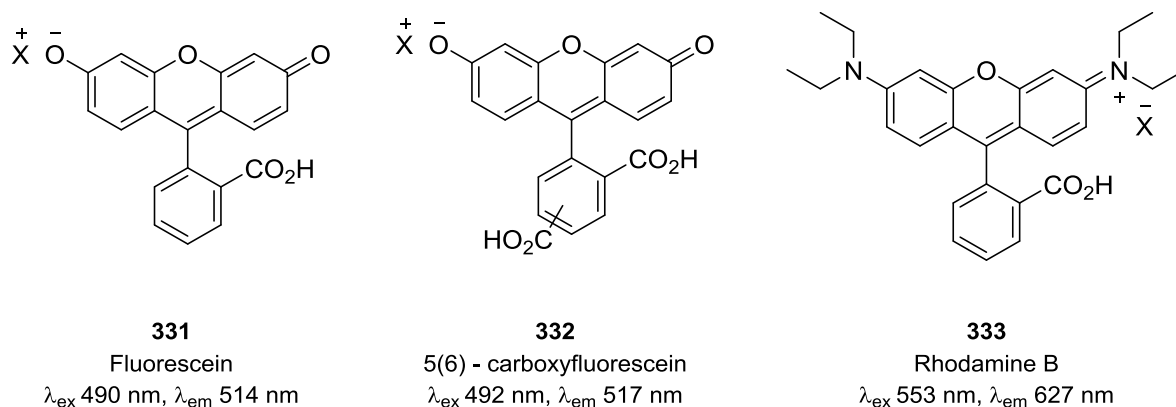
Figure 5.8. Chemical structure of two fluorescein fluorophores and rhodamine B, with corresponding photophysical properties.

A small selection of peptoids were tagged with fluorescein (see **Table 5.5** for a list of the sequences), including those that were biologically active and those with no activity in order to gather mechanistic information. Two peptides sequences from the temporin family of AMPs, were also synthesised and tagged for comparison. Both peptides and peptoids were synthesised on Rink Amide resin and a glycine spacer was added between the sequence and the fluorophore using manual SPPS. Fluorescein was chosen as a dye due to its biocompatibility, low cost and chemical stability under a variety of conditions.

The addition of fluorescein to the peptide/peptoid sequences is straightforward as commercially available fluorescein exists with a free carboxy group, so a simple amide bond formation reaction is sufficient to add the dye to a sequence. For peptoids, standard fluorescein (**331**) dye was used, for the peptides, 5(6)-carboxyfluorescein was used (**332**) due to availability in the lab at this stage of synthesis. Both fluorescein dyes are very similar, with comparable wavelengths for excitation and emission, as shown in **Figure 5.8**, therefore comparisons should be able to be drawn between these compounds.
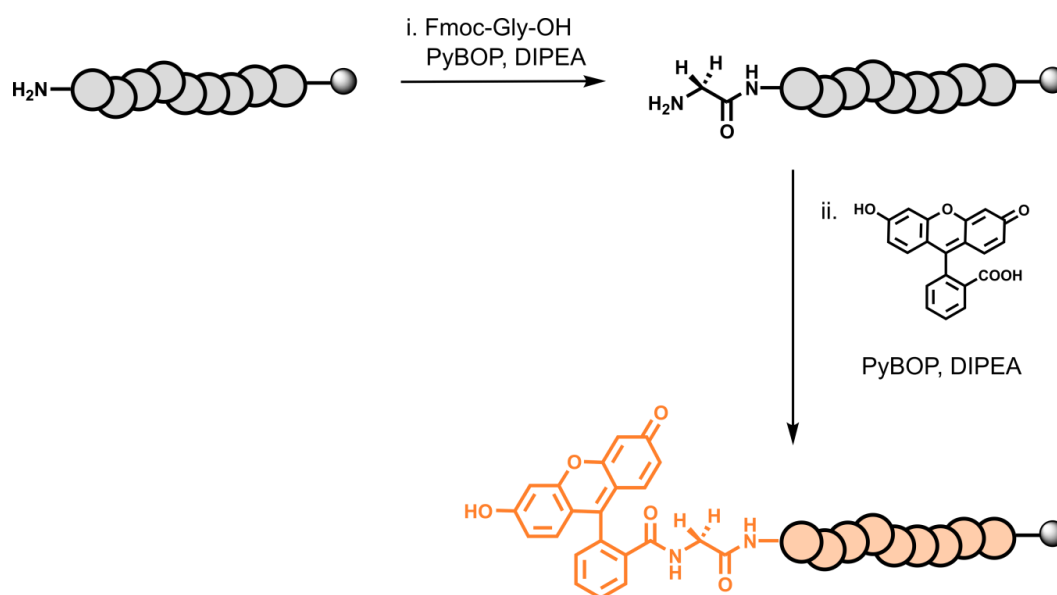
Scheme 5.1. Synthesis of fluorescein-tagged peptoid sequences for microscopy; i. Addition of glycine spacer using standard SPPS; ii. fluorescein coupling using activating agents to form fluorescent sequence. A similar pathway follows for the peptides but with 5(6)-carboxyfluorscein and different activating agents, as explained below.

All fluorescein additions were made manually. For peptoids, PyBOP was used as an activating agent in combination with DIPEA. For the temporin peptides, a few different conditions were trialled since those used to add fluorescein to the peptoids failed. These conditions are summarised in **Table 5.4** and for the peptides, the only successful coupling conditions where the target mass was seen from a test cleave was condition 4, using DIC/HOBt activation. It is suggested that aggregation of the temporin peptides on resin caused these difficulties and that use of the sterically less bulky activating agent DIC was able to overcome the problematic aggregation.[33]

Conditions		Dye	Activator	Conditions	Target *m/z* by LC-MS
Peptoids	1	Fluorescein	4 eq PyBOP 4 eq DIPEA	1 hour, RT	☑

Peptides	1	5(6)-carboxyfluorescein	4 eq PyBOP 4 eq DIPEA	1 hour, RT	☒
	2	5(6)-carboxyfluorescein	4 eq PyBOP 4 eq DIPEA	1 hour, RT Double coupling	☒
	3	5(6)-carboxyfluorescein	1.1 eq HATU 1.1. eq DIPEA	1 hour, RT	☒
	4	5(6)-carboxyfluorescein	1.1 eq DIC 1.1 eq HOBt	1 hour, RT	☑

Table 5.4. Summary of conditions used for the manual coupling of fluorescein to peptoid and peptide sequences.

Table 5.5 shows the sequences that were successfully fluorescently labelled. Following the addition of dye to the peptides and peptoids, compounds were cleaved from the resin and purified by RP-HPLC to > 95 % purity for use in the microscopy experiments (see **Figure 5.9**).

	Sequence
334	Fluorescein-G-(*N*Lys*N*spe*N*spe)$_2$
335	Fluorescein-G-(*N*Lys*N*spe*N*spe)$_4$
336	Fluorescein-G-(*N*ae*N*spe*N*spe)$_4$
337	Fluorescein-G-(*N*Lys*N*phe*N*phe)$_4$
338	Fluorescein-G-(*N*Lys*N*hLeu*N*spe)$_4$
339	Fluorescein-G-(*N*Lys*N*nVal*N*spe)$_4$
340	Fluorescein-G-[(*N*amy*N*spe*N*spe)(*N*Lys*N*spe*N*spe)]$_2$
341	Fluorescein-G-[(*N*Lys*N*pfb*N*pfb)(*N*Lys*N*spe*N*spe)]$_2$
342	5(6)-carboxyfluorescein-FLPLIGRVLSGIL-NH$_2$ *(Temporin A)*
343	5(6)-carboxyfluorescein-GLLPIVGNLLKSLL-NH$_2$ *(Temporin B)*

Table 5.5. The fluorescent peptoid and peptides synthesised for microscopy.
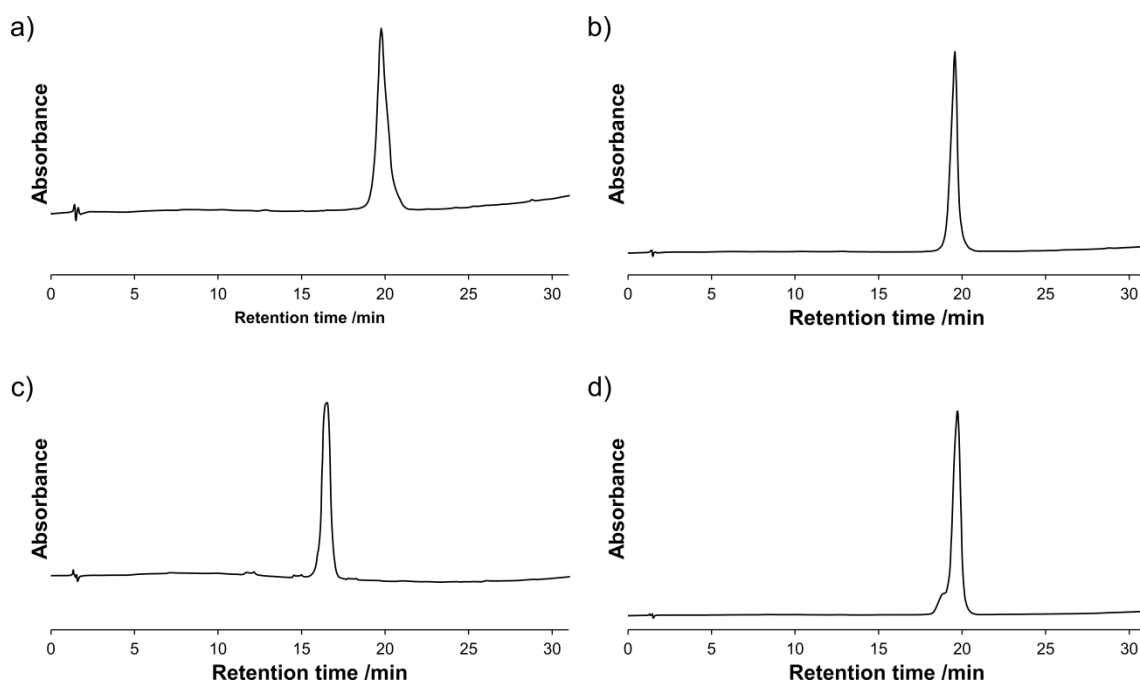

Figure 5.9. Analytical RP-HPLC chromatograms for selected fluorescently labelled peptoids; a) **335**; b) **341**; c) **339**; d) **338**. Gradient 0–100 % solvent B (solvent A = 95 % H$_2$O, 5 % MeCN, 0.1 % TFA; solvent B = 95 % MeCN, 5 % H$_2$O, 0.1 % TFA); column oven at 40 °C; λ = 220 nm.

5.3.2   Confocal fluorescent microscopy and co-localisation experiments

In a series of preliminary experiments, the interactions between fluorescently labelled peptoid sequences **334** and **335** and mammalian cells were investigated using confocal fluorescent microscopy.[†] The two fluorescein-tagged peptide sequences, **342** and **343**, were also studied to provide a comparison with known AMPs.

Two cell lines were chosen for live imaging; NIH-3T3 murine fibroblasts and PC3 human prostate cancer cells derived from bone metastases. Different incubation conditions were used and the addition of commercially available cell stains addressed several questions relating to the mode of action of these compounds. For example, the concentration and time dependence of uptake into the cell, whether compounds were taken up via an active or passive transport process and the site(s) of compound localisation within the cell (see **Figure 5.10** for a diagram of the cell and possible organelles in which compounds may accumulate).
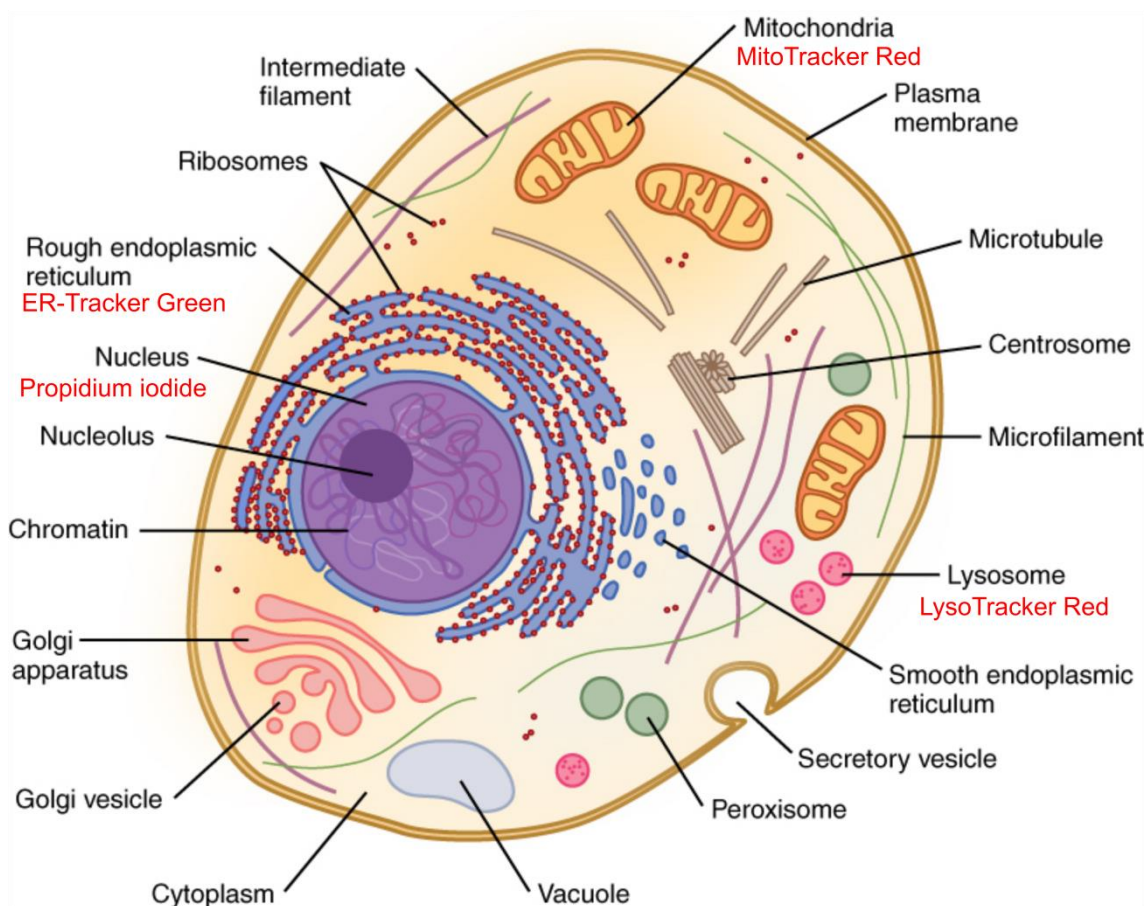
Figure 5.10. A diagram of the complex mammalian cell, to show the different organelles in which a compound may accumulate. For organelles studied in this work, the particular cellular probe used has been labelled.[‡]

[†] **All microscopy images can be found in supplementary information accompanying this report.**

[‡]   Image reproduced from Dr. Duncan Casey, Liverpool John Moores University from http://widnesscibar.blogspot.co.uk/2016/04/single-cell-experiments.html [accessed 21/10/16]

Since the peptide and peptoid sequences were tagged with fluorescein, a green fluorescent dye, orthogonal cell stains from Invitrogen were used. MitoTracker® Red (MTR) is a far red-fluorescent dye and accumulates in the mitochondria of live cells, dependent on membrane potential, ER-Tracker™ Green (ERTG) is a highly selective stain for the endoplasmic reticulum (ER) and LysoTracker® Red (LTR) has very high selectivity for acidic organelles so tends to accumulate in lysosomes.[34-36] Lastly, propidium iodide (PI) was used, which is a red-fluorescent and membrane impermeable dye that is able to stain dead cells by binding to DNA or RNA in non-viable cells.[37]

The conditions used in microscopy experiments with NIH-3T3 cells and the peptoids, **334** and **335**, are summarised in **Table 5.6**. Both peptoids are both based upon compound **22**, the (*N*Lys*N*spe*N*spe)$_x$ motif; where **334** is 6 residues in length and **335** is 12 residues long (i.e. x = 2 and 4 respectively).

Compound	Condition	Time (min)	Concentration (μM)	
	1	15	40	
	2	30	40	
334	*3*	60	40	
	4	120	40	
	5	60	4	
	2	30	40	
	3	60	40	
335	*6*	30	2	
	7	30	2	MTR
	8	30	20	4°C, PI
	9	30	20	MTR

Table 5.6. Time and concentration of peptoids **334** and **335** incubated with NIH-3T3 cells. All incubations were at 37 °C, unless stated. MitoTracker® Red (MTR) and propidium iodide (PI) were also added in conditions *7* and *8*.

Concentration and time dependent uptake of peptoids 334 and 335

To determine the effect of peptoid concentration or incubation time on cellular uptake and the optimum conditions for imaging, conditions *1–5* were trialled. After addition of 40 μM peptoid solution (made in cell media), the cells were incubated between 15 and 120 minutes. For the shorter 6 monomer sequence **334**, after 30 minutes peptoid gathered around the cell membrane but was only detected inside the cells after incubation in excess of 60 minutes. Due to large fluorescence outside the cells the **334** solution was reduced to 4 μM (*condition 5*) and under these conditions, a low amount of green-fluorescence of the peptoid was seen inside the cell, presumably entering via membrane permeabilisation. Microscopy images for these conditions can be found in the Appendix.

The same conditions *1–4* were also applied to **335**, the longer 12 residue peptoid of the same sequence. Compared to **334**, peptoid **335** was able to translocate into the NIH-3T3 cells at a much faster rate. As seen in **Figure 5.11**, a 30 minute incubation was sufficient to see a large amount of green fluorescence from within the cell (*condition 2*). Compound **335** was also significantly more toxic towards the mammalian cells, so a lower concentration (2 µM) was used in *conditions 6–9*. *Condition 6* was determined to be optimal for imaging (2 µM, 30 minute incubation time) and was used to inform the further experiments outlined below.
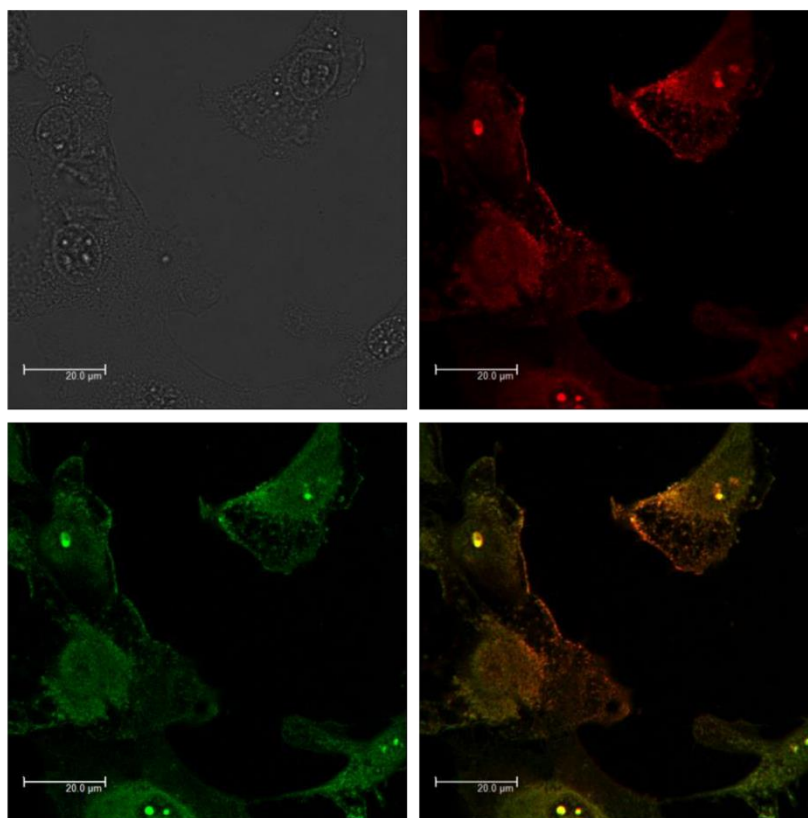

Figure 5.11. Peptoid **335** fluorescein-Gly-(*N*Lys*N*spe*N*spe)$_4$ enters cell following 30 minute incubation of 40 µM **335** with NIH-3T3 cells at 37 ˚C. Showing optical cell images (top left), cell autofluorescence under UV (top right), **335** fluorescence (bottom left), merge (bottom right). Scale bar 20 µm.

Cellular compartmentalisation of peptoid 335

Using the MTR probe (*condition 7*), it was shown that peptoid **335** interacted with and localised in the cellular mitochondria as there is a very good overlay between the peptoid green fluorescence and the MTR detection (see **Figure 5.12C**). Peptoid **335** was shown to diffuse through the outer mitochondrial membrane and then sits in the intermembrane space, with the uptake dependent on an intact mitochondrial membrane potential.[38]
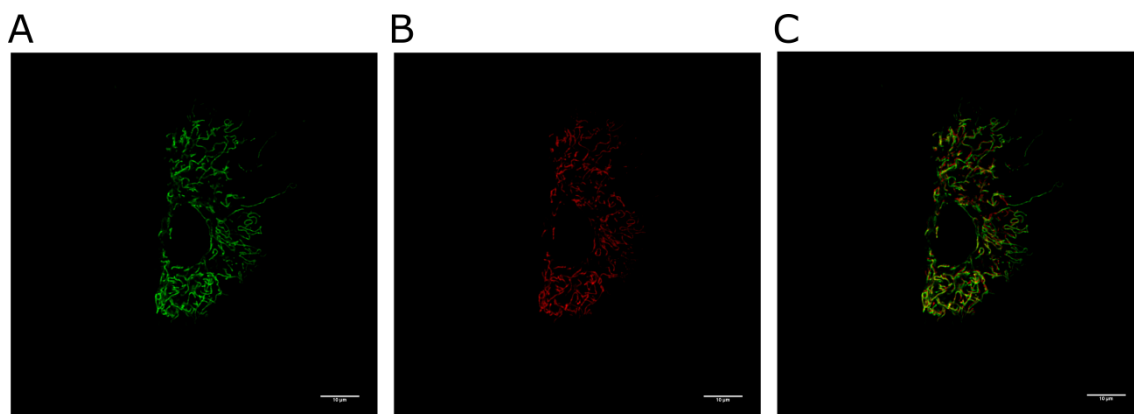
Figure 5.12. Peptoid localisation in mitochondria. Images from incubation of 2 μM peptoid **335** fluorescein-Gly-(*N*Lys*N*spe*N*spe)$_4$ with NIH-3T3 cells and MTR at 37 °C for 30 minutes. Scale bar 10 μm. **A** peptoid **335** fluorescence; **B** MTR fluorescence; **C** merge.

Peptoid 335 enters cells via a passive transport mechanism

In the aforementioned experiments, peptoid **335** was shown to cross the cell membrane and enter cells efficiently. In order to determine whether **335** entered the cell via an active or a passive transport mechanism, peptoids were incubated with NIH-3T3 cells at 4 °C; a lower temperature that should prevent active transport.

As shown in **Figure 5.13B**, peptoid **335** is detected inside cells even with an incubation temperature of 4 °C (*condition 8*) so a passive transport mechanism across the cell is suspected. PI was also added to differentiate between healthy and non-viable cells. Any cell with red fluorescence from PI is assumed to be dead, with a compromised cell membrane. Although in **Figure 5.13C** PI is seen inside the cells after 4 °C incubation, this occurs during transport of cells from the incubator to the microscope, so cannot infer anything about the mechanism of cell death at this stage.
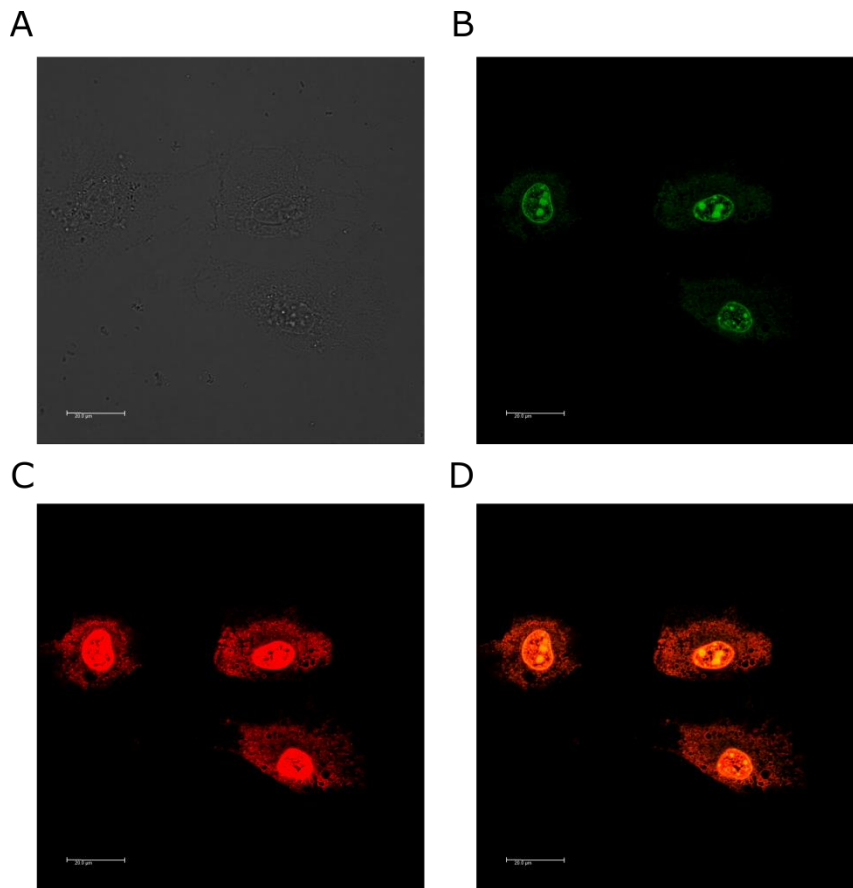
Figure 5.13. Peptoid enters the cell during incubation of 20 μM peptoid **335** fluorescein-Gly-(NLysNspeNspe)$_4$ with NIH-3T3 cells at 4 °C for 30 minutes. PI added immediately before imaging. Scale bar 20 μm. **A** optical image of cells; **B** peptoid **335** fluorescence can be seen inside the cell; **C** propidium iodide fluorescence; **D** merge.

Mode of toxicity for peptoid 335 – apoptotic or necrotic?

Finally, a comparison of the cell morphologies shows that the majority of cells that died during treatment by peptoid **335** under *condition 9* were killed via an apoptotic mechanism. Apoptosis is a regulated process of programmed cell death, whereas necrosis occurs due to accidental cell damage and the two modes of cell death have distinct morphological features. In apoptosis, often membrane blebbing occurs or the formation of membrane bound vesicles without a loss of membrane integrity, a shrinking cytoplasm or condensed cell nucleus and the mitochondria typically become 'leaky'.[39,40] This can be seen in **Figure 5.14** where apoptotic and necrotic cells are compared (necrotic cells **A-D**, apoptotic cells **E-G**).

Only a few cells from those studied were found to be necrotic, where a loss of membrane integrity is seen and typically organelles are seen to swell and ends in total cell lysis.[39,40] This total cell lysis can be seen in image A, where cell efflux is occurring.
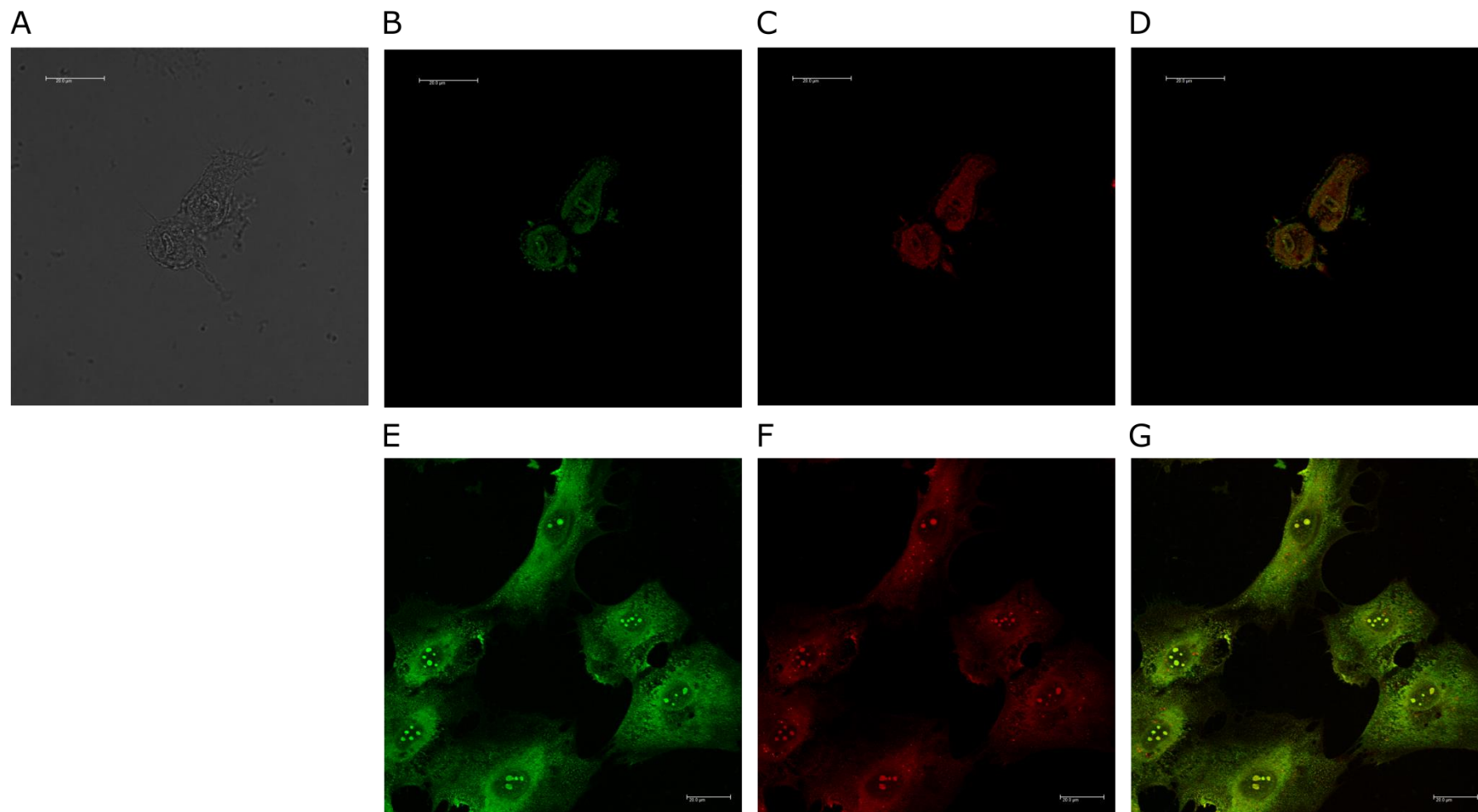
Figure 5.14. Comparison of necrotic and apoptotic cells following incubation of 20 μM peptoid **335** fluorescein-Gly-(*N*Lys*N*spe*N*spe)$_4$ with NIH-3T3 cells and MTR at 37 ˚C for 30 minutes. Scale bar 20 μm. Necrotic cells can be seen in images A-D, apoptotic cells in images E-G. **A** image of cells; **B/E** peptoid **335** fluorescence; **C/F** MTR fluorescence; **D/G** merge.

Similar confocal fluorescence microscopy experiments were undertaken with peptides **342** and **343** and the cell incubation conditions are shown in **Table 5.7**.

Compound	Experiment	Time (min)	Concentration (μM)		Cell
	1	30	20	PI	NIH-3T3
	2	30	20	LTR	NIH-3T3
	3	120	20	LTR	NIH-3T3
	4	24 h	20	LTR	NIH-3T3
342	*5*	30	20	4 °C	NIH-3T3
	6	30	20	LTR	PC3
	7	4 h	20	ERTR	PC3
	8	30	20	ERTR	PC3
	1	30	20	PI	NIH-3T3
	2	30	20	LTR	NIH-3T3
	3	120	20	LTR	NIH-3T3
	4	24 h	20	LTR	NIH-3T3
343	*5*	30	20	4 °C	NIH-3T3
	6	30	20	LTR	PC3
	7	4 h	20	ERTR	PC3
	8	30	20	ERTR	PC3

Table 5.7. Incubation conditions for peptides **342** and **343** with NIH-3T3 or PC3 cells. All incubations were at 37 °C, unless stated. Stains added: ER-Tracker™ Red (ERTR), LysoTracker® Red (LTR), propidium iodide (PI).

Membrane permeability of temporin peptides 342 and 343

To examine the membrane permeability of the temporin peptides, NIH-3T3 cells were first incubated at 37 °C with a 20 μM solution of either **342** or **343** (*condition 1* in **Table 5.7**). Fluorescently labelled temporin A (**342**) was seen around the outer membrane of the cells, and also in lipid droplets indicating surface activity. The peptide fluorescence around the outside of the cell membrane can be seen in **Figure 5.15B**. Exposure of temporin B (**343**) also showed green fluorescence around the cell membrane, with a higher concentration of peptide detected inside the cells (i.e. higher fluorescence intensity). Both **342** and **343** are surface active, causing cell death to a number of cells with the relative proportion of compound found inside the cell correlating with the number of dead cells seen; for temporin A (**342**) approximately 20 % of cells are dead whereas for temporin B (**343**), around 50 % have undergone cell death.[§]

When PI was added immediately before imaging (*condition 1*), PI fluorescence signal was only detected inside a minority of cells showing that the peptides **342** and **343** are not toxic to the mammalian cells under these conditions, unlike the peptoids **334** and **335**.

[§] Cell death estimated by counting cells within a defined field of view.
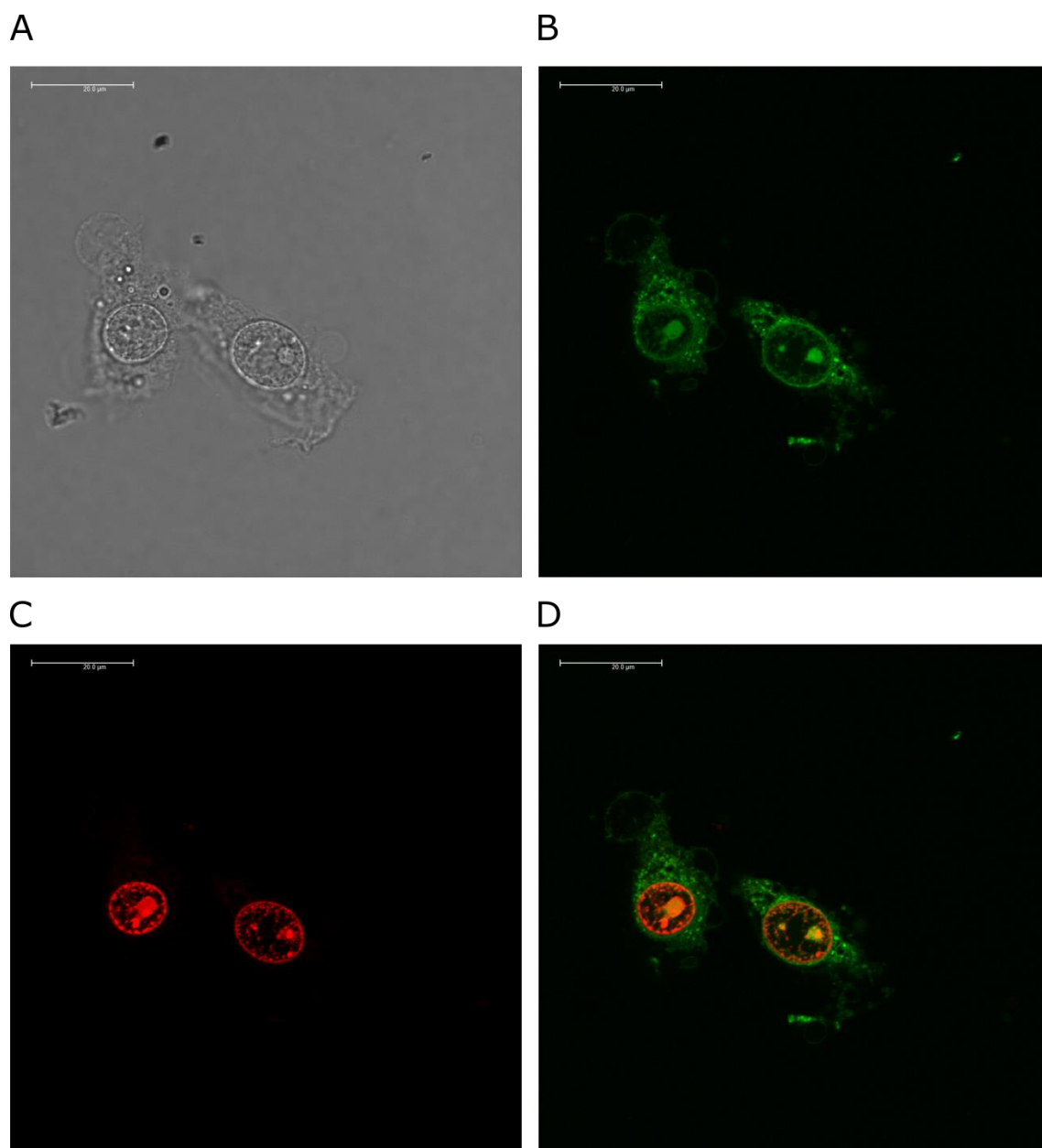
A

B

C

D

Figure 5.15.Temporin A, **342** can be seen to localise around the surface of NIH-3T3 cells following incubation at 37 ˚C with a 20 µM peptide solution and PI for 30 minutes. Scale bar 20 µM. **A** cell image; **B** peptoid fluorescence in green; **C** PI fluorescence in red to show the cell nuclei; **D** merge.

Peptides 342 and 343 enter cells via an active transport mechanism

As with the peptoid sequences, incubation of NIT-3T3 cells with the fluorescently labelled **342** and **343** was undertaken at 4 ˚C (*condition 5*). Since no fluorescence was seen after a 30 minute incubation[**] it is suggested that unlike peptoids **342** and **343**, both peptide **342** and **343** enter the cells via an active transport mechanism. (See Appendix for the image obtained – showing mitochondrial autofluorescence only)

Cellular compartmentalisation of temporin peptides 342 and 343

Since the formation of lipid droplets occurred, LTR was used to determine whether the peptides localised in lysosymes of the NIH-3T3 cells. It is well known that lipid droplets interact with many other structures within the cell to maintain cellular homeostasis so it is possible that the peptides within the droplets interact with other cellular machinery. For example, lipid droplets have been shown to form associations with organelles such as the mitochondria, vacuoles or lysosomes and the endoplasmic reticulum.[41] Therefore LTR and ERTG were deployed to examine possible cellular localisation of **342** and **343**. The LTR is a probe for the acidic lysosomes, which are key for the degradation and recycling of macromolecules in the cell. ERTG is a common tracker for the endoplasmic reticulum, a continuous membrane system made of various domains that perform different functions for the cell such as translocation, folding or modification of proteins.[42,43]

Using *condition 2* with the LTR probe showed no overlay of peptide green fluorescence and the red LTR signal, showing that the peptides do not localise in the lysosymes after a short 30 minute incubation. At longer incubation times (i.e. 120 minutes in *condition 3*), larger lipid droplets were seen and as before, higher concentrations of peptide **343** could be detected inside the cell compared to **342** At the longest incubation time of 24 hours (*condition 4*) an overlay of MTR is seen with the peptide fluorescence. Images to illustrate this are shown in **Figure 5.16** for peptide **343**.

After 24 hour incubation, intracellular **342** fluorescence has an approximate an approximate 40% overlay with LTR and for **343** this overlay increases to around 60 %, suggesting localisation of the compounds in the lysosomes. Imperfect alignment is due to cellular homeostatic movement during the slow scanning of the microscope during image acquisition. In the cells incubated with **342** or **343** for 24 hours, cell death occurred via an apoptotic mechanism, since cell membranes remain intact.

[**] A small amount of peptide fluorescence is seen inside the cell when incubated at 37 ˚C for 30 minutes.
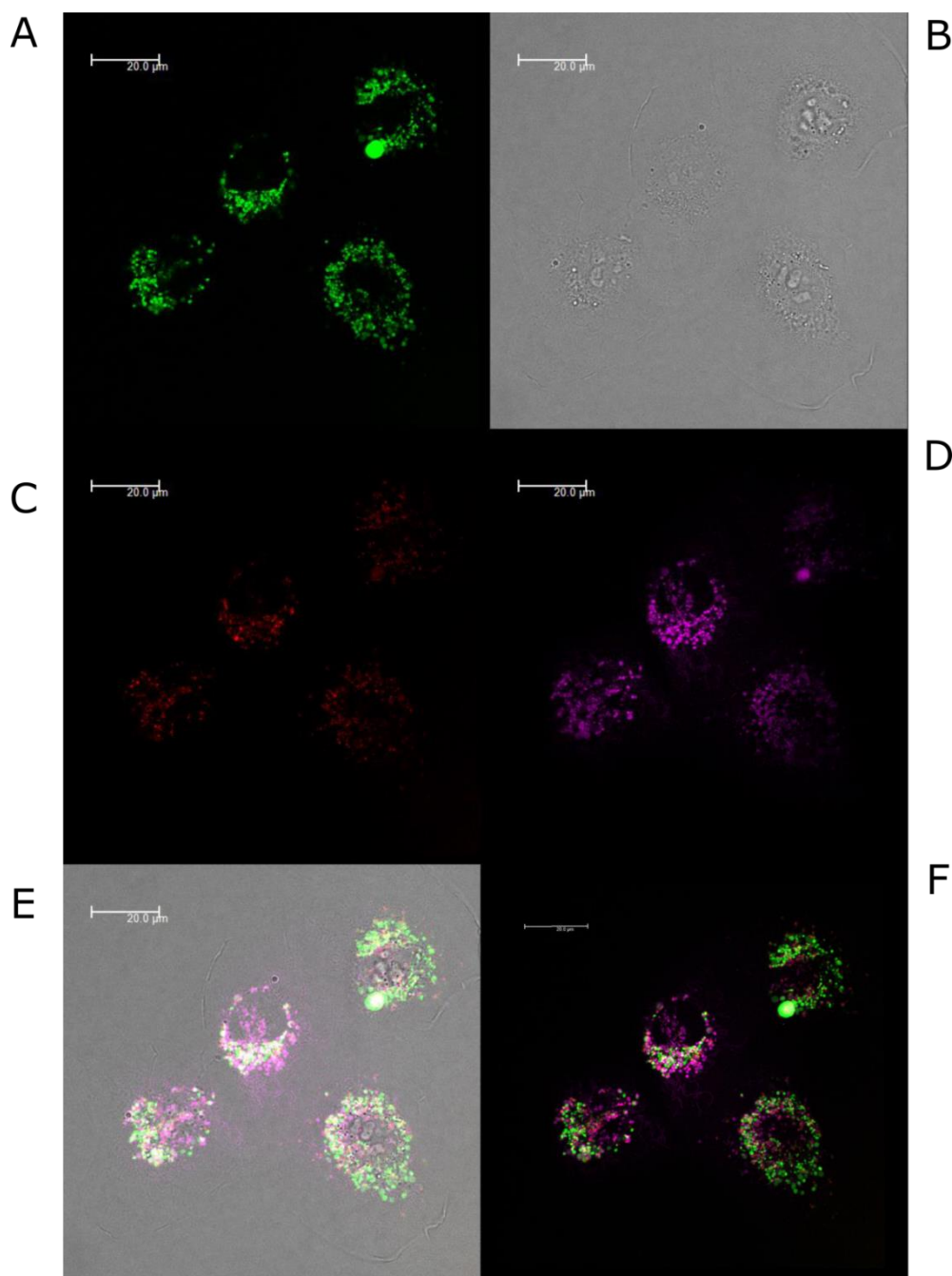
Figure 5.16.Images to show the overlay of peptide **343** fluorescence with LTR after 24 h incubation at 37 ˚C with a 20 μM solution of **343**, LTR and NIH-3T3 cells. Scale bar 20 μm. **A** peptoid fluorescence shown in green; **B** cell image; **C** LTR fluorescence shown in red; **D** mitochondrial autofluorescence shown in pink; **E** merge of A, B, C and D; **F** merge of A, C and D.

To corroborate results in a second cell line, the PC3 cells were used. Again, a partial overlay of LTR and peptide fluorescence is seen for both **342/343** after a 30 minute incubation (*condition 6*) with the PC3 cells. The partial overlay of F9 and LTR can be seen in **Figure 5.17**.

Since the overlay with LTR was not adequate to conclusively confirm that peptides were localising in the acidic lysosymes, ERTG was also used in *conditions* 7 and *8*. Again, partial overlap was seen with the tracker and **342/343**. These images are shown in the Appendix. The formation of lipid droplets within the cells may increase the fluorescently labelled peptide signals in this case, therefore future investigations into the exact compartmentalisation of the peptides is necessary.
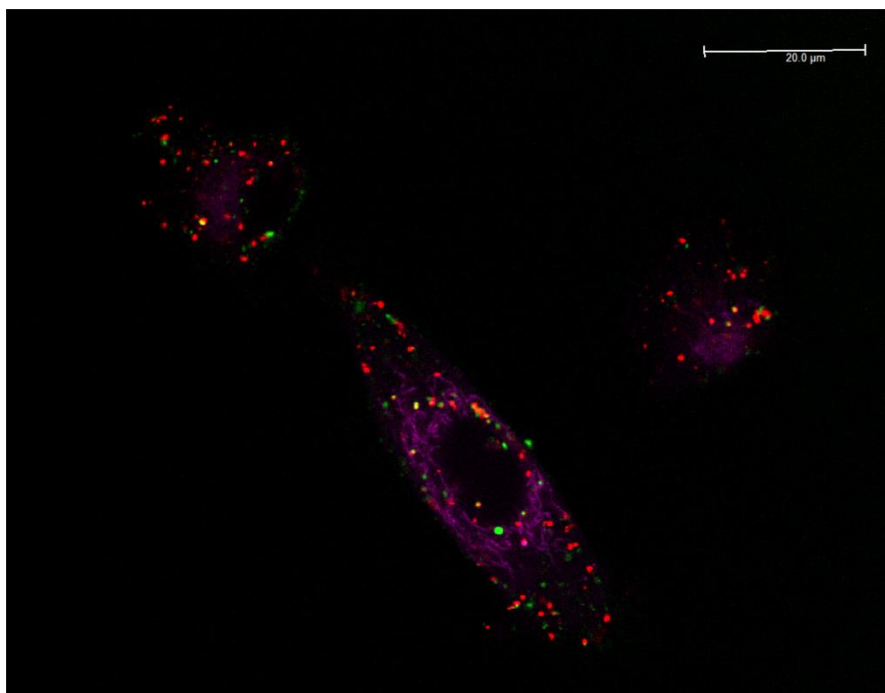
Figure 5.17. Image shows partial overlay of 20 μM peptide **342** solution with LTR. **342** fluorescence (green), LTR fluorescence (red), mitochondrial autofluorescence (pink) following 30 min incubation with PC3 cells at 37 ˚C. Scale bar 20 μm.

5.3.3 Conclusions from confocal fluorescence microscopy

In conclusion, fundamental differences between the antimicrobial peptoids (**334** and **335**) and the temporin peptides (**342** and **343**) have been revealed using confocal fluorescence microscopy and fluorescein labelled sequences. Whilst the peptides show surface activity and gather around the cell membrane before entering mammalian cells, the peptoids permeate through the cell membrane much more efficiently and at a faster rate. The behaviour of peptoid **335** agrees with the work of Olsen *et al*, who showed that fluorescently labelled α-peptide β-peptoids localised inside HeLa cells, with little surface activity.[44] When examining the surface activity of the peptides, temporin A (**342**) shows an increased surface activity *cf* temporin B (**343**), which is found at higher concentrations inside the cell via its higher fluorescence intensity. The rapid transport of peptoid **335** inside the cell is very interesting; many studies suggest that antimicrobial peptoids act on the cell membrane in order to affect their biological effect. However, the fact that **335**

localises inside the cells efficiently may suggest that this is not the only mode of action for this peptoid sequence.

Peptoid **335** was more cytotoxic to the cells studied in the microscopy experiments[††] than the peptides (**342** and **343**). However when cell death occurred, an apoptotic mechanism[‡‡] was responsible for the majority of cells treated by both the peptoids and peptides. Again, the lack of necrosis seen in cells treated by peptoid **335**, suggests that this antimicrobial sequence does not disrupt cell membranes as severely as other peptoids in the literature. For example, cyclic peptoids synthesised by the Kirshenbaum group were shown to significantly damage *S. aureus* cell membranes via pore formation, visualised using SEM in Chapter 1.[2]

The use of several organelle-specific trackers showed that peptoid **335** is transported into the mitochondria, whereas for the peptides localisation in the lysosomes or the ER are suspected (although the overlay between peptide fluorescence and the tracker was not perfect, so this needs to be investigated further in the future). The peptides **342** and **343** are not taken up into cells at 4 °C, however peptoid **335** is able to translocate into the NIT-3T3 cells at 4 °C, suggesting active and passive mechanisms respectively.

In the study by the Bräse and Schepers groups, peptoids with a critical level of lipophilicity were also shown to localise in the mitochondria, although their highly charged sequences (with 3 or more *N*Lys monomers) were taken into the cell by endocytosis (an active transport mechanism) and accumulated in endosomes.[6] In this study, peptoid **335** is both highly charged with 4 *N*Lys monomers (net charge +4) and also fairly lipophilic with a large number of *N*spe monomers, so has both of these properties. In the Bräse study, peptoid sequences were only four monomers in length so it is only to be expected that our compounds may behave differently and therefore it is necessary to undertake more work in this direction for longer antimicrobial peptoid sequences.

Although only four sequences were studied, this preliminary work has laid the groundwork for future microscopy studies which will allow these conclusions to be compared a larger peptoid library and in order to rationalise biological activity and toxicity. Compounds **336**–**341** (**Table 5.5**) are currently being applied in similar microscopy experiments to study their cell permeability and where the sequences localise in mammalian cells. Study of less lipophilic sequences such as **338** and **339**, or the less charged peptoid **340** (net charge +2) will allow further comparisons to the Bräse and Schepers work with longer sequences. In this work, more controls need to be undertaken to ensure that the fluorescein dye is not altering the properties of the peptoid compounds, such as their membrane permeability or cytotoxicity. The direction of this research is discussed in greater detail in Chapter 6: Conclusions and Future Work.

[††] Additionally, peptoid **335** has an ED_{50} of 20 μM for HaCaT and 29 μM for HepG2 (both mammalian cell lines).

[‡‡] In apoptosis the cell membrane remains largely intact.

Finally, it is hoped that the information gathered from this study may allow more rational and an improved design of antimicrobial peptoids in the future; for example, knowledge of the organelles in which the compounds localise can allow us to target specific cellular processes or to alter the compound's structure to decrease toxicity.

5.4   References

1.   P.T. Smith, M.L. Huang, K. Kirshenbaum, *Biopolymers,* **2015**, *103*, 227.
2.   M.L. Huang, M.A. Benson, S.B.Y. Shin, V.J. Torres, K. Kirshenbaum, *Eur. J. Org. Chem.,* **2013**, 3560.
3.   S. Gottschalk, D. Ifrah, S. Lerche, C.T. Gottlieb, M.T. Cohn, H. Hiasa, P.R. Hansen, L. Gram, H. Ingmer, L.E. Thomsen, *BMC Microbiol.,* **2013**, *13*, 1.
4.   W.L. Zhu, Y.M. Song, Y. Park, K.H. Park, S.-T. Yang, J.I. Kim, I.-S. Park, K.-S. Hahm, S.Y. Shin, *Biochim. Biophys. Acta,* **2007**, *1768*, 1506.
5.   W.L. Zhu, K.-S. Hahm, S.Y. Shin, *J. Pept. Sci.,* **2007**, *13*, 529.
6.   Dominik K. Kölmel, Daniel Fürniss, Steven Susanto, Andrea Lauer, Clemens Grabher, Stefan Bräse, U. Schepers, *Pharmaceuticals,* **2012**, *5*, 1265.
7.   B. Mojsoska, R.N. Zuckermann, H. Jenssen, *Antimicrob. Agents Chemother.,* **2015**.
8.   C.A. Olsen, H.L. Ziegler, H.M. Nielsen, N. Frimodt-Moller, J.W. Jaroszewski, H. Franzyk, *ChemBioChem,* **2010**, *11*, 1356.
9.   A.M. Czyzewski, H. Jenssen, C.D. Fjell, M. Waldbrook, N.P. Chongsiriwatana, E. Yuen, R.E.W. Hancock, A.E. Barron, *PLOS ONE,* **2016**, *11*, e0135961.
10.   N.P. Chongsiriwatana, J.A. Patch, A.M. Czyzewski, M.T. Dohm, A. Ivankin, D. Gidalevitz, R.N. Zuckermann, A.E. Barron, *Proc. Natl. Acad. Sci. USA,* **2008**, *105*, 2794.
11.   G.A. Eggimann, H.L. Bolt, P.W. Denny, S.L. Cobb, *ChemMedChem,* **2015**, *10*, 233.
12.   J.A. Patch, A.E. Barron, *J. Am. Chem. Soc.,* **2003**, *125*, 12092.
13.   N. Ramarao, C. Nielsen-Leroux, D. Lereclus, *J. Vis. Exp.,* **2012**, e4392.
14.   A.P. Desbois, P.J. Coote, *Adv. Appl. Microbiol.,* **2012**, *78*, 25.
15.   H.-M. Shin, C.-M. Kang, M.-H. Yoon, J. Seo, *Chem. Comm.,* **2014**, *50*, 4465.
16.   C.W. Wu, T.J. Sanborn, R.N. Zuckermann, A.E. Barron, *J. Am. Chem. Soc.,* **2001**, *123*, 2958.
17.   C.W. Wu, T.J. Sanborn, K. Huang, R.N. Zuckermann, A.E. Barron, *J. Am. Chem. Soc.,* **2001**, *123*, 6778.
18.   B. Sanii, R. Kudirka, A. Cho, N. Venkateswaran, G.K. Olivier, A.M. Olson, H. Tran, R.M. Harada, L. Tan, R.N. Zuckermann, *J. Am. Chem. Soc.,* **2011**, *133*, 20808.
19.   H. Tran, S.L. Gael, M.D. Connolly, R.N. Zuckermann, *J. Vis. Exp.,* **2011**, e3373.
20.   J. Sun, X. Jiang, R. Lund, K.H. Downing, N.P. Balsara, R.N. Zuckermann, *Proc. Natl. Acad. Sci. USA,* **2016**, *113*, 3954.
21.   J. Seo, A.E. Barron, R.N. Zuckermann, *Org. Lett.,* **2010**, *12*, 492.
22.   B.C. Gorske, H.E. Blackwell, *J. Am. Chem. Soc.,* **2006**, *128*, 14378.
23.   C.B. Gorske, R.C. Nelson, Z.S. Bowden, T.A. Kufe, A.M. Childs, *J. Org. Chem.,* **2013**, *78*, 11172.
24.   S.A. Fowler, R. Luechapanichkul, H.E. Blackwell, *J. Org. Chem.,* **2009**, *74*, 1440.
25.   H.L. Bolt, G.A. Eggimann, P.W. Denny, S.L. Cobb, *MedChemComm,* **2016**, *7*, 799.
26.   S.K. Poole, C.F. Poole, *J. Chromatogr. B,* **2003**, *797*, 3.
27.   M. Kah, C.D. Brown, *Chemosphere,* **2008**, *72*, 1401.

28. Y.C. Tang, C.M. Deber, *Biopolymers,* **2002**, *65*, 254.

29. E. Birtalan, B. Rudat, D.K. Kolmel, D. Fritz, S.B. Vollrath, U. Schepers, S. Brase, *Biopolymers,* **2011**, *96*, 694.

30. D.K. Kölmel, A. Hörner, F. Rönicke, M. Nieger, U. Schepers, S. Bräse, *Eur. J. Med. Chem.,* **2014**, *79*, 231.

31. B. Rudat, E. Birtalan, S.B.L. Vollrath, D. Fritz, D.K. Kölmel, M. Nieger, U. Schepers, K. Müllen, H.-J. Eisler, U. Lemmer, S. Bräse, *Eur. J. Med. Chem.,* **2011**, *46*, 4457.

32. T. Schröder, N. Niemeier, S. Afonin, A.S. Ulrich, H.F. Krug, S. Bräse, *J. Med. Chem.,* **2008**, *51*, 376.

33. M.A. Fara, J.J. Díaz-Mochón, M. Bradley, *Tetrahedron Lett.,* **2006**, *47*, 1011.

34. C. Cruz, E. Cairrao, S. Silvestre, L. Breitenfeld, P. Almeida, J.A. Queiroz, *PLOS ONE,* **2011**, *6*, e27078.

35. B. Chazotte, *Cold Spring Harb. Protoc.,* **2011**, 5571.

36. T. Miyake, J.C. McDermott, A.O. Gramolini, *PLOS ONE,* **2011**, *6*, e28628.

37. T. Suzuki, K. Fujikura, T. Higashiyama, K. Takata, *J. Histochem. Cytochem.,* **1997**, *45*, 49.

38. S. Jakobs, *Biochim. Biophys. Acta,* **2006**, *1763*, 561.

39. G. Majno, I. Joris, *J. Pathol.,* **1995**, *146*, 3.

40. S. Rello, J.C. Stockert, V. Moreno, A. Gámez, M. Pacheco, A. Juarranz, M. Cañete, A. Villanueva, *Apoptosis,* **2005**, *10*, 201.

41. Q. Gao, J.M. Goodman, *Front. Cell Dev. Biol.,* **2015**, *3*, 49.

42. H. Appelqvist, P. Wäster, K. Kågedal, K. Öllinger, *J. Mol. Cell Biol.,* **2013**, 5, 214.

43. G.K. Voeltz, M.M. Rolls, T.A. Rapoport, *EMBO Rep.,* **2002**, *3*, 944.

44. C. Foged, H. Franzyk, S. Bahrami, S. Frokjaer, J.W. Jaroszewski, H.M. Nielsen, C.A. Olsen, *Biochimica Et Biophysica Acta-Biomembranes,* **2008**, *1778*, 2487.

Chapter 6

Conclusions and Future Work

In conclusion, the library synthesised as part of this project represents one of the largest and most functionally varied library of antimicrobial peptoids reported to date. In addition to the library synthesis, novel chemical methodology has been developed. In particular, the efficient synthesis of peptoids with both lysine- and arginine-type monomers within the same sequence was described in Chapter 2 and the ligation of peptide and peptoid fragments via a copper catalysed click reaction in Chapter 5.

From work undertaken in Chapter 3, certain peptoid sequences were shown to have potent micromolar potencies against clinically relevant protozoa, including those responsible for the neglected tropical diseases of cutaneous and visceral leishmaniasis, African sleeping sickness and Chagas disease. Additionally some selective peptoids were identified with sub-micromolar against *P. falciparum*, one of the species responsible for fatal malaria infection. This work has provided the first examples of peptoids with activity against trypanosomatid protozoa (i.e. *Leishmania* and *Trypanosoma* species).

In Chapter 4, peptoids have also been successfully applied against planktonic bacteria and cross kingdom biofilms containing multiple bacterial and fungal species. Peptoids have been shown to be active, and significantly species specific, for the treatment of cross kingdom, mixed species biofilms. Detailed SAR discussions regarding peptoid action against protozoa and bacteria or fungi can be found in the conclusions for Chapters 3 and 4 respectively.

The analysis in Chapter 5 provides a large correlation of antimicrobial and toxicity screening, thus it should help inform and direct future research into biologically active peptoids. Chapter 5 also describes further investigation into the biophysical properties of our sequences and it was shown for the first time that HPLC-derived retention times are not the best measure of peptoid hydrophobicity as a means to rationalise compound activity; instead the fundamental log D parameter is suggested to be more appropriate. Additionally, the confocal fluorescence microscopy experiments described in Chapter 5 show that the peptoid sequence tested entered mammalian cells via a passive mechanism and localised in the mitochondria.

Peptoids have been presented as a class of antimicrobial compounds which are less likely to develop resistance than traditional small molecule drugs, due to their proposed mode of action against cell membranes and the significant advantages that peptoids have over peptide analogues due to their reduced susceptibility to proteolysis and resulting higher stability *in vivo*. However, there are still many aspects of peptoids that need to be investigated before they can be applied as pharmaceutical compounds, for example, few studies have looked into the immunogenicity of peptoid sequences and as highlighted in Chapter 1, pharmacokinetic properties still have yet to be optimised; the oral availability of peptoids will need to be improved for applications with enteral administration and the fast excretion rates currently recorded would have to be addressed.[1,2]

One particular challenge highlighted in Chapter 5 is the design of peptoid sequences with high therapeutic indices. The results presented as part of this project show that selectivity has often been problematic since many active sequences have either had some level of toxicity to mammalian cells, or have shown hemolytic activity. In certain circumstances some level of toxicity may be acceptable; for example, in topical applications for cutaneous leishmaniasis, or where current treatments already have significant toxicity and side effects. However, in preliminary studies using a *G. mellonella* model as an *in vivo* measure of toxicity, treatment using high concentrations of peptoid does not lead to larvae death. Overall, in order to enable the further development of peptoids as a new class of antimicrobial compounds, the gaps in our knowledge around the toxicity and *in vivo* efficacy of peptoids need to be addressed and it is clear new models are needed to evaluate toxicity.

A large amount of SAR data was collected from peptoids that covered a large area of the chemical space available and analysis of this has identified several further immediate directions of research in section 6.1. Collection of extra biological activity data is suggested in sections 6.2 and 6.3 outlines possible directions of research to further elucidate the mode of action of antimicrobial peptoids.

Finally, there is an increasing trend in the field of peptide chemistry for N-methylation and removal of hydrogen bonding sites, particularly for medicinal applications. Such changes to peptides are inspired by naturally occurring N-methylated peptides such as the cyclic immunosuppressant drug cyclosporine.[3] N-methylation is reported to increase the biostability of a peptide, prevent aggregation and to assist with membrane permeability due to the removal of hydrogen bonding sites.[4-8] Peptoids by their design already have groups attached to the amide nitrogen and therefore lack hydrogen bonding sites on the backbone, so may provide an alternative platform in the future. Whether peptoids are used as therapeutics themselves or as additions to current bioactive molecules, for example as a targeting moiety or to assist with transit across membranes, peptoids will no doubt begin to feature in an increasing number of lead molecules in the future.

6.1   Improving peptoid selectivity - suggested peptoid syntheses

One of the aims of this project was to synthesise a library that covered a large sector of the chemical space available to peptoids and this was achieved with a great range of varied monomers included across several different design motifs. However, there are some structures, not yet investigated, that may help with the design of selective and biologically active peptoids.

In the antiparasitic screening undertaken, it was shown that chirality was important to overall activity against *Leishmania mexicana* with the *N*-(*S*-phenylethyl) glycine monomers (*N*spe) showing more potent activity than the *N*-benzyl glycine analogues (*N*phe). Although chirality was not quite so important in the antibacterial evaluation of the same compounds, chiral sequences were often the most active. It is suggested that the success of the chiral sequences comes from the induced helical secondary structure, rather than the associated increase in hydrophobicity from inclusion of an extra methyl group.[*]

So far in the library, the chiral residues necessary to induce helical structure have included aromatic residues (*N*spe, *N*sfb or *N*rpe) and it would be advantageous to reduce the proportion of such α-chiral aromatic residues included in the sequence as they have the potential to be hemolytic, more toxic to human cells and also have a poor atom efficiency due the their relatively high molecular weight. It is suggested that inclusion of α-chiral monomers with alkyl character may be a simple approach to balance the toxicity of peptoid sequences with good antimicrobial activity.

A large range of chiral amines are cheap and commercially available, due to their wide use in asymmetric catalysis. Of these many have alkyl functionality, such as those shown in **Figure 6.1**. Inclusion of the *sec*-butyl type monomers have already been shown via CD spectroscopy to induce a helical structure in a peptoid sequence.[9] Adding these residues to a peptoid may allow the fraction of α-chiral aromatic residues to be reduced, or removed entirely, in order to reduce toxicity and hemolytic activity, whilst still retaining the necessary helical structure for antimicrobial activity.
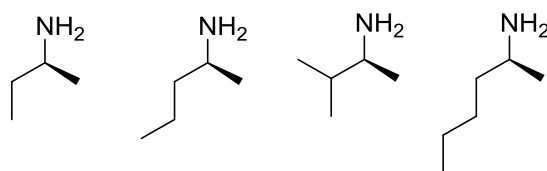

Figure 6.1. Commercially available amines that could be introduced into the submonomer method of peptoid synthesis to achieve peptoids with α-chiral alkyl monomers that would induce a helical structure.

---

[*] See partitioning experiments in Chapter 5.

Additionally in Chapter 2 it was shown that there is a lack of data concerning peptoid conformation in the literature; certain CD spectra published by other groups suggest that related peptoid sequences can form a range of stable helical conformations, however these have yet to be elucidated and characterised in detail. If peptoid secondary structures were clarified, it would allow the diversity of peptoid libraries to be improved. It is known that α-chiral substituents can induce helicity, but the requirement for approximately half of side chains to be bulky α-chiral monomers[9-11] places certain restrictions on the synthesis of diverse peptoid libraries. Future studies should focus upon the development of novel peptoid monomers or side chains that do not rely upon this steric control to stabilise peptoid folding to allow a more through exploration of chemical space and potentially improve the selectivity of peptoids.

6.2   Advancing peptoids as antimicrobial compounds

6.2.1   Future screening

In Chapter 2, the synthesis of 20 lipopeptoids (compounds **158–177**) was described. Lipopeptides are synthesised nonribosomally in bacteria and fungi and can be highly active against multidrug resistant species of bacteria, with the lipid tail facilitating insertion into lipid bilayers of prokaryotic cell membranes.[12] Due to time constraints, these compounds have not yet been biologically evaluated so in the future these could be tested against a variety of bacteria or fungi to determine their activity and toxicity.

Additional testing could also include further investigation into the anti-biofilm activity of the peptoid library. In the initial crystal violet assay, all the biofilms were treated with peptoid solutions at 100 μM which is a very high concentration. Three peptoids (**180**, **216** and **26**) were identified at this stage and taken forward into the qPCR study against mixed biofilms. However, the activity of these sequences at concentrations less than 100 μM were less promising. Therefore, in the future it would be useful to determine if activity is retained at lower concentrations using the crystal violet assay, before utilisation of the more expensive qPCR method. This may allow the identification of the most active sequences at an earlier stage.

In Chapter 3, peptoids **259** (NLysNspe)$_6$ and **260** (NaeNspe)$_6$ were identified that had only mild toxicity to mammalian cells and negligible hemolytic activity but potent activity against *P. falciparum*, (IC$_{50}$ 2.60 μM and 4 μM; TI of 10.2 and 49.2 respectively). Therefore these sequences may be interesting candidates for further development. The sequences of peptoids **259** and **260** both follow an alternating design of hydrophobic and charged monomers which is different to the typical three residue repeat often seen in antimicrobial peptides. In the future, it would be useful to evaluate the toxicity, hemolytic activity and antiparasitic activity of a variety of peptoids with different charge : hydrophobicity ratios and to change the hydrophobic monomer (for both **259** and **260**, α-chiral Nspe is used). This would allow further investigation into whether it is the

increased net cationic charge, the increased number of hydrophobic residues, a structural difference or combination of the above factors that causes the improved antimicrobial effect and lower toxicity/hemolytic activities.

In addition, it may be of merit to investigate a potential synergism between routinely prescribed antibiotic or antiparasitic drugs and the peptoid sequences. Synergy between AMPs and commercially available drugs[13-15] or between peptoids and AMPs[16] has proven successful in previous studies. It would be simple to repeat the assays already performed and treat relevant pathogens with a mixture of some of the most potent peptoid sequences and a relevant drug to see if the membrane permeabilisation properties of the peptoids cause an enhancement in activity of the known drug. This strategy could potentially be useful against multi-drug resistant bacteria, parasites or fungi since the peptoids may disrupt the cell membrane and allow the small molecule therapeutic to target the appropriate mechanism in a compromised cell.

Finally, the large amount of biological data collected as part of this project has been analysed qualitatively in SAR studies, however it may benefit from a further bioinformatics approach to correlate activity with specific features of active sequences. Tests such as the Pearson correlation could be applied to the entire data set to statistically determine if positive or negative correlations exist between activity and characteristics such as hydrophobicity, chirality, net charge or specific monomers within the sequence. These tests should be applied to data obtained from assays against each bacteria or parasite to draw out the trends for these different species.

6.2.2   Investigation into the role of *C. albicans* in polymicrobial biofilms

Biofilms containing *Candida albicans* are responsible for a large number of infections in the clinic, including those associated with medical devices.[17-19] Recently it has been suggested that the presence of *C. albicans* can significantly modify the physical environment and structure of a biofilm.[20] Additionally, the presence of fungi can affect the action of antibiotics and bacteria can influence antifungal activity.[21]

In the biofilm testing carried out as part of Chapter 4, several peptoids were identified that were active against *C. albicans* but had no significant effect upon *S. aureus* or *E. coli,* such as sequences **152** (*N*hArg*N*spe*N*spe)$_4$, **153** (*N*hArg*N*mfb*N*mfb)$_4$ and **181** (*N*hArg*N*hLeu*N*spe)$_4$. Use of such compounds could provide a starting point for further investigation into the role of *C. albicans* in cross-kingdom biofilms. It is anticipated that these molecules could act as probes to determine if inhibition of *C. albicans* alone could perturb or prevent polymicrobial biofilms. With increasing bacterial resistance observed against many conventional antibiotics in polymirobial biofilms containing *C. albicans,* these experiments would be very useful and may provide a starting point for new anti-biofilm treatments.[22]

6.3   Further investigations into peptoid mode of action

6.3.1 The nature of the peptoid helix: further investigations using circular dichroism

This section describes ongoing collaboration with Dr Beth Bromley (Physics Department, Durham University).

Following from Chapter 3, where peptoids **259** (*N*Lys*N*spe)$_6$ and **260** (*Nae*N*spe)$_6$ were identified with potent activity and therapeutic indices greater than 10, a further investigation into the nature of the peptoid helix is suggested. These sequences have an alternating pattern of hydrophobic and cationic monomers which differs from the typical trimer repeat motif (*NxNyNy*)$_n$ that the majority of the library is based upon. It is proposed that the differential activity profile could be due to different secondary structures of these two design patterns. It has already been shown that there is a lack of information regarding the peptoid helix, with CD spectra published by other groups suggesting that related peptoid sequences can form a range of stable helical conformations.

In order to address this issue, a group of peptoids were synthesised with the same side chains, but different repeat motifs as shown in **Table 6.1** and **Figure 6.2**. In these sequences a cationic monomer (*N*ae or *N*Lys) is used with the hydrophobic monomer *N*spe, with the cationic monomer placed in an alternating manner (**259**, **260**), in the typical trimer repeat (**156**, **22**) or in the 4 residue repeat motif (**344** and **345**).

	Sequence	Motif
260	(*NaeN*spe)$_6$	2 repeat
259	(*N*Lys*N*spe)$_6$	
156	(*NaeN*spe*N*spe)$_4$	3 repeat
22	(*N*Lys*N*spe*N*spe)$_4$	
344	(*NaeN*spe*N*spe*N*spe)$_3$	4 repeat
345	(*N*Lys*N*spe*N*spe*N*spe)$_3$	

Table 6.1. Sequences synthesised for investigation of the peptoid helix via CD.
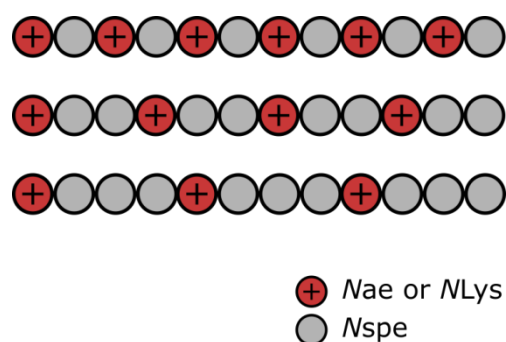

+ *N*ae or *N*Lys
○ *N*spe

Figure 6.2. Repeat motifs used in the 12 residue peptoids shown in **Table 6.1**.

The peptoids absorb the circularly polarised light according to their conformation in space. In the typical CD spectrum of a helical peptoid, two absorption bands are seen around 200 nm and 220 nm, attributed to the π → π* and n → π* transitions of the amide backbone respectively.[23,24] The appearance of the CD spectra for helical peptoids is often very different to that obtained from a typical α-helical peptide. In particular, the minima of the 200 nm and 220 nm transitions are often dissimilar, whereas with α-helical peptides they are mostly even at a similar MRE value. This suggests very different conformations are present, potentially with different helix pitches or different molecular interactions, for example π-π stacking of the aromatic residues. The literature also reports peptoid CD spectra with uneven minima and a suggestion is made that these different shapes are due to different side chains.[9-11,25-27] However, in Chapter 5, the CD spectra of peptoids with the same side chains showed different minima (either biased towards the 200 nm or 220 nm transition), so this cannot be the case and the different characteristic CD signals must mean different conformations are being adopted.

As a starting point to try and elucidate the different conformations present in the peptoids, the partitioning behaviour of the peptoids in **Table 6.1** and their CD spectra in PBS (aqueous) and octanol (hydrophobic solvent) are currently being collected. In addition molecular dynamics is being used by the group of Dr Beth Bromley in an ambitious project to help identify the lowest energy conformations to populate a Ramachandran plot to help identify the allowed regions for the backbone dihedral angles for these peptoids and to predict the energetically accessible helical conformations in different solvents. Molecular dynamics and combined molecular dynamics-quantum mechanical simulations have been used previously to evaluate accessible peptoid backbone conformations, but these have never been used to study the conformations of helical peptoids or to link structures obtained from modelling to the CD data.[28-31]

6.3.2 Peptoid action against model membranes

This section describes ongoing collaboration with Dr Beth Bromley and Dr Kislon Voitchovsky (Physics Department, Durham University).

It is clear that certain peptoid sequences can interact with and pass through the cell membranes of both eukaryotic and bacterial cell membranes from the microscopy work (Chapter 5) and from the membrane permeabilisation assay using SYTOX® Green (Chapter 4). Continuing collaborations are investigating how peptoids act upon different model membranes. Firstly, neutral 1,2-dioleoyl-*sn*-glycero-3-phosphocholine (DOPC) and anionic 1,2-dioleoyl-*sn*-glycero-3-phospho-l-serine (DOPS) vesicles are being studied, as well as some lipids doped with cholesterol to provide a representative chiral membrane surface. These DOPC and DOPS vesicles are a model for cell membranes and the vesicles are labelled with rhodamine and fluorescein dye is trapped inside. Following treatment by peptoid, the dye leakage and appearance of the micelles can be studied.

Additionally, atomic force microscopy (AFM) is being used to examine the interactions between a peptoid sequence and a model bilayer. Two peptoids, based upon sequence **22** are currently being investigated (see **Figure 6.3**). Both peptoid **346** and reteropeptoid **347** have one N terminal cysteine residue and an aminohexanoic acid linker to allow the sequences to be added to a gold coated AFM probe via sulphur-gold affinity.
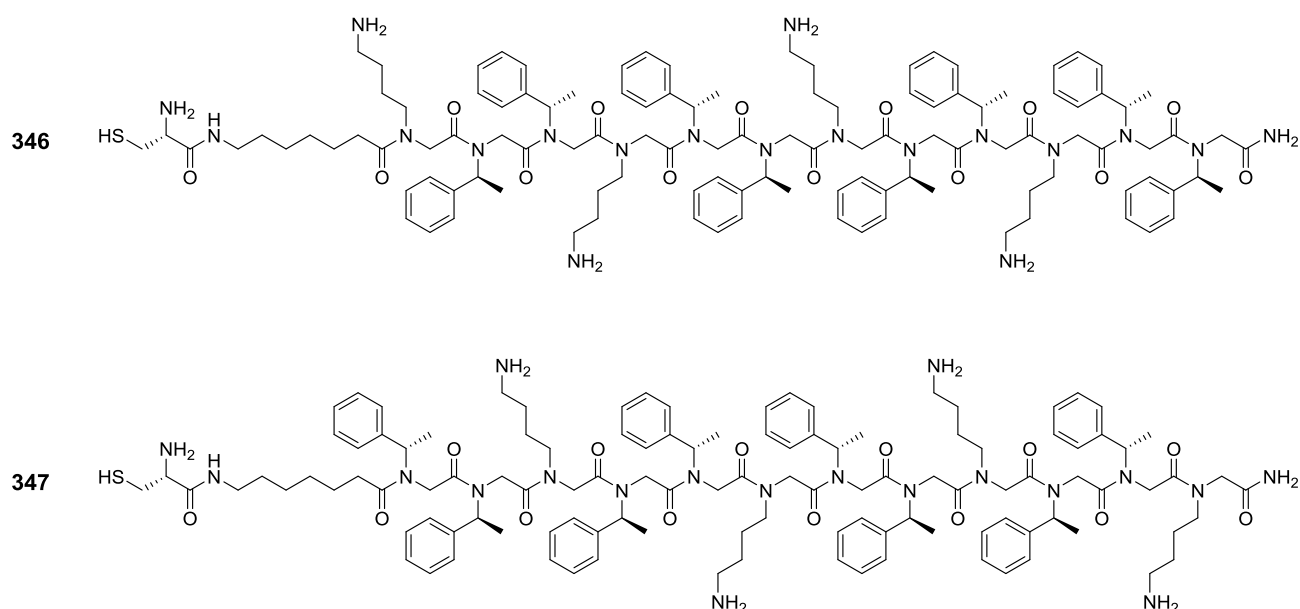

Figure 6.3. Peptoid **346** and reteropeptoid **347** synthesised for attachment to AFM probe.

6.3.3 Confocal fluorescence microscopy

The microscopy experiments described in Chapter 5 provide preliminary investigations into the behaviour of peptoids inside living cells. Currently, compounds **336–341** (see fluorescent peptoid library in Chapter 5.3 .1, as yet unstudied) are being used in further microscopy experiments to ascertain the mechanism of entry into mammalian cells and where these compounds accumulate in mammalian cells. These sequences include peptoids that are less lipophilic than those already studied and also with a lower net charge and should allow more information to be obtained regarding the chemical structures needed to target peptoids to specific organelles. This may help to rationalise the biological activity and toxicity of the sequences in the future. In this work, the cytotoxicity of the labelled compounds should also be obtained, to gauge the effect of the fluorescein dye on the overall compound toxicity. Additionally, it is planned to treat bacteria with the fluorescently labelled peptoids library to further investigate the mode of action of these compounds against prokaryotes.

Biological testing as part of Chapters 3 and 4 highlighted some interesting trends when comparing the activity of lysine- and arginine-type peptoids. Against planktonic bacteria, sequences comprised exclusively of the arginine peptoid monomers were consistently more active than the lysine-only derivative peptoids. However, the arginine-type peptoids were typically less efficacious against the biofilms and this was supported by the SYTOX® Green assay, which shows that lysine sequences are able to cause a greater extent of membrane disruption to the species within the biofilm. This could be a point of further investigation utilising fluorescent microscopy, to examine the localisation of fluorescently labelled lysine-only, arginine-only and mixed peptoids in planktonic bacteria or within a biofilm in an attempt to explain this phenomenon.

Finally, the effect of cyclic peptoids against biological targets has been studied in traditional assays and also using SEM to image the cell membrane of *S. aureus*[32], however as yet, cyclic peptoids have not been studied using fluorescent microscopy. None of the cyclic peptoids synthesised as part of this project (**130–134**) showed any activity against protozoa or bacteria. Although the peptoids obtained from the Kirshenbaum lab (**135–144**) showed no anti-protozoan activity they have been reported as potent antibacterial compounds.[32,33]

It is suggested that differences in activity could be investigated in more detail if a selection of the cyclic library was resynthesised with fluorescent tags, to compare their mode of action. The method developed for the synthesis of mixed arginine- and lysine-type peptoids using Dde-protection could also be adapted to make these fluorescently tagged cyclic peptoids.

A proposed synthetic route to the synthesis of an example compound (**348**) is suggested in **Scheme 6.1**. This involves the solid-phase synthesis of linear peptoid precursor on 2-chlorotrityl chloride resin, Dde deprotection using 2% hydrazine DMF and on-resin fluorescein addition using standard coupling conditions. Following cleavage from the resin using HFIP, which leaves Boc protection on side chains untouched, the peptoid can be cyclised as before and then a final treatment with TFA used to deprotect the Boc groups. It is anticipated that efficient macrocyclisation will occur, even with the bulky fluorescein attached to one sidechain.
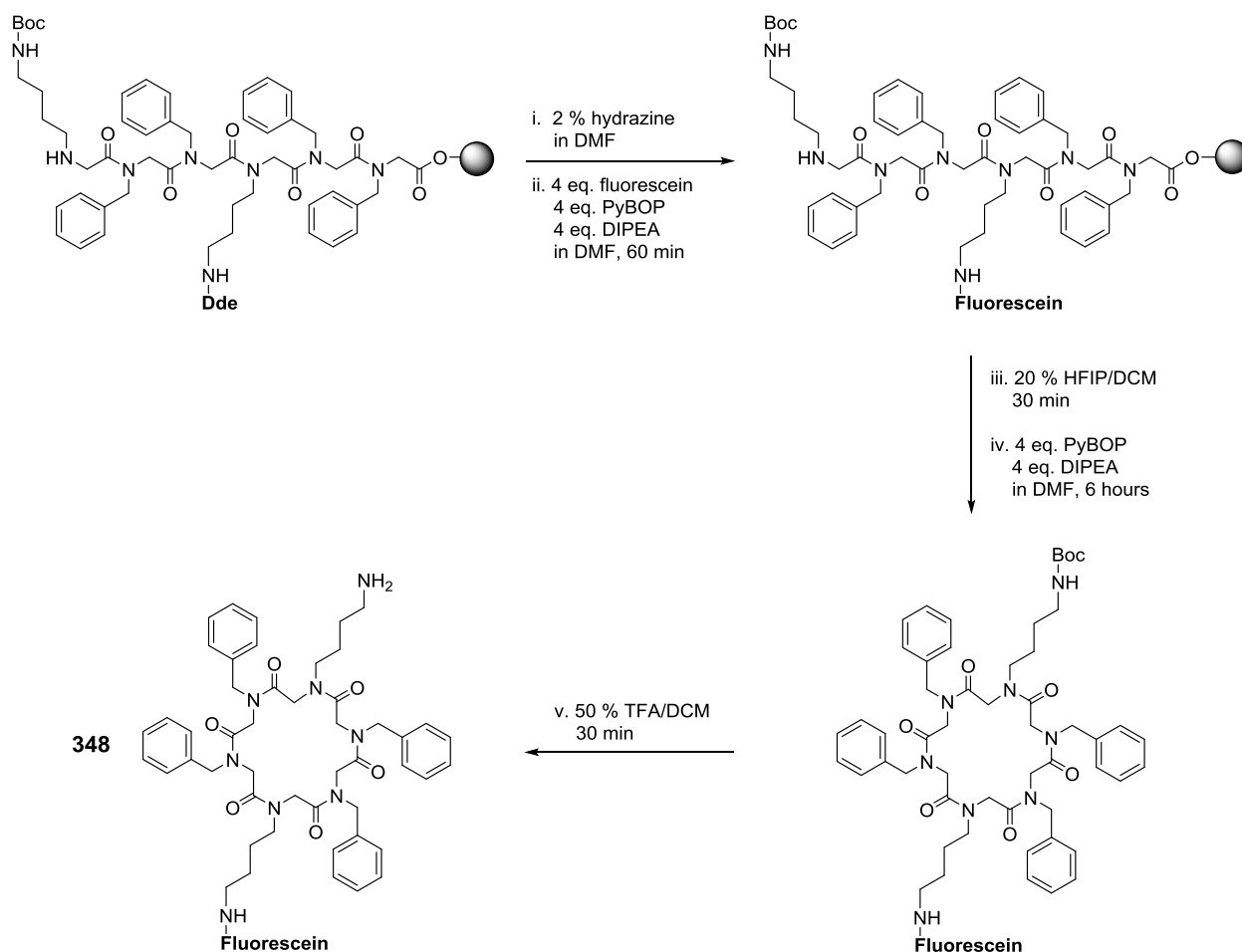
Scheme 6.1. The proposed synthetic route to synthesise fluorescently tagged, cyclic peptoid **348** using the submonomer method of peptoid synthesis on 2-chlorotrityl chloride resin, using orthogonal Boc and Dde protection of sidechains.

6.4   References

1.   J. Seo, G. Ren, H. Liu, Z. Miao, M. Park, Y. Wang, T.M. Miller, A.E. Barron, Z. Cheng, *Bioconjugate Chem.,* **2012**, *23*, 1069.

2.   J.A. Patch, K. Kirshenbaum, S.L. Seurynck, R.N. Zuckermann, A.E. Barron In *Pseudopeptides in Drug Development*; Nielsen, P. E., Ed.; Wiley-VCH: Germany, 2004, p 1

3.   D. Tedesco, L. Haragsim, *J.Transplantation,* **2012**, *2012*, 230386.

4.   T. Uhlig, T. Kyprianou, F.G. Martinelli, C.A. Oppici, D. Heiligers, D. Hills, X.R. Calvo, P. Verhaert, *EuPA Open Proteom.,* **2014**, *4*, 58.

5.   J. Chatterjee, F. Rechenmacher, H. Kessler, *Angew. Chem. Int. Ed.,* **2013**, *52*, 254.

6.   J. Chatterjee, C. Gilon, A. Hoffman, H. Kessler, *Acc. Chem. Res.,* **2008**, *41*, 1331.

7.   K. Fosgerau, T. Hoffmann, *Drug Disc. Today,* **2015**, *20*, 122.

8.   D.J. Craik, D.P. Fairlie, S. Liras, D. Price, *Chem. Biol. Drug Des.,* **2013**, *81*, 136.

9.   C.W. Wu, K. Kirshenbaum, T.J. Sanborn, J.A. Patch, K. Huang, K.A. Dill, R.N. Zuckermann, A.E. Barron, *J. Am. Chem. Soc.,* **2003**, *125*, 13525.

10.   C.W. Wu, T.J. Sanborn, R.N. Zuckermann, A.E. Barron, *J. Am. Chem. Soc.,* **2001**, *123*, 2958.

11.   C.W. Wu, T.J. Sanborn, K. Huang, R.N. Zuckermann, A.E. Barron, *J. Am. Chem. Soc.,* **2001**, *123*, 6778.

12.   S.M. Mandal, A.E. Barbosa, O.L. Franco, *Biotechnol. Adv.,* **2013**, *31*, 338.

13.   L. Fassi Fehri, H. Wroblewski, A. Blanchard, *Antimicrob. Agents Chemother.,* **2007**, *51*, 468.

14.   H. Yan, R.E.W. Hancock, *Antimicrob. Agents Chemother.,* **2001**, *45*, 1558.

15.   S. Nuding, T. Frasch, M. Schaller, E.F. Stange, L.T. Zabel, *Antimicrob. Agents Chemother.,* **2014**, *58*, 5719.

16.   N.P. Chongsiriwatana, M. Wetzler, A.E. Barron, *Antimicrob. Agents Chemother.,* **2011**, *55*, 5399.

17.   F.L. Mayer, D. Wilson, B. Hube, *Virulence,* **2013**, *4*, 119.

18.   N.C. Lim, D.K. Lim, M. Ray, *Eye Contact Lens,* **2013**, *39*, 348.

19.   S. Cairns, J.G. Thomas, S.J. Hooper, M.P. Wise, P.J. Frost, M.J. Wilson, M.A. Lewis, D.W. Williams, *PLOS ONE,* **2011**, *6*, e14759.

20.   M.L. Falsetta, M.I. Klein, P.M. Colonne, K. Scott-Anne, S. Gregoire, C.H. Pai, M. Gonzalez-Begne, G. Watson, D.J. Krysan, W.H. Bowen, H. Koo, *Infect. Immun.,* **2014**, *82*, 1968.

21.   H.F. Jenkinson, L.J. Douglas In *Polymicrobial Diseases*; K.A. Brogden, J.M. Guthmiller, Eds.; ASM Press: Washington DC, 2002, p 357.

22.   M.M. Harriott, M.C. Noverr, *Antimicrob. Agents Chemother.,* **2010**, *54*, 3746.

23.   S.M. Kelly, N.C. Price, *Curr. Protein Pept. Sci.,* **2000**, *1*, 349.

24.   D.H.A. Correa, C.H. I. Ramos, *Afr. J. Biochem. Res.,* **2009**, *3*, 164.

25.   J.A. Patch, A.E. Barron, *J. Am. Chem. Soc.,* **2003**, *125*, 12092.

26.   K. Kirshenbaum, A.E. Barron, R.A. Goldsmith, P. Armand, E.K. Bradley, K.T.V. Truong, K.A. Dill, F.E. Cohen, R.N. Zuckermann, *Proc. Natl. Acad. Sci. USA,* **1998**, *95*, 4303.

27.   N.P. Chongsiriwatana, J.A. Patch, A.M. Czyzewski, M.T. Dohm, A. Ivankin, D. Gidalevitz, R.N. Zuckermann, A.E. Barron, *Proc. Natl. Acad. Sci. USA,* **2008**, *105*, 2794.

28.   R.V. Mannige, T.K. Haxton, C. Proulx, E.J. Robertson, A. Battigelli, G.L. Butterfoss, R.N. Zuckermann, S. Whitelam, *Nature,* **2015**, *526*, 415.

29. G.L. Butterfoss, B. Yoo, J.N. Jaworski, I. Chorny, K.A. Dill, R.N. Zuckermann, R. Bonneau, K. Kirshenbaum, V.A. Voelz, *Proc. Natl. Acad. Sci. USA,* **2012**, *109*, 14320.

30. G.L. Butterfoss, K. Drew, P.D. Renfrew, K. Kirshenbaum, R. Bonneau, *Biopolymers,* **2014**, *102*, 369.

31. G.L. Butterfoss, P.D. Renfrew, B. Kuhlman, K. Kirshenbaum, R. Bonneau, *J. Am. Chem. Soc.,* **2009**, *131*, 16798.

32. M.L. Huang, M.A. Benson, S.B.Y. Shin, V.J. Torres, K. Kirshenbaum, *Eur. J. Org. Chem.,* **2013**, 3560.

33. M.L. Huang, S.B.Y. Shin, M.A. Benson, V.J. Torres, K. Kirshenbaum, *ChemMedChem,* **2012**, 7, 114.

Chapter 7

Experimental

7.1   Materials and reagents

All reagents used in this project were purchased from commercial sources and used without further purification unless otherwise specified. In particular, peptide synthesis grade DMF was obtained from AGTC Bioproducts (Hessle, UK), PyBOP from Apollo Scientific (Stockport, UK) and NMR solvents which were purchased from Cambridge Isotopes Inc., supplied by Goss Scientific (Crewe, UK). All resins and amino acids were purchased from Novabiochem by Merck (Darmstadt, Germany). Amines used in submonomer peptoid synthesis were obtained either from Sigma Aldrich (Gillingham, UK) or TCI Europe (Zwijndrecht, Belgium). These chemicals were used without further purification and stored under appropriate conditions, as detailed in the manufacturer's instructions. Bond Elut solid phase extraction cartridges (20 mL, polypropylene with two polypropylene frits) were purchased from Crawford Scientific and used as reaction vessels for solid phase synthesis.

Solvents were removed under reduced pressure using a Büchi Rotavapor R11. The following centrifuges were used: an Eppendorf centrifuge 5415D (for 1.5 mL tubes) or a Beckman-Coulter Allegra X-22R (for 15mL or 50 mL tubes). A Radleys Discovery Technology shaker was also used to mix solutions where indicated and aqueous solutions were lyophilised using a Christ Alpha 1-2 LD Plus freeze-drier.

Abbreviations for common reagents and protecting groups are as follows: tert-butoxycarbonyl (Boc); 9-fluorenylmethoxycarbonyl (Fmoc); triphenylmethyl or trityl (Trt); *N*-(1-(4,4-dimethyl-2,6-dioxocyclohexylidene)ethyl (Dde); trifluoroacetic acid (TFA); triisopropylsilyl (TIPS); *N,N*-dimethylformamide (DMF); *N,N*-diisopropylcarbodiimide (DIC); dimethylsulphoxide (DMSO); dichloromethane (DCM).

7.2   Characterisation

7.2.1   Liquid chromatography electrospray ionisation mass spectrometry

Analytical LC-MS data were obtained using a triple quadrupole mass spectrometer equipped with an Acquity UPLC (Waters Ltd, UK) and a photodiode array detector. Samples were injected onto the Acquity UPLC BEH C18 column (1.7 µm, 2.1 mm × 50 mm) with a flow rate of 0.6 mL min^{-1} and a linear gradient of 5–95 % of solvent B over 3.8 min (A = 0.1 % formic acid in H$_2$O, B = 0.1 % formic acid in acetonitrile). The flow was introduced into the electrospray ion source of the Aquity TQD mass spectrometer.

7.2.2   Quadrupole time-of-flight mass spectrometry

Measurements were performed using a QToF Premier mass spectrometer with an Acquity ultra-performance liquid chromatography system (Waters Ltd, UK). Samples were injected to the Acquity UPLC BEH C18 column (1.7 µm, 2.1 mm x 100 mm) with a flow rate of 0.6 mL min^{-1} and a linear gradient of 0–99 % of solvent B over 6 min (A = 0.1 % formic acid in H$_2$O, B = 0.1 % formic acid in acetonitrile). The solvent flow from the UPLC was injected into a 0.2 mL/min flow of acetonitrile which was introduced into the electrospray ion source.

7.2.3   Matrix-assisted laser desorption/ionisation mass spectrometry

MALDI-ToF analysis was obtained using an Autoflex II ToF/ToF mass spectrometer (Bruker Daltonik GmBH) equipped with a 337 nm nitrogen laser. The sample solution (ideally at 1 mg mL^{-1}) was mixed with matrix solution, typically α-cyano-4-hydroxycinnamic acid (~ 50 mg mL^{-1}) in the ratio 9:1 matrix to sample. 1 µL of the matrix/sample solution was spotted to the MALDI target and allowed to evaporate prior to analysis, where the metal target is placed into the MALDI ion source. The samples were analysed in positive detection mode with reflectron enhanced mass resolution for m/z between 500 and 5000. Internal mass calibration with known standards was used to established the mass accuracy. Variable laser intensities were used to ensure the most representative mass spectra for samples were produced.

MALDI MS/MS was performed using LIFT technology (MALDI LIFT-ToF-ToF) which enables detection of product ions that result from elevated laser power.

7.2.4 Nuclear magnetic resonance spectroscopy

^{1}H, ^{13}C, ^{19}F NMR spectra were obtained on the following machines; Varian Mercury-400 MHz, Varian VNMRS-600 MHz and Bruker Avance-400 MHz spectrometers.

Chemical shifts are reported in parts per million (δ ppm) and relative to residual solvent peaks. J couplings are reported in megahertz (MHz). Multiplicities: s = singlet, d = doublet, t = triplet.

Chemical Synthesis and Solid Phase Synthesis Methods

7.3   Linear peptoid synthesis

7.3.1   Manual synthesis at room temperature

Rink Amide resin:

Modified protocol following the submonomer synthesis of peptoids.[1] Fmoc-protected Rink Amide resin (normally 100–300 mg, 0.1–0.3 mmol, typical loading between 0.6–0.8 mmol g^{-1}) was swollen in DMF (at least 1 hour, overnight preferred, at room temperature) in a 20 mL polypropylene syringe fitted with two polyethylene frits. The resin was deprotected with piperidine (20 % in DMF *v/v*, 2 x 20 min) and washed with DMF (3 x 2 mL). The resin was treated with haloacetic acid (either bromo- or chloroacetic acid dependent on monomer to be installed, 1 mL, 0.6 M in DMF) and DIC (0.20 mL, 50 % *v/v* in DMF) for 20 minutes at room temperature at 400 rpm. The resin was washed with DMF (3 x 2 mL), before the desired amine sub-monomer was added (1 mL, 0.8–2.0 M in DMF) and allowed to react for 60 minutes at room temperature on the shaker. The resin was again washed with DMF (3 x 2 mL) and the bromoacetylation and amine displacement steps were repeated until the final submonomer had been added and the desired peptoid sequence had been obtained. The resin was shrunk in diethyl ether to remove DMF in preparation for cleavage, as in section 7.12.1. The products on resin were stored at -18 °C and purified using RP-HPLC (section 7.13.1).

2-chlorotrityl chloride resin:

2-chlorotrityl chloride resin (normally 100–250 mg, 0.1–0.2 mmol, typical loading 1.22 mmol g^{-1}) was swollen in dry DCM (45 minutes at room temperature) in a 20 mL polypropylene syringe fitted with two polyethylene frits. The resin was washed with dry DCM (3 x 2 mL) and loaded with bromoacetic acid (1 mL, 0.6 M in DMF) and neat DIPEA (16 eq. with respect to the resin) for 30 minutes at RT on a shaker at 400 rpm. The resin was washed with DMF (3 x 2 mL), before the desired amine sub-monomer was added (1 mL, 1.5 M in DMF) and allowed to react for 60 minutes at RT on the shaker. The resin was again washed with DMF (3 x 2 mL) and the resin was treated with bromoacetic acid (1 mL, 0.6 M in DMF) and DIC (0.2 mL, 50 % *v/v* in DMF) for 20 minutes at RT on the shaker. The resin was washed again with DMF (3 x 2 mL) and amine displacement and bromoacetylation steps repeated until the final sub-monomer had been added and the desired linear peptoid precursor had been obtained. The resin was shrunk in diethyl ether to remove DMF in preparation for cleavage (section 7.12.2). If required, the products on resin were stored at -18 °C

7.3.2 Automated synthesis at room temperature

Automated peptoid synthesis using an Aapptec Apex 396 synthesiser. Fmoc-protected Rink Amide resin (0.1 mmol, loading typically 0.54 mmol g^{-1}) was swollen in DMF (2 mL, 2 min, 475 rpm at RT) and deprotected with 4-methylpiperidine (20 % in DMF v/v, 1 mL for 1 min, 475 rpm at RT; then 2 mL for 12 min, 475 rpm at RT). The resin was treated with haloacetic acid solution (either bromo- or chloroacetic acid, 1 mL, 0.6 M in DMF) and DIC (0.18 mL, 50 % v/v in DMF) for 20 min at 475 rpm, RT. The resin was washed with DMF (2 mL DMF for 1 min at 475 rpm, x 5) before the desired amine sub-monomer was added (1 mL, 1.5M in DMF) and shaken for 60 minutes at 475 rpm (90 min if chloroacetic acid was used as the acetylating agent). The resin was washed again with DMF (2 mL DMF for 1 min at 475 rpm, x 5) and the acetylation and amine displacement steps were repeated until the desired sequence was achieved. The resin was shrunk in diethyl ether in preparation for resin cleavage, as in section 7.12.1. The products on resin were stored at -18 °C and purified using RP-HPLC (section 7.13.1).

7.4   Addition of glycine-glycine spacer to N terminus of peptoids

The linear peptoid was synthesised via manual SPPS, as in section 7.3 and the glycine spacer added as follows. Peptoids on resin were swollen in DMF in a polypropylene syringe fitted with a polyethylene frit (at least 1 hour, overnight preferred, at RT). PyBOP (4 eq. with respect to the resin), Fmoc-Gly-OH (4 eq.) and DIPEA (4 eq.) were dissolved in the minimum volume of DMF and left to preactivate for several minutes, before being added to the resin and placed on the shaker at 400 rpm at room temperature for 1 hour. The resin was washed with DMF (3 x 2 mL) and the resin deprotected using piperidine (20 % in DMF v/v, 2 x 20 min). The resin was washed with DMF (3 x 2 mL) and the second glycine residue added as above, followed by a second deprotection step. The resin was shrunk in diethyl ether to remove DMF and if necessary, the products on resin were stored at -18 °C prior to cleavage, as in section 7.12.

7.5   Addition of Ahx to peptoid sequence

The linear peptoid was synthesised via manual or automated SPPS on Rink Amide, as in section 7.3. Peptoids on resin were swollen in DMF in a polypropylene syringe fitted with a polyethylene frit (at least 1 hour, overnight preferred, at RT). PyBOP (4 eq. with respect to the resin), Fmoc-Ahx-OH (4 eq.) and DIPEA (4 eq.) were dissolved in the minimum DMF and left to preactivate for several minutes, before being added to the resin and placed on the shaker at 400 rpm at room temperature for 1 hour. Fmoc-Ahx-OH coupling repeated. The resin was then washed with DMF (3 x 2 mL) and deprotected using piperidine (20 % in DMF v/v, 2 x 20 min) and washed as before. PyBOP (4 eq. with respect to the resin), Fmoc-Cys(Trt)-OH (4 eq.) and DIPEA (4 eq.) were dissolved in the

minimum volume of DMF and left to react for several minutes, before being added to the resin and placed on the shaker at 400 rpm at room temperature for 1 hour. Fmoc-Cys(Trt)-OH coupling repeated. The resin was washed with DMF (3 x 2 mL) then the Fmoc-group deprotected immediately prior to final cleavage using piperidine (20 % in DMF *v/v*, 2 x 4 mL, 2 x 20 mins). The resin was washed with DMF (3 x 2 mL) and resin cleavage (section 7.12.1), deprotection and RP-HPLC purification (section 7.13.1) was undertaken as before to afford the desired Cys-Ahx tagged peptoid.

7.6   Addition of fluorescein to peptoid sequence

The linear peptoid was synthesised via manual or automated SPPS, as in section 7.3 on Rink Amide resin and a glycine spacer added prior to the fluorescent dye: peptoids on resin were swollen in DMF in a polypropylene syringe fitted with a polyethylene frit (at least 1 hour, overnight preferred, at RT). PyBOP (4 eq. with respect to the resin), Fmoc-Gly-OH (4 eq.) and DIPEA (4 eq.) were dissolved in the minimum volume of DMF and left to preactivate for several minutes, before being added to the resin and placed on the shaker at 400 rpm at room temperature for 1 hour. The resin was then washed with DMF (3 x 2 mL) and the resin deprotected using piperidine (20 % in DMF *v/v*, 2 x 20 min) and washed as before. PyBOP (4 eq. with respect to the resin), fluorescein (4 eq.) and DIPEA (4 eq.) were dissolved in the minimum DMF and left to react for several minutes, before being added to the resin and placed on the shaker at 400 rpm at room temperature for 1 hour. The fluorescein coupling was repeated and then the resin was washed with DMF (6 x 2 mL) and finally DCM (3 x 2 mL). Resin cleavage (see protocol 7.12.1) and RP-HPLC purification (section 7.13.1) was undertaken to afford the desired fluorescently tagged peptoid. Peptoids on resin and the cleaved product should be stored in the dark.

7.7   Addition of lipid tail groups to peptoid N terminus

The linear peptoid sequence was synthesised via manual or automated SPPS on Rink Amide, see protocol 7.3. The lipid tail was added under standard conditions for the peptoid submonomer method using a variety of lipoamines: acylation of the peptoid sequence using bromoacetic acid solution (1 mL, 0.6 M in DMF) and DIC (0.2 mL, 50 % *v/v* in DMF) for 20 min at 400 rpm at RT. The resin was washed with DMF (3 x 2 mL) before the desired amine submonomer was added (1 mL, between 0.5–2M in DMF, DCM or NMP depending upon amine solubility) and shaken for 60 min at 400 rpm. The resin was washed with DMF (3 x 2 mL) and resin cleavage and deprotection (section 7.12.1) and RP-HPLC purification (section 7.13.1) was undertaken as before to afford the desired peptoid with lipid tail.

7.8   Addition of lipid head groups to peptoid C terminus

The linear peptoid sequence was synthesised via manual or automated SPPS on 2-chlorotrityl chloride resin, as in section 7.3. The peptoid was cleaved from the resin (whilst still protected) using HFIP/DCM cleavage cocktail protocol (section 7.12.2) to afford a lyophilised protected peptoid. The lipohead group was added in a solution phase coupling: the peptoid sequence (1 eq., typically 20 µmol), PyBOP (4 eq. with respect to the peptoid) and DIPEA (4 eq.) were dissolved in the minimum volume of DMF and left to preactivate for several minutes. The required amine was then added (4 eq. with respect to the peptoid in in DMF, DCM or NMP, depending upon solubility) and stirred for 90 minutes at RT. The solvent was removed *in vacuo* in a fumehood, the remaining peptoid residue washed with HCl (0.1 M, ~20 mL) and then the peptoid extracted into DCM. The organic layers were combined, dried over MgSO$_4$, filtered then the DCM was removed *in vacuo.* The peptoid was then deprotected in TFA/DCM (50 % *v/v*) for 30 minutes at room temperature. The TFA solution was removed *in vacuo* and the residue remaining was dissolved in 1 : 1 H$_2$O : MeCN (~5 mL), frozen and lyophilised. RP-HPLC purification was undertaken as in section 7.13.1 to afford the desired peptoid with lipid head group.

7.9   Cyclic peptoids

7.9.1 Synthesis of linear precursors

2-chlorotrityl chloride resin (normally 100–250 mg, 0.1–0.2 mmol, typical loading 1.22 mmol g^{-1}) was swollen in dry DCM (45 minutes at RT) in a 20 mL polypropylene syringe fitted with two polyethylene frits. The resin was washed with dry DCM (3 x 2 mL) and loaded with bromoacetic acid (1 mL, 0.6 M in DMF) and neat DIPEA (16 eq. with respect to the resin) for 30 minutes at RT on a shaker at 400 rpm. The resin was washed with DMF (3 x 2 mL), before the desired amine sub-monomer was added (1 mL, 1.5 M in DMF) and allowed to react for 60 minutes at RT on the shaker. The resin was again washed with DMF (3 x 2 mL) and the resin was treated with bromoacetic acid (1 mL, 0.6 M in DMF) and DIC (0.2 mL, 50 % *v/v* in DMF) for 20 minutes at RT on the shaker. The resin was washed again with DMF (3 x 2 mL) and amine displacement and bromoacetylation steps repeated until the final sub-monomer had been added and the desired linear peptoid precursor had been obtained. The resin was shrunk in diethyl ether to remove DMF in preparation for cleavage (7.12.2). If required, the products on resin were stored at -18 ˚C.

7.9.2 Off-resin cyclisation

The linear peptoid precursors were made as above and cleaved from 2-chlorotrityl chloride resin (as in 7.12.2) to yield the protected linear peptoid. Crude peptoids were used without further purification. Typically the linear peptoid (100 μmol) was dissolved in dry, deoxygenated DMF (10 mL) and added dropwise to a solution of PyBOP (4 eq. with respect to the crude linear peptoid) and DIPEA (4 eq.) in the minimum amount of DMF over 5 hours. The reaction was allowed to proceed for a further hour at room temperature under an inert atmosphere. The solvent was removed *in vacuo* and diluted with DCM (20 mL) and HCl (0.2M, 20 mL). The crude peptoids were extracted using DCM (2 x 20 mL). The organic phases were combined, washed with water and dried over MgSO$_4$ before filtration and solvent removal *in vacuo*. The resulting residue was dissolved in 50 % MeCN in H$_2$O and lyophilised. The protected peptoids were then dissolved in 50 % MeCN in H$_2$O and purified by preparative RP-HPLC; flow rate = 2 mL min^{-1}; injection made at 50 % B and a linear gradient elution 50–100 % solvent B over 60 minutes (solvent A = 0.1 % TFA in 95 % H$_2$O, 5 % MeCN, solvent B = 0.1 % TFA in 5 % H$_2$O, 95 % MeCN). Relevant fractions were collected, lyophilised and analysed by LC-MS. The crude products were deprotected using 50 % TFA in DCM for 30 minutes and the cleavage cocktail then evaporated using a stream of N$_2$. The crude products were dissolved in ~1.5 mL (95 % H$_2$O, 5 % MeCN, 0.1 % TFA) and purified by preparative RP-HPLC flow rate = 2 mL min^{-1}; linear gradient elution 0–50 % solvent B over 60 minutes, then 50–100 % B over 15 minutes. Relevant fractions were collected, lyophilised and analysed by LC-MS.

7.10 Arginine-type peptoids

7.10.1 Synthesis of polyarginine peptoids

For the synthesis of polyarginine peptoids (where all lysine residues are transformed to the guanidine group of arginine residues), the peptoids were made, as in 7.3.1 via manual SPPS, using *N*Lys or *N*ae submonomers, cleaved from the resin and purified using RP-HPLC (section 7.13.1) to afford the unprotected, linear amino-functionalised peptoid. Guanidinylation of the free primary amine chains was undertaken using pyrazole-1-carboxamidine hydrochloride (4 eq. per free amine, with respect to the crude peptoid) and DIPEA (4 eq. per amine), which were dissolved in the minimum amount of DMF and added to the peptoid. The reaction was stirred at room temperature for 6 hours. A mixture of TFA : H$_2$O 10 : 90 was added to quench the reaction until a neutral pH was achieved. The solvent was removed *in vacuo*, the residue dissolved in acidified H$_2$O (0.1 % TFA) and lyophilised before purification using protocol 7.13.1.

7.10.2 On-resin synthesis of mixed *N*Lys and *N*Arg type peptoids

To introduce arginine-type residues during the submonomer procedure, the appropriate unprotected diamine was added under normal submonomer coupling conditions (1.5 M amine in DMF, 60 minutes, RT) in place of the mono-*N*-Boc diamine and the resin washed with DMF (3 x 2 mL). Dde-OH (10 eq. wrt resin in the minimum volume of DMF) was added to the resin and placed on the shaker at RT for 60 minutes and the resin washed well with DMF (3 x 2 mL). Subsequent peptoid couplings were made as normal until the desired sequence was achieved, including any extra Dde-protected residues.

After synthesis of the linear peptoid sequence, on resin deprotection of the Dde group was undertaken using 2 % hydrazine in DMF (4 x 4 mL x 3 mins) and the resin washed with DMF (3 x 2 mL). Guanidinylation of the free amines was achieved using pyrazole-1-carboxamidine (6 eq. per free amine, in the minimum amount of DMF) and DIPEA (6 eq. per free amine) on the shaker at 400 rpm, RT for 60 minutes. The resin was washed with DCM (3 x 2 mL) and shrunk in ether prior to cleavage from the resin (section 7.12)

7.10.3 Synthesis of cyclic mixed *N*Lys and *N*Arg type peptoids

2-chlorotrityl chloride resin (0.1 mmol, typical loading 1.22 mmol g^{-1}) was swollen in dry DCM (45 minutes, at RT) in a 20 mL polypropylene syringe fitted with two polyethylene frits. The resin was washed with dry DCM (3 x 2 mL) and loaded with bromoacetic acid (1 mL, 0.6 M in DMF) and neat DIPEA (16 eq. with respect to the resin) for 30 minutes at RT on a shaker at 400 rpm. The resin was washed with DMF (3 x 2 mL), before the desired amine sub-monomer was added (1 mL, 1.5 M in DMF) and allowed to react for 60 minutes at RT on the shaker. The resin was again washed with DMF (3 x 2 mL) and the resin was treated with bromoacetic acid (1 mL, 0.6 M in DMF) and DIC (0.2 mL, 50 % *v/v* in DMF) for 20 minutes at RT on the shaker. The resin was washed again with DMF (3 x 2 mL) and amine displacement and bromoacetylation steps repeated until the final sub-monomer had been added and the desired linear peptoid precursor had been obtained. The resin was shrunk in ether prior to cleavage. Final cleavage from resin was achieved using HFIP (4 mL, 20 % *v/v* in DCM) for 30 minutes. The resin was removed by filtration and the cleavage cocktail sparged off using a fine stream of N$_2$. The crude product was precipitated in diethyl ether (15 mL) and the precipitate retrieved by centrifuge for 15 min at 5,000 rpm. The ether phase was decanted, the crude, protected product dissolved in a mixture of acidified H$_2$O (0.1 % TFA) and MeCN then lyophilised.

Crude peptoids were cyclised in solution without further purification. Typically, the linear peptoid (100 µmol) was dissolved in dry DMF (10 mL) and added dropwise to a solution of PyBOP and DIPEA (both 6 eq. with respect to the crude linear peptoid, in 10 mL DMF) over 8 hours. The reaction was allowed to proceed for a further 60 minutes at room temperature following the last addition. The DMF solvent was removed *in vacuo* and the crude peptoids were extracted using DCM (2 x 20 mL). The organic phases were combined, washed with water and dried over MgSO$_4$ before filtration and solvent

removal *in vacuo*. The resulting residue was dissolved in 50 % MeCN in H_2O and lyophilised.

The protected peptoids were then dissolved in 50 % MeCN in H_2O and purified by preparative RP-HPLC; flow rate = 2 mL min^{-1}; injection made at 50 % B and a linear gradient elution 50–100 % solvent B over 60 minutes (solvent A = 0.1 % TFA in 95 % H_2O, 5 % MeCN, solvent B = 0.1 % TFA in 5 % H_2O, 95 % MeCN). Relevant fractions were collected, lyophilised and analysed by LC-MS.

At this stage, any Dde-groups were removed using 2 % hydrazine in DMF (4 x 4 mL x 3 mins) and then the resin washed with DMF (3 x 2 mL). Guanidinylation of the free amines was undertaken using pyrazole-1-carboxamidinee (6 eq. per free amine, in the minimum amount of DMF) and DIPEA (6 eq. per free amine) on the shaker at 400 rpm, RT for 60 minutes. The cyclic peptoids were then deprotected using 95 : 2.5 : 2.5 TFA : H2O : TIPS (4 mL) for 1.5 hours. The cleavage cocktail was removed *in vacuo*, the crude product precipitated in diethyl ether (45 mL) and the precipitate retrieved by centrifuge for 15 min at 5,000 rpm. The ether phase was decanted, the crude product dissolved in a mixture of acidified H_2O (0.1 % TFA) and MeCN and lyophilised prior to final purification by RP-HPLC (section 7.13.1).

7.11 Peptide synthesis

Fmoc SPPS procedures are detailed in the following sections. Resin swelling was undertaken in a fritted polypropylene reaction vessel (Crawford Scientific) in DMF for a minimum of 1 h (overnight preferred), followed by washing with DMF. Amino acid side chain functionality was protected as follows: FmocArg(Pbf)OH, FmocAsn(Trt)OH, FmocAsp(tBu)OH, FmocCys(Trt)OH, FmocGln(Trt)OH, FmocGlu(tBu)OH, FmocHis(Trt)OH, FmocLys(Boc)OH, FmocSer(tBu)OH, FmocThr(tBu)OH, FmocTrp(Boc)OH and FmocTyr(tBu)OH. Fmoc deprotections were carried out using a 20 % (*v/v*) solution of piperidine in DMF.

7.11.1 Automated peptide synthesis

Automated SPPS was carried out on a CEM Liberty 1 single channel microwave peptide synthesizer equipped with a Discover microwave unit. All reactions were carried out using the 30 mL PTFE reaction vessel, with microwave heating and agitation by bubbling N_2. Couplings were carried out using Fmoc protected amino acid (5 eq.), DIC (10 eq., 0.8 M solution of DIC in DMSO), HOBt (20 eq., 0.5 M solution of HOBt in DMF). For double couplings the reaction vessel was drained after each cycle and fresh reagents were added. Microwave couplings at 0.10 mmol scale were carried out for 10 min at 75 °C and 25 W power unless otherwise stated. Cys and His residues were coupled at low temperature: 10 min at room temperature followed by 10 min at 50 °C (25 W). Arg

residues were double coupled, with the first coupling carried out for 45 min at RT followed by 5 min at 75 ˚C (25 W), and the second using the standard microwave conditions given. Room temperature reactions were carried out using 2 x 1 h couplings (3 x 1 h for Arg residues). The Fmoc group was removed by two successive treatments with piperidine solution (5 min then 10 min). Automated SPPS was continued until the sequence was complete.

7.11.2 Manual peptide synthesis

Manual peptide synthesis was only used for additions of several amino acids to a peptide or peptoid sequence. The linear peptoid was synthesised via manual or automated SPPS as previously described. The sequence on resin was swollen in DMF in a polypropylene syringe fitted with a polyethylene frit (at least 1 hour, overnight preferred, at room temperature). PyBOP (4 eq. with respect to the resin), the Fmoc-protected amino acid (4 eq.) and DIPEA (4 eq.) were dissolved in the minimum DMF and left to preactivate for several minutes, before being added to the resin and placed on the shaker at 400 rpm at room temperature for 1 hour. The resin was then washed with DMF (3 x 2 mL) and deprotected using piperidine (20 % in DMF *v/v*, 2 x 20 min) and washed as before. Further amino acid couplings and Fmoc-deprotection steps were made as necessary. The resin was washed with DMF (3 x 2 mL) and resin cleavage (section 7.12.1) and RP-HPLC purification (section 7.13.1) was undertaken as before.

7.12   Cleavage protocols from acid-labile resins

7.12.1 Rink Amide resin

Final cleavage from resin was achieved using TFA (95 %), H_2O (2.5 %) and TIPS (2.5 %). For test cleaves approximately 1 mL of the cleavage cocktail was used and for cleavage from 100 mg resin, approximately 4 mL of the cleavage cocktail was added. The resin was then placed on the shaker at 400 rpm for 1.5 hours[*] and the resin removed by filtration. The cleavage cocktail was removed *in vacuo*, the crude product precipitated in diethyl ether (45 mL) and the precipitate retrieved by centrifuge for 15 min at 5,000 rpm. The ether phase was decanted, the crude product dissolved in a mixture of acidified H_2O and MeCN and lyophilised.

---

[*] Cleavage times depended on the particular sequence. For peptoids with only Boc protection cleavage of 45 minutes was adequate. For peptide sequences containing Arg(Pbf) cleavage times of around 6 hours were necessary.

7.12.2 2-Chlorotrityl chloride resin

Final cleavage from resin was achieved using hexafluoroisopropanol in DCM (20 % *v/v*). For test cleaves approximately 1 mL of the cleavage cocktail was used and for cleavage from 100 mg resin, approximately 4 mL of the cleavage cocktail was added. The resin was then placed on the shaker at 400 rpm for 30 minutes and the resin removed by filtration. The cleavage cocktail was evaporated using a stream of N_2, the crude product dissolved in a mixture of H_2O and MeCN and lyophilised.

7.13   Purification protocols

7.13.1 Preparative high performance liquid chromatography

Crude peptoids were dissolved into ~1.5 mL (95 % H_2O, 5 % MeCN, 0.1 % TFA) and purified by preparative RP-HPLC using a Perkin Elmer 200 Series LC pump with a Perkin-Elmer 785A UV-vis detector (λ = 250 nm or 220 nm) on a SB Analytical column (ODS-H Optimal), 250 x 10 mm, 5 μm; flow rate = 2 mL min^{-1}; typical linear gradient elution 0–50 % solvent B over 60 minutes, then 50–100 % B over 15 minutes (solvent A = 0.1 % TFA in 95 % H_2O, 5 % MeCN, solvent B = 0.1 % TFA in 5 % H_2O, 95 % MeCN). The gradients chosen were informed by the analytical HPLC retention times of crude products. Relevant fractions were collected, lyophilised and analysed by LC-MS.

7.13.2 Analytical high performance liquid chromatography

Samples were dissolved in 100 μL acidified water and the purity of products was estimated by an injection of 10 μL to analytical RP-HPLC using a Perkin Elmer 200 Series LC pump with a Perkin-Elmer 785A UV-vis detector on an SB Analytical column (ODS-H Optimal), 4.6 x 100mm , 3.5 μm; flow rate = 1 mL min^{-1}; loop size = 20 μL; λ = 220 nm; gradient: 0–100 % solvent B over 30 min (solvent A: 95 % H_2O, 5 % MeCN, 0.05 % TFA; solvent B: 95 % MeCN, 5 % H_2O, 0.03 % TFA).

## 7.14   Preparation of amines for peptoid synthesis

Most amines were commercially available in a useable form (see appendix for table of amine submonomers). Amines that needed treatment or protection before use are described below.

### 7.14.1 Freebasing of ^{t}Bu-β-alanine (127) *N*Glu(^{t}Bu)

127
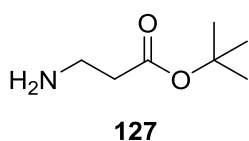
Commercially available ^{t}Bu β-alanine HCl (5.04 g, 27.7 mmol) was dissolved in DCM (15 mL) and neutralised using NaOH (1M, approximately 100 mL). The organic phase was separated and dried over Na$_2$SO$_4$, filtered and the solvent removed from the filtrate *in vacuo* to yield ^{t}Bu β-alanine as a clear oil (2.7 g, 67 %). The product was used without further characterisation or purification.

7.14.2 Trityl protection of thioethylamine (128) *N*Cys(Trt)

128
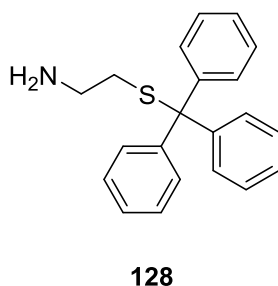
Protocol followed as in the literature[2] and product also commercially available. Thioethylamine HCl (3.00 g, 264 mmol) was dissolved in TFA (50 mL) and cooled to 0 °C. Triphenylmethanol (7.72 g, 264 mmol) was added and the reaction stirred for 3 hours. The TFA was diluted in water (100 mL) and neutralised using solid NaHCO$_3$ (1 M). DCM was added (100 mL) and the organic phase was separated, dried over MgSO$_4$, filtered and the chloroform removed from the filtrate *in vacuo*. The 2-(tritylsulfanyl)ethanamine was found as a white powder and used without further purification (3.01 g, 36 %); ^{1}H NMR (400 MHz, CDCl$_3$) δ 2.47 (4H, s, C*H$_2$*), 7.22–7.45 (15H, m, Ar-*H*); ^{13}C NMR (400 MHz, CDCl$_3$) δ 33.17, 39.84, 66.93, 126.88, 128.04, 129.49, 144.49; IR (cm^{-1}) 3018 (N-H), 1676, 1142, 753, 699; LCMS (ESI-TQD) *m/z*: [M+H]$^+$ mass calculated: 319.1, [2M+H]$^+$ mass observed: 639.2.

7.14.3 Synthesis of *N*-Boc-1,4-diaminobutane (129) *N*Lys(Boc)
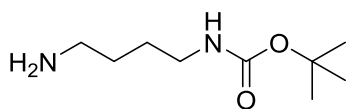
1,4-diaminobutane (17.60 g, 200 mmol) was dissolved in chloroform (100 mL) and cooled to 0 °C. Di-*tert*-butyl dicarbonate (4.40 g, 20 mmol) was dissolved in chloroform (200 mL) and added to the 1,4-diaminobutane solution at 0 °C dropwise over 6 hours. The mixture was then stirred at room temperature for a further 18 hours and washed with deionised water (8 x 200 mL) until the organic phase became clear. The organic phase was separated and dried over MgSO$_4$, filtered and the chloroform removed from the filtrate *in vacuo* to yield *N*-Boc 1,4-diaminobutane as a clear, yellow oil (2.10 g, 76 %); ^{1}H NMR (400 MHz, D$_2$O) δ 1.43–1.48 (9H + 4H, m, C*H*$_3$ + C*H*$_2$), 2.60 (2H, t, *J* 8.0, NH$_2$C*H*$_2$CH$_2$-), 3.06 (2H, t, *J* 8.0, -CH$_2$C*H*$_2$NHBoc); ^{13}C NMR (400 MHz, D$_2$O) δ 26.5, 27.8 (*C*H$_3$), 29.1, 39.9, 40.3, 80.6 (*C*(CH$_3$)$_3$), 158.2 (*C*=O); IR (neat, cm^{-1}) 3345 (N-H), 2960, 2915, 2850, 1700 (C=O), 1560, 1545, 1525, 1475, 1270, 860; LCMS (ESI-TQD) *m/z*: [M+H]$^+$ mass calculated: 188.3, mass observed: 188.7.

7.14.4 Attempted Synthesis of *N*-Dde-1,4-diaminobutane (145) *N*Lys(Dde)
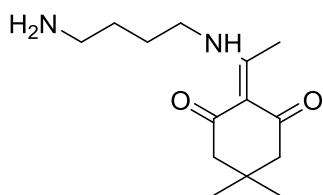
1,4 diaminobutane (2.42 g, 27.44 mmol) was dissolved in chloroform or DCM (100 mL) and cooled to 0 °C. 2-acetyldimedone (0.50 g, 2.74 mmol) was dissolved in chloroform or DCM (100 mL) and added to the amine solution at 0 °C dropwise over 1, 6 or 10 hours. The mixture was then stirred at room temperature for a further 18 hours and washed with deionised water until the organic phase became clear. The organic phase was separated and dried over MgSO$_4$, filtered and the chloroform removed from the filtrate *in vacuo*. The resulting mixture of mono and di-protected 1,4-diaminobutane was separated using silica column chromatography in DCM/MeOH. The mono product **145** was not isolated, only diprotected *N*-*N*-Dde-,4-diaminobutane **146** as a white powder (0.88 g, 77 %); ^{1}H NMR (400 MHz, CDCl$_3$) δ 0.98 (12H, s, C*H*$_3$), 1.79 (4H, m, NHCHC*H*$_2$C*H*$_2$CHNH), 2.31 (8H, s, C*H*$_2$), 2.51 (6H, s, C*H*$_3$), 3.42 (4H, NHC*H*$_2$CH$_2$CH$_2$C*H*$_2$NH), 13.51 (2H, br s, N*H*CH$_2$CH$_2$CH$_2$CH$_2$N*H*); ^{13}C NMR (400 MHz, CDCl$_3$) δ 17.85, 26.45, 28.23, 30.04, 42.78, 52.82, 107.90, 173.53, 197.88; LCMS (ESI-TQD) *m/z*: [M+H]$^+$ mass calculated: 418.6, mass observed: 418.9.

7.15   Nisin-tagged Peptoids

Click reactions to tag peptoid sequences with nisin[A/B] ring fragments were undertaken at the University of Utrecht with Professor Nathaniel Martin and assisted by Laurens Kleijn.

7.15.1 Digestion of nisin to nisin[A/B] ring fragments

Nisin (600 mg, 0.18 mmol) was dissolved in 250 mL Tris buffer (25 mmol, NaOAc, 5 mmol Tris acetate, 5 mmol $CaCl_2$, pH 7.0) and the solution cooled on ice for 15 minutes. Trypsin (50 mg) was added and stirred at room temperature for 15 minutes. The mixture was then heated to 30 °C for 16 hours, then another 50 mg of trypsin was added and after an additional 24 hours the reaction was complete by HPLC. The reaction was acidified with HCl (1 M) to pH 4.0 and solvents removed *in vacuo*. The nisin fragment was isolated by preparative HPLC and product fractions lyophilised to obtain a white powder (80 mg, 39 %).[3]

7.15.2 Amide-coupled azide-nisin[A/B]

Nisin[A/B] was dissolved in DMF (240 µL). BOP (2 eq.), DIPEA (4 eq.) and azidopropylamine (50 eq.) were added. The reaction was stirred for 20 minutes then quenched in the appropriate buffer (95 % H_2O, 5 % MeCN, 0.1 % TFA, 4 mL). The solution was centrifuged for 5 min at 5,000 rpm to remove any insoluble material and the supernatant was purified by RP-HPLC. Relevant fractions were collected and analysed to yield the pure Nisin[A/B]-azide.[3]

7.15.3 Click protocol of alkyne-peptoids with nisin[A/B]-azide

10x stock solutions of $CuSO_4$ (16.2 µmol, 2.59 mg in 1 mL H_2O), 10x sodium ascorbate (32.4 µmol, 6.42 mg in 1 mL H_2O) and 10x TBTA (4.1 µmol, 2.18 mg in 1 mL DMF) were freshly prepared. Nisin[A/B]-azide (1 eq., 8.1 µmol, 10 mg) was dissolved in 200 µL DMF and added to the peptoid in the microwave reaction vessel (1 eq., 8.1 µmol). 100 µL of the $CuSO_4$ solution (0.2 eq., 1.62 µmol), 100 µL of sodium ascorbate stock (0.4 eq., 3.24 µmol) and 100 µL of the TBTA solution (0.05 eq., 0.41 µmol) were added. The vessel was sealed and heated under microwave power for 20 minutes at 80 °C. The reaction mixture was diluted in the appropriate buffer (95 % H_2O, 5 % MeCN, 0.1 % TFA, 4mL) and purified by RP-HPLC on a Reprospher 100 C8- or C18- Aqua column (10 µm x 250 x 20 mm) at a flow rate of 6 mL min^{-1}; λ = 214 nm; linear gradient elution 20–80 % solvent B over 120 minutes (where A = 95 % H_2O, 5 % MeCN, 0.1 % TFA; B = 95 % MeCN, 5 % H_2O, 0.1 % TFA). Relevant fractions were combined and lyophilised from 1 : 1 H_2O : ^{t}BuOH mixture to yield purified peptoid-peptide conjugates as a white powder.

Products

A table to illustrate the monomers used in this library, their abbreviation code and the amine submonomer they are derived from can be found in **Table A1** in the appendix. These monomers are also listed on www.pep-calc.com/peptoid, which is a useful tool for the calculation of peptoid molecular weights or molecular formulae. Yields are expressed as an overall yield calculated from the initial scale of resin used and final amount of pure peptoid obtained. If the whole crude peptoid was not purified, yields are calculated in the same way, but taking account of the proportion of crude product that was purified.

7.15.4 Linear peptoid sequences

Peptoids were synthesised using the submonomer method of peptoid synthesis on Rink Amide resin (typical loading 0.79–0.82 mmol g^{-1}, 0.1 mmol scale) as outlined by the protocol section 7.3 (or section 7.10 for those sequences containing *N*nArg, *N*Arg or *N*hArg) and cleaved from the resin using protocol 7.12.1 to afford the crude deprotected sequence. The crude sample, or a portion of, was purified by procedure 7.13.1 and pure fractions combined to yield the peptoid as a powder. Characterisation data is shown in **Table 7.1** for these sequences.

#	Sequence	Analytical HPLC		Accurate Mass Spectrometry		Yield[†]	
		Retention time[‡] (min)	Approx. purity (%)	Mass calculated	Mass observed	(%)	(mg)
210	(*Nah*N*phe*N*phe*)$_4$	15.8	> 50	[M+2H]$^{2+}$ 910.0473	910.0468	15	15
211	(*Nah*N*phe*N*phe*)$_3$	15.2	> 75	[M+2H]$^{2+}$ 684.9157	684.9141	17	13
212	(*Nah*N*phe*N*phe*)$_2$	14.2	> 50	[M+H]$^+$ 918.5605	918.5634	26	13
186	(*NLys*N*phe*N*phe*)$_4$	16.6	> 99	[M+2H]$^{2+}$ 853.9847	853.9835	24	25
187	(*NLys*N*phe*N*phe*)$_3$	15.4	> 85	[M+2H]$^{2+}$ 642.8688	642.8666	29	22
188	(*NLys*N*phe*N*phe*)$_2$	14.1	> 85	[M+2H]$^{2+}$ 431.7529	431.7513	58	30
180	(*Nae*N*phe*N*phe*)$_4$	15.3	> 99	[M+2H]$^{2+}$ 797.9221	797.9189	22	21
213	(*Nae*N*phe*N*phe*)$_3$	15.8	> 80	[M+2H]$^{2+}$ 600.8218	600.8185	49	35
214	(*Nae*N*phe*N*phe*)$_2$	14.4	> 80	[M+H]$^+$ 806.4354	806.4370	45	22
215	(*Nah*N*spe*N*spe*)$_4$	17.7	> 95	[M+2H]$^{2+}$ 966.6115	966.6127	14	15
216	(*Nah*N*spe*N*spe*)$_3$	16.8	> 95	[M+2H]$^{2+}$ 726.9627	726.9601	16	12
217	(*Nah*N*spe*N*spe*)$_2$	15.2	> 75	[M+2H]$^{2+}$ 974.6232	974.6246	23	12
185	(*NLys*N*spe*N*spe*)$_6$	19.2	> 95	[M+2H]$^{2+}$ 1360.8119	1360.8058	14	57
22	(*NLys*N*spe*N*spe*)$_4$	17.6	> 99	[M+2H]$^{2+}$ 910.0473	910.0483	38	15
26	(*NLys*N*spe*N*spe*)$_3$	17.0	> 95	[M+2H]$^{2+}$ 684.9157	684.9142	34	28
25	(*NLys*N*spe*N*spe*)$_2$	14.4	> 99	[M+2H]$^{2+}$ 459.7842	459.7801	36	20
156	(*Nae*N*spe*N*spe*)$_4$	16.0	> 95	[M+2H]$^{2+}$ 853.9847	853.9841	18	13
218	(*Nae*N*spe*N*spe*)$_3$	17.0	> 95	[M+2H]$^{2+}$ 642.8688	642.8660	37	11
219	(*Nae*N*spe*N*spe*)$_2$	14.1	> 95	[M+2H]$^{2+}$ 862.4980	862.4994	48	25
220	(*NLys*N*pmb*N*pmb*)$_4$	16.5	> 99	[M+2H]$^{2+}$ 974.0269	974.0264	7	13
221	(*NLys*N*pmb*N*pmb*)$_3$	15.9	> 90	[M+2H]$^{2+}$ 1464.7931	1464.7937	6	8
222	(*NLys*N*pmb*N*pmb*)$_2$	14.4	> 75	[M+2H]$^{2+}$ 982.5402	982.5395	52	51
184	(*NLys*N*pcb*N*pcb*)$_4$	20.6	> 99	[M+2H]$^{2+}$ 989.8288	989.8279	22	43
223	(*NLys*N*pcb*N*pcb*)$_3$	19.5	> 99	[M+H]$^+$ 1490.4945	1490.4976	21	31
224	(*NLys*N*pcb*N*pcb*)$_2$	17.9	> 95	[M+H]$^+$ 998.3420	998.3422	28	28
225	(*NLys*N*pfb*N*pfb*)$_4$	17.5	> 95	[M+2H]$^{2+}$ 1850.8861	1850.8865	18	33

[†] Yield is expressed as an overall yield calculated from the final mass recovered following RP-HPLC purification and expressed as a percentage of the original scale of resin used.
[‡] Gradient, solvents and conditions for analytical HPLC as described in section 7.13.2.

226	$(N\text{Lys}N\text{pfb}N\text{pfb})_3$	16.7	> 95	$[\text{M+H}]^+$ 1392.6732	1392.6732	11	15
227	$(N\text{Lys}N\text{pfb}N\text{pfb})_2$	15.0	> 95	$[\text{M+2H}]^+$ 934.4603	934.4601	14	13
228	$(N\text{Lys}N\text{mfb}N\text{mfb})_4$	17.0	> 95	$[\text{M+2H}]^{2+}$ 925.9470	925.9431	34	63
229	$(N\text{Lys}N\text{mfb}N\text{mfb})_3$	16.4	> 95	$[\text{M+H}]^+$ 1392.6732	1392.6746	47	66
230	$(N\text{Lys}N\text{mfb}N\text{mfb})_2$	15.1	> 95	$[\text{M+H}]^+$ 934.4603	934.4610	32	30
183	$(N\text{Lys}N\text{pfb}N\text{spe})_4$	17.6	> 95	$[\text{M+2H}]^{2+}$ 917.9971	917.9981	14	15
231	$(N\text{Lys}N\text{pfb}N\text{spe})_3$	16.6	> 95	$[\text{M+H}]^+$ 1380.7484	1380.7505	21	29
232	$(N\text{Lys}N\text{pfb}N\text{spe})_2$	15.1	> 95	$[\text{M+2H}]^{2+}$ 926.5104	926.5111	26	24
157	$[(N\text{Lys}N\text{pfb}N\text{pfb})(N\text{Lys}N\text{spe}N\text{spe})]_2$	18.4	> 95	$[\text{M+2H}]^{2+}$ 917.9971	917.9983	27	50
233	$(N\text{Lys}N\text{spe}N\text{spe})(N\text{Lys}N\text{pfb}N\text{pfb})(N\text{Lys}N\text{spe}N\text{spe})$	16.5	> 80	$[\text{M+H}]^+$ 1376.7736	1376.7734	23	32
234	$(N\text{Lys}N\text{pfb}N\text{pfb})(N\text{Lys}N\text{spe}N\text{spe})$	15.7	> 80	$[\text{M+H}]^+$ 926.5104	926.5096	28	26
235	$(N\text{Lys}N\text{nVal}N\text{spe})_4$	14.8	> 50	$[\text{M+H}]^+$ 1571.0242	1571.0286	41	64
236	$(N\text{Lys}N\text{nVal}N\text{spe})_3$	14.0	> 95	$[\text{M+H}]^+$ 1182.7767	1182.7771	45	53
237	$(N\text{Lys}N\text{nVal}N\text{spe})_2$	12.7	> 95	$[\text{M+H}]^+$ 794.5992	794.5280	33	26
238	$(N\text{Lys}N\text{Leu}N\text{spe})_4$	16.1	> 99	$[\text{M+H}]^+$ 1627.0868	1627.0897	44	71
239	$(N\text{Lys}N\text{Leu}N\text{spe})_3$	15.4	> 99	$[\text{M+H}]^+$ 1224.8236	1224.8247	20	24
240	$(N\text{Lys}N\text{Leu}N\text{spe})_2$	14.0	> 99	$[\text{M+H}]^+$ 822.5605	822.5604	35	29
182	$(N\text{Lys}N\text{hLeu}N\text{spe})_4$	17.7	> 99	$[\text{M+2H}]^{2+}$ 842.0786	842.0757	18	12
241	$(N\text{Lys}N\text{hLeu}N\text{spe})_3$	17.2	> 90	$[\text{M+2H}]^{2+}$ 1266.8706	1266.8696	18	22
242	$(N\text{Lys}N\text{hLeu}N\text{spe})_2$	15.4	> 95	$[\text{M+H}]^+$ 850.5919	850.5925	21	18
243	$(N\text{amy}N\text{spe}N\text{spe})[(N\text{Lys}N\text{spe}N\text{spe})]_3$	19.4	> 99	$[\text{M+2H}]^{2+}$ 909.5497	909.5507	18	20
244	$(N\text{amy}N\text{spe}N\text{spe})_2(N\text{Lys}N\text{spe}N\text{spe})_2$	22.7	> 95	$[\text{M+2H}]^{2+}$ 909.0521	909.0528	8	9
245	$[(N\text{amy}N\text{spe}N\text{spe})(N\text{Lys}N\text{spe}N\text{spe})]_2$	22.8	> 95	$[\text{M+2H}]^{2+}$ 909.5536	909.5457	8	9
246	$(N\text{Lys}N\text{spe}N\text{spe})_2(N\text{amy}N\text{spe}N\text{spe})(N\text{Lys}N\text{spe}N\text{spe})$	20.0	> 90	$[\text{M+2H}]^{2+}$ 909.5497	909.5483	11	12
293	$(N\text{hArg}N\text{phe}N\text{phe})_4$	16.7	> 99	$[\text{M+2H}]^{2+}$ 938.0283	938.0276	32	12
294	$(N\text{hArg}N\text{phe}N\text{phe})_2$	14.6	> 95	$[\text{M+H}]^+$ 946.5416	946.5424	23	30
152	$(N\text{hArg}N\text{spe}N\text{spe})_4$	17.9	> 99	$[\text{M+2H}]^{2+}$ 994.0909	994.0880	46	34
295	$(N\text{hArg}N\text{spe}N\text{spe})_3$	17.3	> 95	$[\text{M+2H}]^{2+}$ 1494.8890	1484.8894	43	19
153	$(N\text{hArg}N\text{mfb}N\text{mfb})_4$	17.3	> 99	$[\text{M+2H}]^{2+}$ 1009.9906	1009.9874	41	23
296	$(N\text{hArg}N\text{mfb}N\text{mfb})_3$	16.7	> 95	$[\text{M+H}]^+$ 1518.7386	1518.7372	60	26
181	$(N\text{hArg}N\text{hLeu}N\text{spe})_4$	18.3	> 95	$[\text{M+2H}]^{2+}$ 926.1222	926.1262	82	30
297	$(N\text{hArg}N\text{hLeu}N\text{spe})_3$	17.2	> 90	$[\text{M+H}]^+$ 1392.9360	1392.9371	36	27
154	$[(N\text{amy}N\text{spe}N\text{spe})(N\text{hArg}N\text{spe}N\text{spe})]_2$	22.4	> 99	$[\text{M+2H}]^{2+}$ 951.0739	951.0692	22	40

147	(NLysNspeNspe)₂(NhArgNspeNspe)₂	16.6	> 95	[M+2H]²⁺ 952.0691	952.0682	5	6
147	(*N*Lys*N*spe*N*spe)₂(*N*hArg*N*spe*N*spe)₂	16.6	> 95	[M+2H]²⁺ 952.0691	952.0682	5	6
148	(*N*hArg*N*spe*N*spe)₂(*N*Lys*N*spe*N*spe)₂	16.9	> 99	[M+2H]²⁺ 952.0691	952.0693	7	13
149	(*N*Lys*N*spe*N*spe)(*N*hArg*N*spe*N*spe)(*N*Lys*N*spe*N*spe)₂	17.8	> 99	[M+2H]²⁺ 931.0582	931.0579	3	8
150	[(*N*hArg*N*spe*N*spe) (*N*Lys*N*spe*N*spe)]₂	16.6	> 99	[M+2H]²⁺ 952.0691	952.0730	4	8
151	[(*N*nArg*N*spe*N*spe)(*N*ae*N*spe*N*spe)]₂	18.9	> 99	[M+2H]²⁺ 896.0038	896.0026	19	41
155	(*N*nArg*N*spe*N*spe)₄	19.1	> 99	[M+2H]²⁺ 938.0283	938.0297	13	30
247	(*N*ae*N*spe*N*dfea)(*N*ae*N*phe*N*dfea)₃	14.4	> 99	[M+2H]²⁺ 752.8609	752.8582	25	17
248	(*N*ae*N*spe*N*ea)(*N*ae*N*phe*N*ea)₃	13.6	> 99	[M+2H]²⁺ 680.8986	680.8969	19	25
249	(*N*ae*N*spe*N*ea)₄	14.5	> 99	[M+2H]²⁺ 701.9221	701.9249	28	16
250	(*N*ae*N*phe*N*ea)2(*N*ae*N*spe*N*ea)(*N*ae*N*phe*N*ea)	13.4	> 99	[M+H]⁺ 1360.7894	1360.7881	41	18
251	(*N*ae*N*phe*N*dfea)2(*N*ae*N*spe*N*dfea)(*N*ae*N*phe*N*dfea)	14.3	> 99	[M+H]⁺ 1504.7140	1504.7124	36	38
252	(*N*ae*N*pfb*N*spe)₄	17.8	> 99	[M+H]⁺ 1722.8643	1722.8632	25	9
253	[(*N*ae*N*pfb*N*pfb)(*N*ae*N*spe*N*spe)]₂	18.0	> 99	[M+2H]²⁺ 861.9345	861.9322	18	5
254	(*N*Lys*N*pfb*N*Lys*N*spe)₃	13.4	> 99	[M+H]⁺ 1765.0333	1765.0327	14	9
255	(*N*ae*N*pfb*N*ae*N*spe)₃	13.7	> 95	[M+H]⁺ 1596.8456	1596.8475	32	18
256	(*N*Lys*N*pfb*N*rpe)₄	17.6	> 99	[M+2H]²⁺ 917.9971	917.9981	16	13
257	(*N*ae*N*pfb*N*rpe)₄	18.0	> 99	[M+2H]²⁺ 861.9345	861.9346	14	8
258	[(*N*ae*N*pfb*N*spe)(*N*Lys*N*pfb*N*spe)]₂	17.9	> 99	[M+2H]²⁺ 899.9658	899.9665	32	14
259	(*N*Lys*N*spe)₆	13.7	> 99	[M+2H]²⁺ 877.0582	877.0576	31	14
260	(*N*ae*N*spe)₆	14.1	> 99	[M+2H]²⁺ 792.9643	792.9655	48	21
261	(*N*Lys*N*dfb*N*spe)₄	17.9	> 99	[M+H]⁺ 1906.9487	1906.9468	17	6
262	(*N*ae*N*dfb*N*spe)₄	18.7	> 95	[M+2H]²⁺ 897.9157	897.9141	53	16
263	(*N*Lys*N*sfb*N*sfb)₄	18.7	> 99	[M+H]⁺ 1963.0114	1963.0105	23	7
264	(*N*ae*N*sfb*N*sfb)₄	19.5	> 99	[M+2H]²⁺ 925.9470	925.9482	43	16
265	(*N*Lys*N*sfb*N*spe)₄	18.7	> 99	[M+2H]²⁺ 1892.0521	1892.0444	41	13
266	(*N*ae*N*tfe*N*spe)₄	16.2	> 99	[M+2H]²⁺ 809.8632	809.8655	22	18
267	(*N*ae*N*pfp*N*spe)₄	18.4	> 99	[M+2H]²⁺ 909.8592	909.8594	26	18
268	[(*N*Glu*N*pfb*N*spe)(*N*Lys*N*pfb*N*spe)]₂	19.8	> 99	[M+2H]²⁺ 918.9406	918.9448	19	21
269	(*N*Glu*N*pfb*N*spe)(*N*Lys*N*pfb*N*spe)₃	18.5	> 99	[M+2H]²⁺ 918.9725	918.9694	18	20
270	(*N*Glu*N*spe*N*spe)(*N*Lys*N*spe*N*spe)₃	18.3	> 99	[M+2H]²⁺ 910.5211	910.5221	19	21
271	(*N*Glu*N*spe*N*spe)(*N*Lys*N*spe*N*spe)₂(*N*Glu*N*spe*N*spe)	20.4	> 99	[M+2H]²⁺ 910.9949	910.9929	18	9
272	(*N*Lys*N*spe*N*spe)(*N*Glu*N*spe*N*spe)₂(*N*Lys*N*spe*N*spe)	20.0	> 90	[M+2H]²⁺ 910.9949	910.9950	35	16
273	(*N*Glu*N*spe*N*spe)₂(*N*Lys*N*spe*N*spe)₂	19.8	> 99	[M+2H]²⁺ 910.9949	910.9943	36	17

274	(*N*Glu*N*spe*N*spe)₂(Nae*N*spe*N*spe)₂	20.5	> 90	[M+H]⁺ 1764.9194	1764.9165	15	16
275	(*N*Glu*N*spe*N*spe)(Nae*N*spe*N*spe)₂(*N*Glu*N*spe*N*spe)	20.8	> 90	[M+2H]²⁺ 882.9636	882.9627	20	21
276	(Nae*N*spe*N*spe)(*N*Glu*N*spe*N*spe)₂(Nae*N*spe*N*spe)	20.5	> 95	[M+H]⁺ 1764.9196	1764.9194	38	15
277	(*N*Glu*N*spe*N*spe)(Nae*N*spe*N*spe)₃	19.5	> 95	[M+H]⁺ 1735.9404	1735.9377	39	20
278	[(*N*Glu*N*spe*N*spe)(Nae*N*spe*N*spe)]₂	20.1	> 99	[M+2H]²⁺ 882.9636	882.9604	25	16
279	[(*N*Glu*N*spe*N*spe)(*N*Lys*N*spe*N*spe)]₂	20.0	> 99	[M+2H]²⁺ 910.9949	910.9956	29	24
280	(*N*Lys*N*but*N*spe)₄	15.3	> 95	[M+2H]²⁺ 814.0439	814.0473	13	13
281	(Nae*N*but*N*spe)₄	16.9	> 99	[M+H]⁺ 1514.9615	1514.9597	26	3
282	(*N*but*N*spe*N*spe)₂(*N*Lys*N*spe*N*spe)₂	21.8	> 99	[M+2H]²⁺ 895.0364	895.0354	15	17
283	[(*N*but*N*spe*N*spe)(*N*Lys*N*spe*N*spe)]₂	22.0	> 95	[M+2H]²⁺ 895.5380	895.5336	46	11
308	(*N*but*N*spe*N*spe)₂(Nae*N*spe*N*spe)₂	21.9	> 95	[M+2H]²⁺ 867.0051	867.0031	49	11
349	[(*N*but*N*spe*N*spe)(Nae*N*spe*N*spe)]₂	21.5	> 95	[M+2H]²⁺ 867.0051	867.0063	25	26
284	(*N*Lys*N*hHis*N*spe)₄	10.8	> 90	[M+2H]²⁺ 890.0326	890.0314	32	11
285	(Nae*N*hHis*N*spe)₄	11.2	> 85	[M+2H]²⁺ 833.9657	833.9641	15	15
286	[(*N*Lys*N*spe*N*spe)(*N*Lys*N*hHis*N*spe)]₂	13.4	> 99	[M+2H]²⁺ 1799.0677	1799.0692	14	5
287	[(Nae*N*spe*N*spe)(Nae*N*hHis*N*spe)]₂	14.6	> 95	[M+2H]²⁺ 843.9752	843.9747	14	11
288	(*N*Lys*N*hTyr*N*spe)₄	14.0	> 99	[M+2H]²⁺ 942.0371	942.0366	6	4
309	(Nae*N*hTyr*N*spe)₄	14.8	> 95	[M+2H]²⁺ 885.9745	885.9759	13	8
289	[(*N*Lys*N*spe*N*spe)(*N*Lys*N*hTrp*N*spe)]₂	17.0	> 95	[M+H]⁺ 1897.1085	1897.1005	30	6
290	[(Nae*N*spe*N*spe)(Nae*N*hTrp*N*spe)]₂	17.8	> 99	[M+2H]²⁺ 892.9938	892.9956	12	6
291	[(*N*Lys*N*spe*N*spe)(*N*Lys*N*pyr*N*spe)]₂	13.4	> 99	[M+H]⁺ 1793.0459	1793.0468	30	13
310	[(Nae*N*spe*N*spe)(Nae*N*pyr*N*spe)]₂	17.8	> 99	[M+2H]²⁺ 840.9636	840.9643	17	7
292	(*N*Lys*N*hCys*N*spe)₄	14.5	> 99	[M+2H]²⁺ 821.9288	821.9265	13	11
298	(*N*Lys*N*spe*N*spe*N*spe)₃	20.0	> 95	[M+2H]²⁺ 926.5418	926.5414	26	12
344	(Nae*N*spe*N*spe*N*spe)₃	20.8	> 95	[M+2H]²⁺ 884.4949	884.4952	25	14
345	(Nae*N*meo*N*spe*N*spe)₃	17.4	> 95	[M+2H]²⁺ 815.4638	815.4620	27	27
311	(Nae*N*spe*N*moe*N*spe)₃	17.3	> 95	[M+2H]²⁺ 815.4638	815.4659	23	22
299	(*N*Lys*N*phe*N*spe)₄	16.6	> 99	[M+2H]²⁺ 882.0160	882.0151	25	27
300	(Nae*N*phe*N*spe)₄	17.2	> 95	[M+2H]²⁺ 825.9534	825.9551	14	14
301	(*N*Lys*N*rpe*N*rpe)₄	17.6	> 99	[M+2H]²⁺ 910.0473	910.0439	16	17
302	(Nae*N*rpe*N*rpe)₄	18.0	> 95	[M+2H]²⁺ 853.9847	853.9850	34	26
303	(Nae*N*rpe*N*rpe)₃	17.1	> 90	[M+2H]²⁺ 642.8688	642.8653	31	40

Table 7.1. Accurate mass spectrometry data, reverse phase analytical HPLC retention times and approximate purity for the linear peptoid library.

7.15.5 Cyclic peptoids

The cyclic peptoids shown in **Figure 7.1** and **Figure 7.2** were synthesised using the submonomer method of peptoid synthesis using 2-chlorotrityl chloride resin (loading 1.22 mmol g^{-1}, typically 0.1 mmol scale) and cleaved from the resin using as outlined by protocols in section 7.9.1, to afford the protected linear precursor. Peptoids were cyclised in solution to afford the head to tail cyclic product and the crude sample, or a portion of, was purified (as in section 7.9.2). All peptoids were obtained as white powders with characterisation data shown in **Table 7.2**.

130
cyclo (*N*Lys*N*phe*N*phe)$_2$

131
cyclo (*N*Lys*N*pfb*N*pfb)$_2$

132
cyclo (*N*Lys*N*phe)$_3$

133
cyclo (*N*hArg*N*phe)$_3$

134
cyclo (*N*Lys*N*phe*N*hArg*N*phe*N*Lys*N*phe)
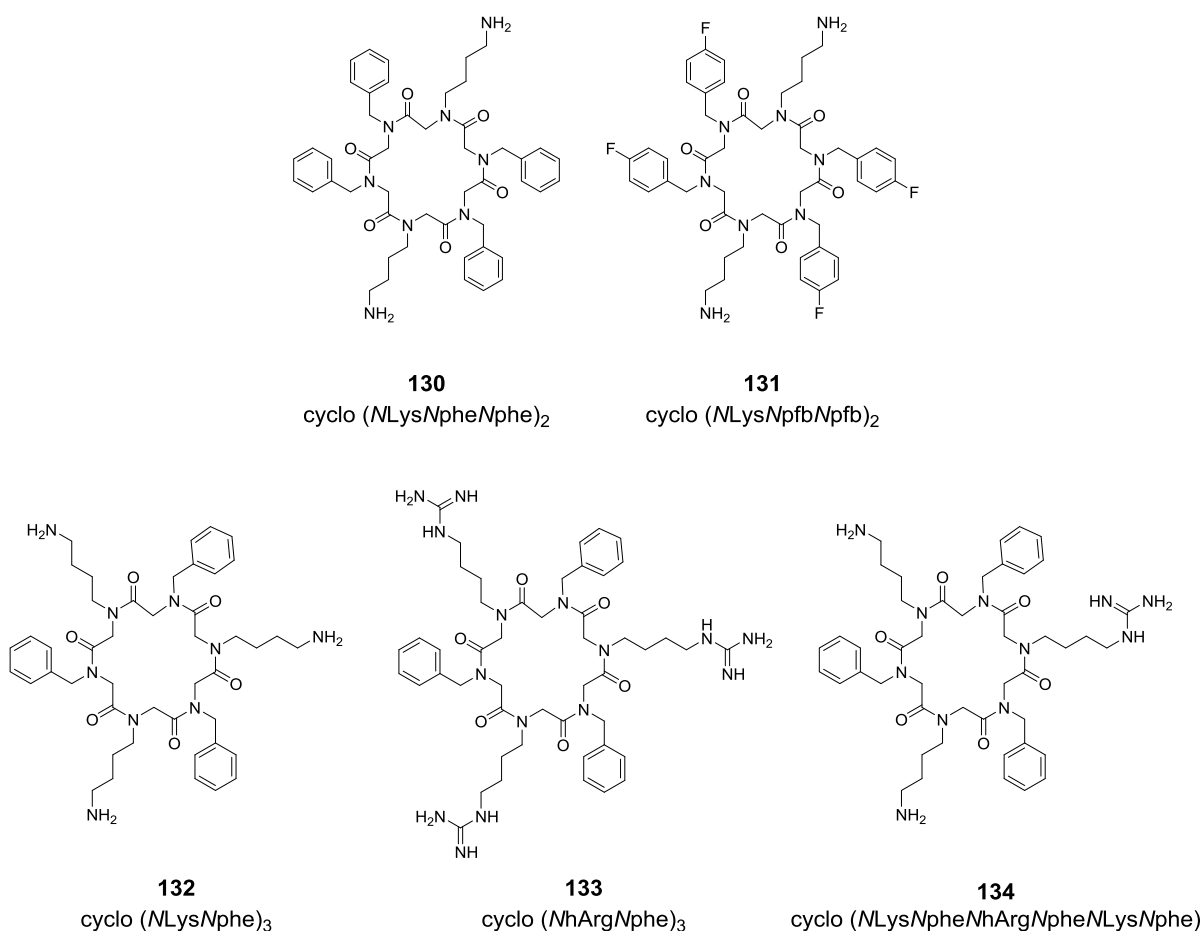
Figure 7.1. Cyclic compounds synthesised, with characterisation data provided in **Table 7.2**.
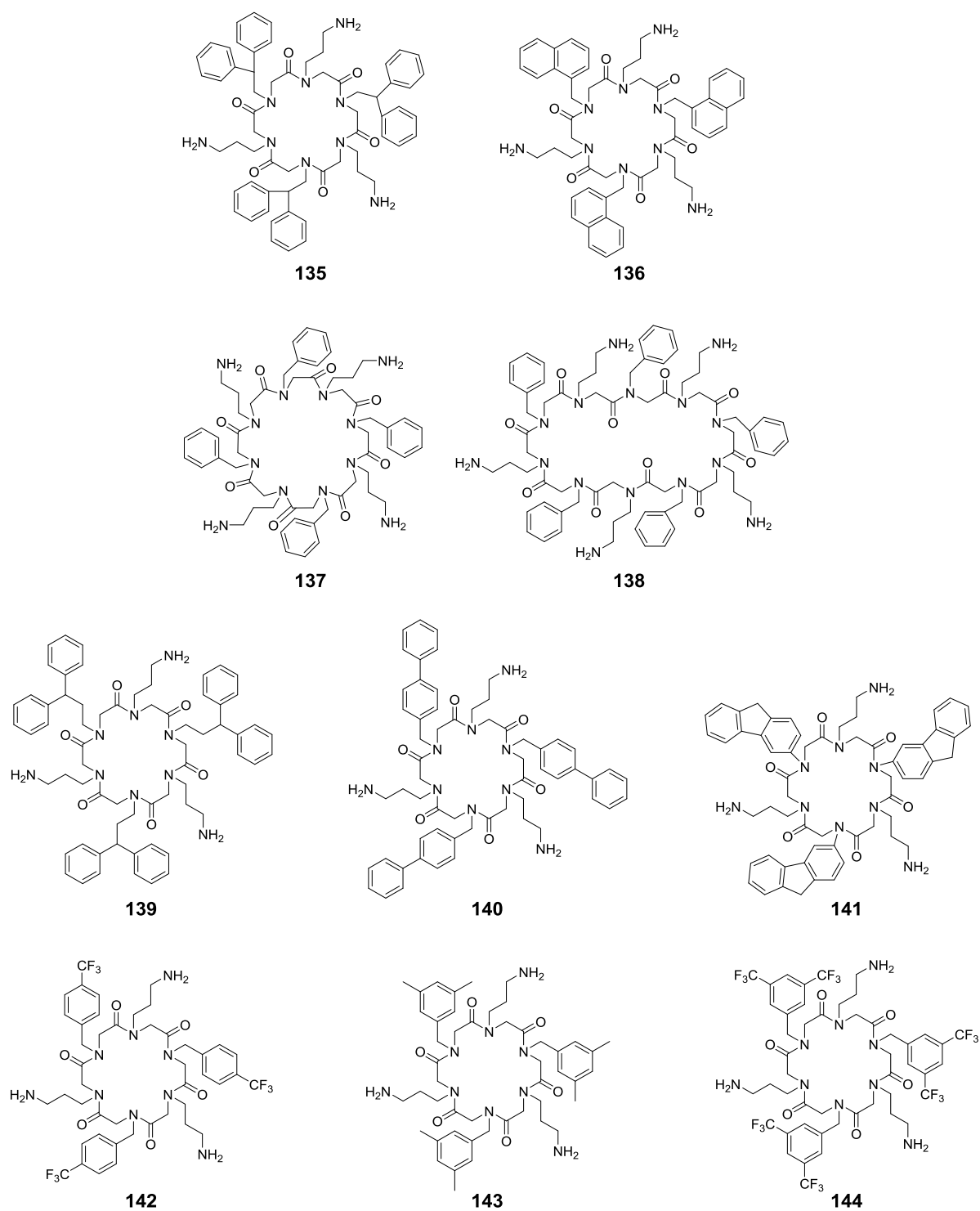
Figure 7.2. Cyclic peptoids synthesised and provided by the Kirshenbaum Group (New York State University, USA).

#	Sequence	Analytical HPLC		Accurate Mass Spectrometry		Yield[§]	
		Retention time[**] (min)	Approx. purity (%)	Mass calculated	Mass observed	(%)	mg
130	cyclo (*N*Lys*N*phe*N*phe)$_2$	13.9	> 95	[M+H]$^+$ 863.4820	863.4823	28	24
131	cyclo (*N*Lys*N*pfb*N*pfb)$_2$	15.5	~ 70	[M+H]$^+$ 917.4337	917.4358	32	32
132	cyclo(*N*Lys*N*phe)$_3$	13.3	> 95	[M+H]$^+$ 826.4980	826.4959	17	14
133	cyclo (*N*hArg*N*phe)$_3$	13.8	> 99	[M+H]$^+$ 952.5634	952.5636	20	3
134	cyclo (*N*Lys*N*phe*N*hArg*N*phe*N*Lys*N*phe)	13.4	> 95	[M+H]$^+$ 868.5198	868.5201	18	2

Table 7.2. Accurate mass spectrometry data, reverse phase analytical HPLC retention times and approximate purity for the cyclic peptoid library.

[§] Yield is expressed as an overall yield calculated from the final mass recovered following RP-HPLC purification and expressed as a percentage of the original scale of resin used.
[**] Gradient, solvents and conditions for analytical HPLC as described in section 7.13.2.

7.15.6 Lipopeptoids

Peptoids with a lipid tail (at the N terminus) were synthesised using the submonomer method of peptoid synthesis on Rink Amide resin (typical loading 0.79–0.82 mmol g^{-1}, 0.1 mmol scale) as outlined by the protocol section 7.3 and 7.7, with the N terminal residue being the appropriate lipoamine submonomer. Peptoids were cleaved from the resin using protocol 7.12.1 to afford the crude deprotected sequence and the crude sample, or a portion of, was purified by procedure 7.13.1 and pure fractions combined to yield the peptoid as a powder. Characterisation data is shown in **Table 7.3**.

Peptoids with a lipid head group (at the C terminus) were synthesised using the submonomer method of peptoid synthesis on 2-chlorotrityl chloride resin (loading 1.22 mmol g^{-1}, 0.1 mmol scale) as outlined by the protocol section 7.8. Peptoids were cleaved from the resin using protocol 7.12.1 to afford the crude deprotected sequence and the lipid head group was added in a solution phase coupling with the appropriate lipoamine and coupling agent, as described in procedure 7.8. The crude sample was purified by procedure 7.13.1 and pure fractions combined to yield the peptoid as a powder. Characterisation data is shown in **Table 7.4**.

#	Sequence	Analytical HPLC		Accurate Mass Spectrometry		Yield[††]	
		Retention time[‡‡] (min)	Approx. purity (%)	Mass calculated	Mass observed	(%)	(mg)
158	*N*C$_7$(*Nae*N*spe*N*spe*)$_4$	20.1	> 99	[M+2H]$^{2+}$ 931.5502	931.5508	30	15
159	*N*C$_{12}$(*Nae*N*spe*N*spe*)$_4$	22.8	> 95	[M+2H]$^{2+}$ 966.5893	966.5894	58	25
160	*N*C$_{16}$(*Nae*N*spe*N*spe*)$_4$	25.2	> 99	[M+2H]$^{2+}$ 994.6206	994.6207	25	10
161	*N*cycloC$_7$(*Nae*N*spe*N*spe*)$_4$	19.3	> 99	[M+H]$^+$ 1860.0769	1860.0771	39	16
162	*N*te(*Nae*N*spe*N*spe*)$_4$	18.5	> 99	[M+2H]$^{2+}$ 955.5425	955.5422	18	12
163	*N*C$_7$[(*N*Lys*N*pfb*N*pfb)(*N*Lys*N*spe*N*spe)]$_2$	18.9	> 99	[M+2H]$^{2+}$ 995.5605	995.5626	25	13
164	*N*C$_{12}$[(*N*Lys*N*pfb*N*pfb)(*N*Lys*N*spe*N*spe)]$_2$	21.6	> 99	[M+2H]$^{2+}$ 1030.6018	1030.6014	31	13
165	*N*C$_{16}$[(*N*Lys*N*pfb*N*pfb)(*N*Lys*N*spe*N*spe)]$_2$	23.7	> 99	[M+2H]$^{2+}$ 1058.6331	1058.6310	23	11
166	*N*cycloC$_7$[(*N*Lys*N*pfb*N*pfb)(*N*Lys*N*spe*N*spe)]$_2$	18.3	> 99	[M+2H]$^{2+}$ 994.5548	994.5518	34	19
167	*N*te[(*N*Lys*N*pfb*N*pfb)(*N*Lys*N*spe*N*spe)]$_2$	17.6	> 99	[M+2H]$^{2+}$ 1019.5550	1019.5535	36	19

Table 7.3. Accurate mass spectrometry data, RP-HPLC retention times and approximate purity for the linear peptoid library with lipid tail groups.

#	Sequence	Analytical HPLC		Accurate Mass Spectrometry		Yield[††]	
		Retention time[‡‡] (min)	Approx. purity (%)	Mass calculated	Mass observed	(%)	(mg)
168	(*Nae*N*spe*N*spe*)$_4$C$_7$H$_{15}$	21.2	> 99	[M+2H]$^{2+}$ 903.0394	903.0374	9	4
169	(*Nae*N*spe*N*spe*)$_4$C$_{12}$H$_{25}$	24.6	> 95	[M+2H]$^{2+}$ 938.0786	938.0784	14	6
170	(*Nae*N*spe*N*spe*)$_4$C$_{16}$H$_{33}$	27.1	> 99	[M+2H]$^{2+}$ 966.1099	966.1111	7	3
171	(*Nae*N*spe*N*spe*)$_{4\text{-cyclo}}$C$_7$H$_{15}$	20.8	> 95	[M+2H]$^{2+}$ 902.0316	902.0325	21	9
172	(*Nae*N*spe*N*spe*)$_4$te	18.9	> 95	[M+2H]$^{2+}$ 927.0318	927.0311	18	8
173	[(*N*Lys*N*pfb*N*pfb)(*N*Lys*N*spe*N*spe)]$_2$-C$_7$H$_{15}$	20.2	> 95	[M+2H]$^{2+}$ 967.0519	967.0496	10	4
174	[(*N*Lys*N*pfb*N*pfb)(*N*Lys*N*spe*N*spe)]$_2$-C$_{12}$H$_{25}$	23.7	> 95	[M+2H]$^{2+}$ 1002.0911	1002.0896	9	4
175	[(*N*Lys*N*pfb*N*pfb)(*N*Lys*N*spe*N*spe)]$_2$-C$_{16}$H$_{33}$	26.0	> 90	[M+2H]$^{2+}$ 1030.1223	1030.1222	22	10
176	[(*N*Lys*N*pfb*N*pfb)(*N*Lys*N*spe*N*spe)]$_{2\text{-cyclo}}$C$_7$H$_{15}$	19.5	> 95	[M+2H]$^{2+}$ 966.0441	966.0430	10	4
177	[(*N*Lys*N*pfb*N*pfb)(*N*Lys*N*spe*N*spe)]$_2$-te	18.4	> 95	[M+2H]$^{2+}$ 991.0443	991.0417	32	14

Table 7.4. Accurate mass spectrometry data, RP-HPLC retention times and purity for the linear peptoid library with lipid head groups.

[††] Yield is expressed as an overall yield calculated from the final mass recovered following RP-HPLC purification and expressed as a percentage of the original scale of resin used.
[‡‡] Gradient, solvents and conditions for analytical HPLC as described in section 7.13.2.

7.15.7 Fluorescently labelled compounds

Peptoids were synthesised using the submonomer method of peptoid synthesis outlined by protocols in section 7.9 and peptides were synthesised using standard SPPS, as in section 7.11. A glycine spacer was added for all peptoids (section 7.4) and the fluorescent dye added to the peptide or peptoid sequence as in section 7.6. Compounds were then cleaved from the resin and purified using protocols 7.12.1 and 7.13.1 respectively, to yield the fluorescently labelled products as yellow powders (fluorescein dye). Characterisation data is shown in **Table 7.5**.

#	Sequence	Analytical HPLC		Accurate Mass Spectrometry		Yield[§§]	
		Retention time[***] (min)	Approx. purity (%)	Mass calculated	Mass observed	(%)	(mg)
334	Fluorescein-G-(*N*Lys*N*spe*N*spe)$_2$	18.9	> 95	[M+H]$^+$ 1289.6399	1289.6406	20	13
335	Fluorescein-G-(*N*Lys*N*spe*N*spe)$_4$	19.7	> 99	[M+2H]$^{2+}$ 1095.5870	1095.5784	8	5
336	Fluorescein-G-(*N*ae*N*spe*N*spe)$_4$	20.1	> 99	[M+2H]$^{2+}$ 1039.5244	1039.5181	9	7
337	Fluorescein-G-(*N*Lys*N*phe*N*phe)$_4$	18.1	> 95	[M+2H]$^{2+}$ 1039.5422	1039.5159	18	2
338	Fluorescein-G-(*N*Lys*N*hLeu*N*spe)$_4$	19.7	> 99	[M+2H]$^{2+}$ 1027.6183	1027.6104	11	7
339	Fluorescein-G-(*N*Lys*N*nVal*N*spe)$_4$	16.6	> 95	[M+H]$^+$ 1942.1035	1942.1025	24	2
340	Fluorescein-G-[(*N*amy*N*spe*N*spe)(*N*Lys*N*spe*N*spe)]$_2$	24.9	> 90	[M+2H]$^{2+}$ 1094.5917	1094.5865	18	<1
341	Fluorescein-G-[(*N*Lys*N*pfb*N*pfb)(*N*Lys*N*spe*N*spe)]$_2$	19.6	> 99	[M+2H]$^{2+}$ 1103.5368	1103.5300	9	6
342	5(6)-carboxyfluorescein-FLPLIGRVLSGIL-NH$_2$ (*Temporin A*)	24.2	> 80	[M+2H]$^{2+}$ 877.9800	877.9785	9	1
343	5(6)-carboxyfluorescein-GLLPIVGNLLKSLL-NH$_2$ (*Temporin B*)	25.7	> 80	[M+2H]$^{2+}$ 904.0062	904.0040	15	2

Table 7.5. Accurate mass spectrometry data, reverse phase analytical HPLC retention times and approximate purity for the linear peptoid library.

[§§] Yield is expressed as an overall yield calculated from the final mass recovered following RP-HPLC purification and expressed as a percentage of the original scale of resin used.
[***] Gradient, solvents and conditions for analytical HPLC as described in section 7.13.2.

7.15.8 Nisin[A/B]-peptoid conjugates

NprpNspeNspe(*NaeNspeNspe*)$_4$ (319)

Synthesis on Rink Amide resin (0.82 mmol g^{-1} loading, 0.1 mmol scale) via manual solid phase peptoid synthesis as outlined by procedure 7.3.1, with propargylamine coupled as the N terminal peptoid submonomer. The global deprotection and resin cleavage was carried out following protocol 7.12.1 and half of the sample was purified as in section 7.13 and pure fractions combined to afford the peptoid as a white powder (33.6 mg, 32 %); RP-analytical HPLC[†††] RT 20.0 min; approximate purity 99 %; accurate QToF MS mass calculated [M+2H]$^{2+}$ 1062.5873, mass observed [M+2H]$^{2+}$ 1062.5857.

NprpNspeNspe[(*NLysNpfbNpfb*)(*NLysNpfbNpfb*)]$_2$ (320)

Synthesis on Rink Amide resin (0.82 mmol g^{-1} loading, 0.1 mmol scale) via manual solid phase peptoid synthesis as outlined by procedure 7.3.1, with propargylamine coupled as the N terminal peptoid submonomer. The global deprotection and resin cleavage was carried out following protocol 7.12.1 and half of the crude sample was purified as in section 7.13 and pure fractions combined to afford the peptoid as a white powder (42.92 mg, 38 %); RP-analytical HPLC[†††] RT 19.0 min; approximate purity > 95 %; accurate QToF MS mass calculated [M+2H]$^{2+}$ 1126.5997, mass observed [M+2H]$^{2+}$ 1126.6017.

Nisin[A/B]-*NspeNspe*(*NaeNspeNspe*)$_4$ (322)

Nisin[A/B]-azide (8.1 µmol, 10.32 mg in 200 µL DMF) and *NprpNspeNspe*(*NaeNspeNspe*)$_4$ (8.1 µmol, 13.89 mg) were conjugated following click protocol 7.15.3 to yield the peptide-peptoid conjugate as a white powder (9.16 mg, 34 %); RP-analytical HPLC[‡‡‡] RT 33.3 min; approximate purity > 99 %; accurate QToF MS mass calculated [M+2H]$^{2+}$ 1678.4032, mass observed [M+2H]$^{2+}$ 1678.3981.

Nisin[A/B]-*NspeNspe*[(*NLysNpfbNpfb*)(*NLysNpfbNpfb*)]$_2$ (323)

Nisin[A/B]-azide (8.1 µmol, 10.10 mg in 200 µL DMF) and *NprpNspeNspe*(*NaeNspeNspe*)$_4$ (8.1 µmol, 18.34 mg) were conjugated following click protocol 7.15.3 to yield the peptide-peptoid conjugate as a white powder (13.86 mg, 49 %); RP-analytical HPLC[‡‡‡] RT 31.8 min; approximate purity >99%; accurate QToF MS mass calculated [M+2H]$^{2+}$ 1742.4156, mass observed [M+2H]$^{2+}$ 1742.4037.

[†††] Conditions for analytical HPLC as described in section 7.13.2; λ = 220 nm; gradient: 0–100 % solvent B over 30 mins (solvent A: 95 % H$_2$O, 5 % MeCN, 0.05 % TFA; Solvent B: 95 % MeCN, 5 % H$_2$O, 0.03 % TFA).
[‡‡‡] Conditions for analytical HPLC as described in section 7.13.2; λ = 220 nm; gradient: 0–100 % solvent B over 60 mins (solvent A: 95 % H$_2$O, 5 % MeCN, 0.1 % TFA; Solvent B: 95 % MeCN, 5 % H$_2$O, 0.1 % TFA).

Biophysical Characterisation

7.16   Circular dichroism spectroscopy (CD)

Circular dichroism experiments were undertaken by the author of this report, Charlotte Williams (MPhys student) and Dr Lara Small (Postdoctoral research assistant) supervised by Dr Beth Bromley, in the Physics Department at Durham University.

Circular dichroism spectroscopy was conducted on sequences with a chiral reporter monomer present using a Jasco J-810 spectropolarimeter, with a 0.1 cm path length and 500 µL quartz cuvette. Samples were made to 5 mM in distilled water, then diluted to 50 µM in a phosphate buffered solution (PBS, 1 M). 300 µL of this solution was transferred to a cuvette for the measurements. All data collection was taken at room temperature and data was collected as an accumulation of 10 measurements, adjusted by the background spectrum of the PBS buffer. Scans were conducted at 50 nm min^{-1} between 260–190 nm, 1 nm data pitch, 5 mdeg sensitivity and a 2 s response.

Mean residue molar ellipticity [θ] was obtained using the equation:

$$[\theta] = \frac{100 \times \theta_{obs} \times M}{n \times l \times c}$$

where θ_{obs} is measured ellipticity (°), M is the molecular weight (g mol^{-1}), n is the number of residues, l is path length (cm), and c is the concentration of peptoid (mg mL^{-1}).

7.17   Partitioning experiments

Partitioning experiments and dynamic light scattering was undertaken by Charlotte Williams (MPhys student), supervised by Dr Beth Bromley, in the Physics Department at Durham University.

Peptoids were dissolved at concentrations between 10 and 300 μM in either Phosphate Buffered Saline (PBS) or 1-octanol. Exact concentrations were measure using UV spectrometry (Shimadzu UV-3600) using the phenylalanine-like peak centred at 258 nm and a molar extinction coefficient of 195 $M^{-1}\,cm^{-1}$ per residue. It was necessary to subtract baselines and the influence of the peptoid backbone absorption at lower wavelengths in order to get accurate concentration data.

Partition experiments were carried out by putting 450 μL of octanol in contact with 450 μL of PBS, which contained between 10 and 100 μL of peptoid. Each peptoid was measured in triplicate. The samples were allowed to equilibrate under gentle agitation for ~150 hours (as 48 hours was not found to be sufficient for the system to reach equilibrium). After this point samples were taken from the PBS half and the octanol half and diluted to produce sufficient volume for spectroscopy. The concentration of peptoid remaining in the PBS and the octanol was measured individually using the phenylalanine peak as before. From these concentrations the ratio K_v of concentration in PBS to concentration in octanol was calculated along with the free energy of insertion into octanol $\Delta G = RT \ln K_v$. All PBS solutions were checked for aggregation both by inspection of the UV spectra to look for scattering effects and by measuring particle size using dynamic light scattering.

7.18   Dynamic light scattering

All of the peptoids tested in partitioning experiments (7.17) were checked at high concentration (~500 μM) in PBS for indicators of aggregation using dynamic light scattering (Malvern Zetasizer Nano). Due to the increase in intensity of scattering with size, the presence of a signal at small hydrodynamic diameters indicates the overwhelming majority of the sample in all cases is present in the smallest peak.

Peptoids that substantially partitioned into the octanol during the partitioning experiments were checked at high concentration (~500 μM) in octanol for indicators of aggregation using dynamic light scattering. Due to the increase in intensity of scattering with size, the presence of a signal at small hydrodynamic diameters indicates the overwhelming majority of the sample is present in the smallest peak.

7.19   Peptoid stability assays

The HPLC based chymotrypsin stability assay was undertaken by Emily Corlett (MSc project student, Durham University).

7.19.1 Chymotrypsin activity assay

1 mL samples were made up 500 µl of 50 mM ammonium bicarbonate buffer (pH 7.8), 467 µL of 1.18 mM BTEE in MeOH/H_2O and 33 µL of chymotrypsin solution, made up at 0.1 mg mL^{-1} in 1 mM HCl solution. The negative control contained 33 µL of 1 mM HCl solution in place of the chymotrypsin solution. Samples were analysed for 1 minute at 256 nm with a spectrophotometer. The chymotrypsin was added to the cuvette in the spectrophotometer so that analysis could begin as soon as the sample had been mixed. Three samples were run for each assay at 22 °C and one negative control. All assays were carried out in triplicate.

7.19.2 Chymotrypsin stability assay

Chymotrypsin was incubated at the digestion temperature of 22 °C in buffer (stock solution containing 5 mL of 50 mM ammonium bicarbonate buffer and 0.33 mL of chymotrypsin solution, made up at 0.1 mg mL^{-1} in 1 mM HCl solution). These volumes were chosen to correspond directly to those used in the chymotrypsin activity assay (section 7.19.1). This stock solution was kept at 22 °C and used to run the chymotrypsin activity assay at 0 h, 8 h and 24 h. Negative controls were made up separately to the same protocol as used in the activity assay.

7.19.3 Chymotrypsin automated digestion protocol

A sample was made up of 187.5 µL of 50 mM ammonium bicarbonate buffer (pH 7.8), containing 2 mM CaCl2 to activate the chymotrypsin, 37.5 µL substrate solution, made up at 5 mg mL^{-1} in DMSO, and 25 µL chymotrypsin solutions, at 0.5 ng µL^{-1}. The negative control contained 25 µL extra buffer in the place of chymotrypsin solution. 10 µL of the sample was pipetted by an auto-sampler at given time points and immediately analysed HPLC with the DAD focused at 215 nm.

7.19.4 Trypsin digestion

Substrate stocks of peptoid or control were prepared in tris-HCl buffer (6 mg mL^{-1} in tris-HCl 50 mM at pH 7.8, with 5 mmol CalCl$_2$[§§§]). *N*-tosyl-L-phenylalanyl chloromethyl ketone treated[****] bovine trypsin solution was freshly made (1 mg in 5 mL tris-HCl, 0.2 mg mL^{-1}). Solutions were preincubated at 37 ˚C[††††] for 20 minutes. 120 μL substrate stock and 80 μL trypsin solution were mixed in 600 μL tris-HCl buffer and incubated at 37 ˚C on a heated shaker platform. After 0 hours (for verification prior to tryptic digestion) or after treatment with trypsin (at several time points) the reaction mixtures were analysed.

For analysis using analytical RP-HPLC, an aliquot of 100 μL was removed from incubation 37 ˚C and acidified by addition of 50 % TFA in acetonitrile (20 μL) to stop further enzyme activity. Samples were analysed following a 10 μL injection to the HPLC instrument, with the DAD focussed at 220 nm.

For analysis using mass spectrometry, a 10 μL aliquot was removed from incubation and analysed using MALDI immediately. The matrix solution was prepared (α-cyano-4-hydroxycinnamic acid in 400 μL MeCN, 800 μL water (+0.1% TFA) as a saturated solution). A solution containing the digestion sample to be analysed was prepared (9 : 1 matrix to sample) and 1 μL of this was spotted to the MALDI target. The plate was dried and then each spot washed carefully with 5 μL of water (+0.1 % TFA) to wash away excess salt. MALDI-TOF MS or MALDI LIFT MS was performed, as outlined in section 7.2.3.

[§§§] CaCl$_2$ added to reduce trypsin autolysis.
[****] Trypsin treated with TPCK to inhibit any chymotrypsin activity which may be present.
[††††] The optimum temperature for trypsin activity.

7.20   Confocal Fluorescence Microscopy

Fluorescent microscopy experiments were undertaken in collaboration with Dr Robek Pal (Durham University, Chemistry Department) and assisted by Sophia Schwartz (Erasmus student). Methods and procedure provided by Dr Robek Pal.

Mammalian cells (either NIH-3T3 or PC3) were subcultured onto sterile, tissue culture treated slides from Ibidi (Thistle Scientific Ltd). Cells were incubated with fluorescent compound alone, or with a variety of trackers prior to imaging (Fisher Scientific).

Visualisation of the peptoids and cell images were obtained using a Leica SP5 II microscope, as previously described.[4] A HeNe laser was used to visualize fluorescein-peptoid/peptide fluorescence and either a He/Ne or Ar ion laser was used to corroborate cellular localisation in combination with commercially available organelle-specific stains (e.g. LysoTrackerRed© or MitoTrackerRed©). All tracker stains were used under conditions and concentrations recommended by the manufacturer(s).

The microscope was equipped with a triple channel imaging detector, comprising two conventional PMT systems and a HyD hybrid avalanche photodiode detector. The latter part of the detection system, when operated in the BrightRed mode, is capable of improving imaging sensitivity above 550 nm by 25 %, reducing signal-to-noise by a factor of 5. The pinhole was always determined by the Airy disc size, calculated from the objective in use (HCX PL APO 63x/1.40 NA LbdBlue), using the lowest excitation wavelength (488 nm). Scanning speed was adjusted to 100 Hz in a bidirectional mode, to ensure both sufficient light exposure and enough time to collect the emitted light from the fluorescent compounds with no field averaging (view area 98 μm x 98 μm, 1024 × 1024 pixel array, a pixel size of 45 × 45 nm at a depth of 380 nm).[4]

The three-dimensional reconstructions wwere achieved using a novel saturation elimination algorithm update of the existing ImageJ 1.46r 3D plug-in using LSCM images recorded on the above detailed Leica SP5 II microscope. In these z-stack images, a deliberate 20% overlap in the applied axial resolution was introduced, determined by the applied optics and experimental parameters detailed above.[4]

Biological Assays

7.21   Antibacterial testing

Antibacterial testing was carried out at Durham University by Dr Gabriela Eggimann (post-doctoral research assistant) and assisted by Mark Laws (MChem Project student) and Sophia Schwartz (Erasmus student).

7.21.1 Bacterial culture preparation

Escherichia coli K-12 wild-type strain (W3110 / ATCC27325, F$^-$, λ$^-$, *rpoS(Am)*, *rph-1*, *Inv*(*rrnD-rrnE*)), *Pseudomonas aeruginosa* PA01 (ATCC 15692) *Staphylococcus aureus* (3R7089 strain Oxford / ATCC9144) and *Staphylococcus epidermidis* (laboratory strain from clinical isolate) were selected for bacteriological studies as representative Gram-negative (*E. coli* and *P. aeruginosa*) and Gram-positive (*S. aureus* and *S. epidermidis*) species. Bacterial cultures were prepared by streaking bacterial strains onto LB agar plates with an inoculation loop and incubated overnight at 37 °C. A single colony was selected and placed in 5 mL of Iso-sensitest broth (Oxoid, ThermoScientific) and incubated with shaking for 16–18 h at 37 °C to provide liquid cultures for testing.

7.21.2 Antibacterial minimum inhibitory concentration determination

MIC values were obtained according to the previously described protocol[5] and were conducted in 96-well plates (Sarsted, Fisher Scientific). Bacteria were grown from overnight cultures in Iso-sensitest broth to an A650nm of 0.07 equivalent to a 0.5 MacFarland standard (240 µM $BaCl_2$ in 0.18 M H_2SO_4). This culture was diluted ten-fold with Iso-sensitest broth before use. Peptoids were initially dissolved in DMSO (5 mM) and diluted further in Iso-sensitest broth to achieve a concentration range of 4–200 µM using 2-fold serial dilutions. 50 µL of inoculum and 50 µL of peptoid solution were added to each test well (final concentration range of 2–100 µM). Experiments were performed in triplicate. A positive control for bacterial growth contained only the inoculum and Iso-sensitest broth. Other controls contained the inoculum and serial dilutions of ampicillin (from 250 µg/mL to 2 µg/mL), serial dilutions of DMSO and the inoculum to confirm no inhibitory effect on bacterial growth, and Iso-sensitest broth alone as a sterile control. The MIC was defined as the lowest concentration which completely inhibited bacterial growth after incubation at 37 °C for 16 h with shaking. Quantitative data was attained from absorbance values using a Biotek Synergy H4 plate reader.

7.22   Anti-leishmanial assays

Initial anti-leishmanial testing was carried out at Durham University by Dr Gabriela Eggimann (post-doctoral research assistant). Subsequent testing was carried out by the author of this thesis.

7.22.1 Cell Culture of *Leishmania mexicana* M379 promastigotes and amastigotes

Leishmania mexicana (M379) promastigote parasites were maintained at 26 °C in Schneider's Insect medium (Sigma-Aldrich) supplemented with heat-inactivated foetal bovine sera (FBS, 15 %; Biosera Ltd). Cells were counted using a Neubauer Improved Hemocytometer. Promastigotes were transformed into axenic amastigotes by a pH and temperature shift as previously described.[6] A culture of recently transformed (three days) promastigotes in the late log phase was transferred into Schneider's Insect medium supplemented with 20 % heat-inactivated FBS (pH 5.5) at 5×10^5 parasites/mL. After 6 days, the parasites were in the metacyclic stage and used for transformation to amastigote-like forms by transfer in the same medium at 32 °C at 5×10^5 parasites/mL. After additional 5–7 days, the parasites should be in the amastigote stage and be ready for cytotoxicity studies and infections.

7.22.2 Cytotoxicity Assays with *L. mexicana* M379 promastigotes and amastigotes

Cytotoxicity analyses were performed in 96-well plates (Costar, Fisher Scientific) using alamarBlue® (Invitrogen) for cell viability detection as previously described.[7] Promastigote and amastigote *L. mexicana* were pre-incubated with the compounds in triplicate (5 mM stock solutions in DMSO; amphotericin B was used as a positive control; untreated parasites with DMSO as a negative control) in 50 μL of the corresponding media at 4×10^6 mL^{-1} for 1 hour. Afterwards, 40 μL were removed from each well before the addition of 90 μL of the corresponding media, followed by incubation for 24 hours at 4×10^5 mL^{-1}. Then, 10 μL alamarBlue® solution (Invitrogen) was added to each well for an incubation of 4 hours prior to assessing cell viability using a fluorescent plate reader (Biotek; λ_{ex} 560 nm, λ_{em} 600 nm). To investigate the effects of serum on the efficacy of the peptoids, the assay described above was modified using serum-free medium for the pre-incubation time. For these assays, the parasites were washed three times in serum-free medium before adding them to the compound solutions. All of the experiments described above were carried out in triplicate on a minimum of two separate occasions to ensure a robust data set was collected.

7.22.3 Cytotoxicity assays with *L. mexicana* intracellular amastigotes

Cytotoxicity analyses were performed in 96-well plates (flat bottom, Costar, Fisher Scientific) using alamarBlue® (Invitrogen) for cell viability detection using a modified protocol as previously described.[4] For the macrophages, RAW 264.7 cells were grown in at 37 °C, 5 % CO_2 in DMEM high glucose supplemented with heat-inactivated foetal bovine sera (FBS, 10 %; Biosera Ltd) and penicillin/streptomycin (P/S, 1 %). The cells were treated with the compounds in quadruplet (5 mM stock solutions in DMSO; amphotericin B was used as a positive control; untreated parasites with DMSO as a negative control).

On day 1, the RAW cells were seeded at 2.5 x 10^5 cells mL^{-1} (200 μL/well) in $DMEM_{10}$ (10% FBS, 1% P/S) followed by an incubation for 24 hours at 37 °C, 5 % CO_2. On day 2, the RAW cells were washed carefully once with $DMEM_2$ (2 % FBS, 1 % P/S). Addition of *L. mexicana* amastigotes at 2.5 x 10^6 cells mL^{-1} (200 μL/well) in $DMEM_2$ (2 % FBS, 1 % P/S) followed by an incubation for 24 hours at 37 °C, 5 % CO_2. On day 3, the infected RAW cells were washed carefully 5 times with $DMEM_2$ (2 % FBS, 1 % P/S) before adding 100 μL/well of fresh $DMEM_2$ (2 % FBS, 1 % P/S) to each well. Peptoids and control solutions were prepared in $DMEM_2$ (2 % FBS, 1 % P/S) and added to the corresponding wells (100 μL/well) for an incubation of 24 hours at 37 °C, 5 % CO_2. On day 4, infected RAW cells were washed carefully 3 times with Schneider's Insect medium (pH 7.0, serum-free) and then lysed with 20 μL/well of SDS (0.05 %, *v/v*) for 30 seconds before addition of 180 μL/well of Schneider's Insect medium (pH 7.0, 15 % FBS). Plates were wrapped with parafilm and incubated for 48 hours at 26 °C. On day 6, 10 μL of alamarBlue® (Invitrogen) was added to each well before a 4 hour incubation at 26 °C prior to assessing cell viability using a fluorescent plate reader (Biotek; $λ_{ex}$ 560 nm, $λ_{em}$ 600 nm). All of the experiments described above were carried out on a minimum of two separate occasions in quadruplet to ensure a robust data set was collected.

7.22.4 Statistical analysis

All ED_{50} data for parasitic assays represent an average of at least 2 independent experiments, undertaken in triplicate. Error bars are plotted to show the variation of data between individual wells as a standard deviation. The Z-factor (Z') was calculated for each assay using the mean (μ) and standard deviation (σ) of both positive (p) and negative (n) controls. Data were only used for assays with Z' between 0.5 and 1.0 to ensure the assay was of high quality.[8]

$$Z' = 1 - \frac{3\,(\sigma_p + \sigma_n)}{|\mu_p - \mu_n|}$$

7.23   Cytotoxicity assays against mammalian cells

7.23.1 Cytotoxicity assays with RAW 264.7 macrophages

Cytotoxicity analyses were performed in 96-well plates (flat bottom, Costar, Fisher Scientific) using alamarBlue® (Invitrogen) for cell viability detection using a modified protocol as described above for the intracellular amastigote cytotoxicity assay. The RAW 264.7 cells were grown in at 37 °C, 5 % CO_2 in $DMEM_{10}$ high glucose supplemented with heat-inactivated foetal bovine sera (FBS, 10 %; Biosera Ltd) and penicillin/streptomycin (P/S, 1 %). The cells were treated with the compounds in quadruplet (5 mM stock solutions in DMSO; amphotericin B was used as a positive control; untreated parasites with DMSO as a negative control). On day 1, the RAW cells were seeded at 2.5 x 10^5 cells mL^{-1} (200 μL/well) in $DMEM_{10}$ (10 % FBS, 1 % P/S) followed by an incubation for 24 hours at 37 °C, 5 % CO_2. On day 2, the RAW cells were washed carefully once with $DMEM_2$ (2 % FBS, 1 % P/S). Addition of 200 μL/well of $DMEM_2$ (2 % FBS, 1 % P/S) followed by an incubation for 24 hours at 37 °C, 5 % CO_2. On day 3, the RAW cells were washed carefully 5 times with DMEM (2 % FBS, 1 % P/S) before adding 100 μL/well of fresh $DMEM_2$ (2 % FBS, 1 % P/S) to each well. Peptoids and control solutions were prepared in $DMEM_2$ (2 % FBS, 1 % P/S) and added to the corresponding wells (100 μL/well) for an incubation of 24 hours at 37 °C, 5 % CO_2. On day 4, 200 μL/well of fresh $DMEM_{10}$ (10 % FBS, 1 % P/S) was added to each well. Then, 10 μL of alamarBlue® (Invitrogen) was added to each well before a 2 hour incubation at 37 °C, 5 % CO_2 prior to assessing cell viability using a fluorescent plate reader (Biotek; λ_{ex} 560 nm, λ_{em} 600 nm). All of the experiments described above were carried out on a minimum of two separate occasions in quadruplet to ensure a robust data set was collected.

7.23.2 Cytotoxicity assays with HepG2 epithelial cells

Cytotoxicity analyses were performed in 96-well plates (Costar, Fisher Scientific) using alamarBlue® (Invitrogen) for cell viability detection using a modified protocol as previously described.[9] The HepG2 cells were grown at 37 °C, 5 % CO_2 in $DMEM_{10}$ high glucose supplemented with heat-inactivated foetal bovine sera (FBS, 10 %; Biosera Ltd) and penicillin/streptomycin (P/S, 1 %). Cells were counted using a Neubauer Improved Hemocytometer. HepG2 cells were seeded 1 day prior to treatment in 96 well plates at a concentration of 2 x 10^5 cells mL^{-1} in 100 μL of medium (2 x 10^4 cells/well). After 24 hours, cells were incubated with the compounds in a dilution series in triplicate from 2–100 μM (5 mM stock solutions in DMSO; untreated cells with DMSO as a negative control) in 50 μL of the media for 1 hour. Afterwards, 40 μL of medium was removed from each well before the addition of 90 μL of the media, followed by incubation for 24 hours at 37 °C, 5 % CO_2. Then, 10 μL of alamarBlue® (Invitrogen) was added to each well before a 2 hour incubation prior to assessing cell viability using a fluorescent plate reader (Biotek; λ_{ex} 560 nm, λ_{em} 600 nm).

7.23.3 Cytotoxicity assay with HaCaT keratinocytes

Cytotoxicity analyses were performed in 96-well plates (Costar, Fisher Scientific) using alamarBlue® (Invitrogen) for cell viability detection. HaCaT cells were subcultured at 37 °C, 5 % CO_2 in $DMEM_{10}$ high glucose supplemented with heat-inactivated foetal bovine sera (FBS, 10 %; Biosera Ltd) and penicillin/streptomycin (P/S, 1 %). Cells were counted using a Neubauer Improved Hemocytometer. HaCaT cells were seeded in the plates 24 hours prior to treatment in 96 well plates at a concentration of 2×10^5 cells mL^{-1} in 100 µL of medium (2×10^4 cells/well). Empty wells were filled with 100 µL PBS. After 24 hours, cells were incubated with the compounds in a dilution series in triplicate from 2–100 µM (5 mM stock solutions in DMSO; and untreated cells with DMSO as a negative control) in 50 µL of the media for 1 hour. Afterwards, 50 µL was removed from each well and cells washed with 100 µL PBS. 100 µL of medium was added to each well and the cells incubated for 24 hours at 37 °C, 5 % CO_2. 10 µL of alamarBlue® (Invitrogen) was added to each well before incubation for 1 hour. Cell viability was determined using a fluorescent plate reader (Synergy H4; λ_{ex} 560 nm, λ_{em} 600 nm).

7.23.4 Hemolysis assay

This assay was undertaken at Queens University, Belfast by Dr Russell Luo (postdoctoral research assistant), under the supervision of Dr Fionnuala Lundy.

Briefly, PBS was added to 2 mL of whole blood to a final volume of 25 mL in a 50 mL centrifuge tube and centrifuged for 5 min at 930 x *g*. The supernatant was discarded and PBS was added again to reach a final volume of 25 mL. This washing procedure was repeated until the supernatant was clear to obtain an 8 % erythrocyte suspension. A total volume of 50 µL of this suspension was pipetted into sterile microtubes. 50 µL of peptoid solution at final concentration of 100 µM, 50 µM, 25 µM, 12.5 µM and 6.25 µM were added to the microtubes and inverted to allowing mixing. 50 µL of 2.5 % Triton-X 100 and 50 µL of PBS were used as positive and negative controls respectively. The hemolytic activity of each peptoid was analysed in triplicate. The microtubes were incubated at 37 ˚C for 1 hour and then centrifuged for 5 minutes at 930 x *g*. 80 µL of supernatant from each microtube was pipetted into a flat bottomed, clear 96-well plate. The absorbance at 570 nm in a microtitre plate reader and the percentage hemolysis was calculated using the following formula:

% Hemolysis = (A–AO)/(AX–AO) × 100%

where A is the OD of the peptoid-treated erythrocytes, AO is OD of the negative control, and AX is OD of the positive control.

7.24   Antiparasitic IC$_{50}$ determination

The antiparasitic testing outlined below was carried out at the Swiss Tropical and Public Health Institute by Dr Marcel Kaiser. Procedures also provided by Dr Marcel Kaiser.

7.24.1 Activity against *Trypanosoma brucei rhodesiense*

This stock was isolated in 1982 from a human patient in Tanzania and after several mouse passages cloned and adapted to axenic culture conditions.[10] Minimum Essential Medium (50 µL) supplemented with 25 mM HEPES, 1g L^{-1} additional glucose, 1 % MEM non-essential amino acids (100x), 0.2 mM 2-mercaptoethanol, 1mM sodium pyruvate and 15 % heat inactivated horse serum was added to each well of a 96-well microtiter plate. Serial drug dilutions of eleven 3-fold dilution steps covering a range from 100 to 0.002 µg mL^{-1} were prepared. Then 4 x 10^3 bloodstream forms of *T. b. rhodesiense* STIB 900 in 50 µL was added to each well and the plate incubated at 37 °C under a 5 % CO$_2$ atmosphere for 70 hours. 10 µL alamarBlue® (resazurin, 12.5 mg in 100 mL double-distilled water) was then added to each well and incubation continued for a further 2–4 hours.[11] The plates were read with a Spectramax Gemini XS microplate fluorometer (Molecular Devices Cooperation, Sunnyvale, CA, USA; λ$_{ex}$ 536 nm, λ$_{em}$ 588 nm) The IC$_{50}$ values were calculated by linear regression[12] from the sigmoidal dose inhibition curves using SoftmaxPro software (Molecular Devices Cooperation, Sunnyvale, CA, USA). Melarsoprol (Arsobal Sanofi-Aventis, received from WHO) is used as control.

7.24.2 Activity against *Trypanosoma cruzi*

Rat skeletal myoblasts (L-6 cells) were seeded in 96-well microtitre plates at 2000 cells/well in 100 µL RPMI 1640 medium with 10 % FBS and 2 mM L-glutamine. After 24 hours the medium was removed and replaced by 100 µL per well containing 5 x 10^3 trypomastigote forms of *T. cruzi* Tulahuen strain C2C4 containing the β-galactosidase (Lac Z) gene.[13] After 48 hours the medium was removed from the wells and replaced by 100 mL fresh medium with or without a serial drug dilution of eleven 3-fold dilution steps covering a range from 100– 0.002 µg mL^{-1}. After 96 hours of incubation the plates were inspected under an inverted microscope to assure growth of the controls and sterility. Then the substrate CPRG/Nonidet (50 µL) was added to all wells. A colour reaction developed within 2–6 hours and could be read photometrically at 540 nm. Data were analysed with the graphic programme Softmax Pro (Molecular Devices), which calculated IC$_{50}$ values by linear regression from the sigmoidal dose inhibition curves. Benznidazole is used as control (IC$_{50}$ 0.5 ± 0.2 g mL^{-1}).

7.24.3 Activity against *Leishmania donovani* axenic amastigotes

Amastigotes of *L. donovani* strain MHOM/ET/67/L82 were grown in axenic culture at 37 °C in SM medium[14] at pH 5.4 supplemented with 10% heat-inactivated foetal bovine serum under an atmosphere of 5 % CO_2 in air. 100 µL of culture medium with 1 x 10^5 amastigotes from axenic culture with or without a serial drug dilution were seeded in 96-well microtitre plates. Serial drug dilutions of eleven 3-fold dilution steps covering a range from 90– 0.002 µg mL^{-1} were prepared. After 70 hours of incubation the plates were inspected under an inverted microscope to assure growth of the controls and sterile conditions. 10 µL of alamarBlue® (12.5 mg resazurin dissolved in 100 mL distilled water)[15] were then added to each well and the plates incubated for another 2 hours. Then the plates were read with a Spectramax Gemini XS microplate fluorometer (Molecular Devices Cooperation, Sunnyvale, CA, USA; λ_{ex} 536 nm, λ_{em} 588 nm). Data were analysed using the software Softmax Pro (Molecular Devices Cooperation, Sunnyvale, CA, USA). Decrease of fluorescence (= inhibition) was expressed as percentage of the fluorescence of control cultures and plotted against the drug concentrations. From the sigmoidal inhibition curves the IC_{50} values were calculated.

7.24.4 Activity against *Plasmodium falciparum*

In vitro activity against erythrocytic stages of *P. falciparum* was determined using a 3H-hypoxanthine incorporation assay[16,17] using the drug sensitive NF54 strain (Schipol airport[18]) or the chloroquine and pyrimethamine resistant K1 strain that originate from Thailand[19] and the standard drug chloroquine (Sigma C6628). Compounds were dissolved in DMSO at 10 mg/mL and added to parasite cultures incubated in RPMI 1640 medium without hypoxanthine, supplemented with HEPES (5.94 g L^{-1}), NaHCO3 (2.1 g L^{-1}), neomycin (100 µg mL^{-1}), AlbumaxR (5 g L^{-1}) and washed human red cells A+ at 2.5 % haematocrit (0.3 % parasitaemia). Serial drug dilutions of eleven 3-fold dilution steps covering a range from 100–0.002 µg mL^{-1} were prepared. The 96-well plates were incubated in a humidified atmosphere at 37 °C; 4 % CO_2, 3 % O_2, 93 % N_2. After 48 hours 50 µL of 3H-hypoxanthine (= 0.5 µCi) was added to each well of the plate. The plates were incubated for a further 24 hours under the same conditions. The plates were then harvested with a Betaplate™ cell harvester (Wallac, Zurich, Switzerland), and the red blood cells transferred onto a glass fibre filter then washed with distilled water. The dried filters were inserted into a plastic foil with 10 mL of scintillation fluid, and counted in a Betaplate™ liquid scintillation counter (Wallac, Zurich, Switzerland). IC_{50} values were calculated from sigmoidal inhibition curves by linear regression using Microsoft Excel. Chloroquine and artemisinin are used as control.

7.24.5 *In vitro* cytotoxicity with L-6 cells

Assays were performed in 96-well microtiter plates, each well containing 100 µL of RPMI 1640 medium supplemented with 1 % L-glutamine (200 mM) and 10 % foetal bovine serum, and 4 x 10^3 L-6 cells (a primary cell line derived from rat skeletal myoblasts).[20,21] Serial drug dilutions of eleven 3-fold dilution steps covering a range from 100–0.002 µg mL^{-1} were prepared. After 70 hours of incubation the plates were inspected under an inverted microscope to assure growth of the controls and sterile conditions. 10 µL of alamarBlue® was then added to each well and the plates incubated for another 2 hours. Then the plates were read with a Spectramax Gemini XS microplate fluorometer (Molecular Devices Cooperation, Sunnyvale, CA, USA; λ_{ex} 536 nm, λ_{em} 588 nm). The IC$_{50}$ values were calculated by linear regression (Huber 1993) from the sigmoidal dose inhibition curves using SoftmaxPro software (Molecular Devices Cooperation, Sunnyvale, CA, USA). Podophyllotoxin (Sigma P4405) is used as control.

7.25 Biofilm prevention and disruption assays

Biofilm testing was carried out at Queens University, Belfast by Dr Yu Luo (postdoctoral research assistant), under the supervision of Dr Fionnuala Lundy. Methods and procedures supplied by Dr Fionnuala Lundy.

7.25.1 Micro-organism strains and growth conditions

C. albicans (NCTC 3179) was subcultured aerobically on Sabouraud agar plates and propagated in yeast peptone dextrose broth. *E. coli* (ATCC 29522) and *S. aureus* (NCTC 6571) were grown on blood agar plates and propagated in brain heart infusion (BHI) broth.

7.25.2 Preparation and treatment of single species biofilms

Overnight cultures of *C. albicans* were washed and resuspended in a modified RPMI-1640 (Sigma-Aldrich, St Louis, USA) medium to yield an inoculum of 1.0×10^6 cells mL^{-1}.[22] Overnight cultures of *S. aureus* or *E. coli* were washed and resuspended in BHI broth (Oxoid, Basingstoke, UK) to yield an inoculum of 5.0×10^6 cells mL^{-1}. A total volume of 100 µL of each inoculum was added to microtitre plate wells (Thermo Fisher Scientific, Roskilde, Denmark). An initial biofilm was allowed to form for 4 hours. Wells were washed three times with 200 µL PBS to facilitate removal of planktonic cells and the biofilms were then treated with 100 µM of peptoids solution in the appropriate broth. Plates were incubated for a further 24 hours to allow biofilm maturation. After removal

of planktonic cells by washing, biofilms were quantified by the crystal violet assay or by PMA-qPCR.

7.25.3 Preparation and treatment of polymicrobial biofilms

Overnight cultures of *C. albicans* were prepared in microtitre plates as outlined above and allowed to adhere for 4 hours to facilitate initial biofilm formation. Planktonic *C. albicans* cells were then removed as outlined above before the addition of 100 μL of *S. aureus* or *E. coli* (5.0×10^6 cells mL^{-1}). Bacteria were allowed to adhere to the *C. albicans* biofilms for 4 hours to facilitate polymicrobial biofilm formation. Following a washing step, the biofilms were then treated with peptoids (100 μM), and incubated for a further 24 hours to allow biofilm maturation. Wells were washed as previously outlined and the polymicrobial biofilms were quantified by PMA-modified qPCR.

7.25.4 Biofilm quantification by crystal violet assay

Washed biofilms were fixed with 100 μL methanol for 10 minutes. Following removal of methanol, the wells were air dried and stained with crystal violet solution (Clin-Tech Ltd, Guildford, UK) for 20 minutes at room temperature. Excess stain was removed by washing, the plate was then air dried and bound crystal violet was re-solubilised in 160 μL 33 % acetic acid prior to reading at 570 nm in a microtitre plate reader (Tecan GENios, Zürich, Switzerland).

7.25.5 Biofilm quantification by PMA-modified qPCR

To determine the bactericidal and fungicidal activity of peptoids against both single species and polymicrobial biofilms, the biofilms were detached from the microtitre plate wells prior to quantification. Wells were washed as previously described before 100 μL of BHI broth was added and the plate was sealed. Biofilm detachment was achieved by sonication for 5 mins in an ultrasonic bath (Dawe, Middlesex, UK). The remaining cells were then collected in 80 μL BHI. Twenty microlitres of PMA (Biotium Inc., California, USA) (2 mM in broth[23]) was added to the biofilm suspensions (180 μL) and incubated at 37 °C (5 min) prior to photoactivation with a broad-spectrum LED floodlight placed at 15 cm from the tubes, (which were mixed by inversion during the 20 min photoactivation step). DNA was extracted using the microLYSIS®-Plus kit (Microzone, Haywards Heath, UK) as per the manufacturer's instructions and qPCR was performed in a Mx3005P qPCR System (Agilent Technologies, California USA).

Table 7.6. Reaction formulation for *C. albicans*:[24]

Component of reaction mix	Volume for 10 reactions (µL)	Final Concentration
FastStart Universal SYBR Green Master (2X) (Roche)	50	1X
Forward primer (60 µM): CCTGTTTGAGCGTCRTTT	0.25	150 nM
Reverse primer (200 µM): TCCTCCGCTTATTGATAT	0.25	500 nM
Template	10	
Nuclease free water	39.5	

Table 7.7. Reaction formulation for *S. aureus*:[25]

Component of reaction mix	Volume for 10 reactions (µL)	Final Concentration
Platinum® qPCR Supermix-UDG	60	1X
Forward primer (200 µM): CAAAGCATCCTAAAAAAGGTGTAGAGA	0.24	400 nM
Reverse primer (200 µM): TTCAATTTTCTTTGCATTTTCTACCA	0.24	400 nM
Probe (100 µM): 6FAM-TTTTCGTAAATGCACTTGCTTCAGGACCA-BHQ1	0.24	200 nM
MgCl2 (50 mM)	2.4	
Template	30	
Nuclease free water	26.88	

Table 7.8. Reaction formulation for *E. coli*:[26]

Component of reaction mix	Volume for 10 reactions (μL)	Final Concentration
FastStart Universal SYBR Green Master (2X) (Roche)	50	1X
Forward primer (200 μM): AGAAGCTTGCTCTTTGCTGA	0.25	500nM
Reverse primer (200 μM): CTTTGGTCTTGCGACGTTAT	0.25	500nM
Template	10	
Nuclease free water	39.5	

Table 7.9. qPCR conditions for *C. albicans* and *E. coli* (instructions provided with FastSart kit, Roche):

Cycles	Target temperature (°C)	Hold time	Analysis Mode
1	50	15 min	None
1	95	10 min	None
45	95	15 s	None
	60	60 s	Single fluorescence acquisition
Melting analysis			
1	95	30 s	None
1	35	60 s	None
1	98	30 s	Continuous fluorescence acquisition
Cooling			
1	40	10 s	None

Table 7.10. qPCR Conditions for *S. aureus* (adapted from instructions provided with Platinum® Quantitative PCR SuperMix-UDG):

Cycles	Target temperature (°C)	Hold time	Analysis Mode
1	50	15 min	None
1	95	5 min	None
45	95	10 s	None
	60	60 s	Single fluorescence acquisition
Cooling			
1	40	10 s	None

7.25.6 Statistical analysis

The susceptibility of *C. albicans*, *S.aureus* and *E.coli* in both single species and polymicrobial biofilms to novel peptoids was determined by biofilm inhibition assays. All data represent an average of 3 independent experiments and were subject to statistical analysis by One-way ANOVA followed by Tukey's post hoc correction for multiple comparisons, where ns: $p>0.5$; * $p< 0.5$; **$p<0.05$, ***$p< 0.001$; **** $p< 0.0001$.

7.25.7 SYTOX® Green assay

Briefly, mid log phase microorganism cultures were adjusted to the appropriate concentration (OD 0.7 at 600nm for *S. aureus* and *E. coli*, OD 2.0 at 600nm for *C. albicans*). A 50 µL of microorganism suspension in Mueller Hinton broth (MHB) was added to each well of a 96 well black flat bottomed plate. 50 µL of each peptoid to be tested at final concentration of 100 µM were added to the wells. SYTOX® Green was added to each well to a final concentration of 5 µM. The plate was covered, protected from light and incubated for 2 hours at 37 °C. Microorganisms which had been heat treated at 99 °C for 10 minutes to permeabilise their membranes served as positive controls. Bacteria without any form of peptoid treatment acted as negative controls. Additional control wells containing SYTOX® Green only were included to ensure there was no background fluorescence. Wells containing SYTOX® Green and peptoid only were included to ensure there were no interactions between the SYTOX® Green and peptoids that could lead to non-specific fluorescence measurements. The plate was read on a fluorimeter (SpectraMax Gemini X fluorimeter; λ_{ex} 480 nm, λ_{em} 530 nm).

7.25.8 Generation of standard curves for PMA-qPCR

To allow quantification of the numbers of *C. albicans*, *S. aureus* and *E. coli* within both single species and polymicrobial biofilms, DNA standards were prepared by extraction of DNA from planktonic organisms using the microLYSIS®-Plus kit and purified using the DNeasy kit (Qiagen, Manchester, UK). DNA standards corresponding to cell numbers from $10–1 \times 10^6$ were used in PMA-qPCR assays to generate standard curves from which the numbers of living organisms within the biofilms could be determined.

7.26 References

1. R.N. Zuckermann, J.M. Kerr, S.B.H. Kent, W.H. Moos, *J. Am. Chem. Soc.,* **1992**, *114*, 10646.
2. H.-Y. Shiu, M.-K. Wong, C.-M. Che, *Chem. Comm.,* **2011**, *47*, 4367.
3. T. Koopmans, T.M. Wood, P. t Hart, L.H.J. Kleijn, A.P.A. Hendrickx, R.J.L. Willems, E. Breukink, N.I. Martin, *J. Am. Chem. Soc.,* **2015**, *29*, 9382.
4. A. Mishra, R. Mishra, S. Gottschalk, R. Pal, N. Sim, J. Engelmann, M. Goldberg, D. Parker, *ACS Chem. Neuroscience,* **2014**, *5*, 128.
5. J.M. Andrews, *J. Antimicrob. Chemother.,* **2001**, *48*, 5.
6. P.A. Bates, *Parasitol.,* **1994**, *108*, 1.
7. F.L. Chadbourne, C. Raleigh, H.Z. Ali, P.W. Denny, S.L. Cobb, *J. Pept. Sci.,* **2011**, *17*, 751.
8. J.H. Zhang, T.D. Chung, K.R. Oldenburg, *J. Biomol. Screen.,* **1999**, *4*, 67.
9. H.L. Bolt, G.A. Eggimann, P.W. Denny, S.L. Cobb, *MedChemComm,* **2016**, *7*, 799.
10. T. Baltz, D. Baltz, C. Giroud, J. Crockett, *EMBO. J.,* **1985**, *4*, 1273.
11. B. Raz, M. Iten, Y. Grether-Buhler, R. Kaminsky, R. Brun, *Acta Tropica,* **1997**, *68*, 139.
12. W. Huber, J.C. Koella, *Acta Tropica,* **1993**, *55*, 257.
13. F.S. Buckner, C.L. Verlinde, A.C. La Flamme, W.C. Van Voorhis, *Antimicrob. Agents Chemother.,* **1996**, *40*, 2592.
14. I. Cunningham, *J. Protozool.,* **1977**, *24*, 325.
15. J. Mikus, D. Steverding, *Parasitol. Int.,* **2000**, *48*, 265.
16. R.E. Desjardins, C.J. Canfield, J.D. Haynes, J.D. Chulay, *Antimicrob. Agents Chemother.,* **1979**, *16*, 710.
17. H. Matile, J.R.L. Pink *Plasmodium falciparum malaria parasite cultures and their use in immunology*; Academic Press: San Diego, 1990.
18. T. Ponnudurai, A.D. Leeuwenberg, J.H. Meuwissen, *Trop. Geogr. Med.,* **1981**, *33*, 50.
19. S. Thaithong, G.H. Beale, M. Chutmongkonkul, *Trans. R. Soc. Trop. Med. Hyg.,* **1983**, *77*, 228.
20. B. Page, M. Page, C. Noel, *Int. J. Oncol.,* **1993**, *3*, 473.
21. S.A. Ahmed, R.M. Gogal, Jr., J.E. Walsh, *J. Immunol. Methods,* **1994**, *170*, 211.
22. C.G. Pierce, P. Uppuluri, A.R. Tristan, F.L. Wormley, Jr., E. Mowat, G. Ramage, J.L. Lopez-Ribot, *Nat. Protoc.,* **2008**, *3*, 1494.
23. J.K. van Frankenhuyzen, J.T. Trevors, C.A. Flemming, H. Lee, M.B. Habash, *J. Ind. Microbiol. Biotechnol.,* **2013**, *40*, 1251.
24. C. Schabereiter-Gurtner, B. Selitsch, M.L. Rotter, A.M. Hirschl, B. Willinger, *J. Clin. Microbiol.,* **2007**, *45*, 906.
25. R.R. McDonald, N.A. Antonishyn, T. Hansen, L.A. Snook, E. Nagle, M.R. Mulvey, P.N. Levett, G.B. Horsman, *J. Clin. Microbiol.,* **2005**, *43*, 6147.
26. D.H. Lee, J.E. Bae, J.H. Lee, J.S. Shin, I.S. Kim, *J. Microbiol. Biotechnol.,* **2010**, *20*, 1463.

Appendices
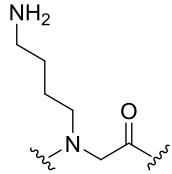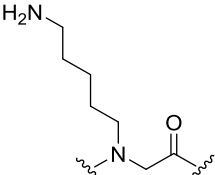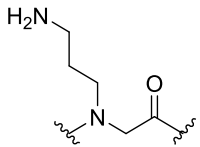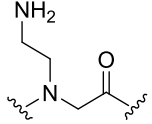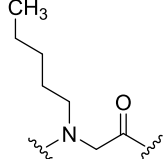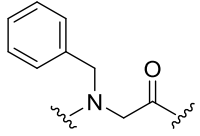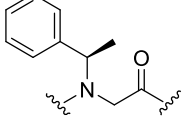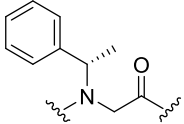
A1. Supplementary information
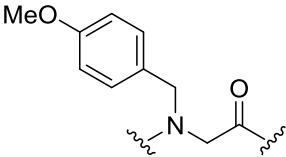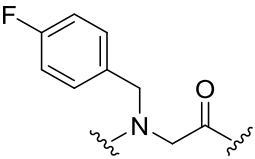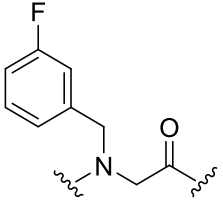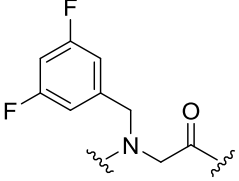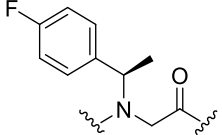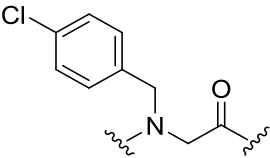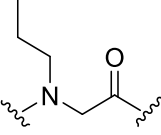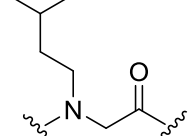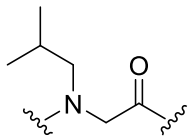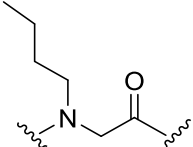
Electronic supplementary information accompanies this thesis, containing characterisation data for all the compounds described in Chapter 7, data from biological testing discussed in Chapters 3–5 and digital copies of the microscopy images discussed in Chapter 5.

A2. Peptoid nomenclature

In an effort to implement a consistent nomenclature across peptoid building blocks in this project, given the ambiguity in the current literature, peptoid monomers described in this thesis have been tabulated below in **Table A1**.

Extra nomenclature and monomers are also listed on www.pep-calc.com/peptoid in collaboration with Sam Lear (which also includes residues not used in this project, but commonly found in the literature).

Monomer	Chemical Structure	Amine Sub-monomer
NLys *N*-(4-aminobutyl) glycine		*N*-Boc-1,4-diaminobutane
Nah *N*-(6-aminohexyl) glycine		*N*-Boc-1,6-diaminohexane
Nap *N*-(3-aminopropyl) glycine		*N*-Boc-1,3-diaminopropyl
Nae *N*-(2-aminoethyl) glycine		*N*-Boc-1,4-diaminoethane
Namy *N*-(pentyl) glycine		amylamine
Nphe *N*-(benzyl) glycine		benzylamine
Nspe *N*-(S)-(1-phenylethyl) glycine		*(S)*-(–)-α-methylbenzylamine
Nrpe *N*-(R)-(1-phenylethyl) glycine		*(R)*-(+)-α-methylbenzylamine

Npmb *N*-(4-methoxyphenylmethyl) glycine		4-methoxybenzylamine
Npfb *N*-(4-fluorophenylmethyl) glycine		4-fluorobenzylamine
Nmfb *N*-(3-fluorophenylmethyl) glycine		3-fluorobenzylamine
Ndfb *N*-(3,5-difluorophenylmethyl) glycine		3,5-difluorobenzylamine
Nsfb *N*(*S*-4-fluorophenylethyl) glycine		(*S*)-4-fluoro-α- methylbenzylamine
Npcb *N*-(4-chlorophenylmethyl) glycine		4-chlorobenzylamine
NnVal *N*-(propyl) glycine		propylamine
NhLeu *N*-(isopentyl) glycine		isopentylamine
NLeu *N*-(isobutyl) glycine		isobutylamine
Nbut *N*-(butyl) glycine		butylamine

NhArg *N*-(4-guanidinobutyl) glycine		*n/a*
NArg *N*-(3-guanidinopropyl) glycine		*n/a*
NnArg *N*-(2-guanidinoethyl) glycine		*n/a*
NGlu *N*-(2-hydroxyethyl) glycine		β-Alanine ᵗBu ester HCl
NhTrp *N*-(2-indole ethyl) glycine		tryptamine
NhTyr *N*-(4-methoxy phenylethyl) glycine		tyramine
Npyr *N*-(pyridyl) glycine		4-(aminomethyl)pyridine
NhHis *N*-(2-imidazole ethyl) glycine		histamine
Ntfe *N*-(2,2,2-trifluoroethyl) glycine		2,2,2 trifluoroethylamine
Npfp *N*-(2,2,3,3,3-pentafluoropropyl) glycine		2,2,3,3,3, pentafluoropropylamine

Ndfea
N-(2,2-difluoroethyl) glycine

2,2 difluroethylamine

NhCys
N-(2-thioethyl) glycine

trityl-thioethylamine

Nea
N-(ethyl) glycine

ethylamine

Nte
N-(2-2(2-methoxyethoxy)ethoxy
ethyl) glycine

2-2(2-methoxyethoxy)ethoxy
ethylamine

Nhept
N-(heptyl) glycine

heptylamine

Nchept
N-(cycloheptyl) glycine

cycloheptylamine

Ndodec
N-(dodecyl) glycine

dodecylamine

Nhexdec
N-(hexadecyl) glycine

hexadecylamine

Nprp
N-(3-propargyl) glycine

propargylamine

Nsch
N-(*S*)-(1-cyclohexylethyl) glycine

(*S*)-(-)-1-cyclohexylethylamine

Nsna
N-(*S*)-(1-napthylethyl) glycine

(*S*)-(-)-1-(2-napthyl)ethylamine

Ncpa
N-(cyclopentyl) glycine

cyclopentylamine
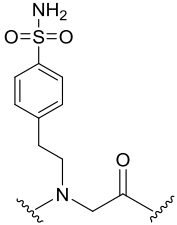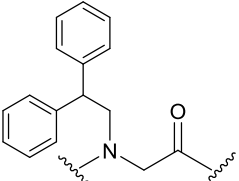
Nbsa *N*-(2-4-aminosulphonamide ethyl) glycine		4-(2 aminoethyl) benzenesulphonamide
Ndpe *N*-(2,2-diphenylethyl) glycine		2-2-diphenylethylamine

Table A1. Peptoid monomers used in the synthesis of the peptoid library and the corresponding amines that the submonomers are derived from.

A3. Synthesis of mixed lysine- and arginine-type peptoids

The following data gives an illustration of the Dde-protection and deprotection steps to synthesise peptoids with both lysine and arginine monomers in the same sequence, as described in Chapter 2.

The synthesis of the peptoids was monitored via LC-MS, using test cleaves on the resin at important steps in the procedure. These spectra are shown below to illustrate the synthesis of linear peptoids with both amino and guanido functionalized monomers. The synthesis of the cyclic peptoid, as monitored by LC-MS, is also shown.

Linear peptoid

Figure A1. Mass spectra and UV chromatograms following the synthesis of a linear mixed Lys/Arg peptoid; **151** [(*N*nArg*N*spe*N*spe)(*N*ae*N*spe*N*spe)]$_2$.

a) After Dde protection step on free amine, **m/z = 1026** [*From test cleave, Boc protection removed by conditions of cleavage but would remain protected on the full resin*]
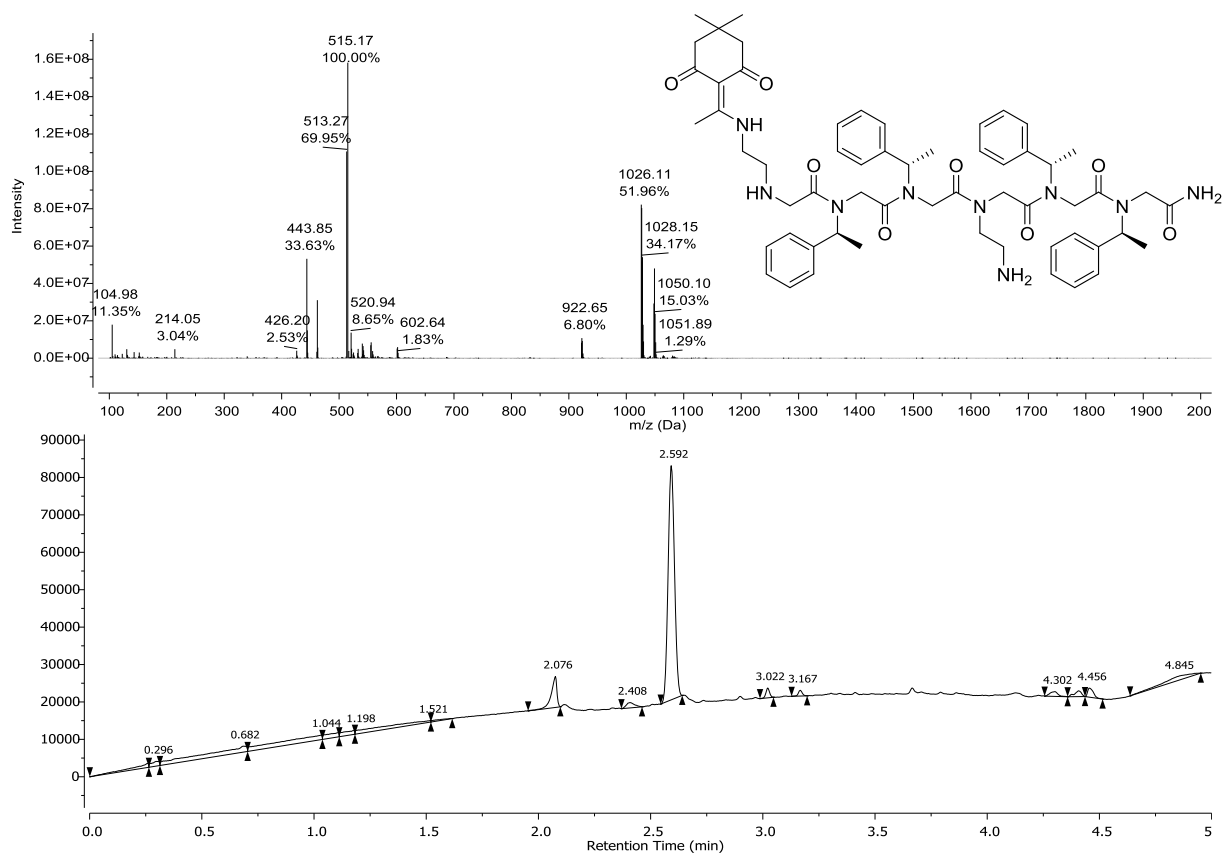
b) After chain elongation and second Dde protection, *m/z* = **2036, see [M+2H]²⁺ at 1017** [*From test cleave, Boc protection removed by conditions of cleavage but would remain protected on the full resin*]
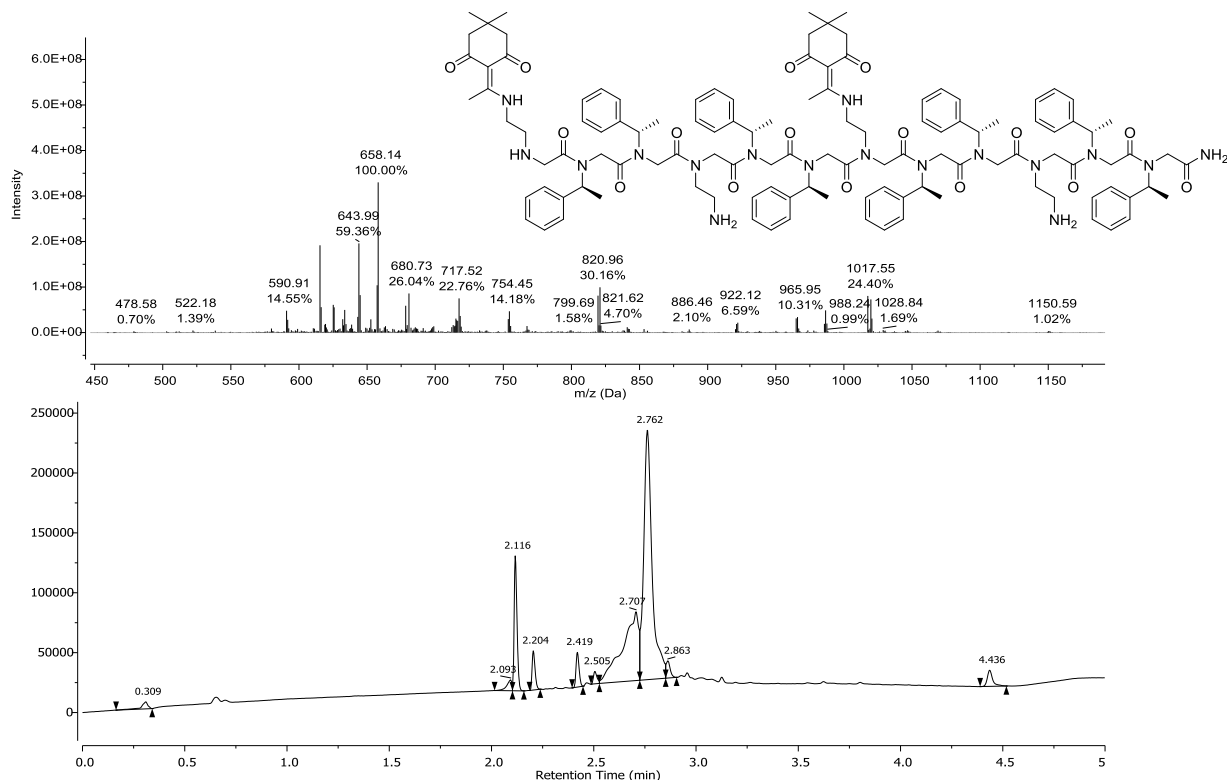
c) Following on-resin Dde-deprotection, *m/z* = **1707** [*From test cleave, Boc protection removed by conditions of cleavage but would remain protected on the full resin*]
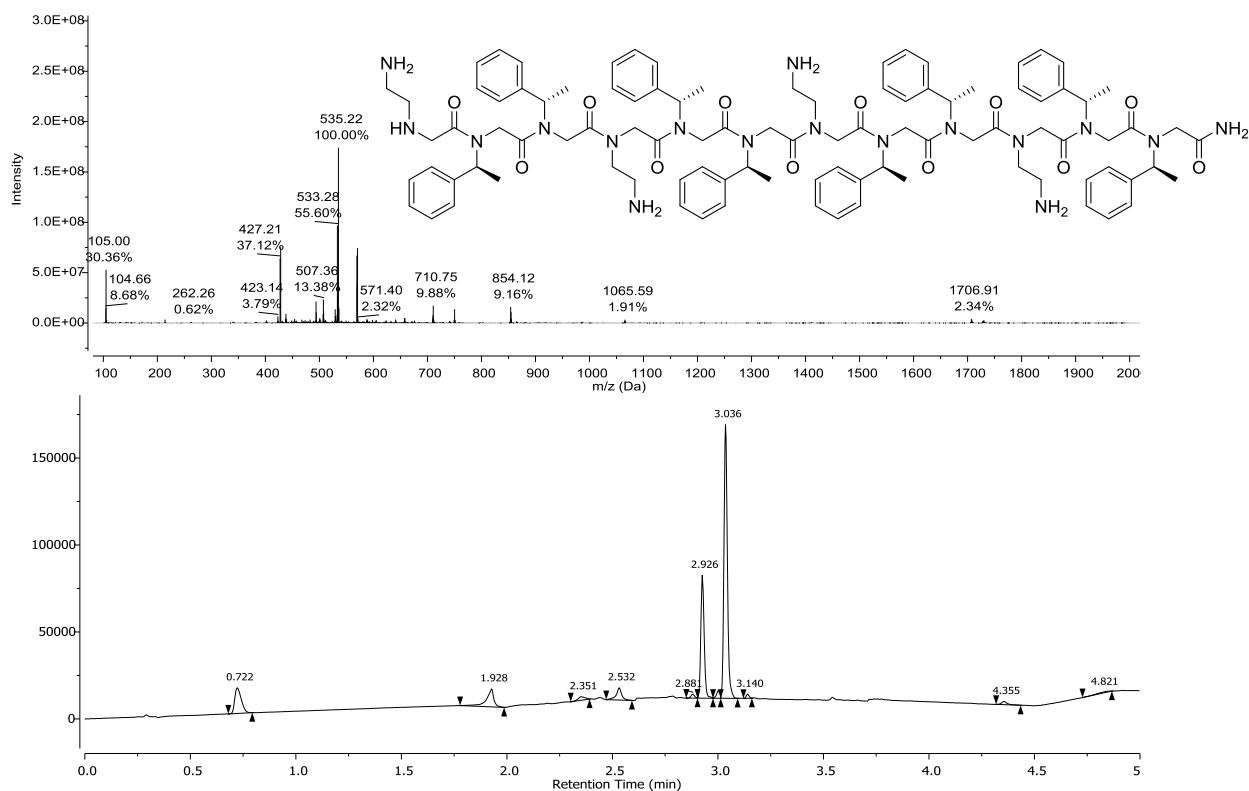
d) Crude peptoid after guanidinylation reaction, **m/z = 1791** [*From test cleave, Boc protection removed by conditions of cleavage but would remain protected on the full resin*]
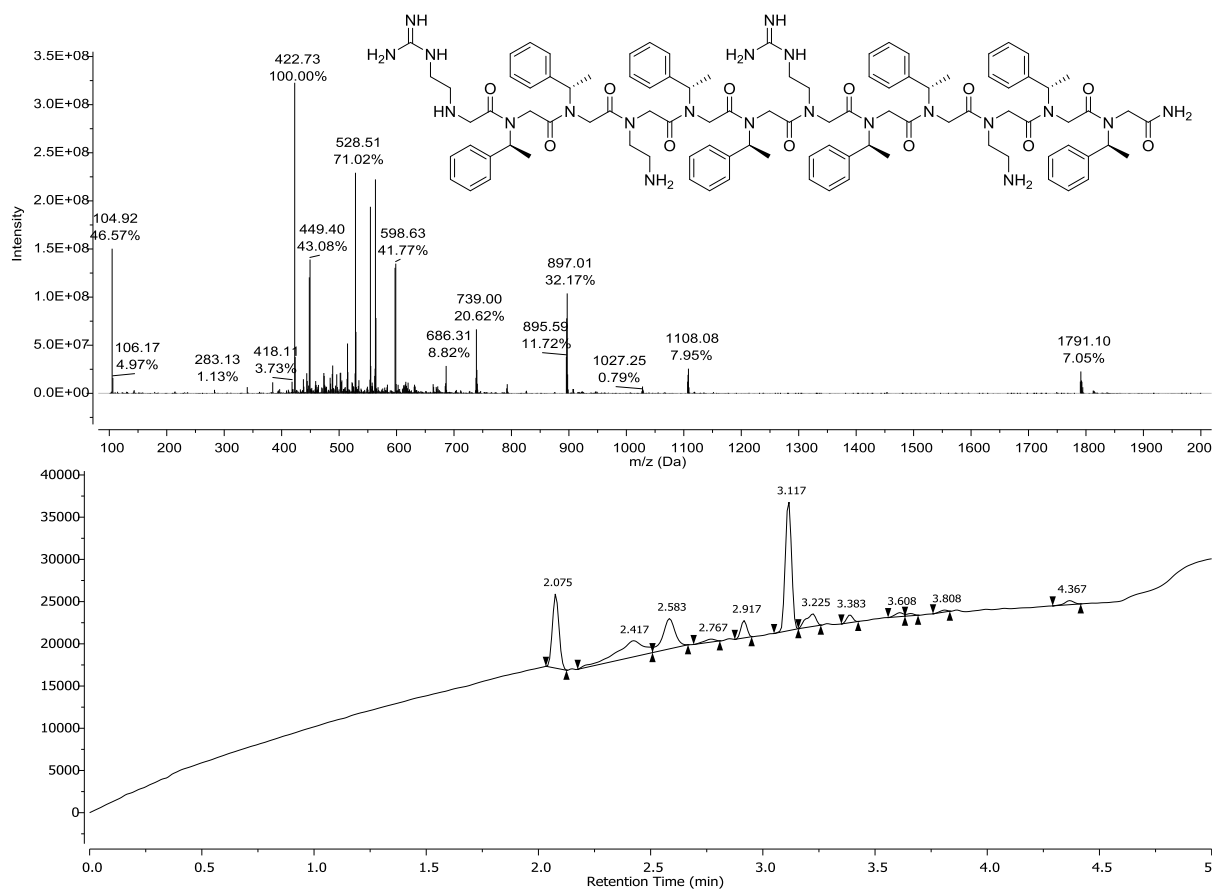
Cyclic peptoid

Figure A2. Mass spectra and UV chromatograms following the synthesis of a mixed Lys/Arg cyclic peptoid; cyclo **134** (*N*hArg*N*phe*N*Lys*N*phe*N*Lys*N*phe).

a) Crude protected linear precursor, *m/z* = **1209**
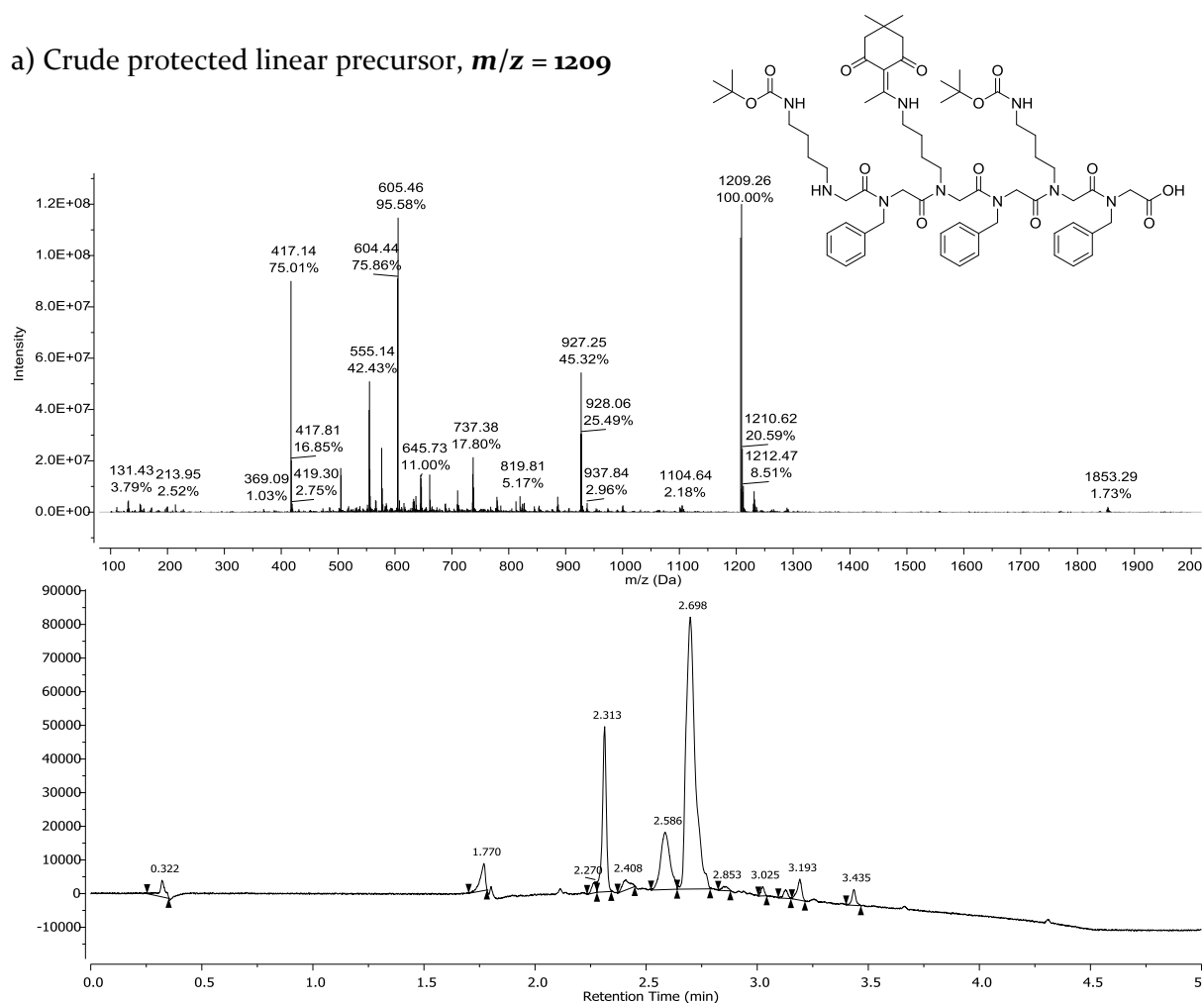
b) Crude cyclised compound, prior to HPLC, *m/z* = **1190**
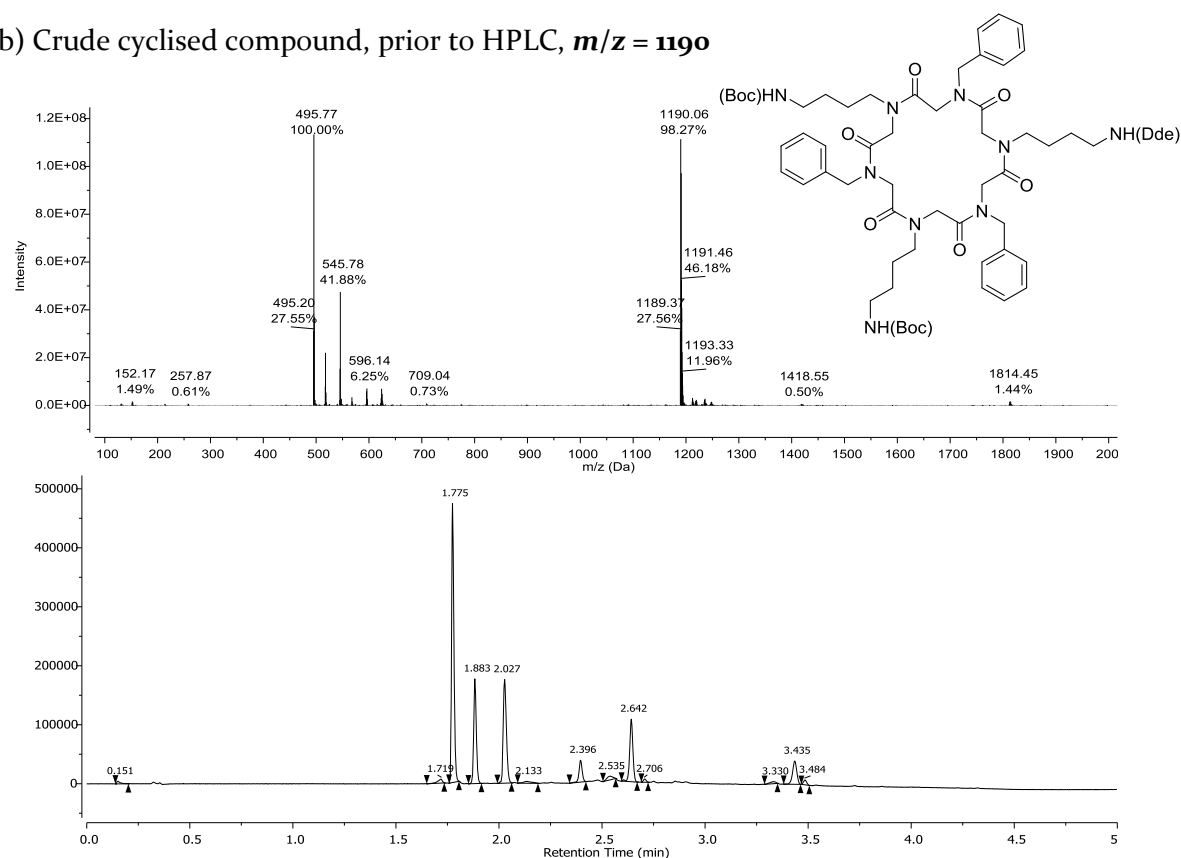
c) Following HPLC, then hydrazine deprotection of Dde group, *m/z* = **1026**
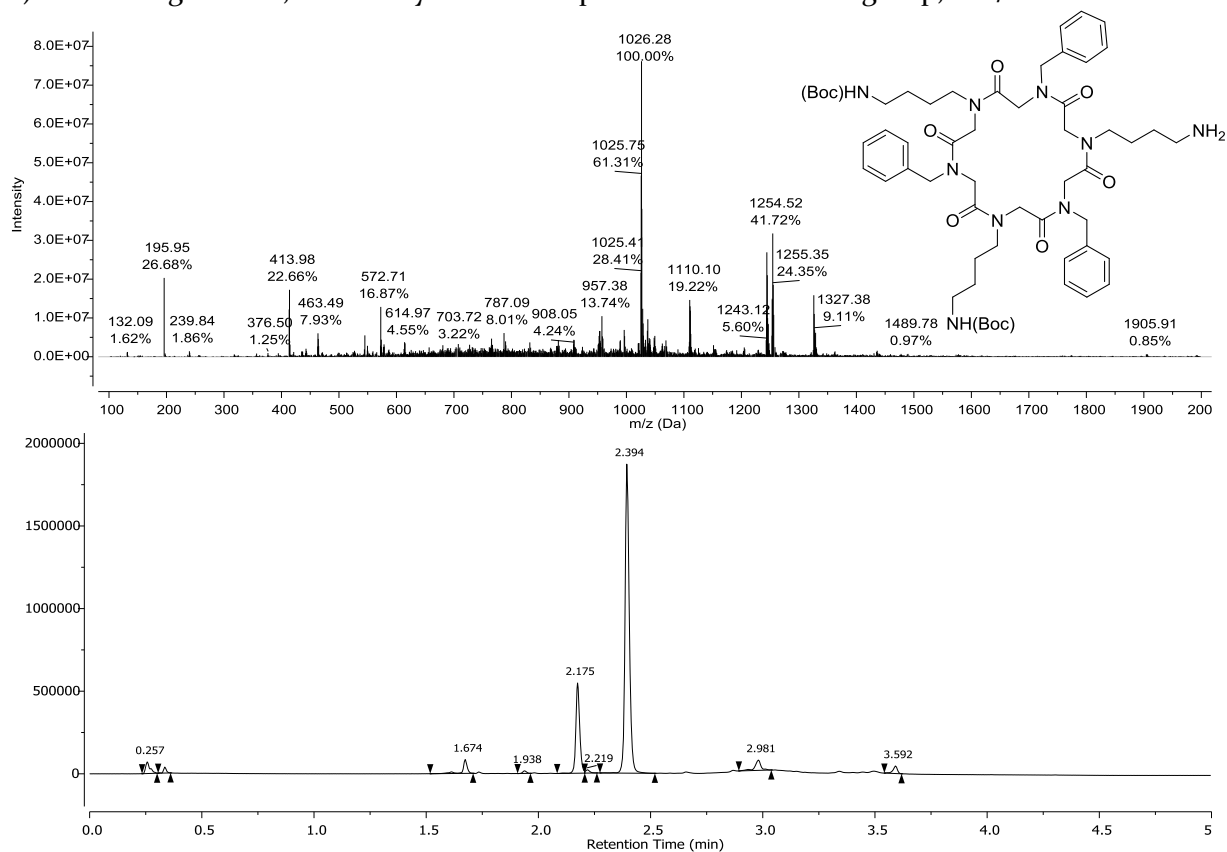
d) Following guanidinylation, *m/z* = 1069
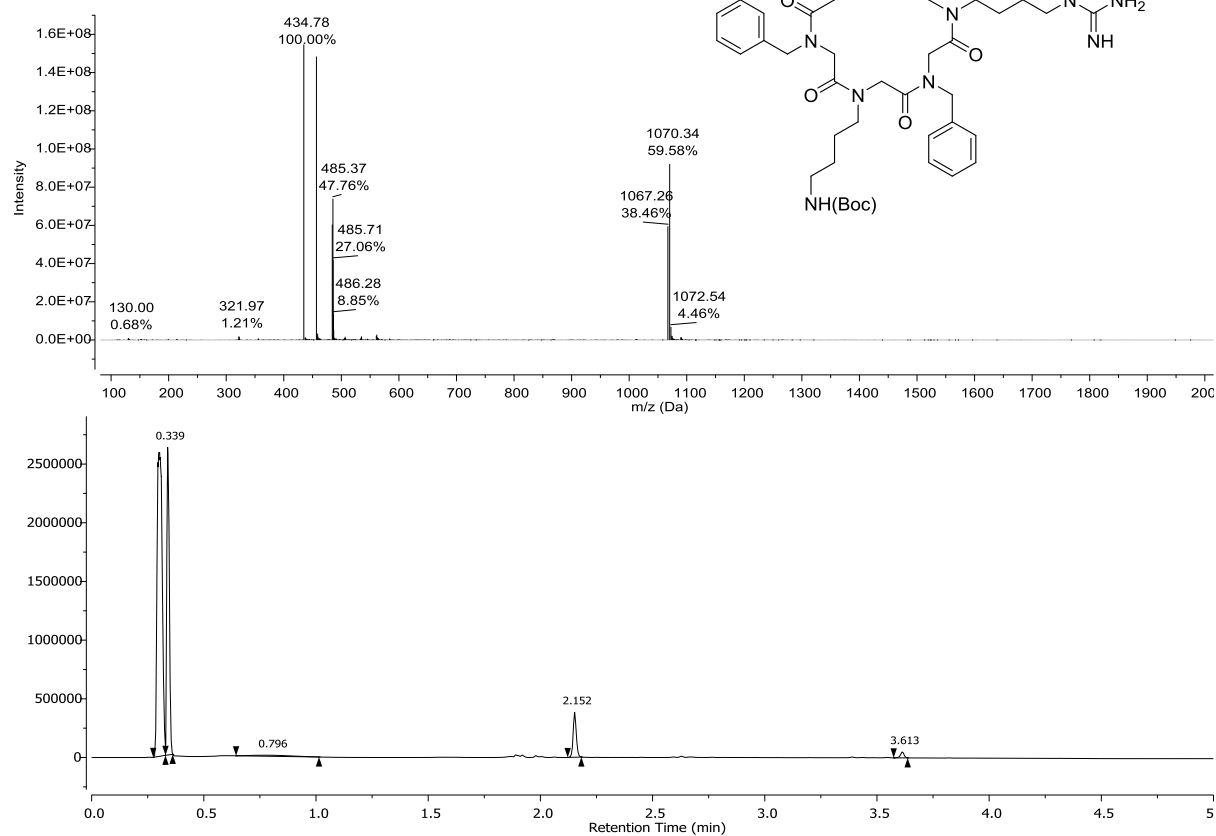
e) Crude product after final Boc deprotection, *m/z* = 868
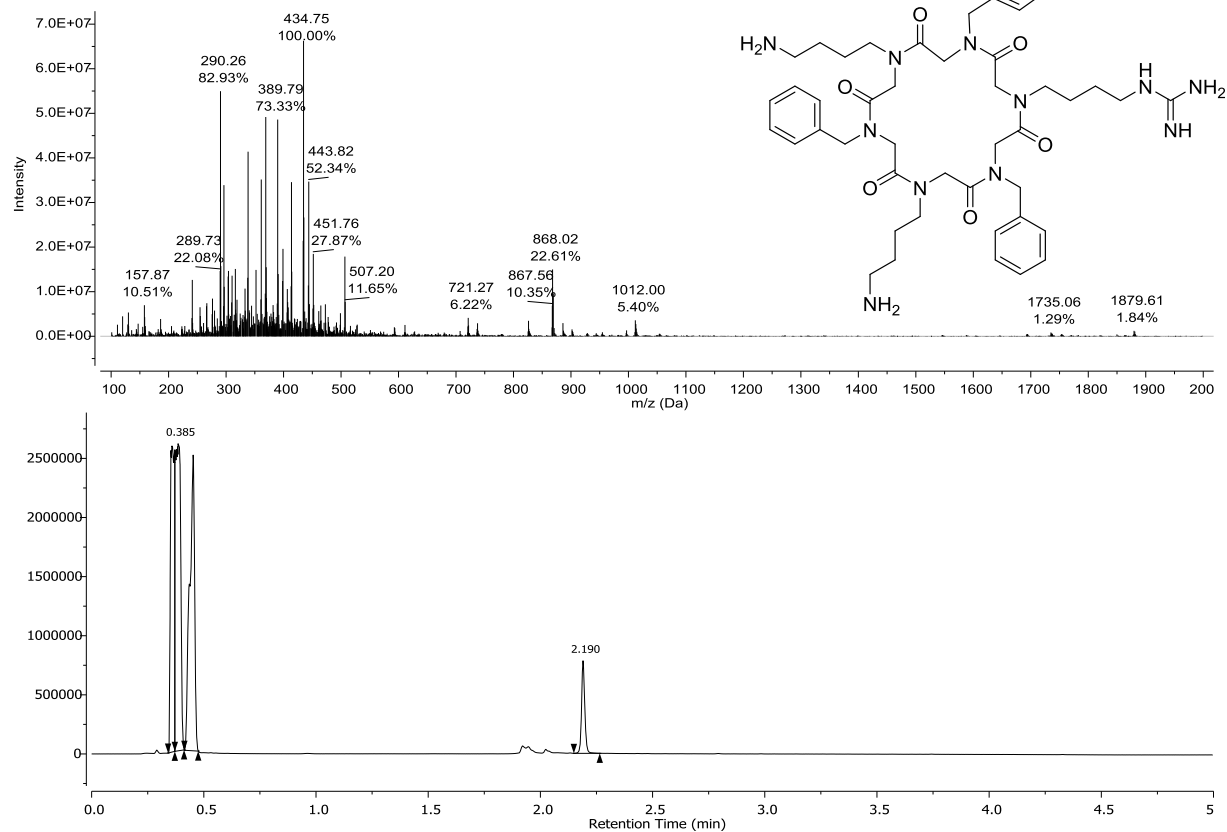
A4. Supplementary information for *L. mexicana* assays

Comparison of peptoid activity against promastigotes and amastigotes in assays with and without serum
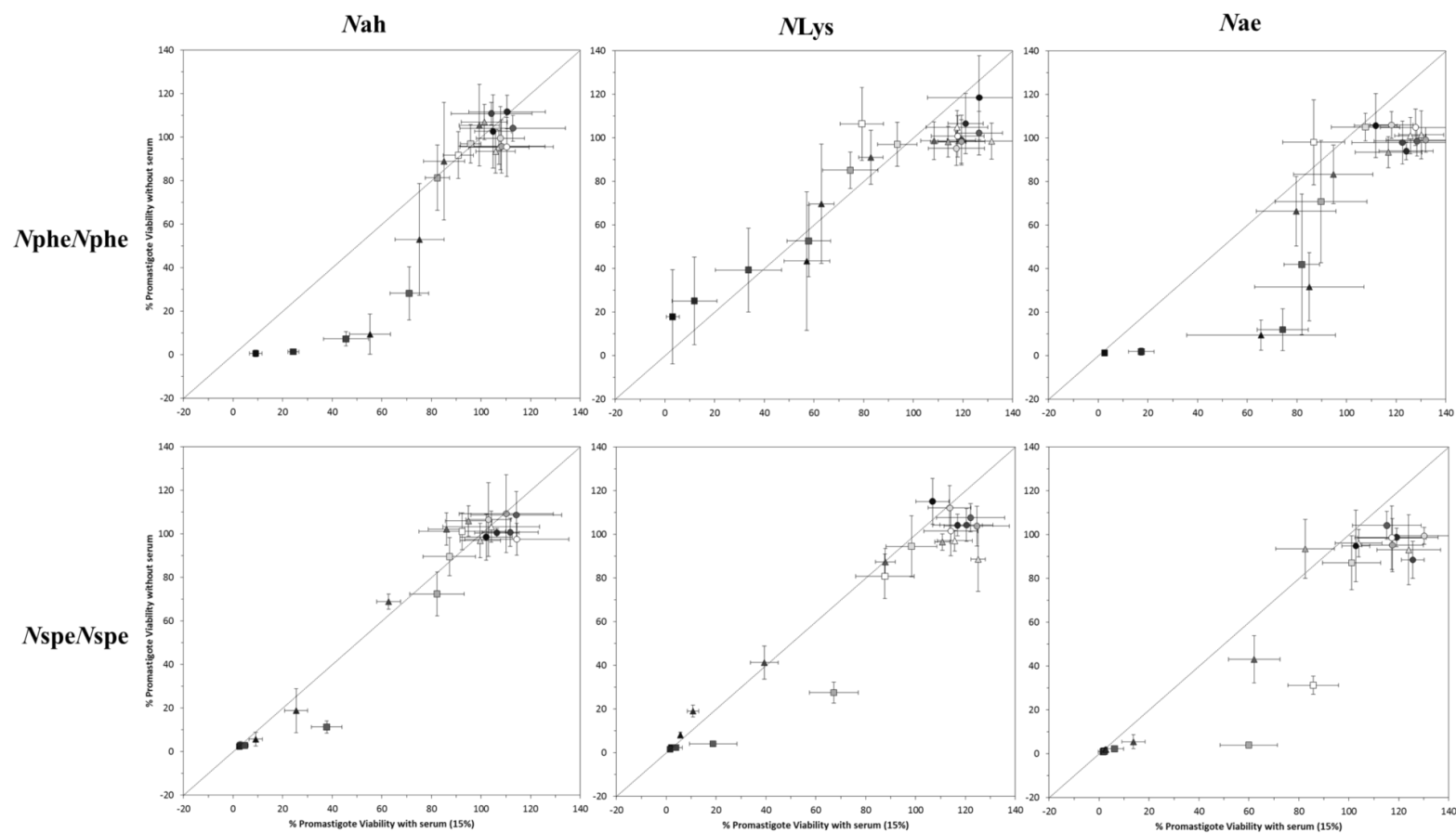
Figure A3. Comparison of serum and serum-free conditions in *L. mexicana* promastigotes; ■ 12 residue, ▲ 9 residue and ● 6 residue peptoids (compounds **210–219**).
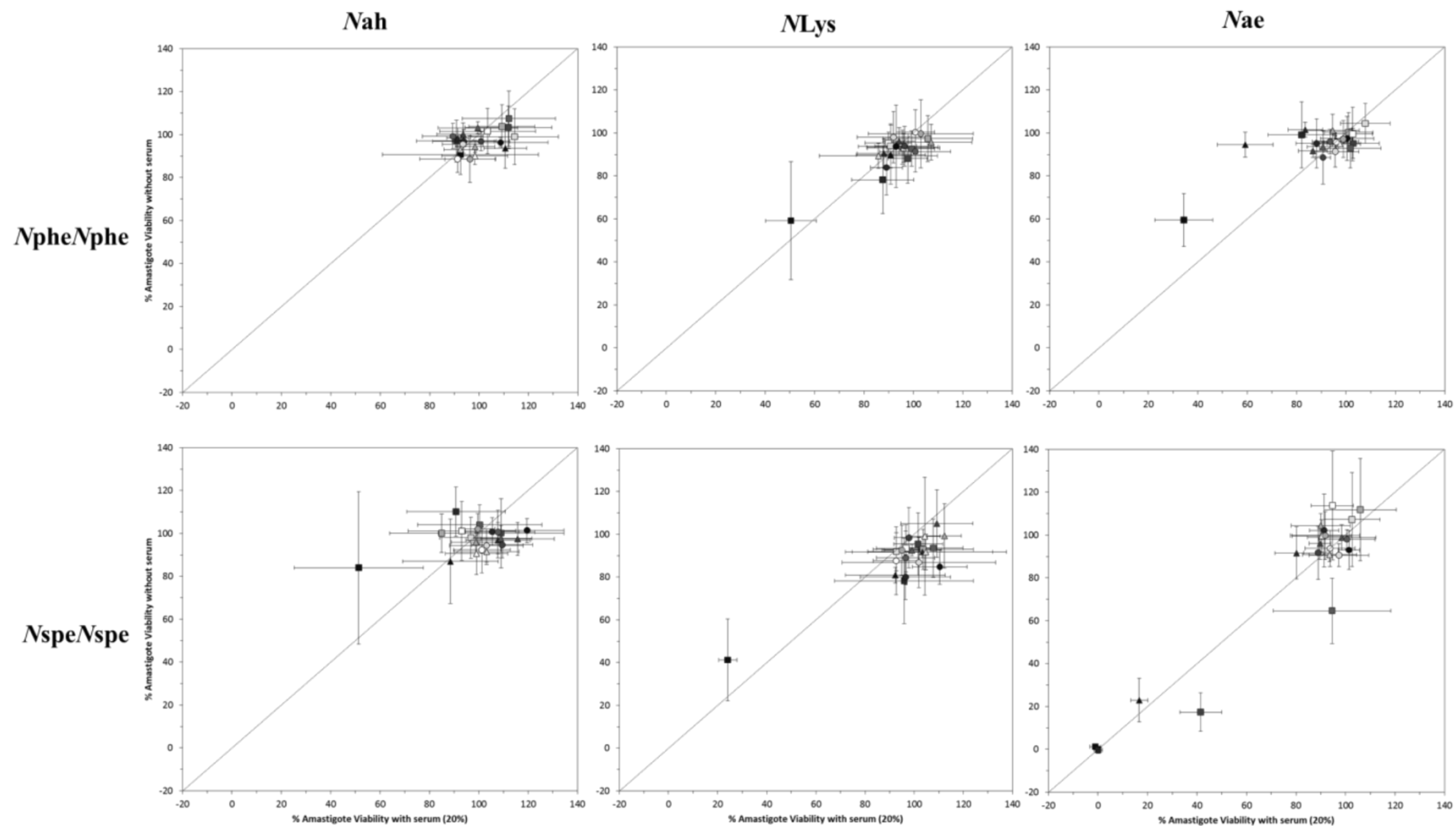
Figure A4. Comparison of serum and serum-free conditions in *L. mexicana* amastigotes; ■ 12 residue, ▲ 9 residue and ● 6 residue peptoids (compounds **210–219**).

Parasite viability graphs for the *L. mexicana* infection assays
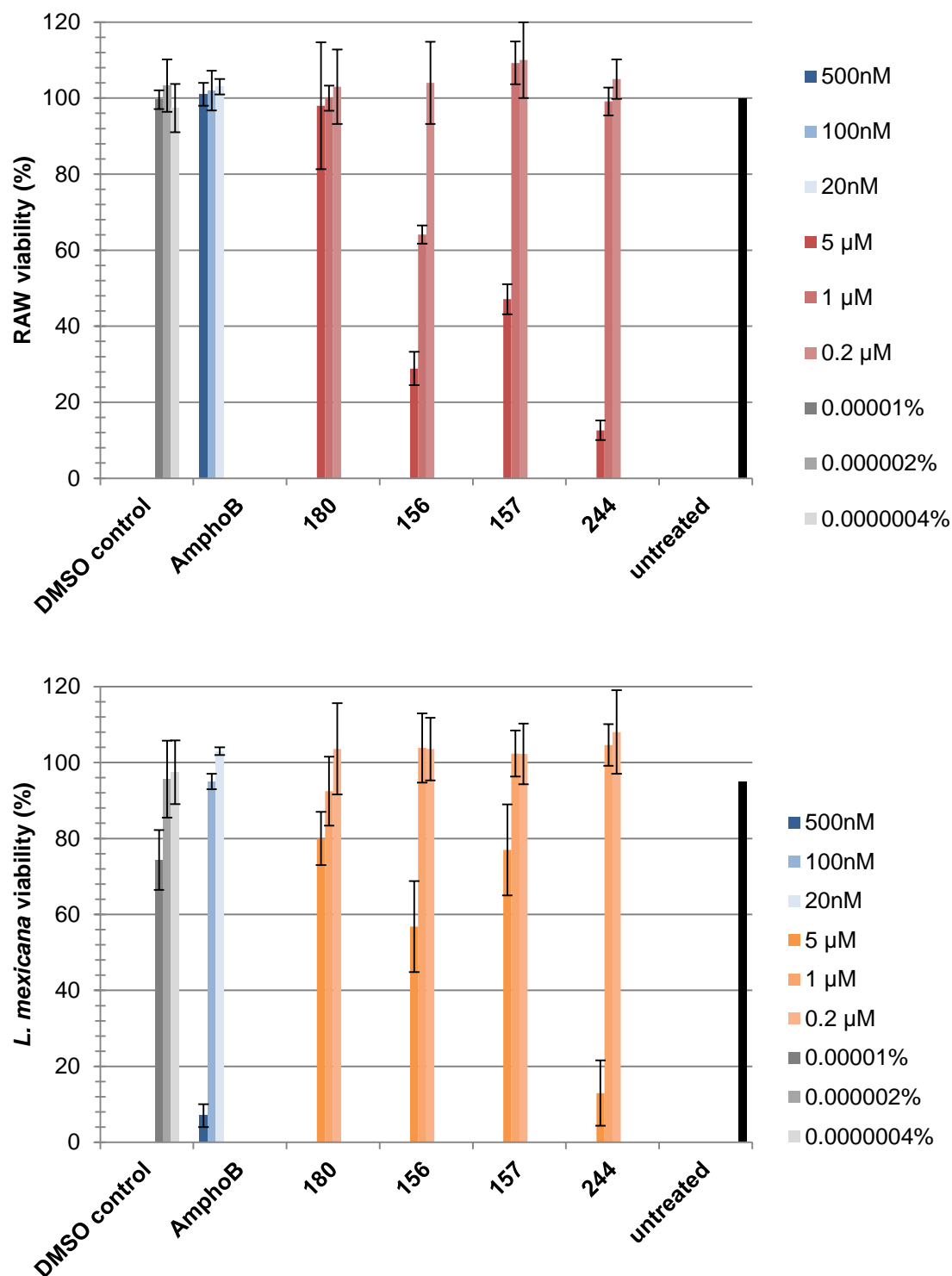
Figure A5. The viability of RAW 264.7 murine macrophages (top) and intracellular *L. mexicana* (bottom) following treatment by peptoids.
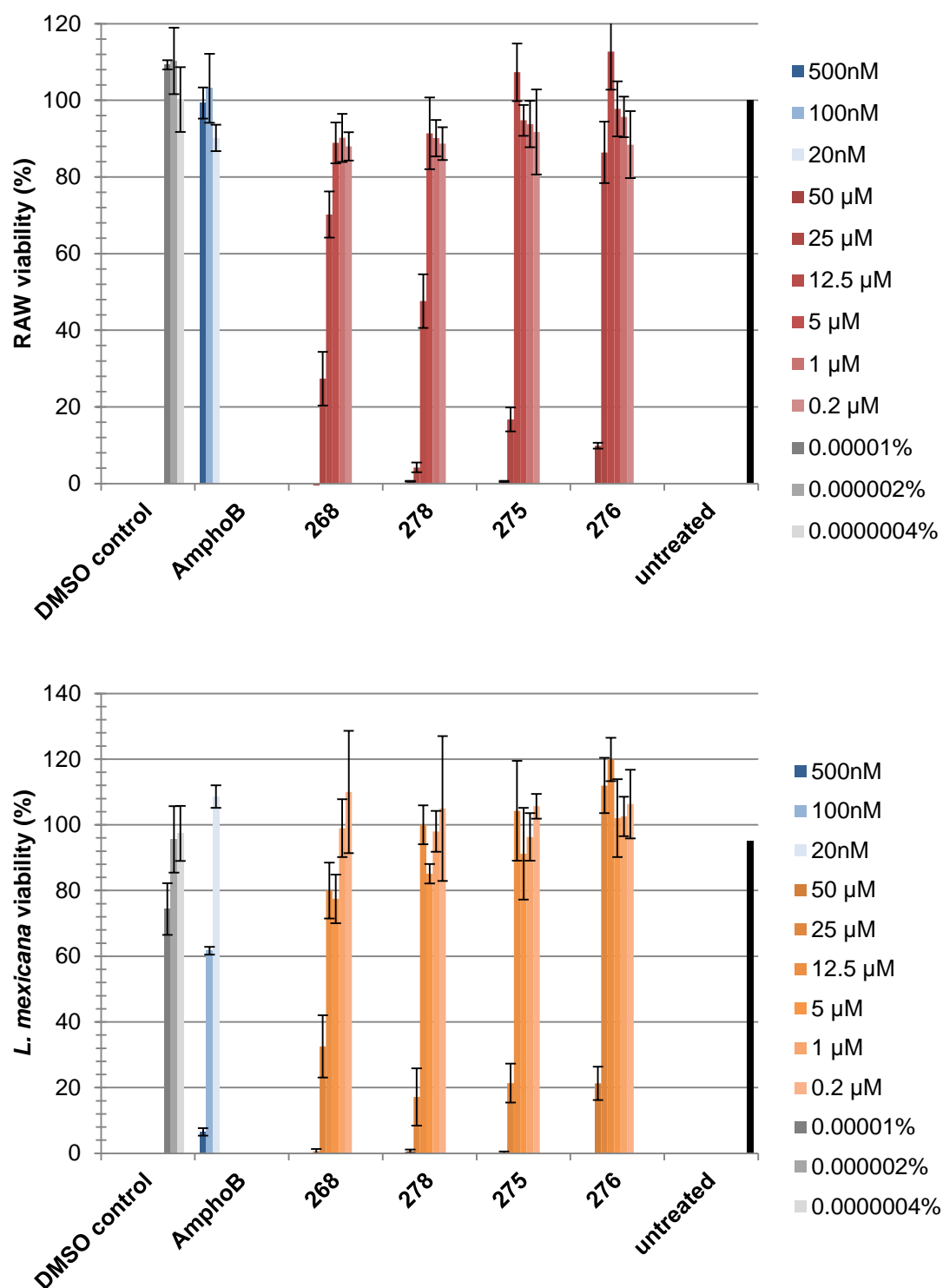
Figure A6. The viability of RAW 264.7 murine macrophages (top) and intracellular *L. mexicana* (bottom) following treatment by peptoids.
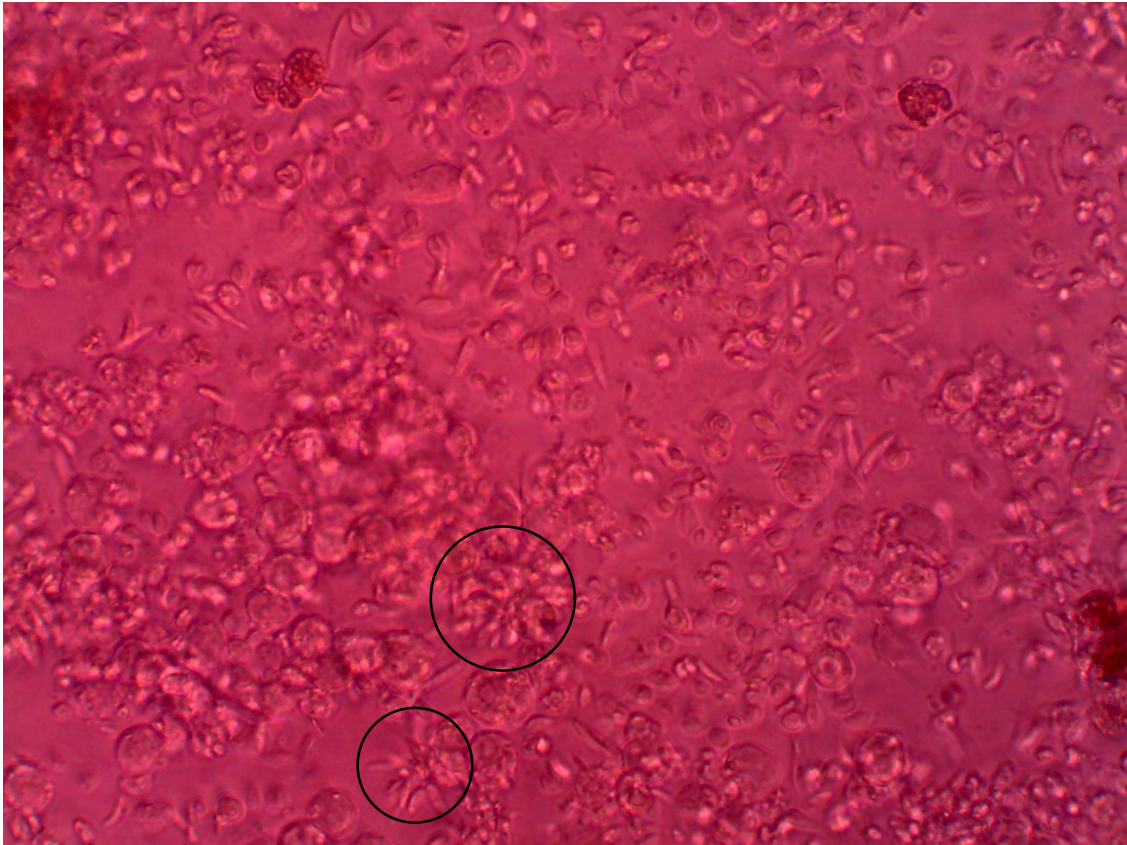
Figure A7. Photograph to show parasites rescued from the infected macrophage assay (in this case from *L. mexicana* infected RAW cells treated with DMSO only). Lysed RAW cell debris is seen as the spherical cells. *L. mexicana* parasites appear similar to the infective, metacyclic promastigote form. Cells appear motile and healthy, with cell splitting and cell bundles seen, as indicated by the highlighted region on the photograph. The pink colour of the culture is due to the alamarBlue® added at the end point of the assay and indicates viable cells.

A5. Nisin stability data

HPLC data from digestion of 322 and 323

Digestion of **322** and **323** was monitored using analytical RP-HPLC. The starting nisin-peptoid conjugate is labelled with a star in **Figure A8 (322)** and **Figure A9 (323)**. At the relevant time point, the digestion was sampled (100 μL), 10 μL TFA added to quench enzyme activity and a 10 μL injection made to the HPLC instrument. Further conditions are described in Chapter 7.
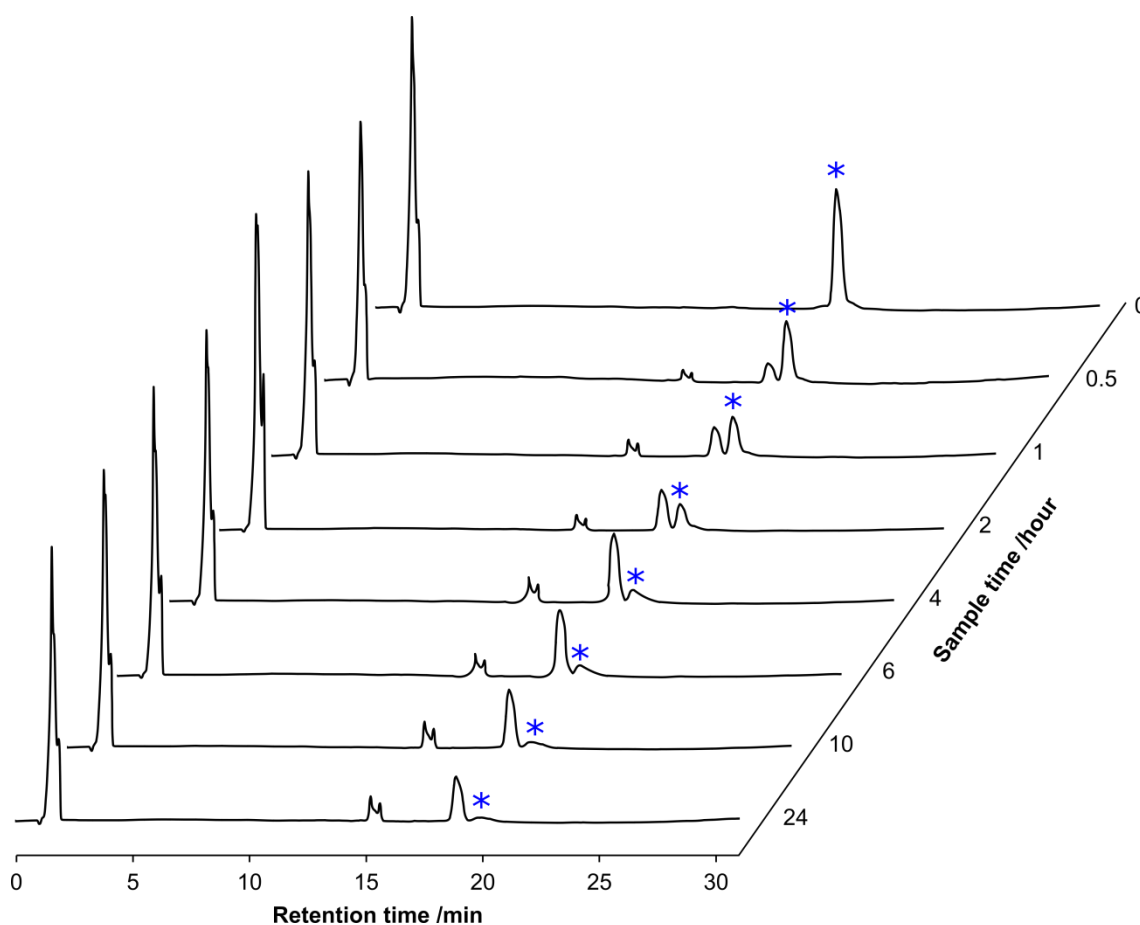
Figure A8. RP-HPLC chromatograms for the digestion of **322** by trypsin in tris-HCl buffer (50 mM at pH 7.8, with 5 mmol CalCl$_2$) over a 24 hour time period. The starting nisin-peptoid conjugate is labelled with a star and cleavage to peptide and peptoid fragments can be seen. Intense peak at approximately 1 minute corresponds to TFA added to quench enzyme activity.
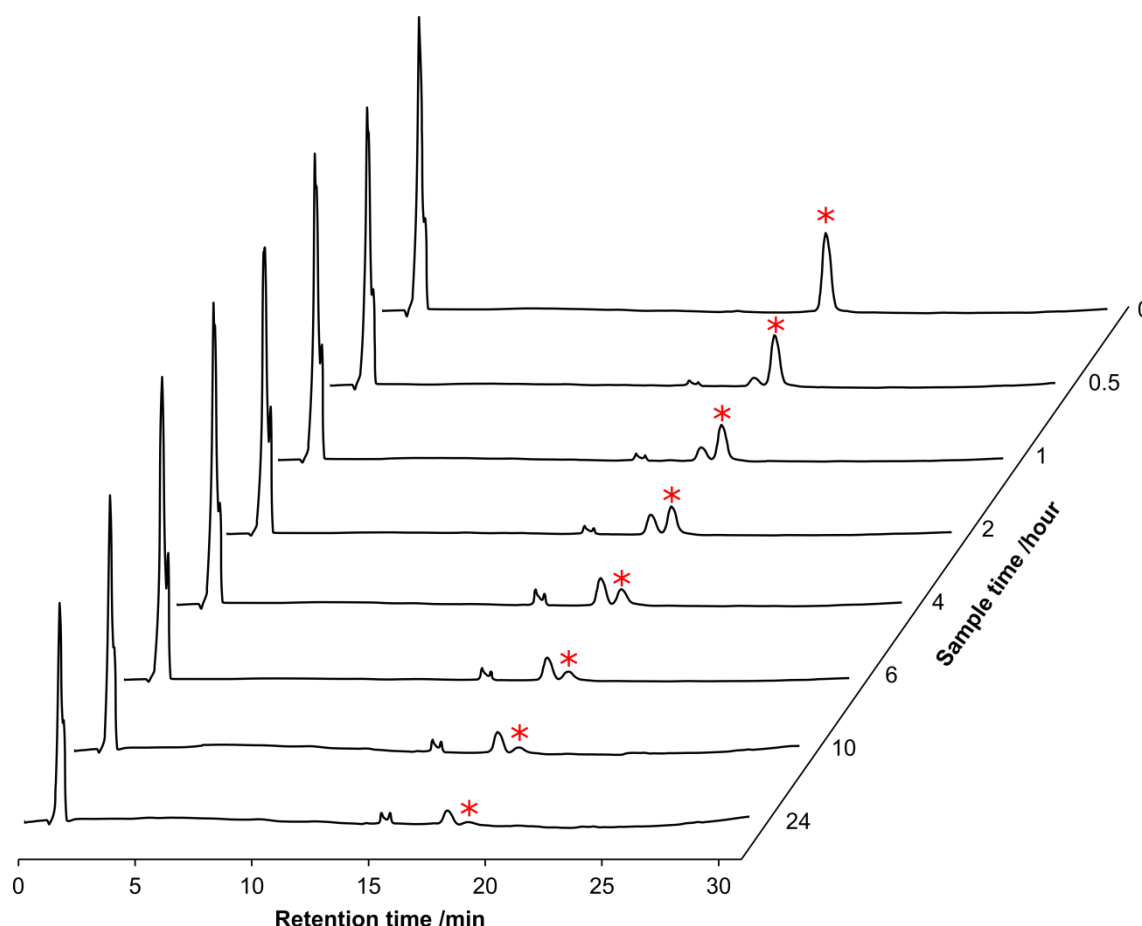
Figure A9. RP-HPLC chromatograms for the digestion of **323** by trypsin in tris-HCl buffer (50 mM at pH 7.8, with 5 mmol CalCl$_2$) over a 24 hour time period. The starting nisin-peptoid conjugate is labelled with a star and cleavage to peptide and peptoid fragments can be seen. Intense peak at approximately 1 minute corresponds to TFA added to quench enzyme activity.

MALDI spectra following 24 hour digestion

MALDI spectra of the nisin-peptoid conjugates and peptoid sequences were recorded before and after sample incubation with trypsin (at t = 0 and t = 24 h). The spectra recorded after 24 hours tryptic degradation are shown in **Figure A10** and **Figure A11** for nisin-peptoid conjugate A (**322**) and nisin-peptoid conjugate B (**323**) respectively. Significant peaks are seen at *m/z* 2225 (fragment **325**) and *m/z* 2353 (fragment **326**) corresponding to cleavage at the nisin[AB] lysine 1$_2$ residue.

MS/MS was also undertaken on the major product ion following degradation experiments using MALDI LIFT to confirm the fragments produced (i.e. cleavage at nisin[AB] lysine 12). MALDI LIFT spectra on ions at *m/z* 2225 (fragment **325**) and *m/z* 2353 (**326**) are shown in **Figure A12** and **Figure A13** respectively.
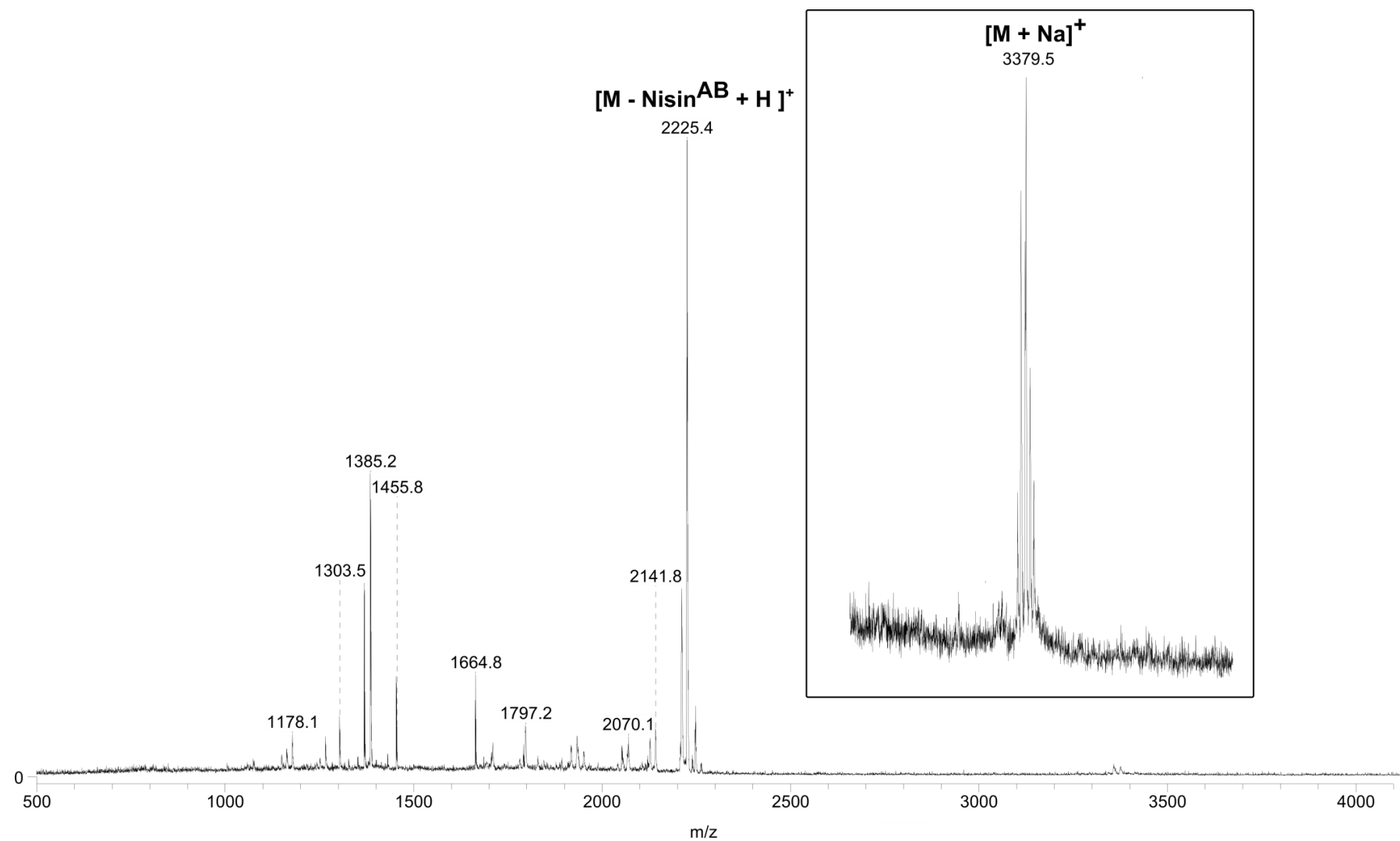
Figure A10. MALDI mass spectrum showing ions following 24 hour trypsin degradation of peptoid **322** with ions labelled. The spectrum has been expanded to show the weak molecular ion peak at *m/z* 3379.5. Suppression of ions at *m/z* < 1000.
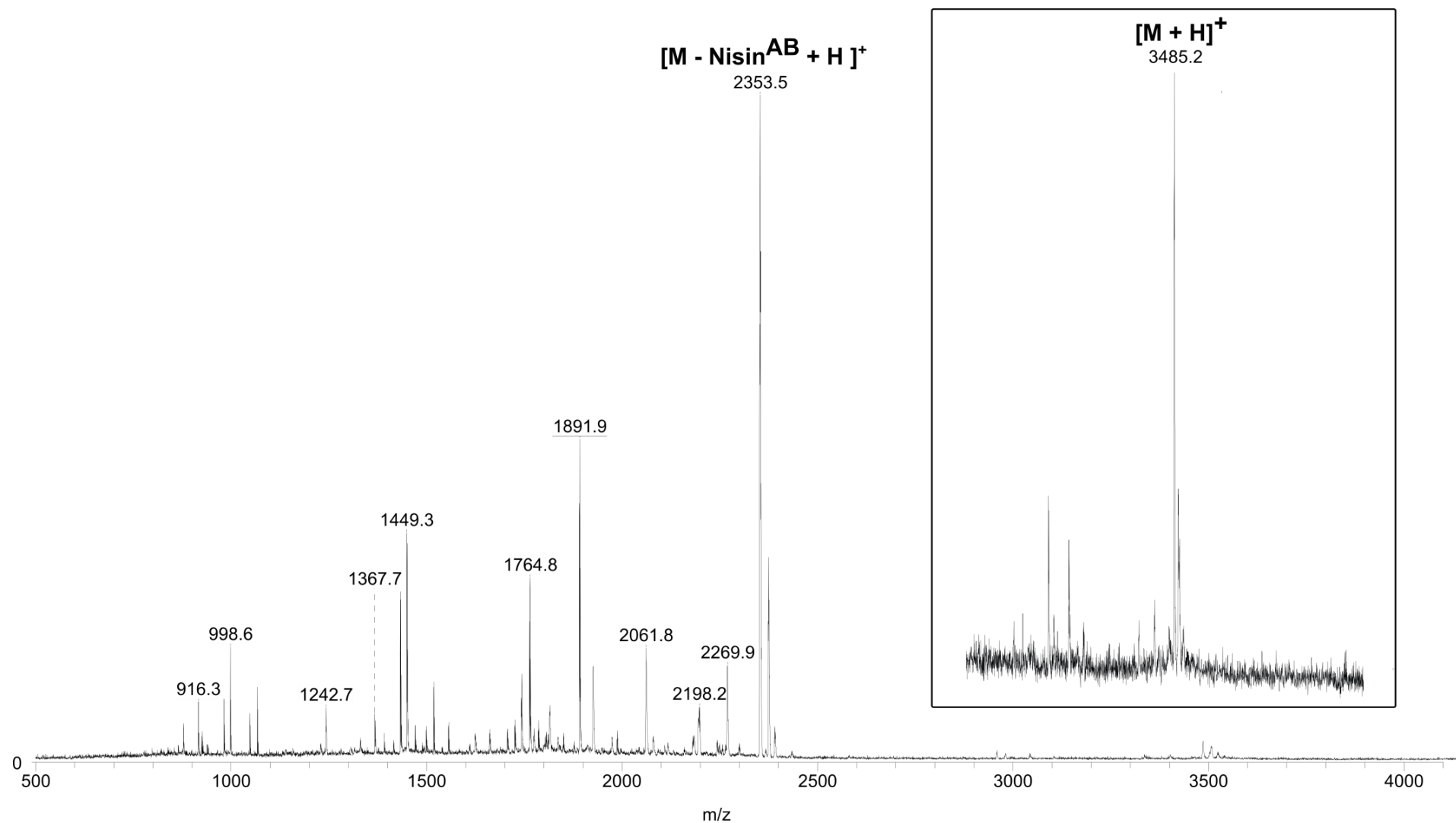
Figure A11. MALDI mass spectrum showing ions following 24 hour trypsin degradation of peptoid **323** with ions labelled. The spectrum has been expanded to show the weak molecular ion peak at *m/z* at 3485.2. Suppression of ions at *m/z* < 1000.
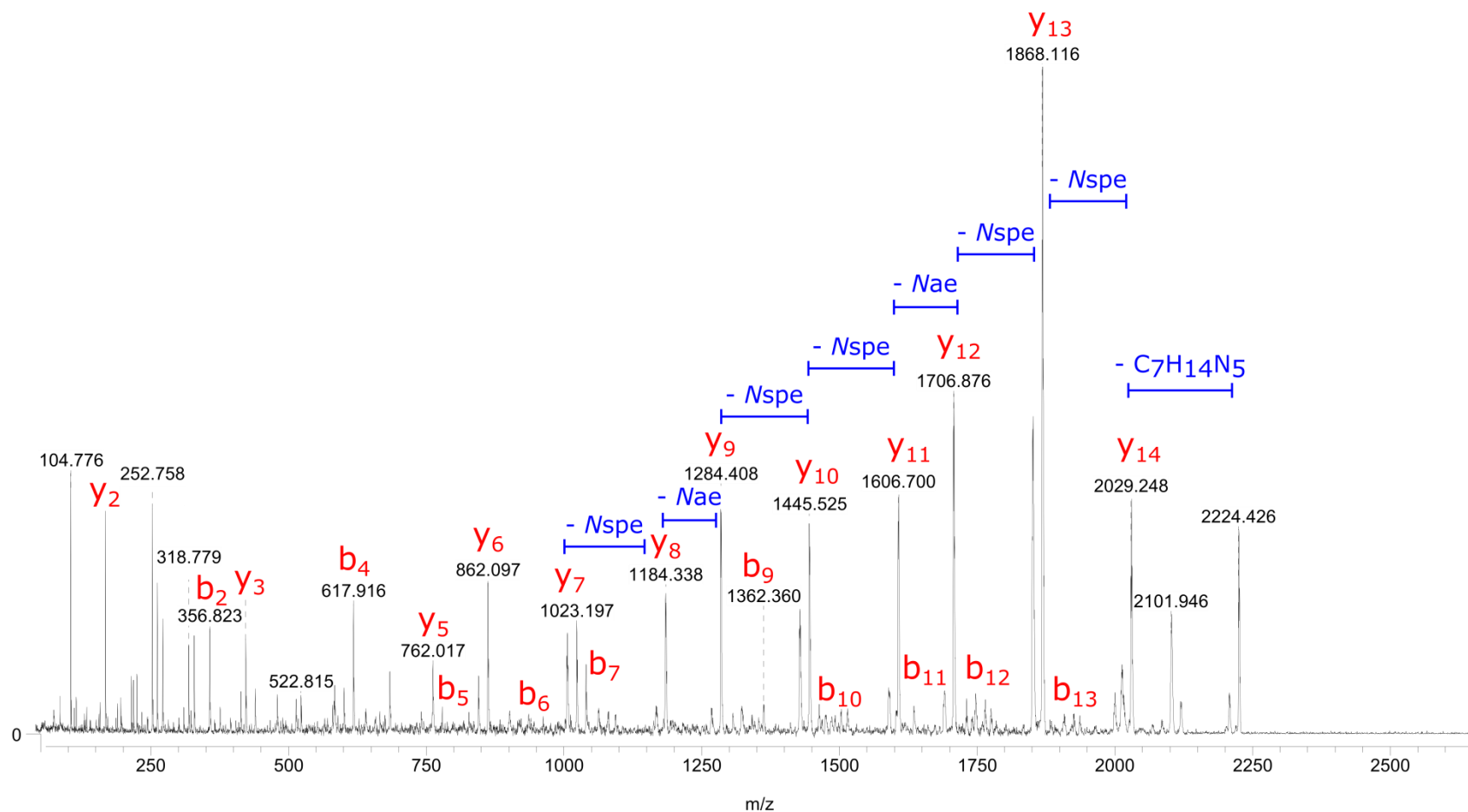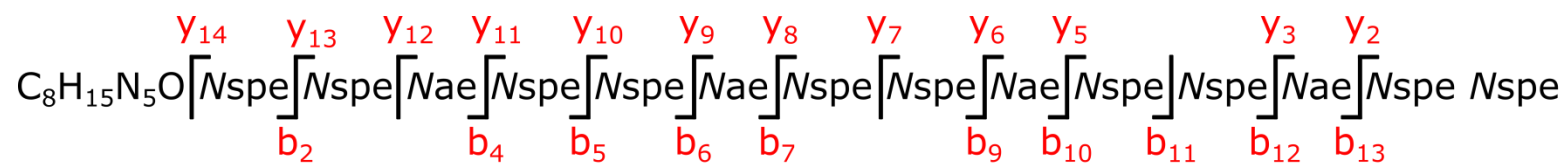
Figure A12. MALDI LIFT TOF/TOF mass spectrum showing fragmentation of ions at m/z 2224 following trypsin degradation of peptoid **322**, with ions labelled. Fragmentation of ions at m/z 2224 is consistent with peptoid fragment **325** obtained from cleavage of nisin[AB] lysine 12 residue in **322**.
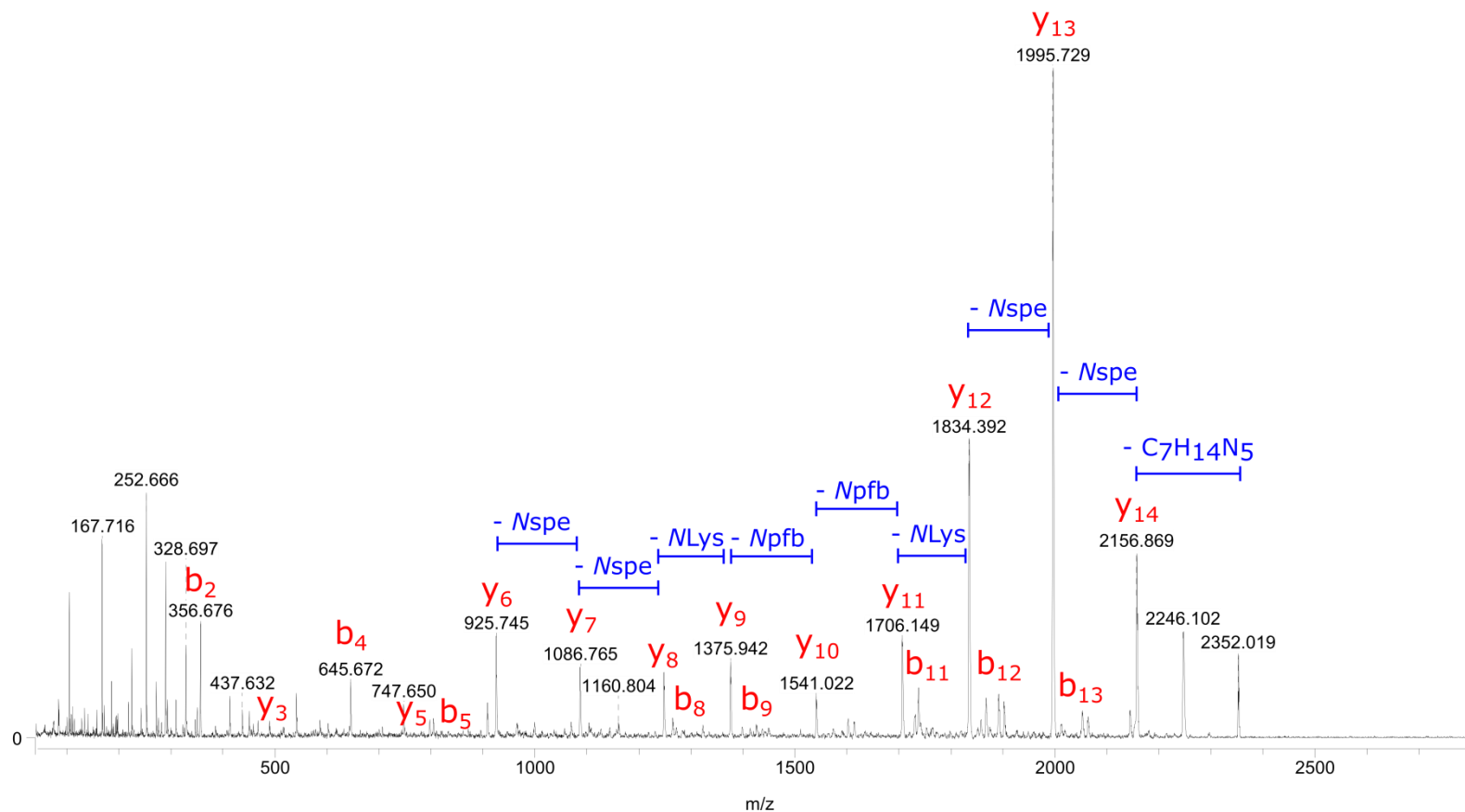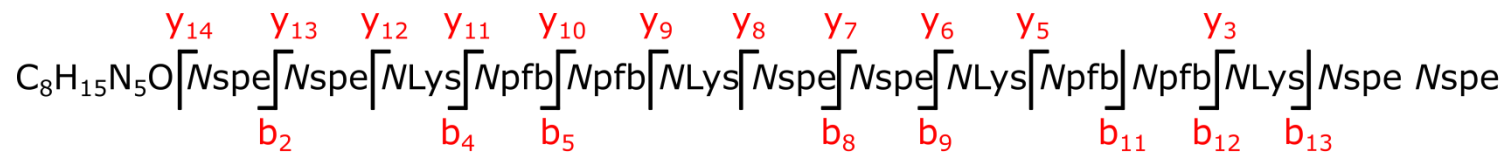
Figure A13. MALDI LIFT TOF/TOF mass spectrum showing fragmentation of ions at *m/z* 2352 following trypsin degradation of peptoid **323**, with ions labelled. Fragmentation of ions at *m/z* 2352 is consistent with peptoid fragment **326** obtained from cleavage of nisin[AB] lysine 12 residue in **323**.

A6. Partitioning experiments

Dynamic light scattering

All of the peptoids used in the hydrophobicity study in Chapter 5 were checked at high concentration (~500 μM) in PBS for indicators of aggregation using dynamic light scattering (**Figure A15**).

Peptoids that partitioned into the octanol substantially during the partitioning experiment were also checked at high concentration (~500 μM) in octanol for indicators of aggregation using dynamic light scattering (**Figure A14**).

Due to the increase in intensity of scattering with size, the presence of a signal at small hydrodynamic diameters indicates the overwhelming majority of the sample is present in the smallest peak.

22 (*N*Lys*N*spe*N*spe)₄
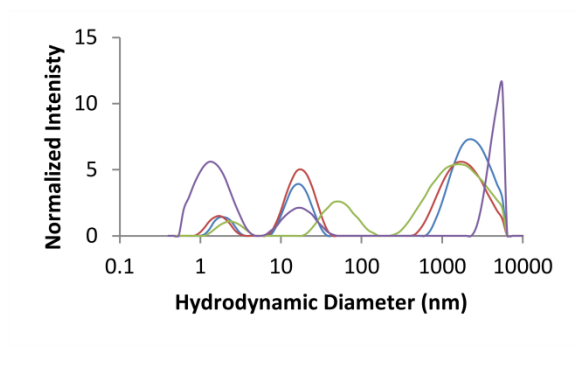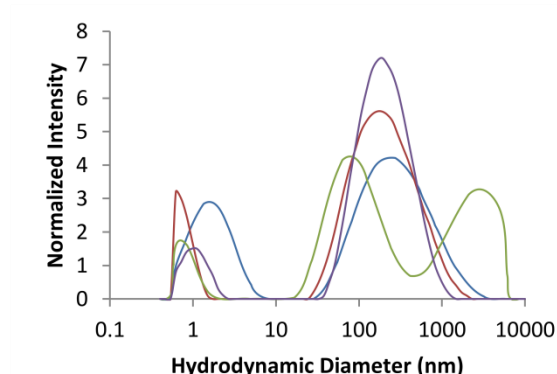
26 (*N*Lys*N*spe*N*spe)₃

156 (*N*ae*N*spe*N*spe)₄
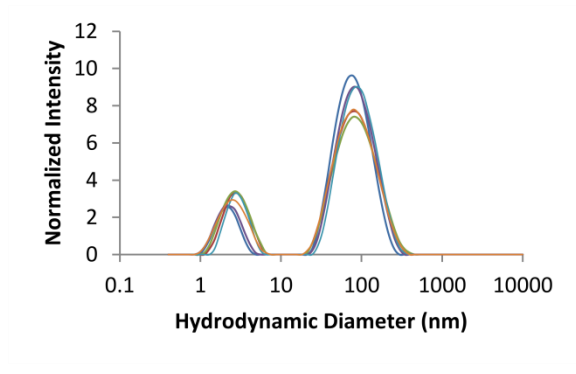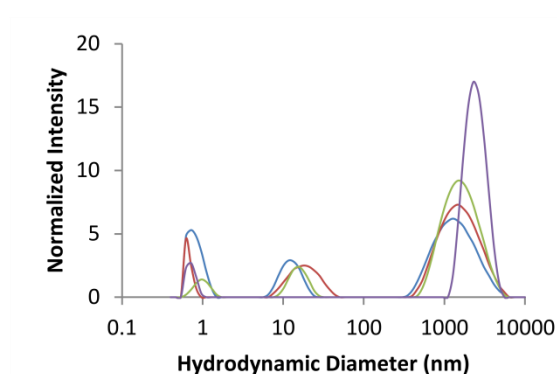
218 (*N*ae*N*spe*N*spe)₃

Figure A14. DLS traces for selected peptoids at 500 μM in octanol.

186 (*N*Lys*N*phe*N*phe)₄
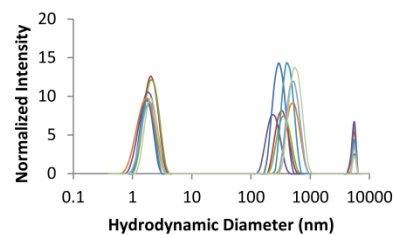
180 (*N*ae*N*phe*N*phe)₄
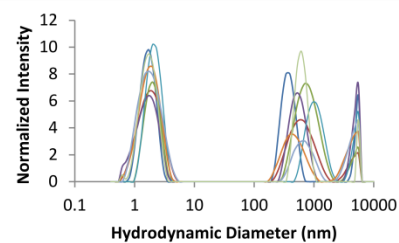
22 (*N*Lys*N*spe*N*spe)₄
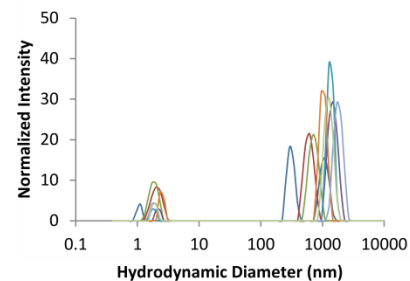
156 (*N*ae*N*spe*N*spe)₄
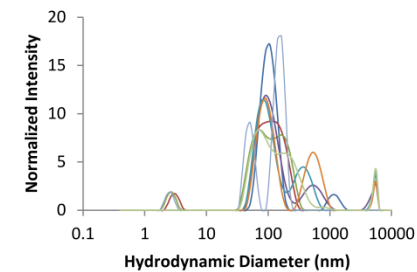
187 (*N*Lys*N*phe*N*phe)₃
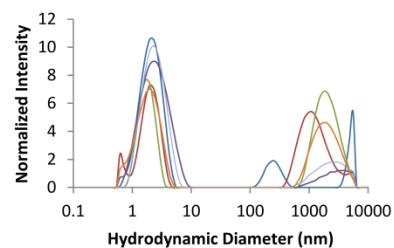
213 (*N*ae*N*phe*N*phe)₃
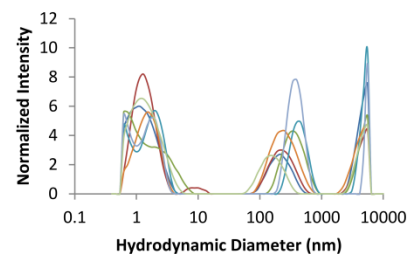
26 (*N*Lys*N*spe*N*spe)₃
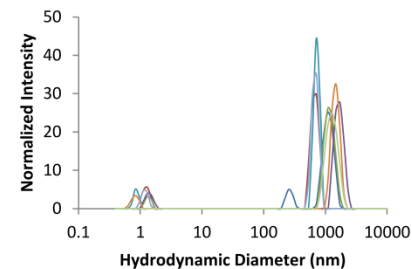
218 (*N*ae*N*spe*N*spe)₃
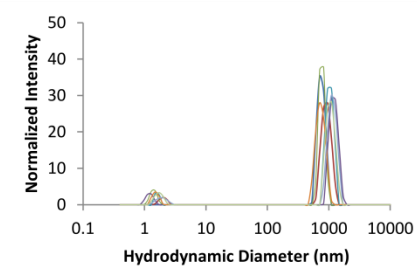
188 (*N*Lys*N*phe*N*phe)₂
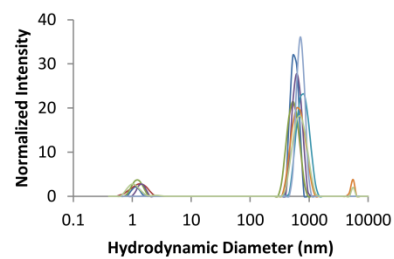
214 (*N*ae*N*phe*N*phe)₂
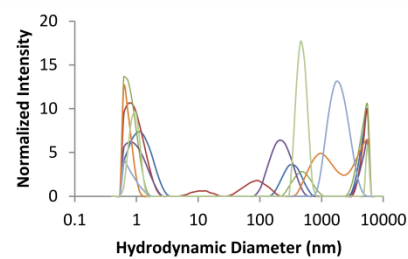
25 (*N*Lys*N*spe*N*spe)₂
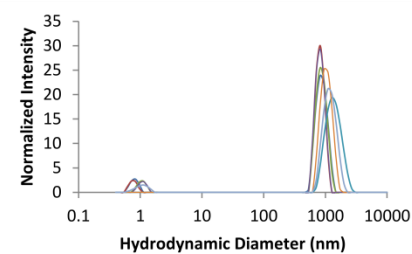
219 (*N*ae*N*spe*N*spe)₂
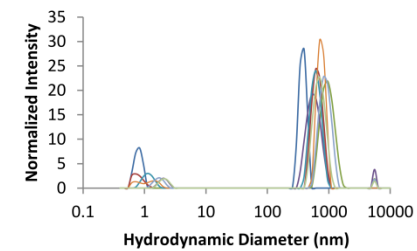
Figure A15. DLS traces for all peptoids tested in partitioning experiments at 500 µM in PBS.

A7. Additional confocal fluorescence microscopy images

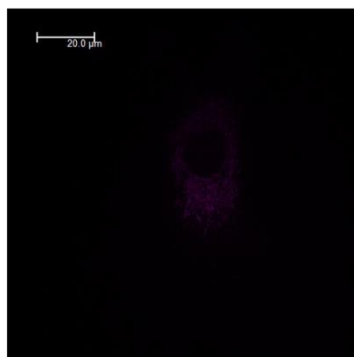The following section contains additional microscopy images, referred to in Chapter 5.
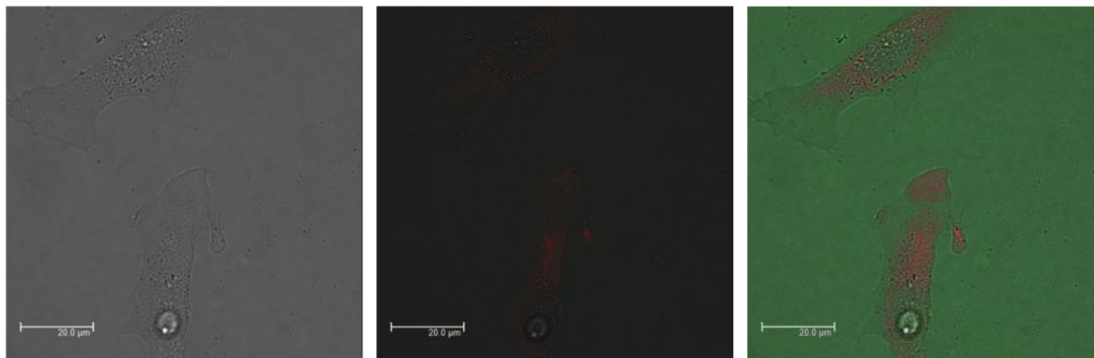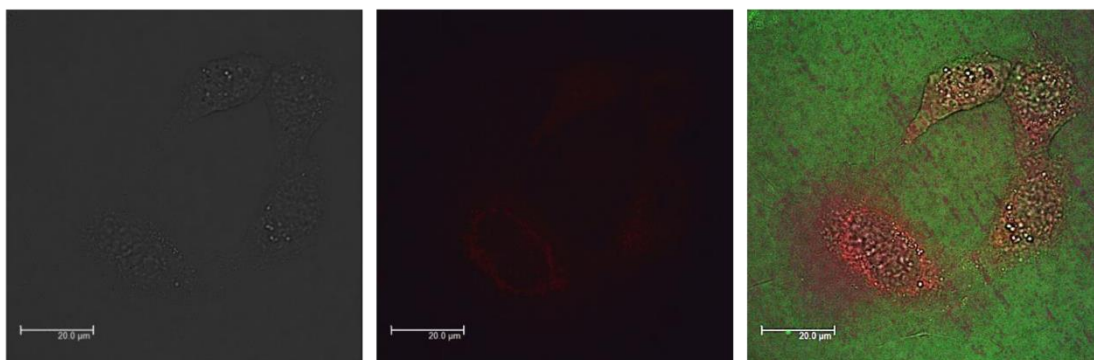
Figure A16. Incubation of 40 µM peptoid **334** fluorescein-Gly-(*N*Lys*N*spe*N*spe)₂ with NIH-3T3 cells at 37 °C. Showing cell images and the green fluorescence seen around the cell, rather than inside the cell. Scale bar 20 µm. **A** incubation time: 15 min; **B** incubation time: 30 min.
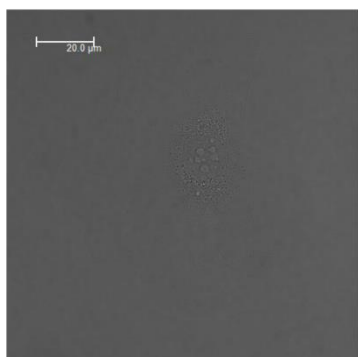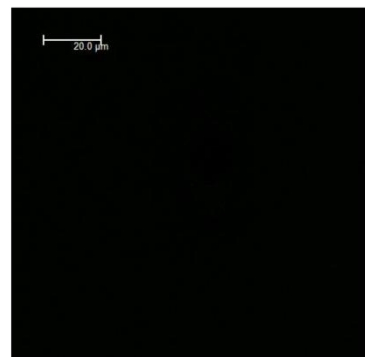

Figure A17. Incubation of 40 µM temporin A peptide **342** with NIH-3T3 cells at 4 °C for 30 min. Cells washed prior to imaging. The lack of peptide fluorescence suggests an active transport mechanism. **A** cell image; **B** mitochondrial autofluorescence (pink); **C** channel where peptide fluorescence is expected.
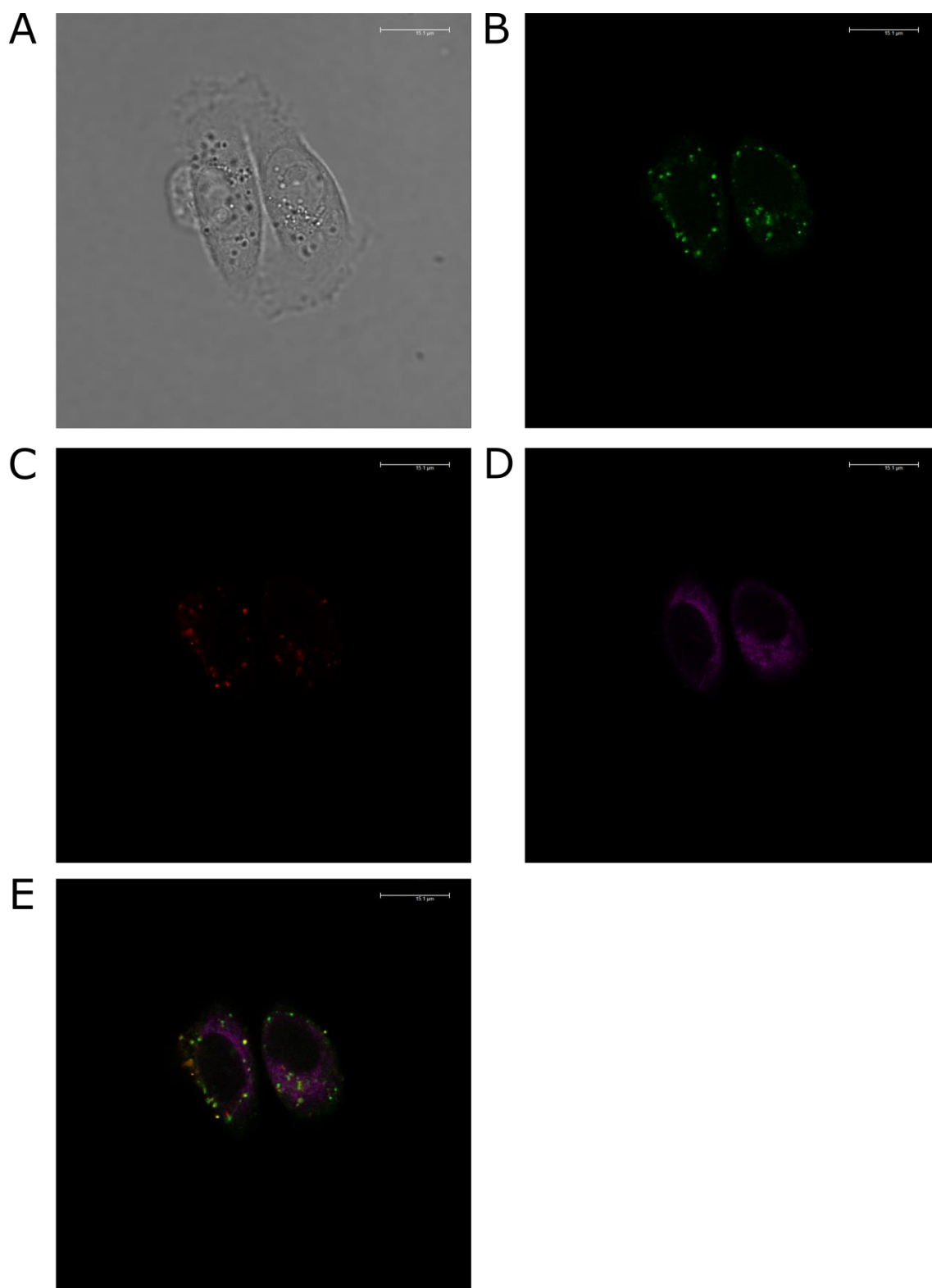
Figure A18. Partial overlap of temporin A peptide **342** and ERTG during incubation of 20 µM **342** with PC3 cells and ERTG at 37 °C for 4 h. **A** cell image; **B** fluorescence of **342** (green); **C** fluorescence of ERTG (red); **D** autofluorescence of mitochondria (pink); **E** merge.
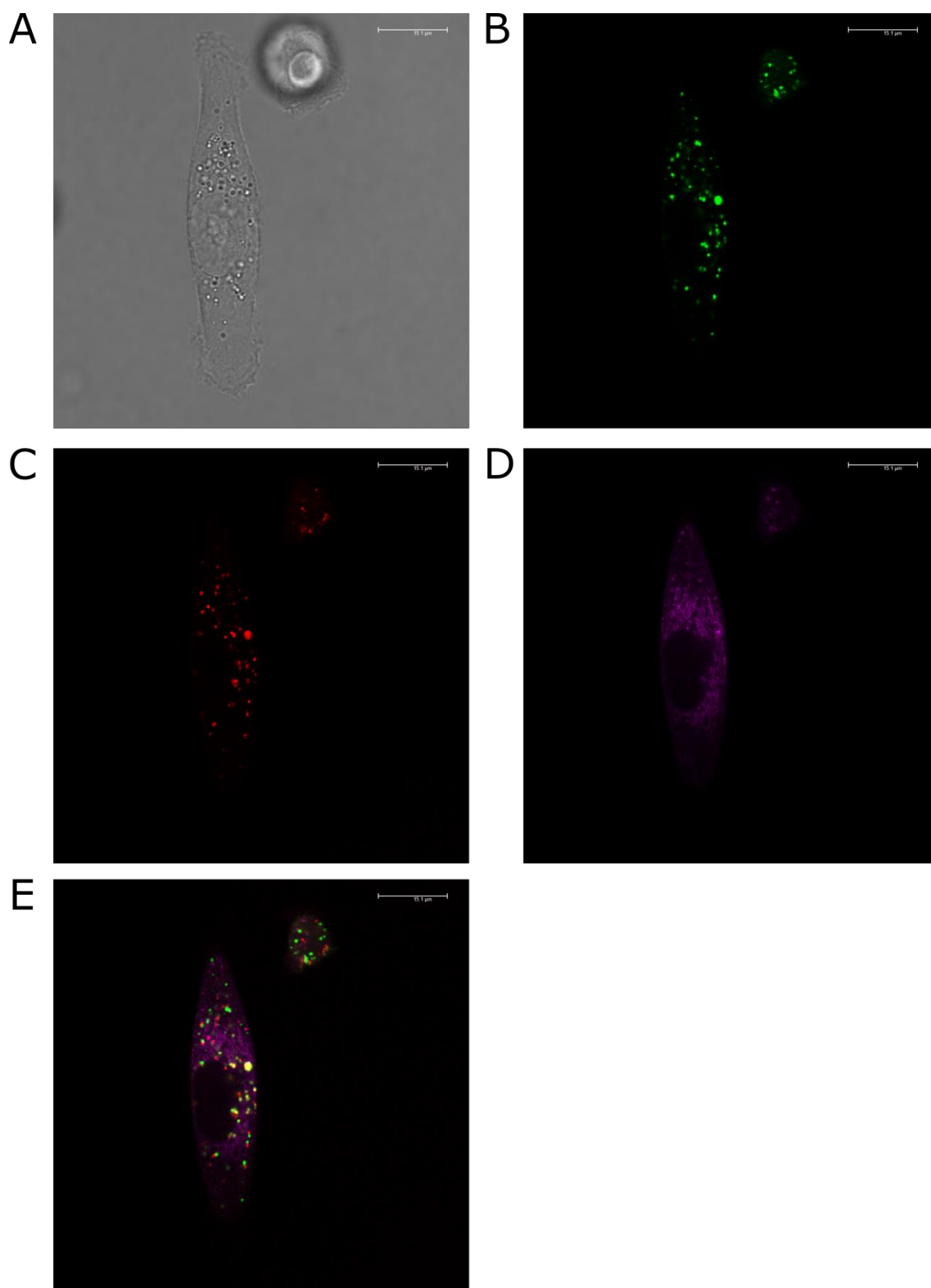
Figure A19. Partial overlap of temporin B peptide **343** and ERTG during incubation of 20 μM **343** with PC3 cells and ERTG at 37 ˚C for 4 h. **A** cell image; **B** fluorescence of **343** (green); **C** fluorescence of ERTG (red); **D** autofluorescence of mitochondria (pink); **E** merge.

A8. Selected additional publications

The following publication describes work using *Leishmania mexicana* mutants, *Δlpg1* and *Δlpg2*, with differing cell membrane compositions (see **Figure A20**) to rationalise the differential activities of the Temporin family of antimicrobial peptides against the amastigote and promastigote forms of the parasite. It is shown that the although the lipophosphoglycan layer (LPG) has little effect, the presence of proteophosphoglycan (PPG) on the parasitic cell membrane is at least partly responsible for the increased susceptibility of promastigotes to the peptides, in comparison to the more resistant amastigotes.
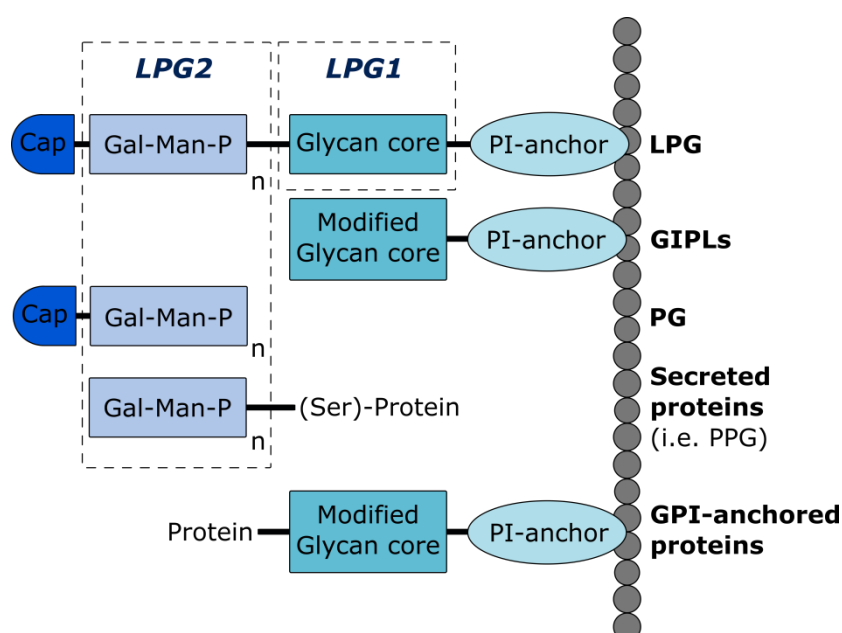

Figure A20. Plasma cell membrane of a typical *Leishmania mexicana* promastigote. The *Δlpg1* parasite is designed to lack LPG, the *Δlpg2* is designed to lack both LPG and PPG.

Article

The Role of Phosphoglycans in the Susceptibility of *Leishmania mexicana* to the Temporin Family of Anti-Microbial Peptides

Gabriela A. Eggimann [1], Kathryn Sweeney [1], Hannah L. Bolt [1], Neshat Rozatian [1], Steven L. Cobb [1,*] and Paul W. Denny [1,2,*]

[1] Biophysical Sciences Institute, Department of Chemistry and School of Biological and Biomedical Sciences, Durham University, South Road, Durham DH1 3LE, UK;
E-Mails: gabriela.eggimann@durham.ac.uk (G.A.E.); kathrynsweeney@hotmail.com (K.S.); h.l.bolt@durham.ac.uk (H.L.B.); neshat.rozatian@durham.ac.uk (N.R.)

[2] School of Medicine, Pharmacy and Health, Durham University, Queen's Campus, Stockton-on-Tees TS17 6BH, UK

* Authors to whom correspondence should be addressed; E-Mails: s.l.cobb@durham.ac.uk (S.L.C.); p.w.denny@durham.ac.uk (P.W.D.); Tel.: +44-191-334-2086 (S.L.C.); +44-191-334-3983 (P.W.D.).

Abstract: Natural product antimicrobial peptides (AMPs) have been proposed as promising agents against the *Leishmania* species, insect vector borne protozoan parasites causing the neglected tropical disease leishmaniasis. However, recent studies have shown that the mammalian pathogenic amastigote form of *L. mexicana*, a causative agent of cutaneous leishmaniasis, is resistant to the amphibian-derived temporin family of AMPs when compared to the insect stage promastigote form. The mode of resistance is unknown, however the insect and mammalian stages of *Leishmania* possess radically different cell surface coats, with amastigotes displaying low (or zero) quantities of lipophosphoglycan (LPG) and proteophosphoglycan (PPG), macromolecules which form thick a glycocalyx in promastigotes. It has been predicted that negatively charged LPG and PPG influence the sensitivity/resistance of promastigote forms to cationic temporins. Using LPG and PPG mutant *L. mexicana*, and an extended range of temporins, in this study we demonstrated that whilst LPG has little role, PPG is a major factor in promastigote sensitivity to the temporin family of AMPs, possibly due to the conferred anionic charge. Therefore, the

lack of PPG seen on the surface of pathogenic amastigote *L. mexicana* may be implicated in their resistance to these peptides.

---

1. Introduction

Leishmaniasis is a neglected tropical disease that is endemic in over 80 countries worldwide. It is caused by *Leishmania* species, insect vector borne protozoan parasites, and affects an estimated 12 million people a year with a further 350 million people living at risk of infection [1]. At the present time a vaccine to prevent leishmaniasis is not available and treatment currently relies entirely on a limited arsenal of chemotherapeutics. For example, treatment of cutaneous leishmaniasis (CL) largely relies on the pentavalent antimonials such as sodium stibogluconate (Pentostam) and meglumine antimoniate (Glucantime) [2,3]. Both Pentostam and Glucantime have been in clinical use for over 70 years despite their associated problems, which include severe side-effects such as cardiotoxicity [4] and the fact that they require parenteral administration [5]. In addition, the use of pentavalent antimonials in the treatment of leishmaniasis is under threat from the emergence of drug resistance [6]. To date resistance has not been widespread in the field but *Leishmania* spp. resistance to Pentostam and Glucantime can be easily induced in the laboratory [7]. Amphotericin B (Fungizone) [8] and diamidine Pentamidine [9] are employed as second-line drugs in the treatment of CL. Like the antimonials, they induce severe side-effects and parasite resistance, although not yet conclusively confirmed in the field, has been observed under laboratory conditions [10]. Given the aforementioned issues with both the current first- and second-line drugs used to treat CL there is clearly a need to develop new and effective therapies for this disease.

In recent years natural product antimicrobial peptides (AMPs) have been investigated as a potential new source of novel antileishmanials [11,12], in part this has been catalysed by the fact that they have displayed promising activity against other cutaneous infectious diseases [13]. The activity of AMPs against *Leishmania* species that give rise to CL has recently been reported. However, despite having promising activity against insect-stage promastigotes, the amphibian-derived temporin family of AMPs has shown limited efficacy against mammalian-stage amastigotes [14]. The predominant surface component of promastigote *Leishmania* is lipophosphoglycan (LPG), a large glycoconjugate which together with cell surface associated proteophosphogycan (PPG) forms a dense glycocalyx protecting the parasite from the mammalian innate immune response on inoculation from the sand fly vector [15]. Subsequently, following infection of macrophage cells and differentiation into the pathogenic amastigote form, expression of cell surface LPG and PPG is massively down-regulated [15,16]. Whilst it has previously been predicted that this thick, negatively charged layer protects the promastigote parasite from cationic AMPs by capturing them and preventing interaction with the cell surface [17], the relative resistance of amastigotes to temporin AMPs suggests the opposite. Herein, we report an extended study of the antileishmanial properties of temporins and the examination of the protective or sensitizing effects of LPG and PPG in *L. mexicana*, a causative agent of CL.

2. Results and Discussion

2.1. The Antileishmanial Properties of Temporin Antimicrobial Peptides

Temporins A, B, 1Sa, F and L were synthesized and analyzed as described in the Experimental Section. The sequences, formulae and accurate mass data are summarized in Table 1. As previously reported [14] temporin A displayed significant activity against *L. mexicana* promastigotes with an ED_{50} of 8 µM. Whilst temporin B demonstrated low potency with an ED_{50} of 38 µM (Figure 1A; Table 2). However, in contrast to the previous study [14] temporin 1Sa demonstrated good activity against these insect stage forms, an ED_{50} of 4 µM (Figure 1). The reasons for this divergence are not clear, however the previously synthesized 1Sa [14] demonstrated similar activity on reanalysis to that shown in Figure 1, indicating that the assay is likely to be the source of this discrepancy. Notably, serum is observed to mask the efficacy of the temporin peptides [14]. Therefore, it is likely that the serum was inadequately removed before assay in the previous study, thereby leading to the underestimation of 1Sa efficacy. To expand this work further temporins F and L were synthesized and purified as described, and then screened against *L. mexicana* promastigotes. Both AMPs showed good activity, F with an ED_{50} of 14 µM and L with an ED_{50} of 5 µM (Figure 1A; Table 2).

Table 1. Tabulated sequences for the peptides tested including accurate mass data. The doubly charged ion was used for accurate mass measurements, *i.e.*, $[M+2H]^{2+}$. All peptides are amidated at the C terminus. Lysine (K) and arginine (R) are positively charged side chains.

Peptide	Sequence	Empirical Formula	Mass Calculated $[M+2H]^{2+}$	Accurate Mass Found $[M+2H]^{2+}$
Temporin A	FLPLIGRVLSGIL-NH$_2$	$C_{68}H_{117}N_{17}O_{14}$	698.9561	698.9548
Temporin B	LLPIVGNLLKSLL-NH$_2$	$C_{67}H_{122}N_{16}O_{15}$	696.4716	696.4735
Temporin 1Sa	FLSGIVGMLGKLF-NH$_2$	$C_{67}H_{109}N_{15}O_{14}S$	690.9078	690.9075
Temporin F	FLPLIGKVLSGIL-NH$_2$	$C_{68}H_{117}N_{15}O_{14}$	684.9531	684.9504
Temporin L	FVQWFSKFLGRIL-NH$_2$	$C_{83}H_{122}N_{20}O_{15}$	820.9792	820.9792

Table 2. ED_{50} for temporins against wild type and mutant *L. mexicana* promastigotes and amastigotes. Mean ED_{50} (and range) shown for the values from at least 3 independent experiments performed in triplicate.

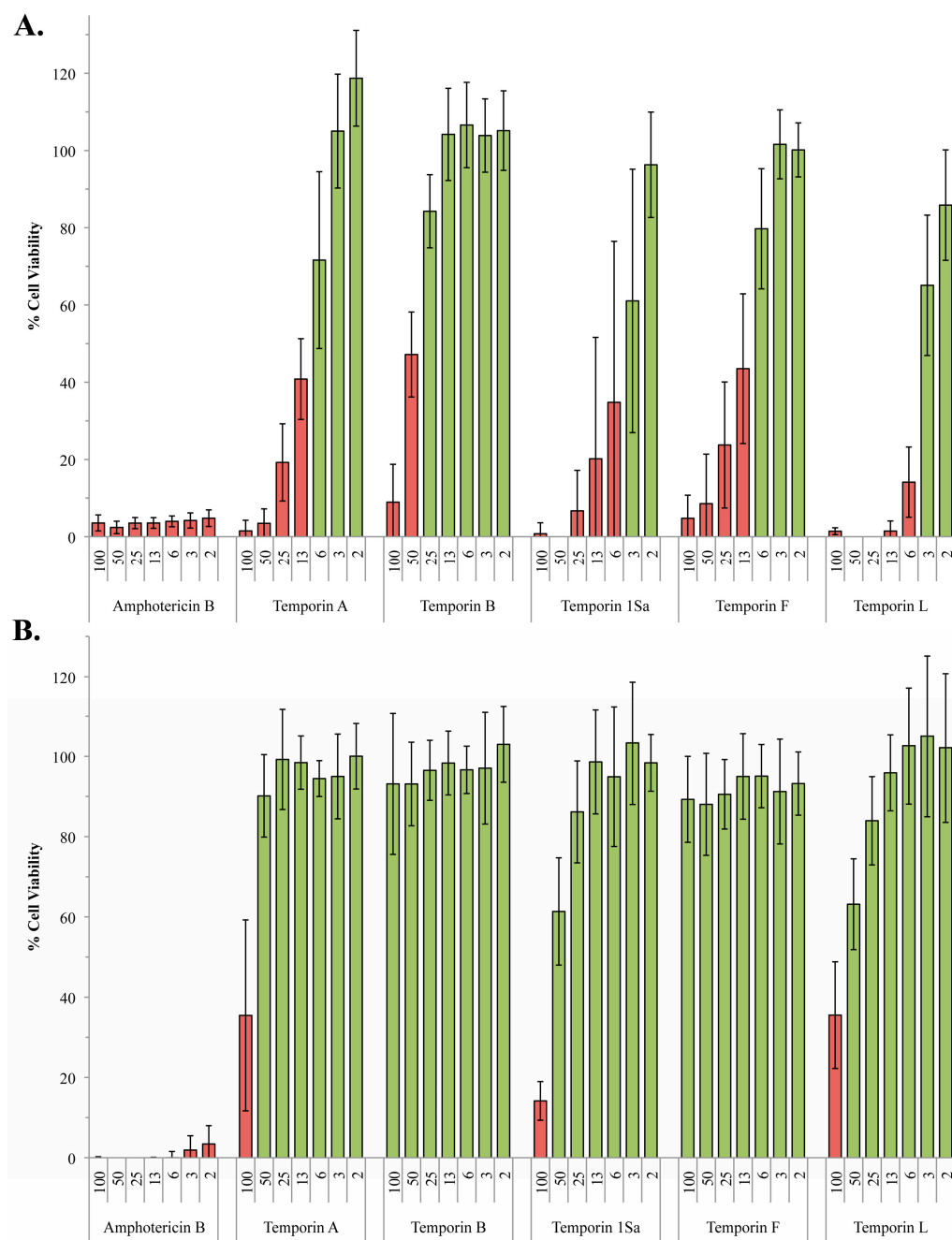| Peptide	ED_{50} (µM)			
	L. mexicana Promastiogte	*L. mexicana* Amastigote	*L. mexicana* $\Delta lpg1$	*L. mexicana* $\Delta lpg2$
Temporin A	8 (6–14)	~100	11 (8–16)	26 (21–39)
Temporin B	38 (24–64)	>100	39 (28–70)	41 (40–41)
Temporin 1Sa	4 (3–13)	42 (35–44)	6 (3–18)	31 (28–35)
Temporin F	14 (10–27)	>100	17 (13–29)	23 (16–49)
Temporin L	5 (5–6)	83 (46–93)	4 (3–6)	9 (8–12)

Figure 1. Activity of the temporin peptides against wild type promastigote and amastigote *L. mexicana.* Using the alamarBlue® assay system, *L. mexicana* promastigote (**A**) and amastigote (**B**) viability in the presence of various concentrations (2–100 µM) of the temporin peptides was determined with respect to a DMSO control. Amphotericin B (2–100 µM) was utilized as a positive control. Data points represent the mean of 3 independent experiments performed in triplicate. Standard deviation indicated. Cell viability <50% indicated by red bars.

However, as previously noted [14], temporin A demonstrated drastically reduced activity against the clinically relevant amastigote form of *L. mexicana* (ED50 of approximately 100 µM), whilst temporin B was inactive at the maximal concentration tested, 100 µM. Similarly, temporin F was

inactive at 100 µM, whilst 1Sa and L had very low levels of activity against amastigote compared to promastigote forms (ED$_{50}$ 42 and 83 µM respectively; Figure 1B; Table 2).

Temporins A, B and 1Sa have all demonstrated significant activity against axenic amastigotes forms of other *Leishmania* species, A and B against *L. pifanoi* [18] and 1Sa against *L. infantum* [19]. *L. infantum* is an Old World species and a member of the *L. donovani* complex, causing visceral disease in the Mediterranean basin, which has subsequently spread to Latin America where it is sometimes known as *L. chagasi* [20]. Like *L. mexicana*, *L. pifanoi* is a New World species, however it is part of the subgenus *Viannia* whereas *L. mexicana* is part of the subgenus *Leishmania* which actually makes it more closely related to *L. infantum* [21]. The considerable evolutionary distance between these different species and subgenra may account for the differing levels of temporin activity observed against amastigotes. The distance is reflected in diversity in the predominant surface glycoconjugates LPG, PPG and glycoinositolphospholipids (GIPLs), macromolecules which play significant roles in the parasite's interface with its insect and mammalian hosts [22]. However, whilst *L. pifanoi* and *L. infantum* have not been extensively analyzed, the levels of LPG and PPG in amastigotes from both Old and New World species are low or zero [15,16] indicating that other factors confer temperin susceptibility. GIPLs are maintained in both lifecycle stages and although *L. pifanoi* and *L. infantum* remain relatively unstudied, significant inter-species variations in GIPL structure have been elucidated. *L. Viannia panamenensis* decorates the conserved galactose-mannose, glycophosphoinositol core with galactose motifs, whereas *L. donovani* GIPLs are highly mannosylated when compared to the simpler *L. mexicana* structures [22]. It is possible that these significant variations account for the differential activity of some temporin AMPs against axenic amastigotes reported in the literature.

2.2. The Role of Phosphoglycans in the Susceptibility of L. Mexiciana to the Temporin Family of Antimicrobial Peptides

Previously it has been postulated that LPG, which forms a thick negatively charged layer, protects the promatigote parasite from cationic AMPs by capturing them and preventing interaction with the cell surface [17]. However, the fact that amastigote *L. mexicana* possess little or no LPG at their surface [16], and yet are considerably more resistant to the temporin AMPs, argues against this hypothesis. Rather it suggests that LPG is a susceptibility factor, with the negatively charged macromolecule perhaps facilitating the concentration of these cationic peptides at the plasma membrane. To test this hypothesis the five temporins were assayed for their activity against *L. mexicana* promastigotes engineered to lack LPG, Δ*lpg1* [23]. Targeted deletion of the β-galactofuranosyl transferase lpg1 in *L. mexicana* specifically blocked LPG expression, leaving the other phosphoglycans unaffected [23]. The results obtained were perhaps surprising, with the temporins showing little or no difference in efficacy against the Δ*lpg1* mutant when compared with the wild type *L. mexicana* promastigotes (Figures 1A and 2A; Table 2). However, it is notable the that efficacy of temporins A and B have previously been reported to be unchanged against a similar, although less defined, *L. donovani* LPG mutant [18,24].
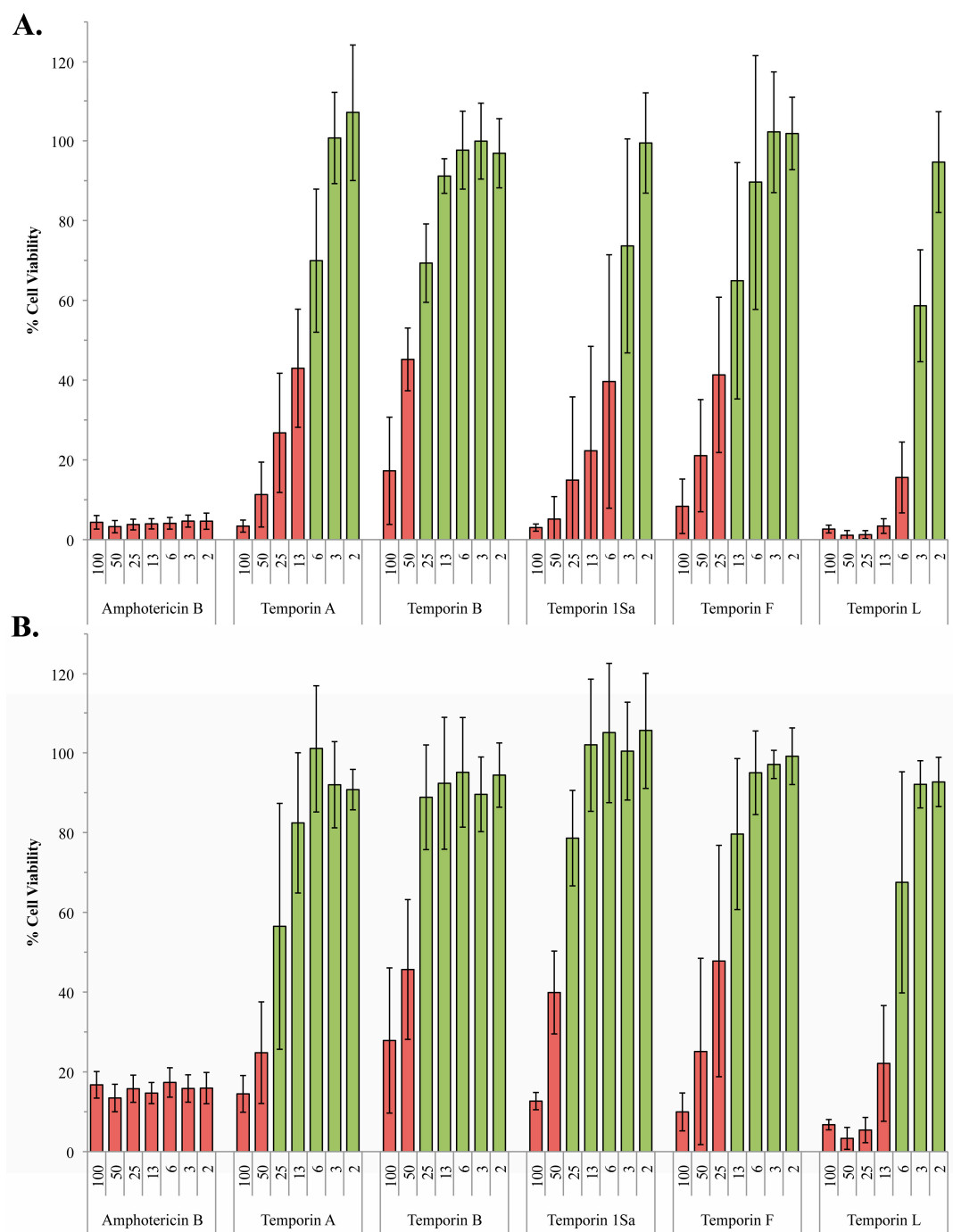
Figure 2. Activity of the temporin peptides against Δ*lpg1 and* Δ*lpg2* promastigote *L. mexicana*. Using the alamarBlue® assay system, *L. mexicana* Δ*lpg1* (**A**) and Δ*lpg2* (**B**) mutant promastigote viability in the presence of various concentrations (2–100 µM) of the temporin peptides was determined with respect to a DMSO control. Amphotericin B (2–100 µM) was utilized as a positive control. Data points represent the mean of 3 independent experiments performed in triplicate. Standard deviation indicated. Cell viability <50% indicated by red bars.

Proteophosphogylcans (PPGs) are a large range of secreted and cell surface associated parasite glycoconjugates which, like LPG, carry a negative charge [25]. Both axenic and intramacrophage *L. mexicana* amastigotes lack cell surface associated PPG, although the intracellular parasites do

secrete a form of PPG known as aPPG [26,27]. Targeted deletion of lpg2, a Golgi GDP-Man transporter, to create Δ*lpg2* [25] prevented the formation of the phosphoglycan repeats that make up the backbone of LPG and PPG leaving the promastigote surface devoid of these negatively charged macromolecules. In contrast to the Δ*lpg1* mutant, the Δ*lpg2* promastigotes appeared less sensitive to all the temporins assayed, with the exception temporin B which was the least active of the AMPs against wild type promastigote forms. Temporins A, 1Sa and L showed the greatest difference in efficacy between wild type and Δ*lpg2* promastigotes (temporin A: ED_{50} 8 μM in wild type *vs.* ED_{50} 26 μM in Δ*lpg2*; 1Sa: 4 *vs.* 31; L: 5 *vs.* 9), with the activity of 1Sa against the mutant close to that of the generically resistant amastigote form (ED_{50} 42 μM in amastigotes *vs.* ED_{50} 31 μM in Δ*lpg2*). This indicated that PPG plays a role in promastigote sensitivity to the temporins (Figures 1 and 2B; Table 2) perhaps due to its negative charge attracting the cationic AMPs to the plasma membrane. However, it is notable that the clinical antileishmanial amphotericin B (used as a control in these experiments) is also less effective against Δ*lpg2 L. mexicana* (Figure 2B) indicating that the lack of PPG is leading to a generic increase in resistance to disruptors of the parasite cell surface. Like the temporins, amphotericin B is a pore forming compound [28].

3. Experimental Section

3.1. Materials and Reagents

Abbreviations for reagents are as follows: *tert*-butoxycarbonyl (Boc); 9-fluorenylmethoxylcarbonyl (Fmoc); trifluoroacetic acid (TFA); triisopropylsilyl (TIPS); *N,N*-dimethylformamide (DMF); dimethyl sulfoxide (DMSO). Solvents and reagents were purchased from commercial sources and used without further purification unless otherwise noted. Rink amide resin (typical loading level 0.6–0.8 mmol/g) was purchased from Merck4Biosciences (Darmstadt, Germany). DMF was purchased from AGTC Bioproducts (National Diagnostics, Hessle, UK). Piperidine and DIPEA were purchased from Sigma Aldrich (Gillingham, UK), PyBOP from Apollo Scientific (Stockport, UK) and Fmoc-protected amino acids from Novabiochem (Merck, Nottingham, UK). Preparative RP-HPLC was performed with a semi-preparative Perkin Elmer (Waltham, MA, USA) Series 200 lc pump fitted with a 785A UV/Vis detector using a SB-Analytical ODH-S optimal column (250 × 10 mm, 5 μm, Waters Ltd, Elstree, UK); flow rate 2 mL/min. Peptides were characterised by accurate LC-MS (QToF mass spectrometer and an Acquity UPLC from Waters Ltd using an Acquity UPLC BEH C8 1.7 μm (2.1 mm × 50 mm) column (Waters Ltd) with a flow rate of 0.6 mL/min and a linear gradient of 5%–95% of solvent B over 3.8 min (A = 0.1% formic acid in H_2O, B = 0.1% formic acid in MeCN). Peptide identities were also confirmed by MALDI-TOF mass spectra analysis (Autoflex II ToF/ToF mass spectrometer Bruker Daltonik GmBH, (Coventry, UK) operating in positive ion mode using an α-cyano-4-hydroxycinnamic acid (CHCA) matrix. Data processing was done with MestReNova Version 8.1.

3.2. Peptide Synthesis

Rink Amide AM resin (200–400 mesh, 0.79 mmol/g loading) and all Fmoc-protected amino acids used were purchased from Novabiochem, Merck. PyBOP™ was purchased from CEM (Buckingham, UK). HPLC grade solvents were obtained from Fisher Scientific (Loughborough, UK) and all other

reagents from Sigma Aldrich. Side chain protecting groups utilised for the Fmoc amino acids were *t*-butyl for Ser, Pbf for Arg, Boc for Lys and Trt for Asn. Temporins A, B and 1Sa were prepared as previously described [14]. Temporins A, B, 1Sa, F and L were prepared via manual Fmoc SPPS. Peptides were synthesised on a 0.1 mmol scale (127 mg of Rink Amide AM resin). Fmoc amino acids (2 equiv.) were coupled using PyBOP (2 equiv.) and DIPEA (4 equiv.) at RT for 1 h on a shaker (380 RPM, manual procedure). For the first C-terminus amino acid, double coupling was used. Also all amino acids from the 7th position were double coupled to increase the yield. Fmoc deprotection was carried out using piperidine/DMF (20% v/v) for 5 and then 10 min at RT. Final peptide cleavage was achieved using TFA:TIPS:H$_2$O 95:5:5 (4 mL) at 25 °C with stirring for a minimum of 4 h. The cleavage cocktail was collected, the solvent removed *in vaccuo*, the crude peptides dissolved in acidified H$_2$O (0.1% TFA) and lyophilised. Crude peptides were purified by semi-preparative RP-HPLC, by use of a Perkin Elmer series 200 LC pump, 785A UV/Vis detector, using a 250 mm × 10.0 mm, 5 µm SB analytical column; flow rate = 2 mL/min linear gradient elution 0%–100% B over 60 min (A = 0.1% TFA in 95% H$_2$O and 5% CH$_3$CN, B = 0.1% TFA in 5% H$_2$O and 95% CH$_3$CN) at λ = 220 or 250 nm. Relevant fractions were collected, lyophilized, and analysed by LC–MS, MALDI-TOF MS and analytical HPLC. See Supplemental Materials for analytical data (MALDI-TOF MS spectra and analytical HPLC spectra). Temporin A [FLPLIGRVLSGIL-NH$_2$], temporin B [LLPIV GNLLKSLL-NH$_2$], temporin 1Sa [FLSGIVGMLGKLF-NH$_2$], temporin F [FLPLIGKVLSGIL-NH$_2$], and temporin L [FVQWFSKFLGRIL-NH$_2$].

3.3. Antileishmanial Assay

Leishmania mexicana (MNYC/BZ/62/M379) wild type and LPG mutant parasites (Δ*lpg1* [23] and Δ*lpg2* [25]) were maintained at 26 °C in Schneider's Drosophila media (Sigma Aldrich) supplemented with heat inactivated foetal bovine sera (15% for promastigotes and mutants, and 20% for amastigotes; Biosera). Promastigotes were transformed into axenic amastigotes by a pH and temperature shift as previously described [29]. Cells were counted using a Neubauer Improved Haemocytometer. Cytotoxicity analyses were performed in 96-well plates (Costar, Corning Inc., Amsterdam, The Netherlands) using alamarBlue® (Life Technologies, Paisley, UK) with some modifications to the published, optimized protocol [14]. Briefly, to mitigate against the effects of serum on the efficacy of the peptides, promastigote and amastigote *L. mexicana* were preincubated (26 °C for promatastigotes; 33 °C for amastigotes) with the temporins (2–100 µM) in 10 µL of serum-free media at 4 × 10^6 mL^{-1} for 1 h before the addition of 90 µL of complete media. Following incubation at the appropriate temperature for 24 h, 10 µL of alamarBlue® was added to each well and the plates incubated for a further 4 h prior to assessing cell viability using a fluorescent plate reader (Biotek UK, Potton, UK; 560EX nm/600EM nm). All data points were in triplicate, with amphotericin B as positive and DMSO as negative controls. All of the experiments described above were carried out on a minimum of three separate occasions to ensure a robust data set was collected.

4. Conclusions

In summary, *L. mexicana* amastigotes are generically resistant to the temporin family of AMPs. This is not attributably to their lack of LPG when compared to the insect stage promastigote form.

However, promastigote *L. mexicana* lacking both LPG and the other major negatively charged surface macromolecule PPG are notably more resistant to the temporin AMPs than either wild type or the LPG mutant promastigotes. Given that amastigote *L. mexicana* lack LPG and surface-associated PPG, it may be considered that the cell surface of these mutant promastigotes resembles that of the mammalian pathogenic form [26,27], leading to the hypothesis that PPG is at least partly responsible for the sensitivity of promastigote compared to amastigote *L. mexicana.* Notably, for temporin 1Sa, the ED_{50} against Δ*lpg2 L. mexicana* promastigotes (lacking both of LPG and PPG; 31 µM) was closer to that established for amastigote form (49 µM) than the wild type promastigote form (4 µM; Table 2; Figures 1 and 2). This indicated that, at least for temporin 1Sa, PPG is a major factor in promastigote sensitivity. As hypothesized, this could be due to the highly negatively charged PPG attracting the cationic temporin peptides towards their site of action, the plasma membrane. However, alternative explanations are conceivable. For example, both LPG and cell surface associated PPG are glycophosphoinositol lipid-anchored to the *Leishmania* plasma membrane [30] and their absence may significantly alter membrane fluidity and, perhaps, AMP sensitivity. Whatever the mechanism it is clear that the loss PPG (together with LPG) increases the resistance of *L. mexicana* to a range of temporin AMPs. Given the lack of these predominant macromolecules in pathogenic amastigote forms this may preclude their development as antileishmanials, however secreted PPG associates with *L. major* promastigotes to form a mucin-like coat [31]. Given that intramacrophage (but not axenic) *L. mexicana* amastigotes secrete a form of PPG, aPPG [26,27], it is possible that the presence of this macromolecule within the phagolysosome, and its potential association with the parasite cell surface, will sensitize the pathogen to the temporin AMPs.

Supplementary Materials

Supplementary materials can be accessed at: http://www.mdpi.com/1420-3049/20/02/2775/s1.

Acknowledgments

Author Contributions

GAE lead the experimental work and performed assays; KS performed assays; HLB and NR synthesized and purified the temporins; SLC and PWD conceived, designed and managed the project.

Conflicts of Interest

The authors declare no conflict of interest

References

1. Stuart, K.; Brun, R.; Croft, S.; Fairlamb, A.; Gurtler, R.E.; McKerrow, J.; Reed, S.; Tarleton, R. Kinetoplastids: Related protozoan pathogens, different diseases. *J. Clin Investig.* **2008**, *118*, 1301–1310.
2. Croft, S.L.; Coombs, G.H. Leishmaniasis—Current chemotherapy and recent advances in the search for novel drugs. *Trends Parasitol.* **2003**, *19* , 502–508.
3. Kedzierski, L.; Sakthianandeswaren, A.; Curtis, J.M.; Andrews, P.C.; Junk, P.C.; Kedzierska, K. Leishmaniasis: Current treatment and prospects for new drugs and vaccines. *Curr. Med. Chem.* **2009**, *16*, 599–614.
4. Chappuis, F.; Sundar, S.; Hailu, A.; Ghalib, H.; Rijal, S.; Peeling, R.W.; Alvar, J.; Boelaert, M. Visceral leishmaniasis: What are the needs for diagnosis, treatment and control? *Nat. Rev. Microbiol.* **2007**, *5*, 873–882.
5. Demicheli, C.; Ochoa, R.; da Silva, J.B.; Falcao, C.A.; Rossi-Bergmann, B.; de Melo, A.L.; Sinisterra, R.D.; Frezard, F. Oral delivery of meglumine antimoniate-beta-cyclodextrin complex for treatment of leishmaniasis. *Antimicrob. Agents Chemother.* **2004**, *48*, 100–103.
6. Croft, S.L.; Sundar, S.; Fairlamb, A.H. Drug resistance in leishmaniasis. *Clin. Microbiol. Rev.* **2006**, *19*, 111–126.
7. Ephros, M.; Waldman, E.; Zilberstein, D. Pentostam induces resistance to antimony and the preservative chlorocresol in Leishmania donovani promastigotes and axenically grown amastigotes. *Antimicrob. Agents Chemother.* **1997**, *41*, 1064–1068.
8. Thakur, C.P.; Singh, R.K.; Hassan, S.M.; Kumar, R.; Narain, S.; Kumar, A. Amphotericin B deoxycholate treatment of visceral leishmaniasis with newer modes of administration and precautions: A study of 938 cases. *Trans. R. Soc. Trop. Med. Hyg.* **1999**, *93*, 319–323.
9. Bray, P.G.; Barrett, M.P.; Ward, S.A.; de Koning, H.P. Pentamidine uptake and resistance in pathogenic protozoa: past, present and future. *Trends Parasitol.* **2003**, *19*, 232–239.
10. Di Giorgio, C.; Faraut-Gambarelli, F.; Imbert, A.; Minodier, P.; Gasquet, M.; Dumon, H. Flow cytometric assessment of amphotericin B susceptibility in Leishmania infantum isolates from patients with visceral leishmaniasis. *J. Antimicrob. Chemother.* **1999**, *44*, 71–76.
11. Cobb, S.L.; Denny, P.W. Antimicrobial peptides for leishmaniasis. *Curr. Opin. Investig. Drugs* **2010**, *11*, 868–875.
12. McGwire, B.S.; Kulkarni, M.M. Interactions of antimicrobial peptides with Leishmania and trypanosomes and their functional role in host parasitism. *Exp. Parasitol.* **2010**, *126*, 397–405.
13. Ulvatne, H. Antimicrobial peptides: Potential use in skin infections. *Am. J. Clin. Dermatol.* **2003**, *4*, 591–595.
14. Chadbourne, F.L.; Raleigh, C.; Ali, H.Z.; Denny, P.W.; Cobb, S.L. Studies on the antileishmanial properties of the antimicrobial peptides temporin A, B and 1Sa. *J. Pept. Sci.* **2011**, *17*, 751–755.
15. Naderer, T.; Vince, J.E.; McConville, M.J. Surface determinants of Leishmania parasites and their role in infectivity in the mammalian host. *Curr. Mol. Med.* **2004**, *4*, 649–665.
16. Bahr, V.; Stierhof, Y.D.; Ilg, T.; Demar, M.; Quinten, M.; Overath, P. Expression of lipophosphoglycan, high-molecular weight phosphoglycan and glycoprotein 63 in promastigotes and amastigotes of *Leishmania mexicana. Mol. Biochem. Parasitol.* **1993**, *58*, 107–121.

17. Torrent, M.; Pulido, D.; Rivas, L.; Rivas, L.; Andreu, D. Antimicrobial peptide action on parasites. *Curr. Drug Targets* **2012**, *13*, 1138–1147.
18. Mangoni, M.L.; Saugar, J.M.; Dellisanti, M.; Barra, D.; Simmaco, M.; Rivas, L. Temporins, small antimicrobial peptides with leishmanicidal activity. *J. Biol. Chem.* **2005**, *280*, 984–990.
19. Abbassi, F.; Oury, B.; Blasco, T.; Sereno, D.; Bolbach, G.; Nicolas, P.; Hani, K.; Amiche, M.; Ladram, A. Isolation, characterization and molecular cloning of new temporins from the skin of the North African ranid Pelophylax saharica. *Peptides* **2008**, *29*, 1526–1533.
20. Mauricio, I.L.; Stothard, J.R.; Miles, M.A. The strange case of Leishmania chagasi. *Parasitol. Today* **2000**, *16*, 188–189.
21. Miranda, A.; Samudio, F.; Saldana, A.; Castillo, J.; Brandao, A.; Calzada, J.E. The calmodulin intergenic spacer as molecular target for characterization of Leishmania species. *Parasit. Vectors* **2014**, *7*, 35, doi:10.1186/1756-3305-7-35.
22. De Assis, R.R.; Ibraim, I.C.; Nogueira, P.M.; Soares, R.P.; Turco, S.J. Glycoconjugates in New World species of Leishmania: Polymorphisms in lipophosphoglycan and glycoinositolphospholipids and interaction with hosts. *Biochim. Biophys. Acta* **2012**, *1820*, 1354–1365.
23. Ilg, T. Lipophosphoglycan is not required for infection of macrophages or mice by *Leishmania mexicana*. *EMBO J.* **2000**, *19*, 1953–1962.
24. King, D.L.; Turco, S.J. A ricin agglutinin-resistant clone of Leishmania donovani deficient in lipophosphoglycan. *Mol. Biochem. Parasitol.* **1988**, *28*, 285–293.
25. Ilg, T.; Demar, M.; Harbecke, D. Phosphoglycan repeat-deficient *Leishmania mexicana* parasites remain infectious to macrophages and mice. *J. Biol. Chem.* **2001**, *276*, 4988–4997.
26. Ho, J.L.; Kim, H.K.; Sass, P.M.; He, S.; Geng, J.; Xu, H.; Zhu, B.; Turco, S.J.; Lo, S.K. Structure-function analysis of Leishmania lipophosphoglycan. Distinct domains that mediate binding and inhibition of endothelial cell function. *J. Immunol.* **1996**, *157*, 3013–3020.
27. Ilg, T.; Craik, D.; Currie, G.; Multhaup, G.; Bacic, A. Stage-specific proteophosphoglycan from *Leishmania mexicana* amastigotes. Structural characterization of novel mono-, di-, and triphosphorylated phosphodiester-linked oligosaccharides. *J. Biol. Chem.* **1998**, *273*, 13509–13523.
28. Ramos, H.; Saint-Pierre-Chazalet, M.; Bolard, J.; Cohen, B.E. Effect of ketoconazole on lethal action of amphotericin B on *Leishmania mexicana* promastigotes. *Antimicrob. Agents Chemother.* **1994**, *38*, 1079–1084.
29. Bates, P.A. Complete developmental cycle of *Leishmania mexicana* in axenic culture. *Parasitology* **1994**, *108*, 1–9.
30. Ilg, T. Proteophosphoglycans of Leishmania. *Parasitol. Today* **2000**, *16*, 489–497.
31. Secundino, N.; Kimblin, N.; Peters, N.C.; Lawyer, P.; Capul, A.A.; Beverley, S.M.; Turco, S.J.; Sacks, D. Proteophosphoglycan confers resistance of Leishmania major to midgut digestive enzymes induced by blood feeding in vector sand flies. *Cell. Microbiol.* **2010**, *12*, 906–918.

Sample Availability: Samples of the temporins discussed are available from the authors on request.